



**JÚLIO CÉSAR PERIN DE MELO**

**CELULOSE E LIGNOCELULÓSICOS COMO SUPORTES NA REMOÇÃO DE  
CONTAMINANTES EM LÍQUIDOS**

**CAMPINAS  
2012**





**UNIVERSIDADE ESTADUAL DE CAMPINAS  
INSTITUTO DE QUÍMICA**

**JÚLIO CÉSAR PERIN DE MELO**

**CELULOSE E LIGNOCELULÓSICOS COMO SUPTORES NA REMOÇÃO DE  
CONTAMINANTES EM LÍQUIDOS**

**Orientador: Prof. Dr. Claudio Airoidi**

**TESE DE DOUTORADO APRESENTADA AO  
INSTITUTO DE QUÍMICA DA UNICAMP PARA  
OBTENÇÃO DO TÍTULO DE DOUTOR EM CIÊNCIAS.**

**ESTE EXEMPLAR CORRESPONDE À VERSÃO FINAL DA TESE DEFENDIDA  
POR (NOME DO ALUNO), E ORIENTADA PELO PROF.DR. (NOME DO ORIENTADOR).**

---

**Assinatura do Orientador**

**CAMPINAS  
2012**

**III**

FICHA CATALOGRÁFICA ELABORADA POR SIMONE LUCAS - CRB8/8144 -  
BIBLIOTECA DO INSTITUTO DE QUÍMICA DA UNICAMP

M49c      Melo, Júlio César Perin de (1982-).  
            Celulose e lignocelulósicos como suportes na  
            remoção de contaminantes em líquidos / Júlio César  
            Perin de Melo. – Campinas, SP: [s.n.], 2012.

            Orientador: Claudio Airoidi.

            Tese (doutorado) - Universidade Estadual de  
            Campinas, Instituto de Química.

            1. Celulose. 2. Lignocelulósicos. 3. Modificação  
            química. 4. Sorção. 5. Química Verde. I. Airoidi, Claudio.  
            II. Universidade Estadual de Campinas. Instituto de  
            Química. III. Título.

Informações para Biblioteca Digital

**Título em inglês:** Cellulose and lignocellulosics as supports toward contaminants removal from liquids

**Palavras-chave em inglês:**

Cellulose  
Lignocellulosics  
Chemical modification  
Sorption  
Green Chemistry

**Área de concentração:** Química Inorgânica

**Titulação:** Doutor em Ciências

**Banca examinadora:**

Claudio Airoidi [Orientador]  
Mara Zeni Andrade  
Éder Tadeu Gomes Cavalheiro  
Inés Joeques  
Edvaldo Sabadini

**Data de defesa:** 11/12/2012

**Programa de pós-graduação:** Química



As lagartas não reconhecem as borboletas e continuam a acreditar em seus deuses, também lagartas.



À Érika Moura, a LORA.



# AGRADECIMENTOS

Ao Prof. Dr. **Claudio Airoidi** pela orientação, dedicação e fé em mim.

Aos colabores científicos, em especial **Sirlane Aparecida de Abreu Santana, Edson Cavalcanti da Silva Filho** e **Ramon Kenned de Souza Almeida** pela amizade e trabalhos realizados.

Ao Professor Dr. **Ulf Friederich Schuchardt**.

Ao amigo Dr. **Cléo Thomáz Gabriel Vilela Menegás Teixeira Pires**.

Ao amigo Dr. **Nilton Geraldo de Oliveira Júnior**.

Ao IQ-UNICAMP, pelo suporte oferecido.

Aos familiares

Aos colegas de laboratório.

À **FAPESP** – Fundação de Amparo à Pesquisa no Estado de São Paulo, pela bolsa concedida e pelo apoio financeiro.



# CURRÍCULO

## 1. Dados pessoais

---

**Nome:** Júlio César Perin de Melo

**Data de nascimento:** 09/11/82

**Estado civil:** Solteiro

**Nacionalidade:** Brasileiro

**Endereço profissional:** Universidade Estadual de Campinas  
Cidade Universitária "Zeferino Vaz"  
Barão Geraldo - Campinas/SP Caixa Postal 6154  
Tel: 19-35213109

**E-mail:** julioperin@yahoo.com.br

## 2. Formação Acadêmica

---

2007-2012 Doutorado em química inorgânica  
Universidade Estadual de Campinas (UNICAMP)

2005-2007 Mestrado em química inorgânica  
Universidade Estadual de Campinas (UNICAMP)

2001-2005 Bacharelado em química com habilitação em indústria  
Universidade Federal de Ouro Preto (UFOP)

## 3. Produção científica

---

### 3.1. Iniciação científica

3.1.1. Projeto: Modificação química do bagaço de cana usando poliaminas. Uso destes materiais na adsorção de íons cobre, cádmio e chumbo. Laboratório de Química Orgânica e Meio Ambiente. Orientador: Prof. Dr. Laurent Frédéric Gil. Instituição Financiadora: Fundação de Amparo à Pesquisa do Estado de Minas Gerais (FAPEMIG). Período: 03/2004-02/2005. CEX 85156/02 UFOP

3.1.2 Projeto: Modificação Química da Medula de bagaço de cana. Aplicação à descontaminação de águas poluídas por metais pesados. Laboratório de Química Orgânica e Meio Ambiente. Orientador: Prof. Dr. Laurent Frédéric Gil. Instituição Financiadora: Fundação de Amparo à Pesquisa do Estado de Minas Gerais (FAPEMIG). Período: 05/2003-02/2004. CEX 85156/02 UFOP

3.1.3 Estágio voluntário no laboratório de Química Ambiental e Análise de Águas e Resíduos do Prof. Dr. Cornélio de Freitas Carvalho. Projeto: desenvolvimento e aprimoramento de uma técnica colorimétrica de dosagem de fosfato em água; Período: 10/2002 a 04/2003

## 3.2. Comunicações apresentadas em congresso

- 3.2.1 OLIVEIRA, Andrea Sales de; DE MELO, Júlio César Perin; AIROLDI, Claudio. NH<sub>2</sub>,SH-BIFUNCTIONALIZED PHYLLOSILICATE: AIMING APPLICATION IN ILED'S In: 13<sup>th</sup> BRAZILIAN MEETING ON INORGANIC CHEMISTRY, 2006, Fortaleza. 2006.
- 3.2.2 DE MELO, Júlio César Perin; DA SILVA FILHO, Edson Cavalcante; AIROLDI, Claudio. SOLVENT FREE MODIFIED CELLULOSE FOR HEAVY METAL ADSORPTION STUDY. In: 13<sup>th</sup> BRAZILIAN MEETING ON INORGANIC CHEMISTRY, 2006, Fortaleza. 2006.
- 3.2.3 DA SILVA FILHO, Edson Cavalcante; DE MELO, Júlio César Perin; AIROLDI, Claudio. MODIFIED CELLULOSE WITH ETHYLENEDIAMINE MOLECULE FOR CATIONS REMOVAL IN AQUEOUS SOLUTION. In: 13<sup>th</sup> BRAZILIAN MEETING ON INORGANIC CHEMISTRY, 2006, Fortaleza. 2006.
- 3.2.4 DA SILVA FILHO, Edson Cavalcante; DE MELO, Júlio César Perin; AIROLDI, Claudio. CALORIMETRIC INVESTIGATIONS OF CATIONS ADSORPTION ON 6-ETHANE-1,2-DIAMINE-6-DEOXYCELLULOSE. In: 2<sup>nd</sup> INTERNATIONAL SYMPOSIUM ON CALORIMETRY AND CHEMICAL THERMODYNAMICS, 2006, São Pedro. 2006.
- 3.2.5 MELO, Julio Cesar Perin de; TOLEDO, Thalita França de; KARNITZ JUNIOR, Osvaldo; BOTARO, Vagner Roberto; GIL, Rossimiriam Pereira de Freitas; GIL, Laurent Frédéric. ESTUDO DA CAPACIDADE DE COMPLEXAÇÃO DE ÍONS Cu<sup>2+</sup> e Cd<sup>2+</sup> PELO BAGACO DE CANA MODIFICADO COM ETILENODIAMINA. In: XLIV CONGRESSO BRASILEIRO DE QUÍMICA, 2004, Fortaleza. 2004.
- 3.2.6 TOLEDO, Thalita França de; KARNITZ JUNIOR, Osvaldo; MELO, Julio Cesar Perin de; BOTARO, Vagner Roberto; GIL, Rossimiriam Pereira de Freitas; GIL, Laurent Frédéric. ESTUDO DA CAPACIDADE DE COMPLEXAÇÃO DE ÍONS Cu<sup>2+</sup>, Cd<sup>2+</sup> e Pb<sup>2+</sup> PELO BAGACO DE CANA MODIFICADA COM ANIDRIDO SUCCÍNICO. In: XLIV CONGRESSO BRASILEIRO DE QUÍMICA, 2004, Fortaleza. 2004.
- 3.2.7 KARNITZ JUNIOR, Osvaldo; TOLEDO, Thalita França de; MELO, Júlio César Perin de; GURGEL, Leandro Vinicius Alves; BOTARO, Vagner Roberto; GIL, Rossimiriam Pereira de Freitas; GIL, Laurent Frederic. ESTUDO DA CAPACIDADE DE COMPLEXAÇÃO DE ÍONS CU<sup>2+</sup>, CD<sup>2+</sup> E PB<sup>2+</sup> PELA CELULOSE MODIFICADA QUIMICAMENTE COM ANIDRIDO SUCCÍNICO. In: XVIII ENCONTRO REGIONAL DA SBQ/MG, 2004, Lavras. 2004.
- 3.2.8 MELO, Júlio César Perin de; TOLEDO, Thalita França de; KARNITZ JUNIOR, Osvaldo; GIL, Rossimiriam Pereira de Freitas; BOTARO, Vagner Roberto; GIL, Laurent Frederic. Estudo da capacidade de complexação de íons Cu<sup>2+</sup>, Cd<sup>2+</sup> e Pb<sup>2+</sup> pelo bagaço de cana modificado com etilenodiamina. In: XVIII ENCONTRO REGIONAL DA SBQ/MG, 2004, Lavras. 2004.
- 3.2.9 GIL, Laurent Frederic; MELO, Júlio César Perin de. MODIFICAÇÃO QUÍMICA DO BAGAÇO DE CANA USANDO POLIAMINAS. USO DESTES MATERIAIS NA ADSORÇÃO DE ÍONS COBRE, CÁDMIO E CHUMBO. In: XII SEMINÁRIO DE INICIAÇÃO CIENTÍFICA DA UFOP, 2004, Ouro Preto. 2004.

- 3.2.10 TOLEDO, Thalita França de; KARNITZ JUNIOR, Osvaldo; MELO, Julio Cesar Perin de; BOTARO, Vagner Roberto; GIL, Rossimiriam Pereira de Freitas; GIL, Laurent Frédéric. ESTUDO DA CAPACIDADE DE COMPLEXAÇÃO DE ÍONS  $\text{Cu}^{2+}$  PELA MEDULA DE BAGAÇO DE CANA MODIFICADA QUIMICAMENTE COM ANIDRIDO SUCCÍNICO. In: XVII ENCONTRO REGIONAL DA SBQ/MG, 2003, Juiz de Fora. 2003.
- 3.2.11 CASTRO, Patricia de Padua; TOLEDO, Thalita França de; KARNITZ JUNIOR, Osvaldo; MELO, Julio Cesar Perin de; BOTARO, Vagner Roberto; GIL, Rossimiriam Pereira de Freitas; GIL, Laurent Frédéric. MODIFICAÇÃO QUÍMICA DA MEDULA DE BAGAÇO DE CANA USANDO POLIAMINAS. APLICAÇÃO À DESCONTAMINAÇÃO DE ÁGUAS POLUÍDAS POR METAIS PESADOS. In: XLIII CONGRESSO BRASILEIRO DE QUÍMICA, 2003, Ouro Preto. 2003.

#### 4. Publicações

---

##### 1. Patente

Data de protocolo: 29.07.10

Número de protocolo: 018100027574

Título: Processo de preparação de mesocarpo do coco de babaçu quimicamente modificado; mesocarpo de babaçu quimicamente modificado, processo de remoção de íons metálicos em soluções hidroetalólicas e uso do mesocarpo do coco de babaçu quimicamente modificado

autores: Claudio Airoidi, Sirlane Aparecida Abreu Santana, Adriana Pires Vieira, Edson Cavalcanti da Silva Filho, Júlio César Perin de Melo, Cícero Wellington Brito Bezerra e Hildo Antonio dos Santos Silva.

Unidade: IQ/UNICAMP

2. R. K. S. Almeida, J. C. P. Melo, C. Airoidi, C, A new approach for mesoporous carbon organofunctionalization with maleic anhydride. *Microporous and Mesoporous Materials* 165 (2013) 168–176.
3. Edson C. Silva Filho, José F. Barros Júnior, Sirlane A. A. Santana, Júlio C. P. Melo, Claudio Airoidi, Thermodynamics of cation/basic center interactions from ethylene-1,2-diamine+pentane-2,4-dione cellulose incorporated, *Global J. Physical Chem.* 2, 2011, 277-286.
4. Júlio C. P. Melo, Edson C. Silva Filho, Sirlane A.A. Santana, Claudio Airoidi, Synthesized cellulose/succinic anhydride as an ion exchanger. *Calorimetry of divalent cations in aqueous suspension*, *Thermochimica Acta* 524 (2011) 29– 34

5. A.V. Pires, S.A.A. Santana, C.W.B. Bezerra, H.A.S. Silva, J.A.P. Chaves, J.C.P. Melo, E.C. Silva Filho, C. Airoidi, "Epicarp and mesocarp of babassu (*Orbignya speciosa*): characterization and application in copper phtalocyanine dye removal", *J. Braz. Chem. Soc.*, 22, 21-29 (2011).
6. S.A.A. Santana, A.P. Vieira, E.C. Silva Filho, J.C.P. Melo, C. Airoidi, "Immobilization of ethylenesulfide on babassu coconut epicarp and mesocarp for divalent cation sorption", *J. Hazard. Mater.*, 174, 714-719 (2010).
7. E.C. Silva Filho, S.A.A. Santana, J.C.P. Melo, F.J.V.E. Oliveira, C. Airoidi, "X-ray diffraction and thermogravimety data of cellulose chlorodeoxycellulose and aminodeoxycellulose", *J. Therm. Anal. Calorim.*, 100, 315-321 (2010).
8. A.P. Vieira, S.A.A. Santana, C.W.B. Bezerra, H.A.S. Silva, J.C.P. Melo, E.C. Silva Filho, C. Airoidi, "Copper sorption from aqueous solutions and sugar cane spirits by chemically modified babassu coconut (*Orbignya speciosa*) mesocarp", *Chem. Eng. J.*, 161, 99-105 (2010).
9. J.C.P. Melo, E.C. Silva Filho, S.A.A. Santana, C. Airoidi, "Exploring the favorable ion-exchange ability of phthalylated cellulose biopolymer using thermodynamic data", *Carbohydr. Res.*, 345, 1914-21 (2010).
10. A.P. Vieira, S.A.A. Santana, C.W.B. Bezerra, H.A.S. Silva, J.A.P. Chaves, J.C.P. Melo, E.C. Silva Filho, C. Airoidi, "Kinetics and thermodynamics of textile dye adsorption from aqueous solutions using babassu coconut mesocarp", *J. Hazard. Mater.*, 166, 1272-78 (2009).
11. J.C.P. Melo, E.C. Silva Filho, S.A.A. Santana, C. Airoidi, "Maleic anhydride incorporated onto cellulose and thermodynamics of cation-exchange process at the solid/liquid interface", *Colloids Surf. A*, 346, 138-145 (2009).
12. E.C. Silva Filho, J.C.P. Melo, M.G. Fonseca, C. Airoidi, "Cation removal using cellulose chemically modified by a Schiff base procedure applying green principles", *J. Colloid Interface Sci.*, 340, 8-15 (2009).
13. L. F. Gil, L.V.A. Gurgel, J.C.P. Melo, J.C. Lena, Adsorption of chromium (VI) ion from aqueous solution by succinylated mercerized cellulose functionalized with quaternary ammonium groups. *Bioresource Technology*, v. 100, p. 3214-3220, 2009.

14. O. Karnitz Junior, L.V.A. Gurgel, J.C.P. Melo, V.R. Botaro, T.M.S. Gil, R.P. Freitas; L.F. Gil, Adsorption of heavy metal ion from aqueous single metal solution by chemically modified sugarcane bagasse. *Bioresource Technology*, 98, **2007**, 1145.
15. E.C. Silva Filho, J.C.P. Melo, C. Airoidi, "Preparation of ethylenediamine-anchored cellulose and determination of thermochemical data for the interaction between cations and basic centers at the solid/liquid interface", *Carbohydr. Res.*, 341, 2842-50 (2006).
16. T.F. Toledo, J.C.P. Melo, L.V.A. Karnitz Junior, O. V. Botaro, R.P.F. Gil, L.F. Gil, Modificação química da celulose usando anidrido succínico. estudo da capacidade de complexação de íons  $\text{Cu}^{2+}$  em solução aquosa pelo material obtido. *Revista da Pesquisa e Pós Graduação da Ufop*, 2004.

## **5. Outros**

---

- 5.1.** Programa de Estágio Docência (PED); Disciplina QF952 – Físico Química Experimental. Coordenador: Fred Yukio Fujiwara. Período 08/2006-12/2006. Departamento de Físico Química. Instituto de Química – UNICAMP
- 5.2.** Curso: FILMS DELGADOS SOL-GEL: SINTESIS Y APLICACIONES. Carga horária: 16 horas. Profa. Dra. Cláudia Longo (UNICAMP) e Prof. Dr. Galo Soler-Illia (Universidade de Buenos Aires). UNICAMP, Campinas, 2006
- 5.3.** Estágio no laboratório de Hidrometalurgia do Prof. Dr. Versiane Albis Leão. Título: Estudo da Remoção de Sulfato de águas ácidas de minas e de lixiviação com ácido sulfúrico por precipitação com  $\text{Fe}^{3+}$  ou por adsorção em goethita natural; Período: 07/2004 – 01/2005); Escola de Minas – UFOP
- 5.4.** Curso: A QUÍMICA DOS PESTICIDAS. XXIII Encontro Nacional dos Estudantes de Química. Carga horária: 08 horas. São Carlos, 2004



## Resumo

O trabalho foi realizado com biopolímeros orgânicos naturais: celulose e lignocelulósicos, modificados quimicamente aumentando a capacidade de sorção de contaminantes em líquidos. Foram caracterizados por IV, RMN de  $^{13}\text{C}$ , DRX, MEV and TG. Assim, as inércias química e física foram superadas através dos seguintes procedimentos sintéticos: esterificação com anidridos de celulose (maleato: 2,82, succinato: 3,07, ftalato: 2,99  $\text{mmol g}^{-1}$ ) e de mesocarpo de babaçu (maleato: 141,79, succinato: 176,99, ftalato: 149,27  $\text{mg g}^{-1}$ ); cloração da celulose com cloreto de tionila (4,95  $\text{mmol g}^{-1}$ ); aminação de celulose com etileno-1,2-diamina (3,03  $\text{mmol g}^{-1}$ ); reação de etilenossulfeto com mesocarpo (86,7  $\text{mg g}^{-1}$ ) e epicarpo de babaçu (20,2  $\text{mg g}^{-1}$ ).

Com as modificações químicas dos biopolímeros as propriedades de sorção se tornaram superiores as dos biopolímeros de partida e as novas capacidades máximas de remoção de contaminantes foram: anidridos de celulose [maleato ( $\text{Ni}^{2+} = 1,75$  e  $\text{Co}^{2+} = 2,40$   $\text{mmol g}^{-1}$ ), succinato: ( $\text{Ni}^{2+} = 2,46$  e  $\text{Co}^{2+} = 2,46$   $\text{mmol g}^{-1}$ ) e ftalato: ( $\text{Ni}^{2+} = 2,26$  e  $\text{Co}^{2+} = 2,43$   $\text{mmol g}^{-1}$ )]; anidridos com mesocarpo de babaçu (maleato: ( $\text{Cu}^{2+} = 19,88$   $\text{mg g}^{-1}$ ), succinato: ( $\text{Cu}^{2+} = 38,58$   $\text{mg g}^{-1}$ ) e ftalato: ( $\text{Cu}^{2+} = 30,63$   $\text{mg g}^{-1}$ ) soluções hidroalcoólicas); aminação de celulose com etileno-1,2-diamina ( $\text{Cu}^{2+} = 2,32$ ,  $\text{Co}^{2+} = 1,35$ ,  $\text{Ni}^{2+} = 1,70$  e  $\text{Zn}^{2+} = 1,65$   $\text{mmol g}^{-1}$ ); reação de etilenossulfeto com mesocarpo ( $\text{Cu}^{2+} = 39,6$   $\text{mg g}^{-1}$ ) e epicarpo ( $\text{Cu}^{2+} = 39,2$   $\text{mg g}^{-1}$ ) de babaçu.

A celulose também foi oxidada com metaperiodato aquoso para dar origem à celulose em sua forma oxidada, o 2,3-dialdeído-celulose, material de partida para outras reações, as quais foram: redução dos grupos aldeído do 2,3-dialdeído-celulose, seguido da reação deste material com os anidridos maléico, succínico e ftálico; em seguida cada um dos materiais na forma ácida foi reagido separadamente com etileno-1,2-diamina, dietil-1,2,4-triamina, trietil-1,2,4,6-tetramina. A outra rota foi a reação do 2,3-dialdeído-celulose com as poliaminas etileno-1,2-diamina, dietil-1,2,4-triamina, trietil-1,2,4,6-tetramina e em seguida, com cada um dos materiais aminados obtidos, reagí-los separadamente com os anidridos maléico, succínico e ftálico.



## Abstract

The natural organic biopolymers, cellulose and lignocellulosics, were chemically modified in order to increase their sorption capacities for contaminants from liquids. The technics employed for characterization were IR,  $^{13}\text{C}$  NMR, XDR, SEM and TGA. Chemical modification and the degree of substitution were: esterification of cellulose with anhydrides [maleate:  $2,82 \text{ mmol g}^{-1}$ , succinate:  $3,07 \text{ mmol g}^{-1}$ , phthalate:  $2,99 \text{ mmol g}^{-1}$ ] and esterification of babassu mesocarp coconut with anhydrides (maleate:  $141,79 \text{ mg g}^{-1}$ , succinate:  $176,99 \text{ mg g}^{-1}$ , phthalato:  $149,27 \text{ mg g}^{-1}$ ); chlorination of cellulose with thionyl chloride ( $4,95 \text{ mmol g}^{-1}$ ); amination of cellulose with ethylene-1,2-diamine ( $3,03 \text{ mmol g}^{-1}$ ); reaction of ethylenesulfide with babaçu coconut mesocarp ( $86,7 \text{ mg g}^{-1}$ ) and epicarp ( $20,2 \text{ mg g}^{-1}$ )

The sorption capacities of these chemically modified biopolymers were outlighted as confirmed by the maxima sorption results and were: cellulose with anhydrides (maleate: ( $\text{Ni}^{2+} = 1,75$  e  $\text{Co}^{2+} = 2,40 \text{ mmol g}^{-1}$ ), succinate: ( $\text{Ni}^{2+} = 2,46$  e  $\text{Co}^{2+} = 2,46 \text{ mmol g}^{-1}$ ) e ftalate: ( $\text{Ni}^{2+} = 2,26$  e  $\text{Co}^{2+} = 2,43 \text{ mmol g}^{-1}$ )); babassu mesocarp coconut with anhydrides [maleate: ( $\text{Cu}^{2+} = 19,88 \text{ mg g}^{-1}$ ), succinate: ( $\text{Cu}^{2+} = 38,58 \text{ mg g}^{-1}$ ) e ftalate: ( $\text{Cu}^{2+} = 30,63 \text{ mg g}^{-1}$ ) hydroalcoholic solution]; aminated cellulose ( $\text{Cu}^{2+} = 2,32$ ,  $\text{Co}^{2+} = 1,35$ ,  $\text{Ni}^{2+} = 1,70$  e  $\text{Zn}^{2+} = 1,65 \text{ mmol g}^{-1}$ ); babaçu coconut thiol-mesocarp ( $\text{Cu}^{2+} = 39,6 \text{ mg g}^{-1}$ ) e epicarp ( $\text{Cu}^{2+} = 39,2 \text{ mg g}^{-1}$ ).

Cellulose was also oxidized with aqueous methaperiodate to produce cellulose-2,3-dialdehyde, which was used in other reactions: reduction of aldehyde groups, followed by reacting it with maleic, succinic and phthalic anhydrides; each of these materials in their acid form was reacted with ethylene-1,2-diamine, diethyl-1,2,4-triamine, triethyl-1,2,4,6-tetramine. The 2,3-dialdehyde-cellulose was also reacted with ethylene-1,2-diamine, diethyl-1,2,4-triamine, triethyl-1,2,4,6-tetramine and the aminated cellulose was separately reacted with maleic, succinic and phthalic anhydrides.



# Índice

|  |        |
|--|--------|
| Lista de siglas e abreviações .....  | XXV    |
| Lista de Figuras.....  | XXVI   |
| Lista de Esquemas.....   | XXVIII |
| Lista de Tabelas.....  | XXIX   |
| 1 Introdução .....   | 1      |
| 2 Objetivos .....  | 17     |
| 3 Parte experimental para celulose oxidada .....                                   | 19     |
| 3.1 Sínteses .....   | 19     |
| 3.1.1 Reação de oxidação da celulose .....   | 19     |
| 3.1.2 Reação de redução do 2,3-dialdeídocelulose.....                              | 20     |
| 3.1.3 Reação entre o material CelOR e os anidridos.....                            | 21     |
| 3.1.4 Reação entre os materiais acilados e as poliaminas.....                      | 22     |
| 3.1.5 Reações de formação das bases de Schiff entre aldeído e poliaminas.....      | 23     |
| 3.1.6 Redução das bases de Schiff .....  | 25     |
| 3.1.7 Reação entre os sólidos aminados e os anidridos.....                         | 26     |
| 3.2 Caracterização .....   | 27     |
| 3.2.1 Espectroscopia na região do IV .....   | 28     |
| 3.2.2 Ressonância magnética nuclear de <sup>13</sup> C aplicada a sólidos .....    | 28     |
| 3.2.3 Termogravimetria.....  | 28     |
| 3.2.4 Difratomia de raios X .....  | 28     |
| 4 Resultados e discussão dos experimentos com celulose oxidada.....                | 29     |
| 4.1 Sobre os artigos publicados .....  | 44     |
| 5 Esterificação de celulose.....   | 45     |
| 5.1 Instrumentação .....   | 45     |
| 5.2 Processos de troca.....  | 46     |
| 5.3 Titulação calorimétrica .....  | 47     |
| 5.4 Esterificação de celulose com anidridos .....                                  | 49     |
| 5.5 Resultados e discussão .....   | 51     |
| 5.6 Conclusão dos três artigos anteriores .....                                    | 65     |
| 6 Bases de Schiff em celulose .....  | 69     |
| 6.1 Materiais e métodos .....  | 69     |
| 6.1.1 Materiais .....  | 69     |
| 6.1.2 Síntese de clorodeoxicelulose (CelCl) .....                                  | 69     |
| 6.1.3 Síntese de copolímeros de etileno-1 ,2-diamina-6-deoxycelulose (Celen) ..... | 69     |
| 6.1.4 Síntese da base de Schiff em celulose (Celenacac).....                       | 70     |
| 6.1.5 Caracterização.....  | 70     |
| 6.1.6 Sorção .....   | 71     |
| 6.2 Resultados e discussão .....   | 73     |
| 6.2.1 Análise elementar .....  | 73     |
| 6.2.2 A espectroscopia de IV .....   | 75     |
| 6.2.3 Ressonância magnética nuclear de carbono-13.....                             | 77     |
| 6.2.4 Termogravimetria.....  | 78     |

|       |  |     |
|-------|--|-----|
| 6.2.5 | Microscopia eletrônica de varredura e espectroscopia de energia dispersiva | 80  |
| 6.2.6 | Adsorção .....   | 81  |
| 6.3   | Conclusão .....  | 84  |
| 6.4   | Parte Experimental.....  | 85  |
| 6.4.1 | Materiais .....  | 85  |
| 6.4.2 | Síntese de 6-clorodeoxicelulose .....                                      | 85  |
| 6.4.3 | Síntese do 6-etileno-1,2-diamino-deoxycellulose .....                      | 85  |
| 6.4.4 | Medidas físicas.....   | 86  |
| 6.5   | Resultados e discussão .....   | 86  |
| 6.6   | Conclusão .....  | 97  |
| 6.7   | Sobre os dois artigos anteriores.....                                      | 98  |
| 7     | Experimentações com Babaçu.....  | 101 |
| 7.1   | Métodos .....  | 101 |
| 7.1.1 | Materiais e reagentes .....  | 101 |
| 7.1.2 | Síntese de derivados .....   | 101 |
| 7.1.3 | Grau de substituição.....  | 102 |
| 7.1.4 | Medidas .....  | 103 |
| 7.1.5 | Ponto de carga zero .....  | 103 |
| 7.1.6 | Estudos de Sorção .....  | 103 |
| 7.2   | Resultados e discussão .....   | 105 |
| 7.2.1 | Efeito do pH e do ponto de carga zero .....                                | 109 |
| 7.2.2 | A cinética de sorção .....   | 110 |
| 7.2.3 | Sorção de amostras aguardentes.....  | 112 |
| 7.3   | Conclusão .....  | 114 |
| 7.4   | Métodos .....  | 114 |
| 7.4.1 | Materiais e reagentes .....  | 114 |
| 7.4.2 | Sínteses.....  | 115 |
| 7.4.3 | Medidas físicas.....   | 115 |
| 7.4.4 | Estudos de pH e ponto de carga zero .....                                  | 116 |
| 7.4.5 | Estudos cinéticos.....   | 116 |
| 7.4.6 | Isotermas de sorção .....  | 116 |
| 7.5   | Resultados e discussão .....   | 117 |
| 7.5.1 | Caracterizações.....   | 117 |
| 7.5.2 | Sorção .....   | 121 |
| 7.6   | Conclusão .....  | 128 |
| 7.7   | Métodos .....  | 129 |
| 7.7.1 | Materiais e reagentes .....  | 129 |
| 7.7.2 | Caracterização da biomassa .....   | 130 |
| 7.7.3 | Sorção .....   | 130 |
| 7.8   | Resultados e Discussão.....  | 132 |
| 7.8.1 | Caracterização da biomassa .....   | 132 |
| 7.8.2 | Sorção .....   | 135 |
| 7.9   | Conclusões .....   | 140 |
| 7.10  | Sobre os três artigos anteriores .....                                     | 141 |
| 8     | Conclusão .....  | 143 |

|    |                               |     |
|----|-------------------------------|-----|
| 9  | Referências.....              | 145 |
| 10 | Anexos .....                  | 155 |
| 11 | Licenças das publicações..... | 215 |

## Lista de siglas e abreviações

- CHN**, análise elementar de carbono, hidrogênio e nitrogênio
- DRX**, Difração de raios X
- DTG**, Termogravimetria derivada
- HPLC**, Cromatografia líquida de alta eficiência
- ICP**, Absorção atômica por plasma indutivamente acoplado
- IV**, Espectroscopia vibracional na região do IV
- LME**, Laboratório de microscopia eletrônica
- RMN**, Ressonância magnética nuclear
- MEV**, Microscopia eletrônica de varredura
- TG**, Termogravimetria
- DMA**, N,N-dimetilacetamida
- AF**, anidrido ftálico
- AM**, anidrido malêico
- AS**, anidrido succínico
- ED**, 1,2-etilenodiamina
- DT**, 1,2,4-dietilenotetramina
- TT**, 1,2,4,6-trietilenotetramina
- Cel**, celulose
- CelO**, celulose oxidada
- CelOR**, celulose oxidada posteriormente reduzida
- CelORA**, celulose oxidada posteriormente reduzida e reagida com anidridos
- CelORAP**, celulose oxidada posteriormente reduzida e reagida com anidridos finalizadas em reações com poliaminas
- CelOp**, celulose oxidada reagida com poliaminas

**CelOP**, celulose oxidada reagida com poliaminas com posterior redução das iminas formadas na reação entre as poliaminas com os aldeídos imobilizados

**CelOPA**, celulose oxidada reagida com poliaminas com posterior redução das iminas formadas na reação entre as poliaminas com os aldeídos imobilizados; finalizadas em reações com anidridos

## Lista de Figuras

|   |    |
|---|----|
| Figura 1 – Precursores da lignina e constituintes aromáticos.....   | 2  |
| Figura 2 – Estrutura genérica da lignina.....   | 3  |
| Figura 3 – Estruturas dos cristais de celulose I $\beta$ e celulose II: a) projeção da cela unitária ao longo do plano a-b; b) projeção da cela unitária paralela ao plano 100 (celulose I) e ao plano 010 (celulose II)..... | 10 |
| Figura 4 – Estrutura molecular da celulose com grau de polimerização n .....  | 11 |
| Figura 5 – Interações intra- e intermoleculares. (a) celulose II (b) celulose I $\beta$ .....   | 12 |
| Figura 6 – Espectro de IV da celulose.....  | 31 |
| Figura 7 – Espectros na região do IV da celulose (a), CelO seco a 363 K por 5 min (b) e CelO tratada com NaCl <sub>(aq)</sub> (c).....  | 33 |
| Figura 8 – Espectros na região do IV da celulose (a), CelO (b), CelOR (c) e CelORA (A = AS (d), AM (e) ou AF (f)).....  | 34 |
| Figura 9 – Espectros na região do IV da celulose (a), CelO (b), CelOR (c) e CelORAP [A = AS (d) e P = ED (e), DT (f) ou TT (g)] .....   | 36 |
| Figura 10 – Espectros na região do IV da celulose (a), CelO (b), CelOR (c) e CelORAP [A = AM (d) e P = ED (e), DT (f) ou TT (g)] .....  | 37 |
| Figura 11 – Espectros na região do IV da celulose (a), CelO (b), CelOR (c) e CelORAP [A = AF (d) e P = ED (e), DT (f) ou TT (g)].....   | 38 |
| Figura 12 - Espectros na região do IV da celulose (a), CelO (b) e CelOP [P = ED (c), DT (d) e TT (e)].....  | 39 |
| Figura 13 – Espectros na região do IV da celulose (a), CelO (b) e CelOPA [P = ED (c) e A = AS (d), AM (e) ou AF (f)].....   | 41 |

|   |     |
|---|-----|
| Figura 14 – Espectros na região do IV da celulose (a), CelO (b) e CelOPA [P = DT (c) e A = AS (d), AM (e) ou AF (f)].....   | 42  |
| Figura 15 – Espectros na região do IV da celulose (a), CelO (b) e CelOPA [P = TT (c) e A = AS (d), AM (e) ou AF (f)].....   | 43  |
| Figura 16 – Espectros de IV de celulose (a), CelAM (b), CelAS (c) e CelAF (d).....  | 52  |
| Figura 17 – Espectros de RMN <sup>13</sup> C de celulose (a), CelAM (b), CelAS (c) e CelAF (d).   | 56  |
| Figura 18 – Difratoogramas de raios X. Celulose (a), CelAM (b), CelAS (c) e CelAF (d)   | 59  |
| Figura 19 – Curvas termogravimétricas. Celulose (a), CelAM (b), CelAS (c) e CelAF (d).....  | 61  |
| Figura 20 – Espectros de IV da celulose (a), CelCl (b), Celen5 (c) e Celenacac5 (d).  | 76  |
| Figura 21 – Espectros de RMN <sup>13</sup> C da celulose (a), CelCl (b), Celen5 (c) e Celenacac5 (d).....   | 78  |
| Figura 22 – Curvas termogravimétricas da celulose, CelCl, Celen5 e Celenacac5....   | 79  |
| Figura 23 – Mapeamento de Cloro da amostra CelCl.....   | 81  |
| <b>Figura 24</b> – Micrografia por MEV de Celenacac5.....   | 81  |
| Figura 25 – Isotermas de adsorção dos cátions: Cu <sup>2+</sup> (■), Co <sup>2+</sup> (●), Ni <sup>2+</sup> (▲) and Zn <sup>2+</sup> (◆) no material Celenacac5, a 298 ± 1 K..... | 83  |
| Figura 26 – Difratoogramas de raios X. Celulose (I) e CelCl (II).....   | 89  |
| Figura 27 – Difratoogramas de raios X de CelenX (X = 1 (a), 2 (b), 3 (c), 4 (d) e 5(e)).  | 92  |
| Figura 28 - Curva termogravimétrica e curva termogravimétrica derivada de celulose (I) e CelCl (II).....  | 95  |
| Figura 29 – Curvas termogravimétricas de CelenX (X = 1 (a), 2 (b) e 5 (c)).....   | 96  |
| Figura 30 – Curvas termogravimétricas de CelenX (X = 1 (a), 2 (b) e 5 (c)).....   | 97  |
| Figura 31 – Espectros de IV de mesocarpo de babaçu (a) e seus derivados modificados com os anidridos succínico (b), malêico (c) e ftálico (d).....                                | 107 |
| Figura 32 – Curvas termogravimétricas de BCM (a), BCMSA (b), BCMFA (c) e BCMMA (d).....   | 108 |
| Figura 33 – Ponto de carga zero para BCMSA (■), BCMFA (●) and BCMMA (▲).  | 109 |
| Figura 34 – Curvas cinéticas de adsorção de cobre em BCMSA (■), BCMFA (●) e BCMMA (▲) em solução aquosa (a) e solução hidroalcoólica (b) a 298 ±1 K.....                          | 111 |

|   |     |
|---|-----|
| Figura 35 – Ajustes aos modelos isotérmicos de Langmuir para adsorção de cobre em BCMSA (■), BCMFA (●) e BCMMA (▲) em água (a) em pH 6.0 em solução hidroalcoólica (b) a 298 ± 1 K..... | 113 |
| Figura 36 – Espectros de IV de BCM (a), BCMS (b), BCE (c) e BCES (d).....   | 118 |
| Figura 37 – Curvas termogravimétricas de BCM, BCMS, BCE e BCES.....   | 119 |
| Figura 38 – Espectros de RMN <sup>13</sup> C de BCM (a), BCMS (b), BCE (c) e BCES (d)...  | 120 |
| Figura 39 – Efeito do pH na adsorção de Cu <sup>2+</sup> aquoso por BCMS (■) and BCES (●) (a) e p <sub>HPZC</sub> (b).....  | 121 |
| Figura 40 – Cinéticas de adsorção de Cu <sup>2+</sup> aquoso por BCMS (■) and BCES (●).   | 123 |
| Figura 41 – Isotermas de Langmuir para adsorção de Cu <sup>2+</sup> aquoso em BCMS e BCES, 298 ± 1 K and pH 6.....  | 127 |
| Figura 42 – Difractogramas de raios X da celulose (a), do mesocarpo (b) e do epicarpo (c) de babaçu.....  | 134 |
| Figura 43 – Curvas termogravimétricas da celulose, mesocarpo e epicarpo.....  | 135 |
| Figura 44 – Efeito do pH no processo adsorptivo do corante turquesa de remazol em mesocarpo (▼) e em epicarpo (■).....  | 139 |

## Lista de Esquemas

|  |    |
|--|----|
| Esquema 1 – Representação do mecanismo através de explosão a vapor para mudanças na morfologia e grau de polimerização de amostras de celulose. ....   | 6  |
| Esquema 2 – Reações para obtenção dos principais ésteres comerciais.....   | 8  |
| Esquema 3 - Principais formas de obtenção da celulose. ....  | 11 |
| Esquema 4 - Oxidação da celulose (a) à 2,3-dialdeídocelulose (b).....  | 14 |
| Esquema 5. - Redução dos grupos aldeídos. CelO (a) e CelOR (b) .....   | 21 |
| Esquema 6 - Esterificação com anidridos. CelOR (a) CelORA (A = AM (a), AS (b) e AF (c)) .....  | 22 |
| Esquema 7 - Reação de poliaminas com CelORA (AM, AS e AF). Para <b>m = 0</b> : 1,2-etilenodiamina (ED); <b>m = 1</b> : 1,2,4-dietilenotriamina (DT); <b>m = 2</b> : 1,2,4,6-trietilenotetramina (TT) ..... | 23 |

|  |     |
|--|-----|
| Esquema 8 - Formação de bases de Schiff entre em CelO por reação com poliaminas. 1,2-etilenodiamina (ED), <b>n = 0</b> , 1,2,4-dietilenotriamina (DT) <b>n = 1</b> e 1,2,4,6-trietilenotetramina (TT) <b>n = 2</b> ..... | 24  |
| Esquema 9 – Redução das bases de Schiff com $\text{BH}_4^-$ (EtOH). Para <b>n = 0</b> tem-se a 1,2-etilenodiamina, <b>n = 1</b> para 1,2,4-dietilenotriamina e <b>n = 2</b> sendo 1,2,4,6-trietilenotetramina.....       | 25  |
| Esquema 10 - Formação de aminadas em CelOPA. CelOPA CelOPA (P = ED, DT e TT e A = AS (a), AM (b), e AF (c)) .....  | 27  |
| Esquema 11 – Esterificação de celulose com anidridos AM (a), AS (b) e AF (c)....   | 50  |
| Esquema 12 – Formação de bases de Schiff. Celen (a) e Celenacac (b).....   | 70  |
| Esquema 13 - Esterificação de mesocarpo de babaçu com anidridos.....   | 102 |
| Esquema 14 – Síntese de BCMS e BCES.....   | 115 |

## Lista de Tabelas

|  |    |
|--|----|
| Tabela 1 – Composição química de alguns materiais celulósicos típicos.....   | 4  |
| Tabela 2 – Exemplos de ésteres e éteres de celulose produzidos comercialmente.....   | 7  |
| Tabela 3 – Grau de cristalinidade ( $X_c$ ), tamanho do cristalito ( $D_{(hkl)}$ ) e dimensões laterais (d) das microfibrilas de celuloses naturais.....   | 9  |
| Tabela 4 – Biopolímeros esterificados CelX (X = AM, AS, AF), temperatura do banho (T), ponto de fusão (PF) e massa (m) dos anidridos utilizados.....   | 49 |
| Tabela 5 – Quantidade de grupos ácidos (n) para CelX (X = AM, AS e AF) determinados por retrotitulação.....  | 50 |
| Tabela 6 – Percentuais determinados para carbono (C), hidrogênio (H), nitrogênio (N), calculado para oxigênio (O), obtidos através de análise elementar, grau de substituição (DS) e concentração dos grupos imobilizados ( $N_o$ )..... | 50 |

|   |     |
|---|-----|
| Tabela 7 – Sumário das bandas típicas encontradas nos espectros de IV para celulose modificada com anidrido succínico.....  | 53  |
| Tabela 8 – Sumário das bandas típicas encontradas nos espectros de IV para celulose modificada com anidrido succínico.....  | 54  |
| Tabela 9 – Sumário das vibrações típicas encontrados em espectros de IV de celulose modificada com anidrido ftálico.....  | 55  |
| Tabela 10 – Sumário dos deslocamentos químicos (DQ) típicos em espectros de RMN <sup>13</sup> C de celulose modificada com anidrido succínico.....  | 57  |
| Tabela 11 – Sumário dos deslocamentos químicos (DQ) típicos encontrados em espectros de RMN <sup>13</sup> C de celulosas modificadas com anidrido ftálico .....   | 58  |
| Tabela 12 – Sumário dos eventos de decomposição térmica e massa final (MF) para alguns biopolímeros celulósicos modificados com anidrido succínico.....   | 62  |
| Tabela 13 – Sumário dos eventos de decomposição térmica e massa final (MF) para alguns lignocelulósicos modificados com anidrido ftálico.....   | 63  |
| Tabela 14 – Entalpia ( $\Delta H$ ), Energia livre de Gibbs ( $\Delta G$ ) e Entropia ( $\Delta S$ ) para as celulosas modificadas CelXC (X = AM, AS e AF; C = Co <sup>2+</sup> e Ni <sup>2+</sup> ).....   | 63  |
| Tabela 15 – Valores termodinâmicos da complexação dos carboxilatos insaturados maleato e fumarato com os metais U(VI) e Eu(III).....  | 64  |
| Tabela 16 – Sumário de parâmetros termodinâmicos da complexação dos succinatos com metais.....  | 64  |
| Tabela 17 – Porcentagens de cloro e nitrogênio em clorodeoxicelulose e etano-1,2-diaminadeoxicelulose, Grau de funcionalização (GF) e porcentagem efetiva de incorporação (EI).....   | 73  |
| Tabela 18 – Número de mols adsorvidos ( $n_f$ ), capacidade máxima de adsorção ( $n^s$ ), coeficientes de correlação ( $r$ ) e a constante ( $b$ ) para o comportamento dos nitratos metálicos em solução e a interação destes metais (M) com Celenacac5 a $298 \pm 1$ K..... | 82  |
| Tabela 19 - Variação da temperatura ( $\Delta T$ ), perda de massa em porcentagem para cada etapa de decomposição térmica ( $\Delta m$ ) e resíduo ( $\Delta m_r$ ) para os biopolímeros (Biop) Cel, CelCl e CelenX (X = 1-5).....  | 93  |
| Tabela 20 – Sumário de materiais obtidos a partir da modificação química de celulose e lignocelulósicos com anidrido succínico.....   | 105 |

|  |     |
|--|-----|
| Tabela 21 – Parâmetros cinéticos para adsorção de $\text{Cu}^{2+}$ em BCMS e BCES. Concentração inicial de $\text{Cu}^{2+}$ $200,0 \text{ mg dm}^{-3}$ , com dose de $1,0 \text{ g dm}^{-3}$ em pH 6.0 a $298 \pm 1 \text{ K}$ ..... | 125 |
| Tabela 22 – Coeficientes das equações de Freundlich e Langmuir da adsorção de $\text{Cu}^{2+}$ por BCMS e BCES a $298 \pm 1 \text{ K}$ .....   | 128 |
| Tabela 23 - Parâmetros cinéticos para sorção de Turquesa de Remazol em babaçu pelo ajuste às equações de pseudo primeira ordem e pseudo segunda ordem.....   | 136 |
| Tabela X - Sumário das reflexões encontrados em difratogramas de raios X para amostras de celulose modificada com anidrido succínico   |     |



## 1 Introdução

A Química de superfícies tem por fundamento a utilização de algum tipo de suporte, para que sejam realizadas as mais diferentes reações, originando um enorme incremento de aplicações aos novos materiais assim sintetizados [1,2]. Dessa forma, algumas pesquisas idealizam um polímero que sirva como suporte para ser funcionalizado e assim apresente alta estabilidade química, térmica e mecânica [3-10].

Dentre esses materiais poliméricos destacam-se os orgânicos: celulose, poliéster, poliamina, uretana, dextrana, quitosana, agarose [11] etc e os inorgânicos: sílica, zeólita, vidro, argila, silicato, hidroxiapatita e óxidos metálicos [12-14]. Os biopolímeros naturais sempre despertam interesse [15], como os lignocelulósicos [16,17] que são formados por celulose, hemicelulose, e ligninas [18].

Tanto a celulose, como os compostos celulósicos e os lignocelulósicos são os mais importantes, principalmente quando se pesquisam fontes de energia renováveis. Assim, nas novas tendências mundiais energéticas [19], os lignocelulósicos são atrativos devido à insuperável disponibilidade, baixo custo, facilidade na manipulação [20], renovação, resistência, durabilidade, dentre outras propriedades [21,22].

Os lignocelulósicos possuem características semelhantes aos componentes que o formaram e a caracterização é obtida praticamente pelas mesmas técnicas utilizadas para os demais biopolímeros, mas a extração química destes compostos, geralmente está associada a mudanças na estrutura e no arranjo [21]. Por exemplo, a lignina é uma policondensação de derivados do grupo 2,3-propenilfenol, tendo os alcoóis cumarílico, seneapílico, coniferílico, p-hidroxifenílico, guaiacílico e siringílico [19,23] como os principais resíduos estruturais da lignina. As razões entre esses resíduos aromáticos são absolutamente dependentes das bioespécies formadoras e são arranjadas aleatoriamente, culminando em estruturas diferentes até mesmo dentro de uma mesma espécie. Esses resíduos são mostrados na **Figura 1**.

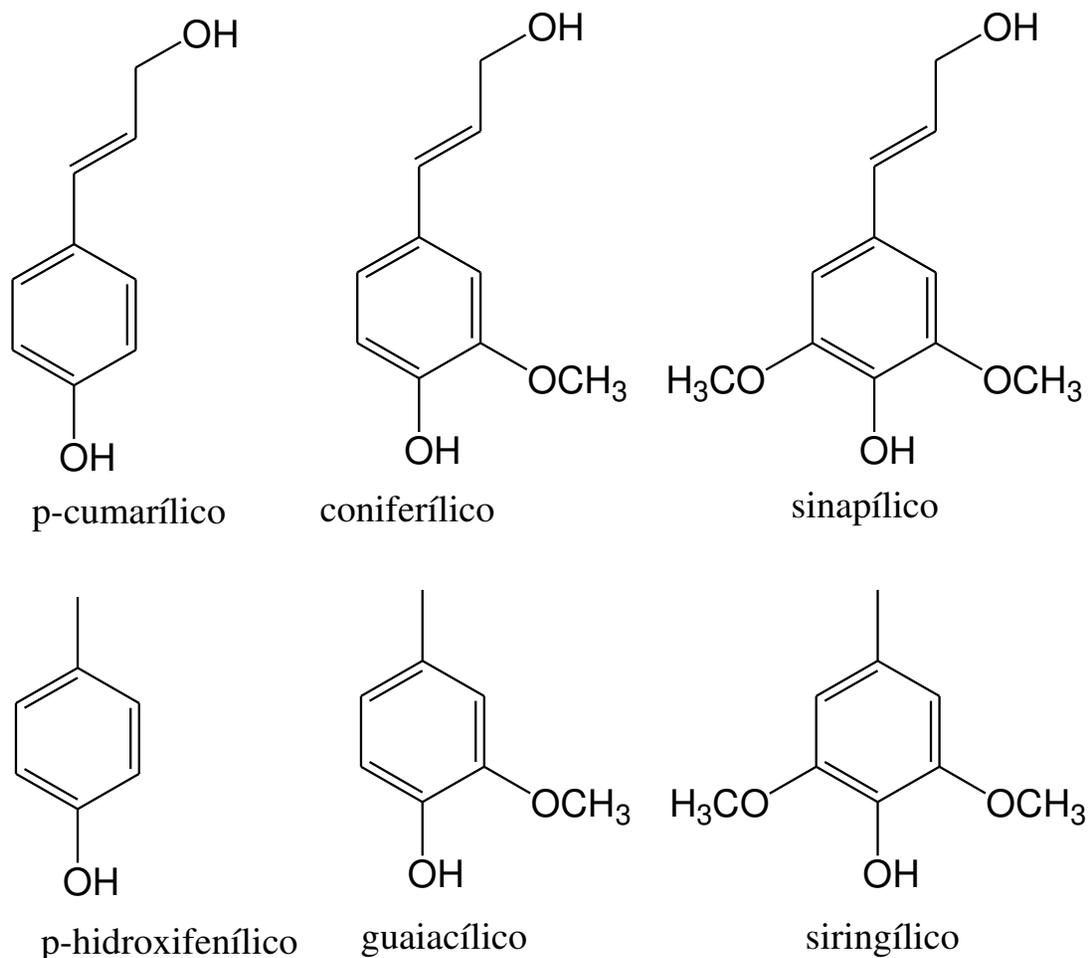


**Figura 1.** Precursores da lignina e constituintes aromáticos.

Uma estrutura genérica de lignina é apresentada na **Figura 2** e como se observa, a estrutura da lignina é praticamente toda formada por reações entre insaturações e hidroxilas e entre insaturações e anéis aromáticos. Dentre as reações, as mais importantes, quanto à robustez da estrutura formada, estão os éteres, os quais são muito estáveis frente às reações, as quais uma lignina está disposta, como meio salino, irradiação, exposição a oxigênio etc.

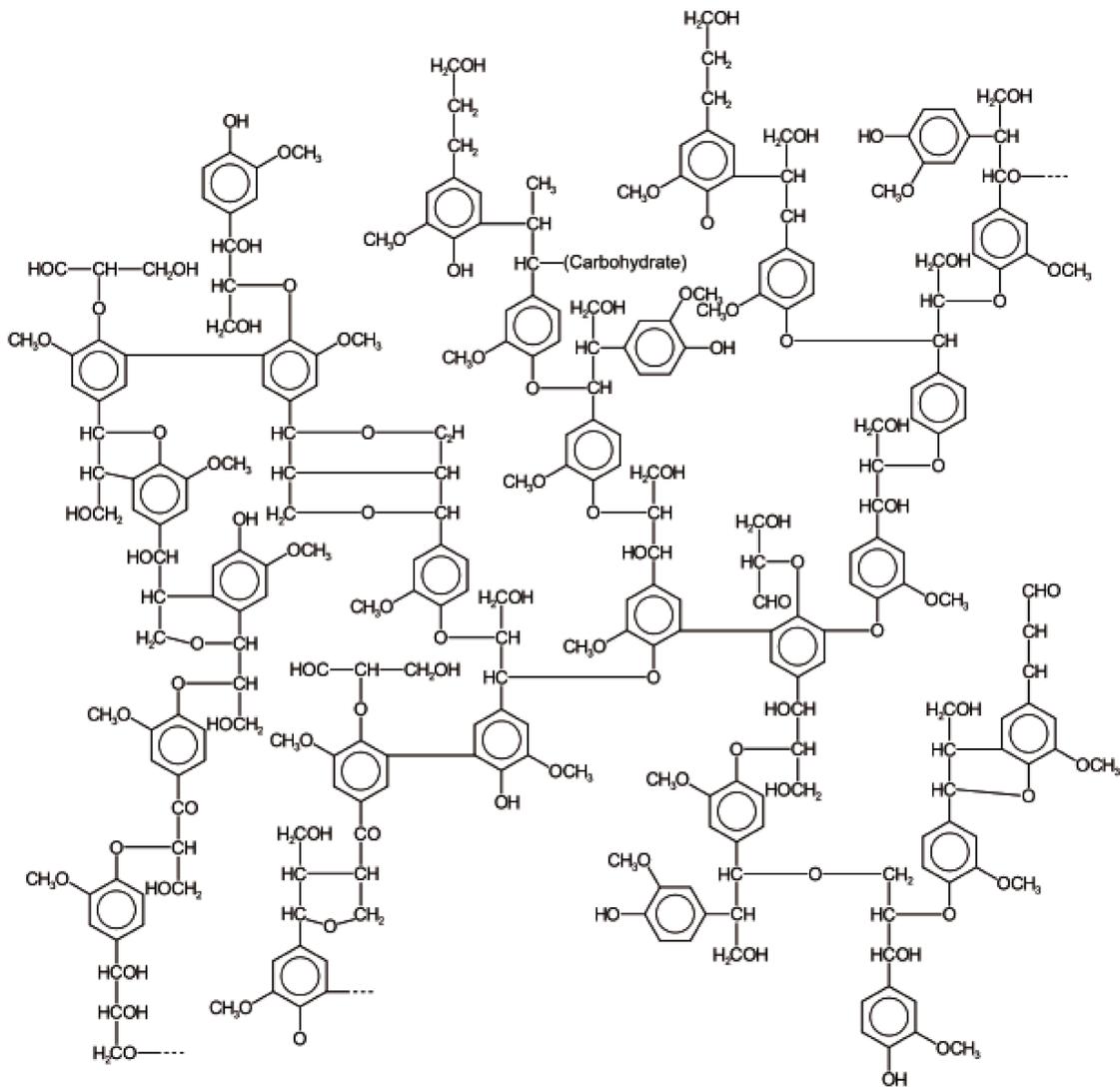


**Figura 2.** Estrutura genérica da lignina.

A composição dos biopolímeros em suas frações está estritamente associada às matrizes vivas produtoras e a fração lignina é a responsável por conferir dureza ou maciez ao produto final, e quanto maior sua proporção maior a maciez conferida ao compósito [24]. Outros exemplos fazem parte da **Tabela 1**. Isso se deve principalmente ao fato de a celulose ser um conjunto fibroso de elevado índice de empacotamento e uma rígida bem definida estrutura de ligações hidrogênio, não havendo sequer águas estruturais entre as cadeias celulósicas; já a lignina não há nenhuma organização em sua complexa e aleatória estrutura formada por moléculas também complexas, quanto

aos grupos existentes, estruturando-se de forma a ocupar um volume grande. Logo, se a proporção dessa estrutura volumosa for grande a maciez também será maior.

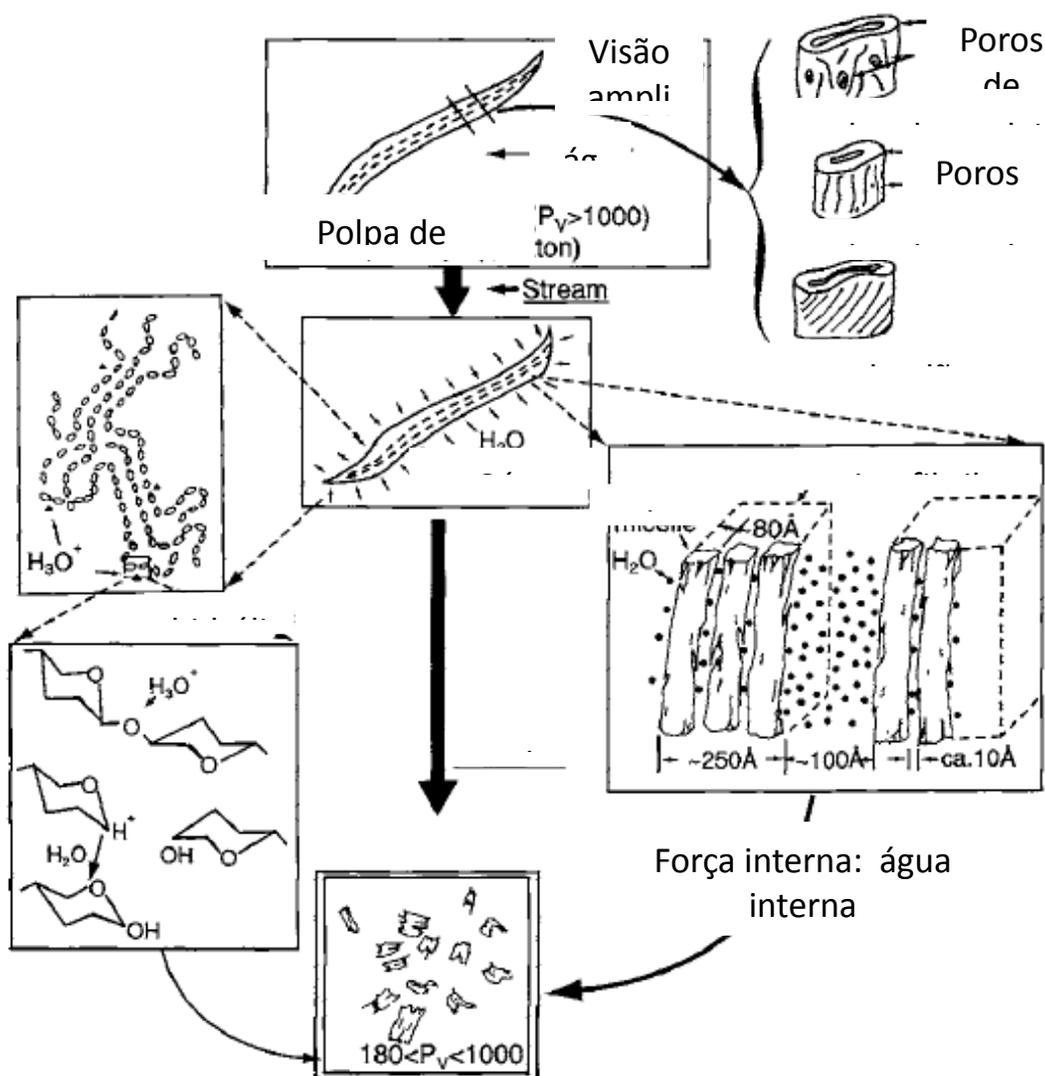
Como apresentado na **Tabela 1** observa-se uma grande distinção entre cada uma das espécies lignocelulósicas e a possibilidade de bioossínteses que culminam em fontes quase puras de celulose, como o caso do algodão com cerca de 95 % de celulose, até a capa dura que reveste o coco com 43-49 % de lignina. Assim, nota-se claramente a dependência entre as bioespécies e o grau de maciez.

**Tabela 1.** Composição química percentual de alguns materiais celulósicos típicos.

| Fonte           | Celulose (%) | Hemicelulose (%) | Lignina (%) | Extratável (%) |
|-----------------|--------------|------------------|-------------|----------------|
| Madeira dura    | 43-47        | 25-35            | 16-24       | 2-8            |
| Madeira macia   | 40-44        | 25-29            | 25-31       | 1-5            |
| Bagaço          | 40           | 30               | 20          | 10             |
| Capa do coco    | 32-43        | 10-20            | 43-49       | 4              |
| Sabugo de milho | 45           | 35               | 15          | 5              |
| Caule de milho  | 35           | 25               | 35          | 5              |
| Algodão         | 95           | 2                | 1           | 0,4            |
| Linho moído     | 71           | 21               | 2           | 6              |
| Linho não moído | 63           | 12               | 3           | 13             |
| Cânhamo         | 70           | 22               | 6           | 2              |
| Henequem        | 78           | 4-8              | 13          | 4              |
| Istel           | 73           | 4-8              | 17          | 2              |
| Juta            | 71           | 14               | 13          | 2              |
| Kenaf           | 36           | 21               | 18          | 2              |
| Rami            | 76           | 17               | 1           | 6              |
| Sisal           | 73           | 14               | 11          | 2              |
| Sunn            | 80           | 10               | 6           | 3              |
| Palha de trigo  | 30           | 50               | 15          | 5              |

## Capítulo 1 – Introdução

A lignina é menos interessante industrialmente [25,26], bem como a hemicelulose, devido à complexidade de suas estruturas e dificuldades em se obterem altos rendimentos, enquanto a celulose desperta mais interesse como insumo químico e suporte [27]. É importantíssimo ressaltar que essa realidade vem mudando rapidamente e as lignina e as hemiceluloses vem encontrando cada vez mais seu lugar no desenvolvimento de biocombustíveis, bioenergia e *químicos* de plataforma. Assim, separar a celulose dos outros componentes dos lignocelulósicos é possível [28,29] e uma forma industrial de obtenção destas fibras celulósicas é por explosão a vapor e tratamento químico [30] como mostrado no **Esquema 1**. Muitas vezes a lignina é usada como fonte de energia nas usinas de celulose ou suas misturas com hemiceluloses são transformadas em fertilizantes ou em insumos químicos.



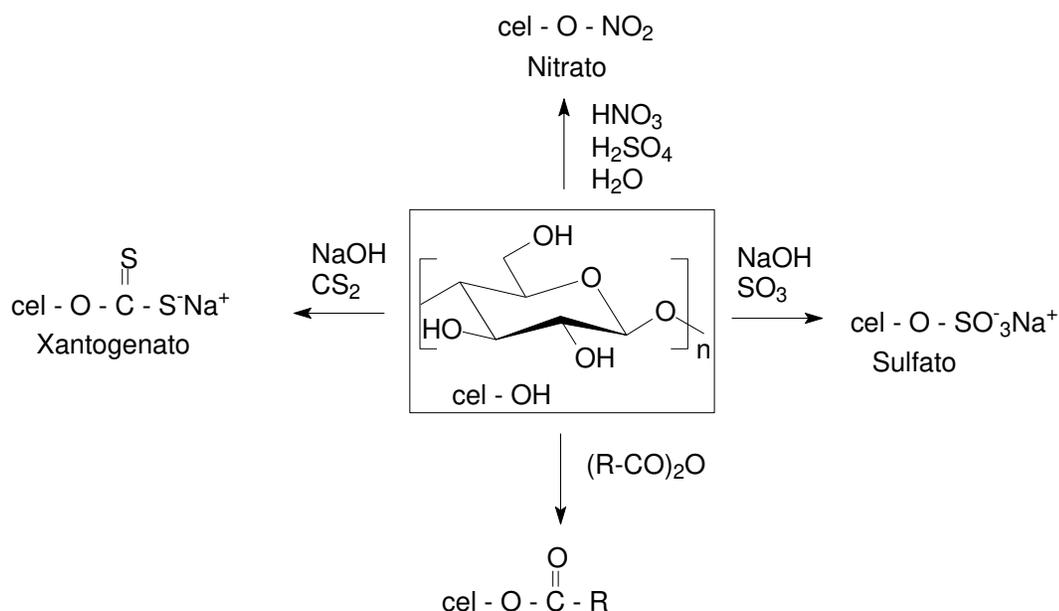
**Esquema 1.** Representação do mecanismo através de explosão a vapor para mudanças na morfologia e grau de polimerização de amostras de celulose.

A polpa de madeira é a fonte de matéria prima mais importante na produção de celulose para a indústria de papel e papelão [31], sendo que apenas 2 % são usados na produção de fibras, filmes, síntese de ésteres e éteres. Os ésteres celulósicos mais produzidos mundialmente são listados na **Tabela 2**. As reações para formação destes ésteres estão exemplificadas no **Esquema 2**.

**Tabela 2.** Exemplos de ésteres e éteres de celulose produzidos comercialmente.

| produto         | Produção anual / (t/ano) | Grupo funcional:<br>Cel O-                          | Grau de funcionalização | Solubilidade                                |
|-----------------|--------------------------|---|-------------------------|---|
| acetato         | 900.000                  | -C(O)CH <sub>3</sub>                                | 0,6 – 0,9               | Água,                                       |
|                 |                          |   | 1,2 – 1,8               | 2-metoxi etanol,                            |
|                 |                          |   | 2,2 – 2,7               | Acetona,                                    |
|                 |                          |   | 2,8 – 3,0               | Clorofórmio                                 |
| acetopropionato | -                        | -C(O)CH <sub>3</sub>                                | 2,4                     | Acetona                                     |
|                 |                          | -C(O)CH <sub>2</sub> CH <sub>3</sub>                | 0,2                     | Acetato de Etila                            |
| acetobutirato   | -                        | -C(O)CH <sub>3</sub>                                | 0,2                     | Acetona                                     |
|                 |                          | C(O)(CH <sub>2</sub> ) <sub>2</sub> CH <sub>3</sub> | 2,7                     | Diisobutil cetona                           |
| nitrato         | 200.000                  | -NO <sub>2</sub>                                    | 1,8 – 2,0               | Etanol                                      |
|                 |                          |   | 2,0 – 2,3               | Metanol<br>acetona,<br>metil-etil<br>cetona |
| xantato         | 3.200.000                | -C(S)SNa  | 0,5 – 0,6               | NaOH<br>Aquoso                              |
| metil           | 150.000                  | -CH <sub>3</sub>                                    | 0,4 - 2,6               | NaOH 4%                                     |
|                 |                          |   | 1,3 – 2,6               | Água fria                                   |
|                 |                          |   | 2,5 – 3,0               | Solventes orgânicos                         |
| carboximetil    | 300.000                  | -CH <sub>2</sub> COONa                              | 0,5 -2,9                | Água  |
| etil            | 4.000                    | -CH <sub>2</sub> CH <sub>3</sub>                    | 0,5 – 0,7               | NaOH 4%                                     |
|                 |                          |   | 0,8 – 1,7               | Água fria                                   |
| hidroxietil     | 50.000                   | -CH <sub>2</sub> CH <sub>2</sub> OH                 | 0,1 – 0,5               | NaOH 4%                                     |
|                 |                          |   | 0,6 – 1,5               | água  |

Esses ésteres de celulose são aplicados em muitas indústrias como a farmacêutica, a alimentícia, a de construção e bricolagem, a de explosivos, a bélica etc, e hoje com as diretrizes de sustentabilidade os ésteres de celulose são especialmente importantes devido à baixa toxicidade e alta degradabilidade destes compostos.



**Esquema 2.** Reações para obtenção dos principais ésteres comerciais. (R = CH<sub>3</sub>, CH<sub>2</sub>-CH<sub>3</sub> e (CH<sub>2</sub>)<sub>2</sub>CH<sub>3</sub> .).

Vale a pena ressaltar do **Esquema 2** que o xantogenato de celulose é aplicado na indústria de viscose e o nitrato na indústria de explosivos; estas indústrias vêm crescendo bastante desde a década de 1950.

A degradação parcial das cadeias celulósicas produz celulose pulverizada com características microcristalinas e grau de polimerização entre 150 a 300 unidades glicosídicas, tendo fibras de 3 a 5 nm [32]. O biopolímero celulose representa cerca de  $1,5 \times 10^{12}$  toneladas da produção total de biomassa, como fonte de matéria prima quase inesgotável, mesmo com o aumento da demanda por produtos ambientalmente seguros e biocompatíveis, com várias estruturas cristalinas: I $\alpha$ , I $\beta$ , II $\alpha$ , II $\beta$ , III e IV. Nessas estruturas estão envolvidas ligações hidrogênio entre as hidroxilas das cadeias poliméricas, acarretando uma supraestrutura de baixa reatividade. Essas características dificultam as modificações químicas, daí o grande interesse em torná-la útil em aplicações por ser matéria prima de baixo custo [33-40]. Alguns comparativos das cristalinidades encontradas em fontes naturais de celulose são mostrados na **Tabela 3**. As estruturas tridimensionais de celulose I $\beta$  e II são mostradas na **Figura 3**.

## Capítulo 1 – Introdução

As algas e as bactérias são mais especializadas na construção de paredes celulares mais robustas que os vegetais, como demonstrado pelas celuloses extraídas destas paredes, as quais apresentam altos graus de cristalinidade. O algodão, por exemplo, biossintetizado a 95 – 98 % de celulose, apresenta celulose com grau de cristalinidade de apenas 56 – 65 %. Os trabalhos da literatura com modificação química de celulose são procedidos quase em sua maioria com celulose de procedência vegetal. A celulose microbiana é empregada no desenvolvimento de materiais biomédicos de alto desempenho e também em estudos cristalográficos, termodinâmicos etc.

**Tabela 3.** Percentagem do grau de cristalinidade ( $\chi_c$ ) %, tamanho do cristalito ( $D_{(hkl)}$ ) (nm) e dimensões laterais (d) das microfibrilas de celuloses naturais

| Fonte    | $\chi_c$ | $D_{(hkl)}$ |        |        | d[nm] |
|----------|----------|-------------|--------|--------|-------|
|          |          | D(110)      | D(110) | D(020) |       |
| Alga     | >80      | 10,1        | 9,7    | 8,9    | 10-35 |
| Bactéria | 65-79    | 5,3         | 6,5    | 5,7    | 4-7   |
| Algodão  | 56-65    | 4,7         | 5,4    | 6,0    | 7-9   |
| Rami     | 44-47    | 4,6         |        | 5,0    | 3-12  |
| Linho    | 44(56) * | 4-5         | 4-5    | 4-5    | 3-18  |
| Cânhamo  | 44(59) * | 3-5         | 3-5    | 3-5    | 3-18  |

grau de cristalinidade comparado à celulose\*

Além das plantas, certas bactérias, algas e fungos também produzem celulose, que devido às estruturas supramoleculares específicas, são frequentemente usadas como substâncias molde para posterior pesquisa em aspectos estruturais, cristalinos e de reatividade. Assim, como acontece no desenvolvimento de novos biomateriais com aplicações mais nobres como em implantes e outras interfaces com a área da medicina e saúde.

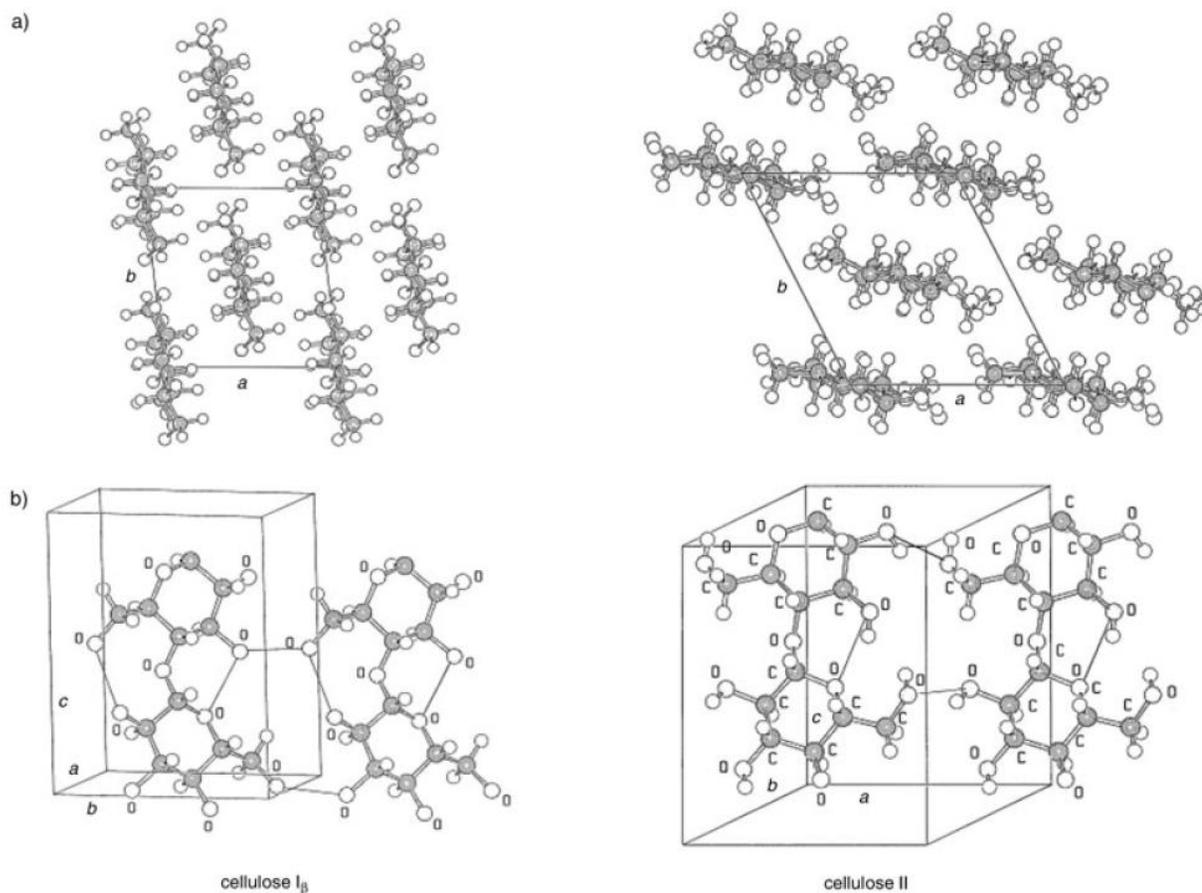
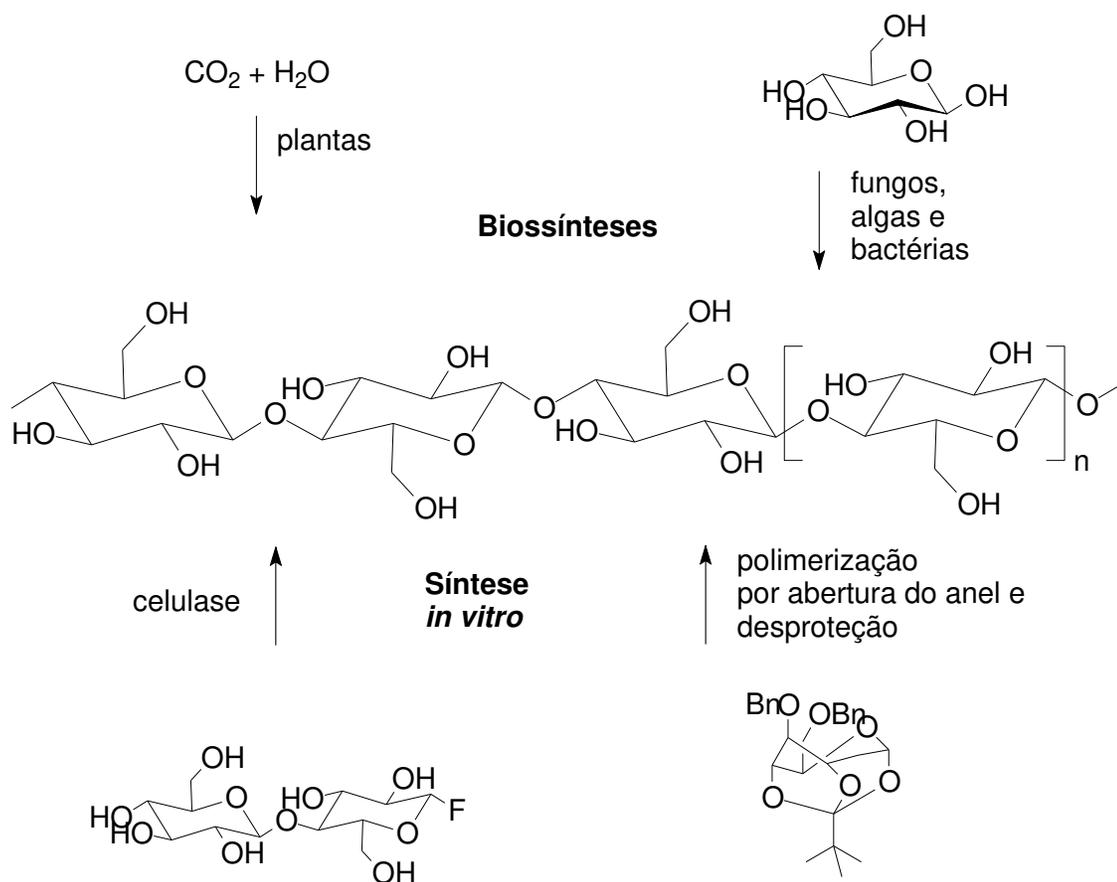


**Figura 3.** Estruturas dos cristais de celulose I $\beta$  e celulose II: a) projeção da cela unitária ao longo do plano a-b; b) projeção da cela unitária paralela ao plano 100 (celulose I) e ao plano 010 (celulose II).

A biossíntese da celulose é parte do ciclo de vida de cianobactérias e a sua síntese *in vitro* deve ser adicionalmente destacada como importante desenvolvimento na atualidade [35]. O primeiro relato da formação de celulose catalisado por celulase foi baseado no fluoreto de celobiosil [41] e a primeira quimiossíntese obtida através da polimerização de D-glicose substituída e com anéis abertos “coroados” seguidos por desproteção [42]. Um Esquema geral sobre esse processo de obtenção de celulose pode ser visto no **Esquema 3**.



**Esquema 3.** Principais formas de obtenção da celulose. Klemm

A estrutura molecular da celulose apresentada na **Figura 4**, gerada pela repetição de unidades  $\beta$ -D-glucopiranosídicas, as quais estão covalentemente ligadas através de funções acetais entre o grupo OH equatorial do átomo de carbono 4 e o átomo de carbono 1; há uma hidroxila primária situada no carbono 6 e duas secundárias nos carbonos 2 e 3. Assim, um glucano  $\beta$ -1,4 com 20 – 30 unidades de glicose oferece todas as propriedades da celulose [34], geralmente encontrada com centenas e centena de milhares de unidades de glicose [43].

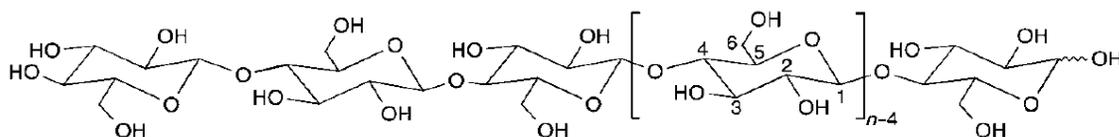


**Figura 4.** Estrutura molecular da celulose com grau de polimerização n.

A celulose microcristalina contém grupos carbonílicos e carboxílicos adicionais como resultado do processo de isolamento e purificação. As terminações reductoras aldeídos em equilíbrio com suas formas cetais e hemicetais implicam em novos grupos funcionais, além das hidroxilas, o que permite oxidação aos ácidos carboxílicos, os quais podem ser decompostos ou reagirem com uma hidroxila próxima [44].

Como é de se esperar, a celulose forma redes em ligações hidrogênio entre os grupos hidroxila [35,36], confirmadas pelas ligações intermoleculares entre as hidroxilas 3(C)...6(C) e 2(C)...5(O) e intramoleculares entre 3(C)...O(5) e 2(C)...6(C), como mostra a **Figura 5b**. Outras ligações intermoleculares [37] aparecem entre C(3)...C(6) e as intramoleculares entre 3(C)...O(5) e 2(C)...6(C), como mostra a **Figura 5a**.

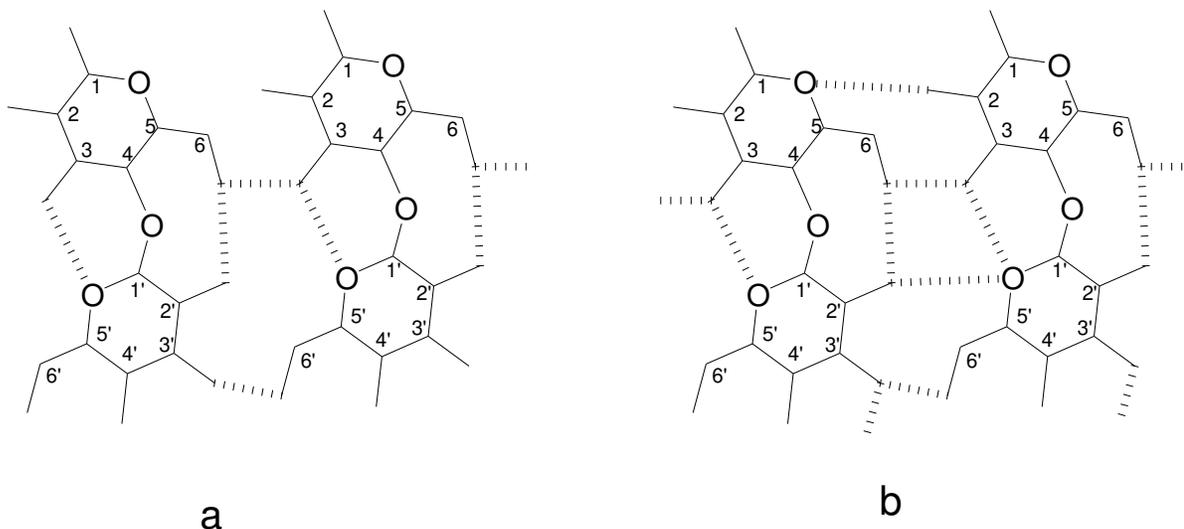


**Figura 5.** Interações intra- e intermoleculares da celulose II (a) e da celulose I $\beta$  (b).

Essas estruturas poliméricas com ligações hidrogênio são responsáveis pela formação de estrutura robusta e supra estrutural, que quando se alinham resulta em microfibrilas, as quais formam as fibrilas, que por sua vez se ordenam para dar sucessivas fibras empilhadas. Desse modo, as características químicas do biopolímero estão relacionadas ao grupo OH primário de C6 e outros dois secundários de C2 e C3 de cada unidade repetitiva [33-40,45].

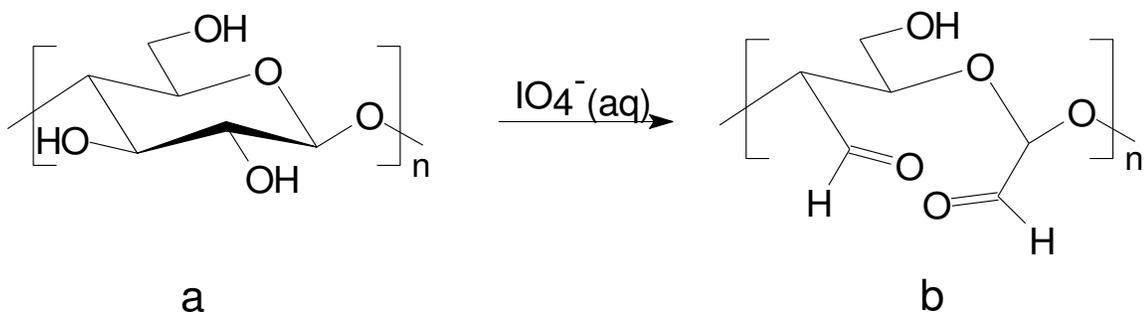
A celulose e os lignocelulósicos apresentam baixa ou nenhuma solubilidade em água, mas pode ocorrer de durante o processo de modificação química das cadeias estas adquirirem maior caráter hidrofílico e até mesmo solubilizá-la. Então se os derivados quimicamente modificados permanecem insolúveis após a síntese, estes potencialmente podem atuar em sorções de possíveis contaminantes em meio aquoso ou líquido [9,10]. Todavia, algumas aplicações da celulose mostram as vantagens da biocompatibilidade e quiralidade como na imobilização de proteínas [46], anticorpos [47], na separação de moléculas enantioméricas [48,49], assim como na formação de compostos entre polímeros sintéticos, biopolímeros [50,51] e remoção de metais [3-10].

Nas reações heterogêneas com compostos lignocelulósicos as hidroxilas e os aldeídos da lignina são os principais centros, sendo possíveis também as modificações nos anéis aromáticos. Já as hemiceluloses possuem os grupos hidroxila como centro reativo [52]. A acessibilidade e reatividade dos grupos OH são determinadas pela etapa de ativação por ruptura das ligações hidrogênio, cujo controle da ativação permite uma síntese efetiva de produtos para atingir um desejável grau de modificação. Portanto, nas sínteses com celulose, experiência e perspicácia no conduzir o estudo são ainda requeridas e tem grande valia [44, 53-82].

Do ponto de vista experimental, as reações com os biopolímeros podem acontecer em meio homogêneo ou heterogêneo. Porém, para que um solvente dissolva a celulose, o mesmo deve romper a rede de ligações hidrogênio, processo difícil, mas possível. Quando as reações são feitas em meio heterogêneo para se modificar quimicamente o polissacarídeo, os princípios seguidos são os mesmos estabelecidos para outros polímeros, como ocorre nos inorgânicos em geral com suspensões em solventes apropriados ou reações no estado sólido.

Um exemplo é a abertura dos anéis glicosídicos celulósicos pela oxidação *via* o rompimento da ligação C2-C3 [36,83-85], como ilustrado no **Esquema 4**. Entretanto, essa oxidação de alta seletividade apresenta desvantagens, centradas principalmente em sobreoxidações, despolimerizações *via*  $\beta$ -eliminações e escamações. Esses processos erosivos são causados pela diminuição/perda de parte do efeito anomérico dos anéis glicopiranosídicos, mudando a robustez da cadeia celulósica, pelo aumento do grau de liberdade do novo polímero formado. Há uma tendência desse composto

polimérico em se separar devido às diferenças mecânicas, físicas e químicas entre esses dois polímeros, celulose e 2,3-dialdeídocelulose [85]. O **Esquema 4** mostra a oxidação da celulose em um composto com maior grau de liberdade aos grupos que não são da cadeia principal.



**Esquema 4.** Oxidação da celulose (a) a 2,3-dialdeídocelulose (b).

Considerando a potencialidade de possíveis reações nas superfícies de polímeros, o presente trabalho é focado na modificação química dos biopolímeros, facilmente encontrados na natureza, como a celulose e os lignocelulósicos, com o intuito de imobilizar covalentemente moléculas com centros básicos. Da mesma forma, como já observado por outros autores com a quitosana, os sítios básicos podem atuar na coordenação de cátions de soluções aquosas [86-89].

O presente trabalho refere-se à reunião de uma série de publicações desenvolvidas no decorrer do tempo estipulado para essa tese numa linha centralizada na síntese de derivados celulósicos e lignocelulósicos sólidos, com o intuito de remover contaminantes em líquidos. Os biopolímeros foram caracterizados através das técnicas de análise elementar, espectroscopia na região do IV, ressonância magnética nuclear de sólidos para o núcleo de carbono 13, termogravimetria e difratometria de raios X. Os modelos matemáticos utilizados para todas as sorções foram os de Langmuir e ou Freundlich e altos coeficientes de correlação foram obtidos. Bem como os modelos, as devidas linearizações das equações foram empregadas para obtenção das devidas constantes e para determinação dos máximos de sorção dos suportes.

## Capítulo 1 – Introdução

Outros modelos empregados foram os de determinação de parâmetros cinéticos, os modelos de pseudoprimeira-ordem e pseudossegunda-ordem.

Ressalta-se ainda que nem todos os materiais foram caracterizados pelo mesmo conjunto de técnicas. A capacidade de sorção e/ou troca de íons foi estudada para os materiais sintetizados e realizou-se ainda para alguns materiais a titulação calorimétrica da interação cátions/centros básicos, em meio heterogêneo.



## 2 Objetivos

Numa geral pretendeu-se trabalhar com biopolímeros capazes de remover contaminantes de soluções. Os materiais que não apresentaram sorção em quantidades relevantes foram modificados para se ter uma melhora no desempenho das superfícies frente aos processos de sorção. Assim, os objetivos específicos desse trabalho foram:

- a) sintetizar materiais insolúveis;
- b) desenvolver rotas sintéticas simples para modificar celulose e lignocelulósicos com moléculas orgânicas contendo grupos funcionais ativos para coordenação com metais em solução;
- c) estudar a capacidade de sorção e/ou troca de íons ou corantes nas superfícies modificadas, através da coordenação do centro básico existente na molécula modificadora com o cátion metálico em solução;
- d) determinar as grandezas termodinâmicas (entalpia, energia de Gibbs e entropia) da interação cátion/centro básico na interface sólido/líquido.



## 3 Parte experimental para celulose oxidada

### 3.1 Sínteses

Para facilitar o entendimento dos vários procedimentos que serão expostos a seguir, é apresentada uma sequência de reações a partir de celulose oxidada. Os principais tópicos a serem descritos estão listados abaixo tendo a sigla dos produtos, seguidos dos procedimentos de reações que levaram a obtenção dos novos biopolímeros.

- a) CelO - Reação de oxidação da celulose. (esquema 4)
- b) CelOR - Reação de redução do 2,3-dialdeído-celulose. (esquema 5)
- c) CelORA (A = AM, AS e AF) - Reação entre o material CelO reduzido e os anidridos. (esquema 6)
- d) CelORAP (A = AS, AM e AF; P = ED, DT e TT) - Reação entre os materiais acilados e as poliaminas. (esquema 7)
- e) CelOp (p = ED, DT e TT) - Formação das bases de Schiff entre aldeído e poliaminas. (esquema 8)
- f) CelOP (P = ED, DT e TT) - Redução das bases de Schiff. (esquema 9)
- g) CelOPA (P = ED, DT e TT; A = AM, AS e AF) - Reação entre os sólidos aminados e os anidridos. (esquema 10)

#### **3.1.1 Reação de oxidação da celulose**

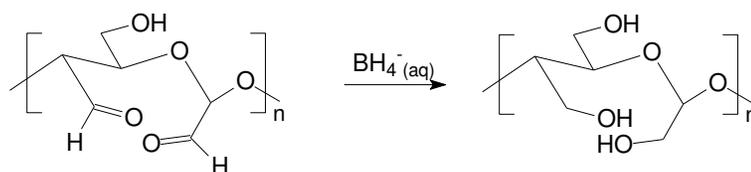
A princípio a celulose utilizada nos estudos foi a celulose do tipo microcristalina, a qual foi substituída posteriormente por celulose de papel de filtro, devido às fibras serem maiores.

O metaperiodato é capaz de oxidar seletivamente a ligação entre os carbonos 2 e 3 do anel glicopiranosídico, reação na qual são formados grupos aldeído. Para a

oxidação à 2,3-dialdeído-celulose, dissolveu-se uma massa de metaperiodato de sódio ( $\text{NaIO}_4$ ) em água, sob agitação magnética e ao abrigo da luz, finalizando numa solução de concentração de  $\text{IO}_4^-$ (aq)  $0,30 \text{ mol dm}^{-3}$  e a razão molar celulose: $\text{IO}_4^-$  foi 1,0:1,3. Suspendeu-se a celulose em água e tratou-se com ultrassom por 0,5 h, verteu-se a suspensão à solução oxidante e agitou-se magneticamente a mistura a por 24 h a 298 K, adaptada [75]. Ao final desse tempo adicionou-se  $200 \text{ cm}^3$  de uma solução 30% (v/v) de etilenoglicol/água, para consumir o  $\text{IO}_4^-$ (aq) não reagido, agitou-se por 1 h, cujo material de aparência gelatinosa foi lavado exaustivamente com  $3 \text{ dm}^3$  de água. Com auxílio de uma centrífuga (3500 rpm) separou-se o decantado e este foi suspenso em água, tratado por 5 min sob ultrassom e novamente centrifugado. repetiu-se o procedimento até que o material final não apresentasse mais as bandas referentes à vibração  $\nu(\text{I-O})$ , em  $530$  e  $850 \text{ cm}^{-1}$ . O biopolímero oxidado foi lavado com acetona, a fim de se facilitar a secagem, foi seco em linha de vácuo por 6 h, sob um lento fluxo de  $\text{N}_{2(g)}$  seco em ácido sulfúrico concentrado. O material foi pulverizado por moagem convencional em almofariz de porcelana e passado por uma peneira de aço inox de 150 mesh. Nomeou-se este material, 2,3-dihidroxi-celulose, como CelO e a reação proposta é mostrada na **Esquema 4**.

### ***3.1.2 Reação de redução do 2,3-dialdeídocelulose***

A redução de grupos aldeídicos com boridreto leva à formação de álcoois primários, os quais são mais reativos que os secundários. Assim, a redução do 2,3-dialdeído-celulose produz o 2,3-diidroxi-celulose, este material foi obtido suspendendo-se uma massa de 2,3-dialdeído-celulose em água, em banho de gelo sob agitação magnética, e em seguida adicionada uma solução recém-preparada de  $\text{BH}_4^-$ (aq)  $0,90 \text{ mol dm}^{-3}$  e de razão molar aldeído: $\text{BH}_4^-$  de 1,0:1,3 [58]. Considerou-se 100 % de reação de oxidação para as futuras etapas a partir desta rota. A reação proposta é mostrada no **Esquema 5**.



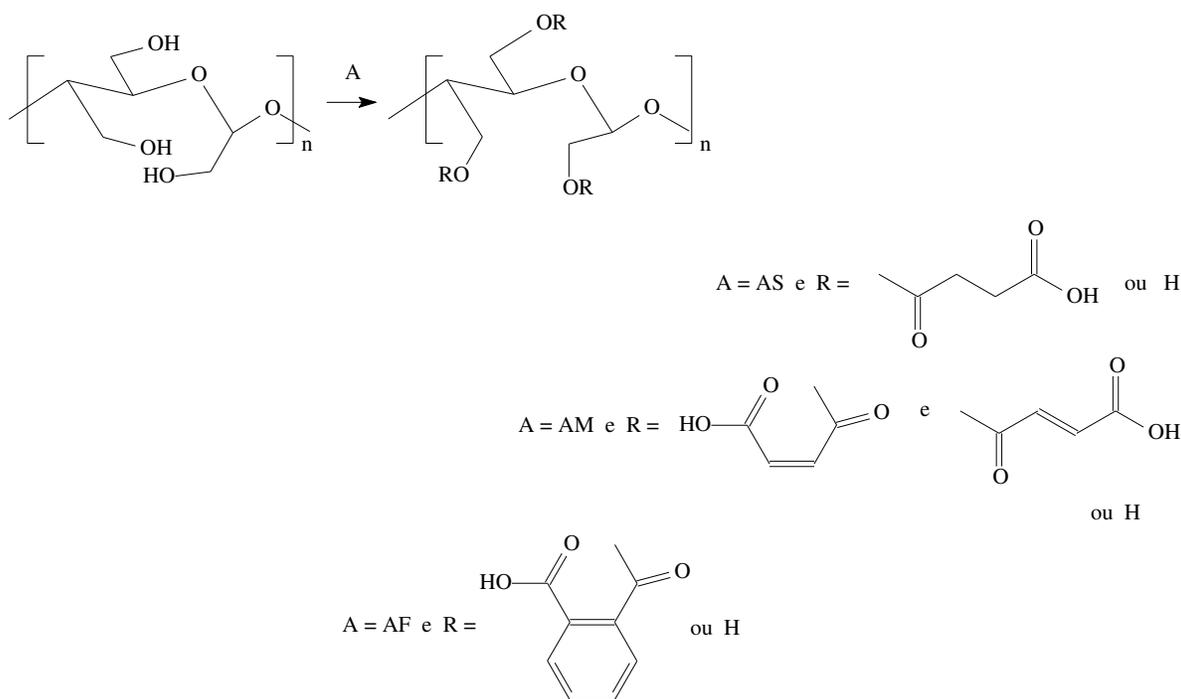
**Esquema 5.** Redução dos grupos aldeídos. CelO (a) e CelOR (b)

### 3.1.3 Reação entre o material CelOR e os anidridos

A esterificação de hidroxilas primárias com anidridos é favorável graças à reatividade desses anéis tensionados. A reação se passa através de um ataque nucleofílico da hidroxila da celulose à carbonila do anidrido. Entretanto, o material oxidado não resiste altas temperaturas utilizando anidridos fundidos e contornou-se este inconveniente ao se experimentar reações sob ultrassom, à temperatura ambiente.

Adicionou-se, separadamente em cada um dos experimentos, os anidridos succínico (AS), malêico (AM) e ftálico (AF), a fim de se estabelecer a razão molar de 3:1 anidrido:2,3-dihidroxi-celulose; a concentração de anidridos em acetona para os experimentos foi de  $1,35 \text{ mol dm}^{-3}$ . Após 24 h de reação, sob agitação magnética à  $298 \pm 2 \text{ K}$ , os materiais obtidos foram lavados com um total de  $300 \text{ cm}^3$  de acetona para remoção de anidrido que não reagiu. O procedimento empregado consistiu em se suspender os materiais acilados em acetona e tratá-los com ultrassom por 5 min em cada uma das lavagens. Filtrou-se a suspensão e por fim lavou-se com  $5 \text{ cm}^3$  de acetona para facilitar a secagem. Os biopolímeros obtidos foram secos em linha de vácuo por 6 h, sob fluxo lento de nitrogênio seco em ácido sulfúrico concentrado. O material foi pulverizado por moagem convencional em almofariz de porcelana e passado por uma peneira de aço inox de 150 Mesh<sup>8</sup>. Nomeou-se estes materiais como CelORA (A = AS, AM e AF) e as reações propostas são mostradas no **Esquema 6**.

Outra metodologia empregada para a esterificação desses materiais foram as reações dos anidridos em acetona.



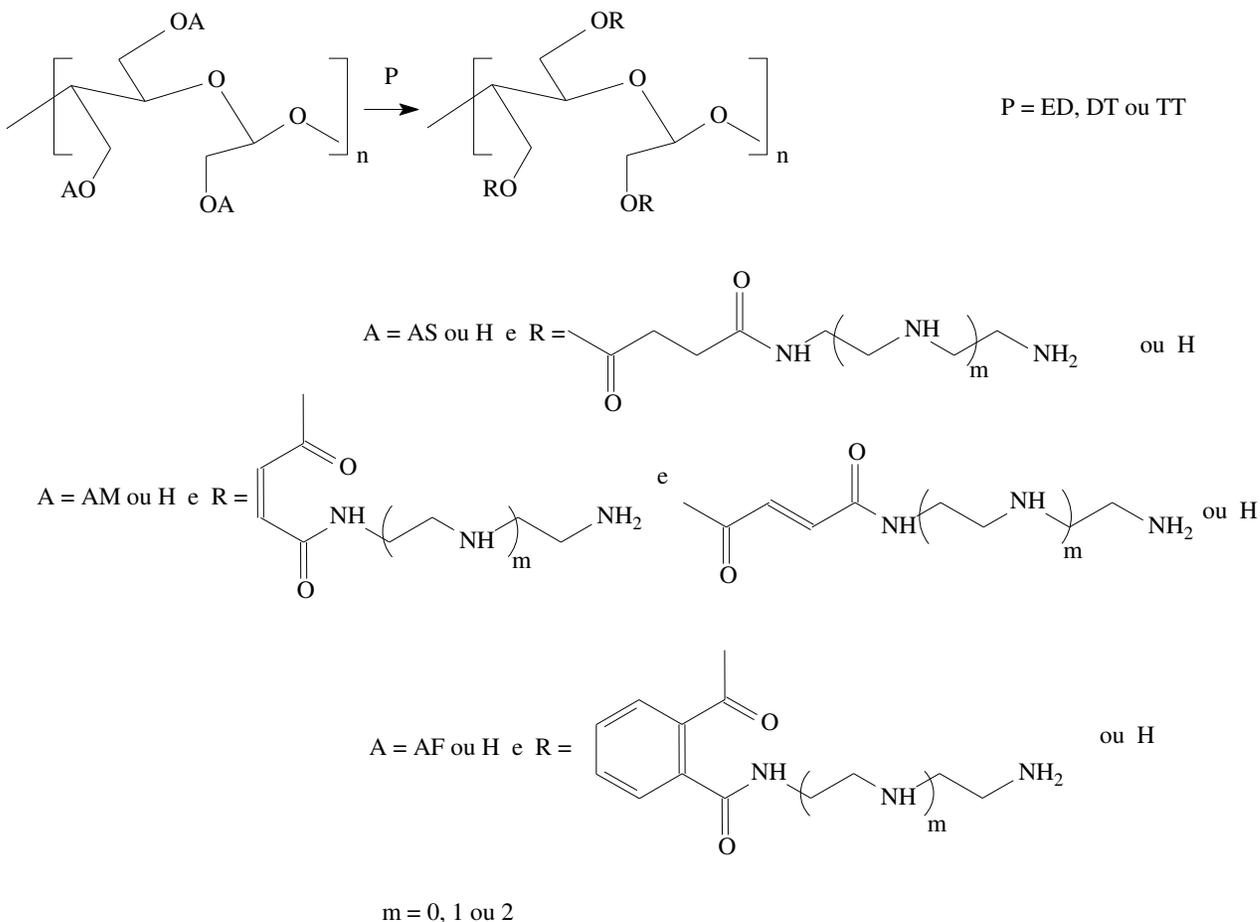
**Esquema 6.** Esterificação com anidridos. CelOR (a) CelORA (A = AM (a), AS (b) e AF (c)).

### 3.1.4 Reação entre os materiais acilados e as poliaminas

A esterificação dos materiais reduzidos, através da reação entre as hidroxilas primárias e os anidridos cíclicos disponibiliza, com a abertura destes anéis, funções ácidos carboxílicos, as quais podem sofrer ataques nucleofílicos por amins primárias e secundárias para formarem amidas. As reações são ditas ancoramentos de amins devido aos ácidos carboxílicos estarem na estrutura de um sólido, a fazer com que as amins que estavam em solução liguem-se covalentemente, através da formação de amidas, ao biopolímero suspenso [10].

Suspendeu-se, em solução DMA/acetona 15 % (v/v), os materiais acilados - CelORA (A = AS, AM e AF) – tratou-se com ultrassom por 5 min, adicionou-se então as poliaminas 1,2-etilenodiamina (ED), 1,2,4-dietilenotriamina (DT) e 1,2,4,6-trietilenotetramina (TT), de modo a apresentar razão molar CelORA:poliamina de 1:3; concentração de poliamina em acetona de 1,35 mol dm<sup>-3</sup>. Deixou-se sob ultrassom por

1 h, agitou-se magneticamente por 12 h; repetiu-se este procedimento três vezes. Filtrou-se, lavou-se com uma solução 20 % (v/v) de acetona em água. Os materiais foram secos e pulverizados como nos casos anteriores. Denominou-se estes materiais como CelORAP (A = AS, AM e AF e P = ED, DT e TT) e as reações propostas são mostradas no **Esquema 7**.

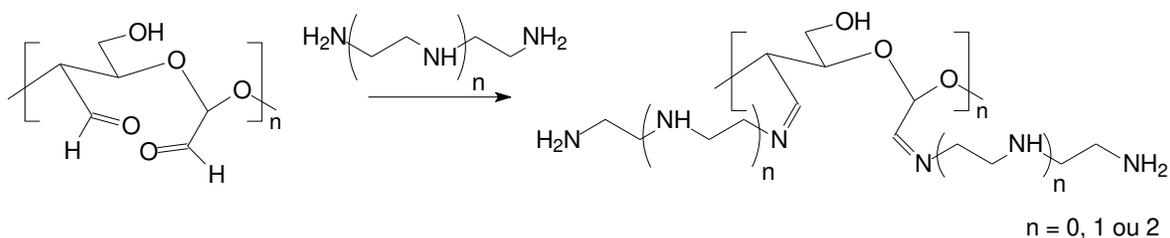


**Esquema 7.** Reação de poliaminas com CelORA (AM, AS e AF). Para **m = 0**: 1,2-etilenodiamina (ED); **m = 1**: 1,2,4-dietilenotriamina (DT); **m = 2**: 1,2,4,6-trietilenotetramina (TT).

### 3.1.5 Reações de formação das bases de Schiff entre aldeído e poliaminas

Sabe-se que as aminas reagem com aldeídos *via* formação de iminas, ou base de Schiff [90]. São reações que se processam em meio aquoso e liberam água como

um dos produtos. Entretanto, o 2,3-dialdeído-celulose é instável em meio básico e ocasiona a despolimerização a ponto de solubilizar-se. Os materiais precipitados a partir dessas soluções permaneciam solúveis em água e em soluções metálicas, o que não era desejado. Portanto, as reações promovidas em meio aquoso culminavam em rendimentos baixos e o meio foi substituído por uma mistura de DMA/acetona, 15 % (v/v). Primeiramente, suspendeu-se nessa solução o 2,3-dialdeído-celulose, tratou-se com ultrassom por 5 min, adicionou-se então a poliamina de modo a apresentar a razão molar 2,3-dialdeído-celulose:poliamina de 1:3. A razão poliamina:acetona também foi de 1,35 mol dm<sup>-3</sup>. Deixou-se sob ultrassom por 1 h, agitou-se magneticamente por 12 h; repetiu-se este procedimento duas vezes. Os sólidos foram filtrados, secos e pulverizados como anteriormente. Nomeou-se estes materiais como CelOp (p = ED, DT e TT) e as reações propostas são mostradas no **Esquema 8**.

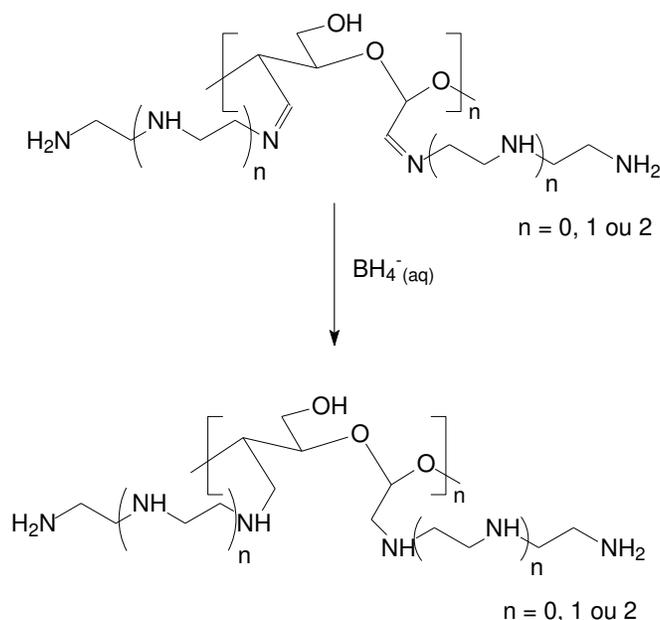


**Esquema 8.** Formação de bases de Schiff entre em CelO por reação com poliaminas. 1,2-etilenodiamina (ED), **n = 0**, 1,2,4-dietilenotriamina (DT) **n = 1** e 1,2,4,6-trietilenotetramina (TT) **n = 2**.

Essas reações foram repetidas em misturas de solventes orgânicos, como em etanol e diclorometano, sem sucesso, mas a diminuição do tempo de 12 h para 2 h, concomitante à diminuição da concentração das poliaminas em água, resultou em um polímero de mais alto teor de centros básicos e com maior rendimento. Exceto para o caso da etilenodiamina, a qual age como solvente para a celulose e seus derivados, funcionalizando a superfície do material ao mesmo tempo em que parte da superfície modificada passa à solução.

### 3.1.6 Redução das bases de Schiff

As iminas formadas na reação das poliaminas com os grupos aldeídicos podem ser reduzidas com  $\text{NaBH}_4$  [91], formando aminas secundárias, e para isso suspendeu-se as bases de Schiff em etanol,  $0,10 \text{ g cm}^{-3}$ . A suspensão foi agitada por 15 min, utilizou-se de um funil de adição coberto com folhas de papel alumínio para que fosse adicionada à suspensão, gota-a-gota, uma solução recém-preparada,  $0,90 \text{ mol dm}^{-3}$  de  $\text{NaBH}_4$ . A reação se procedeu ao abrigo da luz, sob agitação, à temperatura ambiente por 72 h. Os materiais obtidos foram filtrados e lavados com, de 3 a  $4 \text{ dm}^3$  de água, secos em linha de vácuo por 6 h e pulverizados em almofariz. Denominou-se estes materiais como CelOP (P = ED, DT e TT) e as reações propostas são mostradas no Esquema 9.



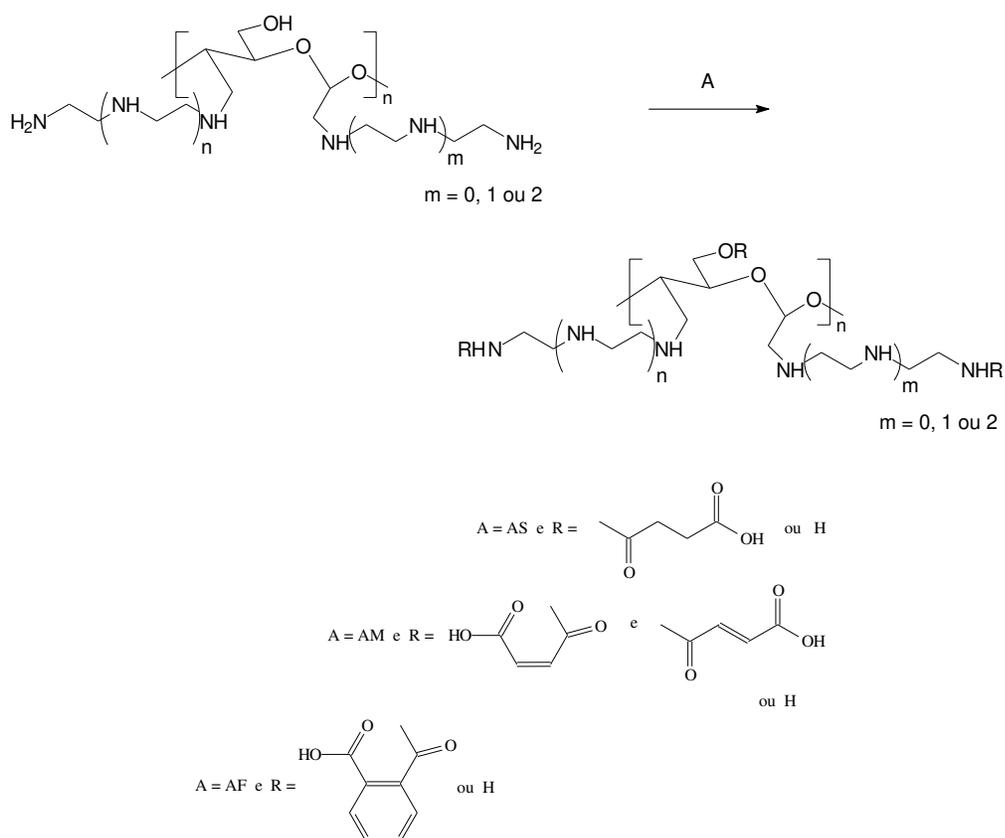
**Esquema 9.** Redução das bases de Schiff em CelOp (p = ED, DT, TT). CelOP (ED, DT, TT). 1,2-etilenodiamina (ED),  $n = 0$ , 1,2,4-dietilenotriamina (DT)  $n = 1$  e 1,2,4,6-trietilenotetramina (TT)  $n = 2$ .

Os ancoramentos das poliaminas nos carboidratos oxidados apresentam algumas limitações como: a) aumento de pH quando são postas em contato com água; b) solubilidade parcial; c) favorecimento de processos erosivos. Assim, a celulose inicial empregada nas modificações, a microcristalina, foi substituída pela de papel de filtro.

### **3.1.7 Reação entre os sólidos aminados e os anidridos**

A esterificação de aminas com anidridos é relativamente fácil de ocorrer graças à reatividade dos anéis cíclicos de cinco membros. A reação se passa através de um ataque nucleofílico da amina à carbonila do anidrido [10]. Entretanto, o material poliamínico não resiste às altas temperaturas utilizando anidridos fundidos, como proposto no projeto inicial, logo se experimentou as reações sob ultrassom, a  $298 \pm 2$  K. Suspendeu-se em solução DMA/acetona 15 % (v/v), os materiais aminados - CelOP (P = ED, DT e TT) – tratou-se com ultrassom por 5 min, adicionou-se, separadamente em cada um dos experimentos, os anidridos succínico (AS), malêico (AM) e ftálico (AF), a fim de se estabelecer a razão molar de 3:1 anidrido: CelOP; concentração de anidrido em acetona de  $1,35 \text{ mol dm}^{-3}$ . Deixou-se sob ultrassom por 1 h, agitou-se magneticamente por 12 h; repetiu-se este procedimento quatro vezes. Filtrou-se, lavou-se com uma solução 20 % (v/v) de acetona em água. Os sólidos obtidos foram secos e pulverizados como já citado. Nomeou-se estes materiais como CelOPA (P = ED, DT e TT e A = AS, AM e AF) e as reações propostas são mostradas na **Esquema 10**.

## Capítulo 3 – Parte experimental (para celulose oxidada)



**Esquema 10.** Formação de aminadas em CelOPA. CelOPA CelOPA (P = ED, DT e TT e A = AS (a), AM (b), e AF (c)).

A rota sintética acima citada esteve limitada ao não uso de ativadores de carbonila, como o DCC e as funcionalizações desses materiais foram pequenos.

### 3.2 Caracterização

As sínteses dos materiais modificados a partir da celulose oxidada apresentaram várias complicações o que levou a uma repetição dos estudos até se obter os materiais purificados. Por isso a técnica de mais baixo custo e disponível, em nosso laboratório, para caracterizar os materiais primariamente, mas com resultados conclusivos de que as reações ocorreram, foi a espectroscopia na região do IV.

### **3.2.1 Espectroscopia na região do IV**

Os espectros na região do IV dos compostos foram obtidos na faixa espectral de 4000 a 400  $\text{cm}^{-1}$ . O método utilizado foi por empastilhamento em KBr, em um espectrômetro Bomem – Hartmann & Braun, série MB, com transformada de Fourier, com resolução de 4  $\text{cm}^{-1}$  e foram realizadas 32 varreduras.

### **3.2.2 Ressonância magnética nuclear de $^{13}\text{C}$ aplicada a sólidos**

Os espectros de ressonância magnética nuclear (RMN) dos núcleos de  $^{13}\text{C}$  foram obtidos no espectrômetro Bruker AC400, utilizando as técnicas polarização cruzada, rotação do ângulo mágico (CP/MAS), com tempo de contato de 3 ms; o tempo de repetição foi de 3 s. A frequência utilizada foi de  $\sim 4$  KHz e um rotor de  $\text{ZrO}_2$  de 7 mm.

### **3.2.3 Termogravimetria**

As curvas termogravimétricas foram obtidas empregando o aparelho termogravimétrico, modelo 9900 da DuPont na faixa de temperatura ambiente até 773 K a uma razão de aquecimento de 0,17  $\text{K s}^{-1}$ , sob atmosfera de nitrogênio.

### **3.2.4 Difractometria de raios X**

Os difratogramas de raios X foram obtidos no difratômetro da Shimadzu modelo XRD7000. A voltagem utilizada foi de 40 kV, corrente de 30 mA, utilizando a fonte de radiação  $\text{CuK}\alpha$  ( $\lambda = 154,06$  pm) e varredura de  $1,4^\circ$  a  $70^\circ$ .

## 4 Resultados e discussão dos experimentos com celulose oxidada

A clivagem oxidativa das ligações C2-C3 pode se sobreoxidar ao ácido carboxílico gerando estruturas instáveis, apesar de serem parcialmente restabilizadas por  $\beta$ -eliminações [38, 44], ocasionando a diminuição do grau de polimerização dos materiais. Se o polímero modificado é solúvel isto o torna desinteressante na busca por suportes sólidos, insolúveis e não expansíveis, os quais terão seus centros básicos testados frente a reações com cátions pesados em solução aquosa.

A aparição da banda em  $1740\text{ cm}^{-1}$  refere-se ao 2,3-dialdeído-celulose [59], região relativa também aos grupos ácidos carboxílicos e cetônico que podem ser formados. As sobreoxidações são observadas principalmente quando: a) os materiais 2,3-dialdeídicos são tratados com  $\text{NaCl}_{(\text{aq})}$ ,  $0,10\text{ mol dm}^{-3}$ , aumentando a intensidade da banda em  $1733\text{ cm}^{-1}$ , devido à formação de ácidos carboxílicos [44]; esta é uma reação controlada cineticamente devido ao aumento da força das ligações hidrogênio, b) os materiais são expostos a altas temperaturas independentemente da presença de oxigênio e c) os materiais são expostos a radiações.

O entumescimento prévio da celulose em água facilita a acessibilidade das espécies reativas,  $\text{IO}_4^-_{(\text{aq})}$ , aos centros que serão oxidados e os materiais obtidos a partir dessa etapa apresentam-se mais homogêneos se comparados aos obtidos sem esta hidratação prévia.

Inicialmente os ésteres de iodo foram removidos suspendendo-se o material oxidado e contaminado em solução de  $\text{NaOH}$   $0,010\text{ mol dm}^{-3}$ . É possível se isolar este biopolímero livre de espécies iodadas precipitando-o em acetona e lavando-o com água até à purificação, contudo para se conseguir tal precipitação a razão 6-8:1 (acetona:solução) foi inviável a ser procedida. A hidrólise básica do material foi então descartada e filtrou-se, despendendo muito tempo para uma lavagem não eficaz na remoção dos compostos de iodo impregnados nos materiais. Estes foram tratados com ultrassom em água e centrifugados, procedimento que se mostrou mais eficaz na eliminação dos compostos iodados.

## Capítulo 4 – Resultados e discussão dos experimentos com celulose oxidada

O tratamento com ultrassom favorece os processos de transferência de massa entre a solução e o interior das fibras, acelerando o processo de purificação dos materiais. Entretanto, o uso de ultrassom também favorece os processos erosivos do polímero, que seriam abertura de fendas na superfície, rompimento de fibras etc.

A redução da celulose oxidada forma novamente uma solução viscosa, a qual é facilmente precipitada em etanol, com aspectos de alta maciez e escorregabilidade ao toque. Contudo, há grande dificuldade em se manter a estrutura fibrosa após a sequência de reações de esterificação e as demais purificações posteriores em meio aquoso, condição em que é perdida praticamente toda a extensão polimérica modificada.

As demais etapas reacionais para obtenção de um material sólido, insolúvel e não expansível em água somente se procede quando o meio aquoso é substituído por DMA/acetona. A substituição do solvente torna o meio heterogêneo, o qual não garante acessibilidade das moléculas reativas aos centros reagentes, a trazer como material modificado um composto disponibilizador de menos centros básicos para reagirem com metais em solução. Devido ao fato de as ondas de pressão causadas pelo ultrassom aumentarem localmente a temperatura, isso aumenta nestes locais os choques entre as moléculas reagentes e os centros reativos, garantindo um aumento na taxa de reação.

### **Espectroscopia na região do IV**

Os espectros vibracionais destes materiais apresentam bandas, das quais é possível qualificar a presença ou não dos grupos incorporados à celulose. Logo, é importante e necessário o entendimento das bandas características do material de partida. Após modificação da matéria prima, esperam-se surgimento de bandas em regiões características, por isso e para facilitar o entendimento através de comparações, fez-se e se detalhou a celulose empregada neste trabalho, como mostrado na **Figura 6**.

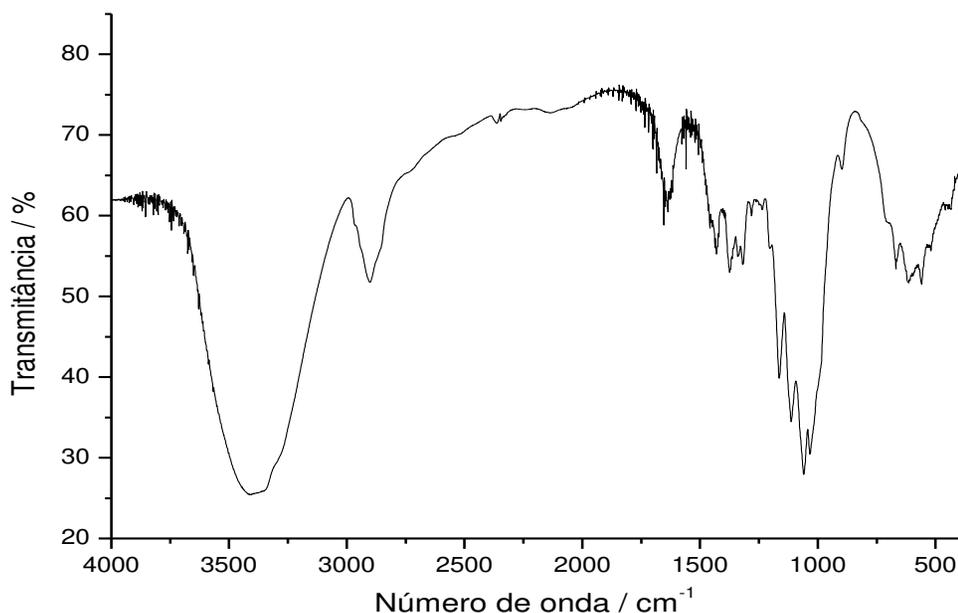


**Figura 6.** Espectro na região do IV da celulose.

A banda existente no intervalo de 3645 a 3200  $\text{cm}^{-1}$  envolve muitos modos vibracionais e os principais são: 3645 a 3620  $\text{cm}^{-1}$   $\nu(\text{O-H})$  de OH livres; 3560  $\text{cm}^{-1}$  água adsorvida fracamente ligada; 3460 a 3412  $\text{cm}^{-1}$   $\nu(\text{O-H})$ ; 3570 a 3450  $\text{cm}^{-1}$  estiramentos de grupos OH intramoleculares; 3455 a 3410  $\text{cm}^{-1}$  ligação intramolecular entre O(2)H...O(6); 3375 a 3340  $\text{cm}^{-1}$  ligação intramolecular O(3)H...O(5); 3310 a 3230  $\text{cm}^{-1}$  ligação intramolecular O(6)H...O(3); 3400 a 3200  $\text{cm}^{-1}$   $\nu(\text{O-H})$ . A banda que surge entre 3000 e 2842  $\text{cm}^{-1}$  refere-se ao  $\nu(\text{C-H})$  de grupos metílicos e metilênicos; 2981 a 2835  $\text{cm}^{-1}$  vibração assimétrica do grupo  $\text{CH}_2$  e  $\text{CH}_2\text{OH}$  (C6); 2940 a 2850  $\text{cm}^{-1}$  vibração de valência simétrica do grupo  $\text{CH}_2$ ; 2840 a 2835  $\text{cm}^{-1}$   $\nu(\text{C-H})$  de metoxila.

Em 1635  $\text{cm}^{-1}$  corresponde à água adsorvida e 1678 a 1650  $\text{cm}^{-1}$   $\nu(\text{C=O})$ . Em 1470 a 1455  $\text{cm}^{-1}$   $\delta(\text{C-H})$  do anel piranosil;  $\sim 1460$   $\text{cm}^{-1}$   $\delta(\text{C-H})$  assimétrico dos grupos metoxilas; 1435  $\text{cm}^{-1}$  deformação da ligação (C-O-H); 1430  $\text{cm}^{-1}$  deformação (C-O-H) de álcoois no plano; 1430 a 1418  $\text{cm}^{-1}$   $\delta(\text{CH}_2)$ ;  $\sim 1374$   $\text{cm}^{-1}$  deformação (C-H); 1350 a 1330  $\text{cm}^{-1}$   $\delta(\text{C-OH})$  no plano; 1319  $\text{cm}^{-1}$   $\delta(\text{CH}_2)$  rotação;  $\sim 1282$   $\text{cm}^{-1}$  deformação (C-H);  $\sim 1235$   $\text{cm}^{-1}$   $\delta(\text{C-OH})$  no plano;  $\sim 1205$   $\text{cm}^{-1}$   $\delta(\text{C-OH})$  no plano; 1162  $\text{cm}^{-1}$  (C-O-C)

vibração de assimétrica; 1120 a 1103  $\text{cm}^{-1}$   $\nu(\text{C-C})$  e  $\nu(\text{C-O})$  assimétrica do anel pirano; 1086  $\text{cm}^{-1}$  deformação  $\delta(\text{C-O})$  em álcoois secundários; 1060  $\text{cm}^{-1}$  estiramento  $\nu(\text{C-O-C})$  éter alifático ( $\beta$ -1,4); 1060 a 1015  $\text{cm}^{-1}$  vibração da ligação C3-O3H; 1047 a 1004  $\text{cm}^{-1}$  ( $\text{C-O-C})$  vibração de metoxila e da ligação  $\beta$ -1,4;  $\sim 1035 \text{ cm}^{-1}$  deformação ( $\text{C-O})$  deformação de álcoois primários e estiramento  $\nu(\text{C=O})$  conjugado;  $\sim 898 \text{ cm}^{-1}$  grupo de carbonos anoméricos e deformação  $\delta(\text{C1-H})$ ; 710  $\text{cm}^{-1}$  deformação ( $\text{CH}_2$ ); 668  $\text{cm}^{-1}$  deformação  $\delta(\text{C-OH})$  fora do plano [58].

Os espectros de IV referentes aos produtos de oxidação estão apresentados na **Figura 7**. O material empregado nas etapas seguintes à oxidativa foi o biopolímero apresentado na **Figura 7b** e, como mostrado, não há significativa mudança se comparado ao biopolímero de partida. O mesmo material após ser disperso em  $\text{KBr}_{(s)}$  e seco por 10 min a 363 K apresentou uma diminuição na intensidade das bandas relativas à água,  $\nu(\text{O-H})$  em 3400  $\text{cm}^{-1}$  e água adsorvida mostrado em 1634  $\text{cm}^{-1}$ ; a banda referente a  $\nu(\text{HC=O})$  aparece em 1740  $\text{cm}^{-1}$  [60], região também atribuída à  $\nu(\text{C=O})$  de cetonas e ácidos carboxílicos, os quais podem ser formados durante o processo de oxidação, como mostrado na **Figura 7b**.

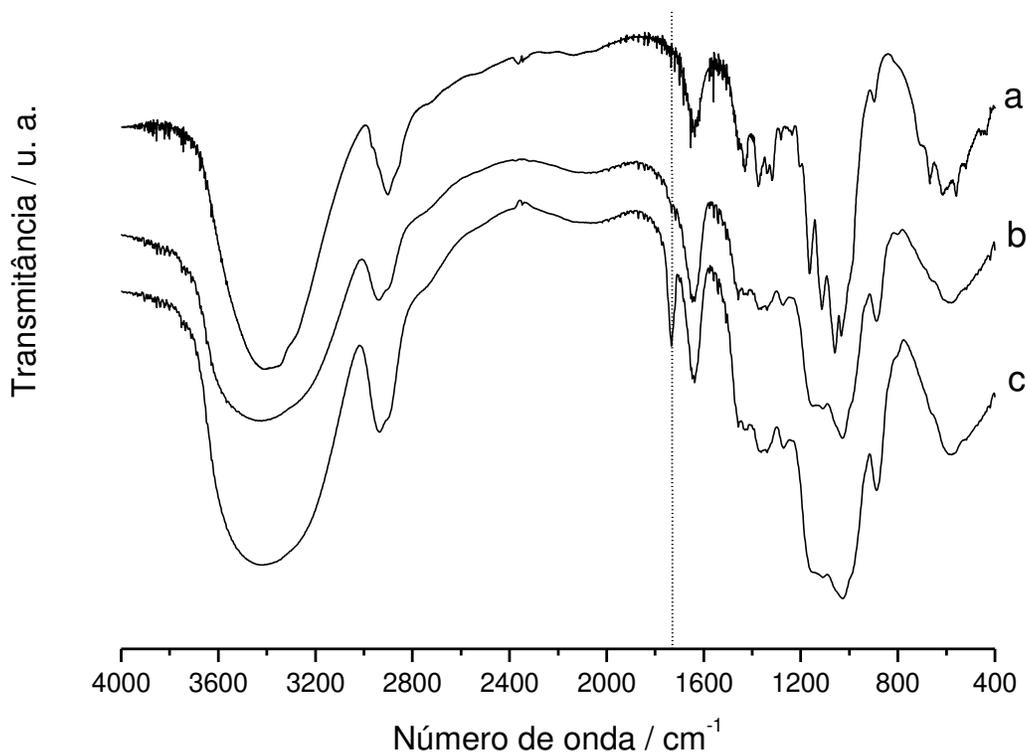


**Figura 7.** Espectros de IV da celulose (a), CelO seco a 363 K por 5 min (b) e CelO tratada com  $\text{NaCl}_{(\text{aq})}$  (c).

Em torno de  $1725 \text{ cm}^{-1}$  observa-se uma banda fraca e alargada referente ao  $\nu(\text{C-H})$  do aldeído. A sensibilidade do material frente ao tratamento salino é justificada pelo aparecimento e intensificação da banda em  $1733 \text{ cm}^{-1}$ , como mostra a **Figura 7c**. Com uma solução de  $\text{NaCl}$   $0,10 \text{ mol dm}^{-3}$  realizou-se os testes de sobreoxidação induzida. Esta sobreoxidação ocorre provavelmente sob controle cinético, no qual a adição do sal aumenta a força das ligações hidrogênio e assim aumento a velocidade de conversão de aldeído para ácido carboxílico. Outras pequenas mudanças são observadas em  $892 \text{ cm}^{-1}$ , referente aos carbonos anoméricos (carbonos que formam o anel glicopiranosídico) e  $\delta(1\text{C-H})$ . Finalmente, em  $846 \text{ cm}^{-1}$  há uma pequena variação da banda referente a acetais, hemiacetais e suas formas hidratadas [61].

Os espectros na região do IV dos sólidos CelOR e CelORA (A = AS, AM ou AF) estão mostrados na **Figura 8c** e **8d-f**. A redução dos grupos aldeídos aos álcoois correspondentes pode ser comprovada com o aumento da banda em  $2930\text{ cm}^{-1}$  referente a  $\nu(\text{HC-H})$ . O sucesso da esterificação com anidridos é comprovado pelo aparecimento da banda em torno de  $1725\text{ cm}^{-1}$  devido a  $\nu(\text{HOC=O})$  e em torno de  $1167\text{ cm}^{-1}$  devido a  $\nu(\text{RO-CO})$ . [60]

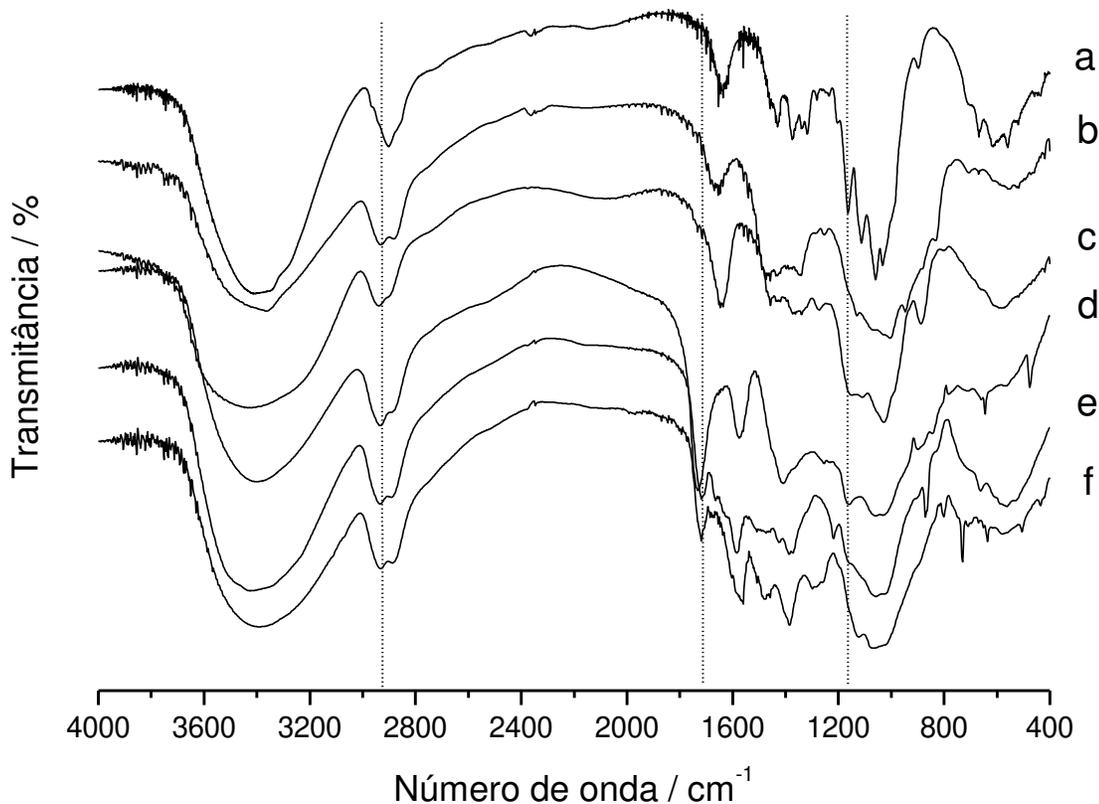


**Figura 8.** Espectros de IV da celulose (a), CelO (b), CelOR (c) e CelORA (A = AS (d), AM (e) ou AF (f)).

A reação de maior rendimento foi com anidrido succínico, pois se tratam de anéis tensionados estabilidade adicional conferida, por exemplo, por insaturações- $\alpha,\beta$ , como no caso dos anidridos maléico e ftálico, os quais são menos reativos nas mesmas

condições. Entretanto, as reações foram procedidas a baixas temperaturas e em solvente de baixa mediação protônica, acetona, ocasionando um baixo grau de modificação.

As reações das três poliaminas com cada uma das celuloses aciladas foi bem limitada, como mostrado nas **Figuras 9 a 11**. Em todos os casos a banda em  $1725\text{ cm}^{-1}$  referente a  $\nu(\text{HOC}=\text{O})$  permanece, ainda que diminuída em intensidade e a permanência indique que nem todos os sítios ácidos reagiram com as aminas. As bandas em  $1655$  e  $715\text{ cm}^{-1}$  referem-se aos estiramentos das amidas secundárias formadas e deformações (N-H) dessas amidas, respectivamente. Os carboxilatos formados devido à desprotonação, com conseqüente protonação dos grupos nitrogenados, formando estruturas zwitteriônicas, correspondem às bandas por volta de  $1588\text{ cm}^{-1}$  [60].

O ancoramento das poliaminas diretamente nos suportes sólidos oxidados teve sucesso como mostrado na **Figura 12**.

A espectroscopia utilizada apresenta certas limitações como, por exemplo, a sobreposição de bandas e o deslocamento destas quando observadas num determinado estado físico, sólido no caso: no estado sólido as possíveis interações deslocam as bandas para números de onda maiores, devido ao aumento relativo da média das massas e diminuição dos graus de liberdade, o que muitas vezes leva à diminuição na intensidade da banda ou sua supressão.

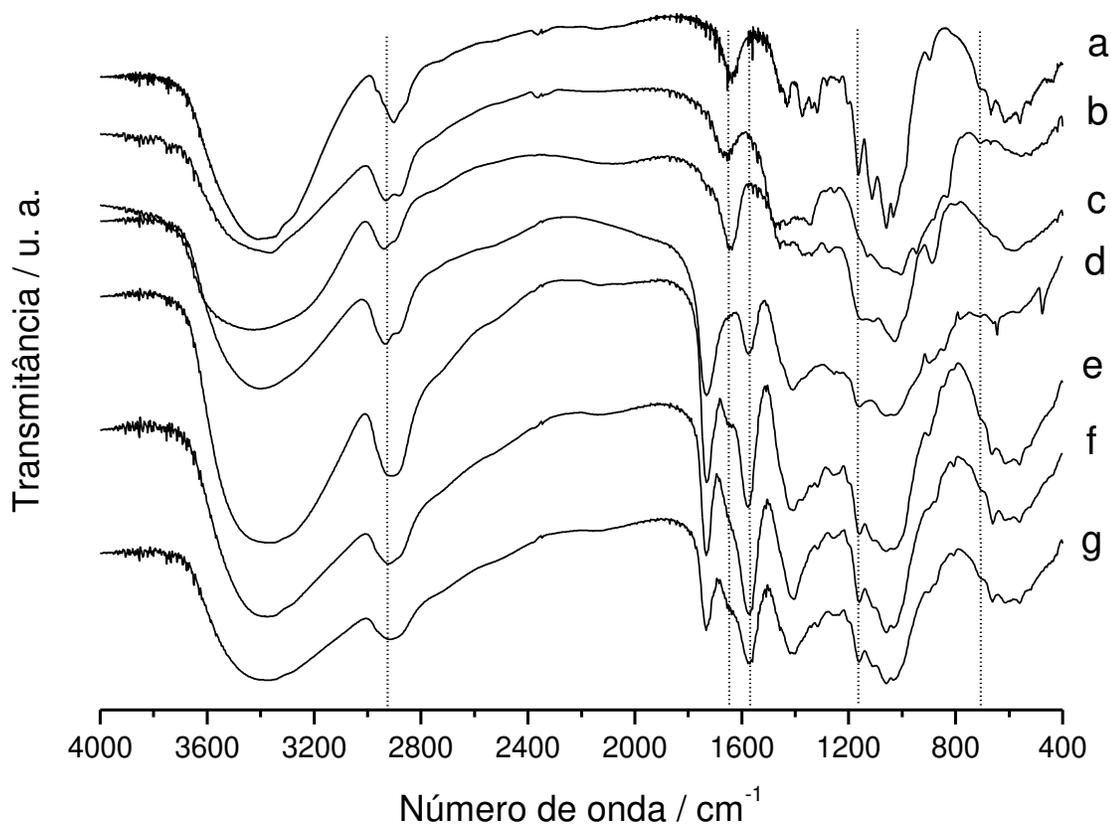


**Figura 9.** Espectros de IV da celulose (a), CelO (b), CelOR (c) e CelORAP [A = AS (d) e P = ED (e), DT (f) ou TT (g)].

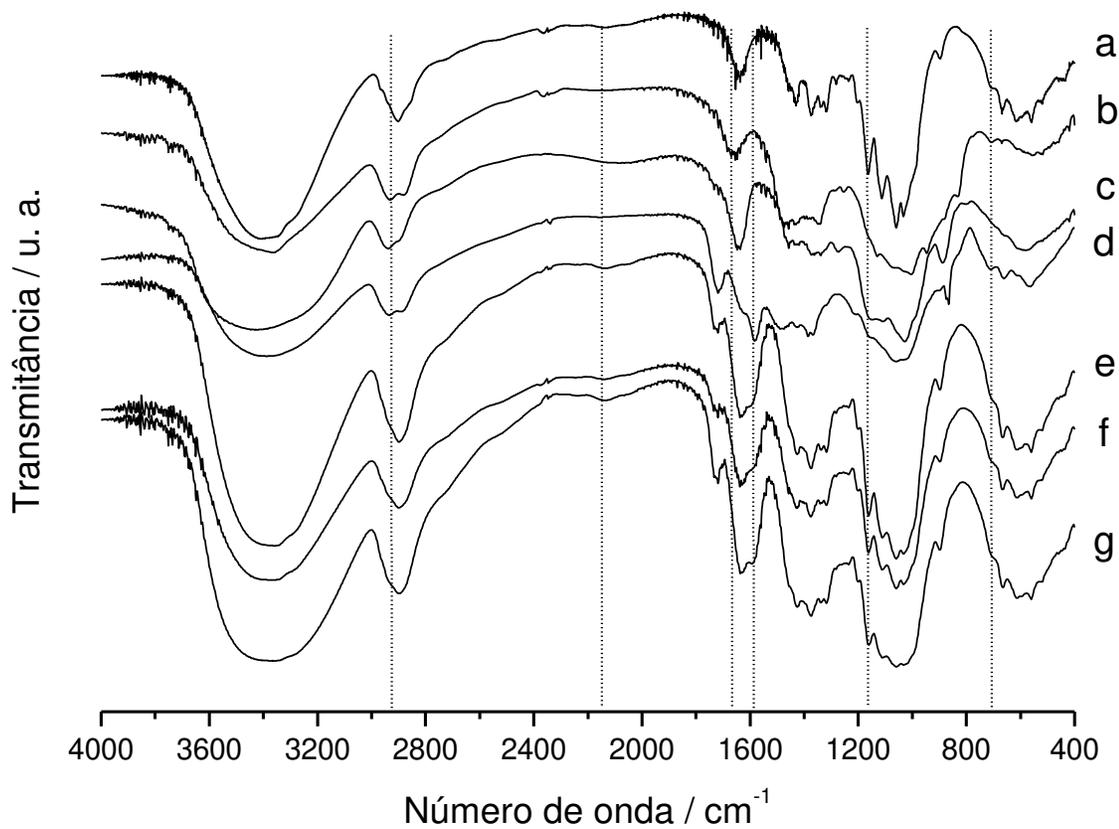


**Figura 10.** Espectros de IV da celulose (a), CelO (b), CelOR (c) e CelORAP [A = AM (d) e P = ED (e), DT (f) ou TT (g)].

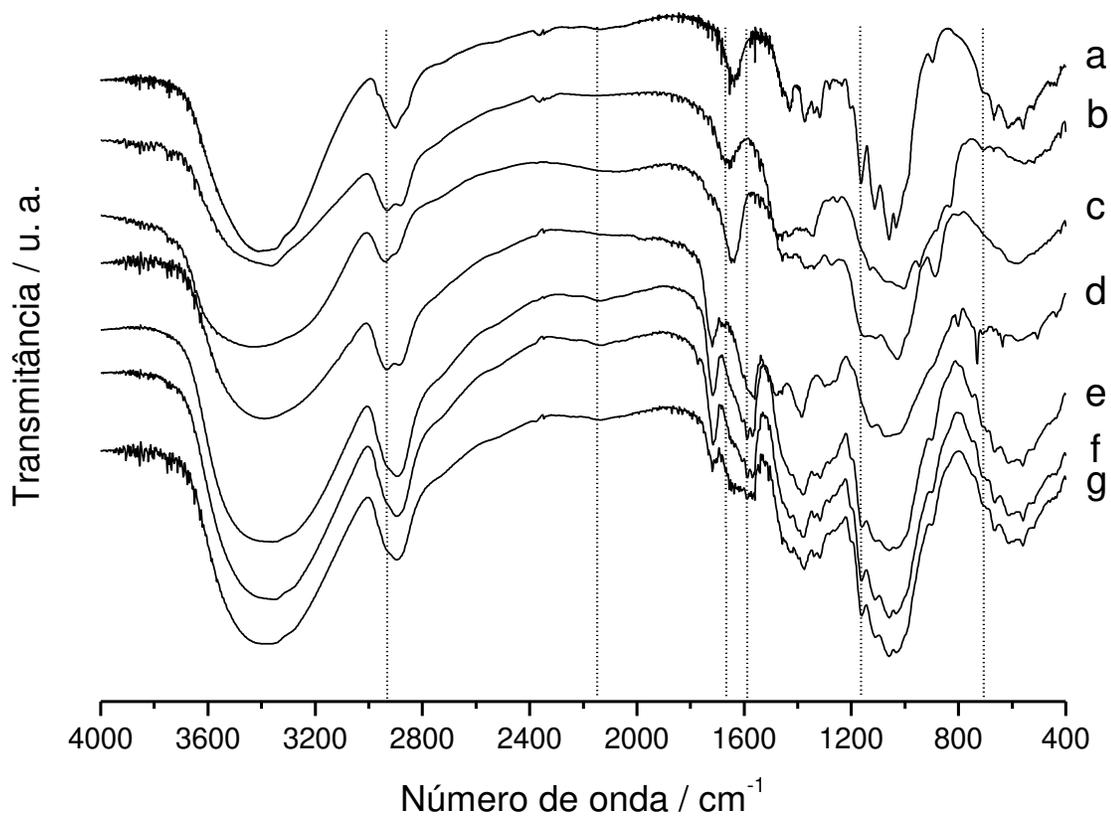


**Figura 11.** Espectros de IV da celulose (a), CelO (b), CelOR (c) e CelORAP [A = AF (d) e P = ED (e), DT (f) ou TT (g)].

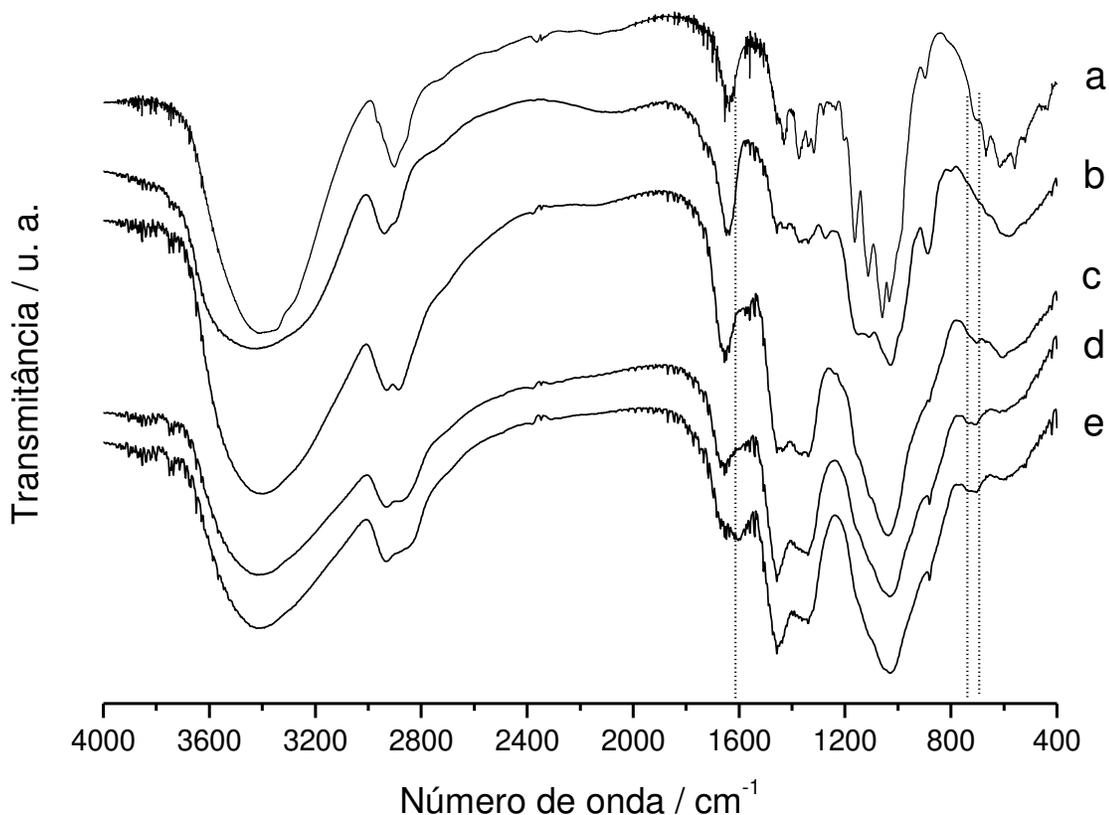


**Figura 12.** Espectros de IV da celulose (a), CelO (b) e CelOP [P = ED (c), DT (d) e TT (e)].

As bandas das amins são difíceis de serem atribuídas, como mostra a **Figura 12**, pois são praticamente todas sobrepostas às bandas do material de partida devido ao relativo baixo grau de modificação. Observa-se, para todos os espectros referentes à aminação, um aumento da banda referente a  $\nu(\text{HC-H})$  em  $2930\text{ cm}^{-1}$  e  $\delta(\text{HC-H})$  em  $1457\text{ cm}^{-1}$ . Os estiramentos (N-H) aparecem sobrepostos aos  $\nu(\text{O-H})$  na alargada e intensa banda em  $3400\text{ cm}^{-1}$ . Entretanto, as deformações (N-H) são observadas principalmente em  $1615$  e em  $715\text{ cm}^{-1}$ . A banda em  $1020 - 1200\text{ cm}^{-1}$ , referente ao  $\nu(\text{C-N})$ , pode estar sobreposta às bandas  $\nu(\text{C-C})$  e  $\nu(\text{C-O})$ , como mostrado no espectro da celulose e do biopolímero oxidado [60].

As reações dos três anidridos cíclicos de cinco membros com cada um dos biopolímeros aminados foram bem sucedidas, como mostrado nas **Figuras 13 a 15**. Em todos os casos a banda em torno de  $1720\text{ cm}^{-1}$  refere-se à formação de lactamas, principalmente no caso das reações com anidrido ftálico e a bandas em  $1655$  e  $710\text{ cm}^{-1}$  referem-se aos estiramentos das amidas secundárias formadas e deformações (N-H) dessas amidas, respectivamente. Os carboxilatos formados devido à desprotonação com formação de grupos pendentes zwitteriônicos, devido à protonação dos grupos nitrogenados, correspondem à banda em  $1588\text{ cm}^{-1}$  [60].

Os espectros mostram o sucesso das reações, entretanto, não é possível extrair informações suficientes a ponto de se determinar, por exemplo, as estruturas formadas. Essas estruturas sugeridas, mostradas nos **Esquemas 4 a 10**, foram idealizadas baseando-se na ordem em que se crescem as cadeias.

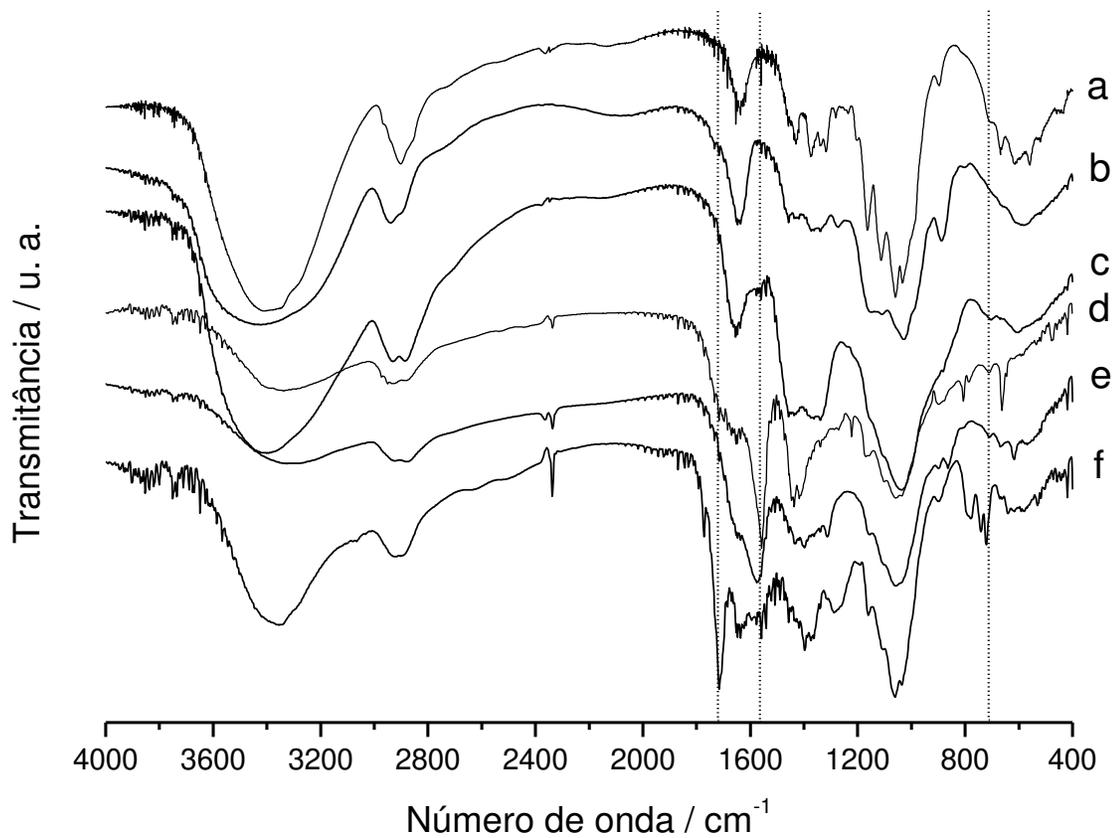


**Figura 13.** Espectros de IV da celulose (a), CelO (b) e CelOPA [P = ED (c) e A = AS (d), AM (e) ou AF (f)].

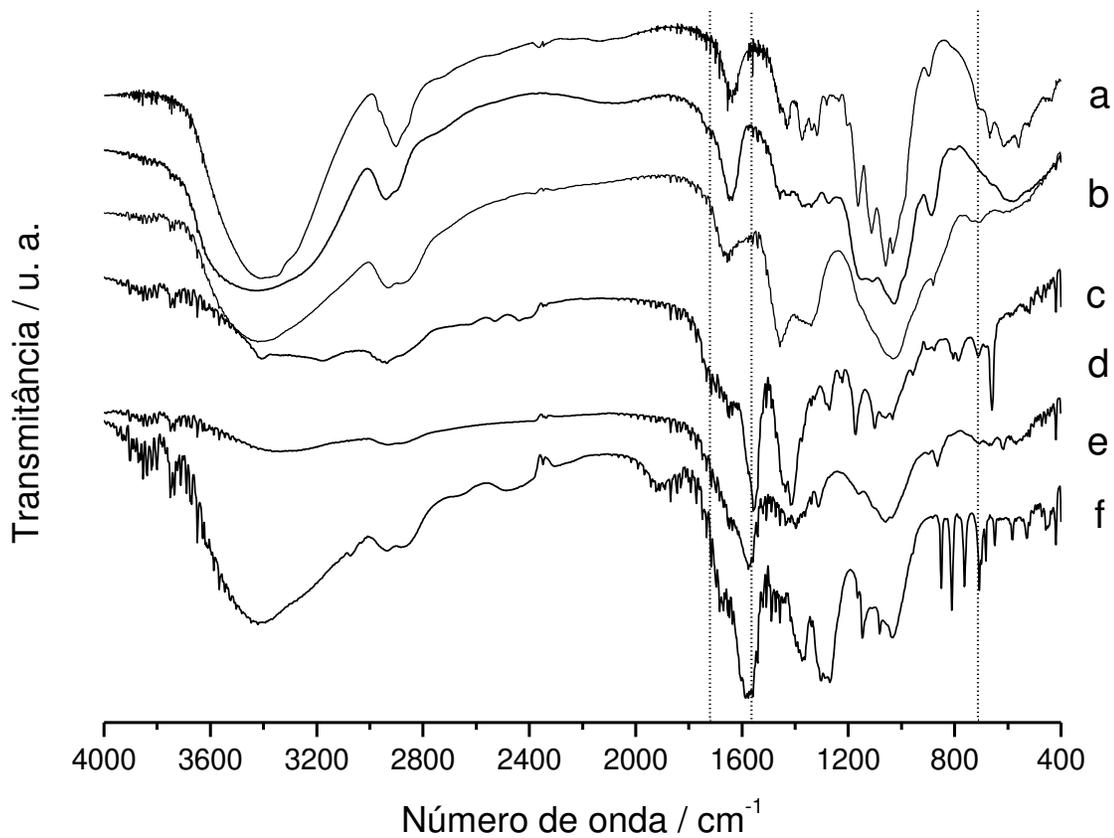


**Figura 14.** Espectros de IV da celulose (a), CelO (b) e CelOPA [P = DT (c) e A = AS (d), AM (e) ou AF (f)].

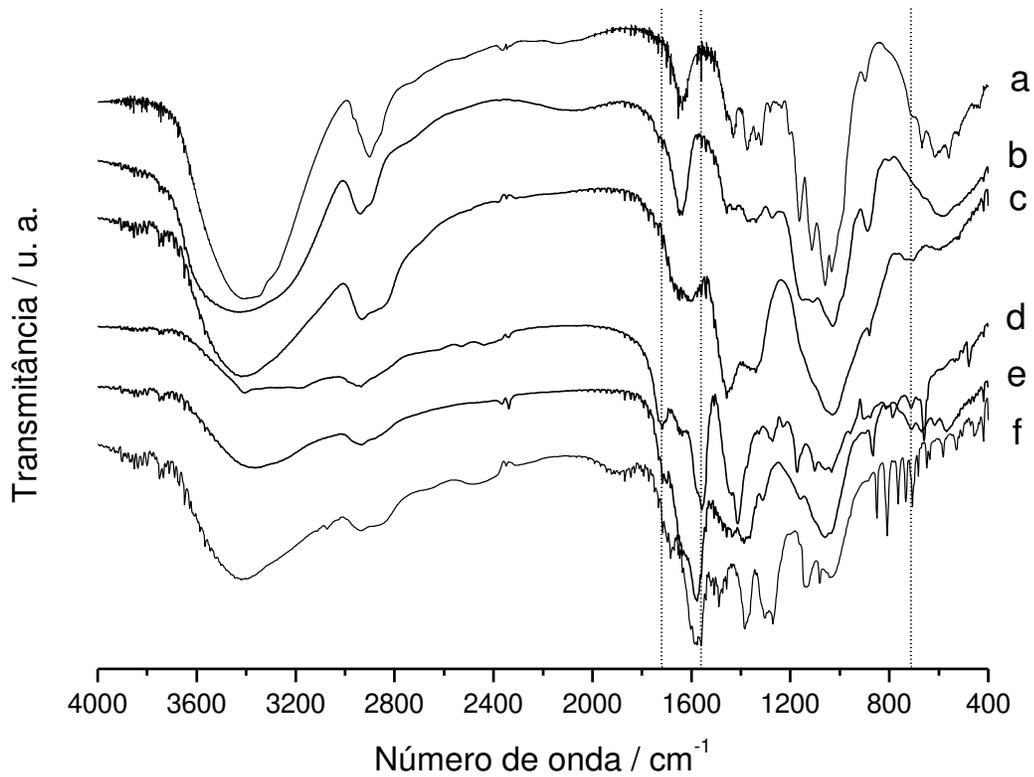


**Figura 15.** Espectros de IV da celulose (a), CelO (b) e CelOPA [P = TT (c) e A = AS (d), AM (e) ou AF (f)].

## 4.1 Sobre os artigos publicados

Como se nota, esta tese trata de uma relação de artigos já devidamente publicados que refletem todo o trabalho de pesquisa desenvolvido pelo aluno no período.

A proposta do plano de pesquisa original e que foi atendido, consistiu na busca do desenvolvimento de materiais, partindo da celulose e de lignocelulósicos. Assim, o enfoque foi a partir dessa biomassa largamente disponível e de baixo custo, para que nos processos de modificações químicas fossem envolvidos reagentes também de baixo custo. O que se pretendeu como linha mestra, também foi usar o mínimo possível de solventes ou até evitá-los, no sentido de seguir os bem traçados princípios estabelecidos pela Química Verde.

Segundo a filosofia do laboratório, a obtenção de novos materiais implica na aplicação dos mesmos, de tal maneira que os suportes sintetizados possam ser úteis na remoção de espécies indesejáveis ao meio. Dentre essas espécies se destacam os catiônicas e os corantes, comumente encontrados em efluentes.

Dessa forma, torna-se importante desenvolver metodologias para a modificação química dos suportes, em especial nessa tese os biopolímeros celulose e lignocelulose, como feito com outros materiais como quitosana, filossilicatos, silicatos mesoporosos bi e tridimensionais, réplicas em estruturas carbonáceas, etc.

Para que os novos suportes aqui representados pelos derivados do biopolímero natural celulose, sejam utilizados com sucesso, esforços foram direcionados à imobilização de moléculas na superfície polimérica, isolando um biopolímero insolúvel, o qual dispõe de cadeias pendentes contendo centros ativos incorporados nas estruturas, para interações químicas com as espécies desejadas.

Como sempre, objetivou-se seguir procedimentos simples para que fossem favoráveis em uma variedade de aplicações, até em casos mais amplos de usos em industriais, muito embora, essa seja uma pretensão pouco viável, em se tratando de que vários aspectos acadêmicos são pouco considerados.

## 5 Esterificação de celulose

As três seguintes publicações:

1) J.C.P. Melo, E.C. Silva Filho, S.A.A. Santana, C. Airoidi, “**Maleic anhydride incorporated onto cellulose and thermodynamics of cation-exchange process at the solid/liquid interface**”, Colloids Surf. A 346, 2009, 138 - 145.

2) J.C.P. Melo, Edson C. Silva Filho, S.A.A. Santana, C. Airoidi, “**Synthesized cellulose/succinic anhydride as an ion exchanger. Calorimetry of divalent cations in aqueous suspension**”, Thermochim. Acta 524, 2011, 29 – 34

3) J.C.P. Melo, E.C. Silva Filho, S.A.A. Santana, C. Airoidi, “**Exploring the favorable ion-exchange ability of modificada cellulose biopolymer using thermodynamic data**”, Carbohydr. Res., 345, 2010, 1914-1921.

possuem os mesmos materiais e métodos e estão descritos abaixo.

### 5.1 Instrumentação

A quantidade de anidridos ligados no biopolímero celulose foi determinada através de retrotitulação dos ácidos carboxílicos formados e a análise elementar em um analisador elementar Perkin-Elmer modelo 2400. Os espectros de FTIR das amostras dispersas em pastilhas de KBr foram obtidos no modo de transmitância através da acumulação de 32 varreduras em um espectrofotômetro FTIR Bomem com  $4\text{ cm}^{-1}$  de resolução, MB-série, no intervalo de número de onda entre  $4000 - 400\text{ cm}^{-1}$ . Os espectros de RMN  $^{13}\text{C}$  em estado sólido foram obtidos num Espectrômetro Bruker AC 400 / P, à temperatura ambiente. As medições foram obtidas a frequências de 75,47 MHz com um ângulo mágico de rotação de 10 kHz. Para aumentar a relação sinal/ruído, a técnica de CP/MAS foi usada, com a repetição de pulso de 5 s e um tempo de contacto de 1 ms. Padrões de difração de raios X foram obtidos num difractômetro de

XRD Shimadzu modelo 7000 com tensão aplicada de 40 kV, corrente de 30 mA, e Cu Ka ( $a = 154,1 \text{ pm}$ ) como fonte de radiação e varredura de  $5^\circ$  a  $45^\circ$ . As curvas termogravimétricas foram obtidas num instrumento TA em atmosfera de argônio, acoplado a uma termobalança B Modelo 1090, com taxa de aquecimento de  $0,167 \text{ K s}^{-1}$ , sob um arraste gasoso com fluxo de  $30 \text{ cm}^3 \text{ s}^{-1}$ , variando desde a temperatura ambiente até  $1273 \text{ K}$ , com uma massa inicial de aproximadamente  $10 \text{ mg}$  de amostra de sólido. Imagens de elétrons secundários foram adquiridos com um microscópio electrónico de varredura JEOL JSM 6360LV, operando a  $20 \text{ kV}$ . As amostras foram fixadas em uma fita de carbono dupla face aderido um suporte de alumínio e de carbono revestido em um instrumento Bal-Tec MD20. Para determinar a quantidade de cátions nas soluções aquosas de OES ICP (espectrometria de emissão óptica por plasma indutivamente acoplado) em um espectrômetro Perkin Elmer, modelo 3000 DV, usado para cada ponto experimental executados em duplicata.

### 5.2 Processos de troca

A capacidade da celulose quimicamente modificada para extrair cátions de uma solução aquosa foi determinada por ensaios em duplicado, utilizando-se um processo em batelada com nitratos divalentes de cobalto ou de níquel, em uma série de frascos de massa ( $m$ ) do sólido suspenso em  $25,0 \text{ cm}^3$  de uma solução aquosa com concentrações de cada metal, variando  $0,10 - 5,0 \text{ mmol dm}^3$ . A partir deste procedimento a melhor isoterma foi obtida com  $25 \text{ mg}$  de trocador de cátions para dar patamares definidos, os quais indicam os máximos da capacidade de troca iônica. A amostra de celulose modificada foi imersa em hidrogenocarbonato de sódio por troca de prótons. O uso de NaCel\_anidrido evita a diminuição do pH durante a suspensão, favorecendo a troca dos metais, o qual foi realizado a um pH isoeletrônica. Para o processo de troca de metal/próton, uma série de frascos contendo as suspensões foi agitada durante  $6 \text{ h}$  numa orbital banho a  $298 \pm 1 \text{ K}$ . Este tempo foi estabelecido anteriormente utilizando métodos semelhantes. Ao final do processo o sólido é separado por centrifugação durante  $10 \text{ min}$  a  $2300 \text{ rpm}$ , e alíquotas do sobrenadante removidas para determinação de cátions por ICP OES. As capacidades de troca ( $N_f$ )

foram calculadas considerando o número de moles:  $N_f = (n_s - n_i) / m$ , em que  $n_i$  e  $n_s$  é o número de moles inicial e que permanece no sobrenadante no final do experimento, respectivamente, e  $m$  é a massa de sólido usado.

O processo de troca iônica ocorre na interface sólido/líquido e envolve a competição entre o solvente (solv) ligado ao sódio da celulose quimicamente modificados (NaCel\_anidrido) que é gradualmente deslocada pelo metal em solução para atingir o equilíbrio, tal como representado na equação 1



A razão entre o número de moles de metal em solução em equilíbrio e o número de moles de metal trocados pelos centros básicos nas cadeias pendentes foi utilizado para obter a equação isotérmica de Langmuir modificada, Equação. 2

$$\frac{C_s}{N_f} = \frac{C_s}{n^s} + \frac{1}{n^s b} \quad (2)$$

onde  $C_s$  ( $\text{mol dm}^{-3}$ ) é a concentração de cátions no sobrenadante e em equilíbrio;  $N_f$  ( $\text{mol g}^{-1}$ ) é o número de moles trocados,  $n^s$  ( $\text{mol g}^{-1}$ ) é a quantidade máxima de soluto trocado por grama de NaCel\_anidrido, que está relacionado com o número de sítios de troca, e  $b$  ( $\text{dm}^3 \text{mol}^{-1}$ ) é uma constante. Os valores de  $b$  e  $n^s$  para cada processo de troca foram obtidas a partir dos coeficientes angulares e lineares, respectivamente, a partir da forma linearizada das isotermas de troca, num gráfico  $C_s / N_f$  versus  $C_s$ , utilizando o método dos quadrados mínimos quadrados.

### 5.3 Titulação calorimétrica

O efeito térmico evoluído a partir da interação entre o cátion e o centro básico ligado nos grupos pendentes na interface sólido-líquido foi medido num aparelho LKB 2277. Para cada operação, uma amostra de cerca de 20 mg de celulose funcionalizado

## Capítulo 5 – Esterificação de celulose

na forma e trocada por sódio foi suspenso em 2,0 cm<sup>3</sup> de água sob agitação a 298,15 ± 0,20 K; as soluções termostatazadas dos cátions, com concentrações de 0,30 mol dm<sup>-3</sup>, foram incrementalmente adicionadas ao recipiente calorimétrico e do efeito térmico da titulação, Q<sub>t</sub>, obtida. Sob as mesmas condições experimentais, o efeito correspondente térmico da diluição da solução de cátion foi obtido em um volume idêntico de solvente calorimétrico, Q<sub>d</sub>. De forma idêntica, o efeito térmico da hidratação em água pelo NaCel\_anidrido também determinado, Q<sub>h</sub>. Sob tais condições, o efeito líquido da troca térmica, Q<sub>r</sub>, foi obtido através da Equação 3, considerando-se que a suspensão do sólido em água originou um valor nulo:

$$\sum Q_r = \sum Q_t - \sum Q_d \quad (3)$$

A variação da entalpia associada com a interação o cátion/matriz pode ser determinada pelo ajuste dos dados a uma equação de troca de Langmuir modificada para calcular a entalpia integral envolvida na formação de uma monocamada por unidade de massa do trocador,  $\Delta_{mono}H$ , [5,19], conforme mostrado na Equação . 4:

$$\frac{\sum X}{\sum \Delta H} = \frac{1}{(K-1)\Delta_{mono}H} + \frac{X}{\Delta_{mono}H} \quad (4)$$

onde  $\sum X$  é a soma da fração molar do cátion em solução depois de trocar, obtido para cada ponto de titulante. Usando a equação modificada de Langmuir, a entalpia integral de troca de íons, por grama da matriz,  $\Delta H$ , foi obtido dividindo o efeito térmico resultante da troca de íons do número de moles do trocador, enquanto K é a constante de proporcionalidade, que também inclui a constante de equilíbrio. Utilizando os valores angulares e lineares, a partir do gráfico  $\sum X / \sum \Delta H$  contra  $\sum X$  permite o cálculo do valor  $\Delta_{mono}H$ . Em seguida, a entalpia de troca pode ser calculada por meio da equação 5:

$$\Delta H = \frac{\Delta_{mono}H}{n^S} \quad (5)$$

A partir dos valores da constante de equilíbrio, as energias de Gibbs foram calculadas pela equação 6:

$$\Delta G = RT - \ln K \quad (6)$$

e o valor de entropia pode ser calculada através da equação 7:

$$\Delta G = \Delta H - T\Delta S \quad (7)$$

## 5.4 Esterificação de celulose com anidridos

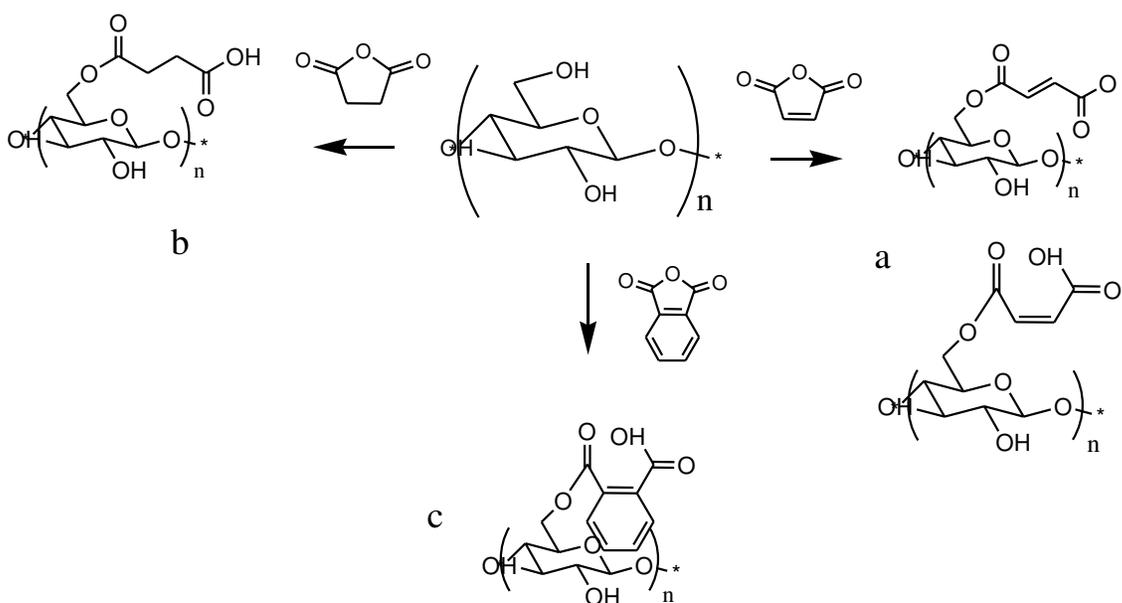
Uma amostra de 5 g de celulose, previamente seca a 383 K por 2 h sob vácuo, foi adicionada ao anidrido X (X = AM, AS e AF) fundido sob agitação magnética, à razão celulose/anidrido de 1:10, em um balão de reação imerso em um banho de areia cujas temperaturas e outros detalhes são mostrados na **Tabela 4**. O balão foi tampado com um *trap* contendo sílica seca a fim de se manter a pressão constante e evitar a umidade do ar. Após 6 h de reação foram adicionados 5 cm<sup>3</sup> de N,N-dimetilacetamida à mistura para que o anidrido fundido não se solidificasse durante a filtração e a mistura foi filtrada a quente; lavada com 100 cm<sup>3</sup> de acetona e então com água até pH neutro, então o sólido foi seco em vácuo a 383 K por 24 h.

O material sintetizado foi tratado com uma solução aquosa 0,9 mol/dm<sup>-3</sup> de bicarbonato de sódio para que os prótons fossem trocados por cátions sódio.

**Tabela 4:** Biopolímeros esterificados CelX (X = AM, AS, AF), temperatura do banho (T), ponto de fusão (PF) e massa (m) dos anidridos utilizados.

| X  | T/ (K) | PF/ (K)   | m/ (g) |
|----|--------|-----------|--------|
| AM | 388    | 324 – 329 | 30,0   |
| AS | 403    | 392 – 393 | 31,0   |
| AF | 413    | 404 – 407 | 47,0   |

## Capítulo 5 – Esterificação de celulose



**Esquema 11:** Esterificação de celulose com anidridos AM (a), AS (b) e AF (c).

**Tabela 5.** Quantidade de grupos ácidos ( $n$ ) para CelX (X = AM, AS e AF) determinados por retrotitulação.

| X  | $n / (\text{mmol g}^{-1})$ |
|----|----------------------------|
| AM | $2,82 \pm 0,05$            |
| AS | $3,07 \pm 0,05$            |
| AF | $2,99 \pm 0,07$            |

**Tabela 6.** Percentuais determinados para carbono (C), hidrogênio (H), nitrogênio (N), calculado para oxigênio (O), obtidos através de análise elementar, grau de substituição (DS) e concentração dos grupos imobilizados ( $\text{No}$ ).

| Composto | C / %            | H / %           | N / %           | O <sup>a</sup> / % | DS    | No / $\text{mmol g}^{-1}$ |
|----------|------------------|-----------------|-----------------|--------------------|-------|---------------------------|
| CMC      | $41,95 \pm 0,04$ | $6,21 \pm 0,08$ | $0,18 \pm 0,02$ | $51,66 \pm 0,11$   | -     | -                         |
| CelAM    | $43,04 \pm 0,01$ | $5,80 \pm 0,04$ | $0,18 \pm 0,05$ | $50,98 \pm 0,01$   | 0,987 | 3,56                      |
| CelAS    | $44,07 \pm 0,19$ | $5,71 \pm 0,01$ | $0,06 \pm 0,06$ | $50,16 \pm 0,28$   | 0,996 | 3,77                      |
| CelAF    | $46,58 \pm 0,19$ | $5,50 \pm 0,09$ | $0,21 \pm 0,04$ | $47,71 \pm 0,14$   | 1,01  | 3,25                      |

## 5.5 Resultados e discussão

Em 1970 foi depositada pela MONSANTO CHEM LTD(MONS-C) a patente abrangente às esterificação de polímeros polihidroxilados com um agente esterificante no estado fundido. Entretanto a técnica defendida é a extrusão, diferentemente do caso estudado e trabalhado nessa tese, na qual a modificação começa a ser analisada quando já há a suspensão do biopolímero em anidridos fundidos; neste estado os anidridos se comportam como um solvente derivatizante. Apesar da técnica estar disponível desde 1970, poucos trabalhos foram publicados sobre a modificação química de celulose com anidrido malêico no estado fundido, pois os pesquisadores descendentes da antiga academia não estiveram muito preocupados com questões sustentáveis e rotas *verdes* de síntese e procederam em solvente. Atualmente os processos de modificação química em extrusoras são amplamente empregados na indústria e, particularmente para o caso das reações com celulose e anidridos, a maior aplicação é no processamento com copolímeros de celulose com polímeros como polietileno etc..

O anidrido malêico é especialmente versátil para esta rota com este reagente no estado fundido pois além de poder reagir nos carbonos carbonílicos podem ainda reagir pela insaturação e esta síntese foi realizada para carbonos mesoporosos pelo nosso grupo [93].

Um resultado recente da literatura, no qual este trabalho já é citado e usado, portanto, como referência, usa a rota com solventes (piridina) se consegue uma funcionalização de 2,7 mmol g<sup>-1</sup>. O método não parece ser mais eficaz que o desenvolvido pelo nosso grupo; além de incluir mais etapas, como a etapa de mercerização da celulose para aumentar a reatividade e acessibilidade às hidroxilas ativas da celulose. Esse método apresenta a desvantagem de possibilitar a formação, em baixa extensão, de poli ácido malêico [94] Uma outra técnica foi a dissolução de celulose de algodão em líquidos iônicos obtendo um grau de modificação de 0,85 a 1,46 mmol g<sup>-1</sup>. Para esta outra técnica o nosso método também se mostrou mais vantajoso [95].

O reagente anidrido maléico possui uma insaturação que forma dois diferentes isômeros quando o anel anidrido é aberto o maléico e o fumárico. A isomerização à formação da estrutura fumárica é irreversível; ainda a capacidade de dessorver o cátion  $\text{Cd}^{2+}$  é maior para o maleato que para o fumarato. [96]

Já para um estudo com resinas contendo os sais reticulados do maleato e fumarato mostraram resultados diferentes, nos quais a troca ocorre com maior intensidade para o maleato e foram estudados  $\text{Pb}^{2+}$ ,  $\text{Cd}^{2+}$  e  $\text{Cu}^{2+}$ . [97]

Nessa direção, esta reação estudada neste trabalho poderia ainda ser aplicável a modificação de outras estruturas contendo carbonos  $\text{sp}^2$  como nanotubos de carbono, fulerenos, estruturas replicadas em carbono etc.

Os espectros de IV da celulose esterificada com anidridos está mostrada na **Figura 16**.

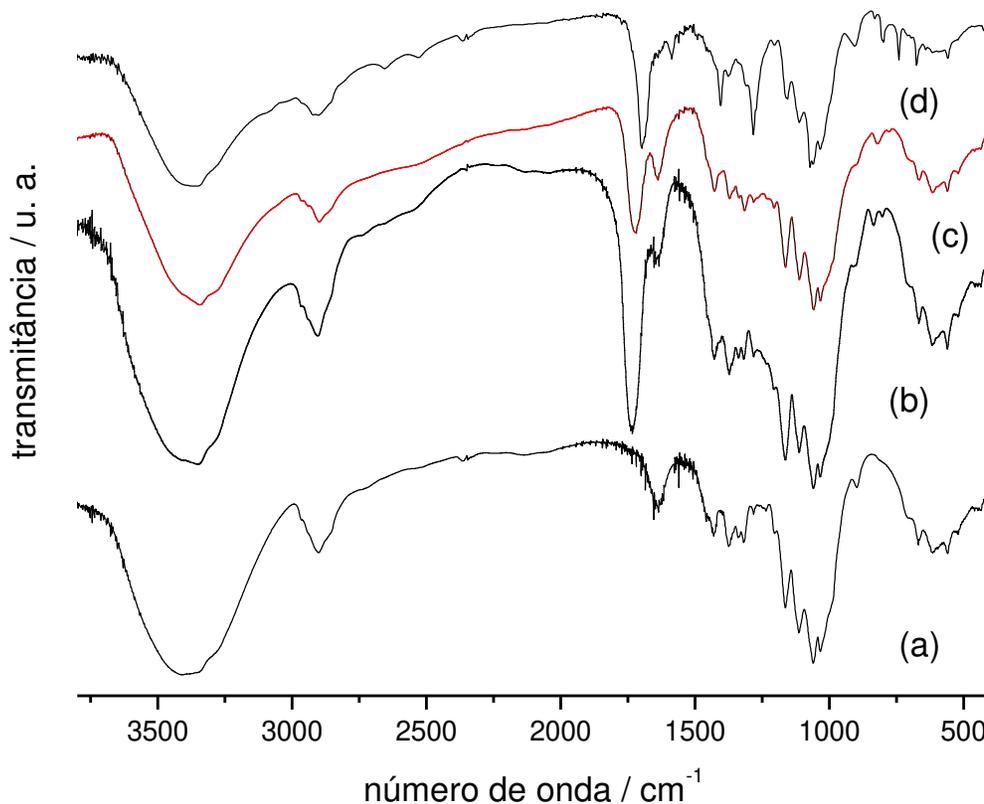


**Figura 16.** Espectros de IV de celulose (a), CelAM (b), CelIAS (c) e CelAF (d).

No espectro de CelAM a banda fraca em  $3045\text{ cm}^{-1}$  é atribuída aos estiramentos de ligações hidrogênio intramoleculares da estrutura malêica e em  $1637 - 1640\text{ cm}^{-1}$   $\nu(\text{C}=\text{C})$ . Dímeros de ácidos carboxílicos são associados à banca centrada em  $2530\text{ cm}^{-1}$  devido à insaturação e as bandas em  $1734$  and  $1162\text{ cm}^{-1}$  são associadas aos  $\nu(\text{C}=\text{O})$  de ésteres; em  $1718$  e  $1282\text{ cm}^{-1}$  estiramentos de ácido carboxílico. O surgimento de uma banda em  $821\text{ cm}^{-1}$  é atribuída às deformações de ácidos carboxílicos fora do plano e a ausência de bandas em  $1850$  e  $1780\text{ cm}^{-1}$  confirmam a ausência de anidrido malêico não reagido. Alguns resultados da literatura estão apresentados na **Tabela 7**.

**Tabela 7.** Sumário das bandas típicas encontradas nos espectros de IV para celulose modificada com anidrido succínico.

| Material modificado | $\nu(\text{C}=\text{O})$ éster / $\text{cm}^{-1}$ | $\nu(\text{C}=\text{O})$ ácido carboxílico / $\text{cm}^{-1}$ | $\nu(\text{C}=\text{C})$ / $\text{cm}^{-1}$ | Referência |
|---------------------|---|---|---|------------|
| madeira             | 1737  | 1737  | 1635  | [98]       |
| Celulose            | 1730  | 1730  | 1637  | [94]       |
| Algodão             | 1729  | 1729  | 1634  | [99]       |
| Metil celulose      | 1735  | 1735  | 1647  | [100]      |
| celulose            | 1730  | 1712  | 1636  | [101]      |

Os espectros de IV da celulose modificada quimicamente (CelAS) mostraram bandas em  $2775$  e  $2500\text{ cm}^{-1}$  relacionados aos dímeros de ácidos carboxílicos, bem como o seus estiramentos em  $1717\text{ cm}^{-1}$ . As bandas a  $1741\text{ cm}^{-1}$  e  $1163\text{ cm}^{-1}$  são atribuídos aos estiramentos e deformações (C=O), respectivamente, de éster, demonstrando o êxito da reacção. A ausência de bandas em  $1860$  e  $1790\text{ cm}^{-1}$  confirma que o produto está isento de anidrido succínico não reagido. Alguns resultados da literatura são apresentados na **Tabela 8**.

**Tabela 8.** Sumário das bandas típicas encontradas nos espectros de IV para celulose modificada com anidrido succínico.

| Material modificado          | $\nu(\text{C=O})$ éster / $\text{cm}^{-1}$ | $\nu(\text{C=O})$ ácido carboxílico / $\text{cm}^{-1}$ | Referência |
|------------------------------|--|--|------------|
| CelS                         | 1741                                       | 1717   | [102]      |
| Celulose de bagaço de cana   | 1750                                       | 1712   | [103]      |
| celulose                     | 1724                                       | 1724   | [104]      |
| Celulose de casca de abacaxi | 1736                                       | 1736   | [105]      |
| Celulose de bambu            | 1735                                       | 1735   | [106]      |
| Caroço de azeitona           | 1742                                       | 1742   | [107]      |
| Bagaço                       | 1725                                       | 1725   | [108]      |
| Bagaço de cana               | 1727                                       | 1727   | [109]      |

O elevado grau de ftalilação na superfície CelAS provoca o aparecimento de uma banda em  $1070 \text{ cm}^{-1}$ , assim como em  $1060 \text{ cm}^{-1}$  estão relacionados ao éter (acetal) alifático  $\nu(\text{C-O-C})$ . Esta nova banda em  $1070 \text{ cm}^{-1}$  sugere a participação efetiva de  $\beta$ -ligações (1,4) glicosídicas de cadeias celulósicas modificadas, que estão presentes no resíduo ftalato, envolvendo interações  $\pi$ - $\pi$ -aromáticos (Ar-Ar) interactions. [referência18artigo] Tais interações parecem ser forte o suficiente para perturbar as ligações  $\beta$ -(1,4) de modo a aparecer outra banda de absorção para esta configuração da parte modificada. A ausência de qualquer banda em  $1800$  e  $1850 \text{ cm}^{-1}$  confirma que o produto está isento de anidrido ftálico não reagido. A **Tabela 9** mostra alguns resultados da literatura.

**Tabela 9.** Sumário das vibrações típicas encontrados em espectros de IV de celulose modificada com anidrido ftálico.

| Material modificado         | $\nu(\text{C=O})$ éster / $\text{cm}^{-1}$ | $\nu(\text{C=O})$ ácido carboxílico / $\text{cm}^{-1}$ | $\delta(\text{C-H})$ aromático / $\text{cm}^{-1}$ | Referência |
|-----------------------------|--|--|---|------------|
| HCeIP                       | 1700                                       | 1700   | 750   | [5]        |
| Celulose de madeira         | 1745                                       | 1645   | -   | [104]      |
| Cellulose de bagaço de cana | 1713<br>1718<br>1722                       | 1713<br>1718<br>1722                                   | 752   | [106]      |
| Celulose de bagaço de cana  | 1716<br>1717<br>1718<br>1719               | 1716<br>1717<br>1718<br>1719                           | 746<br>739<br>741<br>741                          | [110]      |
| Celulose de bagaço de cana  | 1732<br>1724                               | 1732<br>1724   | 742<br>742  | [11 l]     |

A espectroscopia de ressonância magnética nuclear de  $^{13}\text{C}$  também foi empregada, como mostra a **Figura17b** na confirmação das estruturas modificadas e o sucesso da reação está principalmente evidenciado pelo sinal em 165 ppm, relacionado aos carbonos carbonílicos tanto de ésteres quanto de ácidos, estes sobrepostos ao citado deslocamento químico. O sinal encontra-se deslocado para campo alto devido à presença da insaturação  $\alpha,\beta$ -carbonila da molécula modificante. Os carbonos  $\text{sp}^2$  apresentarão deslocamento químico para 136 e 126 ppm para  $\alpha$ -carbonila éster e  $\alpha$ -carbonila ácido, respectivamente. É de se esperar uma porcentagem maior de modificações no carbono 1 como já estudado por outros grupos. [98]

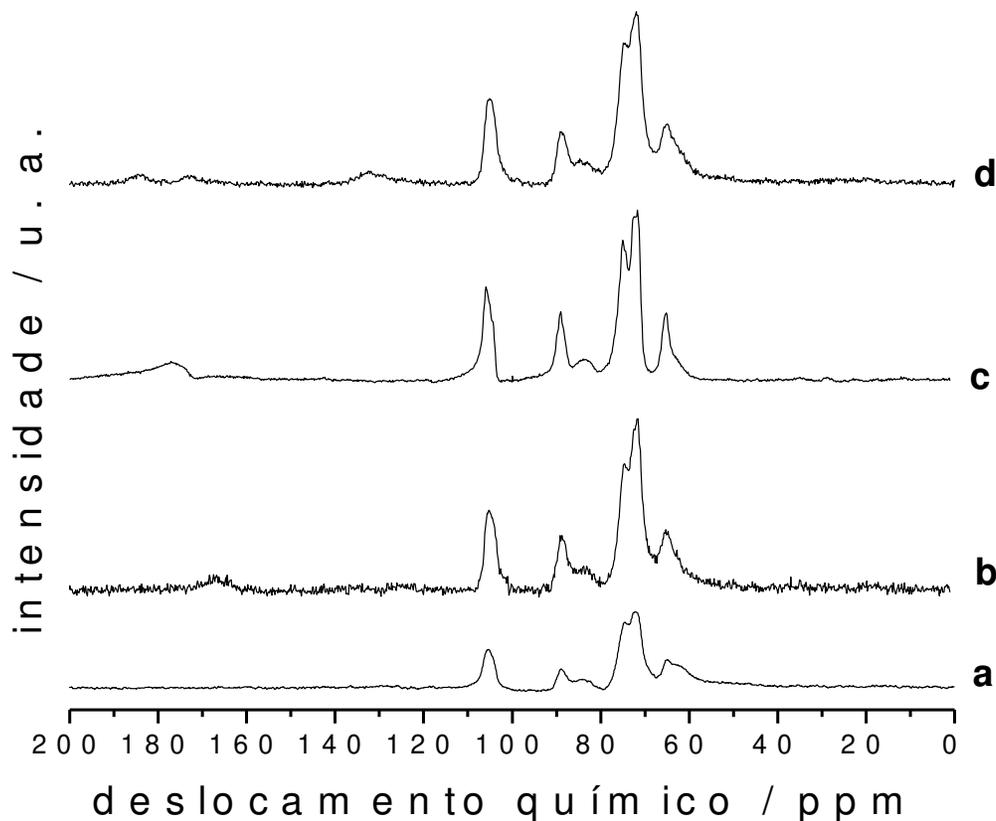


**Figura 17:** Espectros de RMN  $^{13}\text{C}$  de celulose (a), CelAM (b), CelAS (c) e CelAF (d).

Os espectros de RMN  $^{13}\text{C}$  são apresentados na **Figura17c** e comparativos com a literatura são apresentados na **Tabela 10**. Os espectros de RMN de carbono 13 são conclusivos para elucidação da estrutura formada ao final da reação, mas o detalhamento sobre a extensão da reação para cada uma das hidroxilas disponíveis à reação parece estar além das expectativas dos grupos que trabalharam com a modificação de cellulose com anidrido succínico.

**Tabela 10.** Sumário dos deslocamentos químicos (DQ) típicos em espectros de RMN  $^{13}\text{C}$  de celulose modificada com anidrido succínico.

| Celulose modificada         | C6a*/ppm | C6c**/ppm | C2,3/ppm | CO/ppm | Referência |
|-----------------------------|----------|-----------|----------|--------|------------|
| CelS                        | 63       | 65        | 75,5     | 174    | [102]      |
| Cellulose de bagaço de cana | 59,8     | 61,1      | 67,8     | 171    | [103]      |
| Caroço de azeitona          | 60       | 60        | ~ 75     | 173    | [107]      |
| Celulose de bagaço de cana  | 64,5     | 64,5      | 72,4     | 176,5  | [109]      |
| celulose                    | ~ 65     | ~ 65      | ~ 74     | 175    | [112]      |

\* carbono situado em região amorfa

\*\* carbno situado em região cristalina

O sucesso da reação está evidenciado pelos espectros de RMN  $^{13}\text{C}$ , mostrados na **Figura17d**, onde sinais em 184 ppm e 173 ppm estão relacionados aos carbonos carbonílicos de ácido e de éster, respectivamente, presentes na molécula do anidrido, bem como os carbonos aromáticos, os quais são reconhecidos pelo sinal alargado em 130 ppm; de 70 a 75 ppm são os sinais dos carbonos 2, 3 e 5. Finalmente os sinais em 105, 88 e 64 ppm estão relacionados, respectivamente, aos carbonos 1, 4 e 6. Outros resultados são mostrados na **Tabela 11**.

Os carbonos 4 e 6 são esperados de serem reconhecidos distintamente quanto ao ambiente químico: nos espectros de RMN estes carbonos nas regiões cristalinas ou amorfas aparecem como sinais diferentes.

**Tabela 11.** Sumário dos deslocamentos químicos (DQ) típicos encontrados em espectros de RMN  $^{13}\text{C}$  de celuloses modificadas com anidrido ftálico.

| Celulose modificada        | C6/ppm | C2,3/ppm | CO/ppm                                 | C <sub>arom</sub> /ppm | Referência |
|----------------------------|--------|----------|--|------------------------|------------|
| HCeIP                      | 64     | 70-75    | 173 (ácido carboxílico)<br>184 (éster) | 130                    | [5]        |
| Bagaço de cana             | 59,7   | 69,5     | 165                                    | 126                    | [98]       |
| Celulose em madeira        | 61     | 73       | 147                                    | 132                    | [113]      |
| Celulose de bagaço de cana | 63     | 72       | 171 (ácido carboxílico)<br>190 (éster) | 131                    | [110]      |
| Celulose de bagaço de cana | 63     | 72       | 172 (ácido carboxílico)<br>195 (éster) | 126                    | [111]      |
| Celulose em bagaço de cana | 60     | 70       | 205                                    | 126                    | [111]      |

Os difratogramas de raios X mostram, **Figura 18b,c** que não há mudanças significativas em nenhum dos planos de difração da celulose (101, 101', 002, 040) e nota-se que os picos referem-se principalmente aos arranjos originais da celulose natural. O Plano 040 não se encontra evidente nos difratogramas apresentados na literatura, mas os outros planos são equiparáveis aos apresentados na literatura.

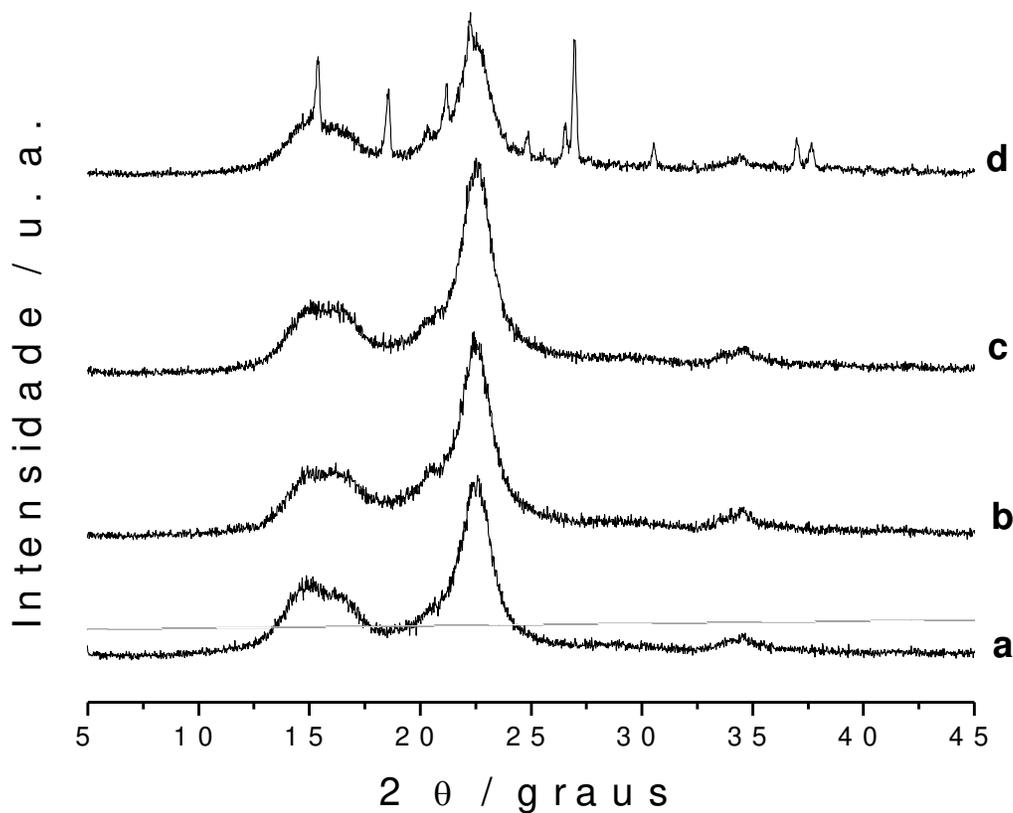


**Figura 18:** Difratogramas de raios X de celulose (a), CelAM (b), CelIAS (c) e CelAF (d).

Em todos os casos ocorre sempre a diminuição do tamanho do cristalito com o aumento do grau de substituição. Ainda é mostrado que as rotas heterogêneas proporcionam materiais ainda com as regiões cristalinas da celulose natural, ao passo que para as reações em fase homogênea a total desconfiguração da cristalinidade não é recuperada devido aos novos grupos introduzidos quimicamente.

**Tabela X.** Sumário das reflexões encontrados em difratogramas de raios X para amostras de celulose modificada com anidrido succínico.

| Celulose modificada      | Reflexões, 2 $\theta$ /grau |      |      |      |        |
|--------------------------|-----------------------------|------|------|------|--------|
|                          | 101                         | 101' | 002  | 040  |        |
| CelS                     | 14,9                        | 15,2 | 22,5 | 34,5 | [102]  |
| Caroço de azeitona       | 8                           | 8    | 20,9 | ~ 35 | [107]  |
| Celulose de madeira dura | 15                          | 16   | 23   | 34   | [114]  |
| Celulose mercerizada     | -                           | -    | -    | -    | [115]. |

O grau de cristalinidade da celulose demonstrou grande interesse de muitos grupos de pesquisa ao passo que para este biopolímero modificado quimicamente com anidrido ftálico esta investigação não é feita. Após a reação, as regiões de mais baixas cristalinidades decrescem, considerando a desorganização e encurtamento do comprimento da fibra. As reações são passíveis e esperadas de ocorrerem primeiramente nas regiões para-cristalinas, localizadas às superfícies poliméricas; os novos padrões de difração surgidos nos difratogramas do material modificado sugere que a intensidade das interações entre os anéis aromáticos de moléculas próximas são fortes o suficiente para garantirem novos planos de difração.

As curvas termogravimétricas apresentadas na **Figura 19b-d** correspondem às análises dos materiais sintetizados em nosso laboratório e estes se comportam de maneira semelhante aos encontrados por outros grupos [94]; mostra eventos de decomposição térmica começando em 450 K e a 650 K mais de 80% do material já está decomposto. A quantidade de resíduo após a análise térmica desses materiais é menor que 20 % enquanto a celulose apresenta cerca de 5 % de resíduo para esta mesma análise.

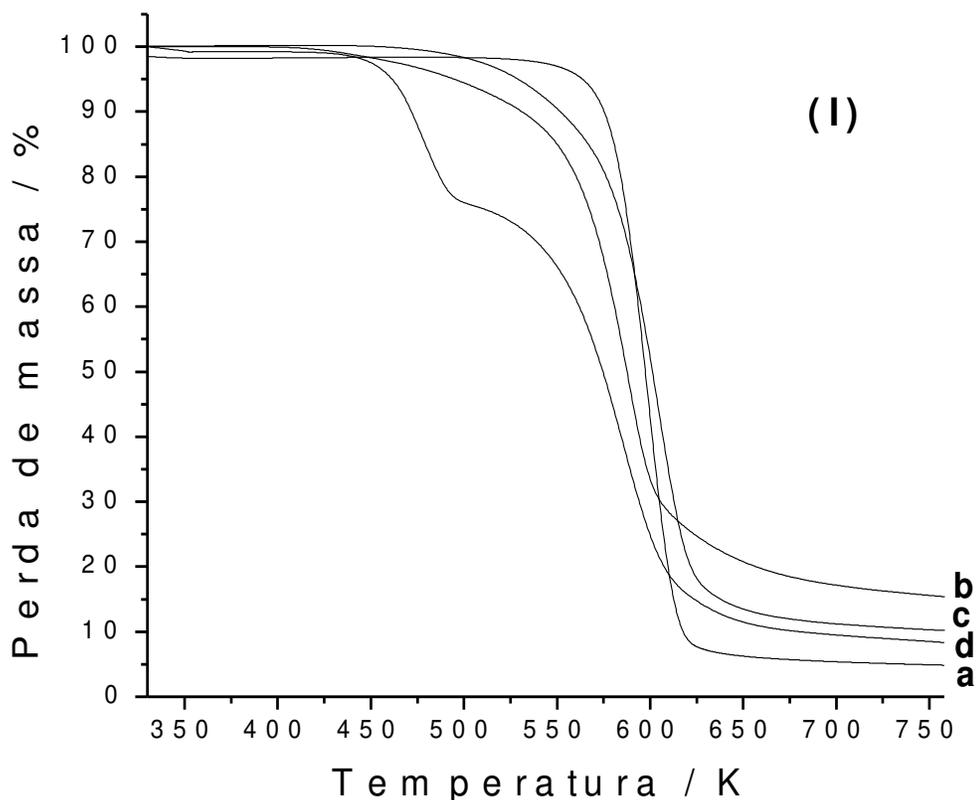


**Figura 19.** Curvas termogravimétricas celulose (a), CelAM (b), CelIAS (c) e CelAF (d).

Para os materiais modificados é sempre esperada a mesma sequência de eventos: perda de qualquer volátil, dessorção de água, perda da modificação, perda de derivados carboxilatos, desidratação acompanhada de policondensação, carbonização do material. Entretanto estes eventos ocorrerão em faixas de temperaturas diferentes de acordo com a estrutura proporcionada após a modificação química. Para rotas heterogêneas de síntese o produto final tem muitas características do biopolímero natural sendo conservado o perfil da curva termogravimétrica para estes materiais. Já as modificações em fase homogênea o perfil das curvas termogravimétricas é diferente e os eventos de decomposição térmica ocorrem a temperaturas anteriores aos esperados para os materiais sintetizados em fase heterogênea. Alguns resultados obtidos por outros grupos são mostrados na **Tabela 12**.

**Tabela 12.** Sumário dos eventos de decomposição térmica e massa final (MF) para alguns biopolímeros celulósicos modificados com anidrido succínico.

| Biopolímero modificado     | Dessorção de água / K | Perda da parte modificada / K | Colapso total da estrutura polimérica / K | MF / % | Referência |
|----------------------------|-----------------------|-------------------------------|---|--------|------------|
| Celulose de bagaço de cana | 323 – 463             | 463 -593                      | > 593                                     | 30     | [103]      |
| CelS                       | 300 – 460             | 475 – 600                     | > 600                                     | < 20   | [102]      |
| Caroço de azeitona         | < 400                 | 473 - 508                     | > 500                                     | < 5    | [107]      |
| Bagaço                     | < 398                 | 398 - 438                     | > 438                                     | < 5    | [108]      |
| Bagaço de cana             | 320 - 450             | 486 - 612                     | > 612                                     | < 40   | [109]      |

Espera-se que o material modificado tenha um desempenho, quanto à inércia térmica, diferente do material de partida e os diferentes fenômenos devido à decomposição térmica foram, os quais foram estudados por análise térmica.

Na celulose ftalilada, até 450 K a água é dessorvida; entre 400-500 K, libertação de espécies aromáticas, que correspondem a 24% da perda da massa de partida e entre 500-700 K correspondente à decomposição da matriz polimérica. Mas entre 500 e 650 K ocorrem muitas reações químicas na matriz polimérica e entre esta e os resíduos do reagente de modificação. Ocorrem desidratações e outros processos oxidativos, gerando insaturações e por fim a oxidação total do material restando 15 % de resíduo. O material HCelP começa a ser decomposto a uma temperatura inferior do que a observada para a celulose, um fenômeno que pode estar associado à facilidade de a cadeia pendente quebrar durante o processo de aquecimento. A celulose microcristalina apresentou apenas um evento de decomposição no intervalo de temperatura de 400-700 K no qual estão inclusos todos os fenômenos citados. Alguns resultados da literatura também são mostrados na **Tabela 13**.

**Tabela 13.** Sumário dos eventos de decomposição térmica e massa final (MF) para alguns lignocelulósicos modificados com anidrido ftálico.

| Biopolímero modificado      | Dessorção de água / K | Perda da parte modificada / K | Colapso total da estrutura polimérica / K | MF / % | Referência |
|-----------------------------|-----------------------|-------------------------------|---|--------|------------|
| HCeIP                       | < 450                 | 400 - 500                     | 500 - 700                                 | 15     | [5]        |
| Bagaço de cana              | < 473                 | 473 - 653                     | 653 - 773                                 | 20     | [111]      |
| Celulose de bagaço de cana  | < 453                 | 453 - 513                     | 513 - 773                                 | < 25   | [113]      |
| Cellulose de bagaço de cana | < 491                 | 491 - 567                     | 567 - 773                                 | 35     | [110]      |
| QF                          | 327                   | 656                           | > 656                                     | < 40   | [117]      |
| QAF                         | 338                   | 447                           | 652                                       | < 10   |            |

**Tabela 14.** Entalpia ( $\Delta H$ ), Energia livre de Gibbs ( $\Delta G$ ) e Entropia ( $\Delta S$ ) para as celulosas modificadas CelXC (X = AM, AS e AF; C =  $\text{Co}^{2+}$  e  $\text{Ni}^{2+}$ ).

| XC                  | $\Delta H/$<br>( $\text{kJmol}^{-1}$ ) | $-\Delta G/$<br>( $\text{kJmol}^{-1}$ ) | $\Delta S/$<br>( $\text{JK}^{-1}\text{mol}^{-1}$ ) | XC                  | $\Delta H/$<br>( $\text{kJmol}^{-1}$ ) | $-\Delta G/$<br>( $\text{kJmol}^{-1}$ ) | $\Delta S/$<br>( $\text{JK}^{-1}\text{mol}^{-1}$ ) |
|---------------------|--|---|--|---------------------|--|---|--|
| AM $\text{Co}^{2+}$ | 0,29±0,02                              | 3,6±0,5                                 | 13±1   | AM $\text{Ni}^{2+}$ | 0,87±0,02                              | 1,9±0,6                                 | 9±1  |
| AS $\text{Co}^{2+}$ | 3,81±0,02                              | 3,2±0,5                                 | 24±1   | AS $\text{Ni}^{2+}$ | 2,35±0,01                              | 3,9±0,6                                 | 21±1   |
| AF $\text{Co}^{2+}$ | 0,14±0,28                              | 2,0±0,5                                 | 46   | AF $\text{Ni}^{2+}$ | 0,13±0,31                              | 2,8±0,6                                 | 49   |

A literatura mostra outros resultados obtidos por experimentos realizados em calorímetros para a interação de dicarboxilatos insaturados. Os valores mostrados na **Tabela 15** foram adaptados da referência 118.

**Tabela 15.** Valores termodinâmicos da complexação dos carboxilatos insaturados maleato e fumarato com os metais U(VI) e Eu(III). [118]

| Carboxilato       | $\Delta H$ (kJ mol <sup>-1</sup> ) | $-\Delta G$ (kJ mol <sup>-1</sup> ) | $\Delta S$ (kJ mol <sup>-1</sup> ) |
|-------------------|------------------------------------|-------------------------------------|------------------------------------|
| Maleato/U(VI)     | 20,4 ± 0,4                         | 26,43                               | 157                                |
| fumarato/U(VI)    | 10,9 ± 0,44                        | 16,67                               | 92,6                               |
| Maleato/Eu(III)   | 20,4 ± 0,4                         | 17,97                               | 96,6                               |
| fumarato/ Eu(III) | 10,1 ± 0,5                         | 13,41                               | 78,8                               |

As energias envolvidas nas reações centro básico/metáforam determinadas experimentalmente em calorímetro ou calculadas indiretamente a partir de parâmetros conseguidos nos ajustes aos modelos matemáticos após estudos de sorção. Para os materiais modificados com anidrido ftálico os parâmetros termodinâmicos determinados encontram-se na **Tabela 16**.

**Tabela 16.** Sumário de parâmetros termodinâmicos da complexação dos succinatos com metais.

| Material/metá         | $\Delta H$ (kJ mol <sup>-1</sup> ) | $-\Delta G$ (kJ mol <sup>-1</sup> ) | $\Delta S$ (J mol <sup>-1</sup> K <sup>-1</sup> ) | Referência |
|-----------------------|------------------------------------|-------------------------------------|---|------------|
| CelP/Ni <sup>2+</sup> | 2,50 ± 0,31                        | 14,4 ± 0,6                          | 56 ± 1  | [5]        |
| CelP/Co <sup>2+</sup> | 2,11 ± 0,28                        | 15,6 ± 0,5                          | 59 ± 1  | [5]        |
| QAF                   | -16,52 ± 0,03                      | 20,7 ± 0,01                         | 16 ± 1  | [117]      |
| QF                    | -11,36 ± 0,02                      | 19,7 ± 0,1                          | 28 ± 1  | [117]      |

Os valores para as troca iônicas são baixos e indicam um processo endotérmico e estes baixos valores para troca iônica são esperados. Já para o caso da quitosana modificada com anidrido ftálico o processo é exotérmico devido a não troca de prótons por sódio

em uma etapa anterior, assim a troca ocorre entre o próton e o metal em solução numa reação exotérmica e espontânea.

## 5.6 Conclusão dos três artigos anteriores

Os biopolímeros sintetizados apresentam a superfície na forma de carboxilatos alcalinos, nos quais o cátion de troca é o sódio. Esse metal é muito menos tóxico que os metais aquosos a serem trocados, e conseqüentemente, removidos do meio, devido a estas superfícies serem sólidas e insolúveis. Ainda, a literatura apresenta relatos sobre o grande número de ciclos possíveis em superfícies análogas preservando o desempenho da capacidade de troca, após reativação dos centros básicos superficiais. O equilíbrio para os processos de troca são alcançados em intervalos diminutos de tempo, a serem menores que trinta minutos, o que torna o processo eficaz na troca de metais em aplicações que requerem tempos curtos de reação.

A técnica de se fundir anidridos cíclicos de ácidos orgânicos é muito vantajosa principalmente por: a) o baixo ponto de fusão dos reagentes, b) o curto tempo de síntese para a funcionalização de superfícies que apresentem grupos nucleofílicos, c) o sistema não requerer condições especiais de síntese. Todo o procedimento não envolve variação de pressão, sem liberação de gases e vapores e os compostos sublimados são prontamente precipitados na torre conectada à entrada do balão de reação, d) a pós-funcionalização dos biopolímeros e/ou a aplicação destes como materiais precursores e e) esse procedimento pode ser aplicável a suportes como quitosana e materiais lignocelulósicos como babaçu, serragem, palhas de arroz etc.

Os estudos calorimétricos acompanhantes das reações de troca em meio aquoso são mais relevantes e importantes como dados acadêmico-científicos que em termos práticos e aplicados das grandezas termodinâmicas determinadas. Quantitativamente esses valores são sempre baixos, como mostram os valores termodinâmicos, relevantes do ponto de vista dos próprios processos de troca.

Para os processos de troca apresentados há um favorecimento entrópico principalmente relacionado à troca de cátions divalentes, antes coordenados apenas por moléculas de água, com liberação de cátions monovalentes pelo suporte, os quais

serão coordenados por moléculas de água do meio reacional. O meio antes está numa situação cujo soluto solvatado apresenta um raio iônico maior que o raio iônico do sódio solvatado ao final do processo de troca, quando superfície e solução estão em equilíbrio. Em termos energéticos significa dizer que o processo é entropicamente favorável, pela desorganização causada ao meio reacional, porém, favorecidos como bem mostram os valores de energia de Gibbs.

A decisão em se trabalhar com biopolímeros derivados quimicamente vem da necessidade em se extrapolar o limite do material natural puro para além das novas perspectivas de aplicações do presente. Essas podem ser simples como na remoção de cobre em bebidas destiladas e biocombustíveis ou até mesmo aplicações nobres como na determinação de grandezas termodinâmicas.

As moléculas ativas a serem imobilizadas nas superfícies são escolhidas pelas inumeráveis características químicas e físicas, podendo ser escolhidas quanto à facilidade em reagirem com os grupos ativos e disponíveis do biopolímero ou ainda quanto à intensidade de interação com espécies contaminante quaisquer. Além desses existem outros motivos para a escolha das moléculas ativas, como o quanto *verdes* ou o quanto sustentável tornam o processo. Ao se tratar de rotas simples não se imagina ser possível encontrá-la obsoleta na literatura e não havendo pesquisas relevantes sobre reações com anidridos ácidos sólidos fundidos.

O ambiente químico desse tipo de reação é propício à modificação química, além de ser muito agressivo. Assim, a reação tende a ocorrer sobre toda a superfície exposta e neste sentido há a extrapolação das hidroxilas primárias, possibilitando também a reação das menos reativas hidroxilas secundárias.

A não utilização de solventes faz com que o processo seja visto, do ponto de vista industrial, como um processo emergente, tendo como tração a Química Verde e a sustentabilidade. Por exemplo, se não há solventes, não há vapores a serem condensados, não há reciclagem dos mesmos nem ainda a necessidade de disposição adequada ou mesmo a incineração deste, processo final que libera gases tóxicos ou estufa.

Outro fato que aumenta o potencial de aplicação industrial é a facilidade de remoção das moléculas que permanecem sem reagir, a qual pode se proceder por: a

## Capítulo 5 – Esterificação de celulose

utilização de diminutas quantidades de acetona, possível de ser recuperada, e a segunda é por sublimação sob atmosfera reduzida com arraste por nitrogênio. Com essa tecnologia uma patente que defende a remoção de cobre de cachaça foi publicada, a qual foi parabenizada. Então o metal contaminante em bebidas pode se acumular e causar males hepáticos, como hepatite e cirrose, e há disponível tecnologia a ser empregada para solucionar este inconveniente, assim que as autoridades acordarem para a necessidade de uma lei que obrigue a remoção deste metal.

Percebeu-se então uma preocupação real em se considerar importante qualquer processo ambientalmente seguro, *verde* e sustentável. Desconsiderar as questões ambientais é negligenciar a vida futura e suas relações.

Ao se aprender a trabalhar com a celulose, o conhecimento gerado pode ser aplicado a uma ampla variedade de biopolímeros lignocelulósicos como serragem, bagaço de cana, palha de arroz etc e todos estes materiais apresentam características próprias como porcentagem de lignina e sílica, por exemplo. Então, estudar a celulose abre portas para se trabalhar com qualquer material lignocelulósico e estes estudos estão além dos interesses acadêmicos.



## 6 Bases de Schiff em celulose

E.C. Silva Filho, J.C.P. Melo, M.G. Fonseca, C. Airoidi, “**Cation removal using cellulose chemically modified by a Schiff base procedure applying green principles**”, J. Colloid Interface Sci., 340, 2009, 8-15.

### 6.1 Materiais e métodos

#### 6.1.1 *Materiais*

A celulose microcristalina na forma de pó (Aldrich), 20  $\mu\text{m}$ , foi seca antes de usar, N,N'-dimetilformamida (DMF) (Synth), cloreto de tionila ( $\text{SOCl}_2$ ) (Fluka), hidróxido de amônio (Aldrich), etileno-1,2-diamina (en) (Aldrich), e pentano-2,4-diona (acac) (Aldrich) eram todos de grau analítico e utilizados sem purificação prévia.

#### 6.1.2 *Síntese de clorodeoxicelulose (CelCl)*

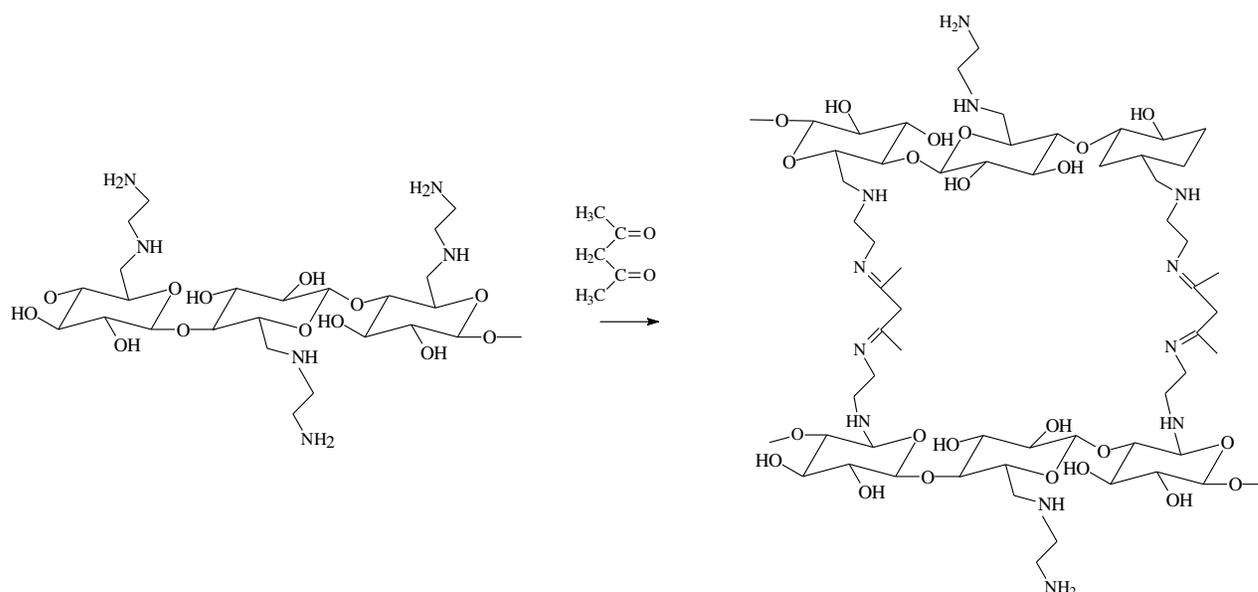
Uma amostra de 10 g de celulose (CEL) suspenso em DMF reagiu com 35  $\text{cm}^3$  de cloreto de tionila sob agitação mecânica por 4 h. O cloreto de celulose (CelCl) obtido foi lavado com solução diluída de hidróxido de amônio até pH neutro. O sólido foi então separado por filtração e seco em vácuo à temperatura ambiente [3].

#### 6.1.3 *Síntese de copolímeros de etileno-1,2-diamina-6-deoxycelulose (Celen)*

Uma amostra de 1,0 g CelCl reagiu com 5,0  $\text{cm}^3$  de en sob refluxo e com agitação mecânica, durante 4 h, com variação das quantidades de água e de um solvente polar ou DMF sob condições livres de solvente. Para uma série de experiências de volumes de 50,0 e 10,0  $\text{cm}^3$  foram utilizados, para dar novos biopolímeros nomeados Celen1 (50,0  $\text{cm}^3$  de DMF), Celen2 (10,0  $\text{cm}^3$  de DMF), Celen3 (50,0  $\text{cm}^3$  de água), Celen4 (10,0  $\text{cm}^3$  de água) e Celen5 (sem solvente). Os produtos sólidos, geralmente representados como CelenX, X = 1-5, foram filtrados e secos em vácuo a temperatura ambiente [119].

### 6.1.4 Síntese da base de Schiff em celulose (Celenacac)

Uma série de sínteses idênticas foram usadas para a incorporação de acac sobre os compostos CelenX. Para isso, amostras de 1,0 g de CelenX foram individualmente suspensas em 7,75 cm<sup>3</sup> de acac com agitação e as suspensões foram suavemente refluxada no ponto de ebulição do reagente durante 4 h. Os sólidos foram filtrados utilizando um filtro de vidro sinterizado e os produtos, com o nome CelenacacX, foram secos em vácuo à temperatura ambiente durante 24 h. A reação proposta está mostrada no **Esquema 12**.



**Esquema 12.** Formação de bases de Schiff. Celen (a) e Celenacac (b).

### 6.1.5 Caracterização

As quantidades de cloreto e das cadeias de moléculas ancoradas pendentes para o CelCl, CelenX (X = 1 – 5), e CelenacacX (X = 1 – 5) superfícies de celulose foram calculadas com base nas percentagens de cloro e nitrogênio determinadas através de análise elementar feitas usando analisador elementar Perkin Elmer, modelo 2400. Os espectros de IV das amostras em pastilhas de KBr foram realizadas por reflectância difusa, acumulando 250 varreduras em um espectrofotômetro Bomem, MB série, em um intervalo de 4000 – 400 cm<sup>-1</sup>, com resolução de 4 cm<sup>-1</sup>. Os espectros de

RMN de C13 das amostras foram obtidos num espectrômetro Bruker AC 300 / P à temperatura ambiente. Para cada ensaio, aproximadamente 1 g de cada amostra de sólido foi compactado em rotores de óxido de zircônio de 7 mm. As medições foram obtidas a uma frequência de 75,47 MHz para núcleos de carbono no ângulo mágico de rotação de 4 Hz. Afim de aumentar a relação sinal-ruído, a técnica por CP/MAS foi realizada e os espectros de  $^{13}\text{C}$  foram obtidos com repetição do pulso de 3 s e um tempo de contacto de 3 ms. As curvas termogravimétricas foram obtidas num instrumento TA em atmosfera de argônio, acoplado a uma termobalança B Modelo 1090, com taxa de aquecimento de  $0,167 \text{ K s}^{-1}$ , sob um arraste gasoso com fluxo de  $30 \text{ cm}^3 \text{ s}^{-1}$ , variando desde a temperatura ambiente até  $1273 \text{ K}$ , com uma massa inicial de aproximadamente 10 mg de amostra de sólido. Imagens de elétrons secundários foram adquiridos com um microscópio electrónico de varredura JEOL JSM 6360LV, operando a 20 kV. As amostras foram fixadas em uma fita de carbono dupla face aderido um suporte de alumínio e de carbono revestido em um instrumento Bal-Tec MD20. Para determinar a quantidade de cátions nas soluções aquosas de OES ICP (espectrometria de emissão óptica por plasma indutivamente acoplado) em um espectrômetro Perkin Elmer, modelo 3000 DV, usado para cada ponto experimental executados em duplicata.

### 6.1.6 Sorção

A capacidade da celulose quimicamente modificada para extrair cátions a partir da solução aquosa foi determinado em duplicado, utilizando-se um processo em batelada com os nitratos metálicos de cobre, de níquel, de cobalto e de zinco, utilizando-se uma massa ( $m$ ) de cerca de 20 mg de Celenacac5 suspensa em  $25,0 \text{ cm}^3$  de uma solução aquosa com concentrações de cada metal variando  $0,050 - 1,0 \text{ mmol dm}^{-3}$ . As suspensões foram mecanicamente agitada à temperatura ambiente durante 4 horas e separou-se o adsorvente do sobrenadante por centrifugação a 2400 rpm durante 10 min. Alíquotas do sobrenadante foram pipetadas e os cátions foram determinados por ICP OES. As capacidades de adsorção ( $n_f$ ) foram calculados considerando o número de moles,  $n_f = (n_i - n_s)/m$ , em que  $n_i$  e  $n_s$  é o número inicial e sobrenadante de moles [88].

A adsorção na interface sólido/líquido exige uma competição entre o solvente (solv) ligado à superfície quimicamente modificada (AS), que é gradualmente deslocado pelo soluto em solução para atingir o equilíbrio, equação 8:



A razão entre o número de moles de metal em solução em equilíbrio e aqueles adsorvidos na superfície quimicamente modificada é utilizada para obter a curva isotérmica de Langmuir modificada, através da aplicação da equação 9:

$$\frac{C_s}{n_f} = \frac{C_s}{n^s} + \frac{1}{nb} \quad (9)$$

onde  $C_s$  é a concentração de cátions sobrenadantes, no equilíbrio,  $n_f$  é o número de moles adsorvidos,  $n^s$  é a quantidade máxima de soluto adsorvido por grama de Celenacac5, que está relacionado com o número de sítios de adsorção, e  $b$  é uma constante. Os valores de  $b$  e  $n^s$  para cada processo de adsorção foram calculados a partir dos coeficientes angulares e lineares, respectivamente, da forma linearizada das isotermias de adsorção,  $C_s/n_f$  contra  $C_s$ , utilizando o método dos quadrados mínimos.

A partir da forma descrita pela isoterma, é possível prever se a adsorção é favorável. Assim, os parâmetros de Langmuir pode ser expressa a partir do fator de separação adimensional,  $R_L$ , definida pela equação 10 [120]

$$R_L = \frac{1}{(1 + b.C_o)} \quad (10)$$

a qual permite a avaliação da forma de isoterma.

## 6.2 Resultados e discussão

### 6.2.1 Análise elementar

A reação eficaz de cloração da celulose deu um grau de substituição completa de um grupo hidroxila (DS) no carbono 6, para atingir o valor de  $0,99 \pm 0,01$ . No entanto, durante o curso das reações com moléculas de etileno-1,2-diamina, uma fracção de átomos de cloro manteve-se no original matrizes, dependendo do procedimento experimental utilizado. A reação originou um grau de funcionalização (DF), que foi calculada com base na quantidade de átomos de nitrogênio incorporado nas cadeias pendentes. A eficácia destas substituições (EI), em percentagem, foi calculada considerando a relação molar entre a etileno-1,2-diamina e a quantidade inicial de cloreto ligado no biopolímero modificado. A partir destes resultados, o valor mais elevado de 61 % foi observado para a reação livre de solvente, o que demonstra a eficácia em substituição átomo de cloro sob estas condições experimentais. Os resultados das análises de cloro e nitrogênio são mostrados na **Tabela 17**.

**Tabela 17.** Porcentagens de cloro e nitrogênio em clorodeoxicelulose e etano-1,2-diaminadeoxicelulose, Grau de funcionalização (GF) e percentagem efetiva de incorporação (EI)

| Matriz | Cl / %           | N / %           | DS   | GF/mmol g <sup>-1</sup> | EI/% |
|--------|------------------|-----------------|------|-------------------------|------|
| CelCl  | $17,58 \pm 0,10$ | -               | 0,99 | $4,95 \pm 0,03$         | -    |
| Celen1 | $11,74 \pm 0,11$ | $3,96 \pm 0,01$ | 0,33 | $1,41 \pm 0,01$         | 28   |
| Celen2 | $4,53 \pm 0,18$  | $5,78 \pm 0,06$ | 0,74 | $2,06 \pm 0,02$         | 42   |
| Celen3 | $16,24 \pm 0,09$ | $1,04 \pm 0,02$ | 0,08 | $0,37 \pm 0,01$         | 7    |
| Celen4 | $5,70 \pm 0,07$  | $5,84 \pm 0,06$ | 0,68 | $2,08 \pm 0,03$         | 42   |
| Celen5 | $7,54 \pm 0,09$  | $8,50 \pm 0,03$ | 0,57 | $3,03 \pm 0,01$         | 61   |

Como esperado, o primeiro passo desta série de reações consistiu na cloração da, um processo favorecido pelo ataque nucleofílico sofrido pelo cloreto de tionila pelo ataque do grupo hidroxila presente no esqueleto do biopolímero, o que resulta em átomos de cloro pendente na estrutura polimérica. Este átomo substituído é muito mais reativo do que o grupo original hidroxila em posteriores reações de substituição, para dar um total de substituição do grupo hidroxila em C6 por cloro. Isto é esperado que o grupo hidroxila nesta posição é mais reativa em comparação com os outros grupos hidroxila, seguindo a ordem [39] C6 > C3 > C2.

O fato mais encorajador para adotar esta metodologia de seqüência de reações é o maior valor para os grupos de nitrogênio para Celen5, que foi sintetizado sem adição de solventes, de acordo com os princípios da química verde [121]. Assim a ordem, da maior para a menor quantidade de grupos incorporados com a quantidade e a polaridade do solvente é claramente demonstrado: Celen5> Celen4> Celen2> Celen1> Celen3.

Para as vias de síntese em que um solvente foi usado a quantidade de moléculas de etileno-1,2-diamina incorporadas aumenta nos biopolímeros com a diminuição do volume empregado. Além disso, quando a comparação é entre solventes diferentes, e mesmo volume (50,0 cm<sup>3</sup>), um maior grau de substituição foi obtido com DMF do que com água. No entanto, para 10,0 cm<sup>3</sup> de solvente o maior grau de substituição foi com água.

Com base nestes resultados, o processo livre de solvente deu um aumento de incorporação de 19 %, em comparação com Celen4, que deu o valor mais elevado, quando utilizados solventes. O aumento favorável no grau de incorporação de uma molécula na cadeia biopolimérica, na ausência de solvente, para a preparação de novos polímeros funcionais, tem benefícios ambientais, além de reduzir os custos, e também simplificando o processo [122]. Outra característica importante a ser analisada é a quantidade de moléculas incorporadas na estrutura polimérica. Por exemplo, Celen2 e Celen4 e foram preparados com 10,0 cm<sup>3</sup> de solventes para se obter 42 % de incorporação, no entanto, a quantidade de átomos cloro remanescentes é maior para

Celen4. Este comportamento sugere que os dois grupos amino podem, simultaneamente, actuar como moléculas bidentadas de ligação adjacentes às cadeias poliméricas, como agente de reticulação.

Os resultados da percentagem de nitrogênio em Celen modificado com pentano-2,4-diona, devido a Schiff formação da base, diminui. Quando a quantidade de nitrogênio livre na matriz Celen é elevada antes da modificação química, a maior quantidade de grupos imina são inscritos, devido à quantidade de grupos acac incorporados nos polímeros, reduzindo assim a percentagem de nitrogênio por grama de biopolímero. As matrizes Celenacac2 e Celenacac4 apresentaram valores reduzidos de grupos amino, um comportamento que pode ser interpretado como ligações cruzadas, com uma conseqüente diminuição nos grupos disponíveis para formação da base de Schiff. Se quaisquer átomos de cloro foram apresentados nas matrizes precursoras, poderia permanecer, mas todos os grupos amino estão disponíveis reagir diretamente com acac para formar a ligação imina.

### **6.2.2 A espectroscopia de IV**

Os úmeros de onda típicos de grupos hidroxila para Cel, como  $-\text{CH}-\text{OH}$  e  $-\text{CH}_2-\text{OH}$  cujos estiramentos aparecem em  $3300 - 3400 \text{ cm}^{-1}$ . O estiramento dos grupos metileno incorporados encontram-se em  $2900 \text{ cm}^{-1}$  e a banda em  $3000 - 2800 \text{ cm}^{-1}$  é atribuída a grupos  $-\text{C}-\text{H}$ , uma vez que a proporção do grupo  $-\text{CH}$  e  $-\text{CH}_2$  da celulose está numa proporção de 5:1 [123,1]. As vibrações OH estão localizados em  $1639 \text{ cm}^{-1}$ , os dobramentos das hidroxilas primárias e secundárias apareceram no intervalo  $1500 - 1200 \text{ cm}^{-1}$  e o estiramento C-O observado em  $1100 \text{ cm}^{-1}$  [123,1].

A diminuição da intensidade das bandas que absorvem em  $1500 - 1200 \text{ cm}^{-1}$  é devida à substituição dos grupos hidroxila por átomos de cloro em CelCl, indicação clara da incorporação da molécula desejada nas cadeias poliméricas. A banda em  $896 \text{ cm}^{-1}$  foi deslocada para  $868 \text{ cm}^{-1}$  após cloração e desapareceu depois de reagir com en. Para a superfície clorodeoxicelulose, as bandas em  $752$  e  $709 \text{ cm}^{-1}$  diminuem de

intensidade, mas são ainda visíveis, devido à substituição incompleta por moléculas de en.

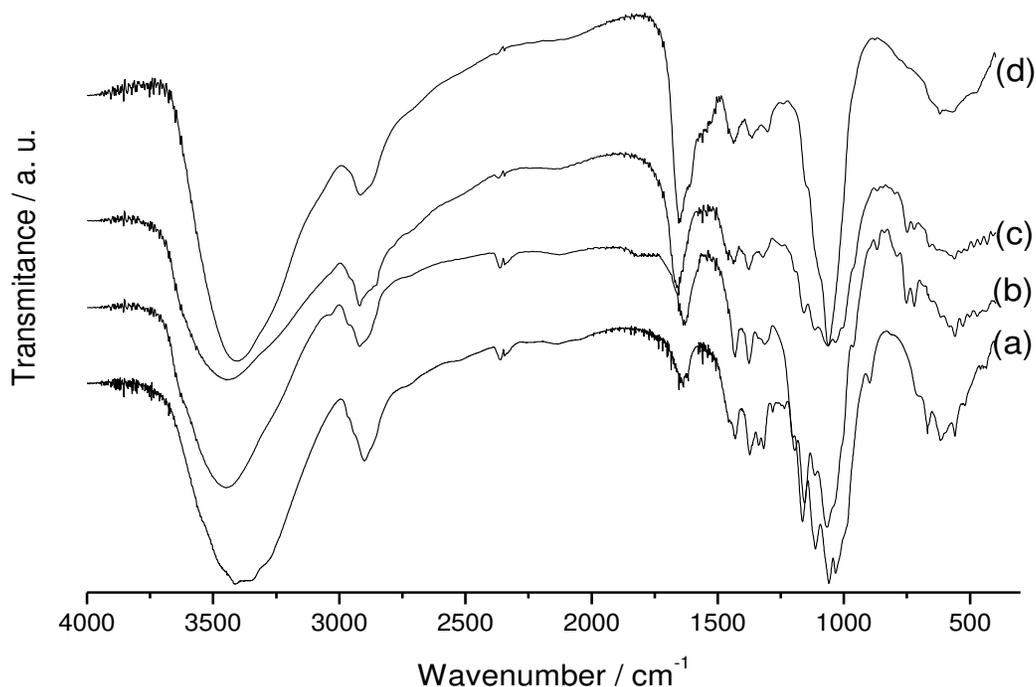


**Figura 20.** Espectros de IV da celulose (a), CelCl (b), Celen5 (c) e Celenacac5 (d).

Para Celen5 os estiramentos típicos  $\text{CH}_2$  são vistos em  $2837 \text{ cm}^{-1}$ , mas agora a razão  $\text{CH}:\text{CH}_2$  diminuiu depois de reagir com a molécula de etileno-1,2-diamina, enquanto uma nova banda fraca em  $1658 \text{ cm}^{-1}$  pode ser atribuída aos dobramentos do grupo amino. Assim, para uma reação completa numa proporção esperada de 5:3 poderia ser obtida, no entanto, nem todos os átomos de cloro disponíveis foram substituídos, mas encontrou-se um valor maior do que 5:1. Por outro lado, a sequência de reação confirma que o processo de incorporação foi realizado em grande parte sobre a superfície do biopolímero. Para o espectro de Celenacac5 observa-se o alargamento da banda em  $2800\text{-}3000 \text{ cm}^{-1}$ , correspondente aos três tipos de diferentes grupos ( $-\text{CH}$ ,  $-\text{CH}_2$  e  $-\text{CH}_3$ ). O aumento da intensidade e da largura da banda em  $1610 \text{ cm}^{-1}$  indica a presença da banda de imina  $\nu(\text{C}=\text{N})$  estiramentos [25,26].

### **6.2.3 Ressonância magnética nuclear de carbono-13**

Para a celulose pura, o primeiro sinal em campo baixo indica o carbono (C1), a 104 ppm, o que está ligado a dois átomos de oxigênio. O carbono 4 é atribuído ao sinal em 88 ppm, o qual encontra-se ligado a um átomo de oxigênio, o qual também forma uma ligação glicosídica  $\beta(1,4)$  [3]. O deslocamento químico em ppm 74 refere-se aos átomos de carbono 2, 3, e 5, que estão localizados em ambientes químicos semelhantes; por exemplo, todos eles estão ligados grupos hidroxila secundários e -CH. Carbono 6 apresentou o menor deslocamento químico devido ao fato de ser um carbono primário, ligado à unidade de anel e também ligado a um grupo hidroxila, correspondendo ao -CH<sub>2</sub> na estrutura de celulose [123,124].

O espectro de clorodeoxicelulose apresentou deslocamentos químicos para campo baixo em comparação com a celulose pura. Por exemplo, o sinal para C1 104 ppm desloca-se para 103 e para C4 o deslocamento ocorre de 88 para 83 ppm, enquanto os carbonos C2, C3, C5 não são deslocados permanecendo na mesma região. Para C6, a substituição da hidroxila por cloreto confere um deslocamento maior de 65 ppm para 44 ppm, fato que indica uma incorporação eficaz de cloreto na superfície da celulose. Assim, a alteração no sinal em campo alto, devido à electronegatividade do átomo de cloro, indica a incorporação de etileno-1,2-diamina. Para a celulose quimicamente modificada com em seguida da reação com acac, ocorreram alterações significativas, e os carbonos insaturados da molécula modificante são vistos em campo baixo, 174 ppm; estes sinais estão relacionados a ligação imina (C=N) na base de Schiff, favorecendo a reticulação. Um sinal nítido em 18 ppm é atribuído aos carbonos metílicos da molécula acac [122,1]. Os espectros de RMN <sup>13</sup>C da celulose e os derivados funcionalizados estão mostrados na **Figura 21**.

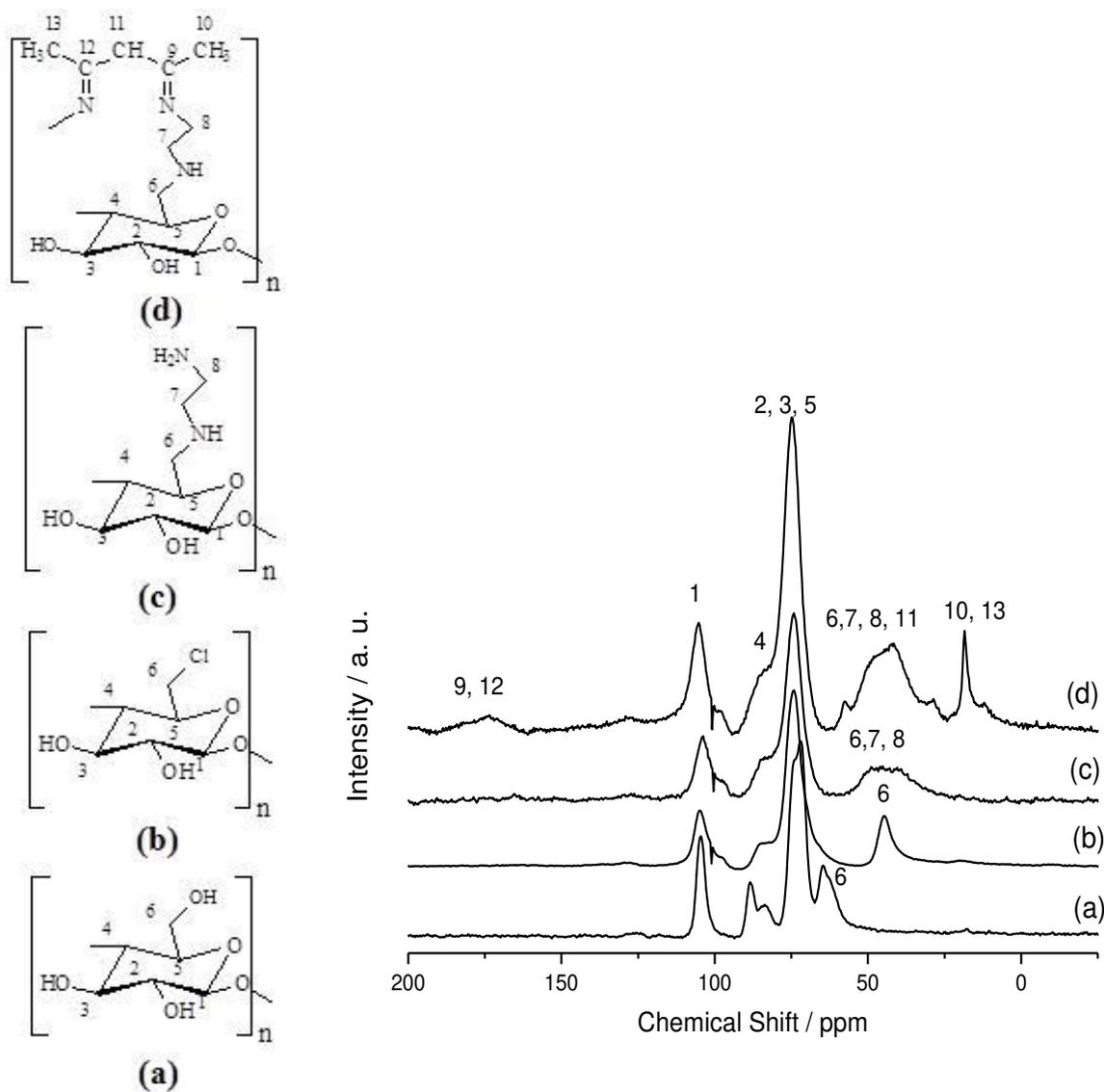


**Figura 21.** Espectros de RMN  $^{13}\text{C}$  da celulose (a), CelCl (b), Celen5 (c) e Celenacac5 (d).

#### 6.2.4 Termogravimetria

A celulose e suas formas funcionalizadas com cloro, nitrogênio e iminas estão mostrados na **Figura 22**.

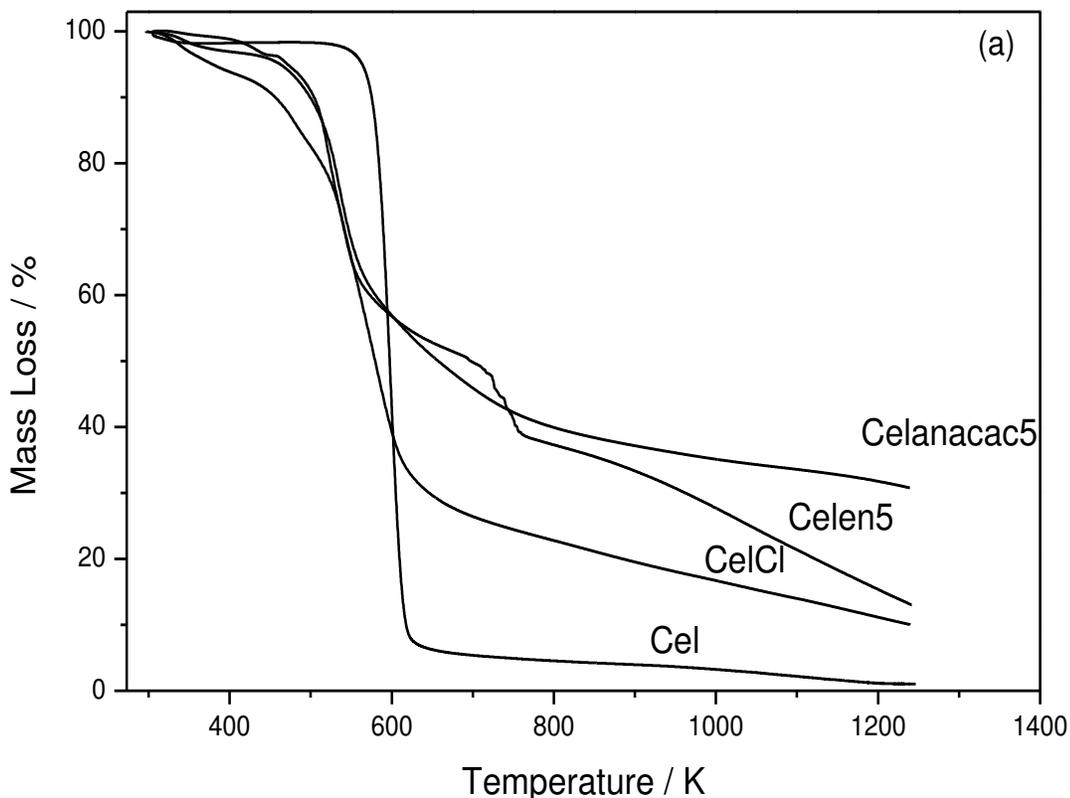


**Figura 22.** Curvas termogravimétricas da celulose, CelCl, Celen5 e Celenacac5.

Para a celulose ocorreu apenas um evento no processo de decomposição, que cobre temperaturas 536 – 647 K, e corresponde a uma perda de massa de 92 %. O biopolímero clorado apresentou uma perda de massa, de 3 % no intervalo de 386 – 430 K, o que pode ser atribuído à água fisicamente adsorvida à superfície; no segundo evento, há a perda 23 % da massa, observado entre 438 e 534 K, sendo a perda de átomos de moléculas de HCl. O último evento neste processo, o que corresponde a uma perda de massa de 64 %, a 521 K pode ser interpretado como a decomposição de fibras de celulose. A curva do biopolímero Celen5 é muito similar ao apresentado pela CelCl, com uma perda de massa inicial de 4 % 320 - 363 K, atribuída à dessorção de água seguido por um evento de decomposição no intervalo 364 – 563 K, com um perda de 34 % massa de, e correspondeu a perda da molécula em incorporada juntamente

com condensação dos grupos hidroxila nos carbonos 2 e 3. A terceira etapa de decomposição, a partir de 564 K, também é atribuída à perda de fibra de celulose, dando uma quantidade de 48 %. A estabilidade térmica dos compostos Celenacac5 e Celen5 foram semelhantes, com perda inicial de massa de 4 % até 442 K. O segundo evento ocorreu no intervalo de 443 - 611 K, com uma perda de massa de 41 %, correspondente a uma perda das moléculas de pentano-2,4-diona imobilizado e de etileno-1,2-diamina com a condensação dos grupos hidroxila dos carbonos 2 e 3 da estrutura polimérica. A última etapa de decomposição ocorre a partir de 613 K K e é atribuída à perda da estrutura fibrosa da celulose, 24 % de perda de massa com cocomitante reestruturação química do suporte. Com base na quantidade de massa perdida, a sequência Celenacac5 <Celen5 <CelCl <Cel é observada. Estes valores estão de acordo com o fato de que a matriz Celenacac5 é mais estável termicamente, seguida por Celen5, CelCl e finalmente por Cel [3,119].

### ***6.2.5 Microscopia eletrônica de varredura e espectroscopia de energia dispersiva***

Uma confirmação adicional da existência de átomos de cloro ligados de forma covalente ao material sintetizado pode ser verificada por uma distribuição homogênea das cadeias pendentes ao longo da superfície e este comportamento está em completo acordo com as vias propostas sintéticas, em que uma distribuição regular dos átomos de cloro à superfície polimérica é esperada. Assim, os microscopia eletrônica de varredura (MEV) para celulose e clorodeoxicelulose apresenta aspectos semelhantes. Para a celulose pura, as características fibrosas e porosas da superfície são observados, mas a cloração altera este aspecto. Para as superfícies modificadas, estas características foram significativamente reduzidas. O mapeamento de cloro é mostrado na **Figura 23** e a microscopia do biopolímero funcionalizado com iminas está mostrado na **Figura 24**.

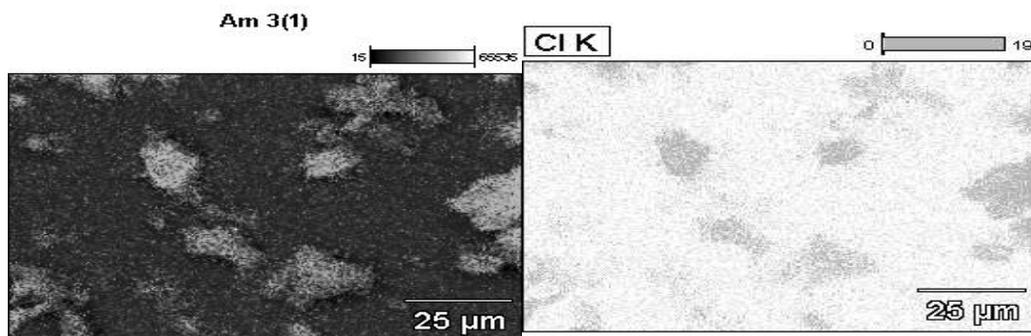


**Figura 23.** Mapeamento de Cloro da amostra CelCl.

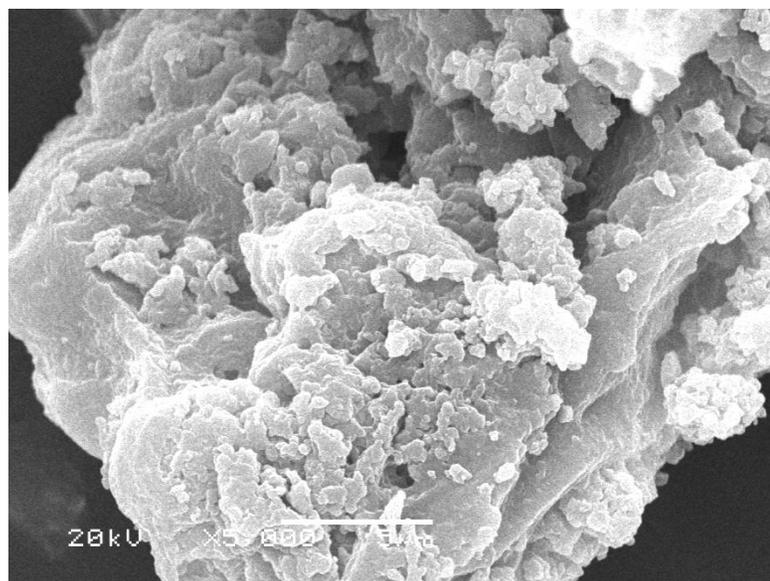


**Figura 24.** Micrografia por MEV de Celenacac5.

### **6.2.6 Adsorção**

A imobilização covalente de moléculas ao suporte que contém centros básicos de nitrogênio, enxofre e oxigênio proporciona condições para a remoção de cátions a partir de solventes aquosos e não aquosos [88,125] que dependem, em certos casos, da hidrofobicidade das matrizes envolvidas. Assim, a superfície quimicamente

modificada, contendo a maior incorporação de en e acac foi estudado para remoção dos cátions divalentes cobre, cobalto e zinco pela metodologia em batelada. A forma da equação linearizada permite o cálculo dos dados lineares e angulares de uma linha reta, para se obter os valores de  $n^s$  e  $b$ ; estes e outros parâmetros relevantes estão mostrados na **Tabela 18**.

**Tabela 18.** Número de mols adsorvidos ( $n_f$ ), capacidade máxima de adsorção ( $n^s$ ), coeficientes de correlação ( $r$ ) e a constante ( $b$ ) para o comportamento dos nitratos metálicos em solução e a interação destes metais (M) com Celenacac5 a  $298 \pm 1$  K.

| M  | $n_f$ (mmol g <sup>-1</sup> ) | $n^s$ (mmol g <sup>-1</sup> ) | $r$    | $b$  |
|----|-------------------------------|-------------------------------|--------|------|
| Cu | 2,32±0,06                     | 2,58±0,04                     | 0,9859 | 718  |
| Co | 1,85±0,02                     | 1,95±0,09                     | 0,9983 | 1935 |
| Ni | 1,70±0,04                     | 1,89±0,05                     | 0,9941 | 1153 |
| Zn | 1,65±0,02                     | 1,78±0,08                     | 0,9979 | 1620 |

Os dados seguem a ordem de adsorção:  $\text{Cu}^{2+} > \text{Co}^{2+} > \text{Ni}^{2+} > \text{Zn}^{2+}$ , como mostrado na **Figura 25**. Esta mesma sequência foi anteriormente observado para o outro biopolímero quitosana [30].

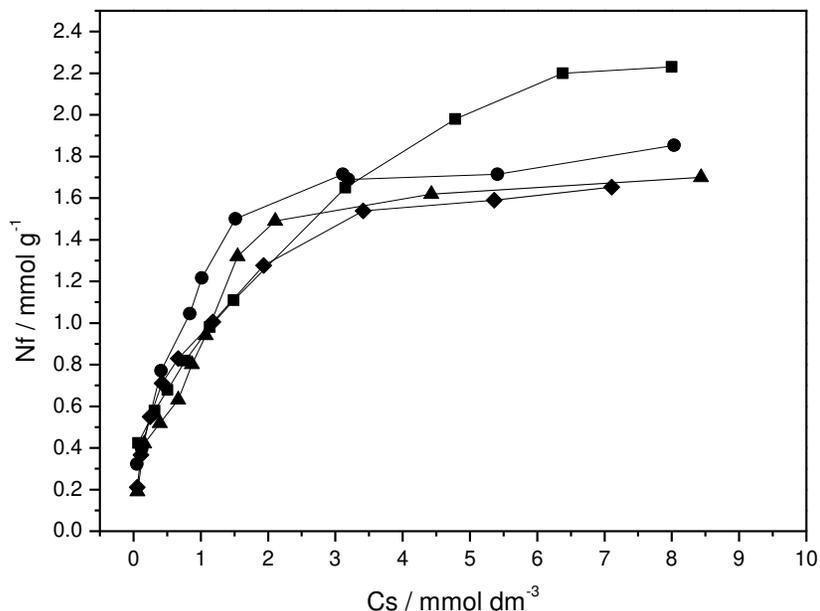


**Figura 25.** Isotermas de adsorção dos cátions: Cu<sup>2+</sup> (■), Co<sup>2+</sup> (●), Ni<sup>2+</sup> (▲) and Zn<sup>2+</sup> (◆) no material Celenacac5, a 298 ± 1 K.

O biopolímero Celenacac5 apresentou a maior capacidade de adsorção de cátions, o que sugere a sua utilização em concentração e de separação. Durante o processo de adsorção as interações na interface sólido-líquido podem ser interpretadas como um centros ácidos em solução aquosa, os quais interagem com os centros básicos disponíveis, as Schiff formadas, para resultar na complexação de cátions para remover a espécie a partir desse meio. Tendo em conta as isotermas obtidas para os cátions, uma estreita correspondência ao esboçado modelo do tipo 2L, como expresso pela classificação de Gilles [126], é observado. Este modelo de isoterma favorável é ilustrada através da afinidade entre cátions e centros básicos para a formação de complexos na interface sólido/líquido [127-128]. Como esperado, algumas possibilidades baseiam-se na disponibilidade centros básicos incorporados nas cadeias pendentes ou unidades de reticulação [3]. Na tentativa de verificar este comportamento isotérmica, todos os parâmetros de cálculo de  $R_L$  deram valores favoráveis, tal como representado pela equação (3), como por exemplo 0,35, 0,21, 0,31, e 0,26, para Cu<sup>2+</sup>,

$\text{Co}^{2+}$ ,  $\text{Ni}^{2+}$ ,  $\text{Zn}^{2+}$  e. Com a exceção de cobalto, os complexos formados seguir a série de Irving-Williams para K1 valores, para dar a ordem de  $\text{Ni}^{2+} < \text{Cu}^{2+} > \text{Zn}^{2+}$  [129].

### 6.3 Conclusão

A molécula de etileno-1,2-diamina, covalentemente incorporada em uma superfície de celulose depois de um passo de cloração anterior, produziu biopolímero modificado, com grande potencial não apenas como um precursor para o crescimento da cadeia pendentes, mas também como suporte para a remoção de cátions. O materiais etileno-1,2-diamina sintetizados pelo procedimento livre de solvente, mostraram-se inovadores, via sintética promissora com a maior eficácia de incorporação da molécula desejada. Usando condições experimentais mais estabelecidas, a melhor síntese em solventes deste biopolímero consiste na utilização de 10,0 cm<sup>3</sup> dos polares DMF ou 10,0 cm<sup>3</sup> de água. Por outro lado, o processo livre de solvente para a incorporação de pentano-2 ,4-diona depende do grupo amino livre no material precursor, que é afetada pelo processo de reticulação.

Uma característica notável associada a estas vias propostas para incorporar a molécula covalentemente e de forma regularmente distribuída em um polissacarídeo natural para o aumento do tamanho da fita polimérica. Tal inovação é importante para o progresso deste campo de pesquisa utilizando biopolímeros naturais disponíveis, abundantes, de baixo custo para melhorar muitas aplicações tecnológicas.

As novas superfícies sintéticas com incorporação de cadeias pendentes contendo átomos de nitrogênio potencialmente básicos são centros potenciais disponíveis para a remoção de cátions, e se comportou como materiais promissores para serem aplicados a esta operação, com boa capacidade de sorção para cátions divalentes, e de grande utilidade para a purificação de ecossistema contaminados com metais na forma iônica.

E.C. Silva Filho, S.A.A. Santana, J.C.P. Melo, F.J.V.E. Oliveira, C. Airoidi, “**X-ray diffraction and thermogravimety data of cellulose chlorodeoxycellulose and aminodeoxycellulose**”, J. Therm. Anal. Calorim., 100, 2010, 315-321.

## **6.4 Parte Experimental**

### **6.4.1 Materiais**

A celulose microcristalina (Merck), cloreto de tionilo (Chemika), N, N0-dimetilformamida (DMF) (Synth), hidróxido de amónio (Aldrich) e de etileno-1,2-diamina (en) (Aldrich) eram todos de grau reagente e foram utilizados sem purificação prévia. Celulose ativada e os correspondentes compostos quimicamente modificados foram armazenadas em frascos em atmosfera de nitrogênio seco.

### **6.4.2 Síntese de 6-clorodeoxicelulose**

Uma amostra de 10 g de celulose (Cel), previamente ativado a 353 K durante 12 h, foi suspenso em 200 cm<sup>3</sup> de DMF, seguida pela adição lenta de 35 cm<sup>3</sup> de cloreto de tionila (SOCl<sub>2</sub>), a 353 K, sob mecânica agitação. Após a adição, a agitação prosseguiu à mesma temperatura durante mais 4 h. A suspensão resfriada contendo o celulose cloreto de (CelCl) foi lavado com várias porções de uma solução diluída de hidróxido de amónio. O sobrenadante em cada operação foi eliminado e o pH controlado até o valor neutro. Para completar a lavagem da suspensão foi tratado exaustivamente com água destilada. Finalmente, o sólido foi então separado por filtração e seco sob vácuo à temperatura ambiente [3].

### **6.4.3 Síntese do 6-etileno-1,2-diamino-deoxycellulose**

Uma amostra de 1,0 g de CelCl foi reagida com 5,0 cm<sup>3</sup> de en sob refluxo, agitação mecânica durante 3 h [3], variação da quantidade de solvente (água ou DMF), seguido por filtração em filtro de vidro sinterizado. O sólido (Celen) foi seco sob vácuo à temperatura ambiente durante 24 h.

### **6.4.4 Medidas físicas**

As quantidades de cadeias pendentes em ancorados na superfície de celulose foram calculadas com base em por cento de nitrogênio, determinado através de análise elementar, com um analisador elementar Perkin Elmer, modelo 2400. Padrões de XRD foram obtidos num difractômetro XRD7000 Shimadzu para amostras em pó. A tensão aplicada foi de 40 kV, corrente de 30 mA, com uma fonte de radiação de CuK $\alpha$  ( $\lambda = 0,154$  nm) varredura de 1,4 -50°. As curvas termogravimétricas para As amostras em pó foram obtidos num instrumento TA Dupont 9900 em atmosfera de argônio sob fluxo de 1,67 cm<sup>3</sup> s<sup>-1</sup>, utilizando-se uma taxa de aquecimento de 0,167 K s<sup>-1</sup>, a partir da temperatura ambiente até 1273 K, com a massa inicial da amostra em aproximadamente 10 mg.

## **6.5 Resultados e discussão**

Análise elementar, com base no nitrogênio incorporado, foi utilizada para determinar a quantidade de moléculas en quimicamente ligadas à fita celulósica para se obter o biopolímero aminado, proveniente da clorodeoxicelulose precursora. A celulose com cloro deu um alto grau de substituição,  $0,99 \pm 0,01$  preferencialmente no carbono 6 (C6) por ser a hidroxila mais reativa; a hidroxila do carbono 3 deveria ser mais ácida que a hidroxila situada no carbono 2 [39] . A modificação química do biopolímero é inequívoca e por RMN de <sup>13</sup>C os espectros demonstraram claramente o deslocamento químico de 65 para 44 ppm para o carbono 6, sem alteração notável para os carbonos 2 e 3 [3]. Os resultados da análise de nitrogênio são mostrados na **TabelaX**(ver artigo anterior)

O biopolímero Celen5 apresenta elevada porcentagem de nitrogênio na estrutura quando a reação foi realizada na ausência de solventes, como é desejável pelos Princípios de Química Verde [121]. Uma sequência de grupos de fixação, cujos valores decrescentes estão de acordo com a quantidade e a polaridade do solvente utilizados nas reações, para dar a seguinte ordem: Celen5 > Celen4 > Celen2 > Celen1 > Celen3. Os biopolímeros preparados utilizando DMF, quanto menos solvente usado, maior a quantidade de moléculas de en ligadas à superfície. O mesmo resultado pode ser observado quando a água foi utilizada como solvente. Por outro lado, quando solventes diferentes são comparados para o mesmo volume final, por exemplo, 50 cm<sup>3</sup>, a síntese foi mais eficaz em DMF do que em água, como refletiu a quantidade de grupos ligados à superfície. No entanto, quando 10 cm<sup>3</sup> de solvente foram utilizados, a água se mostrou mais apropriada, embora as quantidades de nitrogênio fossem próximas.

Para o processo livre de solvente houve um aumento de 31 % de nitrogênio se comparado com Celen4, o que correspondeu ao valor mais elevado quando se utilizou de solventes. Além do grande incremento na no número de moléculas aminadas ligadas, uma vantagem importante é a ausência de solventes para a preparação de novos polímeros funcionais, através de procedimentos ambientalmente sustentáveis, incluindo a redução dos custos e de controle mais fácil do processo [122]. Para Celen5 os dados demonstram que o processo sem solventes apresentaram quantidades maiores de grupos pendentes aminados.

A celulose apresenta uma distinta tendência para a cristalização, provavelmente provocada pela rigidez relativa das cadeias glicosídicas e da capacidade de bem organizar e estabelecer ligações hidrogênio entre suas várias hidroxilas. A forma dos anéis e da distribuição espacial dos grupos hidroxila parecem favorecer a formação de fita em forma de folhas lateralmente ordenadas, que exibem uma anisotropia de três vezes a força de ligação, tanto quanto a força de ligação está em causa [17, 28-30].

Perpendicular às cadeias poliméricas, no plano dos anéis anidroglicose, que representam a direção de um eixo da malha, as ligações hidrogênio entre os grupos hidroxila e os átomos de oxigênio do anel são responsáveis por esta interação. Finalmente, perpendicular às cadeias e ao plano dos anéis anidroglicose, e paralelo ao eixo c do reticulado, a atração existente é apenas devido às interações de van der

Waals entre os anéis anidrogucose e os seus componentes. Este sistema de ligação pode ser considerado como um ponto de partida razoável para a explicação da tendência de cristalização da celulose. Isso leva à existência de finas folhas alongadas com vista lateral elevada, o que pode explicar de uma forma satisfatória as propriedades macroscópicas observadas no estado seco e entumecido [17, 28-30].

Os padrões de difração de raios X de celulose com cloro indicam que o grau correspondente à cristalinidade é menor e este difere do encontrado para a celulose precursora, a qual possui as propriedades originais microcristalinas. O novo conjunto é agora formado por átomos de cloro ligados aos grupos hidroxilas restantes. Comportamento semelhante foi observado para outros biopolímeros onde a ligação hidrogênio ocorre principalmente com grupos hidroxila disponíveis [36, 66, 83, 130]. Assim, quando a celulose é clorada a ligação hidrogênio deve ser parcialmente interrompida, para favorecer a entrada de átomos de cloro simultaneamente com a sua saída do grupo hidroxila, obtendo-se agora uma nova rede de ligações hidrogênio, nas quais os cloros estão envolvidos. A partir da integração do pico principal, entre 20 a 30°, os valores demonstram uma diminuição de 70% da cristalinidade do biopolímero clorado, o que pode ser muito interessante, principalmente quando outras modificações se destinam, tais como o ancoramento de moléculas de etileno-1,2-diamina no copolímero. O processo de cloração oxidativa da celulose consiste em substituir o grupo hidroxila por um átomo de cloro na estrutura do biopolímero original.

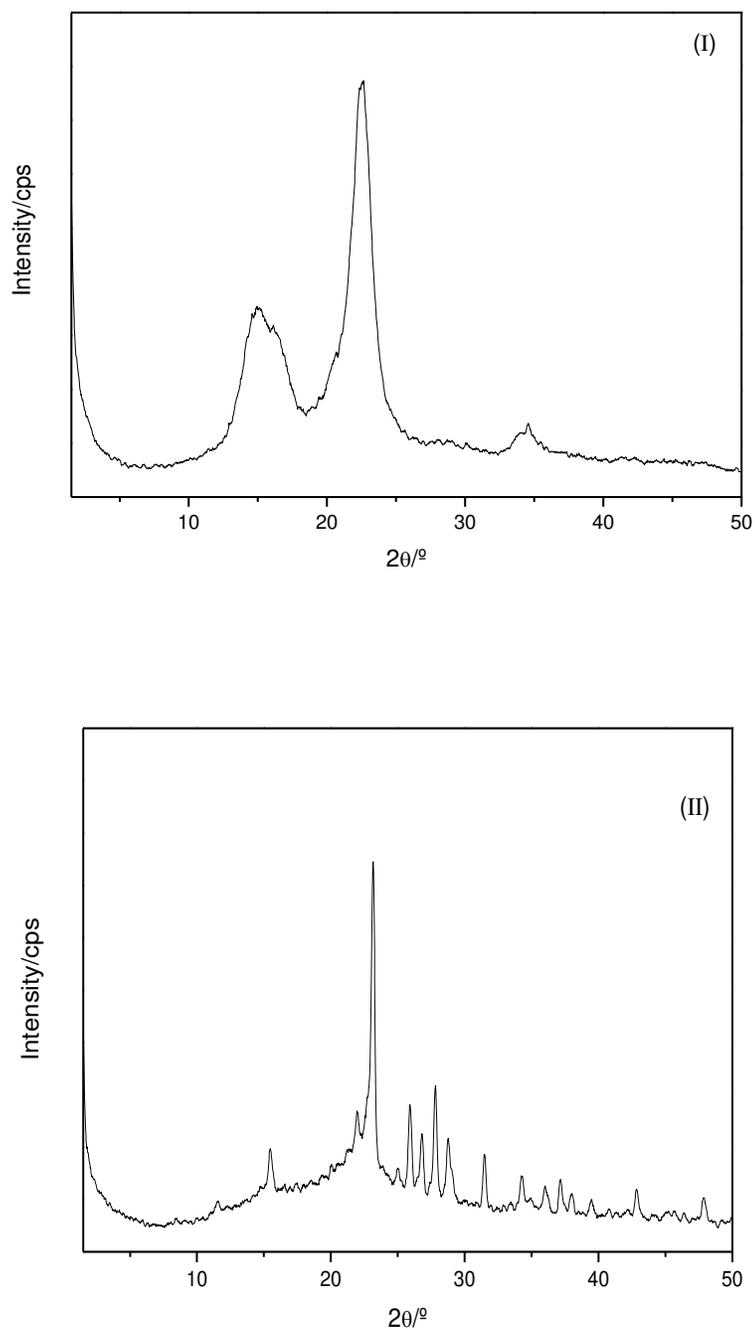


**Figura 26.** Difratoogramas de raios X. Celulose (I) e CelCl (II).

A modificação química ocorre inicialmente nas regiões menos ordenadas poliméricas relacionadas com as regiões para-cristalinas ou amorfas. Os grupos

hidroxila da celulose possuem dois pares de elétrons livres e um de hidrogênio ligados e os átomos de cloro ligados covalentemente ao biopolímero podem potencialmente disponibilizar três pares de elétrons livres para serem compartilhados, através da formação de ligações hidrogênio, com o hidrogênio da hidroxila formadas com características diferentes dos anteriores, por causar novos arranjos químicos estruturais do biopolímero modificado. [36, 66, 83, 130].

Os números de onda típicos de grupos hidroxila para Cel, como  $-\text{CH}-\text{OH}$  e  $-\text{CH}_2-\text{OH}$  cujos estiramentos aparecem em  $3300 - 3400 \text{ cm}^{-1}$ . O estiramento dos grupos metileno incorporados encontram-se em  $2900 \text{ cm}^{-1}$  e a banda em  $3000 - 2800 \text{ cm}^{-1}$  é atribuída a grupos  $-\text{C}-\text{H}$ , uma vez que a proporção do grupo  $-\text{CH}$  e  $-\text{CH}_2$  da celulose está numa proporção de 5:1 [39, 121]. As vibrações OH estão localizados em  $1639 \text{ cm}^{-1}$ , os dobramentos das hidroxilas primárias e secundárias apareceram no intervalo  $1500 - 1200 \text{ cm}^{-1}$  e o estiramento C-O observado em  $1100 \text{ cm}^{-1}$  [39, 121].

A diminuição da intensidade das bandas que absorvem em  $1500 - 1200 \text{ cm}^{-1}$  é devida à substituição dos grupos hidroxila por átomos de cloro em CelCl, indicação clara da incorporação da molécula desejada nas cadeias poliméricas. A banda em  $896 \text{ cm}^{-1}$  foi deslocada para  $868 \text{ cm}^{-1}$  após cloração e desapareceu depois de reagir com en. Para a superfície clorodeoxicelulose, as bandas em  $752$  e  $709 \text{ cm}^{-1}$  diminuem de intensidade, mas são ainda visíveis, devido à substituição incompleta por moléculas de en. O espectro de IV de CelCl está mostrado na **Figura 20b**.

Para Celen5 os estiramentos típicos  $\text{CH}_2$  são vistos em  $2837 \text{ cm}^{-1}$ , mas agora a razão  $\text{CH}:\text{CH}_2$  diminuiu depois de reagir com a molécula de etileno-1,2-diamina, enquanto uma nova banda fraca em  $1658 \text{ cm}^{-1}$  pode ser atribuída aos dobramentos do grupo amino. Assim, para uma reação completa numa proporção esperada de 5:3 poderia ser obtida, no entanto, nem todos os átomos de cloro disponíveis foram substituídos, mas encontrou-se um valor maior do que 5:1. Por outro lado, a sequência de reação confirma que o processo de incorporação foi realizado em grande parte sobre a superfície do biopolímero. O espectro do material aminado com maior porcentagem de nitrogênio está mostrado na **Figura 20c**.

Celulose microcristalina, celulose denominado tipo I, encontra-se normalmente com um grau de cristalinidade compreendida entre 40 e 60%. Algumas reações

heterogêneas são capazes de modificar apenas a superfície do polímero e, por vezes, também pode modificar as camadas internas, bem como tendo uma probabilidade de reagir nas regiões amorfas. Então nos padrões de difração de raios X surgem novos picos, para além dos associados ao sólido original, demonstrando uma estrutura cristalina diferente, embora estejam presentes em baixa intensidade. A diminuição da intensidade dos picos sugere que apenas pequenos cristalitos estão presentes. As novas ligações hidrogênio agora estabelecidas também com átomos de cloro reduzem os espaços entre as fitas, o que resulta no deslocamento dos picos para valores de  $\theta$  mais elevados. As regiões cristalinas presentes no *todo* material, foram formados como uma consequência da intensidade das interações intermoleculares e resultam numa estrutura ordenada. Ao contrário, a região amorfa apresentaram interações fracas, causando uma estrutura ordenada baixo, enquanto os grupos hidroxila têm aumentado capacidades de acesso de produtos químicos. Este fato foi demonstrado através de RMN  $^{13}\text{C}$  com indicações claras que o consumo da parte amorfa da celulose é acompanhada pelo desaparecimento dos sinais dos carbonos C(4) e C(6) na celulose clorada [3]. Estes processos concomitantes de rearranjo das ligações hidrogênio terminam no aumento da cristalinidade como um todo para estas celulosas cloradas, em comparação com a celulose não modificada. Os espectros de RMN  $^{13}\text{C}$  estão mostrados na **Figura 21**.

Para os biopolímeros celulósicos com grupos aminos pendentes, uma diminuição drástica da cristalinidade é observado em comparação com o original e as celulosas contendo cloro, como mostrado na **Figura 27**. Estes dados sugerem que o biomaterial aminada resultou em uma estrutura amorfa. Este resultado é independente da via de síntese e da quantidade de grupos amina ligados às cadeias pendentes [76]. No entanto, nos biopolímeros recentemente obtidos utilizando água como solvente, as características amorfas foram intensificadas. Esta mudança ocorrem devido à substituição de um átomo de cloro por etileno-1,2-diamina. Estas novas moléculas poliaminadas, que substituíram parcialmente os grupos cloro, são grandes demais para serem acomodadas de forma eficiente e organizada a formarem uma estrutura cristalina.

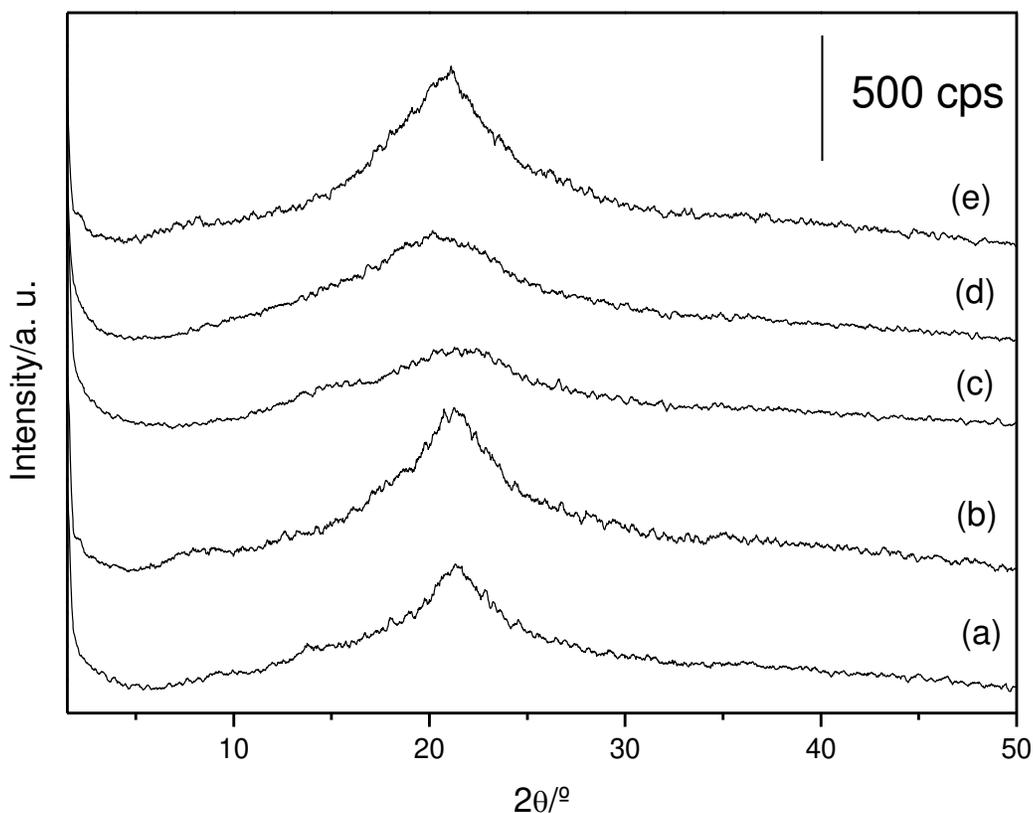


**Figura 27.** Difratogramas de raios X de CelenX (X = 1 **(a)**, 2 **(b)**, 3 **(c)**, 4 **(d)** e 5**(e)**).

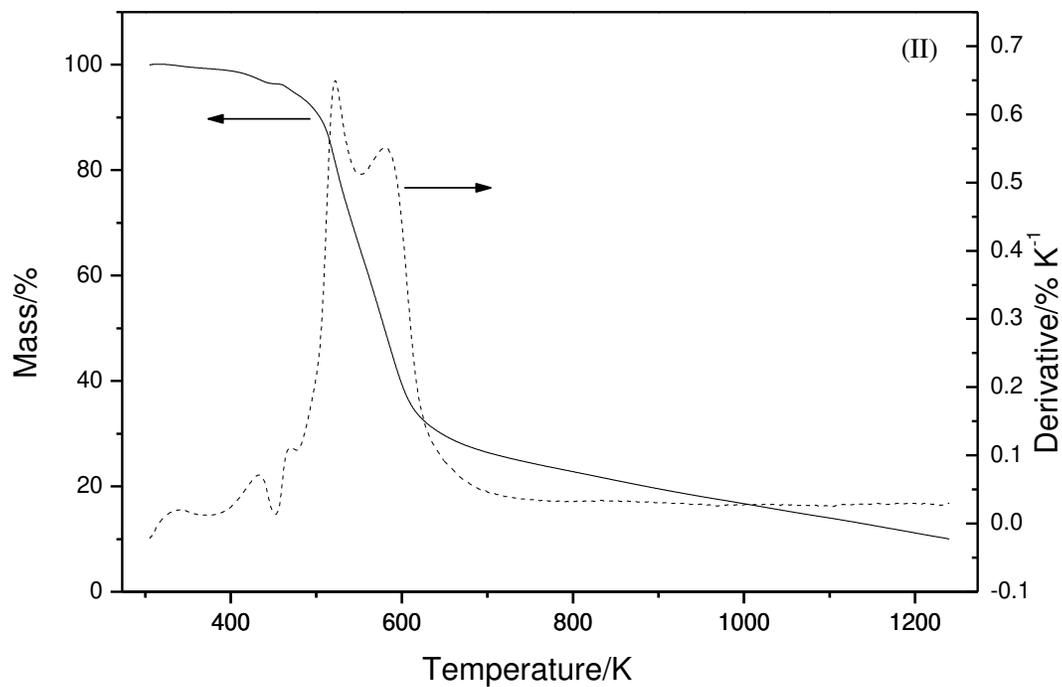
Para celulose pura apenas uma perda de massa entre 563 e 647 K foi observada, constituindo 92% da decomposição térmica. Para CelCl houve três perdas de massa correspondentes a: (i) perda de água adsorvida sobre a superfície no intervalo de 386-430 K, (ii) perda de massa atribuída a perda de ácido clorídrico e a condensação de grupos hidroxila presentes no carbonos 2 e 3, 430-534 K e (iii) a decomposição destrutura orgânica acima 521 K. A **Tabela 19** sumariza os materiais, as temperaturas de decomposição térmica destes materiais.

**Tabela 19.** Variação da temperatura ( $\Delta T$ ), perda de massa em porcentagem para cada etapa de decomposição térmica ( $\Delta m$ ) e resíduo ( $\Delta m_r$ ) para os biopolímeros (Biop) Cel, CelCl e CelenX (X = 1-5).

| Biop   | $\Delta T / K$ | $\Delta m / \%$ | $\Delta m_r / \%$ |
|--------|----------------|-----------------|-------------------|
| Cel    | 298-343        | 2               | 1                 |
|        | 523-647        | 92              |                   |
|        | 647-1273       | 5               |                   |
| CelCl  | 298-430        | 3               | 10                |
|        | 430-534        | 23              |                   |
|        | 534-1273       | 64              |                   |
| Celen1 | 298-452        | 13              | 30                |
|        | 452-1273       | 57              |                   |
| Celen2 | 298-497        | 13              | 27                |
|        | 497-1273       | 60              |                   |
| Celen3 | 298-481        | 13              | 28                |
|        | 481-1273       | 59              |                   |
| Celen4 | 298-481        | 2               | 14                |
|        | 481-1273       | 84              |                   |
| Celen5 | 298-450        | 10              | 13                |
|        | 450-1273       | 77              |                   |

Os biopolímeros modificados com etileno-1,2-diamina também apresentaram três perdas de massa que foram atribuídas à perda de água e, eventualmente, dióxido de carbono, perda do grupo pendente acrescido de condensação de grupos hidroxila e,

finalmente, decomposição térmica do suporte orgânico. As curvas termogravimétricas de CelCl estão mostradas na **Figura 28**.



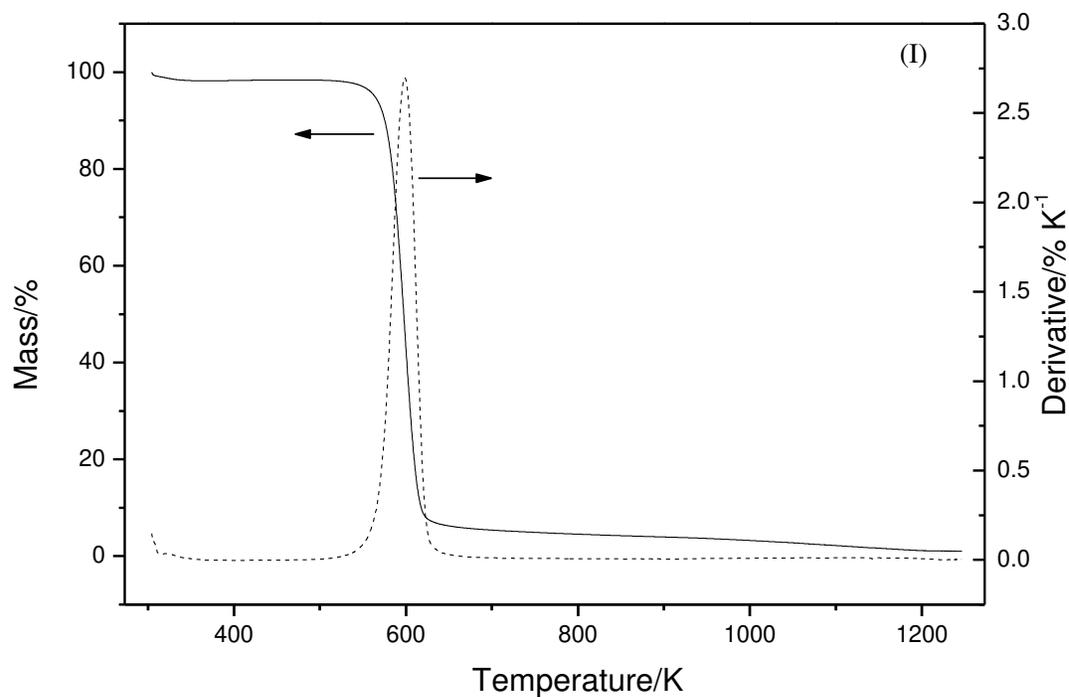


**Figura 28.** Curva termogravimétrica e curva termogravimétrica derivada de celulose (I) e CelCl (II).

A curva termogravimétrica para em celulosas modificadas sintetizados usando DMF como solvente, e também para que a obtida na ausência de solvente são apresentaram a mesma ordem de perda de massa final como anteriormente detetado: Celen1 > Celen2 > Celen5, como mostrado na **Figura 29**.

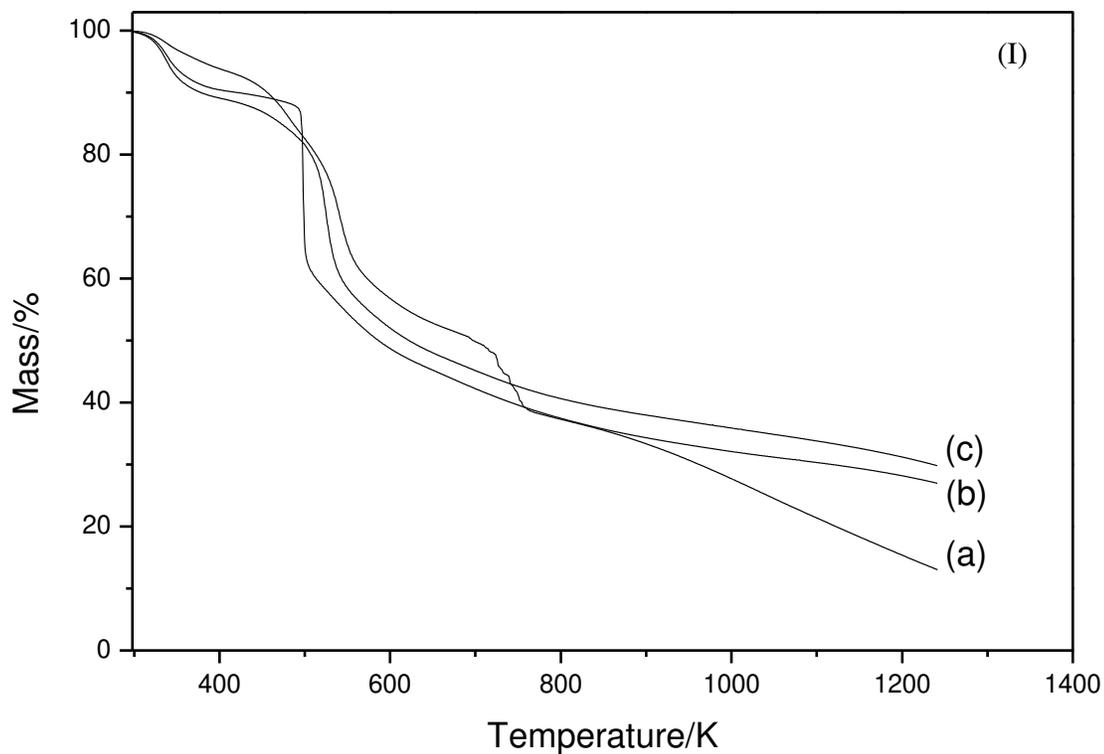


**Figura 29.** Curvas termogravimétricas de CelenX (X = 1 (a), 2 (b) e 5 (c)).

As curvas para a celulose quimicamente modificada, utilizando água como solvente deram o seguinte comportamento quanto ao resíduo final em 1273 K: Celen3 > Celen4 > Celen5, como mostrado na **Figura 30**.

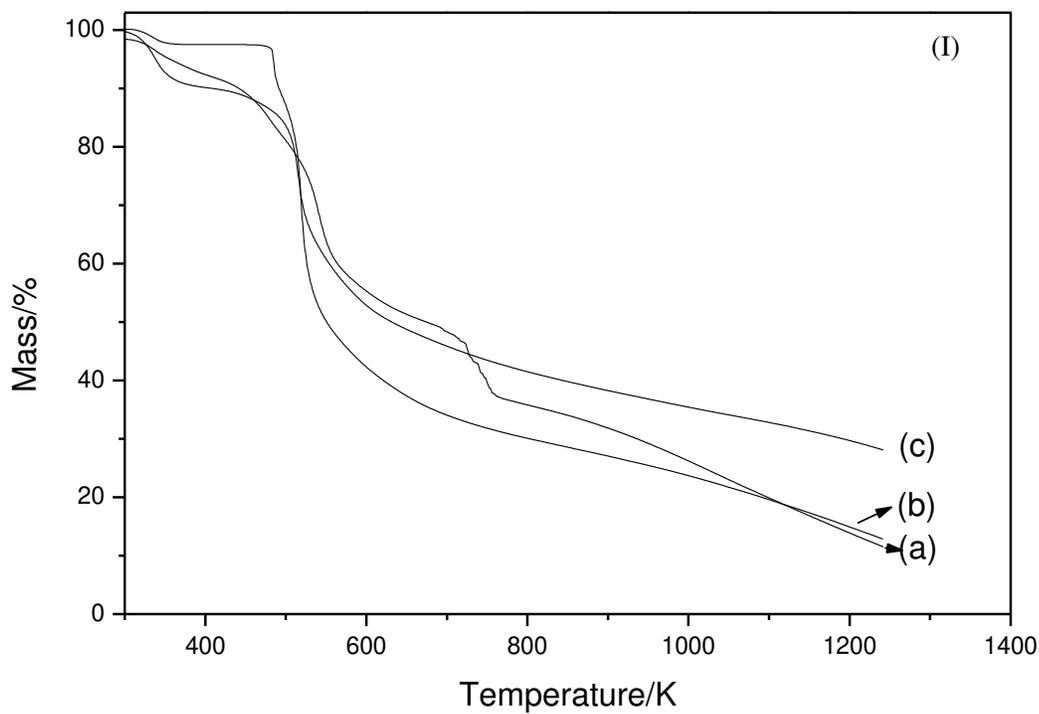


**Figura 30.** Curvas termogravimétricas de CelenX (X = 1 (a), 2 (b) e 5 (c)).

A maior estabilidade térmica é claramente observado quando comparada à celulose não modificada para dar a ordem: Celen > CelCl > Cel, sugerindo que os biopolímeros com menos grupos em ligados apresentaram maior estabilidade térmica.

## 6.6 Conclusão

Os resultados desta investigação são um avanço relevante para este ramo da ciência dos materiais. Os resultados da análise elementar associados às técnicas de difração de raios X e termogravimetria foram aplicadas com sucesso na caracterização da celulose e os derivados quimicamente modificados com cloro e etileno-1,2-diamina; estes derivados podendo ser sintetizados na presença ou ausência de solventes polares, a partir do requerimento do grau de substituição desejado. O método sem

solvente apresenta o conveniente interesse por rotas sintéticas para reduzir a produção de resíduos e também tornar o processo menos dispendioso.

Difração de raios X foi uma técnica útil para seguir a mudança na cristalinidade da celulose, a medida que se avançaram as reações no sentido do de pós funcionalizações. Assim, uma redução na cristalinidade ocorreu depois cloração, com o surgimento de um novo e complexo padrão de difração.

A partir das curvas termogravimétricas dos biopolímeros modificados quimicamente observou-se que a celulose microcristalina apresenta eventos de decomposição muito mais bem definidos que os complexos eventos ocorridos nos materiais modificados.

### **6.7 Sobre os dois artigos anteriores**

Os biopolímeros obtidos a partir da substituição parcial ou total das hidroxilas, principalmente as primárias, dão origem a novas superfícies quimicamente estáveis. No caso da cloro-deoxicelulose cuja liberação dos átomos de cloro, inicialmente ligados covalentemente, faz-se principalmente na forma de cloreto ácido e o próton muitas vezes se envolve na protonação e hidrólise das ligações  $\beta$ -1,4-glicosídicas. Assim, esses materiais devem ser estocados sob condições especiais, como baixa temperatura e são biopolímeros sintetizados já com o intuito de pós-funcionalização. A substituição de cloro pela poliamina, com posterior formação de bases de Schiff ocorre nas superfícies, gerando biopolímeros modificados que não são tão facilmente hidrolisados como as superfícies esterificadas, sendo esperado um maior número de ciclos de uso para estes biopolímeros, em comparação com aqueles que apresentam esterificações.

Essas experimentações, cujos produtos vão dos clorados aos biopolímeros com bases de Schiff superficiais, seriam mais complexas de serem procedidas em escala maior, se comparadas às esterificações de biopolímeros na ausência de solventes. Por exemplo, a etapa de adição do cloreto de tionila é determinante à formação da ligação covalente do cloro à cadeia celulósica e a reação é extremamente exotérmica e ocorre à baixa temperatura. Para se conseguir este controle rápido de temperatura para

grandes volumes, como próximo à escala industrial, pode-se requerer um desenvolvimento de tecnologia, aumentando os custos. Entretanto, o material clorado é interessante, pois dá margem à substituição por praticamente qualquer nucleófilo. Logo, o potencial de obtenção de novos biopolímeros é muito grande.

É importante notar a capacidade de extrapolação da escala laboratorial para a escala industrial, considerando alguns poucos centímetros cúbicos de um solvente qualquer. Esse pouco volume de solvente significa para a indústria um novo reator com sistema adaptado ao solvente que será empregado, pressões no reator, remoção do solvente ao final da operação. Logo, a não utilização de solventes torna o processo mais verde, o qual poderá ser forte candidato num leque de concorrentes cercados por leis de favorecimento ambiental.

Alternativas à obtenção da cloro-deoxicelulose são os outros haletos de celulose, pois possuem bons grupos abandonadores, entretanto, o cloreto de celulose foi escolhido devido à maior estabilidade do biopolímero modificado. E é possível encontrar boa literatura que relata tais substituições da hidroxila celulósica por haletos.

Os biopolímeros com grupos aminados expostos apresentam o inconveniente de reagirem com dióxido de carbono hidratado ou não, dependendo das condições de estocagem, formando carbamato ou bicarbonato; em meio aquoso aumenta o pH favorecendo a sorção de metais divalentes. Os metais podem se ligar aos nitrogênios através dos pares de elétrons não ligados e também à insaturação. Então, muitos estudos no estado sólido podem ser procedidos e questões espectroscópicas dessas interações metal/ligante superficial serem melhores avaliadas, contudo tais estudos estiveram além das perspectivas deste trabalho.

O inconveniente anterior dirige na verdade a outra aplicação que recentemente está em voga: a remoção de gás carbônico ( $\text{CO}_2$ ) de efluentes gasosos. Se propusermos um leito fixo para se tratar milhares de metros cúbicos desse gás efluente, o biopolímero aminado proposto é um forte candidato, pois: a) a celulose é um suporte barato, b) disponível comercialmente, c) baixo custo, ainda d) disponibilidade comercial dos demais reagentes a baixo custo, e) fácil processo de purificação dos materiais, f) alto rendimento para a reação de substituição do cloreto pela etilenodiamina.

O trabalho na parte da reação de substituição do cloreto pela poliamina ainda não atingiu o apogeu, visto que uma considerável quantidade de cloro permanece imobilizada no biopolímero, o que é indesejável. Possibilidades ainda não testadas são o alongamento do tempo de reação do suporte clorado com a poliamina e variações nas temperaturas de síntese.

Para os casos estudados os processos de sorção são esperados de ocorrerem num tempo menor, e cada vez menor, com o aumento da desordem das fibras do biopolímero e exposição dos sítios de adsorção. Esta desordem aumenta proporcionalmente ao número de etapas de reação. Ainda a amorfização mais marcante está na etapa de substituição dos átomos de cloro por poliaminas, pois estas são maiores e dão margem a uma ampla variedade de polimorfos, com conseqüente diminuição da probabilidade de serem formados cristalitos e cristais de tamanho maior.

Finalmente, para um processo de sorção o equilíbrio entre os sítios ativos imobilizados na superfície do sólido e os cátions dissolvidos na solução é esperado de ocorrer num intervalo menor de tempo para biopolímeros com maior grau de amorfização que para os que são mais cristalinos. Logo, em estruturas cristalinas estes sítios ativos podem estar mais envolvidos numa rede de ligação ou estericamente impedidos por isso estar indisponível para tal reação, como uma reação entre um centro básico e um metal em solução, devido às intensas ligações hidrogênio envolvidas na constituição estrutural do biopolímero.

## 7 Experimentações com Babaçu

A.P. Vieira, S.A.A. Santana, C.W.B. Bezerra, H.A.S. Silva, J.C.P. Melo, E.C. Silva Filho, C. Airoidi, “**Copper sorption from aqueous solutions and sugar cane spirits by chemically modified babassu coconut (*Orbignya speciosa*) mesocarp**”, Chem. Eng. J., 161, 2010, 99-105.

### 7.1 Métodos

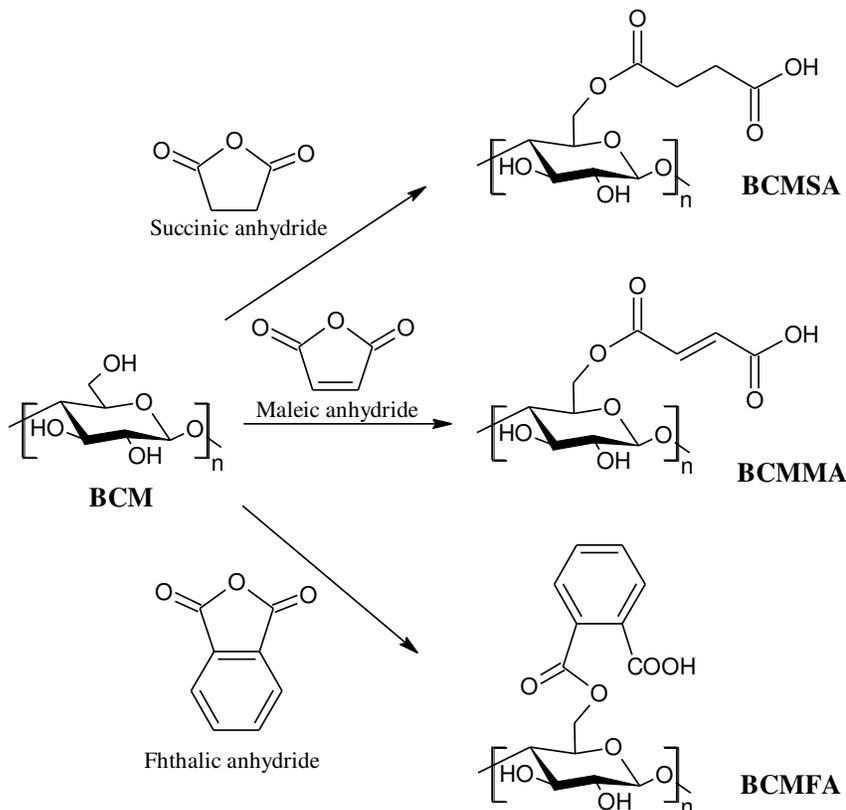
#### 7.1.1 *Materiais e reagentes*

O mesocarpo de babaçu e a aguardente de cana de açúcar comerciais foram obtidos na cidade de São Luís, Estado do Maranhão, na região Nordeste do Brasil. O material em bruto foi triturado para tamanhos de partícula na faixa de 0,88-0,177 milímetros. N, Ndimethylacetamide (DMA), e os anidridos succínico, ácido ftálico e maleico eram todos de grau analítico.

#### 7.1.2 *Síntese de derivados*

Os derivados de lignocelulose contendo grupos carboxílicos livres foram preparadas por reacção do mesocarpo de babaçu (BM) com anidridos succínico, maleico e ftálico fundidos na ausência de solventes [referência]. Este processo consiste em aquecer o mesocarpo seco com uma quantidade de cada um anidrido de um banho de óleo à temperatura de fusão de anidrido. Em cada caso, a razão de anidrido/mesocarpo foi mantida na proporção de 10:1, a mistura foi agitada durante 20 min e a reacção foi parada e adicionou-se DMA. O sólido foi separado por filtração com um filtro sinterizado, lavou-se sequencialmente com acetona e água destilada para remover o anidrido que não reagiu, DMA e produtos provenientes de reacções laterais; secou-se a 353 K durante 12 h. Isto resultou nos biopolímeros modificados

quimicamente BMS, BMP e BMM após a reação com anidridos succínico, maleico ou ftálico, respectivamente [5, 6, 102].



**Esquema 13.** Esterificação de mesocarpo de babaçu com anidridos.

### 7.1.3 Grau de substituição

O grau de substituição dos biopolímeros modificados quimicamente foi determinada por medição da quantidade de grupos carboxílicos ligados à superfície através de retro titulação. Para isso, 0,1000 g de cada material foi tratado com 100,0 cm<sup>3</sup> de uma solução de hidróxido de sódio 400,0 mg dm<sup>-3</sup> por 1 h, sob constante gitação magnética. O sólido foi separado por filtração e três alíquotas de 20,0 cm<sup>3</sup> de cada solução obtida foram tituladas com 365,0 mg dm<sup>-3</sup> ácido clorídrico aquoso.

#### **7.1.4 Medidas**

Os espectros de IV foram obtidos através da acumulação de 32 varreduras no intervalo de  $400 - 4000 \text{ cm}^{-1}$  em um espectrofotômetro de IV com transformada de Fourier MB-Bomem com resolução de  $4 \text{ cm}^{-1}$ , pela técnica de empastilhamento em KBr. As curvas termogravimétricas (TG) foram realizadas com um instrumento TGA-50 Shimadzu sob fluxo de nitrogênio de  $0.50 \text{ cm}^3 \text{ s}^{-1}$ , no intervalo de temperatura de  $298 - 1000 \text{ K}$ , com uma taxa de aquecimento de  $0.167 \text{ K s}^{-1}$ , para uma amostra com cerca de  $10 \text{ mg}$ . Os experimentos de espectrofotometria na região do visível foram realizadas com um instrumento VARIAN-AA 50.

#### **7.1.5 Ponto de carga zero**

O ponto de carga zero dos biopolímeros sintetizados foi determinado pelo método de adição de sólido [referência20]. Para uma série de frascos cônicos de  $100,0 \text{ cm}^3$  foram transferidos  $50,0 \text{ cm}^3$  da solução com pH variando de 1 a 12 e os valores de  $\text{PH}_0$  de cada solução foi ajustado pela adição de  $0,10 \text{ mol dm}^{-3}$  de um ou outro ácido clorídrico ou hidróxido de sódio. O  $\text{PH}_0$  das soluções foi então medida com precisão e  $0,1000 \text{ g}$  de um dos sólidos foi adicionado a cada frasco. As suspensões foram, em seguida, agitadas durante 24 horas e os valores de pH do sobrenadante medidos. A diferença entre o  $\text{pH}_0$  inicial e final  $\text{pH}_F$ , dada por  $\text{pH} = \text{pH}_0 - \text{pH}_F$ , foi representada graficamente contra a  $\text{PH}_0$ .

#### **7.1.6 Estudos de Sorção**

##### **7.1.6.1 Efeito do pH**

Para determinar o efeito do pH sobre a adsorção de íons metálicos, numa quantidade de  $0,1000 \text{ g}$  de cada um dos materiais quimicamente modificados foi suspenso em  $100,0 \text{ cm}^3$  da solução de cobre com uma concentração inicial de  $200 \text{ mg}$

$\text{dm}^{-3}$  sob agitação constante durante 24 h. O intervalo de pH estudado foi 1,0 - 6,0 e estes valores foram ajustados com 0,010 - 1,0  $\text{mol dm}^{-3}$  soluções aquosas de ácido clorídrico. Após filtração, a concentração de cátions no sobrenadante foi determinada por titulação com EDTA

### **7.1.6.2 Cinética**

Para cada estudo 0,1000 g de cada sorvente foi misturado com 100,0  $\text{cm}^3$  de solução aquosa ou uma solução hidroalcoólica de 40 % com concentrações de 200  $\text{mg dm}^{-3}$ , sob agitação, por diferentes intervalos tempos. Após a filtração, a concentração de cátions foi determinada como anteriormente descrito [131].

### **7.1.6.3 Sorção**

Os experimentos de sorção em batelada foram realizados uma série de frascos contendo 0,1000 mg de cada material suspenso em 100,0  $\text{cm}^3$  de soluções aquosas ou hidroalcoólicas a 40% com concentrações de catião de cobre que variaram de 200 a 500  $\text{mg dm}^{-3}$  a  $298 \pm 1$  K. As suspensões foram agitadas durante 30 min com o pH estabelecido a partir das experiências anteriores para assegurar o máximo de adsorção. No final deste processo, o sólido foi separado por filtração e a quantidade de íons metálicos adsorvidos foi determinada por titulação dos metais na solução sobrenadante; pela diferença entre a concentração nas soluções inicial e final que se encontra no sobrenadante por titulação [131].

### **7.1.6.4 Sorção em amostras de aguardente**

Amostras de aguardente obtidas a partir de um mercado local foram dopadas com cobre para simular níveis elevados deste metal na solução. Para esta operação, uma alíquota de 8,0  $\text{cm}^3$  da solução de cobre (etanol 40%) foi diluída em 1 L de aguardente, para resultar em uma aguardente com concentração de metal final de 8.0

mg dm<sup>-3</sup>. As sorções de 1,0 - 4,0 g de cada mesocarpo quimicamente modificado BMS, BMP e BMM foi ensaiado. Para cada biopolímero quatro determinações independentes foram realizadas, utilizando 30 minutos de agitação. A concentração de cobre que permanece na amostra de aguardente foi determinada por uma curva de calibração em espectrofotometria na região do visível. Para cada determinação espectrofotométrica, 1.0 cm<sup>3</sup> de piridina foi adicionado a alíquotas de 9.0 cm<sup>3</sup> do sobrenadante e a absorbância do complexo de cobre-piridina-formada medida em um comprimento de onda de 610 nm.

## 7.2 Resultados e discussão

O método de funcionalização sem solventes se mostrou muito eficaz na funcionalização de lignocelulósicos com anidridos cíclicos resultando em materiais com mais de 3 mmol g<sup>-1</sup> de funções ácidas e estes resultados, bem como outros dados da literatura, são mostrados na **Tabelas 20**.

**Tabela 20.** Sumário de materiais obtidos a partir da modificação química de celulose e lignocelulósicos com anidrido succínico.

| Material modificado      | Solvente         | Temperatura de síntese/K | Grau de modificação       | Contaminante     | Remoção de contaminante   | Referência |
|--------------------------|------------------|--------------------------|---------------------------|------------------|---------------------------|------------|
| Celulose microcristalina | -                | 408                      | 3,07 mmol g <sup>-1</sup> | Ni <sup>2+</sup> | 2,46 mmol g <sup>-1</sup> | [102]      |
| celulose                 | Piridina/tolueno | 363                      | 5,6 meq g <sup>-1</sup>   | Cd <sup>2+</sup> | 1,64 mg g <sup>-1</sup>   | [112]      |
| Celulose mercerizada     | Piridina         | 408                      | 7,2 mmol g <sup>-1</sup>  | Cu <sup>2+</sup> | 1,79 mmol g <sup>-1</sup> | [132]      |
| Bagaço de                | Acetona          | 373                      | 1,92 mmol                 | Ni <sup>2+</sup> | 1,8 mmol                  | [108]      |

Capítulo 7 – Experimentações com Babaçu

|                            |                                    |     |                           |           |                    |       |
|----------------------------|------------------------------------|-----|---------------------------|-----------|--------------------|-------|
| palha de arroz             | (evaporada)                        |     | $g^{-1}$                  |           | $g^{-1}$           |       |
| Bambu                      | Acetato de 1-etil-3-metilimidazol  | 393 | 4,01 mmol $g^{-1}$        | $Cd^{2+}$ | 2,47 mmol $g^{-1}$ | [106] |
| Caroço de azeitona         | Tolueno/piridina                   | 333 | 3,90 mmol $g^{-1}$        | $Cd^{2+}$ | 1,78 mmol $g^{-1}$ | [107] |
| viscose                    | N,N-dimetil sulfóxido              | 343 | 6,2 meq $g^{-1}$          | $Cr^{3+}$ | 1,80 mmol $g^{-1}$ | [108] |
| madeira                    | xileno                             | 398 | 2 mmol $g^{-1}$           | -         | -                  | [133] |
| Bentonita                  | 1,4-dioxano                        | 298 | 1,19 meq $g^{-1}$         | $Cu^{2+}$ | 0,54 mmol $g^{-1}$ | [134] |
| SBA-15 Polihidroxilada     | Trietilamina/N,N-dimetilformamida  | 333 | 1,5 mmol $g^{-1}$         | $Cu^{2+}$ | 0,98 mmol $g^{-1}$ | [135] |
| Casca de abacaxi           | piridina                           | 298 | -                         | $Cu^{2+}$ | 0,44 mmol $g^{-1}$ | [105] |
| celulose                   | Sem solvente – mecano química      | 298 | 2,70 mmol $g^{-1}$        | $Pb^{2+}$ | 2,03 mmol $g^{-1}$ | [104] |
| Celulose de bagaço de cana | Cloreto de 1-butil-3-metilimidazol | 353 | 0,56 – 1,54 mmol $g^{-1}$ | -         | -                  | [103] |

Os espectros dos biopolímeros modificados quimicamente apresentam diferenças notáveis na banda em  $1723\text{ cm}^{-1}$ , atribuídos aos estiramentos  $\text{C}=\text{O}$  [referência22]. A presença de  $\text{CH}_2$  and  $\text{CH}$  groups provenientes dos anidridos adicionados ao estrutura biopoléérica é demonstrado pelas bandas em  $2930$  e  $2890\text{ cm}^{-1}$ , respectivamente [referência14]. Baseado na diferença entre o precursor e as absorções relacionados aos biopolímeros modificados, principalmente o estiramento da carbonila, estes resultados confirmam claramente a ligação das moléculas de anidrido à estrutura polimérica. A **Figura 31** mostra os espectros de IV para os derivados ácidos do mesocarpo de babaçu modificado.

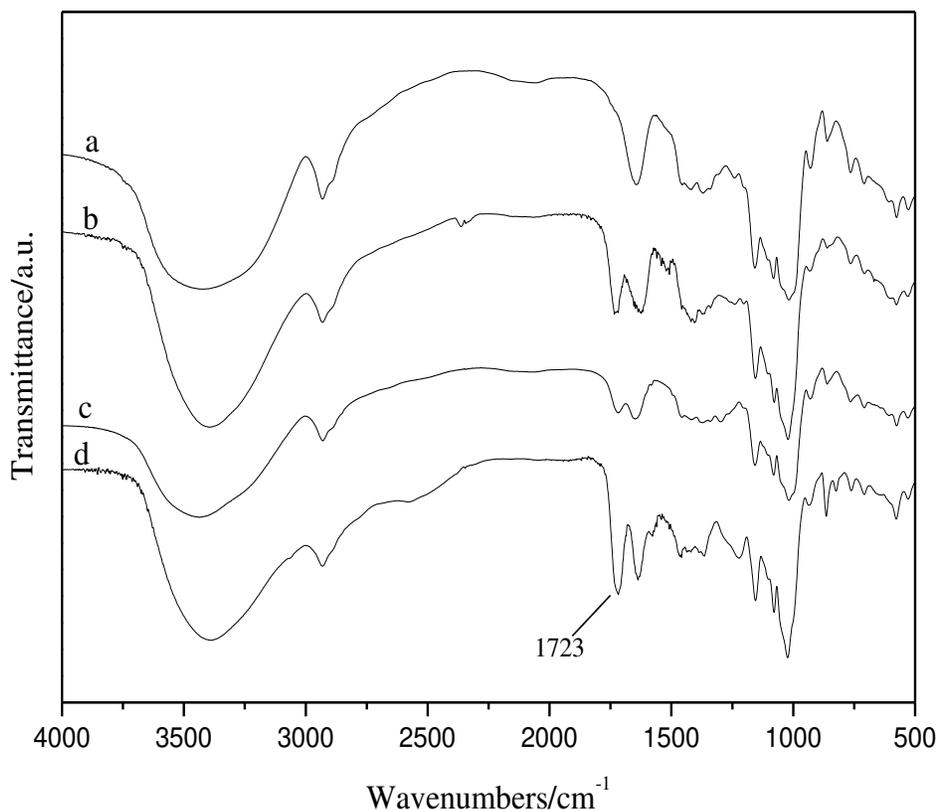


**Figura 31.** Espectros de IV de mesocarpo de babaçu (a) e seus derivados modificados com os anidridos succínico (b), malêico (c) e ftálico (d).

As **Tabelas 7, 8 e 9** resumizam as bandas encontradas para biopolímeros modificados quimicamente com anidridos. As **Tabelas 10 e 11** mostram alguns valores da literatura.

As curvas termogravimétricas para todos os biopolímeros apresentam comportamento muito semelhante ao material de partida [136]. A primeira etapa de decomposição pode ser atribuído à libertação de água fisicamente adsorvida na superfície. Esta fase corresponde a uma perda de massa de 16,0, 4,3, 8,2 e 5,3 %, até 375 K, para o, BM BMS, BMP e BMM, respectivamente, e as curvas termogravimétricas estão mostradas na **Figura 32**.

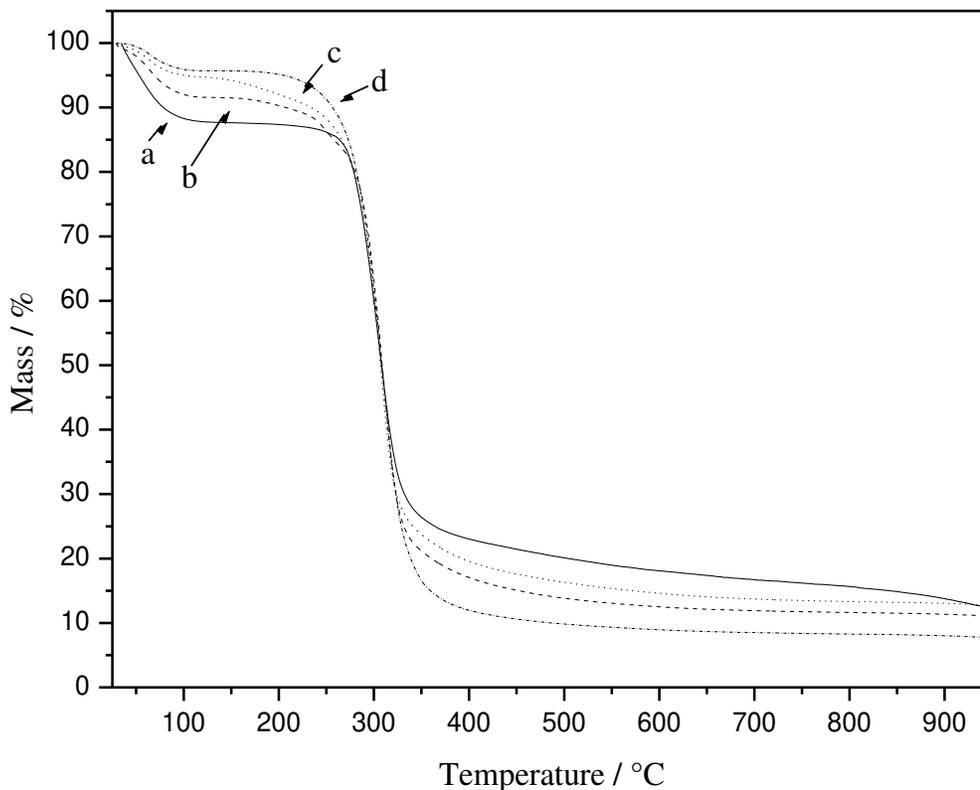


**Figura 32.** Curvas termogravimétricas de BCM (a), BCMSA (b), BCMFA (c) and BCMMA (d).

O segundo estágio corresponde à desfuncionalização do material e surgimento de novos grupos, principalmente devido aos rearranjos da estrutura biopolimérica,

seguido de decomposição de material orgânico, ocorre no intervalo de temperatura de 477 a 623K. A perda de massa, que corresponde a este intervalo de temperatura para BM é de 60%, enquanto que para os MS, BMP e BMM, estas percentagens são 89,3, 81,2, e 82,7%, respectivamente.

As **Tabelas 12 e 13** resumizam as faixas de temperatura, nas quais ocorrem os eventos de decomposição térmica para materiais funcionalizados com anidridos cíclicos.

### 7.2.1 Efeito do pH e do ponto de carga zero

O mesocarpo não modificado BM demonstrou uma capacidade de sorção nula na presença de cátions cobre, nas condições estudadas. Como previamente observado, a sua  $pH_{PZC}$  é de 6,7 e a sorção de espécies de carga positiva será favorecida em  $pH > pH_{PZC}$  [9]. No entanto, espera-se que a um pH superior a 6,7 espécies relacionadas ao hidróxido de cobre são formados, o que afeta a livre sorção de cátions.

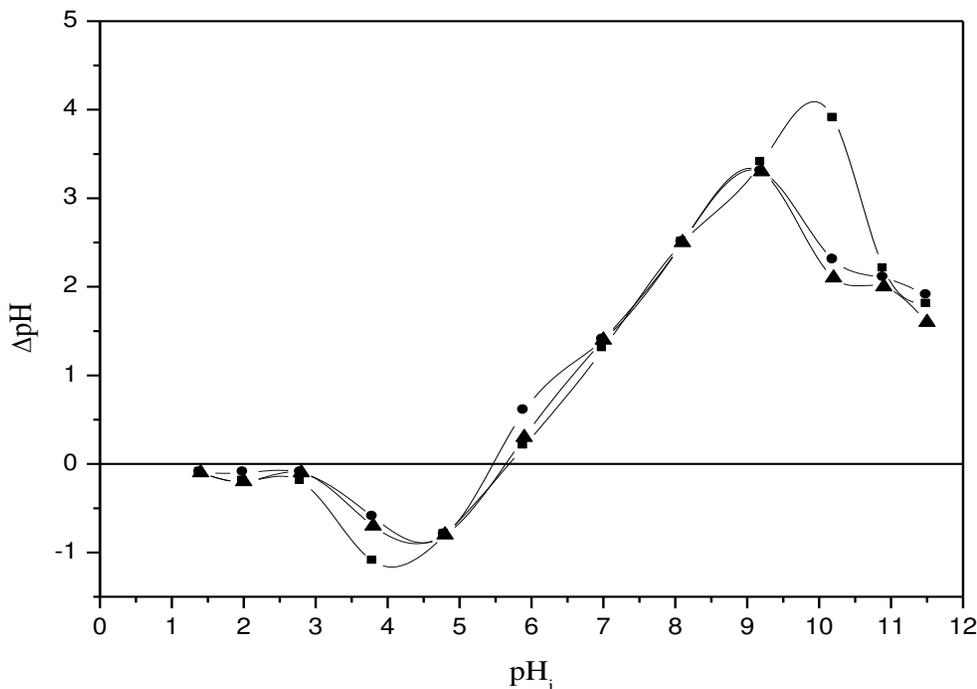


**Figura 33.** Ponto de carga zero para BCMSA (■), BCMFA (●) and BCMMA (▲).

Todos os mesocarpos modificados com anidridos apresentaram um aumento na quantidade de cobre absorvida com o aumento do pH da solução de com um valor máximo em pH 6,0. Os  $pH_{PZC}$  para estes biopolímeros são de 5,6, 5,4 e 5,7 por BMS, BMP e BMM, respectivamente, como mostrados na **Figura 33**. Estes valores indicam que a sorção do cátion é favorecida em soluções com pH mais elevados do que para cada um específico  $pH_{PZC}$  material. Sob condições ácidas, os biopolímeros modificados quimicamente podem ser protonados, devido as maiores concentrações de prótons e a quantidade de cátions sorvida diminui. Por outro lado, o aumento do pH desprotona os grupos carboxilatos, condição que favorece as suas capacidades de coordenação com o metal e, conseqüentemente, a quantidade de  $Cu^{2+}$  sorvidas aumenta; o mesmo comportamento foi observado para outros sistemas [132,137, 138].

### **7.2.2 A cinética de sorção**

A partir das isotermas é claramente evidenciado que o equilíbrio em solução aquosa é alcançada após 20 min de contacto entre o cobre e os sólidos em suspensão. No entanto, em solução hidroalcoólica a quantidade adsorvida torna-se constante a partir de 30, 15 e 20 min para BMS, BMP e BMM, respectivamente. Os resultados dos dados cinéticos foram investigadas pelos modelos de pseudo-primeira ordem [139] e de pseudo-segunda-ordem [140]. O processo de sorção descrita pelo modelo de pseudo-segunda-ordem é o preferido. A correlação deste modelo para estes sistemas corrobora com os estudos quando BM biopolímero foi utilizado como adsorvente de corantes têxteis, demonstrando que todos os corantes examinadas apresentaram melhor ajuste com a equação de pseudo-segunda ordem [9]. Absorventes, tais como turfa [141, 142], quimicamente modificados quitosana [143] e coco verde [144], que também apresentam a capacidade de sorção de cobre, também mostrou um melhor ajuste a este modelo.

Estudos anteriores associadas a sorção de cobre para uma série de materiais, tais como o trigo e lentilha e casca de arroz, sem modificação de [145], bem como materiais tais como o bagaço de cana de açúcar e celulose [132, 146, 147] modificado quimicamente com agentes específicos, revelaram uma tendência para ajuste do

modelo de Langmuir. Os parâmetros relacionados com o presente modelo de reflete a natureza do adsorvente e pode ser utilizada para comparar o desempenho de sorção, no que respeita à sua capacidade máxima. De acordo com a capacidade de adsorção máxima para o cobre por grama de sorvente, a ordem das quantidades adsorvidas nos sistemas estudados foi BMS > BMP > BMM, como mostrado na **Figura 34**.

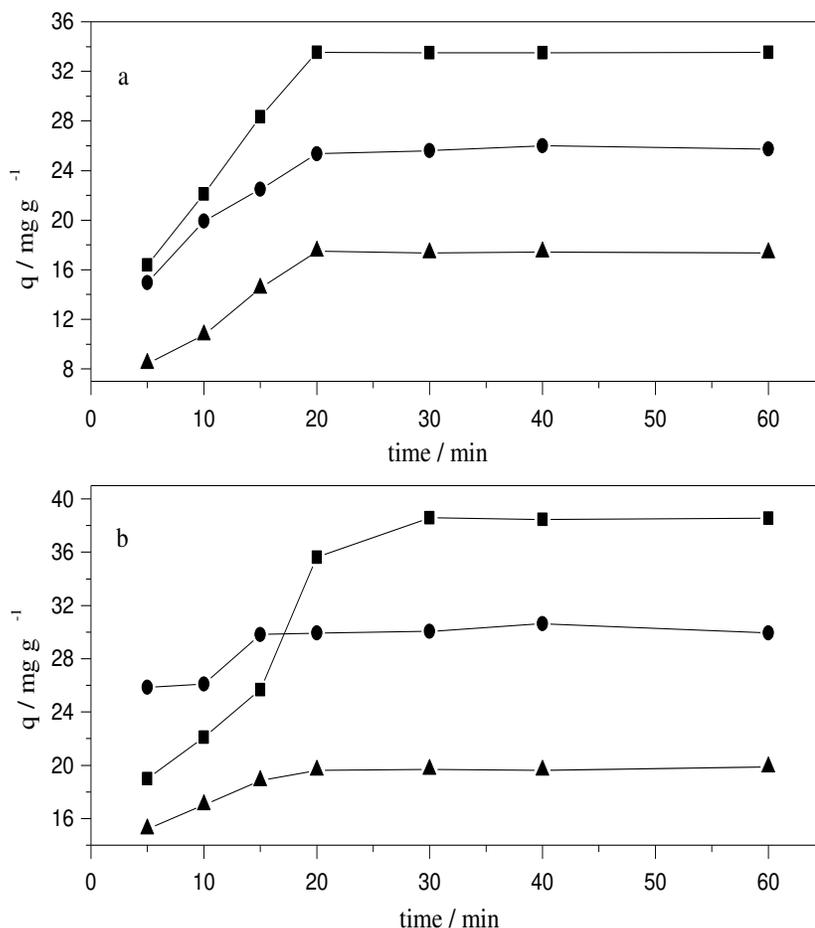


**Figura 34.** Curvas cinéticas de adsorção de cobre em BCMSA (■), BCMFA (●) e BCMMA (▲) em solução aquosa (a) e solução hidroalcoólica (b) a  $298 \pm 1$  K.

Uma sequência semelhante é encontrada para o grau de funcionalização com os ácidos carboxílicos apresentados na estrutura do mesocarpo, 177,0, 149,3, 141.8  $\text{mg g}^{-1}$

<sup>1</sup> para a mesma sequência, respectivamente. Este fato explica a capacidade de sorção de cada um dos materiais, porque a presença destes grupos funcionais é essencial para a absorção dos cátions. A capacidade máxima indica que para a solução hidroalcoólica a sorção de cobre é maior para estes biopolímeros que nas soluções aquosas.

### **7.2.3 Sorção de amostras aguardentes**

O teor de cobre em aguardente de cana de açúcar pode ser reduzido para o permitido pela legislação brasileira, especificado como  $5,0 \text{ mg dm}^{-3}$ , quando apenas  $1,0 \text{ g dm}^{-3}$  de cada sorvente foi usado. Como se pode observar, a concentração inicial de cátions de alta  $8,0 \text{ mg dm}^{-3}$  foi reduzida para  $0,48$ ,  $1,41$ ,  $4,26 \text{ mg dm}^{-3}$  para BMS, BMP e BMM, respectivamente, no final do processo de sorção, como mostrado na **Figura 35**.

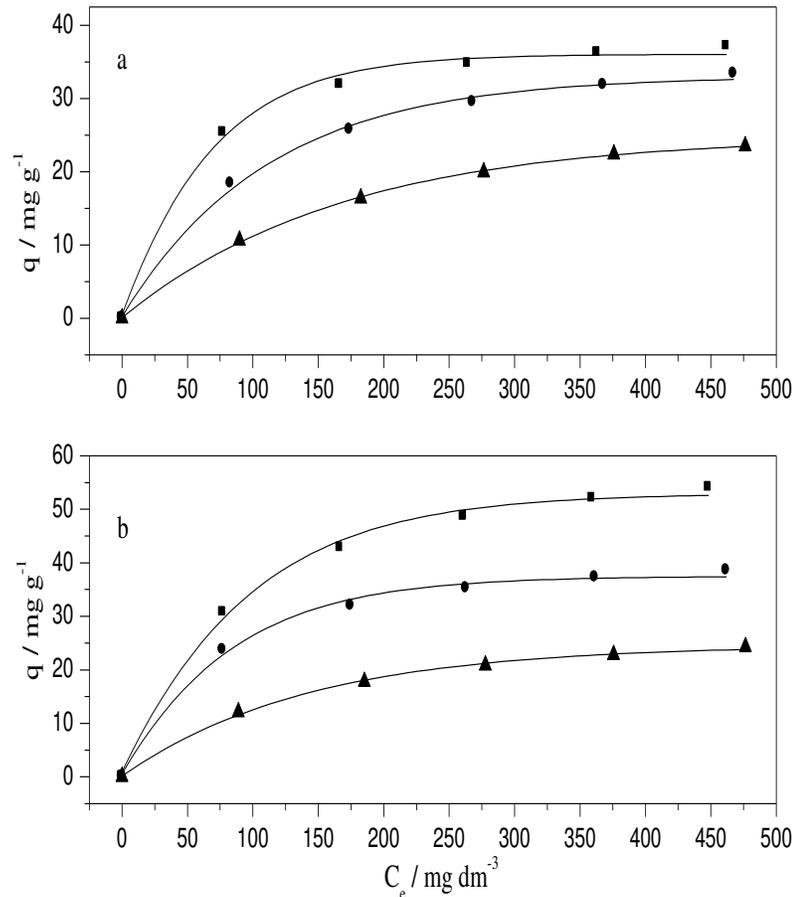


**Figura 35.** Ajustes aos modelos isotérmicos de Langmuir para adsorção de cobre em BCMSA (■), BCMFA (●) e BCMMA (▲) em água (a) em pH 6.0 em solução hidroalcoólica (b) a  $298 \pm 1$  K.

No entanto, países do hemisfério norte permitem até  $2,0 \text{ mg dm}^{-3}$  de cobre em aguardente, o que requer uma dose de  $3,0 \text{ mg dm}^{-3}$  de BMM para caber dentro dos padrões exigidos. O mesocarpo presente quimicamente modificado apresenta maior capacidade de adsorção quando comparado com outros materiais estudados. Por exemplo, a maioria dos estudos com carbono activado, tem a capacidade de remoção de cobre a partir de cana-de-açúcar espírito [148]. Embora os biopolímeros deste estudo demonstraram boa eficiências para remoção de cobre a partir de amostras reais de aguardente de cana de açúcar, uma base sólida para a aplicação comercial requer

mais estudos sobre as mudanças nos perfis dos componentes inorgânicos e orgânicos das aguardentes, viabilidade econômica e as condições ideais de fluxo.

### 7.3 Conclusão

Através de uma metodologia rápida e pronta, foi possível elaborar uma estratégia para introduzir grupos ácidos carboxílicos quelantes no mesocarpo do babaçu. Os biopolímeros sintetizados apresentaram capacidades de sorção boas para o cobre em soluções hidroalcoólicas e aquosa, com valores máximos obtidos a pH 6,0. A cinética de sorção correspondentes é governada por um modelo de pseudo-segunda ordem, com melhor ajuste ao modelo de Langmuir. Os resultados também demonstraram a eficácia de remoção de cobre a partir de uma amostra de aguardente de cana, exigindo apenas 1,0 g dm<sup>-3</sup> de sorvente e 30 min de contato para atender às exigências da legislação brasileira.

S.A.A. Santana, A.P. Vieira, E.C. Silva Filho, J.C.P. Melo, C. Airoidi, “**Immobilization of ethylenesulfide on babassu coconut epicarp and mesocarp for divalent cation sorption**”, J. Hazard. Mater., 174, (2010) 714-719.

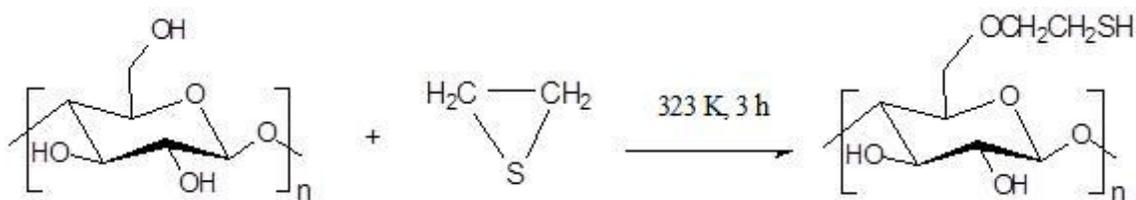
### 7.4 Métodos

#### 7.4.1 *Materiais e reagentes*

Nitrato de cobre hidratado divalente (Carlo Erba) foi utilizado sem purificação e a concentração foi determinada através de titulação com solução padronizada de EDTA. Etilenossulfeto (ES) (Aldrich) foi usado como recebido. Todos os outros químicos foram de grau analítico.

### 7.4.2 Sínteses

Em ambos os casos, 5 g de mesocarpo ou de epicarpo, com tamanhos de partícula na gama de 0,088, 0,177 milímetros, foram individualmente misturadas com 7,0 cm<sup>3</sup> (114,56 mmol) de Etilenossulfeto, tal como anteriormente estabelecido para a incorporação em quitosana [149]. As suspensões foram mantidas em banho de areia durante 3 horas a 323 K para dar o produto final. Os biomateriais quimicamente modificados foram separados por filtração utilizando um filtro sinterizado, lavado com água destilada e depois com acetona. Os produtos foram nomeados BCMS e BCES, respectivamente, foram secos em estufa a 353 K durante 1 hora e num dessecador durante a noite.



**Esquema 14.** Síntese de BCMS e BCES.

### 7.4.3 Medidas físicas

Os espectros de IV foram obtidos com um espectrofotômetro FTIR MB-Bomem com uma resolução de 4 cm<sup>-1</sup>, utilizando pastilhas de KBr, na região entre 4000 – 400 cm<sup>-1</sup>. O Carbono, nitrogênio e enxofre dos compostos foram analisadas por meio de um espectrofotômetro Perkin-Elmer 2400 Série II analisador de microelementos. As curvas termogravimétrica (TG) foram realizadas em um instrumento TGA-50 Shimadzu sob fluxo de nitrogênio de 0,50 cm<sup>3</sup> s<sup>-1</sup>, no intervalo de temperatura de 298 – 1000 K, com uma taxa de aquecimento de 0,167 K s<sup>-1</sup> e massa da amostra inicial de 10 mg. Os espectros de RMN 13C CP/MAS no estado sólido foram obtidos num espectrômetro Bruker AC 400 /, utilizando frequências de 75,47 MHz no ângulo mágico de rotação de 4 kHz. As medidas de pH foram obtidos utilizando um instrumento MS-21 Digimed.

#### **7.4.4 Estudos de pH e ponto de carga zero**

O efeito do pH de sorção foi realizada utilizando uma série de frascos contendo cobre aquoso adicionou-se 100 mg de cada um dos biomaterial modificados, mantendo-se sob agitação por 24 h. O pH da solução na faixa de 1,0 - 6,0 foi ajustado, quando necessário, com 0,10 mol dm<sup>-3</sup> de ácido clorídrico ou solução de hidróxido de sódio. O teor de cobre livre no sobrenadante foi determinada como anteriormente. Os pontos de carga zero para BCMS e biopolímeros BCES foram determinadas pelo método de adição de sólido [18]. Para uma série de 100 cm<sup>3</sup> frascos foram transferidos 20 cm<sup>3</sup> de solução com pH variando de 1 a 12. Os valores PH<sub>0</sub> da solução foram ajustados através da adição de ácido clorídrico ou hidróxido de sódio 0,10 mol dm<sup>-3</sup>. O PH<sub>0</sub> das soluções foi então observado com precisão e 0,10 g cada uma BCMS ou biomaterial BCES foi individualmente adicionados a cada frasco, que foi fechado imediatamente de forma segura. As suspensões foram em seguida agitadas e deixou-se equilibrar durante 24 horas, o valor do pH do sobrenadante de cada frasco determinado.

#### **7.4.5 Estudos cinéticos**

Primeiramente determinou-se o tempo de equilíbrio para a adsorção do metal nos biopolímeros modificados em estudando o intervalo de 5 a 60 min. Assim, quantidades de 100 mg de BCMS ou BCES foram suspensas em 100,0 cm<sup>3</sup> de uma solução de cobre em cada um dos balões, as quais foram filtradas e o teor de cobre no sobrenadante determinado por titulação directa com 0,010 mol dm<sup>-3</sup> de EDTA a pH 10, usando murexida como indicador [131].

#### **7.4.6 Isotermas de sorção**

O termo sorção expressa todo processo que ocorre não só na superfície, mas também por meio da penetração difusiva nos biopolímeros. As isotermas de sorção para BCMS e BCES e para os respectivos biomateriais nativos foram obtidas usando o método descontínuo, que consiste na suspensão de 100,0 mg de cada biomaterial em 100,0 cm<sup>3</sup> da solução de cobre aquoso com várias concentrações, variando de 100 a 500 mg dm<sup>-3</sup>. Em todos os casos, cada determinação de sorção individual foi obtida em

duplicada, em frascos sob agitação mecânica, a  $298 \pm 1$  K. A concentração de metal no sobrenadante foi determinada por titulação com EDTA.

## 7.5 Resultados e discussão

### 7.5.1 Caracterizações

Com base no conteúdo de enxofre de  $2,00 \pm 0,05$  e  $8,67 \pm 0,01\%$ , a quantidade de  $20,2 \pm 0,07$  e  $86,7 \pm 0,01$  mg g<sup>-1</sup> foi calculada para a molécula de Etilenosulfeto ancorada nos biopolímeros BCES e BCMS, respectivamente. A eficácia da reação com etilenosulfeto em polissacáridos naturais pode ser comparada às reações em quitosana. Para esta último biopolímero foram incorporados 20,39 % de enxofre, com dois moles de ethylenesulfite covalentemente ligados a cada unidade de quitosana [149]. Este valor também é alto devido à disponibilidade do grupo amino reativo, que contrasta com o grupo hidroxilo menos reativos na estrutura de carbono lignocelulósico 6 polimérico.

O mesocarpo apresenta uma grande predominância do componente celulósico sobre a estrutura principal polimérica com grupos hidroxila disponíveis, ao passo que para as unidades de epicarpo o componente lignina está disponível com grupos aldeídicos e cetônicos [9]. Do ponto de vista estrutural, a presença de grupos hidroxila faz com que haja um aumento na tensão do anel de três membros, favorecendo a sua abertura no curso da reação e, conseqüentemente, reativo com mesocarpo [150].

As principais bandas observadas nestes biopolímeros modificados são uma banda larga no intervalo de  $3200 - 3600$  cm<sup>-1</sup> que corresponde aos estiramentos (O-H); as bandas bem definidas no intervalo de  $2800-3000$  cm<sup>-1</sup> atribuídas aos estiramentos (C-H) e os estiramnetos dos grupos carbonílicos bandas na região de  $1550 - 1750$  cm<sup>-1</sup>. A banda fraca em  $2544$  cm<sup>-1</sup> é atribuída ao estiramento (S-H) [150]. Os espectros de IV para os derivados tiolados do babaçu são mostrados na **Figura 36**.

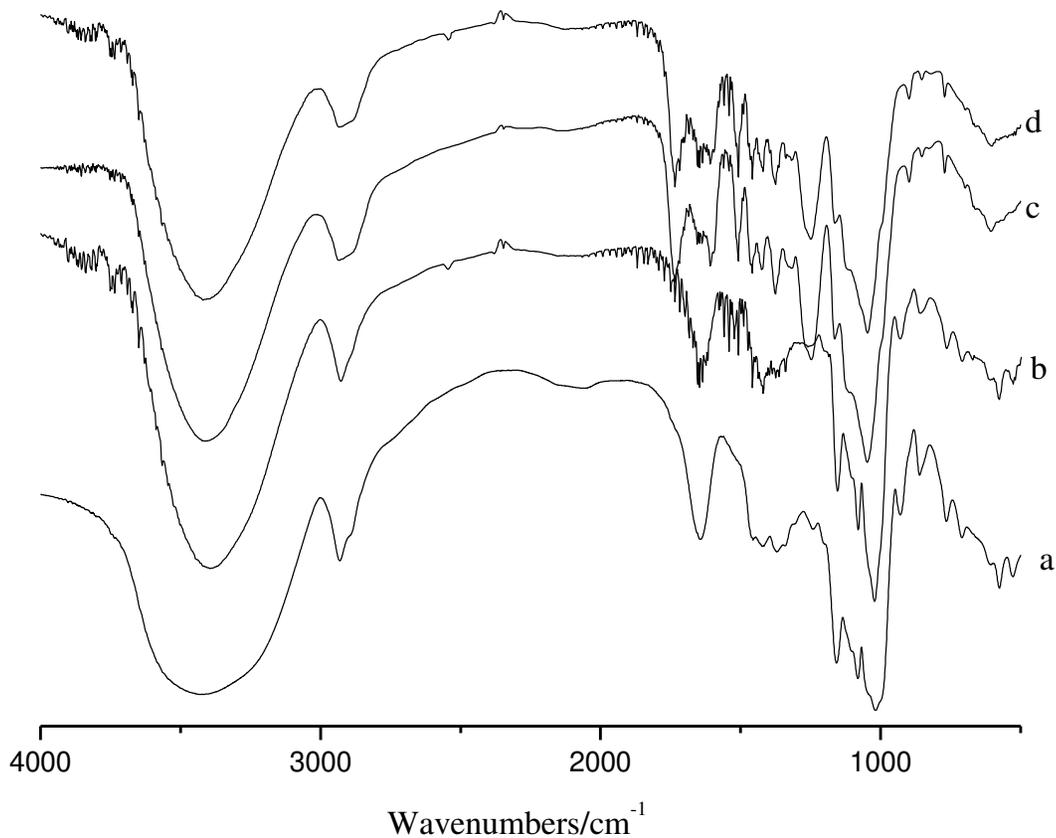


**Figura 36.** Espectros de IV de BCM (a), BCMS (b), BCE (c) e BCES (d).

O efeito da modificação química sobre o comportamento térmico do mesocarpo e epicarpo também foi estudado. Para mesocarpo do material nativo começou decomposição a 375 K, o que corresponde a uma perda de massa de 12 %, seguido de uma outra perda de 62 % no intervalo de 477 -623 K. A primeira evento térmico é atribuído à liberação de água fisicamente adsorvida, enquanto a segunda etapa é devido à perda da modificação do biopolímero e finalmente o terceiro evento com o colapso total da estrutura perdendo suas características de fibra, transformando-se em um *bulk* como resíduo final. Para os estudo com epicarpo, o este apresentou perdas de massa de 11 %, a 353 K e de 56 % no intervalo 609 – 638 K, nas mesmas condições experimentais. Para BCMS e BCES as perdas de massa ocorrerão a temperaturas mais elevadas que para os biopolímeros naturais de partida fazendo com que a

funcionalização desses biopolímeros de babaçu com etilenossulfeto apresentem maior desempenho térmico, como mostrados na **Figura 37**.

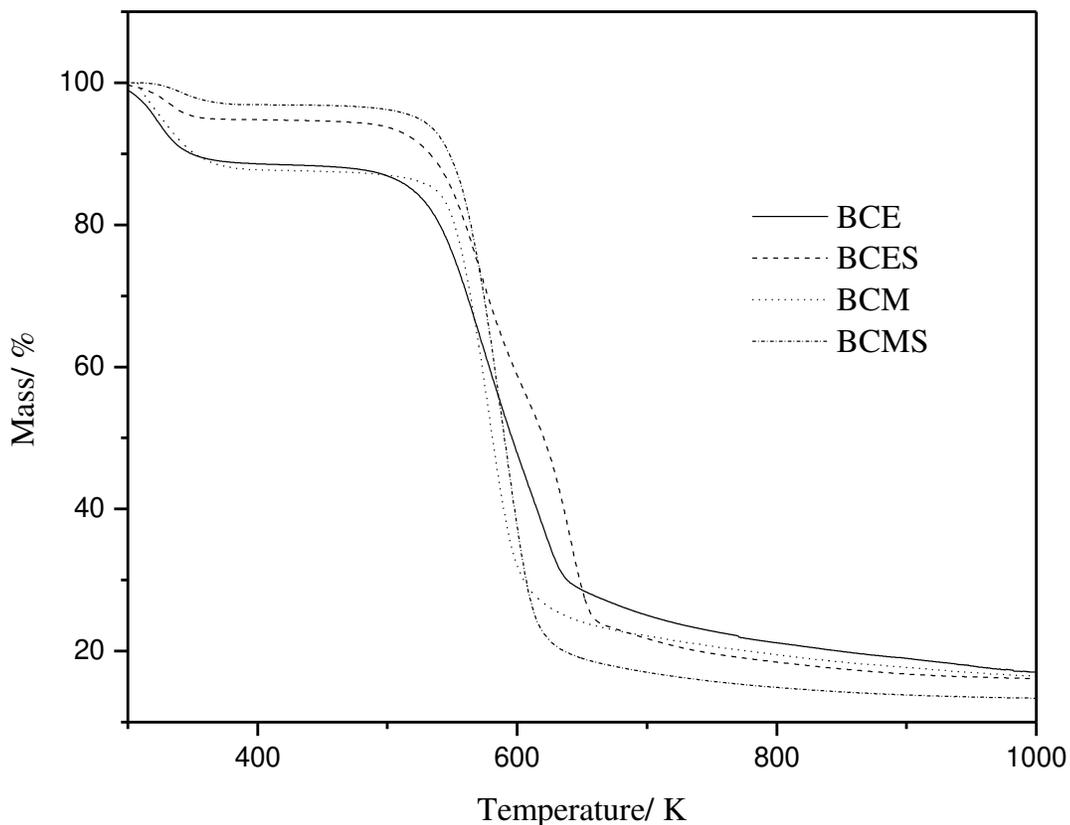


**Figura 37.** Curvas termogravimétricas de BCM, BCMS, BCE e BCES.

Nos espectros de RMN  $^{13}\text{C}$  CP/MAS para o mesocarpo e epicarpos são evidentes o sinal em 101 e 83 ppm atribuídos aos carbonos C1 e C4 no celulósicos, respectivamente, e os carbonos C2, C3 e C5 apresentaram sinais em 71 - 75 ppm. Os sinais entre 64 e 62 ppm foram atribuídos aos carbonos C6 celulósicos em regiões cristalinas e amorfas, respectivamente. Devido ao fato de que o epicarpo é mais rico em lignina, componente na estrutura de biopolímeros, aparece sinal em 22 ppm carbonos metílicos encontrados na lignina; os sinais em 116 - 120, 133 e 149 - 153 ppm atribuídos aos carbonos aromáticos presentes, também presentes na lignina. Por outro

lado, os sinais largos a 160 e 178 ppm correspondem a cetonas, a aldeídos e a funções éster, originados também da complexa estrutura da lignina [123]. No entanto, os biomateriais modificados mostraram sinais em 40, 36, 34 e 31 ppm, atribuídos aos carbonos incorporados na estrutura biopolimérica após a reação com etilenossulfeto. Os espectros de RMN  $^{13}\text{C}$  desses derivados tiolados do babaçu são mostrados na **Figura 38**.

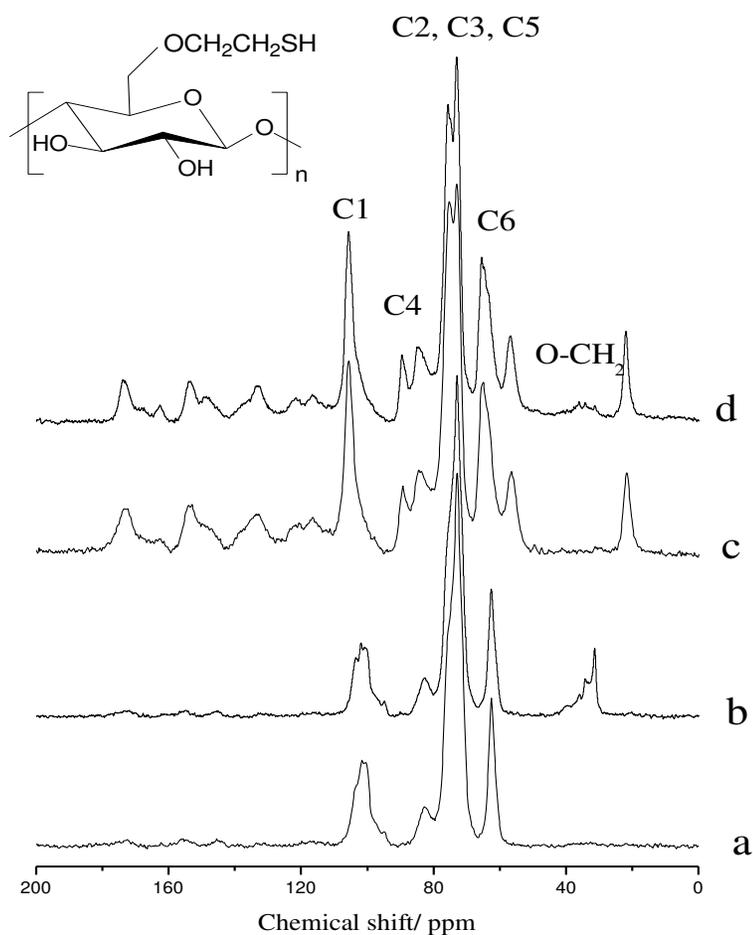


**Figura 38.** Espectros de RMN  $^{13}\text{C}$  de BCM (a), BCMS (b), BCE (c) e BCES (d).

## 7.5.2 Sorção

### 7.5.2.1 Efeito do pH e do ponto de carga zero

Uma vez que a eficiência dos processos de sorção é fortemente dependente do pH, o que afecta a carga superficial do adsorvente, o grau de ionização, e as espécies de sorbato, experimentos comparativos foram realizados em pH entre 1 e 6, como mostrado na **Figura 39**. O efeito do pH na eficiência de sorção de  $\text{Cu}^{2+}$  em íon BCMS e BCES diferem dos valores nulos, determinada para os derivados naturais. A sorção dos íons metálicos aumenta com o aumento do pH e atinge um valor máximo, a pH 6 para ambos os biomateriais BCMS e BCES. Deve-se notar que as alterações superficiais dos sorventes altera sua polarização de acordo com o valor do pH da solução e para o  $\text{pH}_{\text{PZC}}$  do sólido. A um pH mais baixo que o  $\text{pH}_{\text{PZC}}$  a superfície torna-se carregada positivamente e é o oposto para o pH mais elevado do que  $\text{pH}_{\text{PZC}}$ . As sorções de várias espécies aniônicas e catiônicas em tais sorventes podem ser explicados com base na concorrência de íons  $\text{H}^+$  ou  $\text{OH}^-$  com os sorbatos. É uma observação comum que a superfície absorve ânions favoravelmente a um pH mais baixo, devido à presença de íons  $\text{H}^+$ , enquanto que a superfície é ativa para a absorção de cátions em pH mais elevado, devido à acumulação de íons  $\text{OH}^-$ .

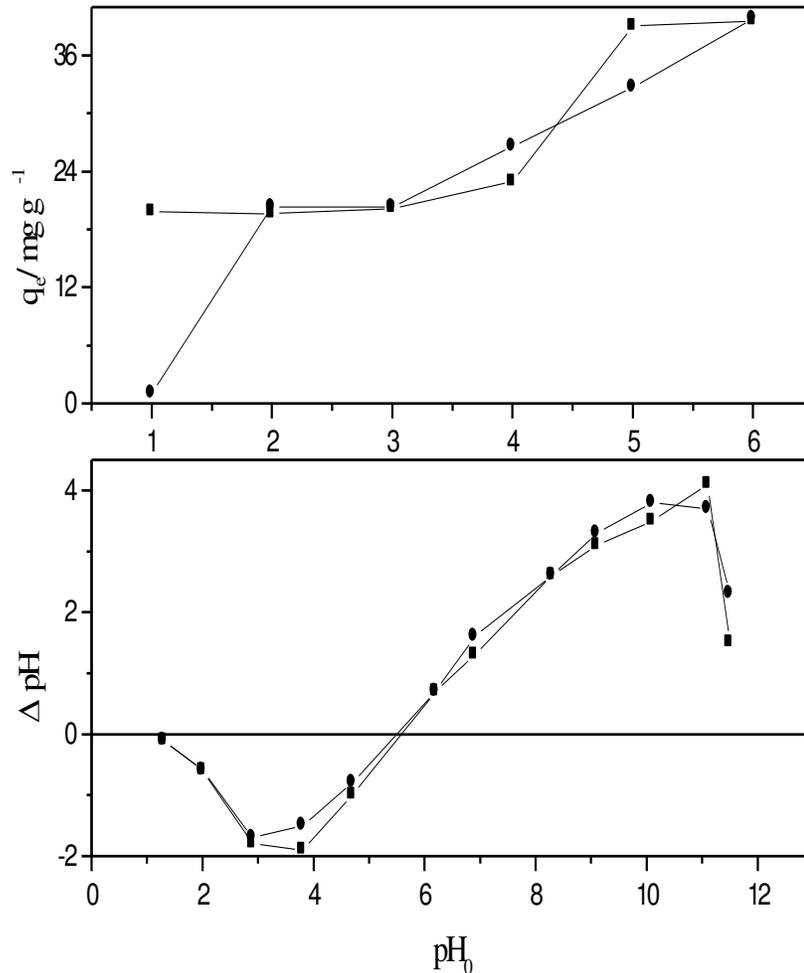


**Figura 39.** Efeito do pH na adsorção de  $\text{Cu}^{2+}$  aquoso por BCMS (■) and BCES (●) (a) e  $\text{pH}_{\text{PZC}}$  (b).

Para compreender o mecanismo de sorção, é necessário determinar o ponto de carga zero ( $\text{pH}_{\text{PZC}}$ ) do sorvente. Sorção de cátions é favorecida a um  $\text{pH} > \text{pH}_{\text{PZC}}$ , enquanto sorção de ânions comportar na condição oposta. Os valores de  $\text{pH}_{\text{PZC}}$  para BCMS e BCES são 5,6. Espera-se que em pH mais elevado a sorção seja favorável. Os experimentos de sorção foram, portanto, procedidos em pH 6. O perfil de adsorção de íons de metal nos biomateriais BCMS e BCES em função do  $\text{pH}_0$  também pode ser explicada com base na densidade de carga superficial de grupos funcionais, tais como hidroxilas, ácidos carboxílicos etc.. O aumento na absorção com  $\text{pH}_0$  pode ser atribuído

ao facto de que os cátions metálicos carregados positivamente são repelidos menos a valores de pH mais elevados, os resultados estão de acordo com relatos anteriores [24,25].

### 7.5.2.2 Efeito do tempo

Encontrou-se o equilíbrio em cerca de 30 minutos a  $298 \pm 1$  K, com um carregamento de  $1,0$  g de sorvente  $\text{dm}^{-3}$ , para uma concentração de sorbato de  $200$   $\text{mg dm}^{-3}$ , como mostrado na **Figura 40**.

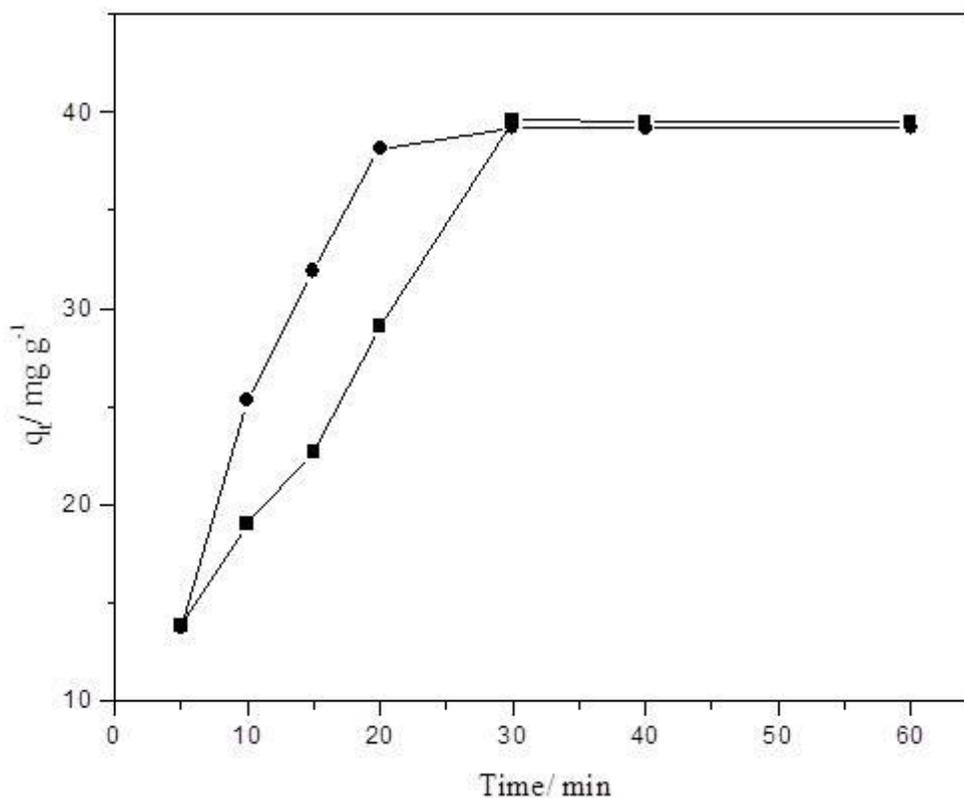


**Figura 40.** Cinéticas de adsorção de  $\text{Cu}^{2+}$  aquoso por BCMS (■) and BCES (●).

Os resultados foram semelhantes aos relatados na literatura para cobre, cádmio e chumbo em sorções com bagaço de cana [132]. Por outro lado, o tempo de equilíbrio

é menor do que outros, tais como em estruturas carbonáceas a partir de esterco de vaca [151] e de cascas de trigo, lentilha e arroz [145].

Os dados cinéticos foram ajustados ao modelo cinético de pseudo-primeira ordem cinética [28], expresso pela equação 11:

$$\log(q_e - q_t) = \log q_e - \frac{k_1 t}{2.303} \quad (11)$$

onde  $q_e$  e  $q_t$  referem-se à quantidade de cátion adsorvido ( $\text{mg g}^{-1}$ ), no equilíbrio e em qualquer outro tempo,  $t$  (min), respectivamente, e  $k_1$  é a constante de equilíbrio da taxa de pseudo-primeira ordem de sorção ( $\text{min}^{-1}$ ).

A constante de velocidade para a equação de primeira ordem foi determinada a partir do declive do  $\log (q_e - q_t)$  versus tempo. Se a cinética de primeira ordem é aplicável ao sistema em estudo, o  $\log (q_e - q_t)$  versus tempo, conforme representado pela equação 11, deve dar uma relação linear. Além disso, o  $q_e$  obtido a partir do gráfico deve também estar perto da  $q_e$  obtida experimentalmente a partir da concentração de cátions de  $200 \text{ mg dm}^{-3}$ . O coeficiente de correlação ( $R^2$ ) da equação de primeira ordem foi razoável, os valores calculados de  $q_e$  da plotagem do modelo cinético de primeira ordem foram pequenos, em comparação com os valores experimentais. Inaplicabilidade da equação Lagergren para descrever a cinética de adsorção de cobre foi também observada para a sorção utilizando turfa [152]. Os dados experimentais obtidos foram analisados utilizando um modelo de pseudo-segunda-ordem [140] de acordo com a seguinte equação 12:

$$\frac{t}{q_t} = \frac{1}{k_2 q_e^2} + \frac{t}{q_e} \quad (12)$$

onde  $k_2$  é a taxa constante de equilíbrio de pseudo-segunda-ordem de sorção ( $\text{g mg}^{-1} \text{ min}^{-1}$ ). Se o modelo cinético de pseudo-segunda ordem é aplicável ao sistema em estudo, a parcela de  $t/q_t$  contra o tempo, como dado na equação (12), deve dar uma relação linear. A taxa constante de adsorção de segunda ordem  $q_e$  foram determinados

a partir da inclinação e interceptação na plotagem  $t/qt$  versus tempo e os coeficientes de correlação na plotagem linear são melhores que 0,96 para BCMS e BCES. Os valores calculados  $q_e$  do modelo de pseudo-segunda ordem estão de acordo com os valores experimentais de  $q_e$ . Isto sugere que o sistema de adsorção segue o modelo de pseudo-segunda-ordem. Os parâmetros cinéticos estão mostrados na **Tabela 21**.

**Tabela 21.** Parâmetros cinéticos para sorção de  $\text{Cu}^{2+}$  em BCMS e BCES. Concentração inicial de  $\text{Cu}^{2+}$   $200,0 \text{ mg dm}^{-3}$ , com dose de  $1,0 \text{ g dm}^{-3}$  em pH 6,0 a  $298 \pm 1 \text{ K}$ .

| Ssorbente | $Q_{e, \text{exp}}$<br>( $\text{mg g}^{-1}$ ) | Pseudo-primeira-ordem                        |                                |       | Pseudo-segunda-ordem                         |  |  |       |
|-----------|---|--|--------------------------------|-------|--|--|--|-------|
|           |   | $q_{e,\text{cal}}$<br>( $\text{mg g}^{-1}$ ) | $k_1$<br>( $\text{min}^{-1}$ ) | $R^2$ | $q_{e,\text{cal}}$<br>( $\text{mg g}^{-1}$ ) | $k_2 \times 10^3$<br>( $\text{g mg}^{-1} \text{ min}^{-1}$ ) | $h$<br>( $\text{mg g}^{-1} \text{ min}^{-1}$ ) | $R^2$ |
| BCMS      | 39,6  | 69,5   | 0,13                           | 0,887 | 51,6   | 1,2  | 3,44   | 0,966 |
| BCES      | 39,2  | 80,2   | 0,19                           | 0,985 | 45,7   | 2,9  | 6,18   | 0,980 |

### 7.5.2.3 Isotermas

As isotermas modelo de Langmuir e Freundlich foram avaliados através de experimentos de sorção em solução aquosa em tempo de equilíbrio e condições de pH ideal. A isoterma de Langmuir [31] é apresentada aqui de uma forma geral linearizada:

$$\frac{C_e}{q_e} = \frac{1}{Q_{\text{max}}b} + \frac{C_e}{Q_{\text{max}}} \quad (13)$$

onde  $C_e$  é a concentração de equilíbrio do soluto ( $\text{mg dm}^{-3}$ ),  $q_e$  é a quantidade de soluto adsorvido por unidade de massa de sorvente ( $\text{mg g}^{-1}$ ),  $Q_{\text{max}}$  é a capacidade máxima de sorvente do sistema ( $\text{mg g}^{-1}$ ), e  $b$  é uma constante de equilíbrio de adsorção relacionado com a energia da sorção.

A equação de Freundlich descreve a isotérmica de sorção com a equação 14 [153]:

$$q_e = K_f C_e^{1/n} \quad (14)$$

onde  $q_e$  e  $C_e$  são as quantidades ( $\text{mg g}^{-1}$ ) adsorvidas no estado de equilíbrio e o concentração no equilíbrio do *todo* ( $\text{g dm}^{-3}$ ), respectivamente, e  $1/n$  e  $K_f$  são as constantes de Freundlich que correspondem a intensidade de sorção e da capacidade de sorção, respectivamente. Na isoterma de Langmuir o parâmetro  $Q_{\text{max}}$  indica a capacidade máxima de sorção do material. Dos coeficientes de correlação  $R^2$ , a aplicabilidade das equações isotérmicas de Langmuir e Freundlich podem ser comparadas, evidenciado ajuste favorável para o primeiro modelo.

O gráfico de sorção para o cobre sobre BCMS e biomateriais BCES e isoterma de Langmuir é mostrado na **Figura 41**, indicando uma homogeneidade da superfície dos sorventes. A maioria dos sistemas de iões metálicos relatados sugerem a aplicabilidade da equação de Langmuir, o qual assume uma cobertura monocamada e energia de sorção constante sobre a superfície adsorvente. [154]

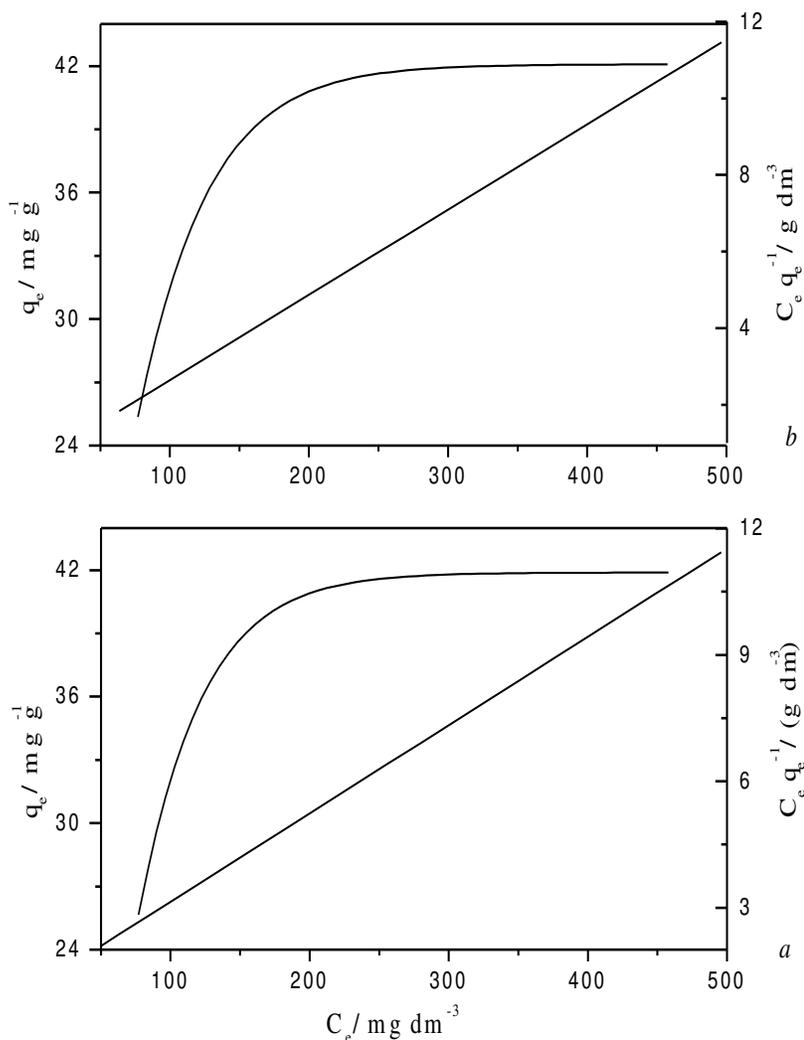


**Figura 41.** Isotermas de Langmuir para adsorção de  $\text{Cu}^{2+}$  aquoso em BCMS e BCES,  $298 \pm 1$  K and pH 6.

Os resultados de adsorção de cobre em BCMS e BCES foram comparados com outros sistemas e mostram maior desempenho para estes biomateriais sintetizados. A investigação de sorção de cobre sobre a casca de arroz modificado por ácido tartárico apresentou a capacidade máximo de sorção de cobre de  $29 \text{ mg g}^{-1}$  [155].

A eficiência da serragem na remoção de cobre e a capacidade de sorção baseada no modelo de Langmuir deu  $6,92 \text{ mg g}^{-1}$  álamo de serraem e  $12,70 \text{ mg g}^{-1}$

para outras serragens [108]. O efeito do tratamento com ácido sulfúrico em serragem de choupo deu uma capacidade de sorção de 13,95 mg g<sup>-1</sup> contra 5,43 mg g<sup>-1</sup> para a serragem tratada, que se seguiu a uma isotérmica de Langmuir [156]. No caso de absorção de cobre por espigas de milho tratadas com ácido sulfúrico concentrado, a capacidade máxima obtida a partir da isotérmica de Langmuir foi 31,45 mg g<sup>-1</sup> [153]. A sorção de íons metálicos bivalentes, particularmente de cobre, zinco, níquel, cobalto e chumbo em casca de banana e laranja tratadas com ácido ou álcali foi realizado e os relatados das capacidades máximas de adsorção de cobre com cascas de banana e de laranja foram 4,75 e 3,65 mg g<sup>-1</sup>, respectivamente [157]. A capacidade máxima de 47,5 e 47,7 mg g<sup>-1</sup> obtidos a partir das isotérmicas de Langmuir para o mesmo cátion para BCMS e BCES são maiores do que os anteriormente relatados, o que sugere que estes biomateriais sintetizados tem um alto desempenho na remoção de cátions na interface sólido/líquido. Os parâmetros do ajuste às equações linearizadas de Langmuir e Freundlich estão mostrados na **Tabela 22**.

**Tabela 22.** Coeficientes das equações de Freundlich e Langmuir da adsorção de Cu<sup>2+</sup> por BCMS e BCES a 298 ± 1 K.

| Sorvente | Freundlich     |      |   | Langmuir       |                                      |  |
|----------|----------------|------|---|----------------|--------------------------------------|--|
|          | R <sup>2</sup> | n    | K <sub>f</sub> (dm <sup>3</sup> g <sup>-1</sup> ) | R <sup>2</sup> | b(dm <sup>3</sup> mg <sup>-1</sup> ) | Q <sub>max</sub> (mg g <sup>-1</sup> ) |
| BCMS     | 0,892          | 3,70 | 8,73  | 0,996          | 0,0207                               | 47,5                                   |
| BCES     | 0,896          | 3,58 | 8,30  | 0,995          | 0,0200                               | 47,7                                   |

## 7.6 Conclusão

Os resíduos agrícolas de babaçu natural BCM e BCE demonstraram ser absorventes impróprios para íons metálicos de soluções aquosas. No entanto, os novos biopolímeros sintetizados, BCES e BCMS, adquiriram propriedades relevantes a

atuarem favoravelmente na remoção de cátion no pH máximo de sorção, pH 6. Com base na diferença de funcionalização de  $20,2 \pm 0,07$  e  $86,7 \pm 0,01$  mg g<sup>-1</sup> para os derivados de mesocarpo e de epicarpo derivados, deve ser esperado a melhor sorção para BCES. No entanto, para além dos átomos de enxofre básicos ligados às cadeias pendentes, ainda há outros grupos disponíveis como os cetônicos, os aldeídicos e os ácidos carboxílicos na superfície BCES, os quais também podem participar da complexação do cobre, para se obter quase as mesmas quantidades de soluto adsorvido, 39,6 e 39.2 mg g<sup>-1</sup> para BCMS e BCES, respectivamente.

A sorção de equilíbrio ajustou-se mais adequadamente ao modelo cinético de pseudo-segunda ordem cinética para cobre pelos biopolímeros BCMS e BCES, como demonstrado pela isoterma de sorção típicas e os resultados foram melhor ajustados ao modelo matemático de Langmuir. O equilíbrio entre os íons de metal na interface sólido/líquido nos biomateriais quimicamente modificadas foi alcançado rapidamente, no curto espaço de tempo de 30 minutos. Os resultados mostraram que estes materiais biológicos podem ser usados com sucesso como adsorventes para a remoção de cobre a partir de águas residuais.

A.V. Pires, S.A.A. Santana, C.W.B. Bezerra, H.A.S. Silva, J.A.P. Chaves, J.C.P. Melo, E.C. Silva Filho, C. Airoidi, “**Epicarp and mesocarp of babassu (*Orbignya speciosa*): characterization and application in copper phthalocyanine dye removal**”, J. Braz. Chem. Soc., 22, 21-29 (2011).

## 7.7 Métodos

### 7.7.1 *Materiais e reagentes*

Os componentes mesocarpo e epicarpo foram extraídos dos frutos naturais do babaçu, adquiridas na cidade de São Luís, Maranhão, Brasil. As partes individuais foram utilizadas após o esmagamento do material em bruto em tamanhos de partícula na gama de 0,088 - 0,177 mm. O corante Turquesa de remazol, CI 74160, foi fornecido pela Indústria de Toalhas de São Carlos, localizado no Estado de São Paulo, Brasil. O

produto reagentes químicos NaOH, HCl, KCl, biphtalata de potássio (C<sub>8</sub>H<sub>5</sub>O<sub>4</sub>K) e Na<sub>2</sub>B<sub>4</sub>O<sub>7</sub> · 10H<sub>2</sub>O foram todos de grau analítico. Celulose microcristalina na forma de pó (Aldrich), ca. 20 mm, foi utilizada como uma referência na caracterização dos biopolímero estudados no presente trabalho.

### **7.7.2 Caracterização da biomassa**

Os espectros de IV foram obtidos com um espectrofotômetro FTIR MB-Bomem com uma resolução de 4 cm<sup>-1</sup>, utilizando pastilhas de KBr, na região entre 4000 – 400 cm<sup>-1</sup>. O Carbono, nitrogênio e enxofre dos compostos foram analisadas por meio de um espectrofotômetro Perkin-Elmer 2400 Série II analisador de microelementos. As curvas termogravimétrica (TG) foram realizadas em um instrumento TGA-50 Shimadzu sob fluxo de nitrogênio de 0,50 cm<sup>3</sup> s<sup>-1</sup>, no intervalo de temperatura de 298 – 1000 K, com uma taxa de aquecimento de 0,167 K s<sup>-1</sup> e massa da amostra inicial de 10 mg. Os espectros de RMN <sup>13</sup>C CP/MAS no estado sólido foram obtidos num espectrômetro Bruker AC 400 /, utilizando frequências de 75,47 MHz no ângulo mágico de rotação de 4 kHz. Os padrões de difração de raios X foram registados utilizando um difratômetro Shimadzu XD3-A para amostras em pó com radiação Cu-K $\alpha$ ,  $\lambda$  = 1,5418 nm, a 30 kV, 20 mA e 2 $\theta$  na faixa de 5 a 50 °. As medições de pH foram obtidos usando instrumento DM-21 Digimed.

### **7.7.3 Sorção**

A capacidade das superfícies para extrair o corante têxtil turquesa de remazol a partir de soluções de água duplamente destilada foi avaliada através das isotérmicas de adsorção em pH 6,0. A variação de adsorção em função do pH (1,00 - 13,0) foi analisada pela utilização de soluções tampão adequadas. Em condições de equilíbrio, os processos de troca na interface sólido/líquido pode ser caracterizado por a quantidade (mg) sorvido por grama de suporte. As experiências de adsorção foram realizadas em batelada sob agitação a 298 ± 1 K, utilizando 100 mg do mesocarpo ou epicarpo modificados suspensos em 10,0 cm<sup>3</sup> de soluções aquosas com concentrações de corante variando de 13,6 - 54,4 mg dm<sup>-3</sup>. As suspensões foram agitadas durante 60

min e o tempo necessário foi estabelecida a partir de experiências anteriores, para garantir a absorção máxima. No final deste processo, o sólido foi separado por filtração e as concentrações do corante sorvido pela biomassa foram determinadas pela diferença entre as concentrações inicial e final da solução aquosa encontrada no sobrenadante, utilizando um espectrofotômetro Varian AA 50 no comprimento de onda 620 nm. A quantidade de corante adsorvido, [158]  $q_e$  (mg g<sup>-1</sup>), foi calculada com a equação 15:

$$q_e = \frac{C_i - C_f}{W} \times V \quad (15)$$

onde  $C_i$  e  $C_f$  são as concentrações inicial e final de corante em equilíbrio na fase aquosa (mg dm<sup>-3</sup>), respectivamente,  $V$  é o volume de solução de corante (dm<sup>3</sup>) e  $W$  (g) é a quantidade de mesocarpo ou epicarpo empregada.

O mecanismo proposto de adsorção foi investigado através do ajuste dos resultados dos dados cinéticos das reações de pseudo primeira e segunda ordem [159], como dado pelas equações 16 e 17, respectivamente.

$$\log(q_e - q_t) = \log q_e - \frac{k_1}{2.303} \times t \quad (16)$$

$$\frac{t}{q_t} = \frac{1}{k_2 q_e^2} + \frac{1}{q_e} \times t \quad (17)$$

onde  $q_e$  e  $q_t$  são as quantidades de corante adsorvido (mg g<sup>-1</sup>), no equilíbrio e no tempo  $t$ , respectivamente,  $k_1$  (min<sup>-1</sup>) é a constante de velocidade de adsorção de primeira ordem e  $k_2$  (g mg<sup>-1</sup> min<sup>-1</sup>) é a constante de velocidade de adsorção de segunda ordem.

As isotermas de Langmuir e de Freundlich isotermas foram empregados para analisar os dados experimentais de adsorção em suas formas linearizadas[160], equações 18 e 19, respectivamente. A isoterma do modelo escolhido foi aquele cujo linearização forneceu o melhor ajuste aos dados experimentais, isto é, o melhor valor de coeficiente de correlação (R).

$$\frac{C_e}{q_e} = \frac{1}{q_{\max} K_{ads}} + \frac{C_e}{q_{\max}} \quad (18)$$

$$\log q_e = \frac{\log C_e}{n} + \log K_f \quad (19)$$

onde  $C_e$  é a concentração de corante no equilíbrio,  $q_e$  é a quantidade de corante adsorvido,  $q_{\max}$  é a capacidade máxima de adsorção,  $K_{ads}$  é a constante de Langmuir, e  $n$  e  $K_f$  são constantes de Freundlich.

## 7.8 Resultados e Discussão

### 7.8.1 Caracterização da biomassa

Análise elementar deu para mesocarpo 39,23, 6,70, 0,33 %; epicarpo 46,72, 6,12, 0,51 % e celulose 41,95, 6,21, 0,18 % para o carbono, hidrogênio e nitrogênio, respectivamente. Estes resultados mostram que os biopolímeros mesocarpo e epicarpo obtidos a partir de derivados de baixo custo de babaçu têm composições elementares próximas as da celulose.

A celulose apresentou bandas em em 3400-3300  $\text{cm}^{-1}$  atribuídas aos estiramentos (O-H). As bandas no intervalo de 2800-3000  $\text{cm}^{-1}$  são de estiramentos (C-H) de  $\text{CH}_2$  e  $\text{CH}_3$ . A banda em 1639  $\text{cm}^{-1}$  corresponde as deformações (O-H) dos grupos hidroxila celulósicos e de moléculas de água adsorvida; entre 1200 – 1000  $\text{cm}^{-1}$

estão relacionadas aos estiramentos (C-O) [3]. No mesocarpo as bandas em 860, 769 e 710  $\text{cm}^{-1}$  são relacionadas às vibrações de ésteres e anéis aromáticos monosubstituídas devido à fracção de lignina. Para o epicarpo, as diferenças mais significativas são em 1740  $\text{cm}^{-1}$  estiramento (C=O) de ésteres, e em 1650  $\text{cm}^{-1}$   $\delta(\text{C-O-H})$  de álcoois aromáticos. As bandas em 1610 - 1460  $\text{cm}^{-1}$  referem-se a  $\nu(\text{C=C})$  de anéis aromáticos, vibrações dos esqueletos aromáticos, deformação do anel aromático. As bandas em 1248  $\text{cm}^{-1}$  são atribuídas a  $\nu(\text{C-O-C})$  e em 1161  $\text{cm}^{-1}$  estão associados às ligações  $\beta$ -1,4. As bandas associadas ao benzeno tetra- e trissubstituídos vibrações [136] aparecem em 853 e 772  $\text{cm}^{-1}$ , respectivamente. Como apresentado na **Figura 36**.

Os espectros de RMN os polissacarídeos apresentaram para o carbono 1 celulósico, um sinal em 104 ppm. Para o carbono 4 dois picos distintos estão disponíveis a 88 e 83 ppm, os quais foram atribuídos ao átomo de carbono associado a regiões cristalinas e amorfas, respectivamente [6]; carbonos 2, 3 e 5, com ambientes químicos próximos, foram atribuídos aos sinais em 71 – 75 ppm. Os sinais entre 64 e 62 ppm foram atribuídos ao carbono 6 em regiões cristalinas e amorfas[3], respectivamente. O espectro epicarpo é afectado pela presença de uma maior quantidade de lignina nesta parte do fruto de babaçu, evidenciada através do sinal a 22 ppm, relacionado aos grupos metílicos da lignina. Os outros sinais tais como 116 – 120, 133 e 149 – 153 ppm, são atribuídos aos carbonos aromáticos. Os sinais alargados em 160 e 178 ppm correspondem aos carbonos carbonílicos de aldeídos, cetonas, ésteres e ácidos, também provenientes da lignin, de hemiceluloses e as ligaões destes na formação do compósito natural [123]. Como mostrados na **Figura 38**.

Padrões de difração de raios X para a celulose e para os componentes lignocelulósicos e as reflexões dos planos cristalinos são todos provenientes dos padrões de difração celulósicos,  $2\theta = 22^\circ$ , como mostrado na **Figura 42**. O mesocarpo por apresentar alta concentração de celulose, em  $2\theta = 14^\circ$  e  $16^\circ$  surgirão dois picos distintos. Nos dois componentes de babaçu, dois picos são indentificados nesta região, e o alto teor de celulose define mais o pico, mas quando a fibra contém uma maior quantidade de componentes como a lignina, hemicelulose e celulose amorfa, os dois picos são aparecem como um único alo ampla [136].

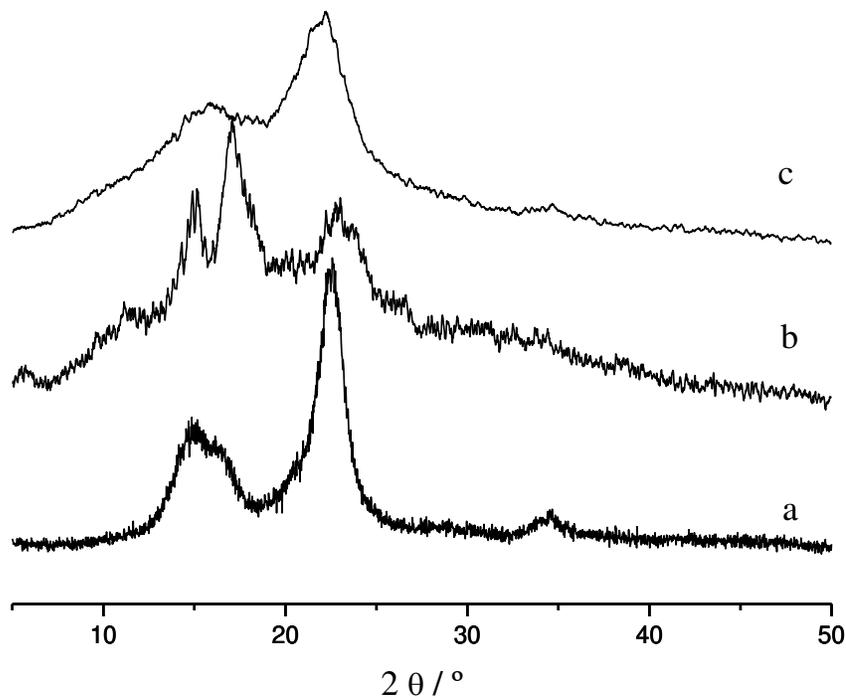


**Figura 42.** Difratoigramas de raios X da celulose (a), do mesocarpo (b) e do epicarpo (c) de babaçu.

As curvas termogravimétricas obtidos em atmosfera inerte para a celulose, mesocarpo e epicarpo apresentaram apenas um evento no processo de decomposição térmica abrangendo o intervalo de temperatura de 536 - 647 K, correspondendo a uma perda de massa de 92 % [3]. No caso do mesocarpo a primeira etapa ocorre até 375 K, corresponde à perda de massa de 12 %, seguido de uma outra perda de massa de 62 % no intervalo de 477 – 623 K; o epicarpo mostrou perdas de massa de 11 % a 353 K e de 56 % entre 609 e 638 K, para as mesmas condições experimentais, como mostrados na **Figura 43**.

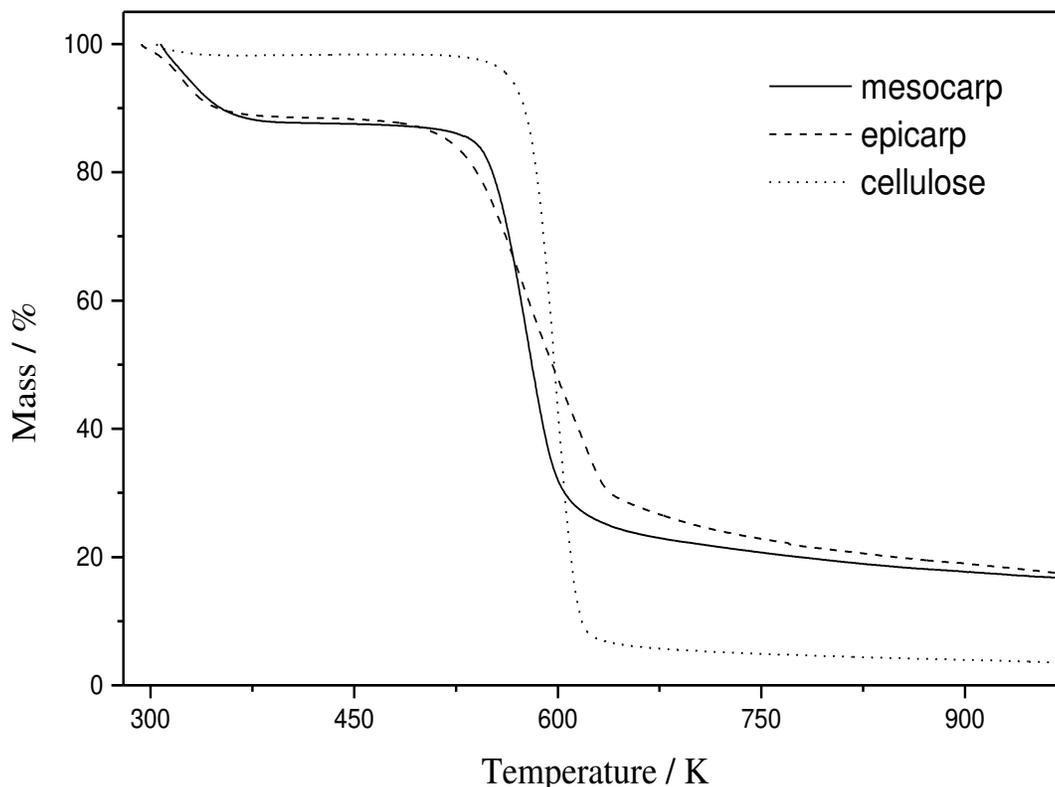


**Figura 43.** Curvas termogravimétricas da celulose, mesocarp e epicarp.

A primeira etapa de decomposição pode ser atribuído à liberação de moléculas ricas em carbono e água sorvida, enquanto o segundo estágio é devido à decomposição de material orgânico, por exemplo, quebra de fibras, processos de caramelização e formação de estruturas grafênicas, assemelhando-se a outros materiais lignocelulósicos cujos componentes principais são a celulose, lenhina e hemiceluloses[136,161]

### 7.8.2 Sorção

As curvas de adsorção do corante turquesa de remazol pelo mesocarp e epicarp em função do tempo atingiu o equilíbrio, em 20 e 60 min, respectivamente,

mantendo-se constante até 3 h. Os dados de adsorção foram ajustados aos modelos cinéticos de pseudo primeira ordem e de pseudo segunda ordem. O modelo de pseudo-primeira ordem apresentou coeficientes de correlação linear mais baixos para o mesocarpo e epicarpo, com valores de  $q_e$  de 0,03 e 0,17  $\text{mg g}^{-1}$ , respectivamente, com a maior diferença em relação aos valores experimentais  $q_e$ . Os melhores coeficientes de correlação para os mesocarpo ( $R = 0,999$ ) e epicarpo ( $R = 0,999$ ) foram fornecidos pelos ajustes ao modelo de pseudo-segunda ordem, indicando uma quimissorção como etapa determinante no mecanismo de adsorção. A constante de velocidade obtida foi um  $k_2$  de 1,43 e 0,31  $\text{g mg}^{-1} \text{min}^{-1}$  para o mesocarpo e epicarpo, respectivamente. Outros parâmetros cinéticos estão mostrados na **Tabela 23**.

**Tabela 23.** Parâmetros cinéticos para sorção de Turquesa de Remazol em babaçu (BB) pelo ajuste às equações de pseudo-primeira-ordem (P1) e pseudo-segunda-ordem (P2) para mesocarpo (Mc) e epicarpo (Ep)

| BB | $q_{e,exp}$        |                                     | P1                       |       |  | P2                       |       |  |
|----|--------------------|-------------------------------------|--------------------------|-------|--|--------------------------|-------|--|
|    | $\text{mg g}^{-1}$ | $k_1 \times 10^2 / \text{min}^{-1}$ | $q_e / \text{mg g}^{-1}$ | $R^2$ | $k_2 / \text{g mg}^{-1} \text{min}^{-1}$ | $q_e / \text{mg g}^{-1}$ | $R^2$ | $h / \text{mg g}^{-1} \text{min}^{-1}$ |
| Mc | 1.44               | 2.1                                 | 0.03                     | 0.701 | 1.43                                     | 1.40                     | 0.999 | 2.8                                    |
| Ep | 2.38               | 2.7                                 | 0.17                     | 0.766 | 0.31                                     | 2.36                     | 0.999 | 1.7                                    |

Os valores de  $q_e$  obtidos pela equação 3 foram 1,40 e 2,36  $\text{mg g}^{-1}$ , demonstrando boa concordância com os valores experimentais de 1,44 e 2,38  $\text{mg g}^{-1}$ . A partir dos valores  $k_2$  e  $q_e$ , as velocidades iniciais de adsorção ( $h$ ) foram determinadas a serem 2,8 e 1,7  $\text{mg g}^{-1} \text{min}^{-1}$ , pela equação 6.

$$h = k_2 \times q_e^2 \tag{6}$$

Deste modo, a adsorção inicial em mesocarpo foi quase duas vezes maior do que no epicarpo.

A cinética de adsorção de muitos corantes em materiais diferentes é frequentemente considerada de segunda ordem [9]. A aplicabilidade do modelo de pseudo segunda ordem sugere que a quimissorção pode ser a etapa limitante na

velocidade, a qual controla os processos de adsorção. Em geral, este modelo tem a seguinte vantagem: a capacidade de adsorção, a taxa constante de pseudo segunda ordem e a taxa de adsorção inicial podem ser determinadas [162].

A isoterma de adsorção representa as concentrações de corante adsorvido no equilíbrio ( $q_e$ ) de acordo com a quantidade adsorvida por grama de sorvente. O perfil das isotermas de adsorção de turquesa de remazol atinge um patamar a medida em que se aumenta a concentração do corante. Assim, a quantidade máxima do corante adsorvido pelas matrizes foi de 1,44 e 2,38 mg g<sup>-1</sup> para o mesocarpo e epicarpo, respectivamente.

As análises dos coeficientes de correlação mostraram que o melhor ajuste para os dados experimentais seguiram o modelo de Freundlich tanto para epicarpo e mesocarpo. Os parâmetros  $n$  e  $K_f$  são as constantes do sistema, que atuam como indicadores da capacidade de adsorção e intensidade, respectivamente, foram determinados a partir da interseção e a inclinação da linha reta da equação obtida através da representação gráfica  $\log q_e$  versus  $\log C_e$ .

O modelo de Langmuir não apresentou ser o melhor modelo para ajustar os dados experimentais culminando em resultados com ajuste linear pobre para a adsorção do corante sobre ambos epicarpo e mesocarpo. O mesocarpo de babaçu e outros adsorventes de baixo custo, têm sido investigados para a remoção de vários corantes. Os resultados obtidos também indicam que a adsorção isotérmica se ajusta melhor ao modelo de Freundlich que ao análogo modelo de Langmuir [9, 163] cinzas ricas em cálcio, foram estudadas para a adsorção de Vermelho do Congo a partir de solução aquosa e o processo de adsorção obedeceu ao modelo cinético de pseudo segunda ordem e a isoterma de adsorção seguindo o modelo de Freundlich [164]. Por outro lado, a adsorção de verde brilhante sobre o pó de folhas de Neem produziu bons ajustes ao modelo de Langmuir, bem como para o de Freundlich [165].

No entanto, a equação de Freundlich foi preferida para a descrição das isotermas de corantes reativos, embora as isotermas de corantes ácidos e básicos foram melhores ajustados ao modelo de Langmuir, dependendo da concentração do corante. Estas investigações confirmam que a equação empírica de Freundlich é aplicável para

a adsorção de solutos individuais dentro de um intervalo fixo de concentration [166], como mostrado na **Tabela 24**.

**Tabela 24.** Parâmetros do ajuste ao modelo isotérmico de Freundlich para adsorção em babaçu.

| <b>Biomass</b> | n    | $K_f$ | $R^2$ |
|----------------|------|-------|-------|
| Mesocarp       | 0.90 | 0.03  | 0.931 |
| Epicarp        | 0.96 | 0.11  | 0.923 |

### 7.8.2.1 Efeito do pH

A adsorção do corante turquesa de remazol pelos epicarpo e mesocarpo de babaçu aumenta consideravelmente com o aumento da acidez, como mostrado na **Figura 44**. De acordo com estes resultados, o pH ótimo para a remoção de corante da amostra é, aparentemente, de 1,0. Nesta condição, as quantidades máximas de o corante adsorvido foram 3,94 e 3,97 mg g<sup>-1</sup>, o que corresponde a 96,6 e de 99,5 % para o mesocarpo e epicarpo, respectivamente. Embora a adsorção em pH 6,0 deu valores mais baixos, 1,44 e 2,38 mg g<sup>-1</sup>, parece que a condição mais adequada para as aplicações em soluções aquosas. Uma tendência semelhante foi observado para a adsorção do corante Vermelho Direto em medula banana [167], com máximo de remoção de 80% com um pH inicial de 3,0. A adsorção de Vermelho do Congo em fibra tem explicação por dois mecanismos possíveis para o efeito de pH: (a) a interação eletrostática entre os grupos possíveis desprotonados com o corante ácido e (b) da reação química entre o sorbato e os sorventes [168]. Resultados semelhantes do efeito do pH também foram relatados para a adsorção de Amarelo Ácido e Vermelho Reativo Red 189 [169-171].

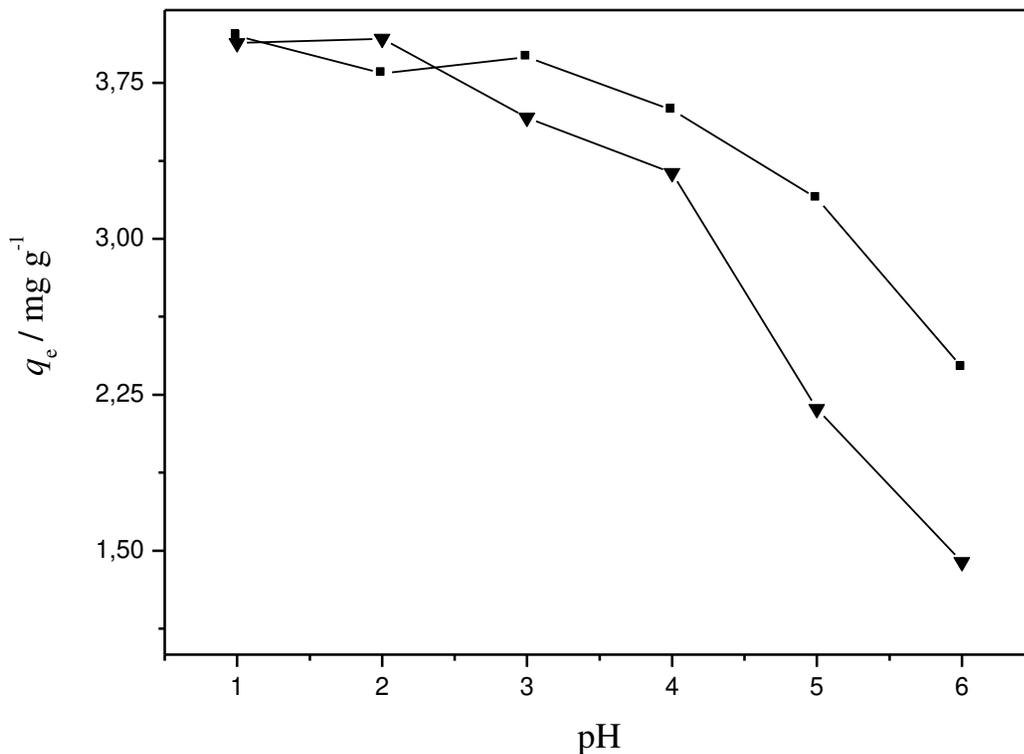


**Figura 44.** Efeito do pH no processo adsorptivo do corante turquesa de remazol em mesocarpo (▼) e em epicarpo (■).

Os principais componentes do mesocarpo e epicarpo são a celulose, lignina e hemicelulose. Estes produtos naturais contêm um grande número de grupos funcionais, incluindo hidroxilas fenólicas bem como grupos ácidos carboxílicos. A interação entre as moléculas de corante com esses grupos funcionais podem seguir um padrão extremamente complicada. À medida que o pH do sistema diminui, o número de sítios de carga negativa superficiais também diminui, com o conseqüente aumento do número de sítios positivos sobre na superfície, favorece a adsorção dos corantes aniônicos devido à atração eletrostática, tal como é esperado para o processo de eletroneutralização.

Como mencionado anteriormente, os materiais lignocelulósicos têm sido estudados extensivamente como sorventes para a remoção do corante. No entanto, ainda há muito a ser feito para compreensão dos mecanismos. Em particular, as

moléculas de corante apresentam várias estruturas diferentes e este é um dos fatores mais importantes que influenciam a adsorção e seus mecanismos [172, 173]. No entanto, algumas sugestões são feitas levando em conta a composição e os cromóforos a serem sorvidos no biopolímero. Conforme relatado aqui, o mesocarpo e epicarpo do fruto do babaçu apresentam os grupos funcionais capazes de estabelecer interações, tais como ligações hidrogênio, interações  $\pi$ - $\pi$  aromática e interações de van der Waals. Aqui, o estabelecimento de ligações hidrogênio entre prótons ou pares de elétrons não ligantes dos materiais lignocelulósicos com os elétrons  $\pi$  da ligação dupla disponíveis ou os centros ácidos dos corantes é proposto. Outra possibilidade é a de considerar que os anéis aromáticos presentes na lignina podem interagir com o cobre localizado na estrutura de corante Turquesa de Remazol

### 7.9 Conclusões

Os estudos de difração de raios X indicaram que os componentes do mesocarpo e epicarpo obtidos a partir de frutos de babaçu apresentam uma fração de baixa cristalinidade, como observado para outros materiais lignocelulósicos. Este resultado é também apoiado por dados de RMN  $^{13}\text{C}$ , onde os sinais de deslocamento químico para o mesocarpo, dessas porções cristalinas, são atribuídos a celulose, enquanto o epicarpo mostra sinais característicos de lignina. A análise térmica das fibras revelaram que os processos de degradação ocorrem de acordo com os seus constituintes celulose, hemicelulose e lignina. Os resultados de IV revelaram absorções típicas de O-H, C-H e C-O, característicos das frações químicas destes materiais, os quais podem adsorver o corante Turquesa de Remazol em um processo dependente do pH. A cinética de adsorção é melhor descrita pelo modelo de pseudo segunda ordem e as isotermas de ajustar ao modelo de Freundlich. Com base na capacidade de adsorção significativa demonstrada por estes materiais para remoção do turquesa de remazol, pode ser proposto como uma alternativa a baixo custo para remoção em soluções aquosas. Por outro lado, a capacidade de adsorção foi maior para o epicarpo, devido às maiores quantidades de grupos funcionais disponíveis neste compósito de celulose, ligninas e hemiceluloses. Tendo em conta este conjunto de resultados, é

razoável inferir que os componentes dos frutos do babaçu podem ter muitas aplicações potenciais na remoção de corantes.

## 7.10 Sobre os três artigos anteriores

O Brasil hoje é exportador de cachaça e esperamos em breve poder contar com mais esta necessidade para conseguir que o governo sancione uma lei, sobre a necessidade do desenvolvimento de filtros e estes poderiam ser produzidos a partir da tecnologia desenvolvida em nossos laboratórios. Pois, além disso, o problema em se usar carvão ativo como material para sorção do cobre contaminante da cachaça é devido aos aromas também serem removidos nesse processo, ao contrário do nosso material que não retira estes aromas.

Essa vantagem sobre o carvão ativo é muito importante, pois a cachaça é produzida pela indústria de bebidas, assim os aromas são absolutamente relevantes. Assim foram sintetizados três biopolímeros diferentes, os quais podem apresentar diferentes desempenhos na remoção do metal cobre, e outros traços que estiverem presentes. Ainda, os grupos próximos ao centro carboxílico de troca são diferentes, podendo apresentar diferentes interações com as moléculas responsáveis pelo aroma, como é mais esperado para o biopolímero modificado com anidrido ftálico.

É interessante se trabalhar com biomassa lignocelulósica devido aos regionalismos intrínsecos que envolvem o estudo. Nesse conjunto foi empregado o babaçu como matéria prima para ser modificada e então, os biopolímeros obtidos aplicados em estudos de remoção de cobre em cachaça, remoção de cobre aquoso com um babaçu modificado quimicamente com tiol e remoção de corante. O babaçu é uma palmeira muito comum no Maranhão e as aplicações mais nobres são na alimentação de animais e de seres humanos como foco de pesquisa para erradicação da fome entre estudantes de escolas públicas em comunidades de baixa renda, empregado sempre como um aditivo alimentício. Com a extração do ácido láurico das amêndoas, este pode ser empregado na manufatura de artesanatos nas comunidades locais maranhenses. Outra aplicação histórica seria a queima para produção de energia em aplicações rurais ou em aplicações de baixa demanda energética.

## Capítulo 7 – Experimentações com Babaçu

O procedimento de funcionalização de celulose com anidridos fundidos se mostrou bem aplicável no desenvolvimento de ‘filtros’ para remoção de cobre em cachaça. Assim, caso a tecnologia fosse aplicada, seria possível encontrar um alambique maranhense com produção de cachaça livre de cobre e destilação realizada com energia proveniente da queima também do babaçu. A tecnologia desenvolvida para um suporte ‘técnico’ foi plenamente aplicada a uma matéria prima natural e não tratada e os estudos de troca catiônica aplicados como melhor solução para um problema real. A presença de metal hepatotóxico em bebidas provenientes de destilação em tacho de cobre torna indesejável do ponto de vista de obtenção artesanal, semi-industrial e mesmo industrial.

O babaçu poderia também ser empregado em tinturarias locais como suporte para remoção dos corantes dos efluentes, os quais se não respeitados ocasionam a diminuição da qualidade da água, solo e vida local. A remoção pode se dar sem qualquer modificação química, apenas pelo controle do pH.

## 8 Conclusão

A celulose e os lignocelulósicos do babaçu se mostraram bons suportes para ligação de novas moléculas nas estruturas, através de procedimentos em fase heterogêna, mas apesar de se ter trabalhado em fase heterogênea, elevados graus de substituição nesses materiais foram obtidos.

Desenvolveu-se ou se adaptou os procedimentos para que se obtivessem os maiores graus de funcionalização desses biopolímeros. As reações com esses materiais naturais foram capazes de ligar grandes quantidades de moléculas reagentes nas superfícies de todos os biopolímeros, mostrando que as rotas empregadas são válidas para o desenvolvimento de suportes sólidos modificados para remoção de contaminantes em líquidos.

As reações mais importantes, pensando-se em escala industrial, são os materiais esterificados na ausência de solvente, pois os processos são rápidos, de alto desempenho, com fácil remoção dos reagentes. Essa rota sintética deu origem à patente que defende a remoção de cobre em aguardente através de carboxilatos de sódio imobilizados na superfície de mesocarpo de babaçu.

Quase todos os biopolímeros apresentaram bom desempenho, podendo ser empregados como técnica alternativa aos processos de precipitação química de contaminantes. Outro ponto a ser ressaltado é a possibilidade desses biopolímeros serem reutilizados após a lixiviação dos contaminantes, o que os torna importantes promessas como alternativa aos métodos atualmente empregados em remoção de contaminantes em líquidos.

A oxidação da celulose com periodado é seletiva e a reação é sensível à temperatura, luz e valores extremos de pH, pois do contrário o material é sobre-oxidado ao ácido correspondente, ou mesmo o metaperiodato, através de fotocatalise, poder ser degradado ao gerar ozônio. Trabalhou-se para se otimizar a reação, no sentido de se obter o máximo de oxidação com o mínimo de despolimerização das cadeias celulósicas.

O ancoramento direto das aminas na celulose oxidada apresenta a vantagem de se ter iminas, ou aminas secundárias após a etapa de redução dos grupos imina e

essas são ligações mais estáveis frente à hidrólise, se comparadas às amidas formadas nas reações dos biopolímeros esterificados com aminas ou formadas na reação entre os materiais aminados com os anidridos. Entretanto, a provável separação celulose/celulose modificada quando em soluções aquosas é um problema evidente, principalmente para as reações do 2,3-dialdeído-celulose com etileno-1,2-diamina.

Os biopolímeros, principalmente os aminados, não resistem às severas condições das rotas de esterificação com anidridos fundidos, apesar de serem interessantes, porém, realizou-se tratamento com ultrassom para se aumentar as taxas de reação. Todavia, o não emprego dos ativadores de carbonila acarreta materiais de baixo teor de nitrogênio.

Assim para se estudarem reações ácido/base na interface sólido/líquido é indispensável que os materiais permaneçam sólidos ao longo do tempo, sem a passagem completa, ou parcial, das moléculas componentes à solução e isso é absolutamente válido para os estudos calorimétricos, nos quais os procedimentos se passam em condições muito próximas aquelas realizadas para experimentos de sorção.

A celulose e os materiais lignocelulósicos, com pequenos graus de liberdade das cadeias, são excelentes suportes sólidos para se trabalhar no desenvolvimento destes materiais modificados, conseguindo-se superfícies estáveis para se experimentarem reações ácido/base, bem como se determinar as grandezas termodinâmicas envolvidas nestas reações em superfícies.

Finalmente, é necessário ressaltar que o biopolímero celulose ou mesmo os lignocelulósicos não são tão fáceis de serem utilizados em rotas vantajosas de modificação química, como se constata na literatura, mas os resultados aqui apresentados abrem um amplo campo de pesquisa a ser explorado. Os novos biopolímeros sintetizados por certo trarão aplicações em vários outros ramos da ciência, mesmo para um futuro próximo.

## 9 Referências

- [1] Castro, G. R., Alcântara, I.L., Roldan, P.S., Bozano, D.F., Padilha, P.M., Florentino, A.O., Rocha, J.C., *Mater. Res.*, 7, **2004**, 329.
- [2] Lima, I.S., Airoidi, C., *Thermochim. Acta.*, 421, **2004**, 133.
- [3] Silva Filho, E.C., Melo, J. C. P., Airoidi, C., *Carbohydr. Res.*, 341, **2006**, 2842.
- [4] Santana, S. A. A., Vieira, A. P., Silva Filho, E. C., Melo, J. C. P., Airoidi, C., *J. Hazard. Mater.* 174, **2010**, 719.
- [5] de Melo, J. C. P., da Silva Filho, E. C., Santana, S. A.A., Airoidi, C., *Carbohydr. Res.* 345, **2010**, 1921.
- [6] Melo, J. C. P., Silva Filho, E. C., Santana, S. A. A., Airoidi, C., *Colloids Surf. A*, 346, **2009**, 145.
- [7] Silva Filho, E. C., Melo, J. C. P., Fonseca, Maria G., Airoidi, C. *J. Colloids Int. Sci.* 340, **2009**, 15.
- [8] Gil, L. F., Karnitz Junior, O., Gurgel, L. V. A., Melo, J. C. P., Botaro, V. R., Melo, T. M. S., Gil, R. P. de F., *Biores. Technol.* 98, **2007**, 1297.
- [9] Vieira, A. P., Santana, S., Bezerra, C., Silva, H., Melo, J. C. P., Silva Filho, E. C., Airoidi, C. 166, **2009**, 1272.
- [10] Gil, L. F. ; Gurgel, L. V. A. ; Melo, J. C. P. ; Lena, J. C. . *Bioresour. Technol.*, 100, **2009**, 3220.
- [11] Monteiro Jr, O.A.C., Airoidi, C., *J. Colloid Interface Sci.*, 282, **2005**, 32.
- [12] Babel, S., Kurniawan, T.A., *J. Hazard. Mater.* B97, **2003**, 219.
- [13] Airoidi, C. “Química de Coordenação – Fundamentos e Atualidades”, R. F. Farias, Editor, Editora Átomo, Campinas, p.123, **2005**.
- [14] Jal, P.K., Patel, S., Mishra, B.K., *Talanta* 62, **2004**, 1005.
- [15] Mohanty, A.K., Misra, M., Drzal, L.T. *Comp. Interf.* 8, **2001**, 313.
- [16] Kumar, P., Barrett, D.M., Delwiche, M.J., Stroeve, P. *Ind. Eng. Chem. Res.* 48, **2009**, 3713.
- [17] Faaij, A. *Mitigat. Adapt. Strat. Global Change* 11, **2006**, 343.
- [18] Pu, Y., Zhang, D., Singh, P.M., Ragauskas, A.J., *Biof. Bioprod. Bioref.* 2, **2007**, 58.
- [19] Zaldivar, J., Nielsen, J., Olsson, L., *Appl. Microbiol. Biotechnol.* 56, **2001**, 17.
- [20] Rogalinski, T., Ingram, T., Brunner, G., *J. Supercrit. Fluids* 47, **2008**, 54.

## Capítulo 9 – Referências

- [21] Zavrel, M., Bross, D., Funke, M., Jochen Büchs, Spiess, A.C., *Biotechnol. Res.* 100, **2009**, 2580.
- [22] Berthold, J., Rinaudo, M. Salmefi, L., *Colloids Surf. A*, 112, **1996**, 117.
- [23] Osada, M., Hiyoshi, N., Sato, O., Arai, K, Shirai, M., *Energy Fuels* 21, **2007**, 1854.
- [24] Rajan, A., Kurup, J. G., Abraham, T. E., *Biochem. Eng. J.* 25, **2005**, 237.
- [25] Pessala, P., Schultz, E., Kukkola, J., Nakari, T., Knuutinen, J., Herve, S., Paasivirta, J., *Ecotoxicol. Environ. Safety* 73, **2010**, 1641.
- [26] Jin, Z., Yu, Y., Shao, S., Ye, J., Lin, L., Iiyama, K., *J. Wood Sci.* 56, **2010**, 470.
- [27] Banerjee, G., Car, S., Scott-Craig, J. S., Borrusch, M. S., Aslam, N., Walton, J. D., *Biotechnol. Bioeng.* 106, **2010**, 707.
- [28] van Spronsen, J., Cardoso, M. A. T., Witkamp, G.-J., de Jong, W., Kroon, M. C., *Chem. Eng. Process.* **no prelo**
- [29] Cardona, C. A., Sanchez, O. J., *Biores. Technol.* 98, **2007**, 2415.
- [30] Sivakumar, G., Vail, D. R., Xu, J., Burner, D. M., Lay Jr., O. J., Ge, X., Weathers, P. *J. Eng. Life Sci.* 10, **2010**, 8.
- [31] Hirschier, R., Althaus, H.-J., Werner, F., *Int. J. Life Cycle Assess.*, 10, **2005**, 50.
- [32] Håkansson, H., Ahlgren, P., *Cellulose* 12, **2005**, 177.
- [33] Dumitriu, S., *Polysaccharides in Medicinal Applications*, Editora: Sherbrooke, Quebec, Canadá, **1996**, p. 87.
- [34] Ardizzone, S., Dioguardi, F. S., Mussini, T., Mussini, P. R., Rondinini, S., Vercelli, B., Vertova, A., *Cellulose* 6, **1999**, 57.
- [35] Kobayashi, S., Sakamoto, J., Kimura, S., *Prog. Polym. Sci.*, 26, **2001**, 1525.
- [36] Sullivan, A. C. O., *Cellulose* 4, **1997**, 173.
- [37] *Spring Series in Wood Science*, Ed. T. E. Timell and R. Wimmer, Spring Series, 2008, Cap. 5-7.
- [38] Zugenmaier, P., *Prog. Polym. Sci.* 26, **2001**, 1341.
- [39] Martin, A. I., Sanchez-Chaves, M., Arranz, F., *React. Funct. Polym.* 39, **1999**, 179
- [40] Smole, M.S., PerĐin, Z., Kre, T., Kleinschek, K.S., Ribitsch, V., Neumayer, S., *Mat. Res. Innovat.* 7, **2003**, 275.
- [41] Kobayashi, S., Uyama, H., Ohmae, M., *Bull. Chem. Soc. Jpn.* 74, **2001**, 613.
- [42] Nakatsubo, F., Kamitakahara, H., Hori, M., *J. Am. Chem. Soc.* 118, **1996**, 1677.

## Capítulo 9 – Referências

- [43] Kennedy, B., Phillips, B., Wedlock, B., Willins, P. A., *Cellulose and its derivatives: chemistry, biochemistry and applications*, New York, John Wiley, **1985**.
- [44] Potthast, A., Rosenau, T., Kosma, P. *Adv. Polym. Sci.* 205, **2006**, 1.
- [45] Kadla, J.F., Gilbert, R.D., *Cellul. Chem. Tech.* 34, **2000**, 197.
- [46] Martinez, A. J., Manolache, S., Gonzalez, V., Young, R. A., Denes, F. J., *J. Biomater. Sci. Polym.* 11, **2000**, 415.
- [47] Sun, H., Ge, B., Liu, S., Chen, H., *J. Sep. Sci.* 31, **2008**, 1201.
- [48] Franco, P., Senso, A., Oliveros, L., Minguillon, C., *J. Chromatogr. A* 906, **2001**, 155.
- [49] Felix, G., *J. Chromatogr.*, 906, **2001**, 171.
- [50] Amash, A., Hildebrandt, F.-I., Zugenmaier, P., *Desig. Monom. Polym.* 5, **2002**, 385.
- [51] Linder, A. P., Bergman, R., Bodin, A., Gatenholm, P., *Langmuir* 19, **2003**, 5072.
- [52] Liu, S., *Biotechnol. Adv.* 28, **2010**, 563.
- [53] Schwanninger, M., Rodrigues, J.C., Pereira, H., Hinterstoisser, B., *Vibr. Spectr.* 36, **2004**, 23
- [54] Kato, K., Vasilets, V.N., Fursa, M.N., Meguro, M., Ikada, Y., Nakamae, K., *J. Polym. Sci. A: Polym. Chem.* 37, **1999**, 357.
- [55] Wach, R.A., Mitomo, H., Yoshii, F., Kume, T., *Macromol. Mater. Eng.* 287, **2002**, 285.
- [56] Alberti, A., Bertini, S., Gastaldi, G., Iannaccone, N., MacCiantelli, D., Torri, G., Vismara, E., *Eur. Polym. J.* 41, **2005**, 1787.
- [57] Pelton, R., Geng, X., Brook, M., *Adv. Colloid Interface Sci.* 127, **2006**, 43.
- [58] Li, S., Yang, W., Chen, M., Gao, J., Kang, J., Qi, Y., *Mater. Chem. Phys.* 90, **2005**, 262.
- [59] Zabetakis, D., Dinderman, M., Schoen, P., *Adv. Mater.* 17, **2005**, 734.
- [60] Yue, Z., Cowie, J.M.G., *Polymer* 43, **2002**, 4453.
- [61] Cunha, A.G., Freire, C.S.R., Silvestre, A.J.D., Neto, C.P., Gandini, A., Orblin, E., Fardim, P., *Biomacromolecules* 8, **2007**, 1347.
- [62] Riekerink, M.B.O., Engbers, G.H.M., Wessling, M., Feijen, J., *J. Colloid Interface Sci.* 245, **2002**, 338.

## Capítulo 9 – Referências

- [63] Matsui, Y., Ishikawa, J., Kamitakahara, H., Takano, T., Nakatsubo, F., *Carbohydr. Res.* 340, **2005**, 1403.
- [64] Takano, T., Ishikawa, J., Kamitakahara, H., Nakatsubo, F., *Carbohydr. Res.* 342, **2007**, 2456.
- [65] Torres, J.D., Faria, E.A., Prado, A.G.S., *J. Hazard. Mater.* 129, **2006**, 239.
- [66] Klemm, D., Heublein, B., Fink, H.-P., Bohn, A., *Angew. Chem. Int. Ed.* 44, **2005**, 3358;
- [67] William Tindall, G., Boyd, B.W., Perry, R.L., *J. Chromatogr. A*, 977, **2002**, 247.
- [68] Satge, C., Granet, R., Verneuil, B., Branland, P., Krausz, P., *Comp. Rend. Chim.* 7, **2004**, 135.
- [69] Liu, C.F., Sun, R.C. Zhang, A.P., Ren, J.L., Wang, X.A., Qin, M.H., Chao, Z.N., Luo, W., *Carbohydr. Res.* 342, **2007**, 919.
- [70] Boufi, S., Belgacem, M.N., *Cellulose* 13, **2006**, 81.
- [71] Matsumura, H., Glasser, W.G., *J. App. Polym. Sci.* 78, **2000**, 2254.
- [72] Yin, C., Shen, X. *Europ. Polym. J.* 43, **2007**, 2111.
- [73] Xiao, D., Hu, J., Zhang, M., Li, M., Wang, G., Yao, H., *Carbohydr. Res.* 339, **2004**, 1925.
- [74] Rosenau, T., Renfrew, A.H.M., Chrer, Potthast, A., Kosma, P., *Polymer* 46, **2005**, 1453.
- [75] Vicini, S., Princi, E., Luciano, G., Franceschi, E., Pedemonte, E., Oldak, D., Kaczmarek, H., Sionkowska, A., *Thermochim. Acta* 418, **2004**, 123.
- [76] Kim, U.J., Kuga, S., *J. Chromatogr. A* 919, **2001**, 29.
- [77] Suflet, D.M., Chitanu, G.C. Popa, V.I., *React. Funct. Polym.* 66, **2006**, 1240.
- [78] Granja, P.L., Pouysgu, L., Ptraud, M., De Jso, B., Baquey, C., Barbosa, M.A., *J. Appl. Polym. Sci.* 82, **2001**, 3341.
- [79] Abdelmouleh, M., Boufi, S., Belgacem, M.N., Dufresne, A., Gandini, A., *J. Appl. Polym. Sci.* 98, **2005**, 974
- [80] Heinze, T., Liebert, T., *Progress in Polymer Science, Oxford*, 26, **2001**, 1689.
- [81] Nishiyama, Y., Langan, P., Chanzy, H., *J. Am. Chem. Soc.* 124, **2002**, 9074.
- [82] Atalla, R. H., *ACS Symp. Ser.* **1987**, 340.
- [83] Zugenmaier, P., *Prog. Polym. Sci.* 26, **2001**, 1341.

## Capítulo 9 – Referências

- [84] Aimin, T. Hongwei, Z., Gang, C., Guohui, X., Wenzhi, L., *Ultras. Sonochem.* 12, **2005**, 467.
- [85] Calvini, P., Conio, G. Lorenzoni, M., Pedemonte, E., *Cellulose* 99, **2004**, 107.
- [86] Arakaki, L. N. H., Espínola, J. G. P., Fonseca, M. G., Oliveira, S. F., Sousa, A. N., Arakaki, T., Airoidi, C., *J. Colloid Interface Sci.* 273, **2004**, 211.
- [87] Fonseca, M. G., da Silva Filho, E. C., Machado Jr, R. S. A., Arakaki, L. N. H., Espínola, J. G. P., Oliveira, S. F., Airoidi, C., *Colloids Suf. A* 227, **2003**, 85.
- [88] Fonseca, M. G., da Silva Filho, E. C., Machado Jr, R. S. A., Arakaki, L. N. H., Espínola, J. G. P., Airoidi, C., *J. Solid State Chem.* 177, **2004**, 2316.
- [89] Pyrzynska, K., Cheregi, M., *Water Res.* 34, **2000**, 4215.
- [90] Han, S., Lee, M., Kim, B. K., *J. App. Polym. Sci.* 117, **2010**, 682.
- [91] Weigel, P. H., University of Texas, **1986**, patente: **US4626571-A**.
- [92] Monsanto Chemical Ltd (Mons-C), **1970**, números da patente: FR94723-A, FR94723-E
- [93] Almeida, R. K. S., Melo, J. C. P., Airoidi, C., *Microporous Mesoporous Mater.*, 165, **2013**, 168.
- [94] Zhou, Y., Jin, Q., Hu, X., Zhang, Q., Ma, T., *J. Mater. Sci.*, 47, **2012**, 5019.
- [95] Li, H.F., Li, H., Zhong, X., Li, X., Gibril, M.E., Zhang, Y., Han, K., Yu, M. *Adv. Mater. Res.*, 581, **2012**, 287.
- [96] Naidu, R., Harter, R. D., *Soil Sci. Soc. Am. J.*, 62, **1998**, 644.
- [97] Park, I. H., Rhee, J. M., Jung, Y. S., *Angewandte Makromolekulare Chemie*, 267, **1999**, 27.
- [98] Chang, S.-T., Chang, H.-T., *Polym. Degrad. Stab.*, 71, **2001**, 261.
- [99] Peng, H., Yang, C. Q., Wang, S., *Carbohydr. Polym.*, 87, **2012**, 491.
- [100] Huang, L., Xiao, C., Chen, B., *J. Hazard. Mater.*, 192, **2011**, 832.
- [101] Chadlia, A., Farouk, M'H. M., *Carbohydr. Res.*, 345, **2010**, 264.
- [102] Melo, J. C. P., daSilva Filho, E. C., Santana, S. A. A., Airoidi, C., *Thermochemica Acta* 524, **2011**, 29.
- [103] Liu, C. F., Zhang, A. P., Li, W. Y., Yue, F. X., Sun, R. C., *Crops Prod.* 31, **2010**, 363.
- [104] Zhang, W., Li, C., Liang, M., Geng, Y., Lu, C., *J. Hazard. Mater.*, 181, **2010**, 468.

## Capítulo 9 – Referências

- [105] Hu, X., Zhao, M., Song, G., Huang, H., *Environmental Tech.*, 32, **2011**, 739.
- [106] Zhong, L.-X., Peng, X.-W., Yang, D., Sun, R.-C., *J. Agric. Food Chem.*, 60, **2012**, 5621.
- [107] Aziza, A., Elandaloussia, E. H., Belhalfaouia, B. Oualia, M. S. De Ménorval, L. C., *Colloids Surf., B*, 73, **2009**, 192.
- [108] Nada, A.-A. M. A., Hassan, M. L., *J. App. Polym. Sci.*, 102, **2006**, 1399.
- [109] Liu, C. F., Sun, R. C., Zhang, A. P., Ren, J. L., Wang, X. A., Qin, M. H., Chao, Z. N., Luo, W., *Carbohydr. Res.* 342, **2007**, 919.
- [110] C.F. Liu, C. F., Sun, R. C., Zhang, A. P., Ren, J. L., *Carbohydr. Polym.*, 68, **2007**, 17.
- [111] Liu, C. F., Sun, R. C., Ye, J., *Polym. Degrad. Stab.*, 91, **2006**, 280.
- [112] Belhalfaouia, B., Aziza, A., Elandaloussia, E. H., Oualia, M. S., De Ménorval, L. C., *J. Hazard. Mater.* 169, **2009**, 831.
- [113] Liu, C. -F., Sun, R.-C., Zhang, A. P., Qin, M. H., Ren, J. L., Wang, X. A., *J. Agric. Food Chem.*, 55, **2007**, 2399.
- [114] Safou-Tchiama, R., Jeso, B., Akagah, A. G., Sèbe, G., Pétraud, M., *Crops Prod.* 26, **2007**, 173.
- [115] Karnitz, O., Gurgel, L. V. A., de Freitas, R. P., Gil, L. F., *Carbohydr. Polym.*, 77, **2009**, 643.
- [116] *J. Mater. Sci.*, 47, **2012**, 5019.
- [117] Sousa, K. S., Tese de doutorado, Campinas, Instituto de Química/UNICAMP, **2009**.
- [118] Rawat, N., Bhattacharyy, A., Tomar, B. S., Ghanty, T. K., Manchanda, V. K., *Thermochimica Acta*, 518, **2011**, 111.
- [119] E.C. Silva Filho, S.A.A. Santana, J.C.P. Melo, F.J.V.E. Oliveira, C. Airoidi, *J. Therm. Anal. Calorim.*, 100, **2010**, 315.
- [120] Hall, K. R., Eagleton, C., Acrivos, A., Vermeulen, T., *Ind. Eng. Chem. Fundam.*, 05, **1999**, 212.
- [121] Warner, J.C. Cannon, A. S., Dye, K. M., *Environ. Imp. Asses. Rev.*, 24, **2004**, 775.
- [122] Tanaka, K., Toda, F., *Chem. Rev.* 100, **2000**, 1025.

## Capítulo 9 – Referências

- [123] Pavia, D. L., Bassler, G. M., Morrill, T. C., Introduction to Spectroscopy, second ed., Saunders College Publishing, New York, **1996**.
- [124] Atalla, R. H., VanderHart, D. L., Solid State Nucl. Magn. Reson., 15, **1999**, 1.
- [125] Machado Jr., R. S. A., da Fonseca, M. G., Arakaki, L. N. H., Espínola, J. G. P. Oliveira, S. F., Talanta, 63, **2004**, 317.
- [126] Giles, C. H., MavEvan, T. H., Nakhawa, S. W., Smith, D., J. Chem. Soc., 786, **1960**, 3973.
- [127] Lopes, E. C. N., Sousa, K. S., Airoidi, C., Thermochem. Acta, 483, **2008**, 21.
- [128] Machado, M. O., Lopes, E. C. N., Sousa, K. S., Airoidi, C., Carbohydr. Polym., 77, **2009**, 760.
- [129] J. E. Huheey, E. A. Keiter, R. L. Leiter, Inorganic Chemistry, fourth ed., Harper Collins College Publishers, **1993**.
- [130] Ott E., Spurlin HM, Grafflin MW. Cellulose and cellulose derivatives. New York: Interscience Publishers; **1954**.
- [131] Jeffery, G. H., Bassett, J., Mendham, J., Denney, R. C., Vogel's Textbook of quantitative Chemical Analysis, 5th ed. revised, John Wiley & Sons, New York, **1989**.
- [132] Karnitz, O., Gurgel, L. V. A., de Melo, J. C. P., Botaro, V. R., Melo, T. M. S., Gil, R. P. F., Gil, L. F., Bioresour. Technol. 98, **2007**, 1291.
- [133] Chang, S.-T., Polym. Degrad. Stab. 71, **2001**, 261.
- [134] Anirudhan, T. S., Jalajamony, S., Sreekumari, S. S., App. Clay Sci. 65–66, **2012**, 67.
- [135] Chen, Z., Zhou, L., Zhang, F., Yu, C., Wei, Z., App. Surf. Sci., 258, **2012**, 5291.
- [136] Tserki, V., Matzinos, P., Kokkou, S., Panayiotou, C., Composites: A 36, **2005**, 965.
- [137] Khasbaatar, A. D., Ko, Y. G., Choi, U. S., React. Funct. Polym. 67, **2007**, 312.
- [138] Khasbaatar, A. D., Chun, Y. J., Choi, U. S., Polym. J., 40, **2008**, 302.
- [139] Srivastava, V. C., Mall, I. D., Mishra, I. M., J. Hazard. Mater. 134, **2005**, 257.
- [140] Ho, Y. S., McKay, G., Process. Biochem., 34, **1999**, 451.
- [141] Gosset, T., Trancart, J. L., Thevenot, D. R., Water Res. 20, **1986**, 21.
- [142] Ho, Y. S., Wase, D. A. J., Forster, C. F., Environ. Technol., 17, **1996**, 71.
- [143] Justi, K. C., Favere, V. T., Laranjeira, M. C. M., Neves, A., Peralta, R. A., J. Colloid Interface Sci., 291, **2005**, 369.

## Capítulo 9 – Referências

- [144] Sousa, F. W., Moreira, S. A., Oliveira, A. G., Cavalcante, R. M., Nascimento, R. F., Rosa, M. F., *Quim. Nova* 30, **2007**, 1153.
- [145] Aydın, H., Bulut, Y., Yerlikaya, C., *J. Environ. Manag.* 87, **2008**, 37.
- [146] Gurgel, L. V. A., Freitas, R. P., Gil, L. F., *Carbohydr. Polym.* 74, **2008**, 922.
- [147] Gurgel, L. V. A., Karnitz Jr., O., Gil, R. P. F., Gil, L. F., *Bioresour. Technol.* 99, **2008**, 3077.
- [148] Lima, A. J. B., Cardoso, M. G., Guerreiro, M. C., Pimentel, F.A., *Quim. Nova* 29, **2006**, 247.
- [149] Sousa, K. S., da Silva Filho, E. C., Airoidi, C., *Carbohydr. Res.*, 344, **2009**, 1716.
- [150] Airoidi, C., Arakaki, L. N. H., *Polyhedron*, 20, **2001**, 929.
- [151] Das, D. D., Mahapatra, R., Pradhan, J., Das, S. N., Thakur, R. S., *J. Colloid Interface Sci.*, 232, **2000**, 235.
- [152] Ho, Y. S., Mckay, G., *Water Res.*, 34, **2000**, 735.
- [153] Khan, M. N., Wahab, M. F., *J. Hazard. Mater.*, 141, **2007**, 237.
- [154] Chuah, T. G., Jumariah, A., Azni, I., Katayon, S., Choong, S. Y. T., *Desalination* 175, **2005**, 305.
- [155] Wong, K. K., Lee, C. K., Low, K. S., Haron, M. J., *Chemosphere*, 50, **2003**, 23.
- [156] Acar, F. N., Eren, Z., *J. Hazard. Mater.: B*, 137, **2006**, 909.
- [157] Annadurai, G., Juang, H. S., Lee, D. J., *Water Sci. Technol.*, 47, **2002**, 185.
- [158] Cestari, A. R.; Vieira, E. R. S.; Santos, A. G. P.; Mota, J. A.; Almeida, V. P.; *J. Colloid Interface Sci.*, 280, **2004**, 380.
- [159] Allen, S. J.; Gan, Q.; Matthews, R.; Johnson, P. A.; *J. Colloid Interface Sci.*, 286, **2005**, 101.
- [160] Alley, E. R.; *Water Quality Control Handbook*, McGraw Hill: New York, **2000**, p.125.
- [161] Satyanarayana, K. G.; Guimarães, J. L.; Wypych, F., *Composites: A*, 38, **2007**, 1694.
- [162] Ho, Y. S., *J. Hazard. Mater.*, B136, **2006**, 681.
- [163] Mohan, D.; Singh, K. P.; Singh, G.; Kumar, K., *Ind. Eng. Chem. Res.*, 41, **2002**, 3688.
- [164] Acemioglu, B., *J. Colloid Interface Sci.*, 274, **2004**, 371.

## Capítulo 9 – Referências

- [165] Bhattacharyya, K. G.; Sarma, A.; *Dyes Pigm.*, 57, **2003**, 211.
- [166] Freundlich, H. M. F., *Z. Phys.*, 57A, **1906**, 385.
- [167] Namasivayam, C., Prabha, D., Kumutha, M., *Bioresour. Technol.*, 64, **1998**, 77.
- [168] Namasivayam, C., Kavitha, D.; *Dyes Pigm.*, 54, **2002**, 47.
- [169] Yuzhu, F., Viraraghavan, T., *Adv. Environ. Res.*, 7, **2002**, 239.
- [170] Malik, P. K., *Dyes Pigm.*, 56, **2003**, 239.
- [171] Chiou, M. S., Li, H. Y., *J. Hazard. Mater.*, B93, **2002**, 233.
- [172] Crini, G.; *Bioresour. Technol.*, 97, **2006**, 1061.
- [173] Gupta, V. K., *J. Environ. Managem.*, 90, **2009**, 2313.



## 10 Anexos

### Lista de Publicações

1. J.C.P. Melo, E.C. Silva Filho, S.A.A. Santana, C. Airoidi, "Maleic anhydride incorporated onto cellulose and thermodynamics of cation-exchange process at the solid/liquid interface", *Colloids Surf. A*, 346, 138-145 (2009).
2. Júlio C. P. Melo, Edson C. Silva Filho, Sirlane A.A. Santana, Claudio Airoidi, Synthesized cellulose/succinic anhydride as an ion exchanger. Calorimetry of divalent cations in aqueous suspension, *Thermochimica Acta* 524 (2011) 29– 34
3. J.C.P. Melo, E.C. Silva Filho, S.A.A. Santana, C. Airoidi, "Exploring the favorable ion-exchange ability of phthalylated cellulose biopolymer using thermodynamic data", *Carbohydr. Res.*, 345, 1914-21 (2010).
4. E.C. Silva Filho, J.C.P. Melo, M.G. Fonseca, C. Airoidi, "Cation removal using cellulose chemically modified by a Schiff base procedure applying green principles", *J. Colloid Interface Sci.*, 340, 8-15 (2009).
5. E.C. Silva Filho, S.A.A. Santana, J.C.P. Melo, F.J.V.E. Oliveira, C. Airoidi, "X-ray diffraction and thermogravimetry data of cellulose chlorodeoxycellulose and E.C. Silva Filho, aminodeoxycellulose", *J. Therm. Anal. Calorim.*, 100, 315-321 (2010).
6. A.P. Vieira, S.A.A. Santana, C.W.B. Bezerra, H.A.S. Silva, J.C.P. Melo, E.C. Silva Filho, C. Airoidi, "Copper sorption from aqueous solutions and sugar cane spirits by chemically modified babassu coconut (*Orbignya speciosa*) mesocarp", *Chem. Eng. J.*, 161, 99-105 (2010).
7. S.A.A. Santana, A.P. Vieira, E.C. Silva Filho, J.C.P. Melo, C. Airoidi, "Immobilization of ethylenesulfide on babassu coconut epicarp and mesocarp for divalent cation sorption", *J. Hazard. Mater.*, 174, 714-719 (2010).
8. A.V. Pires, S.A.A. Santana, C.W.B. Bezerra, H.A.S. Silva, J.A.P. Chaves, J.C.P. Melo, E.C. Silva Filho, C. Airoidi, "Epicarp and mesocarp of babassu (*Orbignya speciosa*): characterization and application in copper phtalocyanine dye removal", *J. Braz. Chem. Soc.*, 22, 21-29 (2011).



Contents lists available at ScienceDirect

## Colloids and Surfaces A: Physicochemical and Engineering Aspects

Journal homepage: [www.elsevier.com/locate/colsurfa](http://www.elsevier.com/locate/colsurfa)

### Maleic anhydride incorporated onto cellulose and thermodynamics of cation-exchange process at the solid/liquid interface

Júlio C.P. de Melo<sup>a</sup>, Edson C. da Silva Filho<sup>b</sup>, Sirlane A.A. Santana<sup>c</sup>, Claudio Airoidi<sup>a,\*</sup>

<sup>a</sup> Institute of Chemistry, University of Campinas, UNICAMP, P.O. Box 6154, 13084-971 Campinas, SP, Brazil

<sup>b</sup> Química, Universidade Federal do Piauí, 64900-000 Bom Jesus, PI, Brazil

<sup>c</sup> Departamento de Química/CCET, Universidade Federal do Maranhão, Av. dos Portugueses S/N, Campus do Bacanga, 65080-540 São Luiz, MA, Brazil

#### ARTICLE INFO

##### Article history:

Received 10 March 2009

Received in revised form 26 May 2009

Accepted 2 June 2009

Available online 11 June 2009

##### Keywords:

Modified cellulose  
Maleic anhydride  
Solvent-free  
Adsorption  
Calorimetry  
Thermodynamic

#### ABSTRACT

This investigation explores the chemical modification of cellulose by using a quasi solvent-free procedure, in which the biopolymer was added to molten maleic anhydride, producing a mixture of maleated and fumarated celluloses. Using this pathway mainly surface modifications are observed and more than  $2.82 \pm 0.05$  mmol of modifier per gram of synthesized polymer were obtained. These chemically modified materials were characterized by elemental analysis, solid-state  $^{13}\text{C}$  NMR CP/MAS, FTIR, XRD, TG and SEM. The chemically modified polysaccharides are able to adsorb cations. The data were adjusted to a modified Langmuir equation to give  $1.75 \pm 0.09$  and  $2.40 \pm 0.12$  mmol/g of  $\text{Co}^{2+}$  and  $\text{Ni}^{2+}$ , respectively. The net thermal effects obtained from calorimetric titration measurements were also adjusted to a modified Langmuir equation and the enthalpy of the interaction was calculated to give the endothermic values of  $0.29 \pm 0.02$  and  $0.87 \pm 0.02$  kJ/mol for  $\text{Co}^{2+}$  and  $\text{Ni}^{2+}$ , respectively. The thermodynamic data for these systems are favorable for cation adsorption from aqueous solutions at the solid/liquid interface, suggesting the use of this anchored biopolymer for cation removal from the environment.

© 2009 Elsevier B.V. All rights reserved.

#### 1. Introduction

Cellulose is the most widely available organic biopolymer in nature, mainly encountered as structures and supports algae, fungus and plants cells. Due to this availability, special attention has been given to its chemical properties and its various useful applications. This natural biopolymer presents considerable chemical and physical inertness. Thus, surface and structural modifications can sometimes be hard to achieve, especially without appropriate solvents in the reaction media, in order to acquire new derivatives to improve its usefulness. This polysaccharide bears three hydroxyl groups per anhydroglucose unit, which, through hydrogen bonds, determine the structural design, crystallinity and reactivity of the bulk. Generally, all modifications are based on derivatizations of these hydroxyl groups, but it is also possible to oxidize its ring selectively at almost any bond and break the  $\beta$ -(1,4) glucosidic linkage to yield glucose [1].

Acylation cellulose through the use of anhydrides [2–4] produces stable ester bonds and reactive carboxylic acid end groups. This process is employed in the coating, cosmetic, food and pharmaceutical industries, for antibody, enzyme, protein and ion separation membranes, filters etc [5–7].

Organic solvents are present in almost all kinds of cellulosic modifications, even when heterogeneous synthetic routes are employed, since solvents are often used in many chemical processes, sometimes even without being necessary [8,9]. Nevertheless, the major problems associated with solvents are the toxicity of their vapors when in the atmosphere and the production of volatile molecules, and other combustion product such as carbon dioxide, a principal substance responsible for the greenhouse effect [10] that causes a great impact on the environment. On the other hand, solvents are useful to disrupt the hydrogen bonds in homogeneous routes to free the polymer for the proposed sequence of reactions, while in heterogeneous routes the solvent's function is to dissolve reagents to promote contact of the reactive centers [11].

Cation adsorption on solids, originating from different natural or synthetic sources, is widely explored with the objective to discover utility in many material operations. These solids, can be chemically functionalized or not, and has been intensively investigated in recent decades for heavy cation removal from aqueous and non-aqueous effluents [10,12,13]. To indicate the need for such adsorbents, intoxication with cobalt causes an increase in hepatic glutathione levels and is absorbed by the same active transport mechanism that normally transports iron, while intoxication with nickel causes nasal and lung cancers as well as damage to DNA [14].

Considering these tendencies, the present investigation deals with a novel proposition of chemically modifying cellulose without the use of solvents during the synthesis, by successfully using

\* Corresponding author. Fax: +55 19 35213023.

E-mail address: [airoidi@iqm.unicamp.br](mailto:airoidi@iqm.unicamp.br) (C. Airoidi).

the low melting point of maleic anhydride. Structural chemical modifications of the biopolymer consist in incorporating ester and carboxylic acid as pendant chains covalently bonded to the main polymeric framework. The applicability of these new synthesized celluloses is related to the ability of the available attached basic centers in the chains to adsorb cations from aqueous solution. Their interactions at the solid/liquid interface, whose quantitative features were followed by calorimetry to better understand this important interactive process, are also reported [15–17].

## 2. Materials and methods

### 2.1. Materials

Microcrystalline cellulose as powder (Aldrich),  $\sim 20 \mu\text{m}$ , was dried before use, maleic anhydride (Synth) and the other analytical grade reagents were used without prior purification.

### 2.2. Instrumentation

The amount of maleic anhydride incorporated into the cellulose was determined through elemental analysis on a Perkin Elmer, model 2400, elemental analyzer and through reactive center titration. Infrared spectra of the samples in KBr pellets were obtained by diffuse reflectance by accumulating 32 scans on a Bomem Spectrophotometer, MB-series, in the  $4000\text{--}400 \text{ cm}^{-1}$  range, with  $4 \text{ cm}^{-1}$  of resolution. Solid-state  $^{13}\text{C}$  NMR spectra of the samples were obtained on a Bruker AC 400/P spectrometer at room temperature. The measurements were obtained at frequencies of 75.47 MHz with a magic angle spinning of 10 kHz. To increase the signal/noise ratio, the CP/MAS technique was used, with pulse repetition of 5 s and a contact time of 1 ms. X-ray diffraction patterns were obtained on a Shimadzu model XRD 7000 diffractometer with 40 kV voltage applied, current of 30 mA and  $\text{CuK}\alpha$  ( $\alpha = 154.1 \text{ pm}$ ) radiation source scanned from 5 to  $45^\circ$ . Secondary electron images were acquired with a JEOL JSM 6360LV scanning electron microscope, operating at 20 kV of voltage acceleration applied and a current of 30 mA. The samples were fixed onto a double-faced carbon tape adhered to an aluminum support and carbon-coated in a Bal-Tec MD20 instrument. Thermogravimetric curves in an argon atmosphere were obtained on a TA instrument, coupled to a model 1090 B thermobalance, using a heating rate of  $0.167 \text{ K/s}$ , under a flow of  $30 \text{ cm}^3/\text{s}$ , varying from room temperature to 773 K, with an initial mass of approximately 10 mg of solid sample. The amount of cation adsorbed was determined by the difference between the initial concentration in the aqueous solution and that found in the supernatant, using ICP OES (inductively coupled plasma optical emission spectrometer) on a Perkin Elmer 3000 DV apparatus. For each experimental point, the cation determination in the supernatant, the reproducibility was checked by at least one duplicate run.

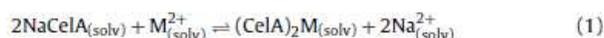
### 2.3. Synthesis of cellulose modified with maleic anhydride

A sample of 10 g cellulose (Cel), previously dried at 383 K for 2 h under vacuum, was added to 60 g of molten anhydride, to maintain a cellulose/maleic anhydride ratio of 1:10, in a reaction flask immersed in a sand bath at 388 K, under magnetic stirring. The flask was fitted with a dried silica trap to maintain constant pressure and to keep out moisture from the air. After 6 h the mixture was filtered while hot. The mixture of as-modified biopolymers was washed intensively with water to a neutral pH and the solid was then dried in vacuum at 383 K for 24 h. The new biopolymer (CeLA) was proton/sodium exchanged before adsorption and calorimetric experiments.

### 2.4. Adsorption

The capacity of the chemically modified cellulose to extract cations from aqueous solution was determined in duplicate runs, using a batch process with divalent cobalt or nickel, by using a series of flasks containing a mass ( $m$ ) of modified cellulose suspended in  $25.0 \text{ cm}^3$  of an aqueous solution with concentrations of each metal nitrate varying from 0.10 to  $5.0 \text{ mmol/dm}^3$ . From this procedure the best isotherm was obtained with 25 mg of adsorbent for each cation to give a defined plateau, indicating the maximum adsorption capacity. Firstly, the as-synthesized matrices were treated with  $0.90 \text{ mol/dm}^{-3}$  of sodium hydrogencarbonate solution at 291 K, to exchange the protons for sodium cations. This exchanging avoids a pH decrease during suspension, favoring metal adsorption, which was carried out at an isoelectronic pH ( $5.5 \pm 0.1$ ). The suspensions were shaken for 3 h in an orbital bath at  $298 \pm 1 \text{ K}$ . This time was previously established by using identical methodology whose results demonstrated that the isotherms reached cation saturation, as was obtained for the concentration study, by giving a well-defined plateau. At the end of the process, the solid was separated by centrifugation for 10 min at 2300 rpm, aliquots of the supernatant were removed and the cations were determined by ICP OES. The adsorption capacities ( $n_f$ ) were calculated by considering the number of moles:  $n_f = (n_i - n_s)/m$ , where  $n_i$  and  $n_s$  are the initial number of moles and the number remaining in the supernatant at the end of the experiment, respectively and  $m$  is the mass of solid used [3,13].

Adsorption at the solid/liquid interface is a competition between the solvent (solv) bonded to the sodium from the chemically modified cellulose (NaCeLA) that is gradually displaced by the solute in solution to reach equilibrium, as represented in Eq. (1):



The ratio between the number of moles of metal in solution at equilibrium and the number of moles of metal adsorbed on the surface was used to obtain the modified Langmuir isotherm, Eq. (2):

$$\frac{C_s}{n_f} = \frac{C_s}{n^s} + \frac{1}{n^s b} \quad (2)$$

where  $C_s$  ( $\text{mol/dm}^3$ ) is the concentration of supernatant cations at the equilibrium,  $n_f$  ( $\text{mol/g}$ ) is the number of moles adsorbed,  $n^s$  ( $\text{mol/g}$ ) is the maximum amount of solute adsorbed per gram of NaCeLA, which is related to the number of adsorption sites, and  $b$  ( $\text{dm}^3/\text{mol}$ ) is a constant. The  $n^s$  and  $b$  values for each adsorption process were obtained from the angular and linear coefficients, respectively, of the linearized form of the adsorption isotherms, by considering  $C_s/n_f$  versus  $C_s$ , using the least squares method.

### 2.5. Calorimetric titration

The thermal effect evolved from the interaction between the cation and the basic center attached on the pendant groups at the solid/liquid interface was measured on a LKB 2277 calorimeter [13]. For each operation, a sample of about 20 mg of functionalized cellulose in the sodium form was suspended in  $2.0 \text{ cm}^3$  of water under stirring at  $298.15 \pm 0.20 \text{ K}$ . The thermostated solutions of the cations with concentration near to  $0.30 \text{ mol/dm}^3$  were incrementally added to the calorimetric vessel and the thermal effect of the titration,  $Q_t$ , was obtained. Under the same experimental conditions, the corresponding thermal effect of the dilution of the cation solution was obtained in an identical volume of the calorimetric solvent,  $Q_d$ . The thermal effect of NaCeLA hydration in water was also determined,  $Q_h$  [13,15–17]. Under such conditions, the net thermal effect of adsorption  $Q_r$  was obtained through Eq. (3), by considering that

the suspension of the solid in water gave a null value:

$$\sum Q_r = \sum Q_t - \sum Q_d \quad (3)$$

The change in enthalpy associated with cation/matrix interaction can be determined by adjusting the adsorption data to a modified Langmuir equation to calculate the integral enthalpy involved in the formation of a monolayer per unit mass of adsorbent  $\Delta_{\text{mono}}H$  [13,15–17], as shown in Eq. (4):

$$\frac{\sum X}{\sum \Delta H} = \frac{1}{(K-1)\Delta_{\text{mono}}H} + \frac{X}{\Delta_{\text{mono}}H} \quad (4)$$

where  $\sum X$  is the sum of the mole fraction of the cation in solution after adsorption obtained for each point of titrant. By using the modified Langmuir equation, the integral enthalpy of adsorption per gram of the matrix,  $\Delta H$ , was obtained by dividing the thermal effect resulting from adsorption by the number of moles of the adsorbate, while  $K$  is the proportionality constant, which also includes the equilibrium constant. Using the angular and linear values from the  $\sum X/\sum \Delta H$  versus  $\sum X$  plot enables the calculation of the  $\Delta_{\text{mono}}H$  value. Then, the enthalpy of adsorption can be calculated by means of expression (5):

$$\Delta H = \frac{\Delta_{\text{mono}}H}{n^s} \quad (5)$$

From the equilibrium constant values, the Gibbs free energies were calculated by the expression (6):

$$\Delta G = -RT \ln K \quad (6)$$

and the entropy value can be calculated through Eq. (7):

$$\Delta G = \Delta H - T\Delta S \quad (7)$$

### 3. Results and discussion

#### 3.1. Characterization

The reaction of cellulose with maleic anhydride produced the chemically modified polysaccharide with a carbon content of  $43.04 \pm 0.01\%$ , which enabled to calculation of the high degree of substitution (DS) of  $0.65 \pm 0.03$  for this new water insoluble material. This amount of carbon in the synthesized polysaccharide differs from  $41.95 \pm 0.04\%$  for the precursor, clearly indicating the success of anhydride incorporation. The proposed scheme of reaction with the structures of reagent and product is shown in Fig. 1. The amount of maleic anhydride covalently bonded to the backbone structure was calculated as  $2.48 \pm 0.05$  or  $2.82 \pm 0.05$  mmol/g, taking into account either the DS or carboxylic acid titration [3] procedures. This difference in values might be associated with the methodology used. For the latter procedure the amount of free sites available was calculated from the covalently bound groups, which is followed by uncertainties that emerge from possible crosslinking reactions [18–20]. Nevertheless, it is worth remembering that due to the large anhydride:hydroxyl ratio the crosslinking effect should be minimized. Based on the carbon percentage obtained for the chemically modified cellulose, another important feature should be considered, which is related to the expected correlation between these values and the proposed chemical structure. Thus, because of the reaction conditions, with the increase in temperature and the presence of dissolved atmospheric oxygen and residual water, an overoxidation can occur that is not taken into account [21].

The appropriate degree of substitution for homogeneous routes requires that the chemical modifications takes place on specific positions that may be selected and achieved. For heterogeneous pathways the degree of substitution is obtained by dissolving the material and analyzing the extension of reaction on each particular position [1,2,22].

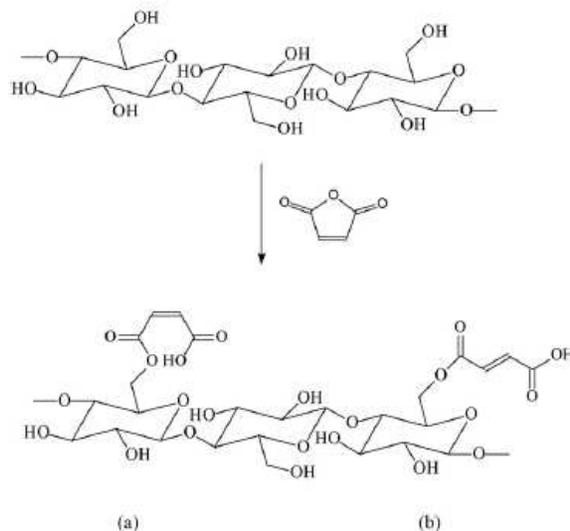


Fig. 1. Synthesis of CelA maleate (a) and fumarate (b) from the reaction of cellulose with maleic anhydride.

As indicated earlier, the present case uses heterogeneous conditions for all chemical modification procedures. However, the degree of substitution was not determined for individual carbon atoms, although for the DS value it was considered that anhydride molecules were covalently bonded preferentially to C6. As already mentioned, the corresponding value of the immobilized amount based on DS and titration procedure differs from the expected value of 3.84 mmol/g. However, the difference may arise from: (1) formation of different structures if some Michael addition occurs [23], (2) oxidized-ends that depend on the degree of polymerization are increased during the reaction due to the carboxylic acid groups formed or to the proton involved in  $\beta$ -(1,4) cleavage [24] and (3) oxidized-opened rings [25].

This degree of incorporation is high due to the absence of solvent in this synthesis, propelled by high temperature and easy availability of the reagent, that suggest surface modification to yield cellulose powder covered with modified polysaccharide, as depicted in Fig. 1. The modifier agent has an unsaturation that, after ring opening will appear as two biopolymer isomers: maleate cellulose (CelM) and fumarate cellulose (CelF), which were identified, but not quantified. This possibility to form both isomers is due to the presence of withdrawn groups near the unsaturation, which can affect the isomerization in agreement with the effect of potential to remove electron and also due to the hindrance caused by these groups [26–28]. Then, reaction of the  $\alpha,\beta$ -unsaturation with C(2)-, C(3)- or C(6)-hydroxyl, via a Michael addition, would yield other compounds as by-products.

Infrared spectra of raw cellulose [29] and the modified polysaccharide are shown in Fig. 2, with a broad band from 3100 to  $3500 \text{ cm}^{-1}$  assigned to OH stretching. The weak band at  $3045 \text{ cm}^{-1}$  is attributed to an intramolecular hydrogen stretching bond from the maleate conformation. Carboxylic acid dimers will produce a band centered at  $2530 \text{ cm}^{-1}$  due to the unsaturation [30] and the bands at  $1734$  and  $1162 \text{ cm}^{-1}$  are assigned to  $\nu(\text{C}=\text{O})$  from ester at;  $1718$  and  $1282 \text{ cm}^{-1}$  for carboxylic acid and at  $1724 \text{ cm}^{-1}$  for ester [29]. The appearance of a new band at  $821 \text{ cm}^{-1}$  is attributed to out of plane deformation for carboxyl groups [31]. The absence of any band at  $1850$  and  $1780 \text{ cm}^{-1}$  confirms the product to be free of non-reacted maleic anhydride [18]. The band at  $1637 \text{ cm}^{-1}$  is attributed to  $\nu(\alpha,\beta \text{ C}=\text{C})$  and  $776 \text{ cm}^{-1}$  to  $\delta(\text{C}=\text{H})$  and at  $1235 \text{ cm}^{-1}$  to  $\nu(\text{CO}-\text{OH})$  plus out of plane hydroxyl bending. The

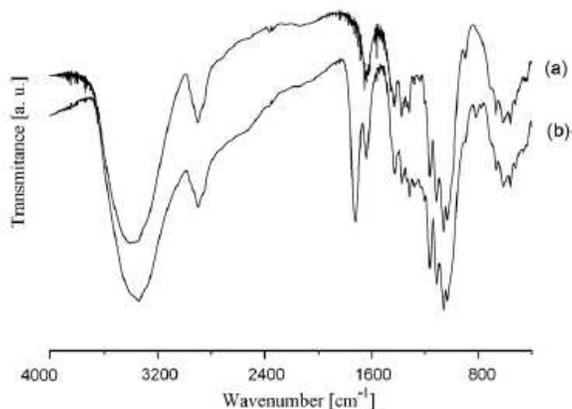


Fig. 2. Infrared spectra of cellulose (a) and its chemically modified form (b).

crystallinity regions are indicated by the observed O(6)H...O(2)H and O(3)H...O(5) vibrations, which are due to anomeric carbons due to the glucopyranose ring. These rings are very sensitive to any change in environment of the pendant groups and changes in crystallinity are reflected in the 1113 to 1110  $\text{cm}^{-1}$  region and 896  $\text{cm}^{-1}$  to a broader band at 893  $\text{cm}^{-1}$ , related to the deformation of the glucopyranose ring in plane and to  $\beta$ -(1,4) glycosidic linkages, respectively. Changes in frequency in the 1060 to 1058  $\text{cm}^{-1}$  interval are related to C(3)O stretching vibrations [31].

The change in crystallinity can also be investigated through signals on carbons 6 and 4 from the  $^{13}\text{C}$  NMR CP/MAS spectrum [32,33], as shown in Fig. 3. The carbon-6 atom bears the primary hydroxyl that is involved in intramolecular hydrogen bonds with the hydroxyl on C2, and intermolecular bonds, with the hydroxyl on C3' in the adjacent chains. As C6 is structured in this fashion it will be affected by any change in these hydrogen bonds. It is quite important to report that its C6 features are related to crystallinity only in non-chemically modified cellulose, such as the pristine polysaccharide. Thus, crystalline C6 are more downfield shifted than the amorphous form with a shoulder upfield at 65 ppm. The C4 signal is independent on the region where it is located, so the disappearance

of the amorphous C6 signal can occur, but not the one for amorphous C4. These carbons are sensitive to conformational effects and tensions on the chains to give a broader signal at 83 ppm, referring to amorphous regions, and at 89 ppm for crystalline ones. Although C1 and C4 hold oxygens that are located between two glucose units, these carbons cannot be related to crystallinity aspects [34,35].

The success of the reaction is evidenced by the signal at 165 ppm related to carbonyl groups, in which signals are overlapped, and are expected to show both an ester and a carboxylic acid. This signal is upfield shifted mainly due to the conjugated  $\pi$ -system of the two different isomers. The  $\alpha,\beta$ -unsaturated carbons of the modifier agent will shift the signal to 126 and 136 ppm for C8 and C9, respectively, and carbons 2, 3 and 5 are assigned to signals from 70 to 74 ppm.

The degree of crystallinity [20] of the cellulose in the solid-state has evoked great interest for several research groups and a way to calculate such a feature is by comparing the relative intensity between the 002 planes through Bragg [36] and Scherrer [37] laws. X-ray diffraction patterns obtained from these new materials, produced from microcrystalline cellulose through a heterogeneous route, are dominated by the original and not by novel crystalline arrangements of these new biopolymers. Thus, in these syntheses, modifications are expected to occur first on the more available hydroxyl groups in the para-crystalline region, located on the polymeric surface. Thus, it is expected that the diffraction patterns do not change in the chemically modified cellulose, as shown in Fig. 4.

As previously discussed from the  $^{13}\text{C}$  NMR spectra the regions of lower crystallinity decreased, proven by regarding the external chain disorganization and fiber length shortening, as confirmed by the peak at 34.5°, corresponding to the 040 plane [38].

The SEM images for cellulose and its modified biopolymer are shown in Fig. 5. The image in Fig. 5a displays the porous and fibrous morphology of the raw material. These characteristics change in the acylated cellulose in Fig. 5b, by slightly decreasing the rugosity, porosity and fibrous aspects.

The thermogravimetric curves for cellulose and the chemically modified biopolymer are shown in Fig. 6. Both biopolymers presented only one event due to decomposition, covering the intervals of temperature from 536 to 647 K and from 450 to 650 K for cellulose and chemically modified Cella (A–M and F), respectively. These events include losses of water physically adsorbed onto the surface,

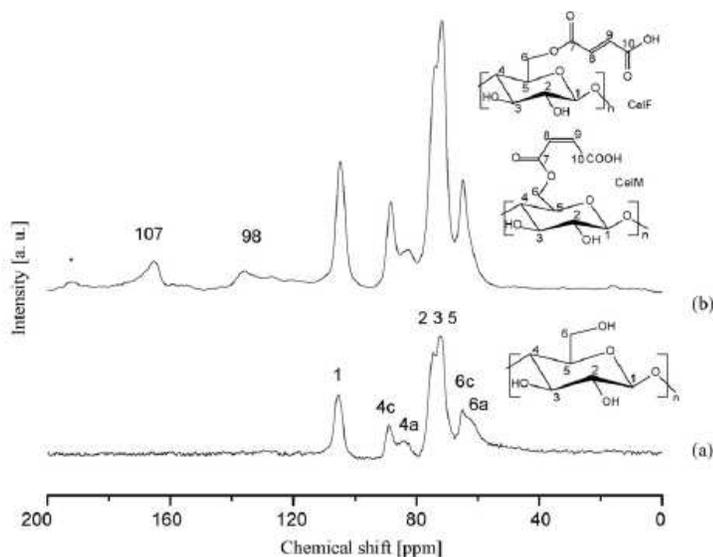


Fig. 3.  $^{13}\text{C}$  CP/MAS NMR spectra of cellulose (a) and its chemically modified form (b).

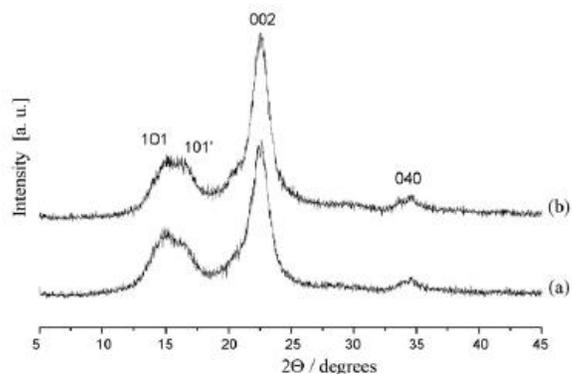


Fig. 4. X-ray diffraction patterns for cellulose (a) and its chemically modified form (b).

condensation of hydroxyl groups on carbons 2 and 3 and cellulose fiber decomposition [13].

3.2. Adsorption

For effectiveness of the interaction between divalent cations and the chemically modified cellulose, the main characteristics of the biopolymer should be considered. Thus, the available carboxylic acid groups covalently bonded to the cellulose backbone have the ability to act as sorbents from aqueous solution, due to the complexing ability of these basic centers at the solid/liquid interface [39,40].

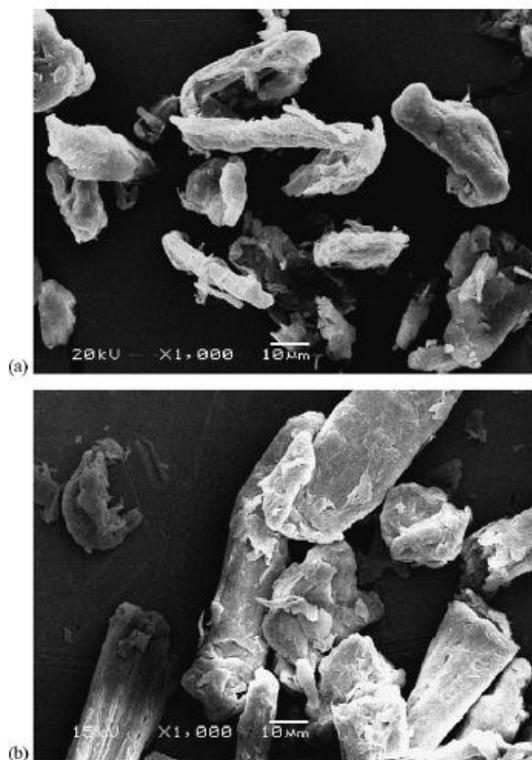


Fig. 5. SEM photographs of cellulose (a) and its chemically modified form (b).

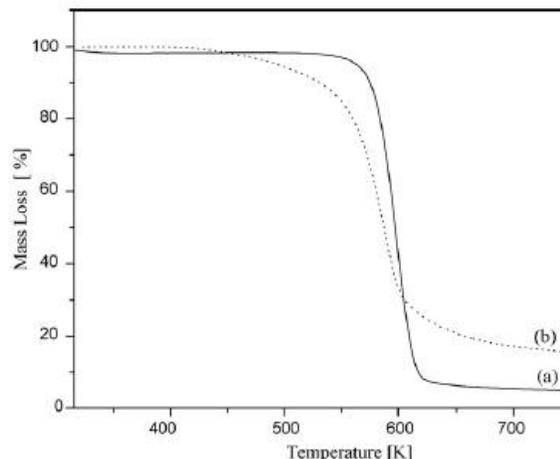


Fig. 6. Thermogravimetric curves of cellulose (a) and CeIA (b).

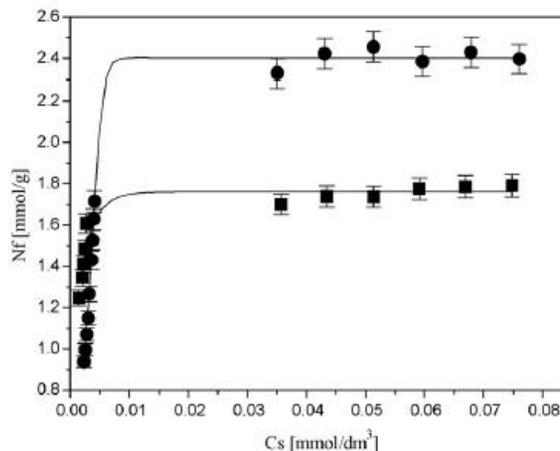


Fig. 7. Adsorption isotherms of  $\text{Co}^{2+}$  (■) and  $\text{Ni}^{2+}$  (●) on the chemically modified cellulose surface at  $298 \pm 1$  K.

To increase complexation by minimizing any lowering in pH, the protons were exchanged by sodium. The isotherms of cation adsorption with the modified biopolymer are shown in Fig. 7, using the best adsorption condition of 25 mg of adsorbent stirring 3 h at  $298 \pm 1$  K. The maximum amounts adsorbed ( $n^s$ ) were  $1.75 \pm 0.09$  and  $2.40 \pm 0.12$  mmol/g for cobalt and nickel, respectively. These values were obtained after fitting the results to a modified Langmuir equation (Eq. (2)), as successfully applied for other systems, to obtain the parameters of adsorptions at the solid/liquid interface [13,15–17]. The linearized form for nickel adsorption is given by  $C_s/n_f$  as a function of  $C_s$ , shown in Fig. 8, and enables the calculation of the linear and angular data from the straight line,  $n^s$  and  $b$  values, are listed in Table 1. These values confirmed the fit of the proposed model for cation complexation onto the NaCeIA surface,

Table 1  
Number of moles adsorbed ( $n_f$ ), maximum adsorption capacity ( $n^s$ ), constant ( $b$ ), and correlation coefficient ( $r$ ) for the interaction of divalent metal (M) nitrates with modified cellulose surface at  $298 \pm 1$  K.

| M                | $n_f$ (mmol/g)  | $n^s$ (mmol/g)  | $b$ ( $\text{dm}^3/\text{mol}$ ) | $r$    |
|------------------|-----------------|-----------------|----------------------------------|--------|
| $\text{Co}^{2+}$ | $1.75 \pm 0.09$ | $1.79 \pm 0.01$ | 1124                             | 0.9998 |
| $\text{Ni}^{2+}$ | $2.40 \pm 0.12$ | $2.53 \pm 0.01$ | 332                              | 0.9995 |

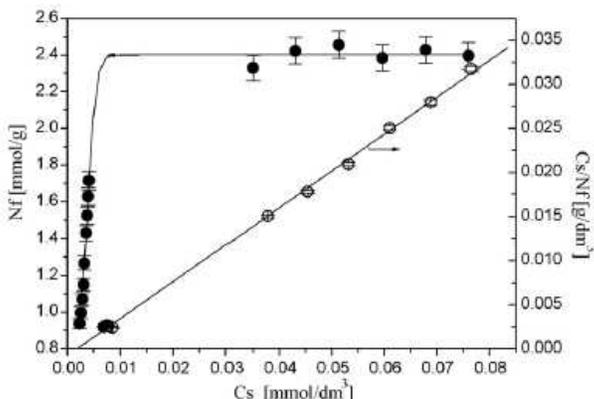
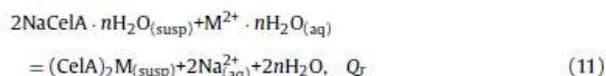
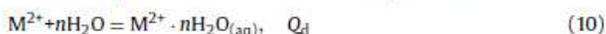


Fig. 8. Adsorption isotherms of Ni<sup>2+</sup> (●) and the linearized Langmuir isotherm (○) on chemically modified cellulose surface at 298 ± 1 K.

whose possible ways of metal interactions are proposed as shown in Fig. 9. The participation of the counter anion to neutralize the free cation charge is also presented, where the cation can bond to individual available carboxylate group or by bridging two distinct basic centers.

3.3. Calorimetric titration

The resulting thermal effects due to the interaction of cations with NaCeLA are obtained by considering the deduction of the dilution effect in water from the total thermal effect, as given by Eq. (3). The effects of the thermodynamic cycle for this series of interactions involving a suspension (susp) of NaCeLA (A–M and F) in aqueous (aq) solution with divalent cations (M<sup>2+</sup>) can be represented by the following reactions:



The net thermal effects obtained from the calorimetric titration ( $\sum Q_r - \sum Q_t - \sum Q_d$ ), as given by Eq. (11), are represented in Fig. 10 and the corresponding linearization involving cobalt and nickel adsorptions are shown in Fig. 11. From Eq. (4) and the linearized data for both cations, the enthalpy of interaction,  $\Delta_{int}H$ , can enable the calculation of the enthalpy, as given by Eq. (5). From calorimetric titration the equilibrium constant and enthalpy were

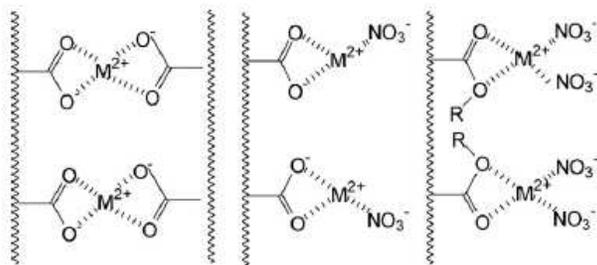


Fig. 9. Possible structures for divalent cation complex formation on CeLA.

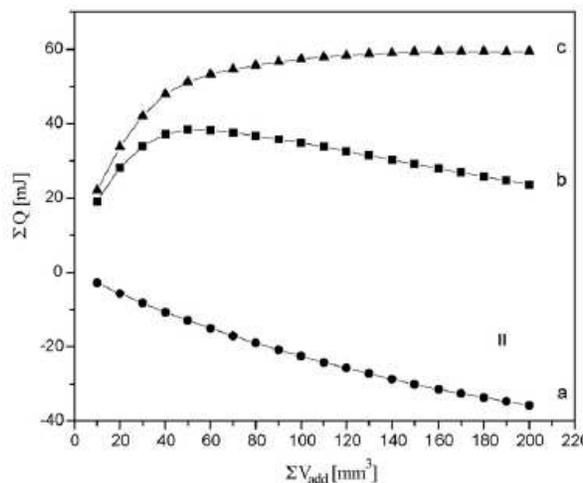
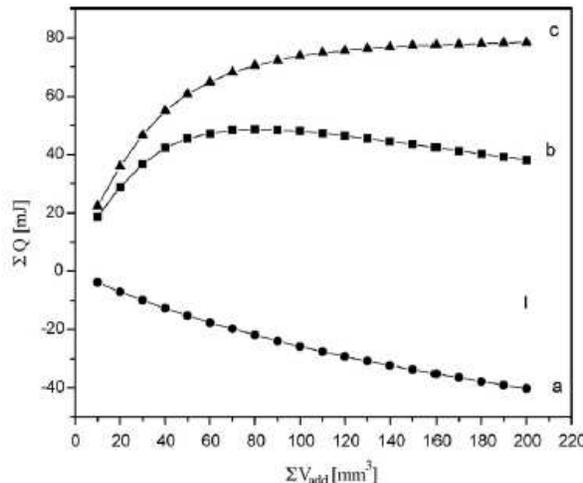


Fig. 10. The resulting thermal effects of the adsorption isotherms of the divalent cations; (I) Co<sup>2+</sup> and (II) Ni<sup>2+</sup> on the CeLA surface at 298.15 ± 0.20 K. Cation/basic center interaction enthalpy (■), dilution enthalpy (●) and reaction enthalpy (▲).

simultaneously obtained, which enable the calculation of the Gibbs free energy and the entropy as listed in Table 2. The magnitude of the values presented is indicative of ion exchange [41] favoring Co<sup>2+</sup> adsorption. The negative free energy indicates spontaneous processes of complexation/ion exchange with the same order of enthalpies, as also previously observed for anchored cellulose. Both systems presented positive entropic values that contribute to the occurrence of favorable reactions. These entropic values suggested that during complex formation the cation desolvation and sodium solvation processes disturbed the original structure of the solvent, by causing a disorganization of the system with an increase in entropy. On the other hand, another contribution to the entropic value comes from the displacement of the water molecules hydrogen-bonded to acidic centers attached to the pendant chains,

Table 2 Summary of thermodynamic values for the interaction of divalent metal nitrates on the CeLA (A–M and F) surface at 298.15 ± 0.20 K.

| CeLA                 | $\Delta H$ (kJ/mol) | $-\Delta G$ (kJ/mol) | $\Delta S$ (J/Kmol) |
|----------------------|---------------------|----------------------|---------------------|
| CeLACo <sup>2+</sup> | 0.29 ± 0.02         | 3.6 ± 0.5            | 13 ± 1              |
| CeLANi <sup>2+</sup> | 0.87 ± 0.02         | 1.9 ± 0.6            | 9 ± 1               |

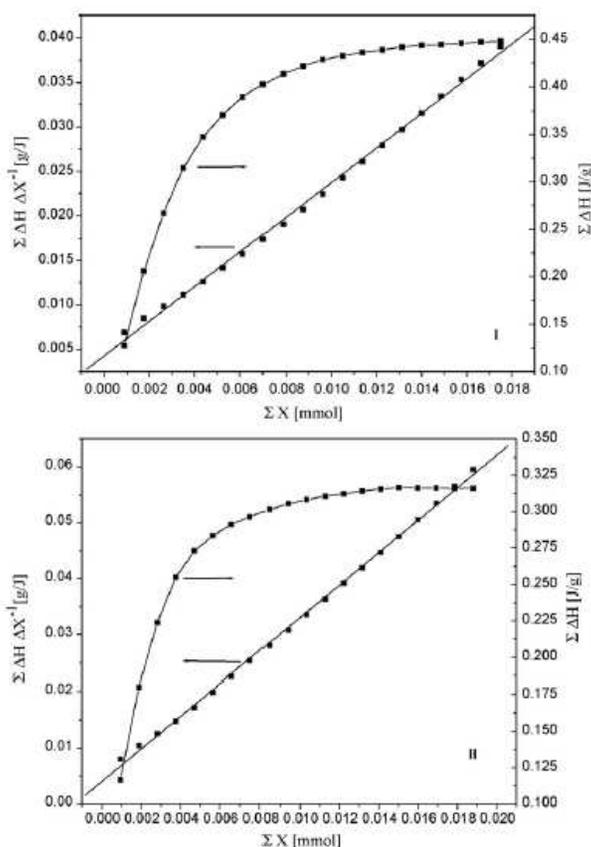


Fig. 11. Isotherms from calorimetric titration and their linearized forms for  $\text{Co}^{2+}$  (I) and  $\text{Ni}^{2+}$  (II) on the CeIA surface at  $298.15 \pm 0.20$  K.

as the complexation is in progress, to form the final rearrangement in structure [13]. The thermodynamic data are in agreement with the adsorption of those cations at the solid/liquid interface, suggesting an application for this anchored polysaccharide for cation removal.

#### 4. Conclusions

The strategy presented to modify the world's most widely available biopolymer surface under solvent-free conditions was plainly achieved. The well-characterized product formed presented a high degree of covalently bound pendant molecules bearing a carboxylic group that is able to adsorb cations.

Instead of proceeding under high temperature as normally used, the present conditions for melting maleic anhydride favor a decrease in reaction time, although it is difficult to avoid overoxidation caused by residual humidity and atmospheric oxygen, which will favor dark and radical processes. The biopolymer generated probably has in the same cellulosic chain both maleate and fumarate isomers, it being impossible to separate them. The conversion (maleate to fumarate) is favored by higher temperatures.

The new synthetic surface with incorporation of pendant chains containing potentially basic centers are potential available centers for cation removal, and behaved as promising materials to be applied for this operation, with good sorption capacity for divalent cations, and of great utility for ecosystem purification. The quantitative interactions between cation and carboxylic basic centers at the solid/liquid interface obtained from calorimetry gave favor-

able thermodynamic data, such as endothermic enthalpy, negative Gibbs free energy and positive entropy. These thermodynamic values suggest the application of this material, available worldwide, to improve the environment.

#### Acknowledgements

The authors are indebted to FAPESP for financial support and for fellowships to J.C.P.M. and E.C.S.F., and also to CNPq and CAPES for fellowships to C.A. and S.A.A.S. Prof. C. Collins is also acknowledged for suggestions and revision of English.

#### References

- [1] D. Klemm, B. Heublein, H.P. Fink, A. Bohn, Cellulose: fascinating biopolymer and sustainable raw material, *Angew. Chem. Int. Ed.* 44 (2005) 3358–3393.
- [2] T. Heinze, T. Liebert, Unconventional methods in cellulose functionalization, *Prog. Polym. Sci.* 26 (2001) 1689–1762.
- [3] O. Karnitz Jr., L.V.A. Gurgel, J.C.P. Melo, V.R. Botaro, T.M.S. Melo, R.P.F. Gil, L.F. Gil, Adsorption of heavy metal ion from aqueous single metal solution by chemically modified sugarcane bagasse, *Bioresour. Technol.* 98 (2007) 1291–1297.
- [4] M.I. Hassan, R.M. Rowell, N.A. Fadl, S.F. Yacoub, A.W. Christensen, Thermoplasticization of bagasse. I. Preparation and characterization of esterified bagasse fibers, *J. Appl. Polym. Sci.* 76 (2000) 561–574.
- [5] C. Vaca-Garcia, G. Gozzelinoi, W.G. Glasser, M.E. Borredon, Dynamic mechanical thermal analysis transitions of partially and fully substituted cellulose fatty esters, *J. Polym. Sci. B* 41 (2003) 281–288.
- [6] T. Heinze, T. Liebert, K. Pfeiffer, M.A. Hussain, Unconventional cellulose esters: synthesis, characterization and structure–property relations, *Cellulose* 10 (2003) 283–296.
- [7] K.J. Edgar, C.M. Buchanan, J.S. Debenham, P.A. Rundquist, B.D. Seiler, M.C. Shelton, D. Tindall, Advances in cellulose ester performance and application, *Prog. Polym. Sci.* 26 (2001) 1605–1688.
- [8] D. Klemm, B. Philipp, T. Heinze, U. Heinze, W. Wagenknecht, *Comprehensive Cellulose Chemistry*, Wiley, Weinheim, 1998.
- [9] I.M. Smallwood, *Handbook of Organic Solvent Properties*, Arnold, London, 1996.
- [10] S.E. Manahan, *Fundamentals of Environmental Chemistry*, CRC Press LLC, Boca Raton, 2001.
- [11] R.P. Swatoski, S.K. Spear, J.D. Holbrey, R.D. Rogers, Dissolution of cellulose with ionic liquids, *J. Am. Chem. Soc.* 124 (2002) 4974–4975.
- [12] S. Babel, T.A. Kurniawan, Low-cost adsorbents for heavy metals uptake from contaminated water: a review, *J. Hazard. Mater.* 97 (2003) 219–243.
- [13] E.C. Silva Filho, J.C.P. Melo, C. Airolti, Preparation of ethylenediamine-anchored cellulose and determination of thermochemical data for the interaction between cations and basic centers at the solid/liquid interface, *Carbohydr. Res.* 341 (2006) 2842–2850.
- [14] E. Hodgson, *A Textbook of Modern Toxicology*, Ernest Hodgson, New Jersey, 2004.
- [15] A.L.P. Silva, K.S. Sousa, A.F.S. Germano, V.V. Oliveira, J.G.P. Espinola, M.G. Fonseca, C. Airolti, A new organofunctionalized silica containing thioglycolic acid incorporated for divalent cations removal—a thermodynamic cation/basic center interaction, *Colloids Surf. A* 332 (2009) 144–149.
- [16] R.K. Dey, F.J.V.E. Oliveira, C. Airolti, Mesoporous silica functionalized with diethylenetriamine moieties for metal removal and thermodynamics of cation-basix center interactions, *Colloids Surf. A* 324 (2008) 41–46.
- [17] E.C.N. Lopes, K.S. Sousa, C. Airolti, Chitosan-cyanuric chloride intermediary as a source to incorporate molecules—thermodynamic data of copper/biopolymer interactions, *Colloids Surf. A* 483 (2008) 21–28.
- [18] A.C. Wibowo, S.M. Desai, A.K. Mohanty, L.T. Drzal, M. Misra, A solvent free graft copolymerization of maleic anhydride onto cellulose acetate butyrate bioplastic by reactive extrusion, *Macromol. Mater. Eng.* 291 (2006) 90–95.
- [19] W. Qiu, T. Endo, T. Hirotsu, A novel technique for preparing of maleic anhydride grafted polyolefins, *Eur. Polym. J.* 41 (2005) 1979–1984.
- [20] C.J. Garvey, I.H. Parker, G.P. Simon, On the interpretation of X-ray diffraction powder patterns in terms of the nanostructure of cellulose. I. *Fibres, Macromol. Chem. Phys.* 206 (2005) 1568–1575.
- [21] J.W. Tindall, B.W. Boyd, R.L. Perry, Determination of acid substituents and unesterified hydroxyl groups in cellulose esters, *J. Chromatogr. A* 977 (2002) 247–250.
- [22] R. Dicke, A straight way to regioselectively functionalized polysaccharide esters, *Cellulose* 11 (2004) 255–263.
- [23] J.W. Larsen, D.M. Quay, J.E. Roberts, Reactions of Pittsburgh No. 8 coal with maleic anhydride. Evidence for the existence of reactive diene structures in coal, *Energy Fuels* 12 (1998) 856–863.
- [24] H. Zhao, J.H. Kwak, Z.C. Zhang, H.M. Brown, B.W. Arey, J.E. Holladay, Studying cellulose fiber structure by SEM, XRD, NMR and acid hydrolysis, *Carbohydr. Polym.* 68 (2007) 235–241.
- [25] S. Margutti, S. Vicini, N. Proietti, D. Capitani, G. Conio, E. Pedemonte, A.L. Segre, Physical-chemical characterisation of acrylic polymers grafted on cellulose, *Polymer* 43 (2002) 6183–6194.
- [26] G.S. Hammond, J. Saliel, A.A. Lamola, N.J. Turro, J.S. Bradshaw, D.O. Cowan, R.C. Counsell, V. Vogt, C. Dalton, Mechanisms of photochemical reactions in

- solution, XXII, 1 Photochemical cis-trans isomerization, *J. Am. Chem. Soc.* 86 (1964) 3197–3217.
- [27] H. Matsuda, M. Ueda, K. Murakami, Preparation and utilization of esterified woods bearing carboxyl groups. II. Esterification of wood with dicarboxylic acid anhydrides in the absence of solvent, *Mokuzai Gakkaishi* 30 (1984) 1003–1010.
- [28] C.F. Liu, R.C. Sun, M.H. Qin, A.P. Zhang, J.L. Ren, F. Xu, J. Ye, S.B. Wu, Chemical modification of ultrasound-pretreated sugarcane bagasse with maleic anhydride, *Ind. Crops Prod.* 26 (2007) 212–219.
- [29] M. Schwanninger, J.C. Rodrigues, H. Pereira, B. Hinterstoesser, Effects of short-time vibratory ball milling on the shape of FT-IR spectra of wood and cellulose, *Vib. Spectrosc.* 36 (2004) 23–40.
- [30] R.M. Silverstein, G.C. Bassler, T.C. Morrill, *Spectrometric Identification of Organic Compounds*, Wiley, London, 2005.
- [31] L.V.A. Gurgel, R.P. Freitas, L.F. Gil, Adsorption of Cu(II), Cd(II) and Pb(II) from aqueous single metal solutions by sugarcane bagasse and mercerized sugarcane bagasse chemically modified with succinic anhydride, *Carbohydr. Polym.* 74 (2008) 922–929.
- [32] R.H. Atalla, D.L. VanderHart, The role of solid state  $^{13}\text{C}$  NMR spectroscopy in studies of the nature of native celluloses, *Solid State Nucl. Magn. Reson.* 15 (1999) 1–19.
- [33] H. Kono, S. Yunoki, T. Shikano, M. Fujiwara, T. Erata, M. Takai, CP/MAS  $^{13}\text{C}$  NMR study of cellulose and cellulose derivatives. I. Complete assignment of the CP/MAS  $^{13}\text{C}$  NMR spectrum of the native cellulose, *J. Am. Chem. Soc.* 124 (2002) 7506–7511.
- [34] A.C.O. Sullivan, Cellulose: the structure slowly unravels, *Cellulose* 4 (1997) 173–207.
- [35] P. Zugenmaier, Conformation and packing of various crystalline cellulose fibers, *Prog. Polym. Sci.* 26 (2001) 1341–1417.
- [36] S.M. Smole, Z. Peršin, T. Kreže, K.S. Kleinschek, V. Ribitsch, X-ray study of pretreated regenerated cellulose fibres, *Mater. Res. Innov.* 7 (2003) 275–282.
- [37] H. Zhao, J.H. Kwak, Y. Wang, J.A. Franz, J.M. White, J.E. Holladay, Effects of crystallinity on dilute acid hydrolysis of cellulose by cellulose ball-milling study, *Energy Fuels* 20 (2006) 807–811.
- [38] W.Y. Chiang, C.H. Hu, Approaches of interfacial modification for flame retardant polymeric materials, *Composites A* 32 (2001) 517–524.
- [39] S. Sun, Q. Wang, A. Wang, Adsorption properties of Cu(II) ions onto N-succinyl-chitosan and crosslinked N-succinyl-chitosan template resin, *Biochem. Eng. J.* 36 (2007) 131–138.
- [40] F. Li, X. Sun, H. Zhang, B. Li, F. Gan, Pyromellitic dianhydride-modified beta-cyclodextrin microspheres for Pb(II) and Cd(II) adsorption, *J. Appl. Polym. Sci.* 105 (2007) 3418–3425.
- [41] A. Ramesh, D.J. Lee, J.W.C. Wong, Thermodynamic parameters for adsorption equilibrium of heavy metals and dyes from wastewater with low-cost adsorbents, *J. Colloid Interface Sci.* 291 (2005) 588–592.



Contents lists available at ScienceDirect

Thermochimica Acta

journal homepage: [www.elsevier.com/locate/tca](http://www.elsevier.com/locate/tca)

## Synthesized cellulose/succinic anhydride as an ion exchanger. Calorimetry of divalent cations in aqueous suspension

Júlio C.P. Melo<sup>a</sup>, Edson C. Silva Filho<sup>b</sup>, Sirlane A.A. Santana<sup>c</sup>, Claudio Airoidi<sup>a,\*</sup>

<sup>a</sup> Institute of Chemistry, University of Campinas, UNICAMP, P.O. Box 6154, 13084-971 Campinas, SP, Brazil

<sup>b</sup> LIMAV, Federal University of Piauí, 64049-550 Teresina, Piauí, Brazil

<sup>c</sup> Departamento de Química/CCET, Universidade Federal do Maranhão, Av. dos Portugueses S/N, Campus do Bacanga, 65080-540 São Luiz, MA, Brazil

### ARTICLE INFO

#### Article history:

Received 8 April 2011

Received in revised form 2 June 2011

Accepted 8 June 2011

Available online 15 June 2011

#### Keywords:

Cellulose

Succinic anhydride

Solvent-free

Ion exchange

Calorimetry

### ABSTRACT

A synthetic route to a biopolymer/anhydride ion exchanger adds cellulose directly to molten succinic anhydride in a quasi solvent-free procedure. An amount of  $3.07 \pm 0.05$  mmol of pendant groups incorporated onto the polymeric structure, which was characterized by elemental analysis, solid state carbon NMR, infrared, X-ray and thermogravimetry. The new polysaccharide is able to exchange cations from aqueous solution through a batchwise methodology, to obtain  $2.46 \pm 0.09$  mmol g<sup>-1</sup> for divalent cobalt and nickel cations. The net thermal effects obtained from calorimetric titrations gave endothermic values of  $3.81 \pm 0.02$  and  $2.35 \pm 0.01$  kJ mol<sup>-1</sup>. The spontaneity of this ion-exchange process reflected in negative Gibbs energies and also a positive entropic contribution. These thermodynamic data at the solid/liquid interface suggests a favorable ion exchange process for this anchored biopolymer, for cation removal from the environment.

© 2011 Elsevier B.V. All rights reserved.

### 1. Introduction

Anthropogenic influences due to human impact contribute to heavy metal environmental contamination, mainly to waters and soils [1]. Even though a series of essential metals, as well as enzymes and proteins, are needed for most living beings, undesirable accumulation along the food chain may occur. For example, sorption and intoxication with cobalt causes an increase in hepatic glutathione levels. This metal is absorbed by the same active transport mechanism that normally occurs for iron, while intoxication with nickel causes nasal and lung cancers as well as DNA damage [2].

The potential utility of some native materials is normally associated with agents to improve life. For example, cellulose is the most abundant natural biopolymer, presenting as the main component of the plant cell walls and also is biosynthesized by other organisms such as algae, fungus and bacteria, making it suitable for this. Sorption on such solids, whether or not chemically organofunctionalized, obtained from different natural or synthetic sources, has been widely investigated for heavy cation removal from aqueous and non-aqueous effluents [3–5]. However, this biopolymer presents considerable chemical and physical inertness, so that surface or bulk modifications can sometimes be hard to achieve, especially without appropriate conditions. From the structural

point of view, cellulose bears one primary hydroxyl on carbon 6 and two other hydroxyls on carbons 2 and 3, on which chemical modifications may occur. Some other reactions are able to succeed via an oxidative opening of the pyrane-rings [6,7].

One well-established and intensively explored reaction consists in acylating through anhydrides [4,8,9] that involves, in principle, all three hydroxyl groups of the cellulose unit, to yield stable ester and reactive carboxylic acid end groups, whose hydroxyl groups act as nucleophilic agents. For practical use, these acylating processes are employed for coatings, cosmetics and, in the food and pharmaceutical industries, as antibody, enzyme, protein and ion separation membranes and filters etc [7,10–13].

The pendant carboxylic groups on the as-synthesized insoluble biopolymer can be converted into the sodium carboxylated form, whose suspension in aqueous solution enables it to act as an ion exchanger. In principle, a large number of distinct natural and synthetic materials present ion exchange properties, for example, natural inorganic clays, zeolites and green sands; natural organic polysaccharides, proteins and carbonaceous derivatives; synthetic zeolites, titanates and silico-titanates and transition metal hexacyanoferrates; synthetic organic resins etc [13].

The present investigation deals with a chemical modification process of the natural biopolymer cellulose without using solvents during the synthetic process [4,14], by successfully exploring the relatively low melting point of the chosen reactant, succinic anhydride. The applicability of this synthesized cellulose is related to the ability of the negatively charged carboxylate group in the pendant

\* Corresponding author. Fax: +55 19 35213023.  
E-mail address: [airoidi@iqm.unicamp.br](mailto:airoidi@iqm.unicamp.br) (C. Airoidi).

chains to exchange cations from aqueous solution. The quantitative features associated with the exchange at the solid/liquid interface were calorimetrically followed to better understand this important and little explored interactive process.

## 2. Experimental

### 2.1. Materials

Microcrystalline cellulose powder (Aldrich), with particle size  $\sim 20 \mu\text{m}$ , was dried before use. Succinic anhydride (Aldrich) and the other analytical grade reagents were used without prior purification.

### 2.2. Characterization

First, the protonated form of the as-synthesized material (H-CeLS) was characterized. The amount of succinic anhydride incorporated on the biopolymer cellulose was determined through elemental analysis on a Perkin Elmer model 2400 analyzer and as well as by a titration procedure. Infrared spectra of the samples in KBr pellets were obtained with diffuse reflectance by accumulating 32 scans on a Bomem Spectrophotometer, MB-series, in the  $4000\text{--}400 \text{ cm}^{-1}$  range, with  $4 \text{ cm}^{-1}$  of resolution. Nuclear magnetic resonance in the solid state for the carbon nucleus was obtained on a Bruker AC 400/P spectrometer at room temperature. The measurements were obtained at frequencies of 75.47 MHz with magic angle spinning of 10 kHz. To increase the signal/noise ratio, the CP/MAS technique was used, with pulse repetitions of 5 s and contact times of 1 ms. X-ray diffraction patterns were obtained on a Shimadzu model XRD 7000 diffractometer with 40 kV applied voltage, current of 30 mA and the  $\text{CuK}\alpha$  ( $\lambda = 0.154 \text{ nm}$ ) radiation source scanned from  $5^\circ$  to  $45^\circ$ . Thermogravimetric curves in an inert atmosphere were obtained on a TA instrument, coupled to a model 1090 B thermobalance, with mass of approximately 10 mg, using a heating rate of  $0.167 \text{ K s}^{-1}$ , under a flow of argon at  $30 \text{ cm}^3 \text{ s}^{-1}$ , from room temperature to 773 K. The amount of cation exchanged was determined from the difference between the initial concentration in aqueous solution and that found in the supernatant, using ICP OES (inductively coupled plasma optical emission spectrometry) on a Perkin Elmer 3000 DV apparatus. For each experimental point of the cation determination in the supernatant, the reproducibility was checked by at least one duplicate run.

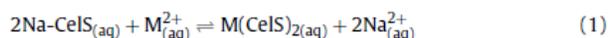
### 2.3. Synthesis of chemically modified cellulose

A sample of 10 g of cellulose (Cel), previously dried at 383 K for 2 h under vacuum, was added to 60 g of molten anhydride, in a cellulose/succinic anhydride ratio of 1:10, under magnetic stirring in a sand bath at 388 K, under anhydrous conditions. The fluid mixture was heated for 6 h, followed by addition of  $50 \text{ cm}^3$  of *N,N'*-dimethylacetamide to avoid recrystallization of free anhydride and was hot filtered. The solid was intensively washed with water to reach a neutral pH and the biopolymer (H-CeLS) was then dried in vacuum at 383 K for 24 h. The proton was exchanged by sodium by immersing the biomaterial in  $0.90 \text{ mol dm}^{-3}$  of a sodium hydrogencarbonate solution at 291 K, producing Na-CeLS, which was then used as an ion exchanger in suspension and also for the calorimetric determinations.

### 2.4. Ion exchange

The sodium from Na-CeLS biopolymer was batchwise exchanged with divalent cobalt and nickel nitrates in aqueous solution in duplicate runs. For this process a given mass ( $m$ ) was suspended in

$25.0 \text{ cm}^3$  of each cation solution in the  $0.10\text{--}5.0 \text{ mmol dm}^{-3}$  range of concentration. The best isotherm was obtained with 25 mg of the exchanger to give a defined plateau with maximum exchange capacity, being carried out at an isoelectronic pH ( $5.5 \pm 0.1$ ), after shaking the suspension for 3 h in an orbital bath at  $298 \pm 1 \text{ K}$ . The isotherms of saturation were obtained by the concentration versus time procedure, which gave a well-defined plateau. In each case, the solid was separated by centrifugation for 10 min at 2300 rpm and the cation concentration was determined by ICP OES, from aliquots of the supernatant. The exchange capacities ( $nf$ ) were calculated through the number of moles:  $nf = (n_i - n_s)/m$ , where  $n_i$  and  $n_s$  are the initial number of moles and those remaining in the supernatant at the end of the experiment, and  $m$  is the mass of the exchanger [4,14]. As expected, the sodium electrostatically bonded to the biopolymer is gradually replaced by cations in the progress of reaction at the solid/liquid interface in aqueous solution (aq) to reach equilibrium:



The experimental data were adjusted to the modified Langmuir isotherm that correlated the number of moles of metal in solution at equilibrium, when the cations are exchanged with sodium bonded on the pendant chains, as given by Eq. (2):

$$\frac{\text{Cs}}{nf} = \frac{\text{Cs}}{n^s} + \frac{1}{n^s b} \quad (2)$$

where  $\text{Cs}$  ( $\text{mol dm}^{-3}$ ) is the concentration of supernatant cations at equilibrium,  $nf$  ( $\text{mol g}^{-1}$ ) is the number of moles exchanged,  $n^s$  ( $\text{mol g}^{-1}$ ) is the maximum amount of solute exchanged per gram of Na-CeLS and  $b$  ( $\text{dm}^3 \text{ mol}^{-1}$ ) is a constant. The  $n^s$  and  $b$  values for each sorption process were obtained from the angular and linear coefficients, respectively, of the linearized form of the isotherms, by considering  $\text{Cs}/nf$  versus  $\text{Cs}$ , using the least squares method [14].

### 2.5. Calorimetric titration

The interaction at the solid/liquid interface due to the cation exchange process is associated with the thermal effects measured on a LKB 2277 calorimeter [4,14]. Briefly, a sample of about 20 mg of the exchanger was suspended in  $2.0 \text{ cm}^3$  of water under stirring at  $298.15 \pm 0.20 \text{ K}$ . The cation solutions with concentrations of  $0.30 \text{ mol dm}^{-3}$  were incrementally added to the calorimetric vessel, to obtain  $Q_t$ . Identically, the thermal effect of dilution,  $Q_d$ , and the thermal effect of Na-CeLS hydration,  $Q_h$ , was determined [4,14,15]. The net thermal effect of the exchanger  $Q_r$  was obtained through Eq. (3), by considering that the suspension of the solid in water gave a null value:

$$\sum Q_r = \sum Q_t - \sum Q_d \quad (3)$$

The enthalpy obtained related to the interaction was also adjusted to a modified Langmuir equation to calculate the integral enthalpy of monolayer formation per unit mass of the ion exchanger,  $\Delta_{\text{mono}}H$  [14], as shown in Eq. (4):

$$\frac{\sum X}{\sum \Delta H} = \frac{1}{(K-1)\Delta_{\text{mono}}H} + \frac{X}{\Delta_{\text{mono}}H} \quad (4)$$

where  $\sum X$  is the sum of the mole fractions of the solute after exchanging, for each addition point of titrant. The integral enthalpy of exchange per gram of biopolymer,  $\Delta H$ , was obtained by dividing the thermal effect resulting from the exchange process by the number of moles of the exchanger and  $K$  includes the equilibrium constant. The angular and linear values of the  $\sum X/\sum \Delta H$  versus  $\sum X$

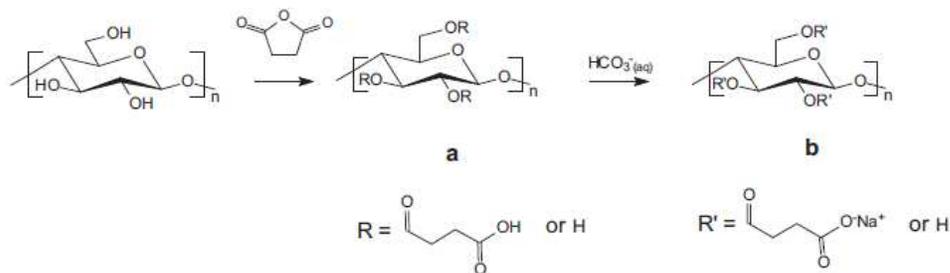


Fig. 1. Synthesis of cellulose (a) and its sodium form (b) from the reaction of cellulose with succinic anhydride.

plot enable calculation of the  $\Delta_{\text{mono}}H$  value, by means of expression (5):

$$\Delta H = \frac{\Delta_{\text{mono}}H}{n^5} \quad (5)$$

From the equilibrium constant values, the Gibbs energies were calculated by expression (6):

$$\Delta G = -RT \ln K \quad (6)$$

and the entropy value can be calculated through Eq. (7):

$$\Delta G = \Delta H - T\Delta S \quad (7)$$

### 3. Results and discussion

The reaction of cellulose with succinic anhydride yielded the chemically modified polysaccharide (H-CeLS) with a carbon content of  $44.07 \pm 0.19\%$ , which enabled calculation of a high degree of substitution (DS) of  $1.00 \pm 0.14$  for this water insoluble biopolymer. Based on the amount of carbon in the precursor biopolymer,  $41.95 \pm 0.04\%$ , the results clearly differ, indicating the success of anhydride incorporation during the chemical reaction and the proposed reaction is shown in Fig. 1a. The amount of succinic anhydride covalently bonded to the biopolymeric backbone structure was calculated as  $3.77 \pm 0.14 \text{ mmol g}^{-1}$ , using the DS value, or  $3.07 \pm 0.05 \text{ mmol g}^{-1}$  through carboxylic acid titration [4,9] procedure. The difference in values might be related to the methodologies. For the latter method the number of free sites available was calculated from the covalently bound groups, which is followed by uncertainties that emerge from possible crosslinking reactions [16,17]. It is worth remembering that in spite of the high anhydride:hydroxyl ratio the crosslinking effect should be minimized, but not completely eliminated. However, the homogeneous route takes place on a specific selected position. On the contrary, for a heterogeneous pathway the degree of substitution is obtained by dissolving the biopolymer and the extension of reaction on each particular position is analyzed [6,7,18].

The success of the heterogeneous conditions leads to a chemical modification procedure that is closely related to the high reactivity on carbon 6. This process can form different structures, due to oxidized-ends that depend on the degree of polymerization increasing during the reaction, due to the carboxylic acid groups formed or to the proton involved in  $\beta$ -(1,4) cleavage [19] and also due to oxidized-opened rings [20]. As a result, the absence of solvent favors incorporations to yield powdered cellulose covered with pendant chains on the polysaccharide, as depicted in Fig. 1.

The infrared spectra of raw cellulose [21] and of the chemically modified polysaccharide (H-CeLS) are shown in Fig. 2. The bands at  $2775$  and  $2500 \text{ cm}^{-1}$  are related to carboxylic acid dimers as well as their stretching at  $1717 \text{ cm}^{-1}$ . The bands at  $1741 \text{ cm}^{-1}$  and  $1163 \text{ cm}^{-1}$  are assigned to  $\nu(\text{C}=\text{O})$  from the ester [16], proving the success of the reaction. The absence of bands at  $1860$  and  $1790 \text{ cm}^{-1}$

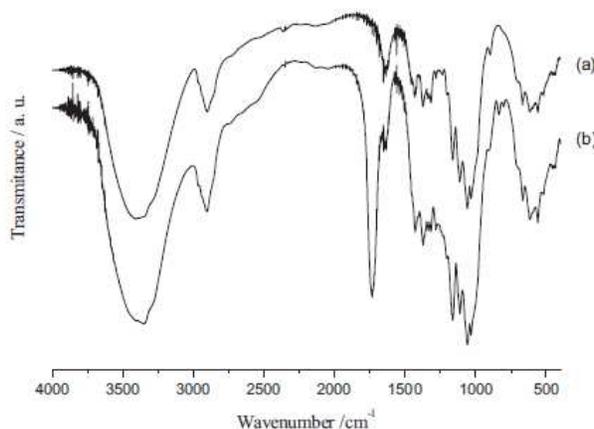


Fig. 2. Infrared spectra of cellulose (a) and its chemically modified form, H-CeLS (b).

confirms that the product is free from unreacted succinic anhydride [14,22].

The main change in the structural organization when comparing pristine and chemically modified cellulose reflects in carbons 6 and 4 from the  $^{13}\text{C}$  NMR CP/MAS spectra [14,23,24], as shown in Fig. 3. The carbon-6 atom bears the primary hydroxyl, as numbered

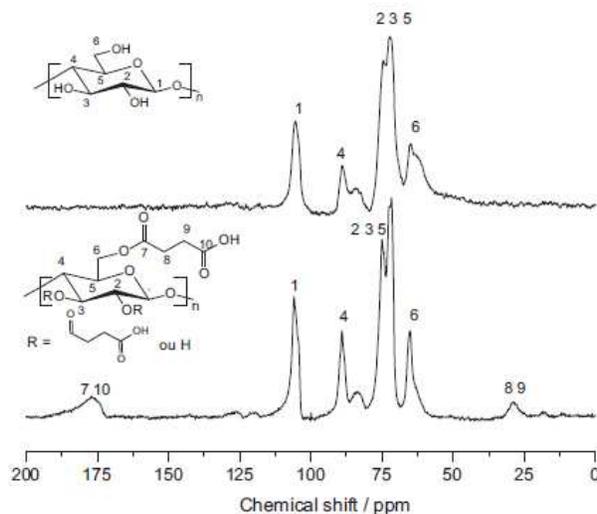


Fig. 3.  $^{13}\text{C}$  CP/MAS NMR spectra of cellulose (a) and its chemically modified form, H-CeLS (b).

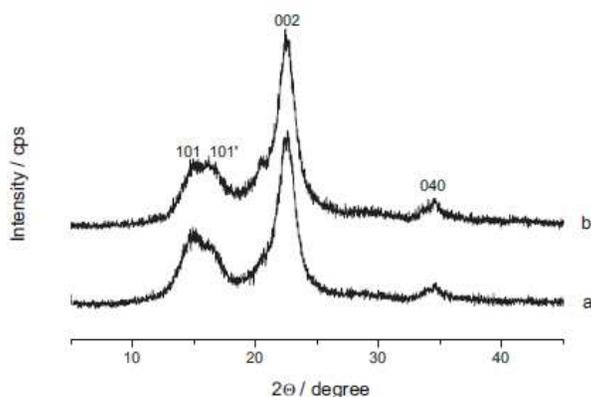


Fig. 4. X-ray diffraction patterns for cellulose (a) and its chemically modified form, H-CeIS (b).

in the inserted structure, that is involved in intramolecular hydrogen bonds with the hydroxyl on C2, and intermolecular bonds, with the hydroxyl on C3' in the adjacent chains. As C6 is structured in this fashion the spectrum will be affected by any change in these hydrogen bonds. It is quite important to note that the C6 features are related to the structural organization only in non-chemically modified cellulose, such as the pristine polysaccharide. The corresponding signal is more downfield shifted than the amorphous form, with a shoulder upfield at 65 ppm. The carbon C4 signal is sensitive to conformational effects and tensions on the chains to give a broader signal at 83 ppm, referring to low organizational structure and at 89 ppm for more crystalline features. Although C1 and C4 hold oxygen atoms that are located between two glucose units, these carbons cannot be related to crystallinity aspects [25,26]. It is worth to mention that the relevant signal at 174 ppm is related to the existence of carbonyl groups of H-CeIS and these signals are overlapped due to the possible presence of both an ester and a carboxylic acid, which is in agreement with these moieties formation. The carbons of the modifier agent appear at 29 ppm for C8 and C9, and carbons 2, 3 and 5 are assigned to signals from 70 to 74 ppm, with signals attributed to side bands at 120 and 125 ppm. The assigned set of signals clearly demonstrated the success of the reaction succinic anhydride/cellulose to yield a new stable polysaccharide.

The degree of structural organization [16] of the cellulose in the solid-state has demonstrated great interest. A way to calculate this feature is by comparing the relative intensity between the 002 planes through Bragg [27] and Scherrer [28] laws. X-ray diffraction patterns obtained from the new material, produced from the original microcrystalline cellulose through a heterogeneous route, are dominated by the original and not by novel crystalline arrangements on the biopolymer. The modifications are expected to occur first on the more available hydroxyl groups in the para-crystalline region, located on the polymeric surface. Thus, it is expected that the diffraction patterns showed no change in the chemically modified cellulose H-CeIS, as shown in Fig. 4. However, as previously discussed, the regions of lower crystallinity decreased, proven by regarding external chain disorganization and fiber length shortening, as confirmed by the peak at  $34.5^\circ$ , corresponding to the 040 plane [29].

Thermogravimetric curves for cellulose and the chemically modified biopolymer are shown in Fig. 5. Both biopolymers presented only one event due to decomposition, covering the intervals of temperature, starting with mass loss from 550 to 475 K for pristine cellulose and chemically modified H-CeIS, respectively, to define plateaus near 700 K. These events include losses of water

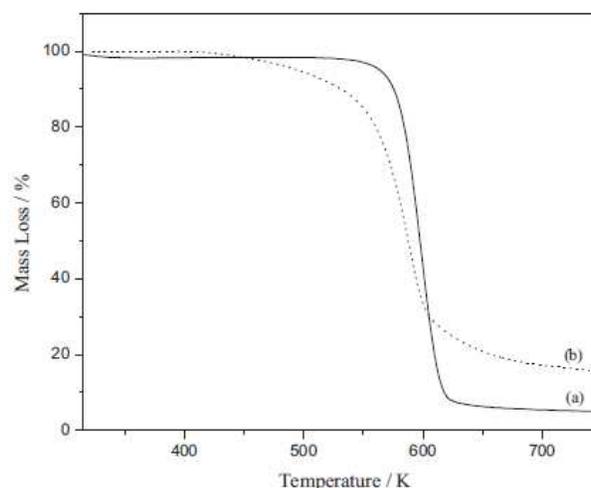


Fig. 5. Thermogravimetric curves of pristine (a) and as-synthesized H-CeIS (b) celluloses.

**Table 1**  
Number of moles sorbed ( $n_f$ ), maximum ion exchange capacity ( $n^s$ ), constant ( $b$ ) and correlation coefficient ( $r$ ) for the interaction of divalent metal (M) nitrates with the modified cellulose surfaces at  $298 \pm 1$  K.

| M                | $n_f/\text{mmol g}^{-1}$ | $n^s/\text{mmol g}^{-1}$ | $b/\text{dm}^3 \text{mol}^{-1}$ | $r$   |
|------------------|--------------------------|--------------------------|---------------------------------|-------|
| $\text{Co}^{2+}$ | $2.46 \pm 0.12$          | $2.53 \pm 0.01$          | 385                             | 0.996 |
| $\text{Ni}^{2+}$ | $2.46 \pm 0.12$          | $2.53 \pm 0.01$          | 87                              | 0.977 |

physically adsorbed onto the surface, condensation of hydroxyl groups on carbons 2 and 3 and cellulose fiber decomposition [4]. As observed, H-CeIS start to decompose at a lower temperature due to the facility of the pendant chain decomposing on heating.

Examination of the interaction of divalent cations and the sodium cation bonded to the chemically modified cellulose is the main characteristic of the biopolymer involved. The original carboxylic acid groups attached to the pendant chains covalently bonded to the cellulose backbone have the ability to act as ion exchangers from aqueous solution at the solid/liquid interface [30,31]. However, to minimize any dependence on pH and also to facilitate the process, the protons were previously exchanged by sodium. The isotherms of cation exchange with the modified biopolymer resulted from the ion exchange represented by the equilibrium summarized in Eq. (1). The exchanging explored the best conditions performed by using 25 mg of ion exchanger, with stirring for 3 h at  $298 \pm 1$  K. This exchanger process gave maximum amounts exchanged ( $n^s$ ) of  $2.46 \pm 0.12 \text{ mmol g}^{-1}$  for both cobalt and nickel cations.

These values were obtained after fitting the results to a modified Langmuir equation (Eq. (2)), as successfully applied for other systems, to obtain the parameters for sorption at the solid/liquid interface [4,14,15]. The linearized form for nickel exchange is given by  $C_s/n_f$  as a function of  $C_s$ , is shown in Fig. 6, and enables the calculation of the linear and angular data from the straight line, to give  $n^s$  and  $b$  values, as listed in Table 1. Although  $n^s$  are very close,  $b$  values differ from each other, demonstrating that they are related to different equilibrium processes. The participation of the anion to neutralize the free cation charge is also presented, where the cation can bond to individual available carboxylate groups or by bridging two distinct basic centers.

The net thermal effects due to the interaction of cations with Na-CeIS are obtained by considering the deduction of the dilution effect in water from the total thermal effect, as given by Eq. (3),

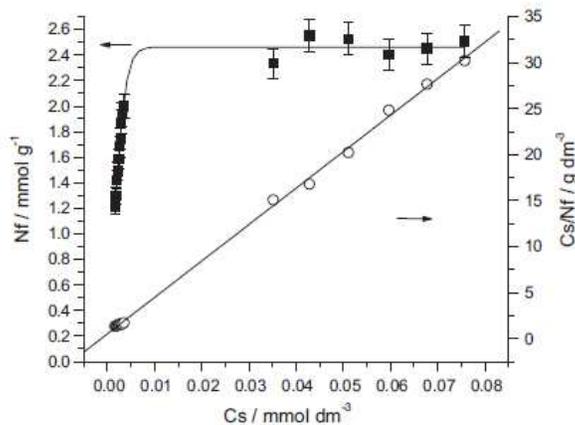
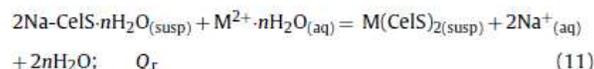
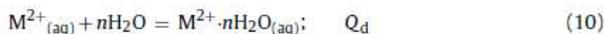
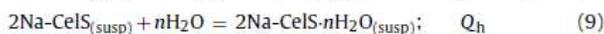


Fig. 6. Ion exchange isotherms for Ni<sup>2+</sup> (●) and the linearized Langmuir isotherm (○) on chemically modified cellulose, Na-CeLS, at 298 ± 1 K.

and the independent titrations for nickel are shown in Fig. 7. The thermodynamic cycle for this series of interactions involving a suspension (susp) of Na-CeLS in aqueous (aq) solution with divalent cations (M<sup>2+</sup>) can be represented by the following reactions:



The net thermal effects obtained from the calorimetric titration ( $\Sigma Q_r = \Sigma Q_t - \Sigma Q_d$ ), as given by Eq. (11), for nickel and the corresponding linearization involving the exchange process is shown in Fig. 8. From Eq. (4) and the linearized data for both cations, the enthalpy of interaction,  $\Delta_{\text{int}}H$ , enables calculation of the enthalpy, as given by Eq. (5). From calorimetric titration the equilibrium constant and enthalpy were simultaneously obtained, from which the

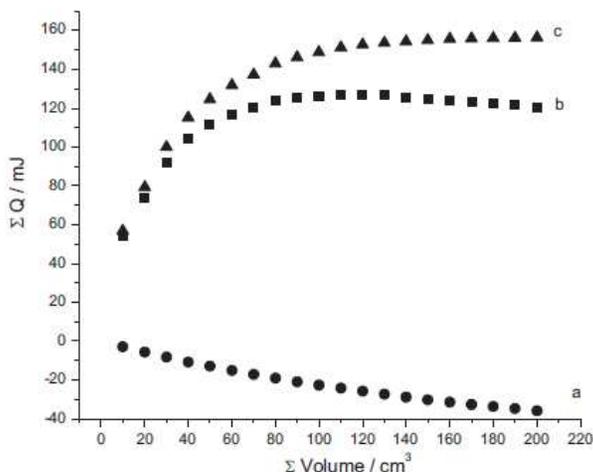


Fig. 7. The resulting thermal effects of the ion exchange isotherms of Ni<sup>2+</sup> on chemically modified cellulose, Na-CeLS, at 298.15 ± 0.20 K, showing cation/basic center interaction (■), dilution (●) and net effect (▲).

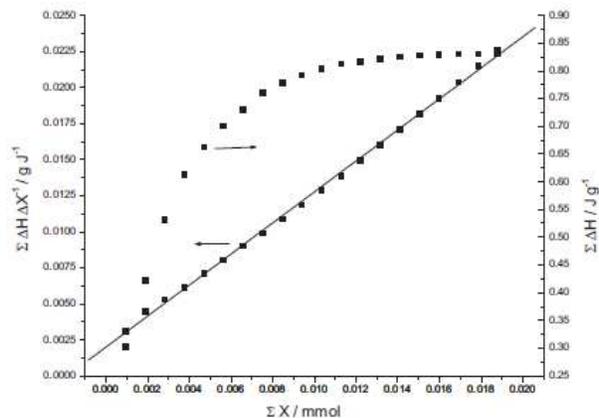


Fig. 8. Isotherms from calorimetric titration and the linearized forms for Ni<sup>2+</sup> on sodium chemically modified cellulose, Na-CeLS, at 298.15 ± 0.20 K.

Table 2

Summary of thermodynamic values for the interaction of divalent metal nitrates on chemically modified cellulose Na-CeLS at 298.15 ± 0.20 K.

| M-CeLS               | $\Delta H/\text{kJ mol}^{-1}$ | $-\Delta G/\text{kJ mol}^{-1}$ | $\Delta S/\text{JK}^{-1} \text{mol}^{-1}$ |
|----------------------|-------------------------------|--------------------------------|---|
| CoCeLS <sup>2+</sup> | 3.81 ± 0.02                   | 3.2 ± 0.5                      | 24 ± 1                                    |
| NiCeLS <sup>2+</sup> | 2.35 ± 0.01                   | 3.9 ± 0.6                      | 21 ± 1                                    |

Gibbs energy and the entropy can be calculated, as listed in Table 2. The low positive magnitude value for enthalpy is in agreement with a general behavior for the ion exchange processes, which normally is followed by positive entropic values [14,32,33].

The negative Gibbs energy indicates spontaneous processes of ion exchange with the positive enthalpies, as also previously observed for other anchored celluloses [4,14]. Both systems presented positive entropic values that contribute to the occurrence of favorable reactions. These entropic values suggest that during the exchange the cation desolvation and free sodium solvation processes disturbed the original structure of the solvent, by causing a disorganization of the system with an increase in entropy [34,35]. Another contribution to the entropic value comes from the displacement of the water molecules hydrogen-bonded to the active centers attached to the pendant chains, as the ion exchange is in progress, to form the final structural rearrangement [4,15]. This set of thermodynamic data demonstrates a spontaneous reaction, whose low positive enthalpic and positive entropic contributions are closely related to the classical sodium/cation exchange process at solid/liquid interfaces, suggesting also an application for this chemically modified polysaccharide for cation removal from aqueous solution in this heterogeneous system.

#### 4. Conclusion

The strategy presented to modify the world's most widely available biopolymer surface under solvent-free conditions was plainly achieved, using a synthetic process that used the mild conditions of melting succinic anhydride, to favor a decrease in reaction time. The well-characterized product formed presented a high degree of covalently bonded pendant molecules bearing a carboxylic group that, when exchanged to the sodium form, is able to remove cations from solution.

The new synthetic surface with incorporation of such pendant chains has attached basic centers potentially available for exchanging divalent cations. This behavior in applications can be useful for ecosystem purification. The quantitative exchange

interactions between the metallic ions and sodium carboxylate at the solid/liquid interface obtained from calorimetry gave low endothermic enthalpies, followed by positive entropies, to result in favorable thermodynamic data, represented by negative Gibbs energies. These thermodynamic values reinforces the proposed applicability of this new chemically modified biopolymer, obtained from most available biopolymer worldwide through a heterogeneous synthetic route as a material to improve environments.

### Acknowledgements

The authors are indebted to FAPESP for financial support and for fellowships to J.C.P.M. and E.C.S. Filho, and also to CNPq and CAPES for fellowships to C.A. and S.A.A.S.

### References

- [1] I. Lerche, W. Glaesser, *Environmental Risk Assessment: Quantitative Measures, Anthropogenic Influences, Human Impact*, Springer, Berlin, 2006, p. 129.
- [2] E. Hodgson, *A Textbook of Modern Toxicology*, Third ed., John Wiley, Hoboken, New Jersey, 2004.
- [3] S.E. Manahan, *Fundamentals of Environmental Chemistry*, CRC Press, Boca Raton, 2001.
- [4] S. Babel, T.A. Kurniawan, Low-cost adsorbents for heavy metals uptake from contaminated water: a review, *J. Hazard. Mater.* 97 (2003) 219–243.
- [5] J.C.P. Melo, E.C. Silva Filho, S.A.A. Santana, C. Airoidi, Maleic anhydride incorporated onto cellulose and thermodynamics of cation-exchange process at the solid/liquid interface, *Colloids Surf. A* 346 (2009) 138–145.
- [6] D. Klemm, B. Heublein, H.P. Fink, A. Bohn, Cellulose: fascinating biopolymer and sustainable raw material, *Angew. Chem. Int. Ed.* 44 (2005) 3358–3393.
- [7] D. Roy, M. Semsarilar, J.T. Guthrie, S. Perrier, Cellulose modification by polymer grafting: a review, *Chem. Soc. Rev.* 38 (2009) 1825–2148.
- [8] J. Otera, *Esterification: Methods, Reactions and Applications*, Wiley/VCH, Weinheim, 2003, p.91.
- [9] O. Karnitz Jr., L.V.A. Gurgel, J.C.P. Melo, V.R. Botaro, T.M.S. Melo, R.P.F. Gil, L.F. Gil, Adsorption of heavy metal ion from aqueous single metal solution by chemically modified sugarcane bagasse, *Bioresour. Technol.* 98 (2007) 1291–1297.
- [10] C. Vaca-Garcia, G. Gozzelino, W.G. Glasser, M.E. Borredon, Dynamic mechanical thermal analysis transitions of partially and fully substituted cellulose fatty esters, *J. Polym. Sci. B* 41 (2003) 281–288.
- [11] T. Heinze, T.F. Liebert, K. Pfeiffer, M.A. Hussain, Unconventional cellulose esters: synthesis, characterization and structure–property relations, *Cellulose* 10 (2003) 283–296.
- [12] K.J. Edgar, C.M. Buchanan, J.S. Debenham, P.A. Rundquist, B.D. Seiler, M.C. Shelton, D. Tindall, Advances in cellulose ester performance and application, *Polym. Sci.* 26 (2001) 1605–1688.
- [13] V.J. Inglesakis, S.G. Pouloupoulos, *Adsorption, Ion Exchange and Catalysis: Design of Operation and Environmental Application*, Elsevier, Amsterdam, 2007, p. 243.
- [14] J.C.P. Melo, E.C. Silva Filho, S.A.A. Santana, C. Airoidi, Exploring the favorable ion-exchange ability of phthalylated cellulose biopolymer using thermodynamic data, *Carbohydr. Res.* 345 (2010) 1914–1921.
- [15] E.C. Silva Filho, J.C.P. Melo, C. Airoidi, Preparation of ethylenediamine-anchored cellulose and determination of thermochemical data for the interaction between cations and basic centers at the solid/liquid interface, *Carbohydr. Res.* 341 (2006) 2842–2850.
- [16] T. Yoshimura, K. Matsuo, R. Fujioka, Novel biodegradable superabsorbent hydrogels derived from cotton cellulose and succinic anhydride: synthesis and characterization, *J. Appl. Polym. Sci.* 99 (2006) 3251–3256.
- [17] C.J. Garvey, I.H. Parker, G.P. Simon, On the interpretation of X-ray diffraction powder patterns in terms of the nanostructure of cellulose I fibres, *Macromol. Chem. Phys.* 206 (2005) 1568–1575.
- [18] R. Dicke, A straight way to regioselectively functionalized polysaccharide esters, *Cellulose* 11 (2004) 255–263.
- [19] H. Zhao, J.H. Kwak, Z.C. Zhang, H.M. Brown, B.W. Arey, J.E. Holladay, Studying cellulose fiber structure by SEM, XRD, NMR and acid hydrolysis, *Carbohydr. Polym.* 68 (2007) 235–241.
- [20] S. Margutti, S. Vicini, N. Proietti, D. Capitani, G. Conio, E. Pedemonte, A.L. Segre, Physical–chemical characterisation of acrylic polymers grafted on cellulose, *Polymer* 43 (2002) 6183–6194.
- [21] M. Schwanninger, J.C. Rodrigues, H. Pereira, B. Hinterstoisser, Effects of short-time vibratory ball milling on the shape of FT-IR spectra of wood and cellulose, *Vib. Spectrosc.* 36 (2004) 23–40.
- [22] C.Q. Yang, X. Wang, Formation of cyclic anhydride intermediates and esterification of cotton cellulose by multifunctional carboxylic acids: an infrared spectroscopy study, *Text. Res. J.* 66 (1996) 595–603.
- [23] R.H. Atalla, D.L. VanderHart, The role of solid state  $^{13}\text{C}$  NMR spectroscopy in studies of the nature of native celluloses, *Solid State Nucl. Magn. Reson.* 15 (1999) 1–19.
- [24] H. Kono, S. Yunoki, T. Shikano, M. Fujiwara, T. Erata, M. Takai, CP/MAS  $^{13}\text{C}$  NMR study of cellulose and cellulose derivatives. 1. Complete assignment of the CP/MAS  $^{13}\text{C}$  NMR spectrum of the native cellulose, *J. Am. Chem. Soc.* 124 (2002) 7506–7511.
- [25] A.C. O'Sullivan, Cellulose: the structure slowly unravels, *Cellulose* 4 (1997) 173–207.
- [26] P. Zugenmaier, Conformation and packing of various crystalline cellulose fibers, *Prog. Polym. Sci.* 26 (2001) 1341–1417.
- [27] M.S. Smole, Z. Peršin, T. Kreže, K.S. Kleinschek, V. Ribitsch, S. Neumayer, X-ray study of pre-treated regenerated cellulose fibers, *Mater. Res. Innovations* 7 (2003) 275–282.
- [28] H. Zhao, J.H. Kwak, Y. Wang, J.A. Franz, J.M. White, J.E. Holladay, Effects of crystallinity on dilute acid hydrolysis of cellulose by cellulose ball-milling study, *Energy Fuels* 20 (2006) 807–811.
- [29] W.Y. Chiang, C.H. Hu, Approaches of interfacial modification for flame retardant polymeric materials, *Composites A32* (2001) 517–524.
- [30] S. Sun, Q. Wang, A. Wang, Adsorption properties of Cu(II) ions onto N-succinyl-chitosan and crosslinked N-succinyl-chitosan template resin, *Biochem. Eng. J.* 36 (2007) 131–138.
- [31] F. Li, X. Sun, H. Zhang, B. Li, F. Gan, Pyromellitic dianhydride-modified cyclodextrin microspheres for Pb(II) and Cd(II) adsorption, *J. Appl. Polym. Sci.* 105 (2007) 3418–3425.
- [32] C. Airoidi, L.M. Nunes, Calorimetric determinations of  $\text{Ba}^{2+}$  and  $\text{La}^{3+}$  in the ion-exchange process involving pure and modified  $\alpha$ -titanium phosphates, *Langmuir* 16 (2000) 1436–1439.
- [33] A. Ramesh, D.J. Lee, J.W.C. Wong, Thermodynamic parameters for adsorption equilibrium of heavy metals and dyes from wastewater with low-cost adsorbents, *J. Colloid Interface Sci.* 291 (2005) 588–592.
- [34] T.R. Macedo, G.C. Petrucelli, C. Airoidi, Sorption and thermodynamic of cation–basic center interactions of inorganic–organic hybrids synthesized from RUB-18, *Thermochim. Acta* 502 (2010) 30–34.
- [35] S. Badshah, C. Airoidi, Layered organoclay with talc-like structure as agent for thermodynamics of cations sorption at the solid/liquid interface, *Chem. Eng. J.* 166 (2011) 420–427.



Contents lists available at ScienceDirect

Carbohydrate Research

journal homepage: [www.elsevier.com/locate/carres](http://www.elsevier.com/locate/carres)

## Exploring the favorable ion-exchange ability of phthalylated cellulose biopolymer using thermodynamic data

Júlio C. P. de Melo<sup>a</sup>, Edson C. da Silva Filho<sup>b</sup>, Sirlane A. A. Santana<sup>c</sup>, Claudio Airoidi<sup>a,\*</sup>

<sup>a</sup> *Institute of Chemistry, University of Campinas, UNICAMP, PO Box 6154, 13084-971 Campinas, SP, Brazil*

<sup>b</sup> *Química, Universidade Federal do Piauí, 64900-000 Bom Jesus, PI, Brazil*

<sup>c</sup> *Departamento de Química/CCET, Universidade Federal do Maranhão, Av. dos Portugueses S/N, Campus do Bacanga, 65080-540 São Luiz, MA, Brazil*

### ARTICLE INFO

#### Article history:

Received 8 April 2010

Received in revised form 9 June 2010

Accepted 21 June 2010

Available online 25 June 2010

#### Keywords:

Modified cellulose

Phthalic anhydride

Solvent-free

Ion-exchange

Calorimetry

Thermodynamic

### ABSTRACT

A phthalylated ion-exchange biopolymer was obtained by adding cellulose to molten phthalic anhydride in a quasi solvent-free procedure. Through this route  $2.99 \pm 0.07 \text{ mmol g}^{-1}$  of pendant groups containing ester and carboxylic acid moieties were incorporated into the polymeric structure that was characterized by elemental analysis, solid-state carbon nuclear magnetic resonance (CP/MAS), infrared spectroscopy, X-ray diffraction, and thermogravimetry. The chemically modified polysaccharide is able to exchange cations from aqueous solution as demonstrated by batchwise methodology. The data were adjusted to a modified Langmuir equation to give  $2.43 \pm 0.12$  and  $2.26 \pm 0.11 \text{ mmol g}^{-1}$  for divalent cobalt and nickel cations, respectively. The net thermal effects obtained from calorimetric titration measurements were also adjusted to a modified Langmuir equation, and the enthalpy of the interaction was calculated to give endothermic values of  $2.11 \pm 0.28$  and  $2.50 \pm 0.31 \text{ kJ mol}^{-1}$  for these cations, respectively. The spontaneity of this ion-exchange process is reflected in negative Gibbs energy and with a contribution of positive entropic values. This set of thermodynamic data at the solid-liquid interface suggests a favorable ion-exchange process for this anchored biopolymer for cation exchange from the environment.

© 2010 Published by Elsevier Ltd.

### 1. Introduction

Metals are essential constituents of a large variety of enzymes and proteins, but excesses of these cations cause problems for living beings, as they accumulate along the food chain. For example, hepatic glutathione levels are increased due to intoxication with cobalt being absorbed by the same active transport mechanism that normally occurs for iron, while higher levels of nickel cause nasal and lung cancers as well as DNA damage.<sup>1</sup>

The major contributing agents to heavy metal environmental contaminations are anthropogenic.<sup>2</sup> To minimize these impacts much effort has expended, mainly on the science of solids and surfaces. This way, sorption on solids, chemically functionalized or not, originating from different natural or synthetic sources has been widely investigated for heavy cation removal from aqueous and non-aqueous effluents.<sup>3–5</sup>

Nowadays, different types of biomass related to natural forests/woodlands, forest plantations, agro-industrial plantations, trees outside forests and woodlands, agricultural crops, crop residues, processed residues, and animal wastes<sup>6</sup> are being largely applied in the development of new materials and surfaces<sup>7,8</sup> mainly due to their biological, chemical, and physical degradabilities.<sup>6</sup> Cellu-

lose is one of the major constituents of biomass, and for this reason special attention has been dedicated to the development of cellulose-based materials.<sup>5</sup>

Taking into account the possible applicability of some native materials as agents to improve life, cellulose is an attractive source material, not only because it is the most widely available organic biopolymer in nature, but also because it is relatively easy to extract from algae and plant cells. This biopolymer presents considerable chemical and physical inertness so that surface or bulk modifications can sometimes be difficult to achieve, especially without appropriate conditions. Thus, the greatest part of these modifications occurs on the cellulose primary hydroxyl groups at C-6, and then on the secondary hydroxyls at C-2 and C-3, although some other reactions are able to succeed via oxidative opening of tetrahydropyran rings, or without disruptions of the rings.<sup>9,10</sup>

Acylation with organic five-membered cyclic anhydrides are well-established reactions,<sup>5,7,11</sup> in which all three hydroxyl groups are involved. The nucleophilic agents attack the carbonyl carbon of strained anhydrides to yield ester bonds, and due to this opening, carboxylic acid groups are formed that are basic centers, which might be involved with sorption and cation-exchange reactions and other applications in, for example, the coating, cosmetic, food, and pharmaceutical industries, for antibody, enzyme, protein, and ion-separation membranes, and filters, among other applications.<sup>10,12–14</sup>

\* Corresponding author. Fax: +55 19 35213023.

E-mail address: [airoidi@iqm.unicamp.br](mailto:airoidi@iqm.unicamp.br) (C. Airoidi).

Ion exchangers are insoluble solid materials that carry exchangeable cations or anions. When the cation exchanger is in contact with an electrolyte solution, the cationic counter ions are exchanged with an equivalent amount of other ions of the same charge. There are a number of different natural and synthetic materials that show ion-exchange properties: (a) natural inorganic ion exchangers: clays, zeolites, and green sands,<sup>15</sup> (b) natural organic ion exchangers: polysaccharides, proteins, and carbonaceous materials, synthetic inorganic ion exchangers, (c) synthetic zeolites, titanate/silicotitanates, and transition metal hexacyanoferrates, and (d) synthetic organic ion exchangers: organic synthetic resins.<sup>14,16</sup>

Phthalic anhydride presents a relatively low melting point, and this investigation deals with the chemical modification processes without using solvents during the synthetic procedure,<sup>5</sup> by successfully exploring the relatively low melting point of the chosen reactant, phthalic anhydride. From this aromatic anhydride some aromatic–aromatic attractive interactions are expected, a behavior which is close to the effective model of interactive processes: (a) the vertical base–base interactions stabilizing the double helical structure that resemble that of DNA, (b) the drug intercalation into DNA, (c) the packing of aromatic molecules in crystals, (d) the protein tertiary structures, and (e) complexation in some host–guest systems.<sup>17,18</sup> The applicability of this synthesized cellulose is related to the ability of the available attached basic centers in the pendant chains to exchange divalent cobalt and nickel from aqueous solution. The quantitative features associated with the interactions at the solid–liquid interface were followed calorimetrically to better understand this important interactive process.

## 2. Materials and methods

### 2.1. Materials

Microcrystalline cellulose as powder (Sigma–Aldrich Chemical Co.), with particle size  $\sim 20 \mu\text{m}$ , was dried before use. Phthalic anhydride (Aldrich) and the other analytical grade reagents were used without prior purification.

### 2.2. Instrumentation

The amount of phthalic anhydride incorporated in the biopolymer cellulose was determined through acid–base titration and elemental analysis on a Perkin–Elmer model 2400 analyzer and through reactive center titration. FTIR spectra of the samples dispersed in KBr pellets were obtained in the transmittance mode by accumulating 32 scans on a Bomem FTIR spectrophotometer, MB-series, in the  $4000$  to  $400 \text{ cm}^{-1}$  range, with  $4 \text{ cm}^{-1}$  resolution.  $^{13}\text{C}$  NMR spectra in solid state of the samples were obtained on a Bruker AC 400/P spectrometer at room temperature. The measurements were obtained at frequencies of  $75.47 \text{ MHz}$  with a magic angle spinning of  $10 \text{ kHz}$ . To increase the signal/noise ratio, the CP/MAS technique was used, with pulse repetition of  $5 \text{ s}$  and a contact time of  $1 \text{ ms}$ . X-ray diffraction patterns were obtained on a Shimadzu model XRD 7000 diffractometer with  $40 \text{ kV}$  applied voltage, current of  $30 \text{ mA}$ , and  $\text{Cu K}\alpha$  ( $\lambda = 154.1 \text{ pm}$ ) radiation source scanned from  $5^\circ$  to  $45^\circ$ . Thermogravimetric curves in an argon atmosphere were obtained on a TA instrument, coupled to a model 1090 B thermobalance, using a heating rate of  $10 \text{ K s}^{-1}$ , under a flow of  $30 \text{ cm}^3 \text{ s}^{-1}$ , varying from room temperature to  $525 \text{ K}$ , with an initial mass of approximately  $10 \text{ mg}$  of solid sample. The amount of cation exchanged was determined by the difference between the initial concentration in the aqueous solution and that found in the supernatant, using an Inductively Coupled Plasma Optical Emission Spectrometer (ICP OES) on a Perkin–Elmer 3000

DV apparatus. For each experimental point, in the cation determination in the supernatant, the reproducibility was checked by at least one duplicate run.

### 2.3. Synthesis of chemically modified cellulose

A sample of  $5 \text{ g}$  of cellulose (Cel), previously dried at  $383 \text{ K}$  for  $2 \text{ h}$  under vacuum, was added to  $45 \text{ g}$  of molten phthalic anhydride,<sup>5</sup> to maintain a cellulose/phthalic anhydride ratio of  $1:10$ , in a reaction flask immersed under magnetic stirring in a sand bath at  $413 \text{ K}$ . The flask was fitted to a dried silica trap to maintain constant pressure and to keep out moisture from the air. The fluid mixture was heated for  $6 \text{ h}$ , when  $50 \text{ cm}^3$  of  $N,N'$ -dimethylacetamide was added to avoid recrystallization of free phthalic anhydride. The fluid was filtered while hot; subsequently,  $100 \text{ cm}^3$  of the same solvent was added to remove a large proportion of unreacted anhydride. The as-modified biopolymer was intensively washed with water until neutral pH, followed by  $50 \text{ cm}^3$  of acetone to make the drying step easier. The solid was then dried in vacuum at  $383 \text{ K}$  for  $24 \text{ h}$ . The new biopolymer (HCElP) was proton–sodium exchanged by immersing a sample of the HCElP in  $0.90 \text{ mol dm}^{-3}$  sodium hydrogencarbonate solution at  $291 \text{ K}$ , to exchange protons with sodium cations, yielding NaCElP for the cation–exchange process and also for calorimetric determinations.

### 2.4. Exchanging process

The capacity of the chemically modified cellulose to extract cations from aqueous solution was determined in duplicate runs, using a batch process with divalent cobalt or nickel nitrates, by using a series of flasks containing mass ( $m$ ) of the solid suspended in  $25.0 \text{ cm}^3$  of an aqueous solution with concentrations of each cation, varying from  $0.10$  to  $5.0 \text{ mmol dm}^{-3}$ . From this procedure the best isotherm was obtained with  $25 \text{ mg}$  of exchanger for each cation to give a defined plateau, indicating the maximum ion-exchange capacity. Firstly, the phthalylated cellulose sample was immersed in sodium hydrogencarbonate for proton exchanges. The use of NaCElP avoids a pH decrease during suspension, favoring metal sorption, which was carried out at an isoelectronic pH ( $5.8 \pm 0.1$ ). For the metal–proton exchange process, a series of flasks containing the suspensions was shaken for  $6 \text{ h}$  in an orbital bath at  $298 \pm 1 \text{ K}$ . This time was previously established using identical methodology, the results of which demonstrated that the isotherms reached cation saturation, as was obtained for the concentration versus time isotherm, which gave a well-defined plateau. At the end of the process, the solid was separated by centrifugation for  $10 \text{ min}$  at  $2300 \text{ rpm}$ , and aliquots of the supernatant were removed for cation determination by ICP OES. The exchanging capacities ( $N_f$ ) were calculated by considering the number of moles:  $N_f = (n_i - n_s)/m$ , where  $n_i$  and  $n_s$  are the initial number of moles and that remaining in the supernatant at the end of the experiment, and  $m$  is the mass of solid used.<sup>5</sup>

The ion-exchange process takes place at the solid–liquid interface that involves a competition between the solvent (solv) bonded to the sodium from chemically modified cellulose (NaCElP) that is gradually displaced by the metal in solution to reach equilibrium, as represented in Eq. 1:



The ratio between the number of moles of metal in solution at equilibrium and the number of moles of metal exchanged by the basic centers on pendant chains was used to obtain the modified Langmuir isotherm, Eq. 2

$$\frac{C_s}{N_f} = \frac{C_s}{n^a} + \frac{1}{n^b} \quad (2)$$

where  $C_s$  ( $\text{mol dm}^{-3}$ ) is the concentration of supernatant cations at equilibrium,  $N_f$  ( $\text{mol g}^{-1}$ ) is the number of moles exchanged,  $n^s$  ( $\text{mol g}^{-1}$ ) is the maximum amount of solute exchanged per gram of NaCelP, which is related to the number of exchanging sites, and  $b$  ( $\text{dm}^3 \text{mol}^{-1}$ ) is a constant. The  $n^s$  and  $b$  values for each exchange process were obtained from the angular and linear coefficients, respectively, of the linearized form of the exchange isotherms, by considering  $C_s/N_f$  versus  $C_s$ , using the least-squares method.

### 2.5. Calorimetric titration

The thermal effect evolved from the interaction between the cation and the basic center attached on the pendant groups at the solid–liquid interface was measured on a LKB 2277 instrument.<sup>5</sup> For each operation, a sample of about 20 mg of functionalized cellulose in the sodium form was suspended in  $2.0 \text{ cm}^3$  of water under stirring at  $298.15 \pm 0.20 \text{ K}$ . The thermostated solutions of the cations, with concentrations of  $0.30 \text{ mol dm}^{-3}$ , were incrementally added to the calorimetric vessel, and the thermal effect of the titration,  $Q_t$ , was obtained. Under the same experimental conditions, the corresponding thermal effect of the dilution of the cation solution was obtained in an identical volume of the calorimetric solvent,  $Q_d$ . Identically, the thermal effect of NaCelP hydration in water was also determined,  $Q_h$ .<sup>5,19</sup> Under such conditions, the net thermal effect of exchanging,  $Q_r$ , was obtained through Eq. 3, by considering that the suspension of the solid in water gave a null value:

$$\sum Q_r = \sum Q_t - \sum Q_d \quad (3)$$

The change in enthalpy associated with cation/matrix interaction can be determined by adjusting the exchange data to a modified Langmuir equation to calculate the integral enthalpy involved in the formation of a monolayer per unit mass of exchanger,  $\Delta_{\text{mono}}H$ ,<sup>5,19</sup> as shown in Eq. 4:

$$\frac{\sum X}{\sum \Delta H} = \frac{1}{(K-1)\Delta_{\text{mono}}H} + \frac{X}{\Delta_{\text{mono}}H} \quad (4)$$

where  $\sum X$  is the sum of the mole fraction of the cation in solution after exchanging, obtained for each point of titrant. By using the modified Langmuir equation, the integral enthalpy of ion exchange per gram of the matrix,  $\Delta H$ , was obtained by dividing the thermal effect resulting from ion exchange by the number of moles of the exchanger, while  $K$  is the proportionality constant, which also includes the equilibrium constant. Using the angular and linear values from the  $\sum X/\sum \Delta H$  versus  $\sum X$  plot enables the calculation of the  $\Delta_{\text{mono}}H$  value. Then, the enthalpy of exchanging can be calculated by means of expression 5:

$$\Delta H = \frac{\Delta_{\text{mono}}H}{n^s} \quad (5)$$

From the equilibrium constant values, the Gibbs energies were calculated by expression 6:

$$\Delta G = -RT \ln K \quad (6)$$

and the entropy value can be calculated through Eq. 7:

$$\Delta G = \Delta H - T\Delta S \quad (7)$$

## 3. Results and discussion

### 3.1. Characterization

Cellulose reacted with molten phthalic anhydride to yield a solid, water-insoluble, chemically modified polysaccharide HCeIP with a carbon content of  $46.58 \pm 0.19\%$ , which permitted the calculation of the degree of substitution (DS) of  $1.01 \pm 0.12\%$ . By considering the amount of carbon in the synthesized polysaccharide that differs from  $41.95 \pm 0.04\%$  for the precursor biopolymer, this datum clearly indicates the success of anhydride incorporation during the chemical reaction, as illustrated in Figure 1, which shows the reagent structures as well as the protonated and sodium products. The amount of phthalic anhydride covalently bonded to the backbone structure was calculated as  $3.25 \pm 0.12$  or  $2.99 \pm 0.07 \text{ mmol g}^{-1}$ , taking into account the DS or carboxylic acid titration procedures.<sup>5,12</sup> This difference in values might be associated with the methodology used. For the second procedure, the amount of free sites available was calculated from the covalently bonded groups, which is followed by uncertainties that emerge from possible crosslinking reactions.<sup>20,22</sup> Nevertheless, it is worth remembering that due to the high anhydride/hydroxyl ratio the crosslinking effect should be minimized. Based on the carbon percentage obtained for the chemically modified cellulose, another important feature should be considered, which is related to the expected correlation between these values and the proposed chemical structure.

The appropriate degree of substitution for the homogeneous route requires that the chemical modifications take place at specific positions on the molecule that may be selected. For the heterogeneous pathway the substitution is obtained by dissolving the material, and the extent of reaction on each particular position is analyzed.<sup>9,10</sup>

The present case uses heterogeneous conditions for all chemical modification procedures. However, the degree of substitution was not determined for individual carbon atoms, although for the DS value it was considered that the anhydride molecules were covalently bonded preferentially on C-6, due to the high reactivity of this primary hydroxyl group. The corresponding values for the immobilized amounts based on both DS and titration differ from the expected  $3.22 \text{ mmol g}^{-1}$ . However, the difference may arise: (a) from the formation of oxidized ends, depending on the degree

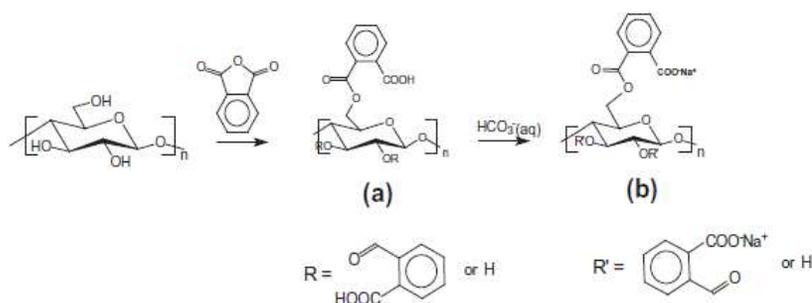


Figure 1. Synthesis of phthalylated cellulose (a) and its sodium form (b) from the reaction of cellulose with phthalic anhydride.

of polymerization, due to the carboxylic acid groups formed or to the proton involved in  $\beta$ -(1 $\rightarrow$ 4) cleavage<sup>23</sup> and (b) due to oxidized open rings.<sup>24</sup>

The absence of solvent in this synthetic methodology explains the high degree of anhydride incorporation that is also propelled by high temperature and the easy availability of the reagent, which suggests a covering of powdered cellulose with aromatic acid ester pendant chains on the polysaccharide, as depicted in Figure 1a.

The infrared spectra of pristine microcrystalline cellulose<sup>25</sup> and the phthalylated polysaccharide are shown in Figure 2.

A strong broad band  $\sim$ 3380  $\text{cm}^{-1}$  is related to O–H stretching from alcohol and acid hydroxyl groups. The band at 3060  $\text{cm}^{-1}$  arises from the intramolecular hydrogen bond between the hydrogen of the acid and the carbonyl of the ester in the same molecule gives. The bands at 2650 and 2520  $\text{cm}^{-1}$  are related to aromatic carboxylic acid dimers as well as their stretching at 1700  $\text{cm}^{-1}$ . The  $\nu$ (C–H) vibration appears at  $\sim$ 2900  $\text{cm}^{-1}$ , and the corresponding deformation is at 1453 and 1373  $\text{cm}^{-1}$ . Aromatic skeletal vibrations are assigned to the 1585, 1450, and 1405  $\text{cm}^{-1}$  bands. A band centered at 1282  $\text{cm}^{-1}$  corresponds to  $\nu$ (C–O) for the aromatic ester and acid.<sup>7</sup> The high degree of phthalylation onto the HCellP surface causes the appearance of a band at 1070  $\text{cm}^{-1}$  as well as that at 1060  $\text{cm}^{-1}$  related to aliphatic ether  $\nu$ (C–O–C). This new band at 1070  $\text{cm}^{-1}$  suggests the effective participation of  $\beta$ -(1 $\rightarrow$ 4) glucosidic linkages from modified cellulosic chains, which are present in the phthalate residue, involving aromatic–aromatic (ar–ar) interactions.<sup>18</sup> Such interactions seem to be strong enough to disturb  $\beta$ -(1 $\rightarrow$ 4) linkages and shift the absorption. The absence of any band at 1800 and 1850  $\text{cm}^{-1}$  confirms that the product is free from unreacted phthalic anhydride.<sup>7,26</sup>

The success of the reaction is evidenced by <sup>13</sup>C NMR CP/MAS spectra in solid state, where signals at 184 (C-14) and 173 ppm (C-7) are related to carbonyl groups of acid and ester components, respectively.<sup>7</sup> The carbons for the aromatic ring that were incorporated as the modifier agent (C-8–C-13) appear as a broad signal centered at 130 ppm. Carbons C-2, C-3, and C-5 are assigned to signals from 70 to 75 ppm, and the signals at 105, 88, and 64 ppm are attributed to C-1, C-4, and C-6, respectively. The remaining carbons, C-4 and C-6, are sensitive to changes in crystallinity, and for this reason their signals vary in both intensity and chemical shift in the spectra,<sup>27–30</sup> as shown in Figure 3.

The degree of crystallinity of cellulose has demonstrated great interest for several research groups,<sup>21</sup> and from the result obtained, a way to calculate such a feature by comparing the relative intensity of 0 0 2 reflections plane through Bragg<sup>31</sup> and Scherrer<sup>32</sup> equations was proposed. X-ray diffraction patterns for HCellP obtained from microcrystalline cellulose through a heterogeneous route are dominated by the original and novel crystalline arrangements of this as-synthesized biopolymer, as shown in Figure 4 for pristine (a) and for modified (b) celluloses. As previously discussed, from the <sup>13</sup>C NMR spectra the regions of lower crystallinity decreased, a fact that was proved by considering the external chain disorganization and fiber length shortening, as confirmed by the peak at 34.5°, corresponding to the 0 4 0 plane.<sup>33</sup> In these syntheses, modifications are expected to occur first on the more available hydroxyl groups in the para-crystalline region, located on the polymeric surface. After surface rearrangement the appearance of new patterns suggests that aromatic–aromatic interactions are evidenced, as shown in Figure 4b.

The thermogravimetric curves for cellulose and the chemically modified biopolymer are shown in Figure 5a, and to illustrate the phthalylated decomposition stages, a derivative curve is also included in Figure 5b.

The chemically modified phthalylated cellulose in acidic form presents two decomposition events in the intervals: (i) 400–500 K due to the release of aromatic species that correspond to 24% and (ii) 500–700 K corresponding to the decomposition event of the polymeric matrix. These mass losses for both stages are clearly shown from two peaks in this synthesized biopolymer in Figure 5b. As observed, HCellP decomposed at a lower temperature than that observed for cellulose, a phenomenon which could be associated with the facility of pendant chain breaking during the heating process, as shown in Figure 5a. Microcrystalline cellulose presented only one event of decomposition in the interval of temperature in the 400–700 K range. This event includes mass losses of water physically sorbed onto the surface and some water from the para-crystalline region, due to polymeric hydroxyl group condensations on heating and also due to cellulose fiber decomposition.<sup>5</sup>

### 3.2. Divalent cation exchanging

For effectiveness of the interaction between divalent cations and the chemically modified cellulose, the main characteristics of

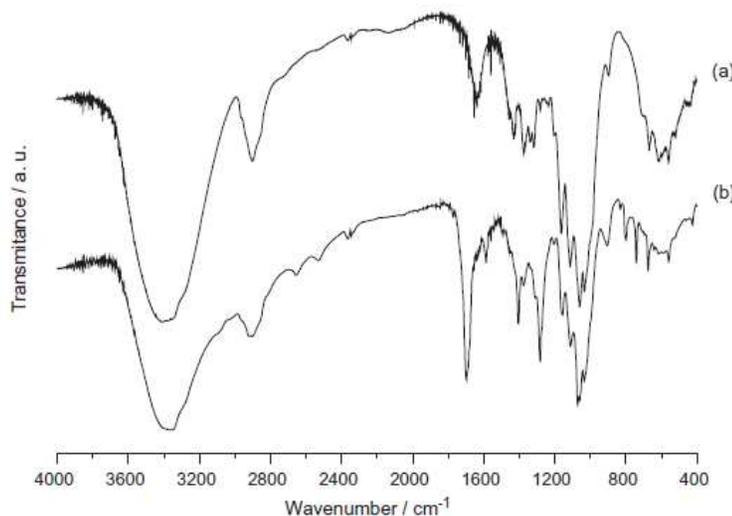


Figure 2. Infrared spectra of cellulose (a) and its phthalylated form (b).

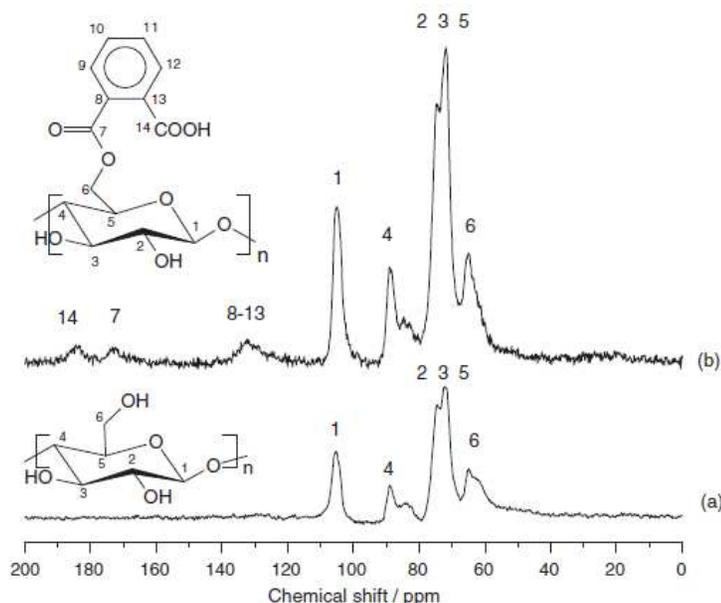


Figure 3. <sup>13</sup>C CP/MAS NMR spectra of (a) cellulose and (b) its phthalylated form.

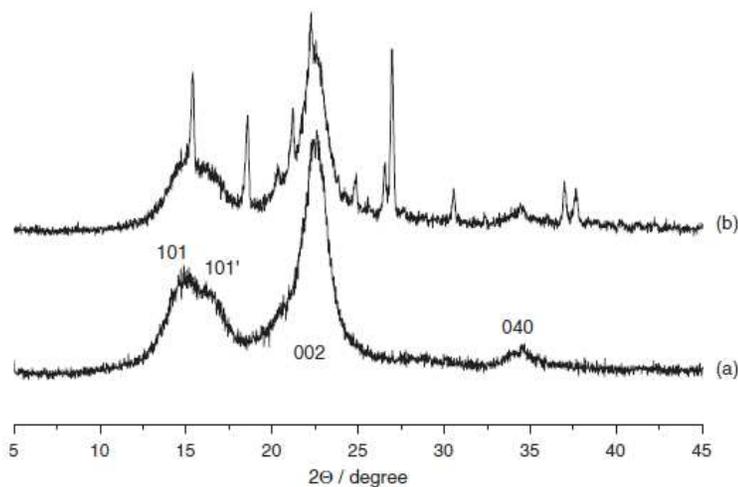


Figure 4. X-ray diffraction patterns for (a) cellulose and (b) its phthalylated form.

the biopolymer should be considered. Thus, the availability of carboxylic acid groups covalently bonded to the cellulose backbone with the ability to act as exchangers from aqueous solution, due to the complexing ability of these basic centers at the solid–liquid interface is important.<sup>34,35</sup>

To increase the ion-exchange process by minimizing any dependence on pH and also to facilitate the process, the protons were previously substituted by sodium. The isotherms of cation exchange with the modified biopolymer are shown in Figure 6. These were determined by exploring the best exchanging conditions, which can be summarized as a mass near 25 mg of the exchanger with stirring for 3 h at 298 ± 1 K.

The maximum amounts exchanged ( $n^s$ ) were 2.43 ± 0.12 and 2.26 ± 0.11 mmol g<sup>-1</sup> for cobalt and nickel, respectively. These values were obtained after fitting the results to a modified Langmuir

equation (Eq. 2), as successfully applied for other systems, to obtain the parameters for exchanging at the solid–liquid interface.<sup>5,19</sup> The linearized exchanged form for nickel is given by  $C_s/N_f$  as a function of  $C_s$  values, as shown in Figure 7, and enables the calculation of the linear and angular data from the straight line, to give  $n^s$  and  $b$  values, as listed in Table 1.

The participation of the counter anion to neutralize its free cation charge is also presented, and under such conditions it can bond to individual available carboxylate groups or can bridge two distinct basic centers.

### 3.3. Calorimetric titration

The net thermal effect results due to the interaction of each cation with NaCelP are obtained by considering the deduction of the

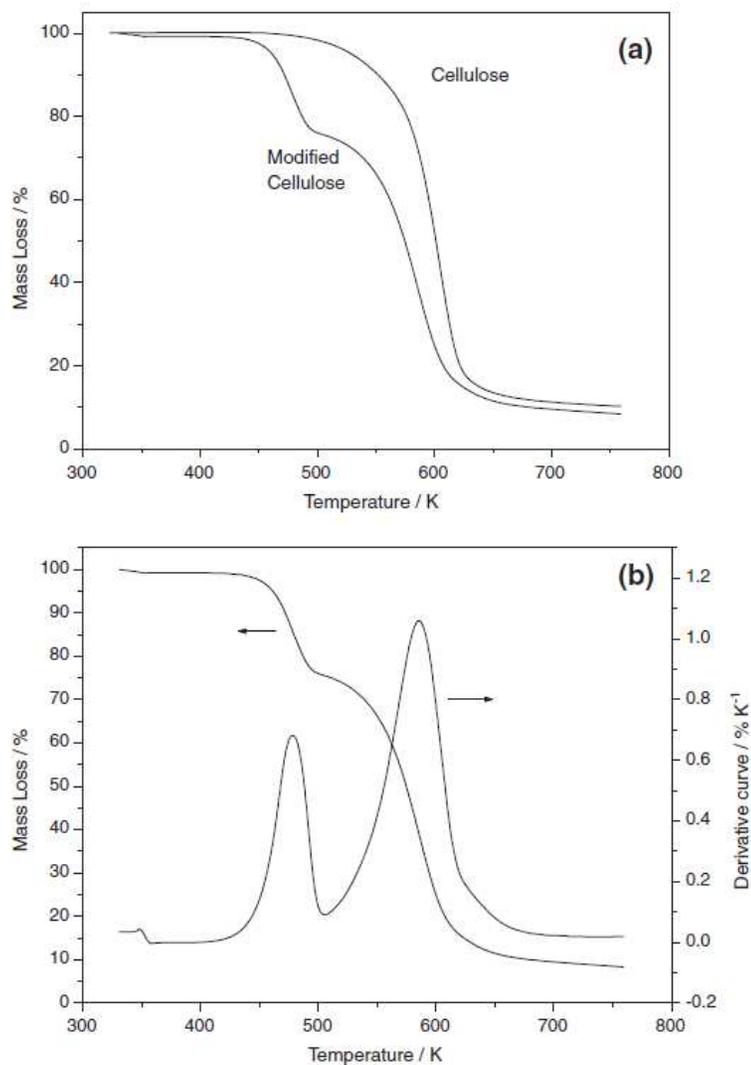


Figure 5. Thermogravimetric curves of (a) pristine phthalylated celluloses and (b) thermogravimetric and derivative curves for phthalylated cellulose.

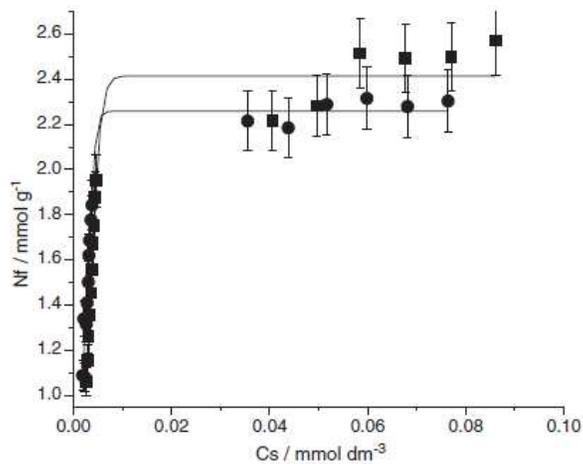


Figure 6. Exchange isotherms of Co<sup>2+</sup> (■) and Ni<sup>2+</sup> (●) on the phthalylated cellulose at 298 ± 1 K.

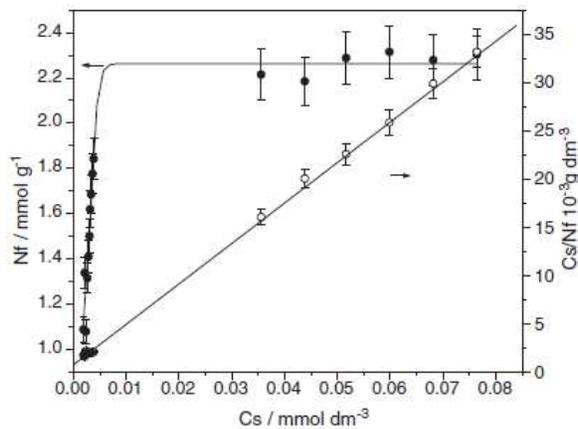
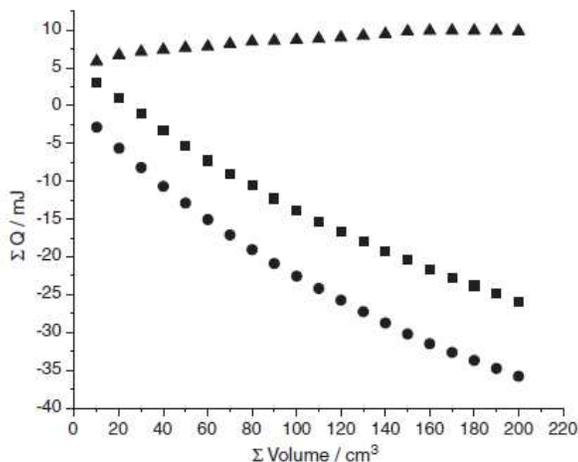


Figure 7. Exchange isotherms of Ni<sup>2+</sup> (●) and the linearized Langmuir isotherm (○) on phthalylated cellulose at 298 ± 1 K.

**Table 1**  
Number of moles exchanged ( $N_i$ ), maximum exchanged capacity ( $n^s$ ), constant ( $b$ ) and correlation coefficient ( $r$ ) for the interaction of divalent metal (M) nitrates with the phthalylated cellulose surface at 298 ± 1 K

| M                | $N_i$ [mmol g <sup>-1</sup> ] | $n^s$ [mmol g <sup>-1</sup> ] | $b$ [dm <sup>3</sup> mol <sup>-1</sup> ] | $r$    |
|------------------|-------------------------------|-------------------------------|--|--------|
| Co <sup>2+</sup> | 2.57 ± 0.01                   | 2.59 ± 0.12                   | 386                                      | 0.9985 |
| Ni <sup>2+</sup> | 2.31 ± 0.01                   | 2.35 ± 0.11                   | 562                                      | 0.9997 |



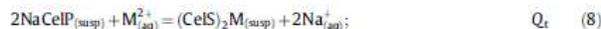
**Figure 8.** The resulting thermal effects of the exchanging isotherms of Ni<sup>2+</sup> on sodium phthalylated cellulose at 298.15 ± 0.20 K, showing cation/basic center interaction (■), dilution (●) and net effect (▲).

dilution effect in water from the total thermal effect, as given by Eq. 3, and the independent titrations for nickel are shown in Figure 8.

The effects of the thermodynamic cycle for this series of interactions involving a suspension (susp) of NaCelP in aqueous (aq) solution with divalent cations (M<sup>2+</sup>) can be represented by the following Eqs. (8)–(11):

**Table 2**  
Summary of thermodynamic values for the ion-exchange process of divalent metal nitrates on chemically modified NaCelP at 298.15 ± 0.20 K

| NaCelP               | $\Delta H$ [kJ mol <sup>-1</sup> ] | $-\Delta G$ [kJ mol <sup>-1</sup> ] | $\Delta S$ [J K <sup>-1</sup> mol <sup>-1</sup> ] |
|----------------------|------------------------------------|-------------------------------------|---|
| CelPCo <sup>2+</sup> | 2.11 ± 0.28                        | 15.6 ± 0.5                          | 59 ± 1  |
| CelPNI <sup>2+</sup> | 2.50 ± 0.31                        | 14.4 ± 0.6                          | 56 ± 1  |



As the hydration thermal effect of the exchanger in water gave null values (Eq. 8), consequently, the net thermal effects obtained from the calorimetric titration is given by  $\sum Q_r = \sum Q_t - \sum Q_d$ , Eq. 11. The isotherm of titration and its linearized form involving cobalt exchange are shown in Figure 9.

The data applied to Eq. 4 enable calculation from the linearized form for both cations of the enthalpy of interaction,  $\Delta_{\text{int}}H$ , as given by Eq. 5. From calorimetric titration the equilibrium constant and enthalpy were simultaneously obtained, from which the Gibbs free energy can be calculated, followed by the entropy, as listed in Table 2.

The low positive magnitude value for enthalpy is in agreement with the ion-exchange process, which is derived from positive entropic values.<sup>36,37</sup> The negative free energy indicates spontaneous processes of ion-exchange, which is normally followed by positive enthalpies, as also previously observed for anchored cellulose. As observed, both systems presented positive entropic values, a contribution that favors the occurrence of these reactions. These entropic values suggest that during the ion-exchange process the cation desolvation and sodium solvation processes disturbed the original structure of the solvent by causing a disorganization of the system with an increase in entropy. On the other hand, another contribution to the entropic value comes from the displacement of the water molecules hydrogen-bonded to basic centers attached to the pendant chains, as the exchanging is in progress, to form the final structural rearrangement.<sup>5,19</sup> This set of thermodynamic data demonstrates a spontaneous reaction, whose low positive enthalpic and positive entropic contributions

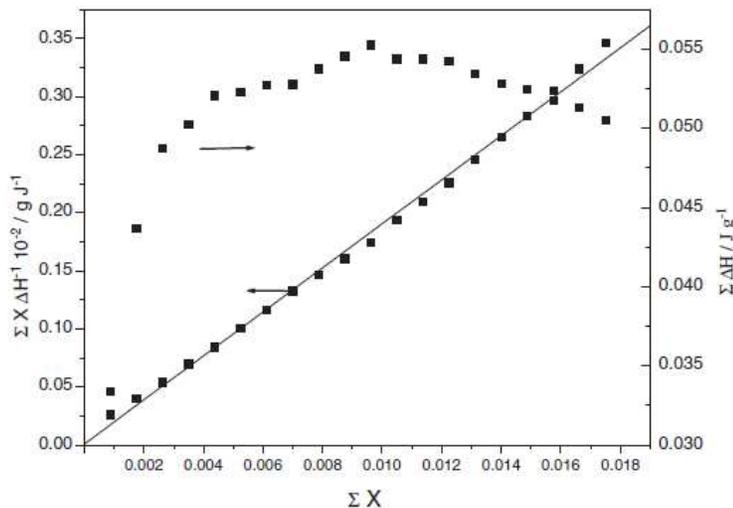


**Figure 9.** Isotherms from calorimetric titration and the linearized form for Co<sup>2+</sup> on sodium phthalylated cellulose at 298.15 ± 0.20 K.

are closely related to the classical sodium–cation exchange process at the solid–liquid interface. The thermodynamic data are in agreement with the exchange of those cations at the solid–liquid interface, suggesting an application for this anchored polysaccharide for cation removal.

#### 4. Conclusions

The pathway investigated to modify the world's most available polysaccharide surface under solvent-free conditions was plainly achieved. The well-characterized product that formed presented a high degree of covalently bonded pendant molecules bearing: (i) carboxylic and/or carboxylate groups that are able to exchange cations and (ii) aromatic rings, from which aromatic–aromatic interactions arise.

The procedure requires a relatively high temperature, and the present conditions for melting phthalic anhydride favor a decrease in reaction time, although it is difficult to avoid overoxidation caused by residual humidity and atmospheric oxygen, which probably favors dark and radical-mediated processes.

The as-synthesized surface with the incorporation of pendant chains containing carboxylated basic centers is a potentially available center for cation removal. These behave as promising materials to be applied for exchanging divalent cations, which is of great utility for ecosystem remediation. The quantitative interactions between cation and carboxylated basic centers at the solid–liquid interface obtained from calorimetry gave favorable thermodynamic data, represented by endothermic enthalpy, negative Gibbs free energy, and positive entropy. These thermodynamic values suggest the applicability of this phthalylated cellulose, available worldwide, to improve environments.

#### Acknowledgments

The authors are indebted to FAPESP for financial support and for fellowships to J.C.P.M. and E.C.S.F., and also to CNPq and CAPES for fellowships to C.A. and S.A.A.S.

#### References

- Hodgson, E. A. *Textbook of Modern Toxicology*; Wiley-Interscience: Hoboken, 2004. pp 49–53.
- Lerche, I.; Claesser, W., *Environmental Risk Assessment: Quantitative Measures, Anthropogenic Influences, Human Impact*; Springer: Berlin, 2006. p 129.
- Manahan, S. E. *Fundamentals of Environmental Chemistry*; CRC Press: Boca Raton, 2001.
- Babel, S.; Kurniawan, T. A. *J. Hazard. Mater.* **2003**, *97*, 219–243.
- de Melo, J. C. P.; da Silva Filho, E. C.; Santana, S. A. A.; Airoidi, C. *Colloids Surf., A* **2009**, *346*, 138–145.
- Rosillo-Calle, F. In *The Biomass Assessment Handbook*; Rosillo-Calle, F., de Groot, P., Hemstock, S. L., Woods, J., Eds.; Earthscan: London, 2007; pp 43–44.
- Liu, C. F.; Sun, R. C.; Ye, J. *Polym. Degrad. Stab.* **2006**, *91*, 280–288.
- Santana, S. A. A.; Vieira, A. P.; da Silva Filho, E. C.; de Melo, J. C. P.; Airoidi, C. *J. Hazard. Mater.* **2010**, *174*, 714–719.
- Klemm, D.; Heublein, B.; Fink, H. P.; Bohn, A. *Angew. Chem., Int. Ed.* **2005**, *44*, 3358–3393.
- Roy, D.; Semsarilar, M.; Guthrie, J. T.; Perrier, S. *Chem. Soc. Rev.* **2009**, *38*, 2046–2064.
- Otera, J. *Esterification: Methods, Reactions and Applications*; Wiley-VCH: Weinheim, 2003. pp 91–123.
- Kamitz, O., Jr.; Gurgel, L. V. A.; Melo, J. C. P.; Botaro, V. R.; Melo, T. M. S.; Gil, R. P. F.; Gil, L. F. *Bioresour. Technol.* **2007**, *98*, 1291–1297.
- Heinze, T.; Liebert, T.; Pfeiffer, K.; Hussain, M. A. *Cellulose* **2003**, *10*, 283–296.
- Inglesakis, V. J.; Pouloupoulos, S. G. *Adsorption, Ion Exchange and Catalysis: Design of Operations and Environmental Applications*; Elsevier: Amsterdam, 2007. p 243.
- Petrus, R.; Warchol, J. *Microporous Mesoporous Mater.* **2003**, *61*, 137–146.
- Lan, Q.; Bassi, A. S.; Zhu, J. X.; Margaritis, A. *Chem. Eng. J.* **2001**, *81*, 179–186.
- Chipot, C.; Jaffe, R.; Maignet, B.; Pearlman, D. A.; Kollman, P. A. *J. Am. Chem. Soc.* **1996**, *118*, 11217–11224.
- Jorgensen, W. L.; Severance, D. L. *J. Am. Chem. Soc.* **1990**, *112*, 4768–4774.
- da Silva Filho, E. C.; de Melo, J. C. P.; Airoidi, C. *Carbohydr. Res.* **2006**, *341*, 2842–2850.
- Malm, C. J.; Genung, L. B.; Kuchmy, W. *Anal. Chem.* **1953**, *25*, 245–249.
- Garvey, C. J.; Parker, I. H.; Simon, G. P. *Macromol. Chem. Phys.* **2005**, *206*, 1568–1575.
- Hassan, M. L.; Rowell, R. M.; Fadl, N. A.; Yacoub, S. F.; Christensen, A. W. *J. Appl. Polym. Sci.* **2000**, *76*, 561–574.
- Zhao, H.; Kwak, J. H.; Zhang, Z. C.; Brown, H. M.; Arey, B. W.; Holladay, J. E. *Carbohydr. Polym.* **2007**, *68*, 235–241.
- Margutti, S.; Vicini, S.; Proietti, N.; Capitani, D.; Conio, G.; Pedemonte, E.; Segre, A. L. *Polymer* **2002**, *43*, 6183–6194.
- Schwanninger, M.; Rodrigues, J. C.; Pereira, H.; Hinterstoisser, B. *Vib. Spectrosc.* **2004**, *36*, 23–40.
- Yang, C. Q.; Wang, X. *Text. Res. J.* **1996**, *66*, 595–603.
- Atalla, R. H.; VanderHart, D. L. *Solid State Nucl. Magn. Reson.* **1999**, *15*, 1–19.
- Kono, H.; Yunoki, S.; Shikano, T.; Fujiwara, M.; Erata, T.; Takai, M. *J. Am. Chem. Soc.* **2002**, *124*, 7506–7511.
- Sullivan, A. C. O. *Cellulose* **1997**, *4*, 173–207.
- Zugenmaier, P. *Prog. Polym. Sci.* **2001**, *26*, 1341–1417.
- Smole, S. M.; Peršin, Z.; Kreže, T.; Kleinschek, K. S.; Ribitsch, V. *Mater. Res. Innovations* **2003**, *7*, 275–282.
- Zhao, H.; Kwak, J. H.; Wang, Y.; Franz, J. A.; White, J. M.; Holladay, J. E. *Energy Fuels* **2006**, *20*, 807–811.
- Chiang, W. Y.; Hu, C. H. *Composites Part A* **2001**, *32*, 517–524.
- Sun, S.; Wang, Q.; Wang, A. *Biochem. Eng. J.* **2007**, *36*, 131–138.
- Li, F.; Sun, X.; Zhang, H.; Li, B.; Gan, F. *J. Appl. Polym. Sci.* **2007**, *105*, 3418–3425.
- Airoidi, C.; Nunes, L. M. *Langmuir* **2000**, *16*, 1436–1439.
- Ramesh, A.; Lee, D. J.; Wong, J. W. C. *J. Colloid Interface Sci.* **2005**, *291*, 588–592.



Contents lists available at ScienceDirect

Journal of Colloid and Interface Science

www.elsevier.com/locate/jcis



## Cation removal using cellulose chemically modified by a Schiff base procedure applying green principles

Edson C. da Silva Filho<sup>a,b,\*</sup>, Júlio C.P. de Melo<sup>c</sup>, Maria G. da Fonseca<sup>d</sup>, Claudio Airoidi<sup>c</sup>

<sup>a</sup> Química, Universidade Federal do Piauí, 64900-000 Bom Jesus, PI, Brazil

<sup>b</sup> Química, Universidade Federal do Piauí, 64800-000 Floriano, PI, Brazil

<sup>c</sup> Institute of Chemistry, University of Campinas, P.O. Box 6154, 13084-971 Campinas, SP, Brazil

<sup>d</sup> Departamento de Química, Universidade Federal da Paraíba, 58059-900 João Pessoa, PB, Brazil

### ARTICLE INFO

*Article history:*  
Received 27 May 2009  
Accepted 7 August 2009  
Available online 12 August 2009

*Keywords:*  
Modified cellulose  
Schiff base  
Free solvent  
Cation adsorption

### ABSTRACT

Pentane-2,4-dione (acetylacetone) molecules were covalently incorporated under several different conditions to ethylene-1,2-diamine (en)-modified cellulose, using polar solvents or without solvents. The quantitative amount of en incorporated was given from  $0.37 \pm 0.01$  to  $3.03 \pm 0.01$  mmol of nitrogen per gram of cellulose, depending on the synthetic routes and after Schiff base formation this percentage was reduced by 1.38–6.12%. The synthetic routes indicated that lower solvent volumes produced higher amounts of en incorporation. However, the highest degree of pendant groups on the polymeric cellulose structure was obtained from a solvent-free reaction route. This procedure was applied for synthesizing all Schiff bases, causing a decrease in the amount of nitrogen. The available basic centers on the best covalently bonded biopolymer were investigated for adsorption of divalent copper, cobalt, nickel, and zinc from aqueous solution, with a capacity order of  $\text{Cu}^{2+} > \text{Co}^{2+} > \text{Ni}^{2+} > \text{Zn}^{2+}$ .

Published by Elsevier Inc.

### 1. Introduction

The chemical modification of cellulose through distinct methodologies, many different methods, using a wide range of solvents, has been developed to obtain new functionalized materials. In particular, some chlorinating agents have been widely applied to these syntheses, by employing thionyl chloride [1,2] and lithium chloride/chlorosuccinimide [3], following either a homogeneous or a heterogeneous route, depending on the agent and the final desired product. The success of the preparative methodology is closely related to the solvents used in these reactions, such as N,N'-dimethylacetamide (DMA), N,N'-dimethylformamide (DMF), pyridine, and xylene [1,3–5]. In addition, an alternative process includes a brominating reaction on cellulose by reacting the biopolymer with lithium bromide [6]. Another typical reaction that has also been explored is based on the transformation of the natural biopolymer to an aldehyde derivative by reacting with sodium metaperiodate, which can cause a ring opening mechanism between carbon 2 and carbon 3 atoms, to yield two aldehyde functions [7].

Many investigations involving these transformation reactions on different molecules, with different synthetic conditions and using a diversity of solvents, have been explored as well [1,3–5]. The molecules more highlighted for modifying the cellulose sur-

faces are ethylene-1,2-diamine [1] thiourea [8], aminobenzoic acid [5], cysteine [8], methyliminodiacetic acid [9], anhydride [10], phosphates [11], and oxides [12] as well as hydroxyquinoline inserted into cellulose previously modified with ethylene-1,2-diamine [13]. Therefore, modified cellulose matrices have been applied in many technological fields, for cation adsorption [1,5,8], as stationary phases in HPLC [14], in hemodialysis [15], as ion exchangers [16], for dye adsorption [17], as sensors [18], and others.

The aim of the present investigation is to synthesize chemically modified cellulose with the commonly used ethylene-1,2-diamine (en) molecule and, in a next step, to react this with the pentane-2,4-dione (acac) molecule, following green chemistry principles [19]. For this, a minimum amount of solvent or even no solvent should be used to establish the best synthetic conditions, to maximize the amount of pendant groups available on biopolymer backbone. The pentane-2,4-dione molecule was incorporated in a solvent-free procedure and the best material was applied as a cation remover for divalent copper, cobalt, nickel, and zinc from aqueous solutions.

### 2. Materials and methods

#### 2.1. Materials

Microcrystalline cellulose as powder (Aldrich),  $\sim 20 \mu\text{m}$ , was dried before use, N,N'-dimethylformamide (DMF) (Synth), thionyl

\* Corresponding author. Address: Química, Universidade Federal do Piauí, 64800-000 Floriano, PI, Brazil. Fax: +55 89 3522 2716.

E-mail address: edsonfilho@ufpi.edu.br (E.C. da Silva Filho).

chloride (SOCl<sub>2</sub>) (Fluka), ammonium hydroxide (Aldrich), ethylene-1,2-diamine (en) (Aldrich), and pentane-2,4-dione (acac) (Aldrich) were all reagent grade and used without prior purification.

### 2.2. Synthesis of chlorodeoxycellulose (CelCl)

A sample of 10 g of cellulose (Cel) suspended in DMF reacted with 35 cm<sup>3</sup> of thionyl chloride under mechanical stirring for 4 h. The cellulose chloride (CelCl) obtained was washed with dilute ammonium hydroxide solution until neutral pH. The solid was then separated by filtration and dried in vacuum at room temperature [1].

### 2.3. Synthesis of ethylene-1,2-diamine-6-deoxycellulose (Celen)

A sample of 1.0 g CelCl reacted with 5.0 cm<sup>3</sup> of en under reflux and with mechanical stirring for 4 h with variation of the amounts of the polar solvent water and DMF or under solvent-free conditions. For a series of experiments volumes of 50.0 and 10.0 cm<sup>3</sup> were used, to give new biopolymers named Celen1 (50.0 cm<sup>3</sup> of DMF), Celen2 (10.0 cm<sup>3</sup> of DMF), Celen3 (50.0 cm<sup>3</sup> of water), Celen4 (10.0 cm<sup>3</sup> of water), and Celen5 (solvent free). The solid products, generally represented as CelenX, X = 1–5, were filtered and dried in vacuum at room temperature [20].

### 2.4. Synthesis of Schiff base on cellulose (Celenacac)

A series of identical syntheses were used for incorporation of acac onto the CelenX compounds. For this, samples of 1.0 g of CelenX were individually suspended in 7.75 cm<sup>3</sup> of acac with stirring and the suspensions were gently refluxed at the boiling point of the reactant for 4 h. The solids were filtered using a sintered glass filter and the products, named CelenacacX, were dried in vacuum at room temperature for 24 h.

### 2.5. Characterization

The amounts of chloride and of the molecules pendant chains anchored onto the CelCl, CelenX (X = 1–5), and CelenacacX (X = 1–5) cellulose surfaces were calculated based on the chlorine and nitrogen percentages determined through elemental analysis made using a Perkin Elmer, Model 2400, elemental analyzer.

The infrared spectra of the samples in KBr pellets were performed by diffuse reflectance, accumulating 250 scans on a Bomem spectrophotometer, MB series, in the 4000–400 cm<sup>-1</sup> range, with 4 cm<sup>-1</sup> of resolution.

Nuclear magnetic resonance spectra of the samples were obtained on a Bruker AC 300/P spectrometer at room temperature. For each run, approximately 1 g of each solid sample was compacted into 7 mm zirconium oxide rotors. The measurements were obtained at frequency of 75.47 MHz for carbon with a magic angle spinning of 4 Hz. In order to increase the signal to noise ratio the CP/MAS technique was performed and <sup>13</sup>C spectra were obtained with pulse repetition of 3 s and contact time of 3 ms.

Thermogravimetric curves were obtained on a TA instrument in an argon atmosphere, coupled to a Model 1090 B thermobalance, using a heating rate of 0.167 K s<sup>-1</sup>, under a flow of 30 cm<sup>3</sup> s<sup>-1</sup>, varying from room temperature up to 1273 K, with an initial mass of approximately 10 mg of solid sample.

Secondary electron images were acquired with a JEOL JSM 6360LV scanning electron microscope, operating at 20 kV. The samples were fixed onto a double-faced carbon tape adhered to an aluminum support and carbon-coated in a Bal-Tec MD20 instrument.

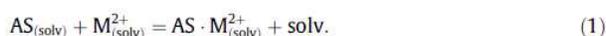
To determine the amount of cation in the aqueous solutions an ICP OES (inductively coupled plasma optical emission spectrome-

ter) Perkin Elmer, Model 3000 DV, was used for each experimental point, and the reproducibility was checked by at least one duplicate run.

### 2.6. Adsorption

The capacity of the chemically modified cellulose to extract cations from aqueous solution was determined in duplicate, using a batch process with divalent copper, cobalt, nickel, and zinc nitrates, by using a mass (*m*) of about 20 mg of Celenacac5 suspended in 25.0 cm<sup>3</sup> of an aqueous solution with concentrations of each metal varying from 0.050 to 1.0 mmol dm<sup>-3</sup>. The suspensions were mechanically stirred at room temperature for 4 h and separated by centrifugation at 2400 rpm for 10 min. Aliquots of the supernatant were pipetted and the cations were determined by ICP OES. The adsorption capacities (*n<sub>f</sub>*) were calculated by considering the number of moles, *n<sub>f</sub>* = (*n<sub>i</sub>* - *n<sub>s</sub>*)/*m*, where *n<sub>i</sub>* and *n<sub>s</sub>* are the initial and supernatant number of moles [21].

The adsorption at the solid/liquid interface demands a competition between the solvent (solv) bonded to the chemically modified surface (AS) that is gradually displaced by the solute in solution to reach equilibrium:



The ratio between the number of moles of metal in solution at equilibrium and those adsorbed on the chemically modified surface is used to obtain the modified Langmuir isotherm, by applying

$$\frac{C_s}{n_f} = \frac{C_s}{n^s} + \frac{1}{n^s b}, \quad (2)$$

where *C<sub>s</sub>* is the concentration of supernatant cations at equilibrium, *n<sub>f</sub>* is the number of moles adsorbed, *n<sup>s</sup>* is the maximum amount of solute adsorbed per gram of Celenacac5, which is related to the number of adsorption sites, and *b* is a constant. The *n<sup>s</sup>* and *b* values for each adsorption process were calculated from the angular and linear coefficients, respectively, of the linearized form of the adsorption isotherms, *C<sub>s</sub>/n<sub>f</sub>* versus *C<sub>s</sub>*, using the method of least squares.

From the outlined form of the isotherm it is possible to foresee if the adsorption is favorable. Thus, the Langmuir parameters can be expressed from the adimensional separation factor, *R<sub>L</sub>*, defined by the equation [22]

$$R_L = \frac{1}{(1 + b \cdot C_0)}, \quad (3)$$

which enables evaluation of the form of isotherm and the values are listed in Table 1 for the proposed models.

## 3. Results and discussion

### 3.1. Elemental analysis

The elemental analyses for all synthesised biopolymeric matrices are listed in Table 2. As observed, an effective chlorinating reaction with cellulose gave a complete degree of hydroxyl group substitution (DS) on carbon 6, to reach the value 0.99 ± 0.01. However, during the course of reactions with ethylene-1,2-diamine

**Table 1**  
Factor of separation, *R<sub>L</sub>*, for the respective isotherm.

| <i>R<sub>L</sub></i>         | Isotherm     |
|------------------------------|--------------|
| <i>R<sub>L</sub></i> > 1     | Unfavorable  |
| <i>R<sub>L</sub></i> = 1     | Linear       |
| 0 < <i>R<sub>L</sub></i> < 1 | Favorable    |
| <i>R<sub>L</sub></i> = 0     | Irreversible |

**Table 2**

Percentages of chlorine and nitrogen in chlorodeoxycellulose and ethane-1,2-diaminedeoxycellulose matrices, degree of functionalization (DF), and percentage of effectiveness of incorporation (EI).

| Matrix | Cl/%         | N/%         | DS   | DF/mmol g <sup>-1</sup> | EI/% |
|--------|--------------|-------------|------|-------------------------|------|
| CelCl  | 17.58 ± 0.10 | –           | 0.99 | 4.95 ± 0.03             | –    |
| Celen1 | 11.74 ± 0.11 | 3.96 ± 0.01 | 0.33 | 1.41 ± 0.01             | 28   |
| Celen2 | 4.53 ± 0.18  | 5.78 ± 0.06 | 0.74 | 2.06 ± 0.02             | 42   |
| Celen3 | 16.24 ± 0.09 | 1.04 ± 0.02 | 0.08 | 0.37 ± 0.01             | 7    |
| Celen4 | 5.70 ± 0.07  | 5.84 ± 0.06 | 0.68 | 2.08 ± 0.03             | 42   |
| Celen5 | 7.54 ± 0.09  | 8.50 ± 0.03 | 0.57 | 3.03 ± 0.01             | 61   |

molecules, a fraction of chlorine atoms remained in the original matrices, depending on the experimental procedure used. The reaction yielded a degree of functionalization (DF), which was calculated based on the amount of nitrogen atom incorporated on the pendant chains. The effectiveness of these substitutions (EI), in percentage, was calculated by considering the molar relationship between the ethylene-1,2-diamine and the initial amount of chloride bonded on the modified biopolymer. From these results the highest value of 61% was observed for solvent-free reaction, demonstrating the effectiveness in chlorine atom substitution under these experimental conditions.

As expected, the first step in this series of reactions consisted in cellulose chlorination, a process favored by nucleophilic thionyl chloride attack on the hydroxyl group in the biopolymer backbone, resulting in pendant chlorine atoms on the polymeric structure. This substituted atom is much more reactive than the original hydroxyl group, to give a total substitution of hydroxyl group at C6 by chlorine. This is expected as the hydroxyl in this position is more reactive in comparison with the other hydroxyl groups, following the order [23] C<sub>6</sub> >> C<sub>3</sub> ≈ C<sub>2</sub>, as shown in Fig. 1.

The most encouraging fact for adopting this sequence of reaction methodology is the highest value for nitrogen groups for Celen5, which was synthesised without adding solvent, in accordance with green chemistry principles [19]. From this series of results a decrease of the incorporated groups with the amount and polarity of solvent is clearly demonstrated to give the order Celen5 > Celen4 > Celen2 > Celen1 > Celen3.

For the synthetic routes in which a solvent was used, but with different quantities in the synthesis, the amount of ethylene-1,2-diamine molecules incorporated in the biopolymer increases with a decrease in the volume employed. In addition, when the comparison is between different solvents with the same volume (50.0 cm<sup>3</sup>), a more effective yield was obtained with DMF than with water. However, when the volume changes to 10.0 cm<sup>3</sup> the more favorable solvent was water, although the nitrogen quantities and the resulting quantities of product were very close.

Based on these obtained results, the solvent-free process gave an increase of incorporation of 19%, in comparison with Celen4, which gave the highest value when using solvents. The favorable increase in the degree of incorporation of a molecule in the biopolymer backbone in the absence of solvent for preparing new functional polymers has environmental benefits, in addition to reducing costs and also simplifying the process [24].

Another important feature to be analyzed is the amount of molecules incorporated into the polymeric structure, by using the

quantitative data from elemental analyses results. For example, Celen2 and Celen4 were prepared with 10.0 cm<sup>3</sup> of solvents to give 42% of incorporation; however, the amount of chlorine atom remaining is higher for Celen4. This behavior suggests that the two amino groups can simultaneously act as bidentate molecules to bond to adjacent polymeric chains, as a crosslinking agent, as illustrated for Celen2 surface, represented in Fig. 2.

The results of nitrogen percentage for Celen modified with pentane-2,4-dione, due to Schiff base formation, are listed in Table 3. From these data it is observed that as Celen reacts with acac, the percentage of nitrogen in the compound decreases, as a consequence of the Schiff base formation. When the amount of free nitrogen in the Celen matrix is high before the chemical modification, the highest amounts of imine groups are attached, due to the quantity of acac groups incorporating into the polymers, thus reducing the percentage of nitrogen per gram of biopolymer. Celenacac2 and Celenacac4 matrices presented reduced values, a behavior that can be interpreted as crosslinking, with a consequent decrease in the available amino groups for Schiff base formation. If any chlorine atoms were presented in the precursor matrices, it could remain, but all available amino groups react directly with acac to form the imine bond. A schematic representation of complete incorporation of pentane-2,4-dione molecules on modified cellulose biopolymer is shown in Figs. 3 and 4.

### 3.2. Infrared spectroscopy

The FTIR spectra of cellulose, chlorodeoxycellulose, and the other two synthesised polymeric biopolymers are shown in Fig. 5. Typical wavenumbers for hydroxyl groups for Cel, such as –CH–OH and –CH<sub>2</sub>–OH stretching in the 3300–3400 cm<sup>-1</sup> interval, are observed in Fig. 5a. The methylene groups stretching, from the incorporated molecule, are located at 2900 cm<sup>-1</sup> and the band in the 3000–2800 cm<sup>-1</sup> range is attributed to –C–H groups, since the –CH and –CH<sub>2</sub> group ratio for cellulose is in a 5:1 proportion [25,26]. The OH bending vibrations for the cellulose surface are located at 1639 cm<sup>-1</sup>, the primary and secondary hydroxyl bending appeared in the 1500–1200 cm<sup>-1</sup> interval, and C–O stretching vibration is observed at 1100 cm<sup>-1</sup> [25,26].

A decrease of the vibrations in the 1500–1200 cm<sup>-1</sup> interval on substitution of hydroxyl groups by chloride atoms in CelCl is a clear indication of the incorporation of the desired molecule in the polymeric chains, as shown in Fig. 5b. The band at 896 cm<sup>-1</sup> was shifted to 868 cm<sup>-1</sup> after chlorination and disappeared after reacting with en. For the chlorodeoxycellulose surface, the bands at 752 and 709 cm<sup>-1</sup> decrease in intensity, but are still visible due to the incomplete substitution by en molecules.

For Celen5 the spectrum shown in Fig. 5c, typical CH<sub>2</sub> stretching at 2837 cm<sup>-1</sup> is seen, but now the CH:CH<sub>2</sub> ratio decreased after reacting with the ethylene-1,2-diamine molecule, while a new weak band at 1658 cm<sup>-1</sup> can be attributed to amino group bending vibrations. Thus, for a complete reaction a 5:3 expected ratio could be obtained; however, not all available chlorine atoms were substituted, but with a value higher than 5:1. On the other hand, the sequence of reaction confirms that the incorporation process was performed to a large extent on the surface of the biopolymer. For the spectrum of Celenacac5, shown in Fig. 5d, it is observed that

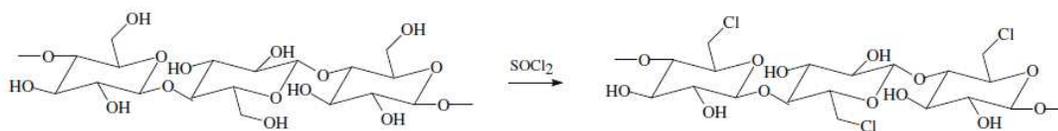


Fig. 1. Reaction for chlorination of cellulose.

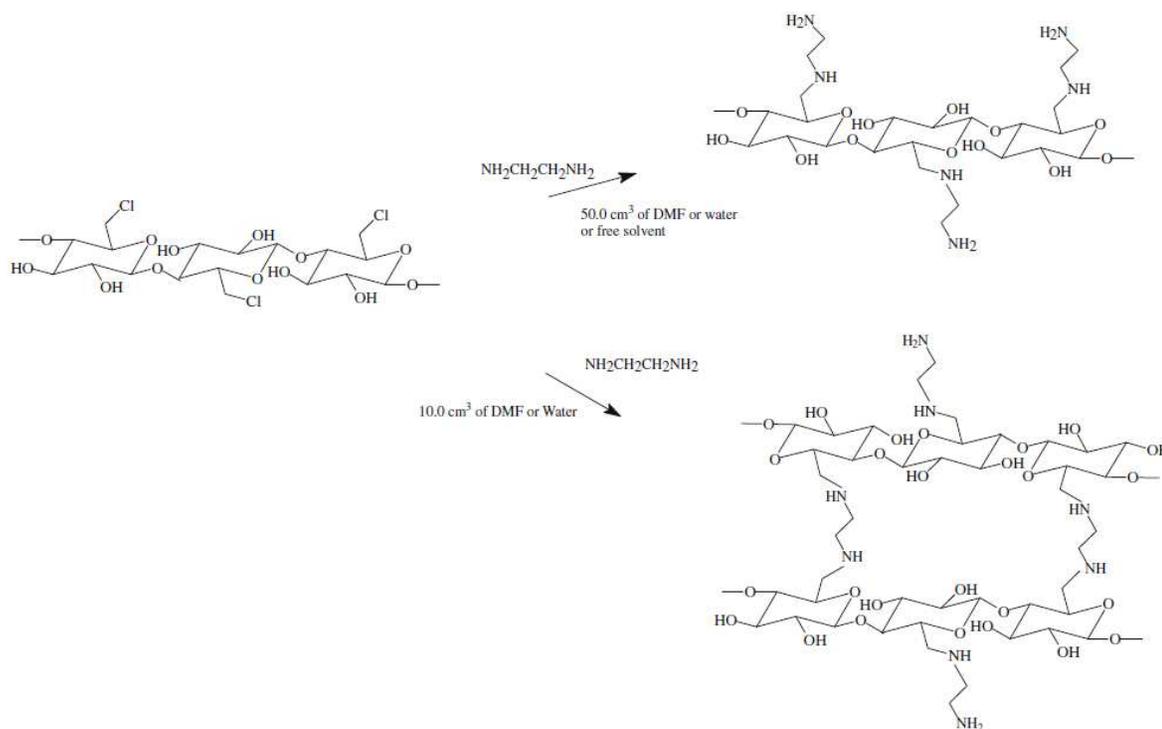


Fig. 2. Reaction of ethylene-1,2-diamine with CeCl.

**Table 3**  
 Percentage of nitrogen (N) in cellulose matrices with Schiff base and variation in amount of nitrogen ( $\Delta N$ ).

| CelenacacX | N/%             | $\Delta N$ /% |
|------------|-----------------|---------------|
| 1          | $3.78 \pm 0.02$ | 4.55          |
| 2          | $5.70 \pm 0.05$ | 1.38          |
| 3          | $0.99 \pm 0.03$ | 4.81          |
| 4          | $5.74 \pm 0.02$ | 2.73          |
| 5          | $7.98 \pm 0.16$ | 6.12          |

in the  $2800\text{--}3000\text{ cm}^{-1}$  interval there is an increase in bandwidth when compared with the spectrum of Celen5. This band, in fact, corresponds to three types of different groups ( $-\text{CH}$ ,  $-\text{CH}_2$ , and  $-\text{CH}_3$ ). The increase in intensity and bandwidth in the  $1610\text{ cm}^{-1}$  region indicates the presence of the band attributed to imine ( $\nu\text{C}=\text{N}$ ) stretching vibrations [25,26].

### 3.3. Nuclear magnetic resonance

For cellulose, chlorodeoxycellulose, and all synthesised compounds the  $^{13}\text{C}$  solid-state NMR spectra had the expected signals, as numbered in the structural representations on the left-hand side in Fig. 6. For pure cellulose, the low field peak corresponded to carbon (C1) at 104 ppm, which is bonded to two oxygen atoms, as shown in Fig. 6a. Carbon 4 is attributed to the peak in the 88 ppm region, which is bonded to one oxygen atom, which also forms a 1,4'- $\beta$ -glycoside bond [1]. The chemical shift at 74 ppm refers to those carbons numbered 2, 3, and 5, which are located in similar chemical environments; e.g., all of them are secondary carbons bonded to hydroxyl and  $-\text{CH}$  groups. Carbon 6 gave the smallest chemical shift due to the fact that it is the only primary carbon atom, attached to the ring unit and also bonded to a hydro-

xyl group, corresponding to  $-\text{CH}_2$  in the cellulose structure [25,27].

The spectrum of chlorodeoxycellulose in Fig. 8b presented down-shift peaks in comparison to pristine cellulose. For example, the C1 peak is shifted from 104 to 103 ppm C4 from 88 to 83 ppm while the C2, C3, and C5 peaks are located at the same region. For C6 where nucleophilic substitution with thionyl chloride occurred, a large shift from 65 to 44 ppm indicates an effective incorporation of chloride onto the cellulose surface. Thus, the change in the high field peak, due to the electronegativity of chlorine atom indicates the incorporation of ethylene-1,2-diamine, as shown in Fig. 6c. For cellulose chemically modified with en followed by the next reaction with acac, significant changes occurred as shown in Fig. 6d. The chemical shifts for C9 and C12 from the pendant chain appeared at 174 ppm; these signals are related to a new imide bond  $\text{C}=\text{N}$  as the Schiff base is formed, to give a crosslinking process, as shown in Figs. 3 and 4. A sharp peak at 18 ppm is assigned to the chemical shift of the other two carbon atoms C10 and C13 that correspond to  $-\text{CH}_3$  terminal groups of acac molecule [24,26]. The signal for C11 appeared close to carbons 6, 7, and 8 for the pendant en moiety, and the chemical shifts for the main biopolymer structure are located at the same positions for other chemically modified celluloses.

### 3.4. Thermogravimetry

The thermogravimetric curves for cellulose and the chemically modified celluloses are shown in Fig. 7a. The curve for pristine cellulose gave only one event in the decomposition process covering temperatures from 536 to 647 K, and corresponded to a mass loss of 92%. The chlorinated biopolymer presented a mass loss of 3% in the 386–430 K range, which can be assigned to the water physically adsorbed onto the surface. The second step, with a mass loss

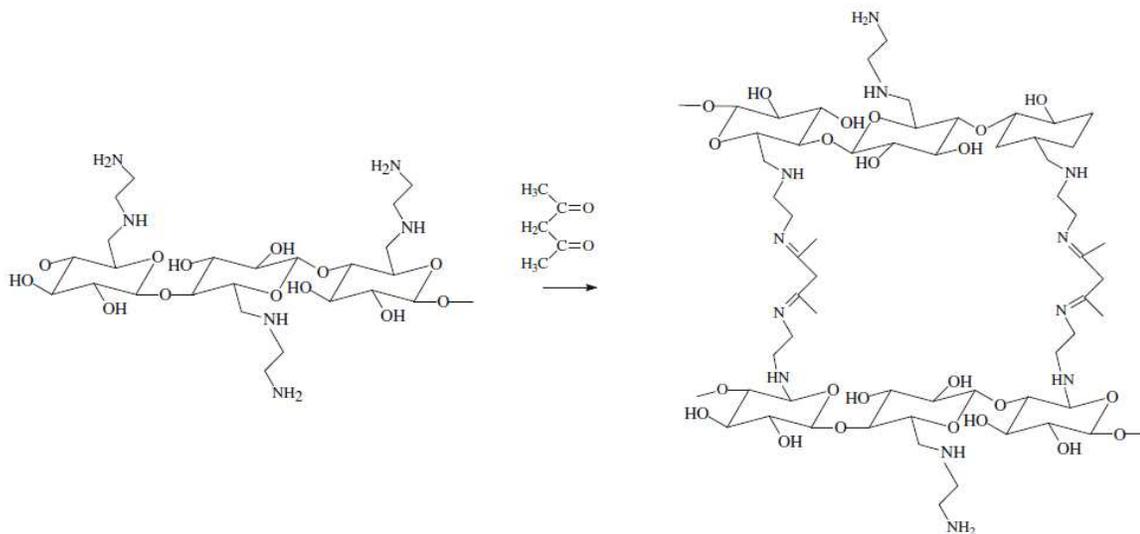


Fig. 3. Possible forms of reaction of CelenX (X = 1, 3, and 5) with pentane-2,4-dione.

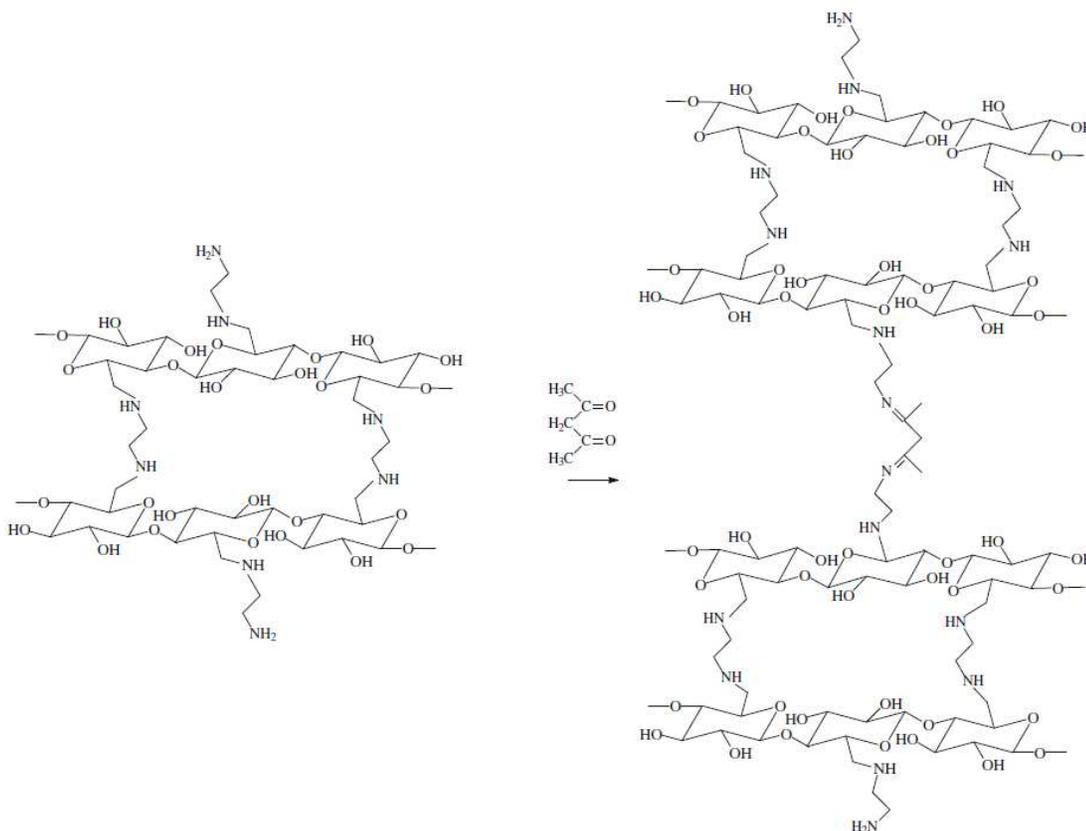
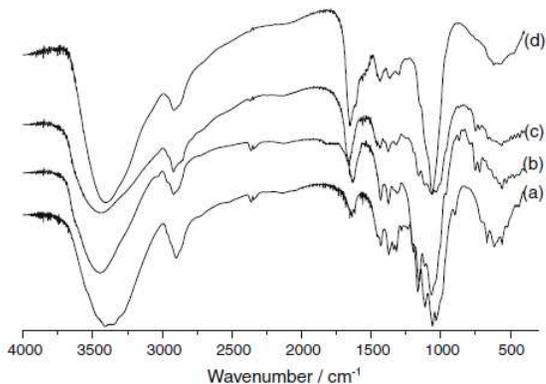


Fig. 4. Possible forms of reaction of Celen2 and Celan4 with pentane-2,4-dione.

of 23%, between 438 and 534 K corresponded to the displacement of the HCl molecule, as the condensation of hydroxyl groups on carbons 2 and 3 occurred. The last event in this process, corresponding to a mass loss of 64%, started at 521 K and can be inter-

preted as cellulose fiber decomposition. The curve of the incorporated biopolymer Celen5 is very similar to that presented by CelCl, with an initial mass loss of 4% from 320 to 363 K, attributed to physisorbed water and a second decomposition event



5. FTIR spectra of Cel (a), CelCl (b), Celen5 (c), and Celenacac5 (d) samples.

occurring in the 364–563 K range, with a mass loss of 34% that corresponded to the loss of the incorporated en molecule together with condensation of the hydroxyl groups on carbons 2 and 3. The third decomposition step, starting from 564 K, also is attributed to the loss of cellulose fiber, giving an amount of 48%. The decomposition of Celenacac5, as identically observed for Celen5, presented an initial mass loss of 4% until 442 K. The second decomposition step occurred in the 443–611 K interval, with a mass loss of 41%, corresponding to the loss of the immobilized pentane-2,4-dione and ethylene-1,2-diamine molecules and the condensation of the hydroxyl groups on carbons 2 and 3 of the polymeric structure. The last decomposition starting from 613 K is assigned to the loss of cellulose fiber, giving an amount of 24%, as shown in derivative curves in Fig. 7b. Based on the quantitative amount of mass loss, a distinct behavior for these decomposition processes can be observed, by presenting the sequence expressed as Celenacac5 < Celen5 < CelCl < Cel. These values are in agreement with

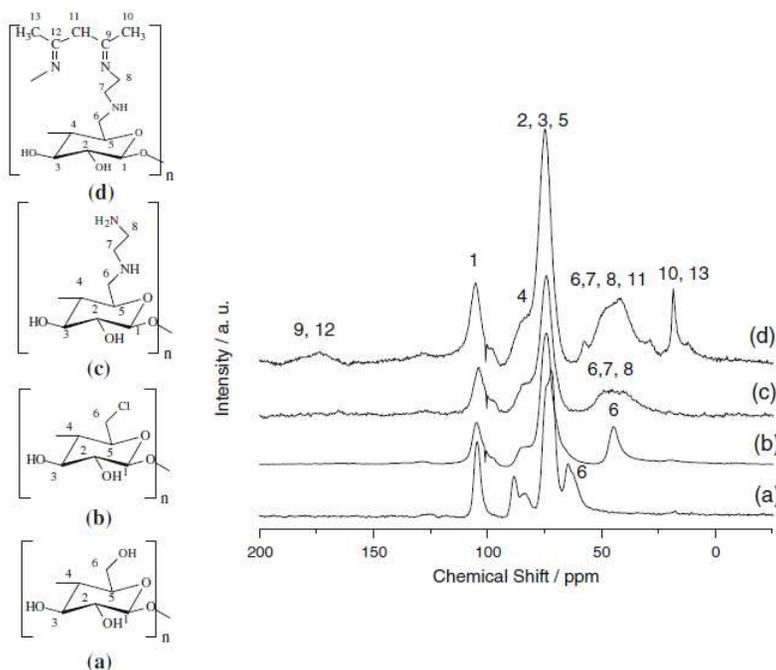


Fig. 6. <sup>13</sup>C NMR spectra of Cel (a), CelCl (b), Celen5 (c), and Celenacac5 (d) samples.

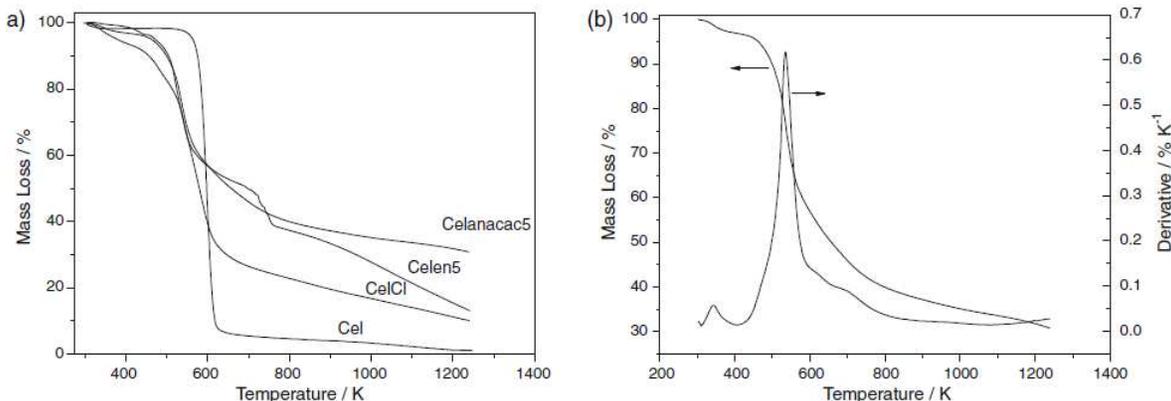


Fig. 7. TG curves of Cel, CelCl, Celen5, and Celenacac5 (a) and TG and DTG of Celenac5 (b).

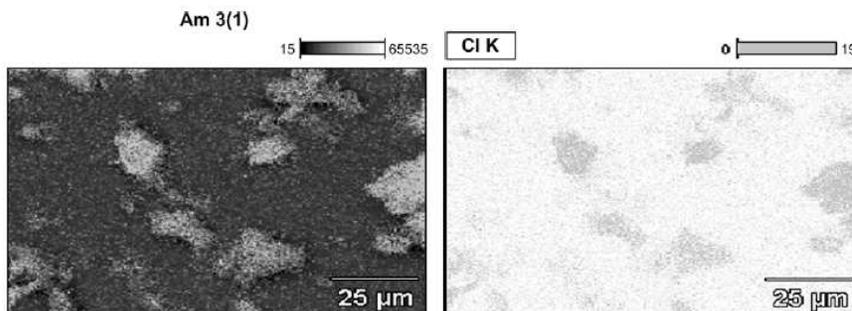


Fig. 8. Chlorine atom mapping for CelCl sample.



Fig. 9. SEM micrographs of Celenacac5 sample.

the fact that Celenacac5 is the most thermally stable matrix, followed by Celen5 and CelCl and finally by Cel [1,20].

### 3.5. Scanning electron microscopy and energy dispersive spectroscopy

An extra confirmation of the existence of the chlorine atom covalently bonded to the synthesised material can be verified for a homogeneous distribution of the pendant chains across the surface and this behavior is in complete agreement with the proposed synthetic routes, where a regular distribution of the incorporated organic moieties bonded to the polymeric backbone is expected, as shown in Fig. 8.

Thus, the scanning electron micrographs (SEM) for cellulose and chlorodeoxycellulose present similar aspects. For pure cellulose, fibrous and porous features on the surface are observed and although the chloride surface is similar, it is not as intensive as in the precursor material. For the modified surfaces, these characteristics decreased significantly in the incorporated cellulose, as shown in Fig. 9, where the original, chlorinated, and Celen5 matrices are compared [1].

### 3.6. Adsorption

The covalent immobilization of molecules in supports containing nitrogen, sulfur, and oxygen basic centers provides conditions for cation removal from aqueous and nonaqueous solvents [21,28,29] that depend in certain cases in the hydrophobicity of the matrices involved. Thus, the chemically modified surface containing the highest incorporation of en and acac was studied for

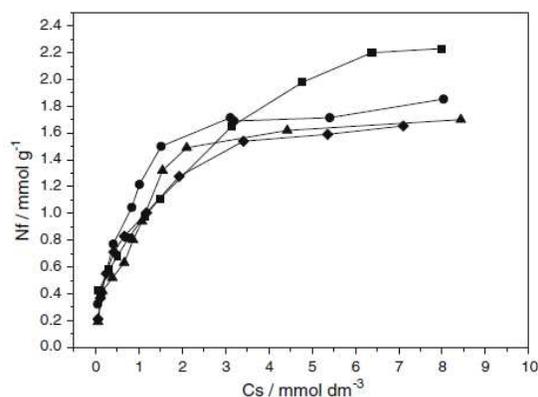


Fig. 10. Adsorption isotherms of the divalent cations: Cu<sup>2+</sup> (■), Co<sup>2+</sup> (●), Ni<sup>2+</sup> (▲), and Zn<sup>2+</sup> (◆) on the Celenacac5 surface at 298 + 1 K.

cation removal using divalent copper, cobalt, and zinc, through batch methodology.

The isotherms of cation adsorption with Celenacac5 biopolymer are shown in Fig. 10. The linearized form of the modified Langmuir equation (Eq. (2)) was applied for zinc adsorption, represented by  $C_s/n_f$  as a function of  $C_s$ , given in Fig. 11 and enables the calculation of the linear and angular data from a straight line, to obtain  $n^2$  and  $b$  values, as listed in Table 4. The data are in agreement with the establishment of the following adsorption order: Cu<sup>2+</sup> > Co<sup>2+</sup> >

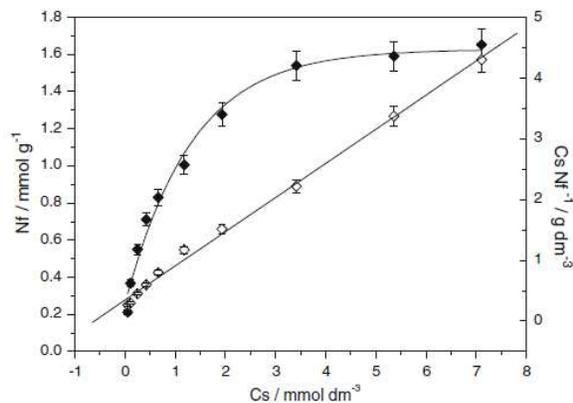
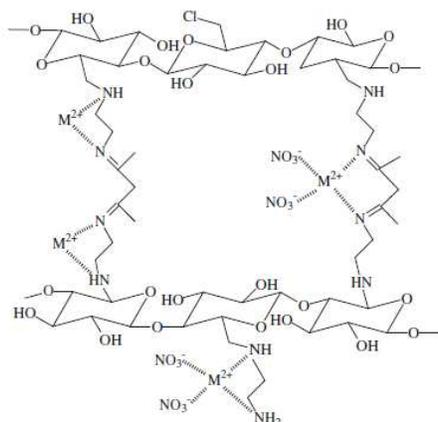


Fig. 11. Adsorption isotherm of Zn<sup>2+</sup>(◆) and the linearized Langmuir isotherm (◇) on Celenacac5 surface at 298 + 1 K.

**Table 4**

Number of moles adsorbed ( $n_f$ ), maximum adsorption capacity ( $n^s$ ), correlation coefficient ( $r$ ), and constant ( $b$ ) for the interaction of divalent metal (M) nitrates with Celenacac5 at 298 + 1 K.

| M  | $n_f$ (mmol g <sup>-1</sup> ) | $n^s$ (mmol g <sup>-1</sup> ) | $r$    | $b$  |
|----|-------------------------------|-------------------------------|--------|------|
| Cu | 2.32 ± 0.06                   | 2.58 ± 0.04                   | 0.9859 | 718  |
| Co | 1.85 ± 0.02                   | 1.95 ± 0.09                   | 0.9983 | 1935 |
| Ni | 1.70 ± 0.04                   | 1.89 ± 0.05                   | 0.9941 | 1153 |
| Zn | 1.65 ± 0.02                   | 1.78 ± 0.08                   | 0.9979 | 1620 |



**Fig. 12.** Possible forms of metal complexation as bidentate on chemically modified cellulose Celenacac5.

$\text{Ni}^{2+} > \text{Zn}^{2+}$ . This same sequence was previously observed for another biopolymer chitosan [30].

However, the biopolymer Celenacac5 presented a larger cation adsorption capacity, suggesting its use in concentration and separation. During the adsorption process the interactions at the solid-liquid interface can be interpreted as a cation acidic center from aqueous solution that interacts with the available basic centers of the formed Schiff base, to result in cation complexation to remove this species from this medium.

Taking into account the obtained isotherm forms for all cations, a close correspondence with the outlined 2L type model, as expressed by Gilles' classification [31], is observed. This favorable isotherm model is illustrated through cation-basic center affinity to complex formation at the solid-liquid interface [32–34]. As expected, some possibilities are based on the availability or basic centers incorporated on pendant chains or crosslinking units [1] and an example is shown in Fig. 12, when cellulose is chemically modified with ethylene-1,2-diamine in the absence of solvent. In attempting to verify this isotherm behavior, all  $R_L$  calculation parameters gave favorable values, as represented by Eq. (3), such as 0.35, 0.21, 0.31, and 0.26, for  $\text{Cu}^{2+}$ ,  $\text{Co}^{2+}$ ,  $\text{Ni}^{2+}$ , and  $\text{Zn}^{2+}$ . With the exception of cobalt, the formed complexes follow the Irving-Williams series for  $K_1$  values, to give the order  $\text{Ni}^{2+} < \text{Cu}^{2+} > \text{Zn}^{2+}$  [35].

#### 4. Summary

The ethylene-1,2-diamine molecule, covalently incorporated onto a cellulose surface after a previous chlorination step, yielded new modified biopolymer, with great potential not only as a precursor for other pendant chain moieties but also as support for cation removal. The ethylene-1,2-diamine material synthesised through a solvent-free route was shown to be an innovative procedure without any solvent participation, which is a promising

synthetic route with the highest effectiveness of incorporation of the desired molecule. Using more established experimental conditions, the best synthesis in solvents of this biopolymer consists in using 10.0 cm<sup>3</sup> of polar DMF or 10.0 cm<sup>3</sup> of water. On the other hand, the solvent-free procedure for incorporation of pentane-2,4-dione depends on the free amino group in the precursor material, which is affected by the crosslinking process.

A remarkable feature associated with these proposed routes to incorporate the covalent molecule regularly distributed in a natural polysaccharide is the increase in size of the new polymeric backbone. Such an innovation is important for the progress of this research field utilizing available, abundant, inexpensive natural biopolymers to improve many technological applications.

The new synthetic surfaces with incorporation of pendant chains containing potentially basic nitrogen atoms are potential centers available for cation removal, and behaved as promising materials to be applied for this operation, with good sorption capacity for divalent cations, and of great utility for ecosystem purification.

#### Acknowledgments

The authors are indebted to FAPESP for financial support and fellowships to E.C.S.F. and J.C.P.M. and to CNPq for fellowships to M.G.F. and C.A.

#### References

- [1] E.C. da Silva Filho, J.C.P. de Melo, C. Airolidi, *Carbohydr. Res.* 341 (2006) 2842.
- [2] T.L. Vigo, D.J. Daigle, *Carbohydr. Res.* 21 (1972) 369.
- [3] B. Tosh, C.N. Saikia, N.N. Dass, *Carbohydr. Res.* 327 (2000) 345.
- [4] S. Nakamura, M. Amano, *J. Polym. Sci. A* 35 (1997) 3359.
- [5] G.R. de Castro, J.D. de Oliveira, I.L. Alcântara, P.S. Roldan, C.C.F. Padilha, A.G.S. Prado, P.M. Padilha, *Sep. Sci. Technol.* 42 (2007) 1325.
- [6] N. Aoki, K. Fukushima, H. Kurukata, M. Sakamoto, K.-I. Furuhashi, *React. Funct. Polym.* 42 (1999) 223.
- [7] L. Frías, L.-S. Jhanson, P. Stenius, J. Laine, K. Stana-Kleinschek, V. Ribitsch, *Colloids Surf., A* 260 (2005) 101.
- [8] E. Mentasti, C. Sarzanini, M.C. Gennaro, V. Porta, *Polyhedron* 6 (1987) 1197.
- [9] M.C. Gennaro, C. Sarzanini, E. Mentasti, C. Baiocchi, *Talanta* 32 (1985) 961.
- [10] J.C.P. de Melo, E.C. Da Silva Filho, S.A.A. Santana, C. Airolidi, *Colloids Surf., A* 346 (2009) 138.
- [11] D.M. Suflet, G.C. Chitanu, V.I. Popa, *React. Funct. Polym.* 66 (2006) 1240.
- [12] Y.-L. Lei, D.-Q. Lin, S.-J. Yao, Z.-Q. Zhu, *React. Funct. Polym.* 62 (2005) 169.
- [13] V. Gurnani, A.K. Singh, B. Venkataramani, *Anal. Chim. Acta* 485 (2003) 221.
- [14] W. Du, G. Yang, X. Wang, S. Yuan, L. Zhou, D. Zu, C. Liu, *Talanta* 60 (2003) 1187.
- [15] V. Panichi, G.M. Rizza, D. Taccola, S. Paoletti, E. Mantuano, M. Migliori, S. Frangioni, C. Filippi, A. Carpi, *Biomed. Pharm.* 60 (2006) 14.
- [16] U.S. Orlando, T. Okuda, A.U. Baes, W. Nishijima, M. Okada, *React. Funct. Polym.* 55 (2003) 311.
- [17] C. Namasivayam, R.T. Yamuna, J. Jayanthi, *Cell. Chem. Technol.* 37 (2003) 333.
- [18] V. Ducéré, A. Bernès, C. Lacabanne, *Sens. Actuators, B* 106 (2005) 331.
- [19] J.C. Warner, A.S. Cannon, K.M. Dye, *Environ. Imp. Asses. Rev.* 24 (2004) 775.
- [20] E.C. da Silva Filho, J.C.P. de Melo, F.J.V.E. Oliveira, C. Airolidi, *J. Therm. Anal. Calorim.* (2009), doi:10.1007/s10973-009-0270-6.
- [21] M.G. da Fonseca, E.C. da Silva Filho, R.S.A. Machado Jr., L.N.H. Arakaki, J.G.P. Espinola, C. Airolidi, *J. Solid State Chem.* 177 (2004) 2316.
- [22] K.R. Hall, C. Eagleton, A. Acrivos, T. Vermeulen, *Ind. Eng. Chem. Fundam.* 05 (1966) 212.
- [23] A.I. Martin, M. Sanchez-Chaves, F. Arranz, *React. Funct. Polym.* 39 (1999) 179.
- [24] K. Tanaka, F. Toda, *Chem. Rev.* 100 (2000) 1025.
- [25] D.L. Pavia, G.M. Bassler, T.C. Morrill, *Introduction to Spectroscopy*, second ed., Saunders College Publishing, New York, 1996.
- [26] G.R. Castro, I.L. Alcântara, P.S. Roldan, D.F. Bozano, P.M. Padilha, A.O. Florentino, J.C. Rocha, *Mater. Res.* 7 (2004) 329.
- [27] R.H. Atalla, D.L. VanderHart, *Solid State Nucl. Magn. Reson.* 15 (1999) 1.
- [28] L.N.H. Arakaki, A.P.M. Alves, E.C. da Silva Filho, M.G. Fonseca, S.F. Oliveira, J.G.P. Espinola, C. Airolidi, *Thermochim. Acta* 453 (2007) 72.
- [29] R.S.A. Machado Jr., M.G. da Fonseca, L.N.H. Arakaki, J.G.P. Espinola, S.F. Oliveira, *Talanta* 63 (2004) 317.
- [30] I.S. Lima, C. Airolidi, *Thermochim. Acta* 421 (2004) 133.
- [31] C.H. Giles, T.H. MavEvan, S.W. Nakhawa, D. Smith, *J. Chem. Soc.* 786 (1960) 3973.
- [32] E.C.N. Lopes, K.S. Sousa, C. Airolidi, *Thermochim. Acta* 483 (2008) 21.
- [33] M.O. Machado, E.C.N. Lopes, K.S. Sousa, C. Airolidi, *Carbohydr. Polym.* 77 (2009) 760.
- [34] D.L. Guerra, R.R. Viana, C. Airolidi, *J. Braz. Chem. Soc.* 20 (2009) 1164.
- [35] J.E. Huheey, E.A. Keiter, R.L. Keiter, *Inorganic Chemistry*, fourth ed., Harper Collins College Publishers, 1993.

## X-ray diffraction and thermogravimetry data of cellulose, chlorodeoxycellulose and aminodeoxycellulose

Edson C. da Silva Filho · Sirlane A. A. Santana ·  
Júlio C. P. Melo · Fernando J. V. E. Oliveira ·  
Claudio Airoidi

Received: 11 March 2009 / Accepted: 22 June 2009  
© Akadémiai Kiadó, Budapest, Hungary 2009

**Abstract** Cellulose was chemically modified with  $\text{SOCl}_2$  to obtain chlorodeoxycellulose, followed by a reaction that gave bonded ethylene-1,2-diamine (en), producing 6-(2'-aminoethylamino)-6-deoxycellulose. The reactions were carried out without the presence of solvent, in water or in *N,N'*-dimethylformamide, in which the highest amount of amino compound was incorporated onto the biopolymer backbone. The X-ray diffraction patterns for the chlorodeoxycellulose indicate new crystallinities that result from hydrogen bonds established through bonded chlorine atoms and the remaining hydroxyl groups, while all the aminodeoxycelluloses were amorphous compounds. Thermal stabilities, for all aminated celluloses gave lower final mass losses than for the chlorinated biopolymer, whose value is lower than unmodified cellulose.

**Keywords** Ethylene-1,2-diamine · Cellulose · Solvent-free · Thermogravimetry · X-ray

### Introduction

A great variety of pristine or chemically modified organic or inorganic polymeric materials have been and continue to be the focus of many studies [1], including the two most abundant biopolymers, cellulose [2, 3] and chitosan [4, 5], as well as synthetic and natural inorganic polymers, such as silicas [6–8], phyllosilicates [9–11], phosphates [12, 13], chrysotile [14], clays [15, 16] etc. The increasing usefulness of these classes of materials is closely related to chemical surface modifications, explored to change the chemical and physical properties and also the activity of the available functional groups attached on pendant chains. For any support, the original hydroxyl reactive centers on the surface are of great utility to graft desirable molecules in single-step procedures or using a sequence of reactions [17].

Many studies concerning the synthesis and characterization of modified surfaces have been reported in the last half-century [18–20]. Thus, surfaces modified with basic centers, such as the ethylene-1,2-diamine moiety, are applied in different areas for cation removal from aqueous solution [20], in chromatography [21], in catalysis [22], for pre-concentration of trace chemical species in solution [23], and in ion-exchange processes [24].

This investigation deals with the most abundant natural biopolymer, cellulose, with the objective to improve its applicability, by exploring the limited reactivity of the hydroxyl groups bonded to the polymeric structure [17, 25]. After cellulose chlorination on carbon 6 the synthetic procedure enables the incorporation of the ethylene-1,2-diamine molecule, exploring different features with polar or solvent-free routes. As the characterization of these synthetic products is not an easy task, the elemental analysis results associated with those obtained from X-ray diffraction and thermogravimetric tools, contribute to

E. C. da Silva Filho (✉)  
Química, Universidade Federal do Piauí, Bom Jesus,  
Piauí 64900-000, Brazil  
e-mail: edsonfilho@ufpi.edu.br

S. A. A. Santana  
Departamento de Química, UFMA, São Luiz,  
Maranhão 65080-540, Brazil

J. C. P. Melo · F. J. V. E. Oliveira · C. Airoidi  
Institute of Chemistry, University of Campinas, UNICAMP,  
P.O. Box 6154, Campinas, SP 13084-971, Brazil

rapidly clarify the chemical and structural changes of the newly synthesized compounds.

### Experimental

#### Materials

Microcrystalline cellulose (Merck), thionyl chloride (Chemika), *N,N'*-dimethylformamide (DMF) (Synth), ammonium hydroxide (Aldrich) and ethylene-1,2-diamine (en) (Aldrich) were all reagent grade and were used without prior purification. Activated cellulose and the corresponding chemically modified compounds were stored in flasks under dry nitrogen.

#### Synthesis of 6-chlorodeoxycellulose

A sample of 10 g of cellulose (Cel) previously activated at 353 K for 12 h was suspended in 200 cm<sup>3</sup> of DMF followed by the slow addition of 35 cm<sup>3</sup> of thionyl chloride (SOCl<sub>2</sub>) at 353 K, under mechanical stirring. After the addition, stirring was continued at the same temperature for another 4 h. The cooled suspension containing the cellulose chloride (CelCl) was washed with several portions of dilute ammonium hydroxide solution. The supernatant in each operation was eliminated with pH control to bring its value to neutral. To complete the washing the suspension was exhaustively treated with distilled water. Finally, the solid was then separated by filtration and dried under vacuum at room temperature [13].

#### Synthesis of 6-ethylenodiamino-deoxycellulose

A sample of 1.0 g of CelCl was reacted with 5.0 cm<sup>3</sup> of en under reflux and with mechanical stirring for 3 h [2, 13] with variation of the quantity of solvent (water or DMF), or without solvent, as shown in Fig. 1, followed by filtration using a sintered glass filter. The solid (Celen) was dried under vacuum at room temperature for 24 h.

#### Physical measurements

The amounts of en pendant chains anchored onto the cellulose surface were calculated based on percent nitrogen,

**Scheme 1** Reaction sequence to prepare CelCl and Celen

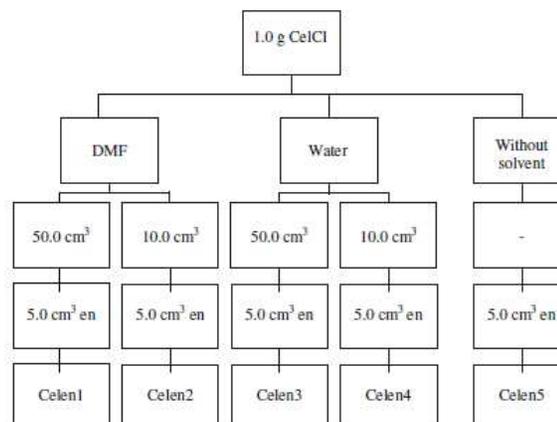
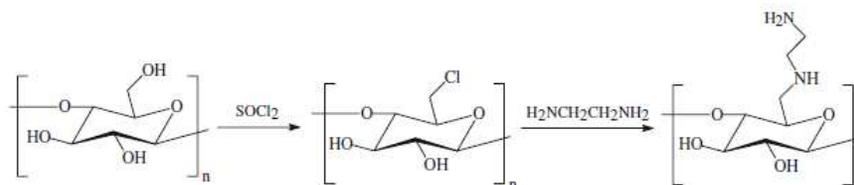


**Fig. 1** Variations in the preparation of the five aminated biopolymers

determined through elemental analysis with a Perkin Elmer, model 2400, elemental analyzer. XRD patterns were obtained on a Shimadzu XRD7000 diffractometer for powdered samples. The voltage applied was 40 kV, current of 30 mA, with a CuK $\alpha$  ( $\alpha = 0.154$  nm) radiation source scanned from 1.4 to 50°. The thermogravimetric curves for powdered samples were obtained on a Dupont TA 9900 instrument in an argon atmosphere of 1.67 cm<sup>3</sup> s<sup>-1</sup>, using a heating rate of 0.167 K s<sup>-1</sup>, from room temperature to 1,273 K, with an initial mass of approximately 10 mg of solid sample.

### Results and discussion

Elemental analysis, based on incorporated nitrogen, was used to determine the amount of en molecules chemically bonded to the cellulose backbone to give the aminated biopolymer, originating from the chlorodeoxycellulose precursor, as shown in Scheme 1 and the results are listed in Table 1. The chlorinated cellulose gave a high degree of substitution,  $0.99 \pm 0.01$ , of the hydroxyl groups preferentially on carbon 6 (C6) and this expected favorable process is due to its high reactivity compared to other positions. Thus, the following decreasing sequence in reactivity of the hydroxyls of the cellulose presents the order: C<sub>6</sub> >> C<sub>3</sub> > C<sub>2</sub>, due to the fact that C<sub>6</sub> bear a primary hydroxyl and the differences between C<sub>3</sub> and C<sub>2</sub>

**Table 1** Percent of nitrogen for CelenX ( $X = 1-5$ ) biopolymers, the degrees of substitution (DS) and incorporation (DI)

| CelenX | N (%)       | DS   | DI (mmol g <sup>-1</sup> ) |
|--------|-------------|------|----------------------------|
| 1      | 3.96 ± 0.01 | 0.28 | 1.41 ± 0.01                |
| 2      | 5.78 ± 0.06 | 0.42 | 2.06 ± 0.02                |
| 3      | 1.04 ± 0.02 | 0.07 | 0.37 ± 0.01                |
| 4      | 5.84 ± 0.06 | 0.42 | 2.08 ± 0.03                |
| 5      | 8.50 ± 0.03 | 0.61 | 3.03 ± 0.01                |

are mainly to their acidities [25]. The unequivocal biopolymer modification was previously confirmed through <sup>13</sup>C NMR, where the spectra clearly demonstrated the chemical shift from 65 to 44 ppm for carbon 6, without notable change for carbons 2 and 3 [2].

The most encouraging fact to support this reaction is the high value found for nitrogen percentage on Celen5, as listed in Table 1, where the incorporation was performed without adding solvents, as is desirable under Green Chemistry principles [26]. A sequence of attaching groups, whose decreasing values are in agreement with the amount and polarity of solvent used in these reactions, to give the following order: Celen5 > Celen4 > Celen2 > Celen1 > Celen3.

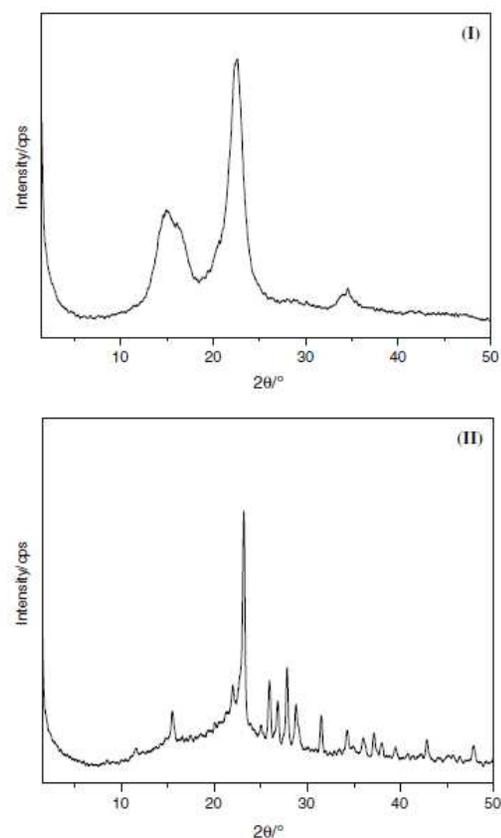
An important feature to compare in these syntheses is related to the same solvent, but the quantities employed varied. For example, for the biopolymers prepared using DMF, as less of this solvent was used, the amount of en molecule bonded to the surface increased. The same result can be observed when water was used as solvent. On the other hand, when the different solvents are compared for the same final volume, for example, 50 cm<sup>3</sup>, the synthesis was more effective in DMF than in water, as reflected the amount of incorporated groups. However, when 10 cm<sup>3</sup> was used the more favorable solvent was water, although the nitrogen quantities were close.

For the solvent-free process of incorporation, an increase of 31% was detected when compared to Celen4, which corresponded to the highest value when solvent was employed. In addition to the great increment on incorporation, an important advantage is the absence of solvent for preparing new functional polymers, a procedure that brings many environmental benefits, including reduction in costs and easier process control [27]. For Celen5 the data demonstrate that the solvent-free procedure gave larger amounts of pendant amino groups.

Cellulose and its various derivatives were among a series of polymers for which phase transitions in the solid and semisolid state were first studied. For instance, when compared with other biopolymers, cellulose shows a distinct tendency for crystallization, probably caused by the relative stiffness of the glucosidic chains and the hydrogen-bonding capacity of the hydroxyl groups. The shape of the

rings and the spatial distribution of the hydroxyl groups appear to favor the formation of ribbon-shaped laterally ordered sheets, which exhibit a three-fold anisotropy as far as bonding strength is concerned [17, 28–30].

Perpendicular to the polymeric chains, in the plane of the anhydroglucose rings, representing the a-axis direction of the lattice, the hydrogen bonds between the hydroxyl groups and the ring oxygen atoms are responsible for this interaction. Finally, perpendicular to the chains and to the plane of the anhydroglucose rings and parallel to the c-axis of the lattice, the only existing attraction is due to van der Waals interactions between the anhydroglucose rings and their constituents. This system of bonding can be considered as a reasonable starting point for the explanation of the crystallization tendency of cellulose. It leads to the existence of elongated thin sheets with high lateral order, which can explain in a satisfactory way the observed macroscopic mechanical and flow properties of cellulose fibers and films in the dry and swollen state [17, 28–30]. To explore such biopolymer properties, the X-ray diffraction patterns are shown in Fig. 2 (I).


**Fig. 2** X-ray diffraction patterns for microcrystalline cellulose (I) and chlorodeoxycellulose (II)

The X-ray diffraction patterns of chlorinated cellulose, shown in Fig. 2 (II), indicate that the corresponding degree of crystallinity is smaller and differs from that found for the precursor cellulose, which has the original microcrystalline properties. The new assembly is now formed through bonded chlorine atoms and remaining hydroxyl groups, where depolymerization processes can occur due to the effect of a hydrochloric acid reaction. Similar behavior was also observed for other biopolymers where mainly hydrogen bonding occurs with available hydroxyl groups [17, 28–30]. Thus, when cellulose is chlorinated the hydrogen bonding should be partially disrupted, to favor the entrance of chlorine atoms concomitantly with the leaving of the hydroxyl group, yielding a new network with distinct features. From the integration of the main peak, between 20 to 30°, the values demonstrate a decrease of 70% in crystallinity for the chlorinated biopolymer, which can be very interesting mainly when other modifications are intended, such as anchoring an ethylene-1,2-diamine molecule.

The oxidative chlorination process on cellulose consists in substituting the hydroxyl group by a chlorine atom in the original biopolymer structure. The chemical modification occurs initially in the less ordered polymeric regions related to the para-crystalline or amorphous regions. The hydroxyl groups of cellulose bear two electron lone pairs and one bonded hydrogen. On the other hand, chlorine atoms covalently bonded to the biopolymer can potentially make available three free pairs of electrons to be shared through the formation of hydrogen bonds. Therefore, as chlorine atoms, in the progress of the reaction, substitute the hydroxyl groups, other hydrogen bonds can be formed with different characteristics from the earlier ones, being established between the chlorine atoms and hydrogen from unreacted hydroxyl groups, by causing new chemical structural arrangements of the modified biopolymer. These characteristics change the crystallinity due to the new chain arrangement [17, 28–30].

The cellulose structure reacting with thionyl chloride to obtain Cel-Cl sample is shown in Scheme 1. According to earlier publication, IR spectra confirm substitution of hydroxyl groups from the original cellulose by the chlorine species [2]. The typical bands assigned at 709 and 752  $\text{cm}^{-1}$  correspond to the stretching vibration of the C–Cl bond, from the branched part of the original polymer. The displacement and decreasing size of the band originally observed in the cellulose at 894  $\text{cm}^{-1}$ , is now shifted to 865  $\text{cm}^{-1}$  in the CelCl compound and has disappeared in Celen. This fact corroborates with the chemical substitution of the OH groups by chlorine atoms in this proposed reaction. The appearance of a new band at 2,844  $\text{cm}^{-1}$  is assigned to C–H stretching of the symmetric  $\text{CH}_2$  group, due to ethylene-1,2-diamine molecule immobilization. The displacement of the band at 1,632  $\text{cm}^{-1}$  that corresponds to

the deformation of OH groups and also the angular deformation for the N–H amine band at 1,659  $\text{cm}^{-1}$  are unequivocal facts that confirm the ethylene-1,2-diamine immobilization on the cellulosic matrix [2].

Microcrystalline cellulose, named type I cellulose, is normally found with a degree of crystallinity between 40 to 60%. Some heterogeneous reactions are able to modify only the surface of the polymer and sometimes can also modify the internal layers, as well as having a high probability of reacting in the amorphous regions. Here, the X-ray diffraction patterns show the appearance of new peaks, in addition to those associated with the original solid, demonstrating a different crystalline structure, even though present at low intensity. The decrease in intensity of the peaks suggests that only small crystallites are present due to the hydrogen bonding involving chlorine atoms. This behavior decreases the space between the chains, resulting in the displacement of the peaks to give higher  $\theta$  values. Again the confinement of bonded chlorine atoms allows them to form hydrogen bonds that could be differentiated from those found on the surface of the material [17, 28–30].

The crystalline regions found in the bulk material were formed as a consequence of the intensity of the intermolecular interactions and result in an ordered lattice dominated by the lower availability of hydroxyl groups. To the contrary, the amorphous region presented weak interactions, causing a low ordered lattice while the hydroxyl groups have increased abilities to access chemicals. This fact was demonstrated through  $^{13}\text{C}$  NMR with clear indications that the consumption of the amorphous part of cellulose is followed by the disappearance of C(4) and C(6) signals of the chloride cellulose [2]. These concomitant processes address the increase crystallinity of cellulose-chloride part in comparison to the unmodified cellulose.

For cellulose with amino pendant groups, as shown in Fig. 3, a drastic decrease in crystallinity is observed in

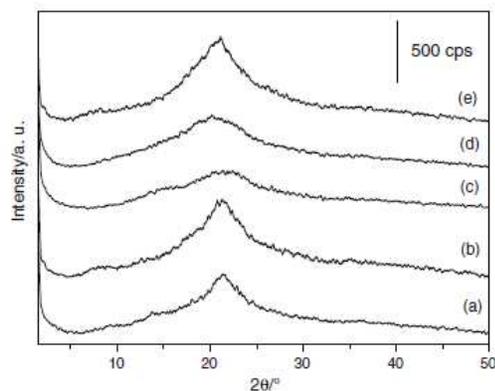


Fig. 3 X-ray diffraction patterns for CelenX: 1 (a), 2 (b), 3 (c), 4 (d) and 5 (e)

comparison with the original and the chlorine-containing celluloses. These data suggest that the aminated biomaterial resulted in an amorphous structure. This result is independent on the synthetic route and the amount of amine groups attached to the pendant chains [31, 32]. However, in the newly obtained biopolymers using water as solvent, the amorphous characteristics were intensified, as observed in Fig. 3c and d. This change occurs due to the substitution of a chlorine atom by ethylene-1,2-diamine, it means that this molecule is capable to increase the effectiveness of the hydrogen bonds. Taking into account the decrease in the crystallization process, the data are in agreement that the bonded en molecules do not establish an ordered assembly, resulting in these amorphous aminated biopolymers.

A careful investigation of the thermal decomposition of the modified materials was performed using thermogravimetry. The curves of pure cellulose, chloride-cellulose and cellulose modified with en, using DMF and water as solvents, as well as that prepared without any solvent, are shown in Figs. 4, 5, 6.

For pure cellulose only one mass loss between 563 and 647 K was observed, composing 92% of the thermal decomposition. These curves are shown in Fig. 4 (I). For

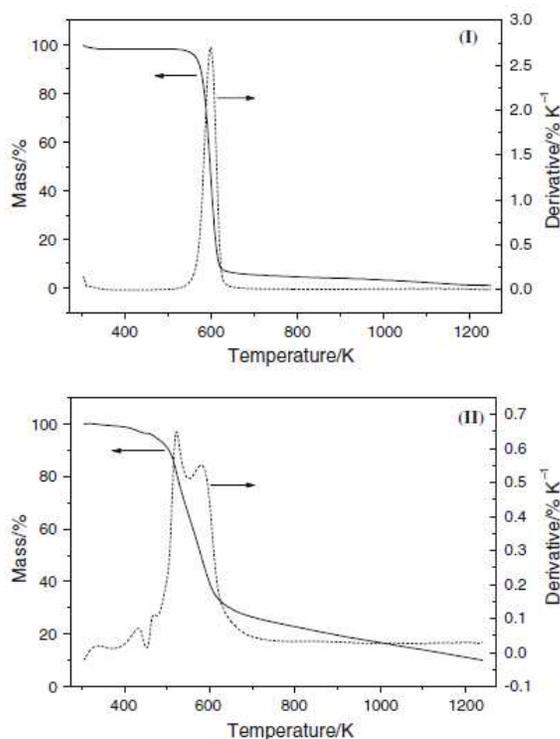


Fig. 4 Thermogravimetric and differential curves for pristine cellulose (I) and chlorodeoxycellulose (II)

CelCl the curve shows three mass losses corresponding to: (i) loss of water adsorbed on the surface in the 386–430 K interval, (ii) mass losses attributed to loss of hydrochloric acid and to condensation of hydroxyl groups present on carbons 2 and 3 in the 430 to 534 K range, and (iii) the decomposition of the organic framework above 521 K. The curves for CelCl are shown in Fig. 4 (II) and the corresponding mass losses are listed in Table 2. Based on these results, it could be supposed that CelCl presented higher mass loss due to formation of hydrochloric acid that catalyzes bulk oxidation.

The ethylene-1,2-diamine incorporated biopolymers also presented three mass losses that were attributed to loss of water and possibly carbon dioxide, pendant group decomposition plus condensation of hydroxyl groups and, finally, thermal decomposition of the organic support.

The thermogravimetric curves for en modified celluloses synthesized using DMF as solvent and also for that obtained without solvent are shown in Fig. 5 (I), presenting the same order of final mass loss as previously detected, given as: Celen1 > Celen2 > Celen5. The curves for cellulose chemically modified using water as solvent are shown in Fig. 6 (I), where the behavior

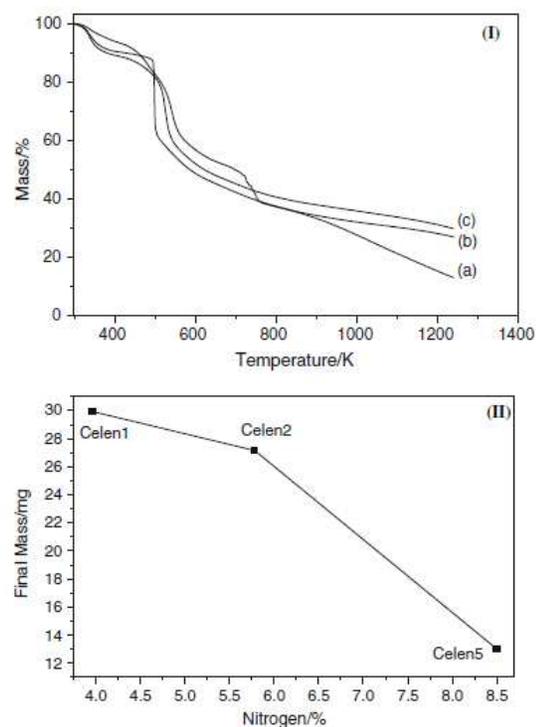
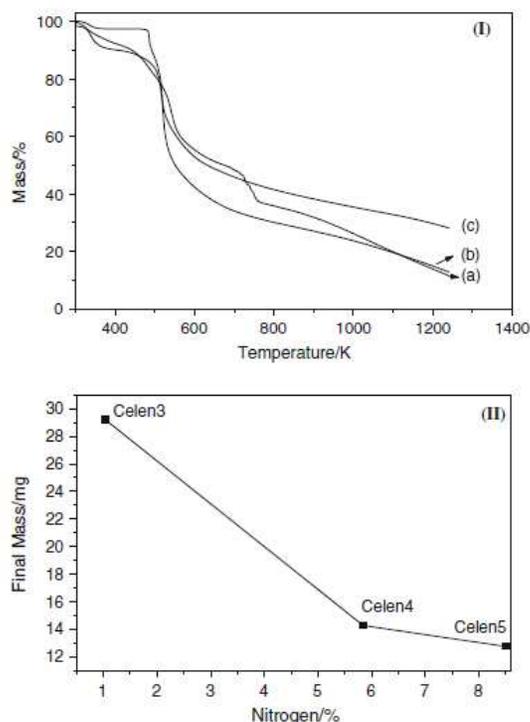


Fig. 5 Thermogravimetric curves for Celen5 (a), Celen2 (b) and Celen1 (c) biopolymers (I) and residue of mass loss from thermogravimetric data as a function of the percentage of nitrogen for Celen5, Celen2 and Celen1 biopolymers (II)



**Fig. 6** Thermogravimetric curves for Celen5 (a), Celen4 (b) and Celen3 (c) biopolymers (I) and residue of mass loss from thermogravimetric data as a function of the percentage of nitrogen for Celen5, Celen4 and Celen3 biopolymers (II)

**Table 2** Variation in temperature ( $\Delta T$ ), percent of mass losses for each step of decomposition ( $\Delta m$ ) and residue ( $\Delta m_r$ ) for biopolymers (Biop) Cel, CelCl and CelenX (X = 1–5)

| Biop   | $\Delta T$ (K) | $\Delta m$ (%) | $\Delta m_r$ (%) |
|--------|----------------|----------------|------------------|
| Cel    | 298–343        | 2              | 1                |
|        | 523–647        | 92             |                  |
|        | 647–1273       | 5              |                  |
| CelCl  | 298–430        | 3              | 10               |
|        | 430–534        | 23             |                  |
|        | 534–1273       | 64             |                  |
| Celen1 | 298–452        | 13             | 30               |
|        | 452–1273       | 57             |                  |
| Celen2 | 298–497        | 13             | 27               |
|        | 497–1273       | 60             |                  |
| Celen3 | 298–481        | 13             | 28               |
|        | 481–1273       | 59             |                  |
| Celen4 | 298–481        | 2              | 14               |
|        | 481–1273       | 84             |                  |
| Celen5 | 298–450        | 10             | 13               |
|        | 450–1273       | 77             |                  |

observed was: Celen3 > Celen4 > Celen5. From this relationship an inverse behavior was obtained for all biopolymers, when the residues were at 1273 K were considered, as shown in Fig. 5 (II). For these an analogous graphical representation is obtained by relating the final residue as a function of the nitrogen percentage, as shown in Fig. 6 (II). As observed, the final mass of the chemically modified cellulose is equivalent to the amount of en immobilized.

A higher thermal stability is clearly observed when compared with the unmodified cellulose and chloride modified biomaterials, to give the thermal stability order as follows: Celen > CelCl > Cel, suggesting that biopolymers with fewer incorporated en groups gave higher thermal stability [3, 31, 33, 34].

A summary of thermogravimetric results is presented in Table 2, indicating all decomposition processes, comparing the precursors and chemically modified biopolymers in all steps involved. As expected, the amount of residue after final decomposition depends on the amount immobilized. For the Celen1-5 biopolymers the second interval presented in Table 2 corresponds to two events of different decompositions, as previously described.

### Conclusions

The results from this investigation are a relevant advance for this branch of materials science, due to the fact that elemental analysis associated with X-ray diffraction and thermogravimetric tools were successfully applied to characterize cellulose chemically modified with ethylene-1,2-diamine, taking into account that the new compounds were synthesized in available polar solvents and in a special methodology without solvent. The highest amine group incorporations were synthesized through the solvent-free condition, which is a very convenient method of great interest for reducing the generation of toxic wastes and also making the process less expensive.

X-ray diffraction is a useful technique to follow the change in cellulose crystallinity as the sequence of reactions progressed. Thus, a decrease in crystallinity occurred after chlorination, probably due to glucosidic chains and the hydrogen-bonding capacity of the hydroxyl groups, which was further reduced in the next step when ethylene-1,2-diamine was incorporated onto the biopolymer backbone.

The thermogravimetric data of the chemically modified biopolymers indicated smaller total decompositions than the respective cellulose and cellulose chloride precursors. Based on the incorporation results, lesser amounts of ethylene-1,2-diamine attached to the precursor lead to higher total decompositions. For all systems, the final mass was inversely proportional to the amount of the en molecule incorporated.

**Acknowledgements** The authors are indebted to FAPESP (ECSF, JCPM, FJVEO) and CNPq (CA) for fellowships and for financial supports.

## References

- Airoldi C. The weighty potentiality of nitrogenated basic centers in inorganic polymers and biopolymers for cation removal. *Quim Nova*. 2008;31:144–53.
- da Silva Filho EC, de Melo JCP, Airoldi C. Preparation of ethylenediamine-anchored cellulose and determination of thermochemical data for the interaction between cations and basic centers at the solid/liquid interface. *Carbohydr Res*. 2006;341:2842–50.
- de Melo JC, da Silva, Santana SA, Airoldi, C. Maleic anhydride incorporated onto cellulose and thermodynamics of cation-exchange process at the solid/liquid interface. *Colloids Surf A*. 2009.
- Lopes ECN, Sousa KS, Airoldi C. Chitosan-cyanuric chloride intermediary as a source to incorporate molecules—thermodynamic data of copper/biopolymer interactions. *Thermochim Acta*. 2009;483:21–8.
- Sousa KS, Silva Filho EC, Airoldi C. Ethylenesulfide as a useful agente of incorporation into the biopolymer chitosan in a solvent-free reaction for use in cation removal. *Carbohydr Res*. 2009. doi: 10.1016/j.carres.2009.05.028.
- Arakaki LNH, Alves APM, da Silva Filho EC, Fonseca MG, Oliveira SF, Espínola JGP, Airoldi C. Sequestration of Cu(II), Ni(II), and Co(II) by ethyleneimine immobilized on silica. *Thermochim Acta*. 2007;453:72–4.
- Sales JAA, Petrucelli GC, Oliveira FJVE, Airoldi C. Some features associated with organosilane groups grafted by the sol-gel process onto synthetic talc-like phyllosilicate. *J Colloid Interface Sci*. 2006;297:95–103.
- Sales JAA, Airoldi C. Calorimetric investigation of metal ion adsorption on 3-glycidioxypropyltrimethylsiloxane + propane-1,3-diamine immobilized on silica gel. *Thermochim Acta*. 2005;427:77–83.
- da Fonseca MG, da Silva Filho EC, Machado Júnior RSA, Arakaki LNH, Espínola JGP, Airoldi C. Zinc phyllosilicates containing amino pendant groups. *J Solid State Chem*. 2004;177:2316–22.
- da Fonseca MG, Airoldi C. Mercaptopropyl magnesium phyllosilicate—thermodynamic data on the interaction with divalent cations in aqueous solution. *Thermochim Acta*. 2001;359:1–9.
- Sales JAA, Petrucelli GC, Oliveira FJVE, Airoldi C. Mesoporous silica originating from a gaseous ammonia epoxide ring opening and the thermodynamic data on some divalent cation adsorptions. *J Colloid Interface Sci*. 2006;297:426–33.
- da Silva OG, da Fonseca MG, Arakaki LNH. Silylated calcium phosphate and their new behavior for copper retention from aqueous solution. *Colloids Surf A*. 2007;301:376–81.
- da Silva OG, da Silva Filho EC, da Fonseca MG, Arakaki LNH, Airoldi C. Hydroxyapatite organofunctionalized with silylating agents to heavy cation removal. *J Colloid Interface Sci*. 2006;302:485–91.
- da Fonseca MG, da Silva Filho EC, Machado Júnior RSA, Arakaki LNH, Espínola JGP, Oliveira SF, et al. Anchored fibrous chrysotile silica and its ability in using nitrogen basic centers on cation complexing from aqueous solution. *Colloids Surf A*. 2003;227:85–91.
- da Fonseca MG, Almeida RKS, Arakaki LNH, Espínola JGP, Airoldi C. Vermiculite as a useful host for guest cyclic aliphatic amine intercalation, followed by cation adsorption. *Colloids Surf A*. 2006;280:39–44.
- Morais CC, da Silva Filho EC, da Silva OG, da Fonseca MG, Arakaki LNH, Espínola JGP. Thermal characterization of modified phyllosilicates with aromatic heterocyclic amines. *J Thermal Anal Calorim*. 2007;87:767–70
- Klemm D, Heublein D, Fink HP, Bohn A. Cellulose: fascinating biopolymer and sustainable raw material. *Angew Chem Int Ed*. 2005;44:3358–93.
- Jal PK, Patel S, Mishra BK. Chemical modification of silica surface by immobilization of functional groups for extractive concentration of metal ions. *Talanta*. 2004;62:1005–28.
- Arakaki LNH, da Fonseca MG, da Silva Filho EC, Alves APM, de Sousa KS, Silva ALP. Extraction of Pb(II), Cd(II), and Hg(II) from aqueous solution by nitrogen and functionality grafted to silica gel measured by calorimetry. *Thermochim Acta*. 2006;450:12–15.
- Tashiro T, Shimura Y. Removal of mercuric ions by systems based on cellulose derivatives. *J Appl Polym Sci*. 1982;27:747–56.
- Silva CR, Airoldi C, Collins KE, Collins CH. Influence of the TiO<sub>2</sub> content on the chromatographic performance and high pH stability of C<sub>18</sub> titanized phases. *J Chrom A*. 2006;1114:45–52.
- Valkenberg HM, Hölderich WF. Preparation and use of hybrid organic-inorganic catalysts. *Catal Rev*. 2002;44:321–74.
- Prado AGS, Airoldi C. Adsorption, preconcentration and separation of cations on silica gel chemically modified with the herbicide 2,4-dichlorophenoxyacetic acid. *Anal Chim Acta*. 2001;432:201–11.
- Pehlivan E, Altun T. The study of various parameters affecting the ion exchange of Cu<sup>2+</sup>, Zn<sup>2+</sup>, Ni<sup>2+</sup>, Cd<sup>2+</sup>, and Pb<sup>2+</sup> from aqueous solution on Drowex 50W synthetic resin. *J Hazard Mater*. 2006;134:149–56.
- Martin AI, Sanchez-Chaves M, Arranz F. Synthesis, characterization and controlled release behaviour of adducts from chloroacetylated cellulose and  $\alpha$ -naphthylacetic acid. *React Funct Polym*. 1999;39:179–87.
- Warner JC, Cannon AS, Dye KM. Green chemistry. *Env Imp Ass Rev*. 2004;24:775–99.
- Tanaka K, Toda F. Solvent-free organic synthesis. *Chem Rev*. 2000;100:1025–74.
- Ott E, Spurlin HM, Grafflin MW. Cellulose and cellulose derivatives. New York: Interscience Publishers; 1954.
- Zugenmaier P. Conformation and packing of various crystalline cellulose fibers. *Prog Polym Sci*. 2001;26:1341–417.
- O'Sullivan AC. Cellulose: the structure slowly unravels. *Cellulose*. 1997;4:173–207.
- Kim UJ, Kuga S. Thermal decomposition of dialdehyde cellulose and its nitrogen-containing derivatives. *Thermochim Acta*. 2001;369:79–85.
- Cunha AP, Freire CRS, Silvestre AJD, Pascoal Neto C, Gandini A, Orblin E, et al. Characterization and evaluation of the hydrolytic stability of trifluoroacetylated cellulose fibers. *J Colloid Interface Sci*. 2007;316:360–6.
- Liu CF, Sun RC, Zhang AP, Ren JL, Geng ZC. *Polym Degrad Stab*. 2006;91:3040–7.
- Yin C, Li J, Xu Q, Peng Q, Liu Y, Shen X. Chemical modification of cotton cellulose in supercritical carbon dioxide: synthesis and characterization of cellulose carbamate. *Carbohydr Polym*. 2007;67:147–54.



Contents lists available at ScienceDirect

Chemical Engineering Journal

journal homepage: [www.elsevier.com/locate/cej](http://www.elsevier.com/locate/cej)Chemical  
Engineering  
Journal

## Copper sorption from aqueous solutions and sugar cane spirits by chemically modified babassu coconut (*Orbignya speciosa*) mesocarp

Adriana P. Vieira<sup>a</sup>, Sirlane A.A. Santana<sup>a,\*</sup>, Cícero W.B. Bezerra<sup>a</sup>, Hildo A.S. Silva<sup>a</sup>, Júlio C.P. de Melo<sup>b</sup>, Edson C. da Silva Filho<sup>c</sup>, Claudio Airoidi<sup>b</sup>

<sup>a</sup> Departamento de Química/CCET, Universidade Federal do Maranhão, Avenida dos Portugueses S/N, Campus do Bacanga, 65080-540 São Luís, MA, Brazil

<sup>b</sup> Institute of Chemistry, University of Campinas, P.O. Box 6154, 13084-971 Campinas, SP, Brazil

<sup>c</sup> Química, Universidade Federal do Piauí, 64900-000 Bom Jesus, Piauí, Brazil

### ARTICLE INFO

#### Article history:

Received 12 March 2010

Received in revised form 16 April 2010

Accepted 19 April 2010

#### Keywords:

Sorption

Babassu coconut mesocarp

Chemical modification

Heavy metal

Kinetic

Isotherm

### ABSTRACT

The present investigation explores the chemical modification of natural dry babassu coconut (*Orbignya speciosa*) mesocarp (BM), using a quasi solvent-free procedure in which the precursor was added to molten succinic (S), maleic (M) or phthalic (P) anhydrides, to give new products named BMS, BMM and BMP (babassu coconut mesocarp modified with succinic, maleic and phthalic anhydride, respectively). These synthesized biopolymers were characterized by infrared spectroscopy and thermogravimetry and the degree of substitution was calculated, based on the number of carboxylic groups covalently attached to the lignocellulosic polymer. The chemically modified biopolymers suspended in aqueous or hydroalcoholic solutions have the ability to remove copper from aqueous or aqueous-alcohol solutions in the order BMS > BMP > BMM. The kinetic process followed a pseudo-second-order model and the results for sorbents were better represented by the Langmuir sorption model. The effectiveness of these biopolymers for application to real samples of sugar cane spirits reflected in using only 1.0 g dm<sup>-3</sup> to reduce the copper to a value lower than 5.0 mg dm<sup>-3</sup> for all sorbents. Thus, these inexpensive chemically modified biopolymers may be useful to permit sugar cane spirits to meet the requirements of Brazilian legislation with respect to copper contamination.

© 2010 Elsevier B.V. All rights reserved.

### 1. Introduction

Annually, agricultural residues, such as the class of lignocellulosic biomass, represent an abundant, inexpensive, and readily available source of sorbents. The potential uses attract increasing interest all over the world, particularly, for production of environmentally friendly, novel materials, mainly when industrially extractable by-products can be chemically modified [1,2]. For example, bagasse-based ion sorbents were prepared by chemically modifying the original materials with acrylonitrile and hydroxylamine, with the aim of enhancing the ability of heavy metal ion removal from wastewater [3].

Raw native wheat, soybean straw, corn stalk and corn cobs were studied to determine their efficiency in removing different heavy metal ions from contaminated samples. In attempting to increase their sorption capacities, efforts were directed to a variety of ways to chemically modify the original material and the effects of these treatments were evaluated in copper removal assays [4].

A great variety of reagents are able to react with lignocellulosic components, due to their high reactivity towards the available hydroxyl groups on the polymeric polysaccharide surfaces. For example, the chemical modification of sugar cane bagasse cellulose components with succinic anhydride in ionic liquids as the reaction medium was successfully accomplished with the carboxylic groups being covalently attached to the main polymeric structure [5]. Another aspect related to such chemical modification consists in the phthalation process under the same experimental condition, but in absence of any catalyst [6]. On the other hand, the ultrasound technique has improved the maleation of the free hydroxyl groups present in sugar cane bagasse, when the respective anhydride was used in pyridine as solvent [7].

Other important features associated with chemical modification are those related to lignocellulose esterification with dicarboxylic acid anhydrides, to yield synthesized material with improved abilities to trap heavy metals from aqueous solutions [8–10]. In addition, sugar cane bagasse was modified by mercerizing with aqueous sodium hydroxide solution, followed by reaction with succinic anhydride and the resulting materials were successfully applied for divalent copper, cadmium and lead sorptions [11,12].

\* Corresponding author. Tel.: +55 98 33019233; fax: +55 98 33018245.

E-mail addresses: [sirlane@ufma.br](mailto:sirlane@ufma.br), [sirlaneufma@hotmail.com](mailto:sirlaneufma@hotmail.com) (S.A.A. Santana).

As a general procedure, the use of low-cost sorbents has been intensively investigated as sources of replacement materials for current costly methods of metal removal. Thus, this procedure was applied for copper with different natural sorbents such as lentil pods, wheat and rice husks. The sorption equilibrium level was determined as a function of the solution pH, temperature, contact time, initial sorbate concentration and sorbent quantity [13].

Babassu coconut mesocarp, an abundant agricultural lignocellulosic by-product, is a fibrous residue left after crushing and extracting the nuts. It is a non-toxic, renewable and modifiable material with wide potential as an excellent industrial material, as recently demonstrated by its high capacity for textile dye sorption from aqueous solutions [14]. From the structural point of view, its hydroxyl and phenolic chemical functions can be converted to carboxylic groups by using succinic, phthalic or maleic anhydrides. The great advantage in introducing some functional groups on these biopolymer structures is related to the increase in cation sorption capacity, which contrasts to the very low capacity before modification. A clear recent illustration is the chemical modification that was carried out by attachment of ethylenesulfide onto the surface; the final biopolymer demonstrated affinity to sorb copper from aqueous solution [15].

As far as the authors are aware, lignocellulosic esterification in the absence of both solvent and catalyst has not been reported. Thus, the present investigation deals with babassu coconut mesocarp chemically modified with succinic, phthalic or maleic anhydrides, which resulted in materials that were applied for copper sorption from aqueous and hydroalcoholic solutions. This last composition resembles sugar cane spirits that, in many cases, are distilled using pot stills made of copper, so that the distillate is contaminated with this metal [16,17]. The level of this undesirable metal is restricted to less than  $5.0 \text{ mg dm}^{-3}$  by Brazilian law and even lower amounts at the  $2.0 \text{ mg dm}^{-3}$  level, are permitted in distillates by northern hemisphere countries [18]. Based on these legal requirements, development of new inexpensive materials that can be useful for removing undesirable species from the environment is an important objective, as is proposed herein.

## 2. Methods

### 2.1. Materials and reagents

The mesocarp from raw babassu coconut and commercial sugar cane spirits were obtained in the city of São Luís, Maranhão state, in the northeast region of Brazil. The raw material was crushed to give particle sizes in the  $0.088\text{--}0.177 \text{ mm}$  range. N,N-dimethylacetamide (DMA) and the succinic, phthalic and maleic anhydrides were all of analytical grade.

### 2.2. Synthesis of derivatives

The lignocellulose derivatives containing free carboxylic groups were prepared by reaction of babassu coconut mesocarp (BM) with succinic, phthalic or maleic anhydrides in the absence of solvent [19]. This procedure consists in heating the dry mesocarp with an amount of each anhydride in an oil bath at the anhydride fusion temperature. In each case, the anhydride/mesocarp ratio was maintained in the 10:1 ratio, the mixture was stirred for 20 min and the reaction was stopped by addition of DMA. The solid was separated by filtration with a sintered filter, washed in sequence with acetone and distilled water to remove the unreacted anhydride, DMA and by products and dried at  $353 \text{ K}$  for 12 h. This resulted in the chemically modified biopolymers BMS, BMP and BMM after reaction with succinic, phthalic or maleic anhydrides, respectively. The complete scheme of the reactions is shown in Fig. 1.

### 2.3. Degree of substitution

The degree of substitution of the chemically modified biopolymers was determined by measuring the amount of carboxylic functions attached on the surface through retro-titration. For this purpose,  $0.1000 \text{ g}$  of each material was treated with  $100.0 \text{ cm}^3$  of  $400.0 \text{ mg dm}^{-3}$  sodium hydroxide solution for 1 h under constant magnetic stirring. The solid was separated by filtration and three aliquots of  $20.0 \text{ cm}^3$  of each solution obtained were titrated with  $365.0 \text{ mg dm}^{-3}$  aqueous hydrochloric acid [11]. The concentration of the carboxylic function was calculated by Eq. (1):

$$C_{\text{COOH}} = \frac{(C_{\text{NaOH}} \times V_{\text{NaOH}}) - (5 \times C_{\text{HCl}} \times V_{\text{HCl}})}{m_{\text{mat}}} \quad (1)$$

where  $C_{\text{NaOH}}$  and  $C_{\text{HCl}}$  are the concentrations of hydroxide and acid ( $\text{mg dm}^{-3}$ ),  $V_{\text{NaOH}}$  and  $V_{\text{HCl}}$  are the volumes of initial hydroxide and hydrochloric acid ( $\text{dm}^3$ ) used in the titration of the excess of non-reacted base and  $m_{\text{mat}}$  (g) is the mass of the final chemically modified material.

### 2.4. Measurements

Infrared spectra were obtained by accumulating 32 scans in the  $4000\text{--}400 \text{ cm}^{-1}$  range on a MB-Bomem FTIR spectrophotometer using KBr pellets with a resolution of  $4 \text{ cm}^{-1}$ . Thermogravimetric curves (TG) were carried out with a Shimadzu TGA-50 instrument under a nitrogen flow rate of  $0.50 \text{ cm}^3 \text{ s}^{-1}$ , in the temperature interval from  $298$  to  $1000 \text{ K}$ , with a heating rate of  $0.167 \text{ K s}^{-1}$  for a sample mass of about  $10 \text{ mg}$ . The experiments of the visible spectrophotometry were carried with VARIAN-AA 50 instrument.

### 2.5. Point of zero charge

The point of zero charge of the synthesized biopolymers was determined by the solid addition method [20]. To a series of  $100.0 \text{ cm}^3$  conical flasks were transferred  $50.0 \text{ cm}^3$  of solution with pH varying from 1 to 12 and the  $\text{pH}_0$  values of each solution were adjusted by adding either  $0.10 \text{ mol dm}^{-3}$  of hydrochloric acid or sodium hydroxide. The  $\text{pH}_0$  of the solutions was then accurately measured and  $0.1000 \text{ g}$  of one of the solids was added to each flask. The suspensions were then shaken for 24 h and the pH values of the supernatant were measured. The difference between the initial  $\text{pH}_0$  and final  $\text{pH}_f$  values, given by  $\text{pH} = \text{pH}_0 - \text{pH}_f$ , was plotted against  $\text{pH}_0$  and the point of intersection of the resulting null  $\Delta \text{pH}$  corresponds to the point of zero charge,  $\text{pH}_{\text{pzc}}$ .

### 2.6. Sorption studies

#### 2.6.1. Effect of pH

The precursor and the three chemically modified mesocarps were assayed. To determine the effect of pH on metal ion adsorption, an amount of  $0.1000 \text{ g}$  of each material was suspended in  $100.0 \text{ cm}^3$  of copper solution having an initial concentration of  $200 \text{ mg dm}^{-3}$  under constant stirring for 24 h. The pH range studied was from 1.0 to 6.0 and these values were adjusted with  $0.010\text{--}1.0 \text{ mol dm}^{-3}$  aqueous hydrochloric acid solutions. After filtration, the cation concentration in the supernatant was determined by EDTA titration [21].

#### 2.6.2. Kinetics

For this study  $0.1000 \text{ g}$  of each sorbent was mixed with  $100.0 \text{ cm}^3$  of aqueous or 40% hydroalcoholic solution having concentrations of  $200 \text{ mg dm}^{-3}$  under stirring for different times. For all experiments in the aqueous solution the pH was adjusted at 6.0, using hydrochloric acid/sodium hydroxide solutions. After fil-

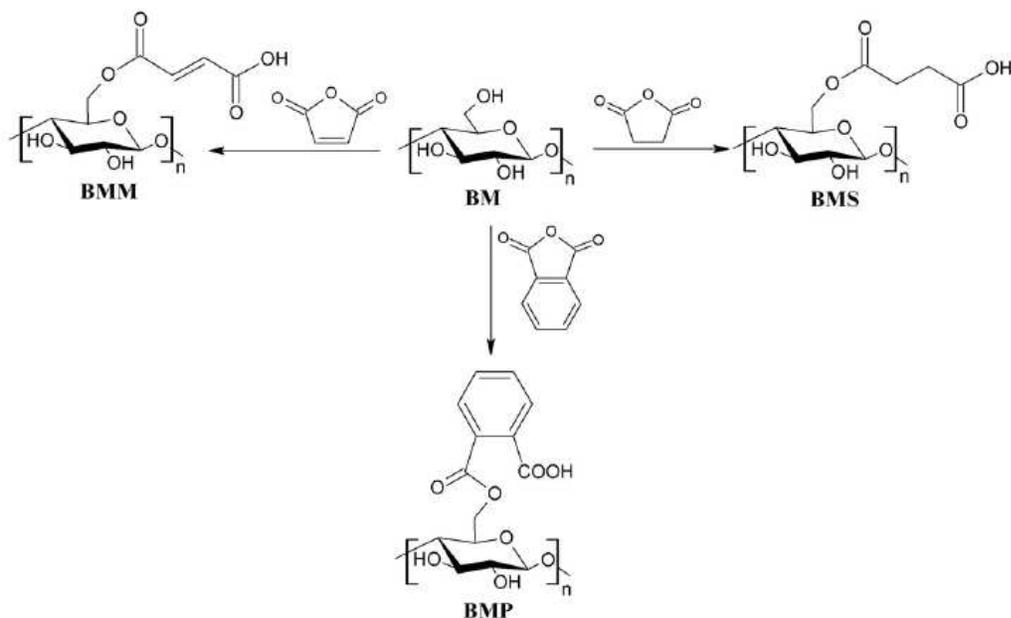


Fig. 1. A general scheme for synthesis of the biopolymers BMS, BMP and BMM.

tration, the cation concentration was determined as previously described [21].

### 2.6.3. Sorption

The batchwise sorption experiments used a series of flasks containing 0.1000 mg of each material suspended in 100.0 cm<sup>3</sup> of the aqueous or the 40% hydroalcoholic solutions having concentrations of copper cation that varied from 200 to 500 mg dm<sup>-3</sup> at 298 ± 1 K. The suspensions were shaken for 30 min at the pH established from the previous experiments to ensure maximum adsorption. At the end of this process, the solid was separated by filtration and the metal ion amount sorbed was determined by difference between the initial solution concentration and that found in the supernatant by titration [21].

### 2.6.4. Sorption from sugar cane spirit samples

Sugar cane spirit samples obtained from a local market were doped with copper to simulate high levels of this metal. For this operation, an aliquot of 8.0 cm<sup>3</sup> of copper solution (40% ethanol) was diluted to 1 L of sugar cane spirits, to result in a sugar cane spirit having a final metal concentration of 8.0 mg dm<sup>-3</sup>. The sorptions by 1.0–4.0 g of each chemically modified mesocarp BMS, BMP and BMM were assayed. For each biopolymer four independent determinations were performed, using 30 min of stirring. The concentration of copper remaining in the sugar cane sample was determined by a calibration curve in visible spectrophotometry. For each spectrophotometric determination 1.0 cm<sup>3</sup> of pyridine were added to aliquots of 9.0 cm<sup>3</sup> of the supernatant and the absorbance of the copper–pyridine complex formed was measured at a wavelength of 610 nm [16].

## 3. Results and discussion

### 3.1. Characterization

The amounts of carboxyl groups covalently attached to the synthesized biopolymers are shown in Table 1. A considerable increase

**Table 1**  
Degree of substitution of the biopolymers.

| Biopolymer | C <sub>COOH</sub> (mg g <sup>-1</sup> ) |
|------------|---|
| BM         | 36.19 ± 0.03                            |
| BMS        | 176.99 ± 0.10                           |
| BMP        | 149.27 ± 0.05                           |
| BMM        | 141.79 ± 0.05                           |

in carboxylic groups is detected when compared to the unmodified precursor, confirming the success of the proposed chemical modification.

The infrared spectra of the unmodified and all chemically modified mesocarps are shown in Fig. 2. The precursor biopolymer BM in Fig. 2a shows a broad and intense band in the 3000–3700 cm<sup>-1</sup>

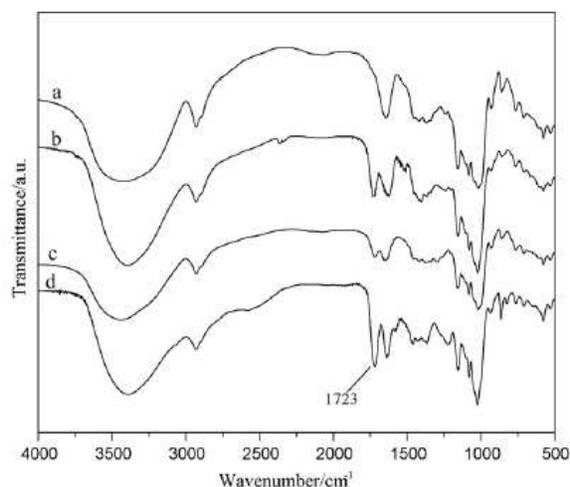


Fig. 2. Infrared spectra of the initial mesocarp BM (a), chemically modified biopolymers BMS (b), BMP (c) and BMM (d).

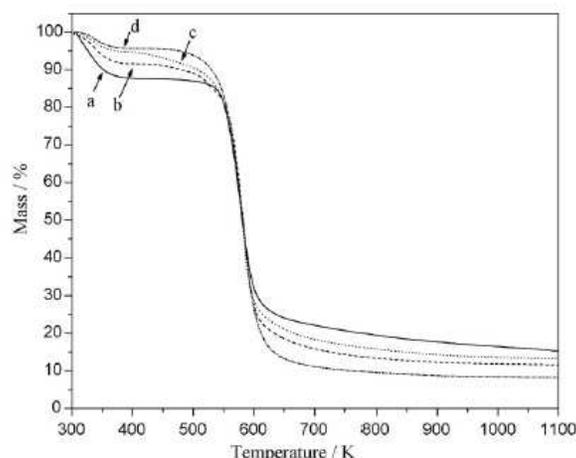


Fig. 3. Thermogravimetric curves for BM (a), BMS (b), BMP (c) and BMM (d).

range due to the presence of free and hydrogen bonded OH stretching vibrations. The hydroxyl groups bonded to the cellulosic structure correspond to the  $\delta(\text{O-H})$  band at  $1640\text{ cm}^{-1}$  and those between  $1200$  and  $1000\text{ cm}^{-1}$  are related to  $\nu(\text{C-O})$  [22]. The spectra of chemically modified biopolymers are very close to that of the precursor, however, the most remarkable differences are the strong band at  $1723\text{ cm}^{-1}$  assigned to the  $\text{C=O}$  stretching vibration [10]. The presence of  $\text{CH}_2$  and  $\text{CH}$  groups proceeding from the anhydrides added to the biopolymer backbone is shown by the stretching bands at  $2930$  and  $2890\text{ cm}^{-1}$ , respectively [14]. Based on the difference from the precursor and the sorptions related to the modified biopolymers, mainly the carbonyl stretching frequency, these results clearly confirm the attachment of the anhydride molecules onto the polymeric structure.

The thermogravimetric curves for all biopolymers are shown in Fig. 3, from which a very similar behavior in decomposition is observed, in agreement to other lignocellulosic materials [23]. The first step of decomposition can be attributed to the release of water physically sorbed on the surface. This stage corresponds to a mass loss of 16.0, 4.3, 8.2 and 5.3% up to 375 K, for the BM, BMS, BMP and BMM, respectively. The second stage corresponds to the decomposition of organic material, as expected for the breakdown of fibers to give the final residue, and occurs in the 477 to 623 K temperature range. The mass loss that corresponds to this interval of temperature for BM is 60%, while for BMS, BMP and BMM, these percentages are 89.3, 81.2, and 82.7%, respectively.

### 3.2. 3.2 pH effect and point of zero charge

The unmodified mesocarp BM demonstrated a null sorptive capacity in the presence of copper cations under the conditions studied. As previously observed, its  $\text{pH}_{\text{pzc}}$  is 6.7 and the sorption of positively charged species will be favored only at  $\text{pH} > \text{pH}_{\text{pzc}}$  [14]. However, it is expected that at pH higher than 6.7 species related to copper hydroxide can be formed, that will affect free cation sorption.

All anhydride-modified mesocarps presented an increase in the amount of copper sorbed with the increase of the pH of the solution with a maximum value at pH 6.0. The  $\text{pH}_{\text{pzc}}$  for these biopolymers are 5.6, 5.4 and 5.7 for BMS, BMP and BMM, respectively, as shown in Fig. 4. These values indicate that cation sorption is favored in solutions with pH higher than  $\text{pH}_{\text{pzc}}$  for each specific material. Under acidic conditions, the chemically modified biopolymers can be protonated, due to the higher concentrations of protons

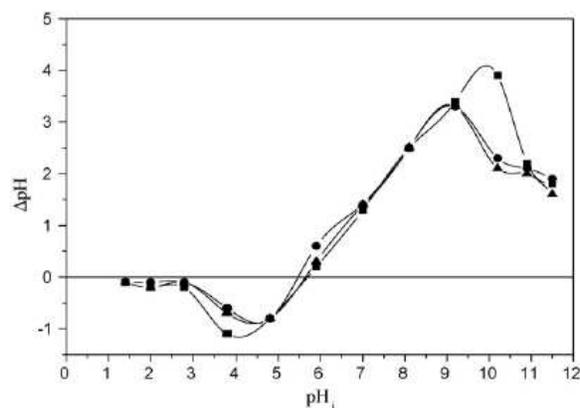


Fig. 4. Point of zero charge for BMS (■), BMP (●) and BMM (▲).

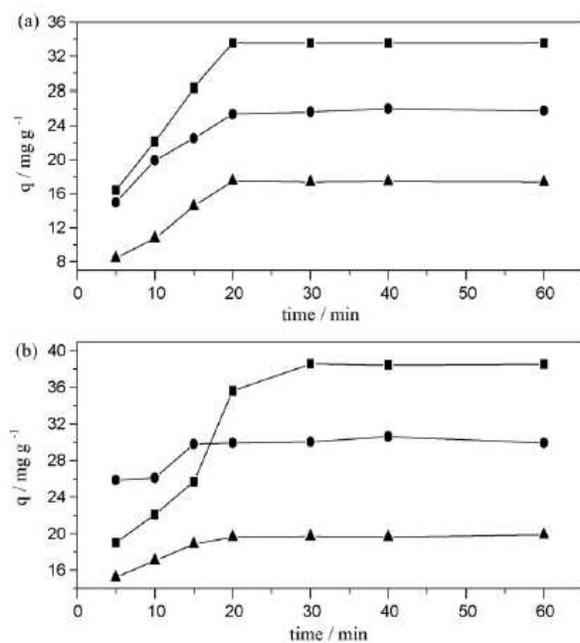


Fig. 5. Kinetics of copper sorption for BMS (■), BMP (●) and BMM (▲) in water (a) and hydroalcoholic (b) solution, both at pH 6.0 and at  $298 \pm 1\text{ K}$ .

and the amount of cations sorbed decreases. On the other hand, the increase in pH deprotonates carboxylate groups, a condition that favors their chelating abilities and, consequently, the amount of sorbed  $\text{Cu}^{2+}$  ions is increased. An identical behavior was previously observed for other systems, in which the attached function, derived from succinic anhydride, chelated bivalent and trivalent cations [10–12,24,25].

### 3.3. Kinetics of sorption

The complete curves of sorbed amount versus time for the three chemically modified mesocarp biopolymers at pH 6.0 are shown in Fig. 5, where the sorption process in aqueous solution is compared with that of hydroalcoholic solutions, as observed in Fig. 5a and b, respectively. From these isotherms it is clearly evidenced that the equilibrium in aqueous solution is reached after 20 min of contact between copper and the suspended solids. However, in

hydroalcoholic solution the amount adsorbed becomes constant after 30, 15 and 20 min for BMS, BMP and BMM, respectively. The results of the kinetic data were investigated by pseudo-first-order [20] and pseudo-second-order [26] models, as given by Eqs. (2) and (3), respectively. The initial rate of sorption,  $h$  ( $\text{mg g}^{-1} \text{min}^{-1}$ ), can be obtained from Eq. (4):

$$\log(q_e - q_t) = \log q_e - \frac{k_1 t}{2.303} \quad (2)$$

$$\frac{t}{q_t} = \frac{1}{k_2 q_e^2} + \frac{1}{q_e t} \quad (3)$$

$$h = k_2 q_e^2 \quad (4)$$

where  $q_e$  and  $q_t$  are the amounts of metal sorbed on sorbent ( $\text{mg g}^{-1}$ ) at equilibrium and at time  $t$  (min), respectively,  $k_1$  and  $k_2$  are the rate constants for first order ( $\text{min}^{-1}$ ) and for second-order ( $\text{g mg}^{-1} \text{min}^{-1}$ ) of such sorption processes.

The parameters obtained from these equations, based on the correlation coefficients for the best fit, are listed in Table 2. The sorption process described by the pseudo-second-order model is preferred. The correlation of this model for these systems corroborates with the studies when BM biopolymer was used as sorbent for textile dyes, demonstrating that all examined dyes showed better fit with the pseudo-second-order equation [14]. Other sorbents such as peat [27,28], chemically modified chitosan [29] and green coconut [30], that also present the ability to sorb copper, also showed a better adjustment to this model.

### 3.4. Sorption Isotherms

The data used to build the sorption isotherms compared two well-known models Langmuir and the Freundlich models. The first model assumes that the sorbate forms a monolayer on a surface containing a finite number of sites with uniform strategies for sorption, without transmigration of sorbate on the plane of surface, while the Freundlich model assumes an energetic and heterogeneous surface. Based on the results obtained from the Langmuir equation, the energetic term varies as a function of surface coverage, as the sorption is in progress [31,32]. Taking into account the correlation coefficients,  $R^2$ , then the applicabilities of these isotherm equations can be compared. Both models permit the linearization of the isotherm data as indicated by Eqs. (5) and (6):

$$\frac{C_e}{q} = \frac{1}{K_L Q_m} + \frac{C_e}{Q_m} \quad (5)$$

$$\log q_e = \log K_f + \frac{1}{n \log C_e} \quad (6)$$

where  $C_e$  is the equilibrium concentration of the sorbate ( $\text{mg dm}^{-3}$ ),  $q_e$  is the amount of sorbate per unit mass of sorbent ( $\text{mg g}^{-1}$ ),  $Q_m$  ( $\text{mg g}^{-1}$ ) and  $K_L$  ( $\text{dm mg}^{-1}$ ) are Langmuir constants related to the capacity and rate of adsorption, respectively,  $K_f$  ( $\text{dm mg}^{-1}$ ) and  $n$  are Freundlich constants and give an indication of how favorable the process and the capacity of the sorbent are, respectively. The values of the parameters of the isotherms and the related correlation coefficients are listed in Table 3, showing that the Langmuir model produces a better fit for all materials investigated. The essential characteristics of the Langmuir isotherm can be expressed in terms of a dimensionless equilibrium parameter ( $R_L$ ) [33], which is defined by:

$$R_L = \frac{1}{1 + K_L C_0} \quad (7)$$

where  $K_L$  is the Langmuir constant and  $C_0$  is the initial concentration of metal ( $\text{mg dm}^{-3}$ ). The value of  $R_L$  indicates the type of isotherm to be either unfavorable ( $R_L > 1$ ), linear ( $R_L = 1$ ), favorable

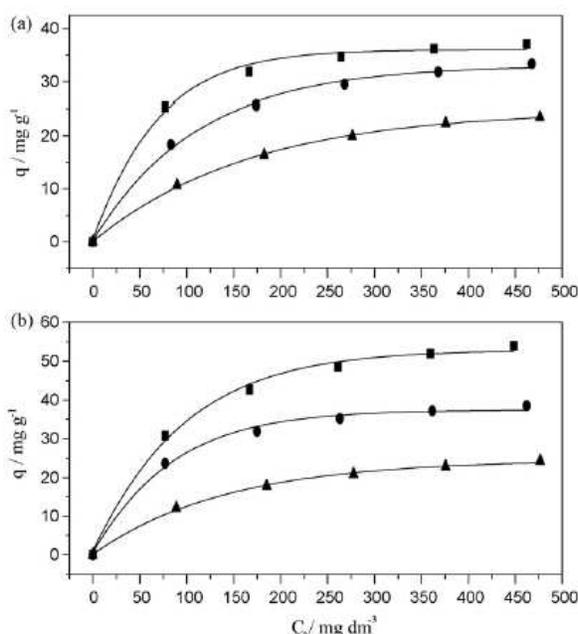


Fig. 6. Adjustment of the data to the Langmuir isotherms for copper sorption by BMS (■), BMP (●) and BMM (▲) in water (a) at pH 6.0 and hydroalcoholic solution (b), both at pH 6.0 and at  $298 \pm 1 \text{ K}$ .

( $0 < R_L < 1$ ) or irreversible ( $R_L = 0$ ). For all biopolymers  $R_L$  values varied between 0 and 1, which confirms that the sorbents are favorable for copper sorption with the conditions used for this study. The sorption curves according to the Langmuir model for the system in aqueous and hydroalcoholic solutions are shown in Fig. 6a and b, respectively.

Earlier studies associated with copper sorption for a series of materials such as wheat and lentil and rice husks without modification [13] as well as materials such as sugar cane bagasse and cellulose [10–12] chemically modified with specific agents, revealed a tendency for Langmuir model adjustment. The parameters related to this model reflect the nature of the adsorbent and can be used to compare the performance of sorption, as regards the maximum capacity. According to the maximum sorption capacity for copper per gram of sorbent,  $Q_m$ , the order of amount adsorbed on the systems investigated was  $\text{BMS} > \text{BMP} > \text{BMM}$ . A similar sequence is found for the degree of functionalization with the carboxylic acids introduced into the mesocarp structure, 177.0, 149.3, 141.8  $\text{mg g}^{-1}$  for the same sequence, respectively. This fact explains the sorption capacity of each material, because the presence of these functional groups is essential for cation sorption. The maximum capacity,  $Q_m$ , indicates for the hydroalcoholic solution that copper sorption is higher for these biopolymers than in the aqueous solutions. This can be explained based on the hydration energies of the hydrated copper ion with coordination number 6, as in alcohol solution, the solvation is hindered, which reduces the solubility of ions and can promote the sorption process [34].

### 3.5. Sorption from sugar cane spirit samples

The variation of the final copper concentrations according to the dosage of each sorbent, varying from 1.0 to 4.0  $\text{g dm}^{-3}$ , is shown in Fig. 7. It is observed that the copper content in sugar cane spirits can be reduced to that permitted by Brazilian law, specified as 5.0  $\text{mg dm}^{-3}$ , when only 1.0  $\text{g dm}^{-3}$  of each sorbent was used. As

**Table 2**

Pseudo-first- and pseudo-second-order rate constants for copper sorption on chemically modified mesocarp at pH 6.0 and 298 ± 1 K.

| Condition      | Biopolymer | $q_{e,exp}$ (mg g <sup>-1</sup> ) | Pseudo-first order                |                            |       | Pseudo-second order               |   |   |       |
|----------------|------------|-----------------------------------|-----------------------------------|----------------------------|-------|-----------------------------------|---|---|-------|
|                |            |                                   | $q_{e,cal}$ (mg g <sup>-1</sup> ) | $k_1$ (min <sup>-1</sup> ) | $R^2$ | $q_{e,cal}$ (mg g <sup>-1</sup> ) | $k_2$ (g mg <sup>-1</sup> min <sup>-1</sup> ) | $h$ (mg g <sup>-1</sup> min <sup>-1</sup> ) | $R^2$ |
| Water          | BMS        | 33.53                             | 62.80                             | 0.202                      | 0.928 | 37.19                             | 0.005   | 7.586                                       | 0.992 |
|                | BMP        | 26.01                             | 9.85                              | 0.085                      | 0.883 | 27.62                             | 0.011   | 8.595                                       | 0.997 |
|                | BMM        | 17.50                             | 15.54                             | 0.127                      | 0.952 | 19.46                             | 0.009   | 3.625                                       | 0.988 |
| Hydroalcoholic | BMS        | 38.58                             | 45.98                             | 0.126                      | 0.951 | 44.86                             | 0.002   | 5.720                                       | 0.982 |
|                | BMP        | 30.63                             | 6.46                              | 0.091                      | 0.944 | 30.66                             | 0.039   | 37.25                                       | 0.999 |
|                | BMM        | 19.88                             | 4.66                              | 0.092                      | 0.753 | 20.43                             | 0.033   | 13.94                                       | 0.999 |

**Table 3**

The Langmuir and the Freundlich parameters for copper adsorption on chemically modified mesocarps at pH 6.0 and 298 ± 1 K.

| Condition      | Biopolymer | Langmuir |                             |   | Freundlich |       |   |       |
|----------------|------------|----------|-----------------------------|---|------------|-------|---|-------|
|                |            | $R^2$    | $Q_m$ (mg g <sup>-1</sup> ) | $K_L$ (dm <sup>3</sup> mg <sup>-1</sup> ) | $R_L$      | $R^2$ | $K_f$ (dm <sup>3</sup> mg <sup>-1</sup> ) | $N$   |
| Water          | BMS        | 0.994    | 40.98                       | 0.021                                     | 0.084      | 0.834 | 8.015                                     | 3.859 |
|                | BMP        | 0.986    | 40.47                       | 0.010                                     | 0.166      | 0.901 | 3.221                                     | 2.557 |
|                | BMM        | 0.946    | 34.36                       | 0.005                                     | 0.263      | 0.901 | 1.048                                     | 1.897 |
| Hydroalcoholic | BMS        | 0.980    | 64.06                       | 0.012                                     | 0.144      | 0.909 | 7.812                                     | 3.094 |
|                | BMP        | 0.995    | 44.11                       | 0.015                                     | 0.120      | 0.939 | 6.526                                     | 3.373 |
|                | BMM        | 0.967    | 31.51                       | 0.007                                     | 0.222      | 0.876 | 1.548                                     | 2.167 |

observed, the initial high concentration of cation of 8.0 mg dm<sup>-3</sup> was reduced to 0.48, 1.41, 4.26 mg dm<sup>-3</sup> for BMS, BMP and BMM, respectively, at the end of the sorption process. However, northern hemisphere countries permit only up to 2.0 mg dm<sup>-3</sup> of copper in sugar cane spirits, which requires a dosage of 3.0 mg dm<sup>-3</sup> of BMM to fit within the required standards.

The present chemically modified mesocarp has considerably higher sorption capacity when compared with other studied materials. For example, the most investigated sorbent activated carbon, has the ability for copper removal from sugar cane spirit [35], showing that it would require concentration of 12.0 g dm<sup>-3</sup> and a stirring time of 60 min to obtain sugar cane spirits with copper levels below the limit allowed under Brazilian law.

Although the biopolymers of this study have demonstrated good efficiencies for copper removal from real samples of sugar cane spirits, a solid base for commercial application requires further studies on the changes in the profiles of inorganic and organic components of the sugar cane spirits, economic feasibility and the ideal flow conditions.

## 4. Conclusion

Through a quick and ready methodology it was possible to devise a strategy to introduce chelating carboxylic acid functions onto natural babassu mesocarp. The synthesized biopolymers presented good sorption capacities for copper in hydroalcoholic and aqueous solutions, with maximum values obtained at pH 6.0. The corresponding kinetics of sorption is governed by a pseudo-second-order model, with better adjustment to the Langmuir model. The results also demonstrated the effectiveness of copper removal from a sample of sugar cane spirits, requiring only 1.0 g dm<sup>-3</sup> of sorbent and 30 min of contact to meet the requirements of Brazilian law.

## Acknowledgements

The authors are indebted to CAPES for financial support, to FAPEMA for a fellowship to APV and to CNPq for a fellowship to CA.

## References

- [1] A. Pandey, C.R. Soccol, P. Nigam, V.T. Soccol, Biotechnological potential of agro-industrial residues. I. Sugarcane bagasse, *Bioreour. Technol.* 74 (2000) 69–80.
- [2] S. Richardson, L. Gorton, Characterisation of the substituent distribution in starch and cellulose derivatives, *Anal. Chim. Acta* 497 (2003) 27–65.
- [3] Y. Jiang, H. Pang, B. Liao, Removal of copper (II) ions from aqueous solution by modified bagasse, *J. Hazard. Mater.* 164 (2009) 1–9.
- [4] M. Šaibani, M. Klačnjak, B. Škrbič, Adsorption of copper ions from water by modified agricultural by-products, *Desalination* 229 (2008) 170–180.
- [5] C.F. Liu, R.C. Sun, A.P. Zhang, J.L. Ren, X.A. Wang, M.H. Qin, Z.N. Chao, W. Luo, Homogeneous modification of sugarcane bagasse cellulose with succinic anhydride using an ionic liquid as reaction medium, *Carbohydr. Res.* 342 (2007) 919–926.
- [6] C.F. Liu, R.C. Sun, A.P. Zhang, J.L. Ren, Preparation of sugarcane bagasse cellulosic phthalate using an ionic liquid as reaction medium, *Carbohydr. Polym.* 68 (2007) 17–25.
- [7] C.F. Liu, R.C. Sun, M.H. Qin, A.P. Zhang, J.L. Ren, F. Xu, J. Ye, S.B. Wu, Chemical modification of ultrasound-pretreated sugarcane bagasse with maleic anhydride, *Ind. Crop. Prod.* 26 (2007) 212–219.
- [8] V. Marchetti, A. Clement, P. Gerardin, B. Loubinoux, Synthesis and use of esterified sawdusts bearing carboxyl groups for removal cadmium (II) from water, *Wood Sci. Technol.* 34 (2000) 167–173.
- [9] A.M.A. Nada, M.L. Hassan, Ion exchange properties of carbohydrate bagasse, *J. Appl. Polym. Sci.* 102 (2006) 1399–1404.
- [10] O. Kamitz Júnior, V.A. L.J.C.P. Gurgel, V.R. Melo, T.M.S. Botaro, R.P.F. Melo, L.F. Gil, Adsorption of heavy metal ions from aqueous single metal solution by chemically modified sugarcane bagasse, *Bioreour. Technol.* 98 (2007) 1291–1297.
- [11] L.V.A. Gurgel, R.P. Freitas, L.F. Gil, Adsorption of Cu(II), Cd(II), and Pb(II) from aqueous single metal solutions by sugarcane bagasse and mercerized sugarcane

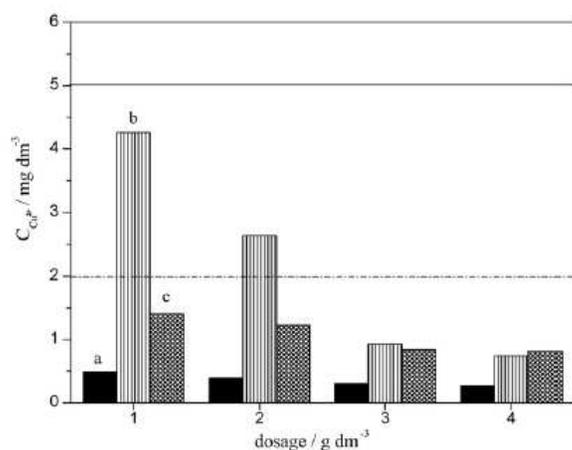


Fig. 7. Copper sorption from a sample of sugar cane spirit by BMS (a), BMM (b) and BMP (c) at 298 ± 1 K after 30 min of contact. (---) maximum allowed by the laws of countries of the northern hemisphere; (—) maximum allowed under Brazilian law.

- bagasse chemically modified with succinic anhydride, *Carbohydr. Polym.* 74 (2008) 922–929.
- [12] L.V.A. Gurgel, O. Karnitz Jr., R.P.F. Gil, L.F. Gil, Adsorption of Cu(II), Cd(II), and Pb(II) from aqueous single metal solutions by cellulose and mercerized cellulose chemically modified with succinic anhydride, *Bioresour. Technol.* 99 (2008) 3077–3083.
- [13] H. Aydin, Y. Bulut, C. Yerlikaya, Removal of copper (II) from aqueous solution by adsorption onto low-cost adsorbents, *J. Environ. Manag.* 87 (2008) 37–45.
- [14] A.P. Vieira, S.A.A. Santana, C.W.B. Bezerra, H.A.S. Silva, J.A.P. Chaves, J.C.P. Melo, E.C. Silva Filho, C. Airoidi, Kinetics and thermodynamics of textile dye adsorption from aqueous solutions using babassu coconut mesocarp, *J. Hazard. Mater.* 166 (2009) 1272–1278.
- [15] S.A.A. Santana, A.P. Vieira, E.C. Silva Filho, J.C.P. Melo, C. Airoidi, Immobilization of ethylenesulfide on babassu coconut epicarp and mesocarp for divalent cation sorption, *J. Hazard. Mater.* 174 (2010) 714–719.
- [16] B.S. Lima Neto, C.W.B. Bezerra, L.R. Polastro, P. Campos, R.F. Nascimento, S.M.B. Furuya, D.W. Franco, O cobre em aguardentes brasileiras: Sua quantificação e controle, *Quím. Nova* 17 (1994) 220–223.
- [17] Y. Boza, J. Horii, Influência do grau alcoólico e da acidez do destilado sobre o teor de cobre na aguardente, *Cienc. Tecnol. Aliment.* 20 (2000) 279–284.
- [18] M.B. Miranda, N.G.S. Martins, A.E.S. Belluco, J. Horri, A.R. Alcarde, Qualidade química de cachaças e de aguardentes brasileiras, *Cienc. Tecnol. Aliment.* 27 (2007) 897–901.
- [19] J.C.P. Melo, E.C. Silva Filho, S.A.A. Santana, C. Airoidi, Maleic anhydride incorporated onto cellulose and thermodynamics of cation-exchange process at the solid/liquid interface, *Colloids Surf. A* 346 (2009) 138–145.
- [20] V.C. Srivastava, I.D. Mall, I.M. Mishra, Characterization of mesoporous rice husk ash (RHA) and adsorption kinetics of metal ions from aqueous solution onto RHA, *J. Hazard. Mater.* 134 (2005) 257–267.
- [21] G.H. Jeffery, J. Bassett, J. Mendham, R.C. Denney, *Vogel's Textbook of Quantitative Chemical Analysis*, 5th ed. revised, John Wiley & Sons, New York, 1989.
- [22] K. Nakamoto, *Infrared and Raman Spectra of Inorganic and Coordination Compounds*, 4th ed., John Wiley & Sons, New York, 1986.
- [23] V. Tserki, P. Matzinos, S. Kakkou, C. Panayiotou, Novel biodegradable composites based on treated lignocellulosic waste flour as filler. Part I. Surface chemical modification and characterization of waste flour, *Composites: Part A* 36 (2005) 965–974.
- [24] A.D. Khasbaatar, Y.G. Ko, U.S. Choi, Adsorption and equilibrium adsorption modeling of bivalent metal cations on viscose rayon succinate at different pHs, *React. Funct. Polym.* 67 (2007) 312–321.
- [25] A.D. Khasbaatar, Y.J. Chun, U.S. Choi, Trivalent metal adsorption properties on synthesized viscose rayon succinate, *Polym. J.* 40 (2008) 302–309.
- [26] Y.S. Ho, G. McKay, Pseudo-second order model for sorption processes, *Process. Biochem.* 34 (1999) 451–465.
- [27] T. Gosset, J.L. Trancart, D.R. Thevenot, Batch metal removal by peat kinetics and thermodynamics, *Water Res.* 20 (1986) 21–26.
- [28] Y.S. Ho, D.A.J. Wase, C.F. Forster, Kinetic studies of competitive heavy metal adsorption by sphagnum moss peat, *Environ. Technol.* 17 (1996) 71–77.
- [29] K.C. Justi, V.T. Fávere, M.C.M. Laranjeira, A. Neves, R.A. Peralta, Kinetics and equilibrium adsorption of Cu(II), Cd(II), and Ni(II) ions by chitosan functionalized with 2[-bis-(pyridylmethyl)aminomethyl]-4-methyl-6-formylphenol, *J. Colloid Interface Sci.* 291 (2005) 369–374.
- [30] F.W. Sousa, S.A. Moreira, A.G. Oliveira, R.M. Cavalcante, R.F. Nascimento, M.F. Rosa, Uso da casca de coco verde como adsorvente na remoção de metais tóxicos, *Quím. Nova* 30 (2007) 1153–1157.
- [31] I. Langmuir, The constitution and fundamental properties of solids and liquids, *J. Am. Chem. Soc.* 38 (1916) 2221–2295.
- [32] H.M.F. Freundlich, Über die adsorption in lösungen, *Z. Phys. Chem.* 57A (1906) 385–470.
- [33] D.A. Fungaro, M.G. Silva, Utilização de zeólita preparada a partir de cinza residual de carvão como adsorvente de metais em água, *Quím. Nova* 25 (2002) 1081–1085.
- [34] L.B. Cantanhede, J.B. Lima, G.S. Lopes, R.F. Farias, C.W.B. Bezerra, Uso de sílica e sílica-titânia organofuncionalizada para a remoção de Cu (II) em aguardentes, *Cienc. Tecnol. Aliment.* 25 (2005) 500–505.
- [35] A.J.B. Lima, M.G. Cardoso, M.C. Guerreiro, F.A. Pimentel, Emprego do carvão ativo para a remoção de cobre em cachaça, *Quím. Nova* 29 (2006) 247–250.



Contents lists available at ScienceDirect

Journal of Hazardous Materials

journal homepage: [www.elsevier.com/locate/jhazmat](http://www.elsevier.com/locate/jhazmat)

## Immobilization of ethylenesulfide on babassu coconut epicarp and mesocarp for divalent cation sorption

Sirlane A.A. Santana<sup>a</sup>, Adriana P. Vieira<sup>a</sup>, Edson C. da Silva Filho<sup>b</sup>, Júlio C.P. Melo<sup>c</sup>, Claudio Airoidi<sup>c,\*</sup><sup>a</sup> Departamento de Química/CCET, Universidade Federal do Maranhão, Av. dos Portugueses S/N, Campus do Bacanga, 65080-540 São Luís, MA, Brazil<sup>b</sup> Química, Universidade Federal do Piauí, 64900-000 Bom Jesus, PI, Brazil<sup>c</sup> Institute of Chemistry, University of Campinas, UNICAMP, P.O. Box 6154, 13084-971 Campinas, SP, Brazil

### ARTICLE INFO

#### Article history:

Received 28 July 2009

Received in revised form 1 September 2009

Accepted 21 September 2009

Available online 24 September 2009

#### Keywords:

Sorption

Ethylenesulfide

Lignocellulosic

Babassu coconut

### ABSTRACT

A new synthetic methodology route consisted in reacting the natural babassu coconut mesocarp (BCM) and babassu coconut epicarp (BCE) with ethylenesulfide, for adding basic sulfur centers in pendant chains that possess high potential activity for coordinating divalent cations from aqueous solution. All biomaterials were characterized by elemental analysis, infrared (IR), <sup>13</sup>C NMR and thermogravimetry. The sulfur elemental analysis gave  $2.00 \pm 0.05$  and  $8.67 \pm 0.01\%$  for BCES and BCMS, which correspond to  $0.60 \pm 0.01$  and  $2.71 \pm 0.01$  mmol of this element per each gram of BCE and BCM, to confer a degree of functionalization of  $20.2 \pm 0.07$  and  $86.7 \pm 0.01$  mg g<sup>-1</sup>. This synthesis enabled from IR weak SH band at  $2544$  cm<sup>-1</sup> due to the incorporation of the reagent into the structure. The basic centers favor copper sorption with increasing pH from 2 to 6 observed by a batchwise methodology and the data obtained from the chosen pH 6 were adjusted to Freundlich and Langmuir models, favoring fit for the latter equation. The kinetics of sorption was established at 30 min for both biopolymers with a pseudo-second-order model.

© 2009 Elsevier B.V. All rights reserved.

### 1. Introduction

The simple presence of a series of metals such as copper, cadmium, lead, nickel, and chromium in the aquatic environment has been of great concern due to their toxicity and non-biodegradable nature [1]. These metallic ions may present acute toxicity to aquatic and terrestrial life, causing noticeable adverse physiological effects in humans and animals [2]. From this viewpoint, to decrease or eliminate the action of these unfavorable polluting effects, investigations to control these metals in the environment have increased significantly in recent decades [3].

Among various methods for toxic metal ion removal from aqueous solutions, sorption is by far the most versatile and widely used for such different pollutants and many efforts have recently been devoted to find cheaper pollution control methods and also available materials to bring efficiency to the proposed methodology [4–7].

Reusing and recycling industrial and agricultural residues can minimize the environmental problems and this has contributed to reconsideration of applying traditional biomaterials, such as natural lignocellulosic fibers, to substitute synthetic polymers, for

example, since in many cases better performance can be attained. These biomaterials contain various organic components such as lignin, cellulose and hemicellulose with a lot of hydroxyl and/or phenolic groups that are chemically reactive centers, yielding biopolymers with new properties [8].

Chemically modified plant wastes originating from various sources for metal ion removal have attracted much attention by considering chemical modification of the polymeric structure to improve the sorption capacity of the sorbents, normally by incorporating a higher number of active binding sites, bringing better ion-exchange properties or forming new functional groups that favor metal uptake [9]. For example, the effect of sulfuric acid treatment on poplar tree sawdust resulted in good removal, removing 92.4% of copper at pH 5, while the untreated biomaterial removed only 47% [10]. When two kinds of sawdust were treated with sodium hydroxide or sodium carbonate solutions, the first reagent markedly increased the sorption capacity for divalent copper and zinc [11].

Sorption of divalent copper, zinc, cobalt, nickel and lead onto acid or alkali treated banana and orange peels demonstrated that the sorption capacity increased for both sorbents [12]. Rice husk treated with sodium hydroxide, sodium carbonate and epichlorohydrin enhanced the sorption capacity for cadmium [13], while sorption investigations carried out with copper and lead on rice husk chemically modified by various kinds of carboxylic acids, showed that the highest sorption capacity was achieved when tartaric acid was used [14].

\* Corresponding author. Tel.: +55 19 35213055; fax: +55 19 35213023.  
E-mail address: [airoidi@iqm.unicamp.br](mailto:airoidi@iqm.unicamp.br) (C. Airoidi).

Etherification, esterification and oxidation of bagasse fibers with the aim to prepare lignocellulosic materials for metal ions removal from wastewater were recently investigated [15], while the incorporation of carboxylic functions via a succinylation reaction was also explored [16]. In both cases the sorption capacities increased in comparison with the original biopolymer.

Taking into account the potentiality of natural sources to give useful materials, the preparation and evaluation of two new biomaterials obtained from babassu coconut mesocarp (BCM) and babassu coconut epicarp (BCE), which are abundant, easily available by-products, in the northeast of Brazil, were explored after chemical modification with ethylenesulfide, in order to adsorb copper from aqueous solution. The sorption studies were performed for different times, with variations in pH and also the metal ion concentrations.

## 2. Experimental

### 2.1. Chemicals

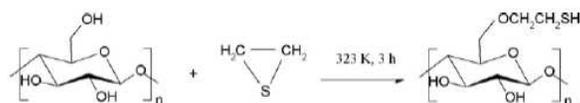
Hydrated divalent copper nitrate (Carlo Erba) was used without purification and the concentration was determined through complexometric titration with standardized EDTA solution. Ethylenesulfide (Es) (Aldrich) for lignocellulose incorporation on coconut epicarp and mesocarp was used as received. All other chemicals were reagent grade.

### 2.2. Syntheses

The general synthetic route for the natural biopolymer chemical modifications is presented in Scheme 1. In both cases, 5 g of mesocarp or epicarp, with particle sizes in the 0.088–0.177 mm range, were individually mixed with 7.0 cm<sup>3</sup> (114.56 mmol) of ethylenesulfide, as previously established for chitosan incorporation [17]. The suspensions were maintained in a sand bath for 3 h at 323 K to give the final product. The chemically modified biomaterials were separated by filtration using sintered filter, washed with distilled water and then with acetone. The products named BCMS and BCES, respectively, were dried at 353 K in an oven for 1 h and in a desiccator overnight.

### 2.3. Physical measurements

Infrared spectra were obtained with a MB-Bomem FTIR spectrophotometer, using KBr pellets in 4000–400 cm<sup>-1</sup> region, with a resolution of 4 cm<sup>-1</sup>. Carbon, nitrogen, and sulfur of the compounds were analyzed by using a Perkin-Elmer 2400 Series II microelemental analyzer. Thermogravimetric curves (TG) was carried out with a Shimadzu TGA-50 instrument under a nitrogen flow rate of 0.50 cm<sup>3</sup> s<sup>-1</sup>, in the temperature interval from 298 to 1000 K, with a heating rate of 0.167 K s<sup>-1</sup> and initial sample mass of 10 mg. Solid-state CP/MAS <sup>13</sup>C NMR spectra were obtained on a Bruker AC 400/P spectrometer, by using frequencies of 75.47 MHz with a magic angle spinning of 4 kHz. The pH measurements were obtained using a DM-21 Digimed instrument.



Scheme 1. Synthetic route used to obtain BCMS or BCES.

### 2.4. pH studies and point of zero charge

The effect of pH sorption was performed by using identical series of flasks containing 100 mg of each biomaterial with same copper concentration, maintaining stirring for 24 h. The pH, in the range from 1.0 to 6.0 of the solution was adjusted when necessary with 0.10 mol dm<sup>-3</sup> hydrochloric acid or sodium hydroxide solutions. The content of free copper in the supernatant was determined as before.

The points of zero charge for BCMS and BCES biopolymers were determined by the solid addition method [18]. To a series of 100 cm<sup>3</sup> conical flasks was transferred 20 cm<sup>3</sup> of solution with pH varying from 1 to 12. The pH<sub>0</sub> values of the solution were roughly adjusted by adding either hydrochloric acid or sodium hydroxide 0.10 mol dm<sup>-3</sup>. The pH<sub>0</sub> of the solutions was then accurately noted and 0.10 g each of BCMS or BCES biomaterial was individually added to each flask, which was securely capped immediately. The suspensions were then manually shaken and allowed to equilibrate for 24 h with intermittent manual shaking, after which the pH value of the supernatant for each flask was noted. The difference between the initial and final pH values ( $\Delta\text{pH} = \text{pH}_0 - \text{pH}_f$ ) was plotted against the pH<sub>0</sub> and the point of intersection of the resulting curve at which  $\Delta\text{pH} = 0$  gave the pH<sub>PZC</sub> value.

### 2.5. Kinetic studies

Experiments for each biomaterial and copper ion were performed to determine the sorption equilibrium time, with intervals from 5 to 60 min. Thus, amounts of 100 mg of BCMS or BCES were suspended in 100.0 cm<sup>3</sup> of copper solution of each flask, which was filtered and the copper content of the supernatant was determined by direct titration with 0.010 mol dm<sup>-3</sup> EDTA at pH 10, using murexide as indicator [19].

### 2.6. Sorption isotherms

The term sorption expresses the whole process that occurs not only on surface, but also through the diffusive penetration in the biopolymers. Such occurrence is due to a general and non-mechanistic way, in which the present biopolymers have ability in cation removal from aqueous solution [20].

The isotherms of sorption for BCMS and BCES and the respective native biomaterials were obtained using the batchwise method, which consisted in suspending a series of 100.0 mg of each biomaterial in 100.0 cm<sup>3</sup> of aqueous copper solution having several concentrations, varying from 100 to 500 mg dm<sup>-3</sup>. In every case, each individual sorption determination was obtained from duplicate run, for flasks mechanically stirred at 298 ± 1 K. Each experiment was performed using the time and the pH from the best sorption obtained from the kinetic and pH studies. Again, the solid was filtered and the metal concentration in the supernatant was determined by titration, as before.

The sorption capacity (mg g<sup>-1</sup>) was calculated through the expression

$$q_e = \frac{C_i - C_f}{W} \times V \quad (1)$$

where  $C_i$  and  $C_f$  are the initial and final copper concentrations in the aqueous phase (mg dm<sup>-3</sup>), respectively,  $V$  is the volume of the solution (dm<sup>3</sup>) and  $W$  is the mass of the chemically modified mesocarp or epicarp used.

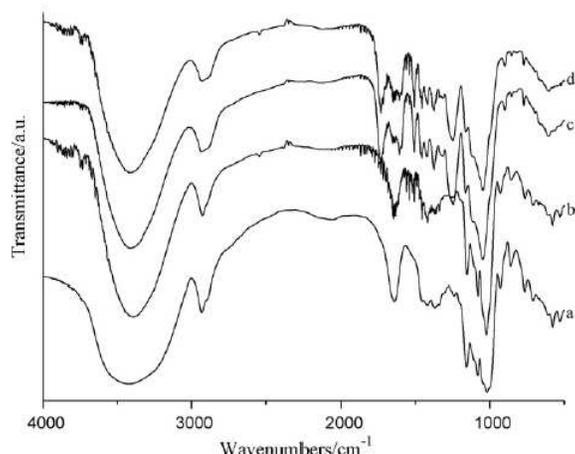


Fig. 1. FTIR of BCM (a), BCMS (b), BCE (c) and BCES (d).

### 3. Results and discussion

#### 3.1. Characterizations

Based on the obtained content of sulfur atom  $2.00 \pm 0.05$  and  $8.67 \pm 0.01\%$ , the amount of  $20.2 \pm 0.07$  and  $86.7 \pm 0.01 \text{ mg g}^{-1}$  was calculated for the corresponding ethylenesulfide molecule anchored on BCES and BCMS biopolymers, respectively. The effectiveness of ethylenesulfide in bonding natural polysaccharides can be compared through the present lignocellulosic components and the biopolymer chitosan. For this last biopolymer the amount of sulfur gave 20.39%, with two moles of ethylenesulfite covalently bonded to each unit of chitosan [17]. This high value is also due to the availability of the more reactive free amino center that contrasts with the less reactive hydroxyl group on carbon 6 lignocellulosic polymeric structure.

Different degree of immobilizations can be explained when structural characteristics between these original biopolymers are considered. Thus, mesocarp presented a large predominance of cellulose component on the main polymeric structure with available hydroxyl groups, while for epicarp lignin units are available with aldehydic and ketone functions [21]. From the structural point of view, the presence of hydroxyl groups causes an increased tension of the ring, favoring its opening in the course of reaction and, consequently, increases its reactivity in the mesocarp form [22].

The infrared spectra of unmodified and modified epicarp and mesocarp are shown in Fig. 1, showing: (i) a broad band in the  $3200\text{--}3600 \text{ cm}^{-1}$  range corresponding to O–H stretching vibration, (ii) well defined bands in the  $2800\text{--}3000 \text{ cm}^{-1}$  interval assigned to CH stretching vibrations and (iii) carbonyl group stretching bands in the  $1550\text{--}1750 \text{ cm}^{-1}$  region. The most remarkable difference between the unmodified and chemically modified spectra is the weak band at  $2544 \text{ cm}^{-1}$  that is assigned to the SH stretching frequency [22].

The effect of chemical modification on the thermal behavior of mesocarp and epicarp is shown in Fig. 2. For mesocarp the native material started decomposition at 375 K, which corresponds to a mass loss of 12%, followed by another loss of 62% in the 477–623 K interval. The first step of this decomposition can be attributed to the release of water physically adsorbed on surface, while the second stage is due to the decomposition of organic material to result in the expected breakdown of fibers to give the final residue. Identically, epicarp presented mass losses of 11% at 353 K and 56% in the 609–638 K interval, for the same experimental condition. For BCMS and BCES higher mass loss values are given when compared with

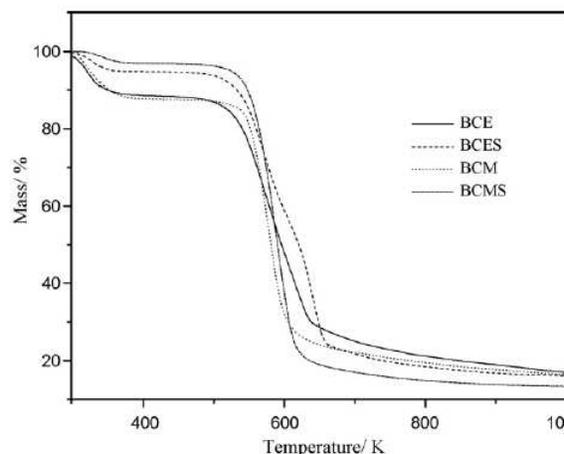


Fig. 2. TG curves of BCM, BCMS, BCE and BCES in inert atmospheres.

the native materials, however, there are no significant differences in thermal stability between unmodified and chemically modified coconut babassu mesocarp and epicarp.

Carbon nuclear magnetic resonance operating in cross polarization procedure presented spectra of unmodified chemically modified mesocarp and epicarp as shown in Fig. 3. mesocarp the peaks at 101 and 83 ppm were attributed to carbon C1 and C4 in the cellulose skeleton, respectively, and carbon C2, C3 and C5 were assigned to the signals at 71–75 ppm. peaks between 64 and 62 ppm were assigned to carbon C6 in cellulose and amorphous regions, respectively. Due to the fact epicarp is richer in lignin component in the biopolymeric structure, its spectrum also showed signal at 22 ppm related to methoxy groups belonging to lignin, while the signals at 116–120, 133–149–153 ppm attributed to aromatic carbons present, which

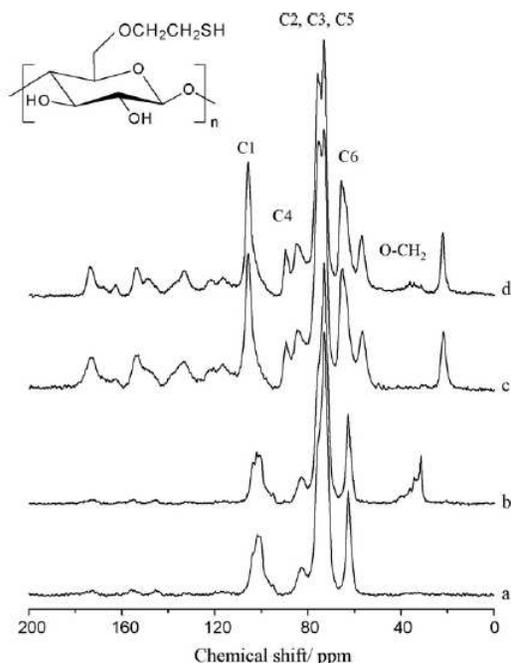


Fig. 3.  $^{13}\text{C}$  NMR of BCM (a), BCMS (b), BCE (c) and BCES (d).

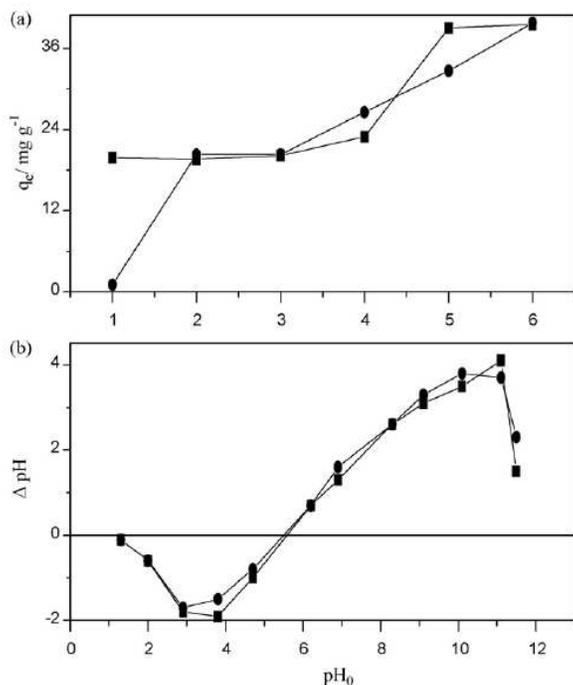


Fig. 4. Effect of pH on sorptions of  $Cu^{2+}$  aqueous solution by BCMS (■) and BCES (●) (a) and  $pH_{PZC}$  (b). Sorbent dose,  $1.0 \text{ g dm}^{-3}$ ; agitation time, 24 h;  $T = 298 \pm 1 \text{ K}$ ;  $[Cu^{2+}] = 200 \text{ mg dm}^{-3}$ .

also present in its same component. On the other hand, the broad signals at 160 and 178 ppm correspond to aldehyde, ketone and ester functions, originating also from the complex structure of the lignin [23]. However, the modified biomaterials showed signals at 40, 36, 34 and 31 ppm, which can be assigned to C7 and C8 carbons incorporated in the biopolymeric structure.

### 3.2. Sorption

#### 3.2.1. pH effect and point of zero charge

Since the efficiency of sorption processes is strongly dependent on the pH, which affects the sorbent surface charge, the degree of ionization, and the species of sorbate, comparative experiments were performed at pH between 1 and 6. The effect of pH on the sorption efficiency of  $Cu^{2+}$  ion on BCMS and BCES is shown in Fig. 4a, which differ from the null values, determined for the native derivatives. The sorption of the metal ion increases with the increase in pH and reaches to a maximum value at pH 6 for both the BCMS and BCES biomaterials. It must be noted that the surface of the sorbent changes its polarization according to the value of the pH of the solution and to the  $pH_{PZC}$  of the solid. At pH lower than  $pH_{PZC}$  the surface becomes positively charged and it is the opposite for pH higher than  $pH_{PZC}$ . Sorption of various anionic and cationic species on such sorbents can be explained on the basis of the competition for sorptives of  $H^+$  or  $OH^-$  ions with the sorbates. It is a common observation that the surface adsorbs anions favorably at lower pH due to the presence of  $H^+$  ions, whereas, the surface is active for the sorption of cations at higher pH, due to the deposition of  $OH^-$  ions.

To understand the sorption mechanism, it is necessary to determine the point of zero charge ( $pH_{PZC}$ ) of the sorbent. Sorption of cations is favored at  $pH > pH_{PZC}$ , while anion sorptions behave in the opposite condition. Fig. 4b shows that  $pH_{PZC}$  for BCMS and BCES gave identical values of 5.6. Then, it is clearly expected that at higher

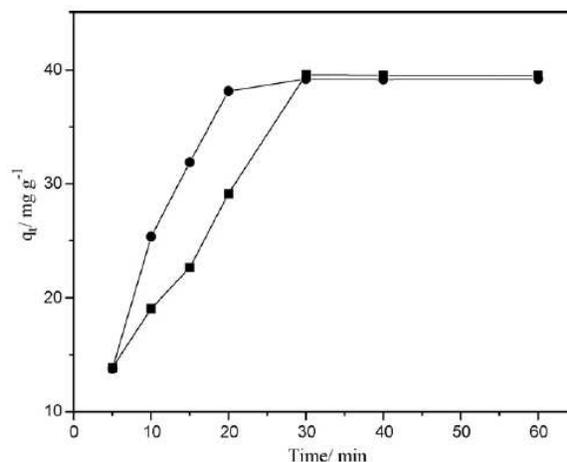


Fig. 5. Kinetics for  $Cu^{2+}$  sorptions by BCMS (■) and BCES (●) at  $298 \pm 1 \text{ K}$  and pH 6.

pH the sorption is favorable, as observed in Fig. 4a, and pH 6 was chosen for all sorption processes.

The sorption profile of metal ion on BCMS and BCES biomaterials as a function of the  $pH_0$  could also be explained on the basis of surface charge density of functional groups, such as hydroxyl, carboxyl, and others. The increase in sorption with  $pH_0$  can be attributed to the fact that the positively charged metal cations are repulsed less at higher pH values, in which results are in agreement with earlier reports [24,25].

#### 3.2.2. Effect of time

Taking into account the sorption property, the solid capacity against time plot defined a well-established kinetic of sorption, as shown in Fig. 5. Although the mesocarp immobilized 86.7 mg of ethylenesulfide per gram of biopolymers, compared with 20.2 mg of the same agent per gram of epicarp, however, the presence of lignin and available organic functions on this last biopolymeric structure favored the complexation of copper. As observed, the equilibrium is promptly achieved in about 30 min at  $298 \pm 1 \text{ K}$  with a sorbent dose of  $1.0 \text{ g dm}^{-3}$  for a sorbate concentration of  $200 \text{ mg dm}^{-3}$ . Thereafter, the obtained plateau remains almost unchanged with respect to large time. The present results are similar to those previously reported for divalent copper, cadmium and lead sorption on sugarcane bagasse [16]. On the other hand, the equilibrium time is shorter than other sorbents such as cow dung carbon [26] and shells of lentil, wheat, and rice [27].

The kinetic sorption data were adjusted to a pseudo-first-order kinetic model [28], as expressed by the equation:

$$\log(q_e - q_t) = \log q_e - \frac{k_1 t}{2.303} \quad (2)$$

where  $q_e$  and  $q_t$  refer to the amount of metal ion adsorbed ( $\text{mg g}^{-1}$ ), at equilibrium and at any other time,  $t$  (min), respectively, and  $k_1$  is the equilibrium rate constant of pseudo-first-order sorption ( $\text{min}^{-1}$ ).

The rate constant for the first-order equation was determined from the slope of the plot  $\log(q_e - q_t)$  versus time. If first-order kinetics is applicable to the system under study, the plot of  $\log(q_e - q_t)$  versus time, as represented by Eq. (2), should give a linear relationship. Further, the  $q_e$  obtained from the plot should also be close to the  $q_e$  experimentally obtained from the metal ion concentration of  $200 \text{ mg dm}^{-3}$ . Even though the correlation coefficient ( $R^2$ ) of the first-order equation was reasonable, the calculated values of  $q_e$  from the first-order kinetic plot were far too small, compared to the experimental values. The inapplicability of the

**Table 1**

 Kinetic parameters for Cu<sup>2+</sup> sorption on BCMS and BCES. Initial copper concentration of 200.0 mg dm<sup>-3</sup> with dosage of 1.0 g dm<sup>-3</sup> at pH 6.0 and 298 ± 1 K.

| Sorbent | $q_{e,exp}$ (mg g <sup>-1</sup> ) | Pseudo-first-order model          |                            |       | Pseudo-second-order model         |   |   |       |
|---------|-----------------------------------|-----------------------------------|----------------------------|-------|-----------------------------------|---|---|-------|
|         |                                   | $q_{e,cal}$ (mg g <sup>-1</sup> ) | $k_1$ (min <sup>-1</sup> ) | $R^2$ | $q_{e,cal}$ (mg g <sup>-1</sup> ) | $k_2$ (× 10 <sup>3</sup> g mg <sup>-1</sup> min <sup>-1</sup> ) | $h$ (mg g <sup>-1</sup> min <sup>-1</sup> ) | $R^2$ |
| BCMS    | 39.6                              | 69.5                              | 0.13                       | 0.887 | 51.6                              | 1.2   | 3.44  | 0.966 |
| BCES    | 39.2                              | 80.2                              | 0.19                       | 0.985 | 45.7                              | 2.9   | 6.18  | 0.980 |

Lagergren equation to describe the kinetics of copper sorption was also observed for sorption using sphagnum moss peat [29].

The obtained experimental data were also analyzed using a pseudo-second-order model [30] according to the following equation:

$$\frac{t}{q_t} = \frac{1}{k_2 q_e^2} + \frac{t}{q_e} \quad (3)$$

where  $k_2$  is the equilibrium rate constant of pseudo-second-order sorption (g mg<sup>-1</sup> min<sup>-1</sup>). If pseudo-second-order kinetic is applicable to the system under study, the plot of  $t/q_t$  against time, as given in Eq. (3), should give a linear relationship. The second-order sorption rate constant and  $q_e$  were determined from the slope and intercept of  $t/q_t$  versus time plot and the correlation coefficients for the linear plot are better than 0.96 for BCMS and BCES. The calculated  $q_e$  values from the pseudo-second-order model are in good agreement with experimental  $q_e$  values. This suggests that the sorption system followed the pseudo-second-order model. The values of kinetic constants and  $q_e$  values for copper sorption onto BCMS and BCES are given in Table 1.

### 3.2.3. Isotherms

The Langmuir and Freundlich model isotherms were evaluated by sorption experiments in aqueous solution under equilibrium time and optimal pH conditions. The Langmuir isotherm [31] is presented here in a general linearized form:

$$\frac{C_e}{q_e} = \frac{1}{Q_{max} b} + \frac{C_e}{Q_{max}} \quad (4)$$

where  $C_e$  is the equilibrium concentration of the solute (mg dm<sup>-3</sup>),  $q_e$  is the amount of solute adsorbed per unit of mass of sorbent (mg g<sup>-1</sup>),  $Q_{max}$  is the maximum capacity of sorbent of the system (mg g<sup>-1</sup>) and  $b$  is an sorption equilibrium constant related to the energy of the sorption.

The Freundlich model describes the sorption isotherm with the equation [32]:

$$q_e = K_f C_e^{1/n} \quad (5)$$

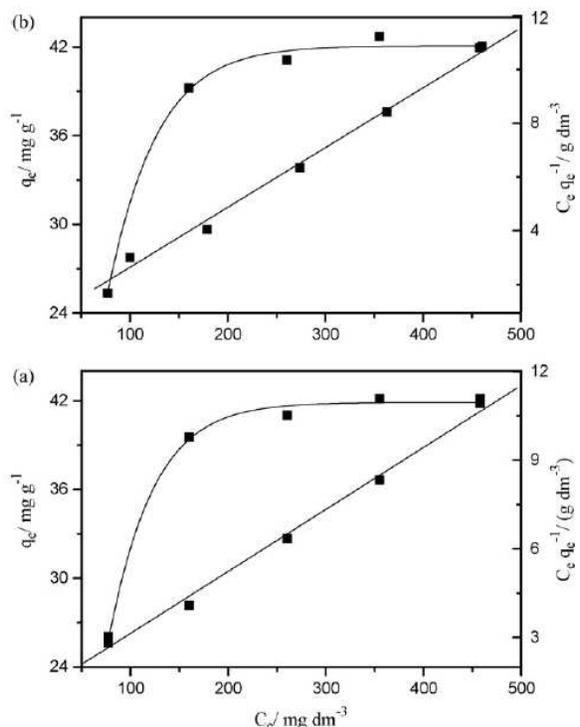
where  $q_e$  and  $C_e$  are the amounts (mg g<sup>-1</sup>) adsorbed at equilibrium and the equilibrium bulk concentration (g dm<sup>-3</sup>), respectively and  $1/n$  and  $K_f$  are the Freundlich constants which correspond to sorption intensity and sorption capacity, respectively.

The related parameters of Langmuir and Freundlich isotherms for BCMS and BCES are summarized in Table 2. The Langmuir isotherm parameter  $Q_{max}$  indicates the maximum sorption capacity of the material, in other words, the sorption of metal ions at high concentrations. From the correlation coefficients,  $R^2$ , the applicability of the isotherm equations can be compared for Langmuir and Freundlich isotherms, evidenced favorable fit for the first model.

**Table 2**

 Freundlich and Langmuir coefficients for Cu<sup>2+</sup> sorption on BCMS and BCES at 298 ± 1 K.

| Sorbent | Freundlich |      |  | Langmuir |   |                                 |
|---------|------------|------|--|----------|---|---------------------------------|
|         | $R^2$      | $n$  | $K_f$ (dm <sup>3</sup> g <sup>-1</sup> ) | $R^2$    | $b$ (dm <sup>3</sup> mg <sup>-1</sup> ) | $Q_{max}$ (mg g <sup>-1</sup> ) |
| BCMS    | 0.892      | 3.70 | 8.73                                     | 0.996    | 0.0207                                  | 47.5                            |
| BCES    | 0.896      | 3.58 | 8.30                                     | 0.995    | 0.0200                                  | 47.7                            |


**Fig. 6.** Isotherms and Langmuir sorption for Cu<sup>2+</sup> onto BCMS and BCES in aqueous solution at 298 ± 1 K and pH 6.

The plot of sorption data for copper on BCMS and BCES biomaterials and the Langmuir isotherm is shown in Fig. 6, indicating a surface homogeneity of the sorbents. Most of the reported metal ion systems suggest the applicability of the Langmuir equation, which assumes a monolayer coverage and constant sorption energy on the sorbent surface [33].

The sorption results for copper on BCMS and BCES were compared with other systems and showed higher capacities for these synthesized biomaterials. The sorption investigation of copper on tartaric acid-modified rice husk gave the maximum sorption capacity for copper with 29 mg g<sup>-1</sup> [14].

The efficiency of sawdust for copper removal and the sorption capacity based on Langmuir model gave 6.92 mg g<sup>-1</sup> for poplar sawdust and 12.70 mg g<sup>-1</sup> for other sawdust [15]. The effect of sulfuric acid treatment on poplar sawdust gave a maximum sorption capacity of 13.95 against 5.43 mg g<sup>-1</sup> for untreated sawdust, which followed a Langmuir isotherm [10]. In the case of copper sorp-

tion by concentrated sulfuric acid-treated corncobs, the maximum capacity obtained from the Langmuir isotherm was  $31.45 \text{ mg g}^{-1}$  [32]. Sorption of divalent metal ions, particularly divalent copper, zinc, cobalt, nickel and lead onto acid- and alkali-treated banana and orange peels was performed and the reported maximum sorption capacities for copper with banana and orange peels were 4.75 and  $3.65 \text{ mg g}^{-1}$ , respectively [12]. The maximum capacity of 47.5 and  $47.7 \text{ mg g}^{-1}$  for BCMS and BCES obtained from the Langmuir isotherms for the same cation are higher than those previously reported, which suggests that these newly synthesized biomaterials have high performance for cation removal at the solid/liquid interface.

#### 4. Conclusion

Agricultural wastes, native babassu coconut BCM and BCE biomaterials demonstrated to be unsuitable sorbents for metal ions from aqueous solutions. However, the new synthesized biopolymers, BCMS and BCES, acquired relevant proprieties to act favorably for cation removal, which depended on pH with maximum sorption occurring at pH 6. Based on the difference in functionalization  $20.2 \pm 0.07$  and  $86.7 \pm 0.01 \text{ mg g}^{-1}$  for mesocarp and epicarp derivatives, it should be expected the best sorption for BCES. However, in addition to sulfur basic atoms attached to the pendant chains, the available ketone and aldehydic centers on BCES surface can be also used for copper complexation, to give nearly the same amounts of solute adsorbed, 39.6 and  $39.2 \text{ mg g}^{-1}$  for BCMS and BCES, respectively.

The equilibrium sorption is best fitted to a pseudo-second-order kinetic equation for this cation by BCMS and BCES biopolymers, as demonstrated for typical sorption isotherms and the results were adjusted to the Langmuir sorption better than to the Freundlich model. The equilibrium between the metal ions at the solid/liquid interface on chemically modified biomaterials was quickly achieved, in the short time of 30 min. The results showed that these biomaterials may be successfully used as a sorbent for copper removal from wastewater. The effectiveness of both sorbents in cation removal from aqueous solution is expressed within concentration range from 100 to  $500 \text{ mg dm}^{-3}$ , with sorbent dose of  $1.0 \text{ g dm}^{-3}$  at pH 6.0, under the minimum equilibration time of 30 min.

#### Acknowledgments

The authors are indebted to CAPES for financial support and for a fellowship to SAAS, to FAPEMA for a fellowship to APV and to CNPq for a fellowship to CA.

#### References

- [1] S. Çay, A. Uyanık, A. Özasiç, Single and binary component sorption of copper(II) and cadmium(II) from aqueous solutions using tea-industry waste, *Sep. Purif. Technol.* 38 (2004) 273–280.
- [2] R.E. Clement, G.A. Eiceman, C.J. Koester, Environmental analysis, *Anal. Chem.* 67 (1995) 221R–225R.
- [3] J. Goel, K. Kadirvelu, C. Rajagopal, V.K. Garg, Removal of lead(II) by sorption using treated granular activated carbon: batch and column studies, *J. Hazard. Mater.* 125 (2005) 211–220.
- [4] V.K. Gupta, I. Ali, Removal of lead and chromium from wastewater using bagasse fly ash—a sugar industry waste, *J. Colloid Interface Sci.* 271 (2004) 321–328.
- [5] A.A. Ali, R. Bishtawi, Removal of lead and nickel ions using zeolite tuff, *J. Chem. Technol. Biotechnol.* 69 (1997) 27–34.
- [6] K.K. Panday, P. Gur, V.N. Singh, Copper(II) removal from aqueous solutions by fly ash, *Water Res.* 19 (1985) 869–873.
- [7] B. Acemioglu, M.H. Alma, Equilibrium studies on sorption of Cu(II) from aqueous solution onto cellulose, *J. Colloid Interface Sci.* 243 (2001) 81–84.
- [8] B. Xiao, X.F. Sun, R. Sun, The chemical modification of lignins with succinic anhydride in aqueous systems, *Polym. Degrad. Stabil.* 71 (2001) 223–231.
- [9] W.S.W. Ngah, M.A.K.M. Hanafiah, Removal of heavy metal ions from wastewater by chemically modified plant wastes as sorbents: a review, *Bioresour. Technol.* 99 (2008) 3935–3948.
- [10] F.N. Acar, Z. Eren, Removal of Cu(II) ions by activated poplar sawdust (Samsun Clone) from aqueous solutions, *J. Hazard. Mater. B* 137 (2006) 909–914.
- [11] M. Ščiban, M. Klačnja, B. Škrbić, Modified softwood sawdust as sorbent of heavy metal ions from water, *J. Hazard. Mater. B* 136 (2006) 266–271.
- [12] G. Annadurai, H.S. Juang, D.J. Lee, Sorption of heavy metal from water using banana and orange peels, *Water Sci. Technol.* 47 (2002) 185–190.
- [13] U. Kumar, M. Bandyopadhyay, Sorption of cadmium from aqueous solution using pretreated rice husk, *Bioresour. Technol.* 97 (2006) 104–109.
- [14] K.K. Wong, C.K. Lee, K.S. Low, M.J. Haron, Removal of Cu and Pb by tartaric acid modified rice husk from aqueous solutions, *Chemosphere* 50 (2003) 23–28.
- [15] A.M.A. Nada, M.L. Hassan, Ion exchange properties of carbohydrate bagasse, *J. Appl. Polym. Sci.* 102 (2006) 1399–1404.
- [16] O. Karnitz Júnior, L.V.A. Gurgel, J.C.P. de Melo, V.R. Botaro, T.M.S. Melo, R.P.F. Gil, L.F. Gil, Sorption of heavy metal ion from aqueous single metal solution by chemically modified sugarcane bagasse, *Bioresour. Technol.* 98 (2007) 1291–1297.
- [17] K.S. Sousa, E.C. da Silva Filho, C. Airoidi, Ethylenesulfide as a useful agent for incorporation into the biopolymer chitosan in a solvent-free reaction for use in cation removal, *Carbohydr. Res.* 344 (2009) 1716–1723.
- [18] L.S. Balistreri, J.W. Murray, The surface chemistry of goethite ( $\alpha\text{-FeOOH}$ ) in major ion seawater, *Am. J. Sci.* 281 (1981) 788–806.
- [19] G.H. Jeffery, J. Bassett, J. Mendham, R.C. Denney, Vogel's textbook of quantitative chemical analysis, in: Longman Scientific & Technical, Co-published with John Wiley and Sons Inc., New York, 1989, pp. 309–322.
- [20] N.J. Barrow, The description of sorption curves, *Eur. J. Soil Sci.* 59 (2008) 900–910.
- [21] A.P. Vieira, S.A.A. Santana, C.W.B. Bezerra, H.A.S. Silva, J.A.P. Chaves, J.C.P. de Melo, E.C. da Silva Filho, C. Airoidi, Kinetics and thermodynamics of textile dye sorption from aqueous solutions using babassu coconut mesocarp, *J. Hazard. Mater.* 166 (2009) 1272–1278.
- [22] C. Airoidi, L.N.H. Arakaki, Immobilization of ethylenesulfide on silica surface through sol-gel process and some thermodynamic data of divalent cation interactions, *Polyhedron* 20 (2001) 929–936.
- [23] D.L. Pavia, G.M. Bassler, T.C. Morrill, Introduction to Spectroscopy, 2nd ed., Saunders College, New York, 1996.
- [24] A. Akli, M. Mouflih, S. Sebti, Removal of heavy metal ions from water by using calcined phosphate as a new sorbent, *J. Hazard. Mater.* 112 (2004) 183–190.
- [25] V.C. Srivastava, I.D. Mall, I.M. Mishra, Characterization of mesoporous rice husk ash (RHA) and sorption kinetics of metal ions from aqueous solution onto RHA, *J. Hazard. Mater.* B134 (2006) 257–267.
- [26] D.D. Das, R. Mahapatra, J. Pradhan, S.N. Das, R.S. Thakur, Removal of Cr(VI) from aqueous solution using activated cow dung carbon, *J. Colloid Interface Sci.* 232 (2000) 235–240.
- [27] H. Aydin, Y. Buluta, Ç. Yerlikayab, Removal of copper (II) from aqueous solution by sorption onto low-cost sorbents, *J. Environ. Manage.* 87 (2008) 37–45.
- [28] K. Periasamy, C. Namasivayam, Process development for removal and recovery of cadmium from wastewater by low-cost sorbent: sorption rates and equilibrium studies, *Ind. Eng. Chem. Res.* 33 (1994) 317–320.
- [29] Y.S. Ho, G. McKay, The kinetics of sorption of divalent metal ions onto sphagnum moss peat, *Water Res.* 34 (2000) 735–742.
- [30] Y.S. Ho, G. McKay, Pseudo-second order model for sorption processes, *Process Biochem.* 34 (1999) 451–465.
- [31] E.C. da Silva Filho, J.C.P. de Melo, C. Airoidi, Preparation of ethylenediamine-anchored cellulose and determination of thermochemical data for the interaction between cations and basic centers at the solid/liquid interface, *Carbohydr. Res.* 341 (2006) 2842–2850.
- [32] M.N. Khan, M.F. Wahab, Characterization of chemically modified corncobs and its application in the removal of metal ions from aqueous solution, *J. Hazard. Mater.* 141 (2007) 237–244.
- [33] T.G. Chuah, A. Jumariah, I. Azni, S. Katayon, S.Y.T. Choong, Rice husk as a potentially low-cost biosorbent for heavy metal and dye removal: an overview, *Desalination* 175 (2005) 305–316.

### Epicarp and Mesocarp of Babassu (*Orbignya speciosa*): Characterization and Application in Copper Phtalocyanine Dye Removal

Adriana P. Vieira,<sup>a</sup> Sirlane A. A. Santana,<sup>\*a</sup> Cícero W. B. Bezerra,<sup>a</sup> Hildo A. S. Silva,<sup>a</sup> José A. P. Chaves,<sup>b</sup> Júlio C. P. de Melo,<sup>c</sup> Edson C. da Silva Filho<sup>d</sup> and Claudio Airoidi<sup>c</sup>

<sup>a</sup>Departamento de Química/CCET, Universidade Federal do Maranhão, Avenida dos Portugueses S/N, Campus do Bacanga, 65080-540 São Luís-MA, Brazil

<sup>b</sup>Colégio Universitário, Universidade Federal do Maranhão, 65080-540 São Luís-MA, Brazil

<sup>c</sup>Institute of Chemistry, University of Campinas, CP 6154, 13084-971 Campinas-SP, Brazil

<sup>d</sup>Química, Campus Amilcar Ferreira Sobral, Universidade Federal do Piauí, 64800-000 Floriano-PI, Brazil

Os componentes mesocarpo e epicarpo do coco babaçu foram utilizados como novos biossorventes alternativos para remoção do corante têxtil ftalocianina de cobre de soluções aquosas. Esses biopolímeros foram caracterizados por análise elementar, RMN de <sup>13</sup>C no estado sólido, espectroscopia de absorção na região do infravermelho, análise termogravimétrica e difratometria de raios X. Os resultados mostraram que a composição do mesocarpo e do epicarpo é similar à de outros materiais lignocelulósicos e que ambos os componentes são efetivos na remoção do corante têxtil Turqueza Remazol. O modelo cinético de pseudo-segunda ordem resultou no melhor coeficiente de correlação tanto para o epicarpo quanto para o mesocarpo ( $R^2 = 0,999$ ), com constantes de velocidade de sorção,  $k_2$ , de 0,31 e 1,43  $\text{g mg}^{-1} \text{min}^{-1}$ , respectivamente. Os modelos de Langmuir e Freundlich foram empregados para analisar os dados experimentais em sua forma linearizada. O segundo modelo apresentou melhor adequação para a adsorção do corante Turqueza Remazol com sorção máxima de 1,44 e 2,38  $\text{mg g}^{-1}$  a pH 6,0 para mesocarpo e epicarpo, respectivamente.

The mesocarp and epicarp components of the babassu palm tree were applied as novel alternative biosorbents for copper phtalocyanine textile dye removal from aqueous solutions. The natural biopolymers were characterized by elemental analyses, solid state <sup>13</sup>C NMR, infrared spectroscopy, thermogravimetric analysis and X-ray diffractometry. Results demonstrated that the compositions of the mesocarp and epicarp are similar to those of other lignocellulosic materials, and that they were very effective for removal of the textile dye Turquoise Remazol. A pseudo second-order kinetic model resulted in the best fit with experimental data for both epicarp and mesocarp ( $R^2 = 0.999$ ), providing rate constants of sorption,  $k_2$ , of 0.31 and 1.43  $\text{g mg}^{-1} \text{min}^{-1}$ , respectively. The Langmuir and Freundlich isotherm models were employed for adsorption analysis of the experimental data in their linearized forms. The second model resulted in the better fit for Turquoise Remazol dye, which presented maximum adsorption of 1.44 and 2.38  $\text{mg g}^{-1}$  at pH 6.0 for mesocarp and epicarp, respectively.

**Keywords:** mesocarp, epicarp, babassu coconut, adsorption, dye textile

## Introduction

Environmental pollution, in general, is one of the most serious problems confronted by society and is directly linked to industrial development, with textile activities

being responsible for the worsening of the situation, generating a considerable amount of colored wastewater.<sup>1</sup> It is estimated that around 15% of the world's production of dyes is lost to the environment during synthesis, processing and applications.<sup>2</sup> From the environmental point of view this is a serious problem, since the disorderly dumping of effluents into aquatic environments such

\*e-mail: sirlane@ufma.br

as rivers, streams and lakes, without prior treatment, decreases the transparency of water and the penetration of solar radiation, affecting photosynthetic activity and solubility of gases and causing serious damage to regional fauna and flora.<sup>3</sup>

Conventional methods used for dye removal from industrial effluents include biodegradation, Fenton and photo-Fenton oxidations, electroflocculation, combined photo catalytic and ozonation processes, adsorption, etc. However, some of these processes may form intermediate compounds with higher degrees of toxicity, as happens with ozone, which makes it necessary to monitor the process through toxicity tests.<sup>4</sup> In addition, most of these methods are often expensive or ineffective, especially for dye removal from dilute solutions.

The adsorption is an efficient treatment process for dye removal from wastewater.<sup>5</sup> The first step for an effective process of adsorption is the choice of a sorbent with high capacity and long life, available on a large scale and at low cost. It is considered low cost if it requires little processing, is naturally abundant or is a by-product or waste from another industry.<sup>6</sup> Normally, the adsorption process is studied on the basis of empirical models such as Langmuir and Freundlich. The first model assumes that the sorbent surface is covered by adsorption sites with identical energies and each sorbed molecule adheres to a single site, predicting the formation of a sorbate monolayer on the surface.<sup>7</sup> On the other hand, the Freundlich model describes a reversible heterogeneous adsorption without restricting the covering to forming a monolayer on the sorbate.<sup>8</sup>

Investigations have recently been directed to alternative sorbents, also known as low-cost or unconventional, based on both the environmental and the economical points of view.<sup>9-20</sup> In order to overcome high cost problems, an increasing interest in producing new alternative sorbent materials to replace the most used activated carbon has been raised, also taking into account local availability, since these new materials are frequently constituted of residues from agricultural activity or sea food processing.<sup>21</sup>

Brazil has a high potential for lignocellulosic fiber production. As an example, this type of material results from babassu (*Orbignya speciosa*) biomass, a very abundant palm tree in the north-central region of the country, especially in the State of Maranhão. The babassu palm tree is of large size, up to 20 m, having a cylindrical trunk with a crown containing a number of fruits in ellipsoidal form. Each fruit is constituted of epicarp, mesocarp, endocarp and almond with 11, 23, 59 and 7% in mass, respectively.<sup>22</sup>

The major exploitation of the babassu almond is for lauric oil production, which can be used for energetic

purposes, such as biodiesel production, or in cooking.<sup>23-25</sup> The most common use for the epicarp is coal production due to its stiffness, while the mesocarp is used by food ration manufacturers, since it is rich in sugars and, consequently, can be useful in nutritional compositions.<sup>21</sup> Normally, most extractive processes consist in collecting the attractive almonds from the fruits, leaving all the other components unexploited.

Recent research has analyzed other applications of the outer layers of the babassu, including the anti-inflammatory and analgesic properties<sup>26-29</sup> of the mesocarp, which is also capable of adsorbing various textile industry dyes.<sup>30</sup> Also, the structural features associated with mesocarp and epicarp permit their use as polymeric supports for the immobilization of ethylenesulfide followed by divalent cation removal from aqueous solutions.<sup>31</sup>

From the environmental point of view, there is some difficulty in color removal from solutions of metallated dyes often encountered in wastewater. For example, copper may be released during the process, and this metal is controlled by environmental regulations. Studies have usually been related to decoloration of azo dyes, which are currently of wide use in the textile industry, with the exclusion of other commercially important classes of textile dyes such as the metallophthalocyanines. Photochemical oxidation has been employed for removal of the latter; however, the method is limited at high dye concentration.<sup>32</sup>

Taking into account the great availability of the byproducts of *Orbignya speciosa* after extraction of the almonds, the present investigation deals with the characterization and evaluation of the mesocarp and epicarp of babassu as sorbents for copper phthalocyanine, the agent in the textile dye Turquoise Remazol, from aqueous solutions. These studies are directly related to the potential uses of abundant, naturally growing palm trees in northeastern Brazil. In this context, the babassu tree is of great importance and the use of its byproducts can contribute to the expected sustainable development of that geographical region.

## Experimental

### *Materials and reagents*

The mesocarp and epicarp components were extracted from raw babassu fruits acquired in the city of São Luís, Maranhão state, Brazil. The individual parts were used after crushing the raw material into particle sizes in the 0.088-0.177 mm range. The dye Turquoise Remazol, CI 74160, shown in Figure 1, was supplied by Indústria de Toalhas de São Carlos, located in the state of São Paulo, Brazil. The

chemical reagents NaOH, HCl, KCl, potassium biphtalate ( $C_8H_5O_4K$ ) and  $Na_2B_4O_7 \cdot 10H_2O$  were all of analytical grade. Microcrystalline cellulose as powder (Aldrich), *ca.* 20  $\mu m$ , was used as a reference biopolymer during the characterization of the materials studied in this work.



Figure 1. Chemical structure of the Turquoise Remazol dye.

#### Biomass characterization

Infrared spectra were obtained in the 4000 to 400  $cm^{-1}$  range by accumulating 32 scans on a MB-Bomem FTIR spectrophotometer using KBr pellets with a resolution of 4  $cm^{-1}$ . Elemental analyses were performed with a Perkin-Elmer 2400 Series II equipment. Thermogravimetric curves (TG) for the powdered samples were obtained out with a Shimadzu TGA-50 instrument under a nitrogen flow rate of 30  $cm^3 min^{-1}$ , in the temperature interval from 298 to 1000 K, with a heating rate of 10 K  $min^{-1}$  and initial sample mass of 10.0 mg.  $^{13}C$  NMR spectra in the solid state were obtained on a Bruker AC 400/P spectrometer, by using the frequency of 75.47 MHz with a magic angle spinning of 10 Hz. X-ray diffraction patterns were recorded using a Shimadzu XD3-A diffractometer for the powdered samples with  $Cu-K_{\alpha}$  radiation,  $\lambda = 1.5418$  nm, at 30 kV, 20 mA and 2 $\theta$  angular regions in the 5 to 50 $^{\circ}$  range. The pH measurements were obtained by using DM-21 Digimed instrument.

#### Adsorption

The ability of the surfaces to extract the textile dye Turquoise Remazol from doubly distilled water solutions was evaluated by measuring adsorption isotherms at pH 6.0. The variation of adsorption as a function of pH (from 1.0 to 13.0) was analyzed by using appropriate buffer solutions. Under equilibrium conditions, the exchange processes at the solid/liquid interface can be characterized by the amount (mg) sorbed per gram of support. The batchwise adsorption

experiments were carried out under stirring at  $298 \pm 1$  K, by using *ca.* 100 mg of mesocarp or epicarp suspended in 10.0  $cm^3$  of aqueous solutions with dye concentrations varying from 13.6 to 54.4  $mg dm^{-3}$ . The suspensions were shaken for 60 min and the required time was established from prior experiments to ensure maximum sorption. At the end of this process, the solid was separated by filtration and the concentration of the dye sorbed by the biomass was determined by difference between the initial concentration of the aqueous solution and that found in the supernatant, by using a Varian AA 50 spectrophotometer at a wavelength of 620 nm.

The amount of dye adsorbed,<sup>15</sup>  $q_e$  ( $mg g^{-1}$ ), was calculated with equation 1:

$$q_e = \frac{C_i - C_f}{W} \times V \quad (1)$$

where  $C_i$  and  $C_f$  are the initial and final dye concentrations at equilibrium in the aqueous phase ( $mg dm^{-3}$ ), respectively,  $V$  is volume of dye solution ( $dm^3$ ) and  $W$  (g) is the amount of mesocarp or epicarp employed.

The proposed mechanism of adsorption was investigated by fitting the results of the kinetic data to pseudo first and second-order reactions,<sup>33</sup> as given by equations 2 and 3 respectively.

$$\log(q_e - q_t) = \log q_e - \frac{k_1}{2.303} \times t \quad (2)$$

$$\frac{t}{q_t} = \frac{1}{k_2 q_e^2} + \frac{1}{q_e} \times t \quad (3)$$

where  $q_e$  and  $q_t$  are the amounts of dye sorbed ( $mg g^{-1}$ ) at equilibrium and at time  $t$ , respectively,  $k_1$  ( $min^{-1}$ ) is the rate constant of first-order adsorption and  $k_2$  ( $g mg^{-1} min^{-1}$ ) is the rate constant of second-order sorption.

The Langmuir and Freundlich isotherm models were employed to analyze the experimental adsorption data in their linearized forms,<sup>34</sup> equations 4 and 5 respectively. The isotherm model chosen was that whose linearization provided the best fit to experimental data, that is, the best correlation coefficient value (R).

$$\frac{C_e}{q_e} = \frac{1}{q_{max} K_{ads}} + \frac{C_e}{q_{max}} \quad (4)$$

$$\log q_e = \frac{\log C_e}{n} + \log K_f \quad (5)$$

where  $C_e$  is the dye concentration at equilibrium,  $q_e$  is the amount of dye adsorbed,  $q_{max}$  is the maximum adsorption capacity,  $K_{ads}$  is the Langmuir constant, and  $n$  and  $K_f$  are Freundlich constants.

## Results and Discussion

### Biomass characterization

Elemental analysis gave for mesocarp 39.23, 6.70, 0.33; epicarp 46.72, 6.12, 0.51 and cellulose 41.95, 6.21, 0.18% for carbon, hydrogen and nitrogen, respectively. These results show that the mesocarp and epicarp biopolymers obtained from low cost babassu byproducts have elemental compositions close to that of cellulose.

The infrared spectra for cellulose, mesocarp and epicarp are presented in Figure 2. Cellulose, as shown in Figure 2 (a), presented bands attributed to H-bonded OH groups at 3400 to 3300  $\text{cm}^{-1}$ . The stretching bands of  $\text{CH}_2$  and  $\text{CH}_3$  appear in the 2800 to 3000  $\text{cm}^{-1}$  interval. The band at 1639  $\text{cm}^{-1}$  corresponds to  $\delta(\text{O-H})$  of the hydroxyl groups of the cellulose structure and those between 1200 to 1000  $\text{cm}^{-1}$  are related to  $\nu(\text{C-O})$ .<sup>35</sup> The spectra of mesocarp and epicarp are shown in Figures 2 (b) and (c), respectively. The most remarkable differences between the mesocarp and the cellulose spectra are at 860, 769 and 710  $\text{cm}^{-1}$ , where the bands related to vibrations of esters and monosubstituted aromatic rings due to the lignin fraction of the material are recorded. For epicarp, the most significant differences are at 1740  $\text{cm}^{-1}$ ,  $\nu(\text{C=O})$  for carboxylic esters, and at 1650  $\text{cm}^{-1}$ ,  $\nu(\text{C-OH})$  for alcohol groups, also due to the presence of lignin. The bands around 1610-1460  $\text{cm}^{-1}$  refer to  $\nu(\text{C=C})$  of aromatic rings, aromatic skeletal vibrations, aromatic ring deformation and  $-\text{CHO}$  out of plane vibrations. Similar bands to those found in cellulose at 1248  $\text{cm}^{-1}$  are attributed to  $\nu(\text{C-O-C})$  and at 1161  $\text{cm}^{-1}$  are associated with the  $\beta$ -1,4 linkage. Based on the appearance of this broad band it is inferred that an overlap occurred involving  $\nu(\text{C-O})$ ,  $\nu(\text{C-C})$  and  $\nu(\text{C-H})$  aromatic bending vibrations.

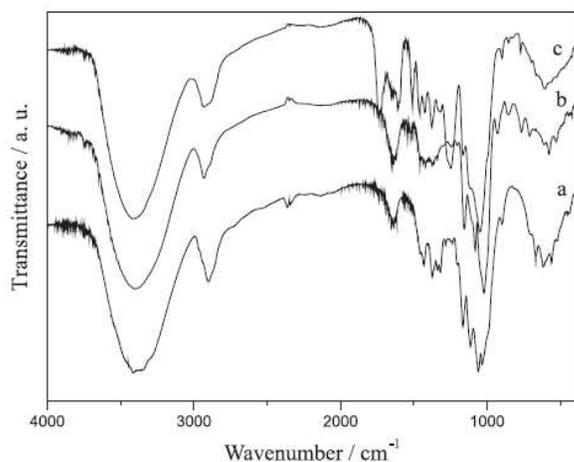


Figure 2. FTIR spectra of cellulose (a) and of the mesocarp (b) and epicarp (c) of babassu fruit.

The bands associated with tetra- and trisubstituted benzene out of plane vibrations<sup>36</sup> are assigned at 853 and 772  $\text{cm}^{-1}$ , respectively.

The solid state  $^{13}\text{C}$  NMR spectra for cellulose (a), mesocarp (b) and epicarp (c) are shown in Figure 3. As observed, both babassu components present similar sets of peaks in the spectra when compared to cellulose. The polysaccharide carbon 1 signal was attributed at 104 ppm, taking into account that it is bonded to two electronegative oxygen atoms, as shown in Figure 3 (a). For carbon 4 two distinct peaks are available at 88 and 83 ppm, which were attributed to the carbon associated with crystalline and amorphous regions, as normally occurs with the morphology of pure cellulose.<sup>37</sup> Carbons 2, 3 and 5, with almost equivalent chemical environments, were attributed to the signals at 71 to 75 ppm. The peaks with small chemical shifts between 64 and 62 ppm were assigned to carbon 6 in the crystalline and amorphous regions,<sup>35</sup> respectively.

In the mesocarp spectrum, as shown in Figure 3 (b), there is a small difference for carbon 4, which is responsible for the 1,4'- $\beta$ -glucosidic linkage. In this case, only one signal at 83 ppm is recorded, in agreement with the existence of the crystalline form of the cellulosic component. The epicarp spectrum is affected by the presence of a higher amount of lignin in this part of the babassu fruit, as shown in Figure 3c. A clear difference is observed by the signal at 22 ppm, which is related to methyl groups due to lignin. Several other small signals emerged when compared to cellulose, all of them due to chemical shifts of the carbonic lignin structure, such as the signals at 116 to 120, 133 and 149 to 153 ppm, assigned to aromatic carbons. The broad signals at 160 and 178 ppm correspond to aldehydes, ketones and esters, also originating from the complex structure of the lignin.<sup>38</sup>

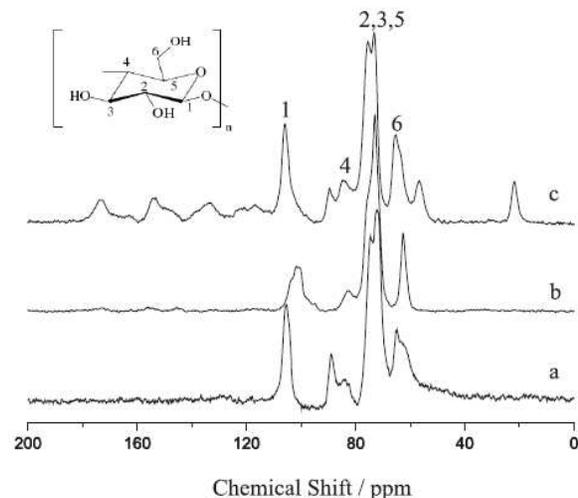


Figure 3.  $^{13}\text{C}$  NMR spectra of cellulose (a), and of the mesocarp (b) and epicarp (c) of babassu fruit.

X-ray diffraction patterns for cellulose and the lignocellulosic components are shown in Figure 4. The diffractogram for cellulose, as shown in Figure 4 (a), is similar to that given by the epicarp, in Figure 4 (c). In fact, the diffraction pattern in 4c probably come from the cellulosic constituents, as observed for a main peak at about  $2\theta = 22^\circ$ . For mesocarp, Figure 4 (b), the principal difference is related to two peaks around  $16^\circ$ . In the two babassu components, two peaks are noted in this region when the cellulose content is high, but when the fiber contains an increased amount of amorphous components such as lignin, hemicelluloses and amorphous cellulose, the two peaks are smeared and appear as a single broad feature like that shown for epicarp in Figure 4 (c).<sup>36</sup>

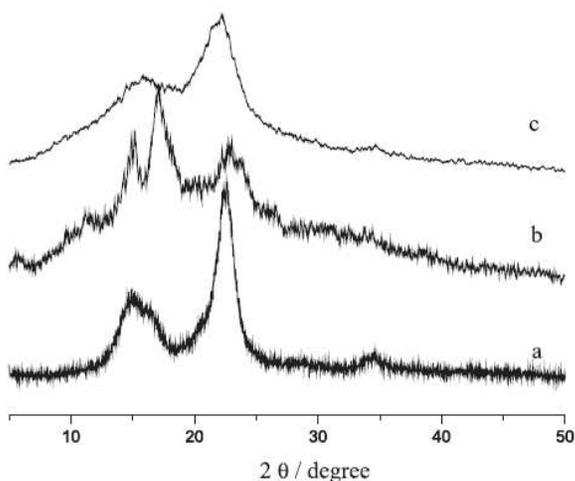


Figure 4. X-ray diffraction patterns of cellulose (a), and of the mesocarp (b) and epicarp (c) of babassu fruit.

The thermogravimetric curves obtained in an inert atmosphere for cellulose, mesocarp and epicarp are shown in Figure 5. Cellulose gave only one event in the

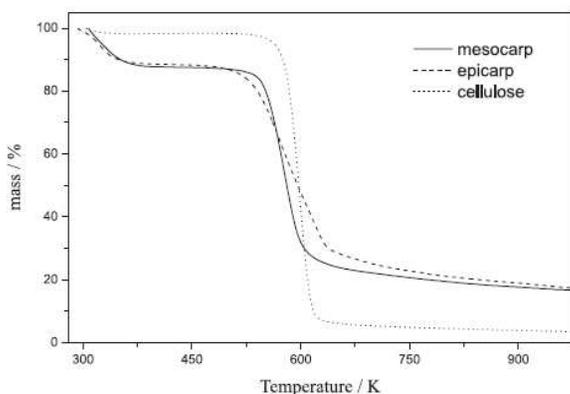


Figure 5. TGA curves obtained for cellulose and for the mesocarp and epicarp of the babassu fruit in an inert atmosphere.

decomposition process covering the interval of temperature from 536 to 647 K, corresponding to a mass loss of 92%.<sup>35</sup> For mesocarp the first stage, up to 375 K, corresponds to the mass loss of 12%, followed by another mass loss of 62% in the 477 to 623 K interval. Epicarp showed mass losses of 11% at 353 K and of 56% between 609 and 638 K, for the same experimental conditions. The first step of decomposition can be attributed to the release of low mass carbon-rich molecules and sorbed water, while the second stage is due to the decomposition of organic material, for example breakdown of fibers with caramel and graphene formation, resembling other lignocellulosic materials whose main components are cellulose, lignin and hemicelluloses.<sup>36,39</sup>

### Adsorption

The curves of adsorption of Turquoise Remazol dye by mesocarp and epicarp as a function of time are shown in Figure 6. For these materials, the adsorption process reached equilibrium in 20 and 60 min, respectively,

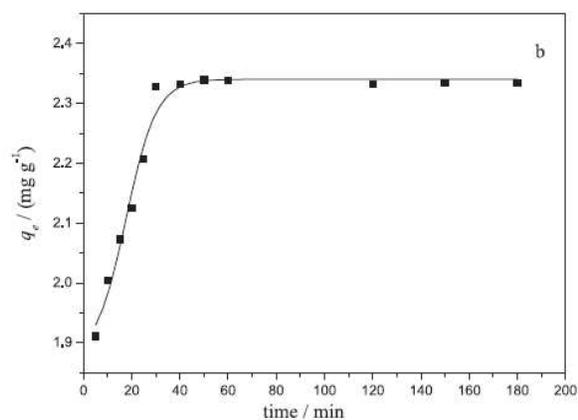
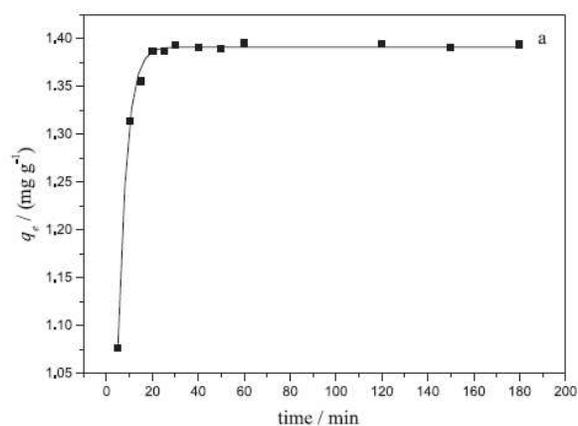


Figure 6. Kinetics of the adsorption of Turquoise Remazol onto mesocarp (a) and epicarp (b) of babassu fruit at  $298 \pm 1$  K and pH 6.0.

remaining constant for 3 h. The adsorption data were fitted to pseudo first-order and pseudo second-order kinetic models. The pseudo first-order model presented lower linear correlation coefficients for mesocarp and epicarp (results not shown), with  $q_e$  values of 0.03 and 0.17  $\text{mg g}^{-1}$ , with greater discrepancy in relation to the experimental  $q_e$  values.

The best correlation coefficients for mesocarp ( $R = 0.999$ ) and epicarp ( $R = 0.999$ ) were provided by the pseudo second-order model, indicating chemisorption as the determinant stage in the adsorption mechanism, as shown in Figure 7. The results obtained with the pseudo second-order model are shown in Table 1, which gives the rate constants  $k_2$  of 1.43 and 0.31  $\text{g mg}^{-1} \text{min}^{-1}$  for mesocarp and epicarp, respectively.

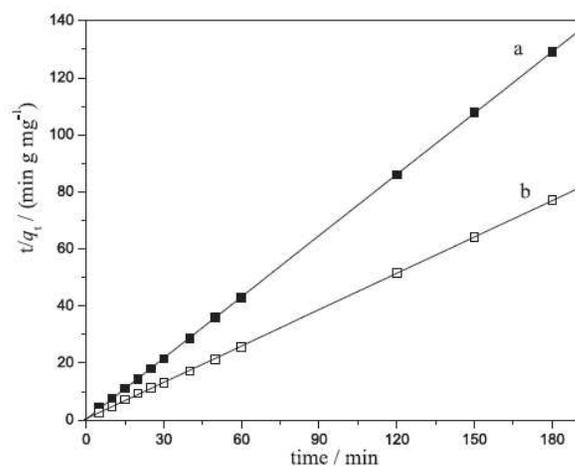


Figure 7. Pseudo-second order model curve for the adsorption of Turquoise Remazol onto mesocarp (a) and epicarp (b) of babassu fruit.

The  $q_e$  values obtained from equation 3 and the slopes of 1.40 and 2.36  $\text{mg g}^{-1}$  demonstrated good agreement with the experimental values of 1.44 and 2.38  $\text{mg g}^{-1}$ . From the  $k_2$  and  $q_e$  values, the initial adsorption rates ( $h$ ) were determined as 2.8 and 1.7  $\text{mg g}^{-1} \text{min}^{-1}$  by equation 6. Thus, the initial adsorption on mesocarp was nearly two times greater than on epicarp.

$$h = k_2 \times q_e^2 \quad (6)$$

Table 1. Kinetic parameters determined for Turquoise Remazol adsorption onto mesocarp and epicarp of the babassu coconut using pseudo first-order and pseudo second-order equations

| Biomass  | $q_{e,exp}/(\text{mg g}^{-1})$ | Pseudo First-order                  |                            |       | Pseudo Second-order                        |                            |       |  |
|----------|--------------------------------|-------------------------------------|----------------------------|-------|--|----------------------------|-------|--|
|          |                                | $k_1 \times 10^2 / \text{min}^{-1}$ | $q_e / (\text{mg g}^{-1})$ | $R^2$ | $k_2 / (\text{g mg}^{-1} \text{min}^{-1})$ | $q_e / (\text{mg g}^{-1})$ | $R^2$ | $h / (\text{mg g}^{-1} \text{min}^{-1})$ |
| Mesocarp | 1.44                           | 2.1                                 | 0.03                       | 0.701 | 1.43                                       | 1.40                       | 0.999 | 2.8                                      |
| Epicarp  | 2.38                           | 2.7                                 | 0.17                       | 0.766 | 0.31                                       | 2.36                       | 0.999 | 1.7                                      |

The kinetics of adsorption of many dyes onto various materials is frequently found to be of second-order.<sup>30</sup> The applicability of the pseudo second-order model suggests that chemisorption might be the rate-limiting step that controls the adsorption processes. In general, this model has the following advantage: the adsorption capacity, the pseudo second-order rate constant and the initial adsorption rate can be determined.<sup>40</sup>

The adsorption isotherm represents the concentrations of dye sorbed at equilibrium ( $q_e$ ) according to the amount adsorbed per gram of sorbent. Profiles of the isotherm of Turquoise Remazol adsorption from aqueous solution on mesocarp and epicarp are shown in Figure 8.

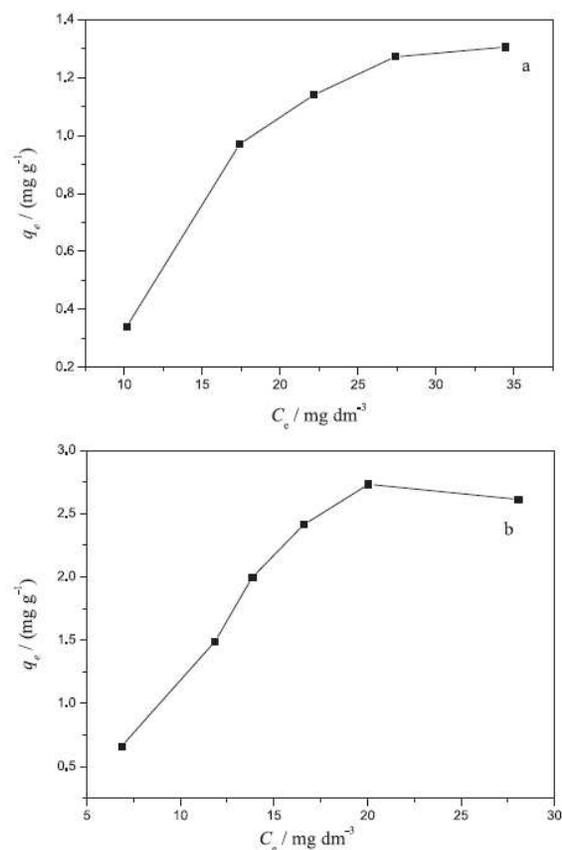


Figure 8. Isotherm of Turquoise Remazol adsorption onto mesocarp (a) and epicarp (b) of babassu fruit at  $298 \pm 1 \text{ K}$  and  $\text{pH } 6.0$ .

From the adsorption curves the plateau was progressively approached as the concentration investigated increased. Thus, the maximum quantity of the dye sorbed by these matrices was 1.44 and 2.38 mg g<sup>-1</sup> for mesocarp and epicarp, respectively.

Analyses of correlation coefficients showed that the Freundlich isotherm provided the best fit for experimental data for both epicarp and mesocarp. The results are listed in Table 2, which was obtained from linearizations following the Freundlich model (Figure S1, Electronic Supplementary Information). The parameters  $n$  and  $K_f$ , the constants of the system, which act as indicators of adsorption capacity and intensity, respectively, were determined from the intercept and the slope of the straight line equation obtained by plotting  $\log q_e$  versus  $\log C_e$ .

**Table 2.** Parameters determined from Freundlich isotherms for adsorption onto the mesocarp and epicarp of babassu fruit

| Biomass  | $n$  | $K_f$ | $R^2$ |
|----------|------|-------|-------|
| Mesocarp | 0.90 | 0.03  | 0.931 |
| Epicarp  | 0.96 | 0.11  | 0.923 |

The results from the Langmuir model presented a poor linear fit for dye adsorption on both epicarp and mesocarp. Babassu mesocarp and fly ash, as low-cost sorbents, have been investigated for the removal of several dyes. The results obtained also indicated that the Freundlich adsorption isotherm fit the data better than the Langmuir analogue.<sup>30,41</sup> Calcium-rich fly ash was studied for the adsorption of Congo Red from aqueous solution and the author reported that the adsorption process obeyed the pseudo second-order kinetic model and the adsorption isotherm followed the Freundlich model.<sup>42</sup> On the other hand, the adsorption of Brilliant Green on Neem leaf powder yielded good fits with the Langmuir isotherm as well as the empirical Freundlich isotherm.<sup>43</sup> However, the Freundlich equation was preferred for the description of the isotherms of reactive dyes although the isotherms of acidic and basic dyes were better fitted by the Langmuir model, depending on the dye concentration. These investigations confirm that the empirical Freundlich equation is applicable to the adsorption of single solutes within a fixed range of concentration.<sup>8</sup>

#### Effect of pH

The adsorption of Turquoise Remazol by the mesocarp and epicarp of babassu increases considerably as the acidity is increased, as shown in Figure 9.

According to these results, the optimal sample pH for dye removal is apparently 1.0. In this condition,

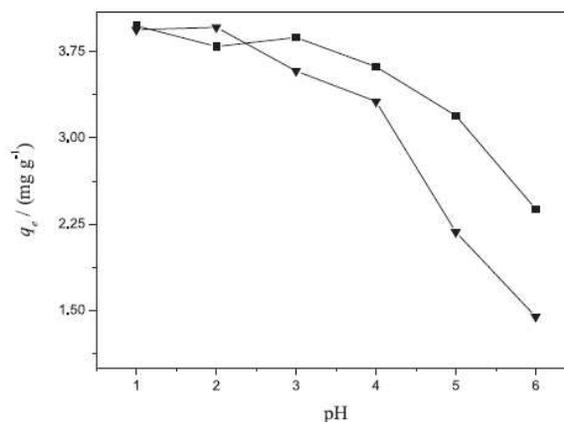


**Figure 9.** Effect of pH on the adsorption of Turquoise Remazol dye onto mesocarp (▼) and epicarp (■) of babassu fruit at 298 ± 1 K.

the maximum quantities of the dye sorbed were 3.94 and 3.97 mg g<sup>-1</sup>, which correspond to 96.6 and 99.5% for mesocarp and epicarp, respectively. Although the adsorption at pH 6.0 gave lower values of 1.44 and 2.38 mg g<sup>-1</sup>, it seems the more appropriate condition for applications to normal aqueous solutions.

A similar trend was observed for the adsorption of Direct Red onto banana pith,<sup>44</sup> which had a maximum removal of 80% at an initial pH of 3.0. For Congo Red adsorption on coir pith two possible mechanisms for the effect of pH were proposed: (a) electrostatic interaction between the possible unprotonated groups and the acidic dye and (b) chemical reaction between the sorbate and the sorbent.<sup>45</sup> Similar results of pH effect were also reported for the adsorption of Acid Yellow 36 and Reactive Red 189.<sup>46-48</sup>

The main components of the mesocarp and epicarp are cellulose, lignin and hemicelluloses. These natural products contain a large number of functional groups, including phenolic OH as well as carboxylic groups. The interaction of the dye molecules with these functional groups may follow an extremely complicated pattern. As the pH of the system decreases, the number of negatively charged surface sites also decreases, with a consequent increase of the number of positive sites on the same surface, which favors the adsorption of anionic dyes due to electrostatic attraction, as is expected for the electroneutralization process.

As mentioned previously, lignocellulosic materials have been studied extensively as sorbents for dye removal. However, there is still much to be accomplished in understanding the mechanisms. In particular, dye molecules have many different and complicated structures and this is one of the most important factors that influence adsorptions and their mechanisms.<sup>1,5</sup> However, some suggestions are made by taking into account the biopolymer composition and the chromophores to be sorbed. As

reported here, in mesocarp and epicarp of the babassu fruit the major functional groups are capable of establishing interactions such as hydrogen bonds and aromatic ring  $\pi$ - $\pi$  interactions, as well as van der Waals interactions. Here the establishment of hydrogen bonds between protons or non-bonding electron pairs on lignocellulosic material with the available  $\pi$  electrons of the double bond or the acidic centers on dyes is proposed. Another possibility is to consider that the aromatic rings present in the lignin may interact with the acidic copper located in the dye structure of Turquoise Remazol.

## Conclusions

X-ray diffraction studies showed that the mesocarp and epicarp components obtained from babassu fruits present a low crystallinity fraction, as observed for other lignocellulosic materials. This result is also supported by  $^{13}\text{C}$  NMR data, where mesocarp signals present chemical shifts similar to those attributed to cellulose, while epicarp shows characteristic lignin signals. Thermal analysis of the fibers revealed that the degradation processes occur according to their cellulose, hemicellulose and lignin constituents. FTIR studies reveal structural features such as O-H and C-H stretching that are characteristic of the chemical fractions of the materials, which can sorb Turquoise Remazol dye in a process that depends on pH. The kinetics of adsorption is described by the pseudo second-order model and the isotherms fit the Freundlich model. Based on the significant adsorption capacity shown by this new material for Turquoise Remazol removal, it can then be proposed as an alternative inexpensive sorbent from aqueous solutions. On the other hand, the adsorption capacity was higher for epicarp, suggesting possible selectivity due to its higher quantities of available functional groups. Taking into account this set of results, it is reasonable to infer that the babassu fruit components may have many potential applications in dye removal. Additional studies are required to fully exploit this possibility, resulting in significant social benefits.

## Supplementary Information

Supplementary data are available free of charge at <http://jbcs.sbq.org.br>, as PDF file.

## Acknowledgments

The authors acknowledge CAPES for financial support, the Indústria de Toalhas São Carlos for the gift of the dye sample, FAPEMA for a fellowship to A. P. V. and CNPq for a fellowship to C. A.

## References

1. Crini, G.; *Bioresour. Technol.* **2006**, *97*, 1061.
2. Guarantini, C. I.; Zanoni, M. V. B.; *Quim. Nova* **2000**, *23*, 71.
3. McKay, G.; Otterburn, M. S.; Aga, D. A.; *Water Air Soil. Pollut.* **1985**, *24*, 307.
4. Langlais, B.; Legube, B.; Beuffe, H.; Doré, M.; *Water Sci. Technol.* **1992**, *25*, 135.
5. Gupta, V. K.; Suhas; *J. Environ. Managem.* **2009**, *90*, 2313.
6. Figueiredo, S. A.; Boaventura, R. A.; Loureiro, J. M.; *Sep. Purif. Technol.* **2000**, *20*, 129.
7. Langmuir, I.; *J. Am. Chem. Soc.* **1916**, *38*, 2221.
8. Freundlich, H. M. F.; *Z. Phys.* **1906**, *57A*, 385.
9. Lima, I. S.; Ribeiro, E. S.; Airoidi, C.; *Quim. Nova.* **2006**, *29*, 501.
10. Özacar, M.; Sengil, A. I.; *Bioresour. Technol.* **2005**, *96*, 791.
11. Chuah, T. G.; Jumariah, A.; Azni, I.; Katayon, S.; Choong, S. T. Y.; *Desalination* **2005**, *175*, 305.
12. Morais, L. C.; Freitas, O. M.; Gonçalves, E. P.; Vasconcelos, L. T.; González Beça, C. G.; *Water Res.* **1999**, *33*, 979.
13. Arami, M.; Limaee, N. Y.; Mahmoodia, N. M.; Tabrizi, N. S.; *J. Hazard. Mater.* **2006** *B135*, 171.
14. Crini, G.; *Prog. Polym. Sci.* **2005**, *30*, 38.
15. Cestari, A. R.; Vieira, E. R. S.; Santos, A. G. P.; Mota, J. A.; Almeida, V. P.; *J. Colloid Interface Sci.* **2004**, *280*, 380.
16. Poots, V. J. P.; McKay, G.; Healy, J. J.; *Water Res.* **1976**, *10*, 1061.
17. Kamel, M. M.; Magda, M. K.; Youseef, B. M.; Waly, A.; *Am. Dyestuff Rep.* **1991**, *80*, 34.
18. Robinson, T.; Chandran, B.; Nigam, P.; *Environ. Int.* **2002**, *28*, 29.
19. Bhattacharyya, K. G.; Sharma, A.; *Dyes Pigment.* **2005**, *65*, 51.
20. Pirillo S.; Pedroni V.; Rueda E.; Ferreira, M. L.; *Quim. Nova.* **2009**, *32*, 1239.
21. Lima, E. C.; Royer, B.; Vaghtti, J. C. P.; Simon, N. M.; Cunha, B. M.; Pavan, F. A.; Benvenuti, E. V.; Cataluña-Veses, R.; Airoidi, C.; *J. Hazard. Mater.* **2008**, *155*, 536.
22. Albiero, D.; Maciel, A. J. S.; Lopes, A. C.; Mello, C. A.; Gamero, C. A.; *Acta Amaz.* **2007**, *37*, 337.
23. Teixeira, M. A.; *Biomass Bioenergy* **2008**, *32*, 857.
24. Teixeira, M. A.; Carvalho, M. G.; *Energy* **2007**, *32*, 999.
25. Freitas, L.; Da Ró, P. C. M.; Santos, J. C.; Castro, H. F.; *Process Biochem.* **2009**, *44*, 1068.
26. Silva, B. P.; Parente, B. P.; *Fitoterapia* **2001**, *72*, 887.
27. Batista, C. P.; Torres, O. J. M.; Matias, J. E. F.; Moreira, A. T. R.; Colman, D.; Lima, J. H. F.; Macri, M. M.; Rauen Jr, R. J.; Ferreira, L. M.; Freitas, A. C. T.; *Acta Cir. Bras.* **2006**, *21*, 26.
28. Azevedo, A. P. S.; Farias, J. C.; Costa, G. C.; Ferreira, S. C. P.; Aragão-Filho, W. C.; Sousa, P. R. A.; Pinheiro, M. T.; Maciel, M. C. G.; Silva, L. A.; Lopes, A. S.; Barroqueiro, E. S. B.; Borges, M. O. R.; Guerra, R. N. M.; Nascimento, F. R. F.; *J. Ethnopharm.* **2007**, *111*, 155.

29. Brito Filho, S. B.; Matias, J. E. F.; Stahlke Júnior, H. J.; Torres, O. J. M.; Timi, J. R. R.; Tenório, S. B.; Tãmbara, E. M.; Carstens, Â. G.; Campos, R. V.; Myamoto, M.; *Acta Cir. Bras.* **2006**, *21*, 76.
30. Vieira, A. P.; Santana, S. A. A.; Bezerra, C. W. B.; Silva, H. A. S.; Chaves, J. A. P.; Melo, J. C. P.; da Silva Filho, E. C.; Airoidi, C.; *J. Hazard. Mater.* **2009**, *166*, 1272.
31. Santana, S. A. A.; Vieira, A. P.; da Silva Filho, E. C.; Melo, J. C. P.; Airoidi, C.; *J. Hazard. Mater.* **2010**, *174*, 119.
32. Osugi, M. E.; Umbuzeiro, G. A.; Anderson, M. A.; Zandoni, M. V. B.; *Electrochim. Acta* **2005**, *50*, 5261.
33. Allen, S. J.; Gan, Q.; Matthews, R.; Johnson, P. A.; *J. Colloid Interface Sci.*, **2005**, *286*, 101.
34. Alley, E. R.; *Water Quality Control Handbook*, McGraw Hill: New York, 2000, p.125.
35. da Silva Filho, E. C.; de Melo, J. C. P.; Airoidi, C.; *Carbohydr. Res.* **2006**, *341*, 2842.
36. Tserki, V.; Matzinos, P.; Kokkou, S.; Panayiotou, C.; *Composites A*, **2005**, *36*, 965.
37. Melo, J. C. P.; da Silva Filho, E. C.; Santana, S. A. A.; Airoidi, C.; *Colloids Surf. A*, **2009**, *346*, 138.
38. Pavia, D. L.; Bassler, G. M.; Morrill, T. C.; *Introduction to Spectroscopy*, 2<sup>nd</sup> ed., Saunders College: New York, 1996.
39. Satyanarayana, K. G.; Guimarães, J. L.; Wypych, F.; *Composites A* **2007**, *38*, 1694.
40. Ho, Y. S.; *J. Hazard. Mater.* **2006**, *B136*, 681.
41. Mohan, D.; Singh, K. P.; Singh, G.; Kumar, K.; *Ind. Eng. Chem. Res.* **2002**, *41*, 3688.
42. Acemioglu, B.; *J. Colloid Interface Sci.* **2004**, *274*, 371.
43. Bhattacharyya, K. G.; Sarma, A.; *Dyes Pigm.* **2003**, *57*, 211.
44. Namasivayam, C.; Prabha, D.; Kumutha, M.; *Bioresour. Technol.* **1998**, *64*, 77.
45. Namasivayam, C.; Kavitha, D.; *Dyes Pigm.* **2002**, *54*, 47.
46. Yuzhu, F.; Viraraghavan, T.; *Adv. Environ. Res.* **2002**, *7*, 239.
47. Malik, P. K.; *Dyes Pigm.* **2003**, *56*, 239.
48. Chiou, M. S.; Li, H. Y.; *J. Hazard. Mater.* **2002**, *B93*, 233.

Submitted: March 3, 2010

Published online: July 22, 2010

FAPESP has sponsored the publication of this article.

### 11 Licenças das publicações

| ELSEVIER LICENSE<br>TERMS AND CONDITIONS  |  | Dec 18, 2012 |
|---|--|--------------|
| <p>This is a License Agreement between Claudio Airoidi ("You") and Elsevier ("Elsevier") provided by Copyright Clearance Center ("CCC"). The license consists of your order details, the terms and conditions provided by Elsevier, and the payment terms and conditions.</p> |  |              |
| <b>All payments must be made in full to CCC. For payment instructions, please see information listed at the bottom of this form.</b>  |  |              |
| Supplier  | Elsevier Limited<br>The Boulevard, Langford Lane<br>Kidlington, Oxford, OX5 1GB, UK                                      |              |
| Registered Company Number   | 1982084  |              |
| Customer name   | Claudio Airoidi  |              |
| Customer address  | Chemistry institute, Unicamp, A1-100<br>Campinas, São Paulo 13083970   |              |
| License number  | 3051900065965  |              |
| License date  | Dec 18, 2012   |              |
| Licensed content publisher  | Elsevier   |              |
| Licensed content publication  | Colloids and Surfaces A: Physicochemical and Engineering Aspects   |              |
| Licensed content title  | Maleic anhydride incorporated onto cellulose and thermodynamics of cation-exchange process at the solid/liquid interface |              |
| Licensed content author   | Júlio C.P. de Melo, Edson C. da Silva Filho, Sirlane A.A. Santana, Claudio Airoidi                                       |              |
| Licensed content date   | 20 August 2009   |              |
| Licensed content volume number  | 346  |              |
| Licensed content issue number   | 1-3  |              |
| Number of pages   | 8  |              |
| Start Page  | 138  |              |
| End Page  | 145  |              |
| Type of Use   | reuse in a thesis/dissertation   |              |
| Portion   | full article   |              |
| Format  | both print and electronic  |              |
| Are you the author of this Elsevier article?  | Yes  |              |
| Will you be translating?  | No   |              |
| Order reference number  |  |              |
| Title of your thesis/dissertation   | Cellulose and Lignocellulosics as supports toward contaminants removal form liquids                                      |              |

## Anexo 1 - Artigos Publicados

|                                  |                   |
|----------------------------------|-------------------|
| Expected completion date         | Dec 2012          |
| Estimated size (number of pages) | 129               |
| Elsevier VAT number              | GB 494 6272 12    |
| Permissions price                | 0.00 USD          |
| VAT/Local Sales Tax              | 0.0 USD / 0.0 GBP |
| Total                            | 0.00 USD          |
| Terms and Conditions             |                   |

### INTRODUCTION

1. The publisher for this copyrighted material is Elsevier. By clicking "accept" in connection with completing this licensing transaction, you agree that the following terms and conditions apply to this transaction (along with the Billing and Payment terms and conditions established by Copyright Clearance Center, Inc. ("CCC"), at the time that you opened your Rightslink account and that are available at any time at <http://myaccount.copyright.com>).

### GENERAL TERMS

2. Elsevier hereby grants you permission to reproduce the aforementioned material subject to the terms and conditions indicated.

3. Acknowledgement: If any part of the material to be used (for example, figures) has appeared in our publication with credit or acknowledgement to another source, permission must also be sought from that source. If such permission is not obtained then that material may not be included in your publication/copies. Suitable acknowledgement to the source must be made, either as a footnote or in a reference list at the end of your publication, as follows:

"Reprinted from Publication title, Vol /edition number, Author(s), Title of article / title of chapter, Pages No., Copyright (Year), with permission from Elsevier [OR APPLICABLE SOCIETY COPYRIGHT OWNER]." Also Lancet special credit - "Reprinted from The Lancet, Vol. number, Author(s), Title of article, Pages No., Copyright (Year), with permission from Elsevier."

4. Reproduction of this material is confined to the purpose and/or media for which permission is hereby given.

5. Altering/Modifying Material: Not Permitted. However figures and illustrations may be altered/adapted minimally to serve your work. Any other abbreviations, additions, deletions and/or any other alterations shall be made only with prior written authorization of Elsevier Ltd. (Please contact Elsevier at [permissions@elsevier.com](mailto:permissions@elsevier.com))

6. If the permission fee for the requested use of our material is waived in this instance, please be advised that your future requests for Elsevier materials may attract a fee.

7. Reservation of Rights: Publisher reserves all rights not specifically granted in the combination of (i) the license details provided by you and accepted in the course of this licensing transaction, (ii) these terms and conditions and (iii) CCC's Billing and Payment terms and conditions.

8. License Contingent Upon Payment: While you may exercise the rights licensed immediately upon issuance of the license at the end of the licensing process for the transaction, provided that you have

disclosed complete and accurate details of your proposed use, no license is finally effective unless and until full payment is received from you (either by publisher or by CCC) as provided in CCC's Billing and Payment terms and conditions. If full payment is not received on a timely basis, then any license preliminarily granted shall be deemed automatically revoked and shall be void as if never granted. Further, in the event that you breach any of these terms and conditions or any of CCC's Billing and Payment terms and conditions, the license is automatically revoked and shall be void as if never granted. Use of materials as described in a revoked license, as well as any use of the materials beyond the scope of an unrevoked license, may constitute copyright infringement and publisher reserves the right to take any and all action to protect its copyright in the materials.

9. **Warranties:** Publisher makes no representations or warranties with respect to the licensed material.

10. **Indemnity:** You hereby indemnify and agree to hold harmless publisher and CCC, and their respective officers, directors, employees and agents, from and against any and all claims arising out of your use of the licensed material other than as specifically authorized pursuant to this license.

11. **No Transfer of License:** This license is personal to you and may not be sublicensed, assigned, or transferred by you to any other person without publisher's written permission.

12. **No Amendment Except in Writing:** This license may not be amended except in a writing signed by both parties (or, in the case of publisher, by CCC on publisher's behalf).

13. **Objection to Contrary Terms:** Publisher hereby objects to any terms contained in any purchase order, acknowledgment, check endorsement or other writing prepared by you, which terms are inconsistent with these terms and conditions or CCC's Billing and Payment terms and conditions. These terms and conditions, together with CCC's Billing and Payment terms and conditions (which are incorporated herein), comprise the entire agreement between you and publisher (and CCC) concerning this licensing transaction. In the event of any conflict between your obligations established by these terms and conditions and those established by CCC's Billing and Payment terms and conditions, these terms and conditions shall control.

14. **Revocation:** Elsevier or Copyright Clearance Center may deny the permissions described in this License at their sole discretion, for any reason or no reason, with a full refund payable to you. Notice of such denial will be made using the contact information provided by you. Failure to receive such notice will not alter or invalidate the denial. In no event will Elsevier or Copyright Clearance Center be responsible or liable for any costs, expenses or damage incurred by you as a result of a denial of your permission request, other than a refund of the amount(s) paid by you to Elsevier and/or Copyright Clearance Center for denied permissions.

### LIMITED LICENSE

The following terms and conditions apply only to specific license types:

15. **Translation:** This permission is granted for non-exclusive world **English** rights only unless your license was granted for translation rights. If you licensed translation rights you may only translate this content into the languages you requested. A professional translator must perform all translations and reproduce the content word for word preserving the integrity of the article. If this license is to re-use 1 or 2 figures then permission is granted for non-exclusive world rights in all languages.

## Anexo 1 - Artigos Publicados

16. **Website:** The following terms and conditions apply to electronic reserve and author websites:  
**Electronic reserve:** If licensed material is to be posted to website, the web site is to be password-protected and made available only to bona fide students registered on a relevant course if:

This license was made in connection with a course,

This permission is granted for 1 year only. You may obtain a license for future website posting, All content posted to the web site must maintain the copyright information line on the bottom of each image,

A hyper-text must be included to the Homepage of the journal from which you are licensing at <http://www.sciencedirect.com/science/journal/xxxxx> or the Elsevier homepage for books at <http://www.elsevier.com> , and

Central Storage: This license does not include permission for a scanned version of the material to be stored in a central repository such as that provided by Heron/XanEdu.

17. **Author website** for journals with the following additional clauses:

All content posted to the web site must maintain the copyright information line on the bottom of each image, and the permission granted is limited to the personal version of your paper. You are not allowed to download and post the published electronic version of your article (whether PDF or HTML, proof or final version), nor may you scan the printed edition to create an electronic version.

A hyper-text must be included to the Homepage of the journal from which you are licensing at <http://www.sciencedirect.com/science/journal/xxxxx> . As part of our normal production process, you will receive an e-mail notice when your article appears on Elsevier's online service ScienceDirect ([www.sciencedirect.com](http://www.sciencedirect.com)). That e-mail will include the article's Digital Object Identifier (DOI). This number provides the electronic link to the published article and should be included in the posting of your personal version. We ask that you wait until you receive this e-mail and have the DOI to do any posting.

Central Storage: This license does not include permission for a scanned version of the material to be stored in a central repository such as that provided by Heron/XanEdu.

18. **Author website** for books with the following additional clauses:

Authors are permitted to place a brief summary of their work online only.

A hyper-text must be included to the Elsevier homepage at <http://www.elsevier.com> . All content posted to the web site must maintain the copyright information line on the bottom of each image. You are not allowed to download and post the published electronic version of your chapter, nor may you scan the printed edition to create an electronic version.

Central Storage: This license does not include permission for a scanned version of the material to be stored in a central repository such as that provided by Heron/XanEdu.

19. **Website** (regular and for author): A hyper-text must be included to the Homepage of the journal from which you are licensing at <http://www.sciencedirect.com/science/journal/xxxxx> . or for books to the Elsevier homepage at <http://www.elsevier.com>

20. **Thesis/Dissertation:** If your license is for use in a thesis/dissertation your thesis may be submitted to your institution in either print or electronic form. Should your thesis be published commercially, please reapply for permission. These requirements include permission for the Library and Archives of Canada to supply single copies, on demand, of the complete thesis and include permission for UMI to supply single copies, on demand, of the complete thesis. Should your thesis

## Anexo 1 - Artigos Publicados

be published commercially, please reapply for permission.

### 21. Other Conditions:

v1.6

**If you would like to pay for this license now, please remit this license along with your payment made payable to "COPYRIGHT CLEARANCE CENTER" otherwise you will be invoiced within 48 hours of the license date. Payment should be in the form of a check or money order referencing your account number and this invoice number RLNK500919347. Once you receive your invoice for this order, you may pay your invoice by credit card. Please follow instructions provided at that time.**

**Make Payment To:  
Copyright Clearance Center  
Dept 001  
P.O. Box 843006  
Boston, MA 02284-3006**

**For suggestions or comments regarding this order, contact RightsLink Customer Support: [customercare@copyright.com](mailto:customercare@copyright.com) or +1-877-622-5543 (toll free in the US) or +1-978-646-2777.**

**Gratis licenses (referencing \$0 in the Total field) are free. Please retain this printable license for your reference. No payment is required.**

# Anexo 1 - Artigos Publicados

## ELSEVIER LICENSE TERMS AND CONDITIONS

Dec 18, 2012

This is a License Agreement between Claudio Airoidi ("You") and Elsevier ("Elsevier") provided by Copyright Clearance Center ("CCC"). The license consists of your order details, the terms and conditions provided by Elsevier, and the payment terms and conditions.

**All payments must be made in full to CCC. For payment instructions, please see information listed at the bottom of this form.**

|  |  |
|--|--|
| Supplier                                     | Elsevier Limited<br>The Boulevard, Langford Lane<br>Kidlington, Oxford, OX5 1GB, UK                                    |
| Registered Company Number                    | 1982084  |
| Customer name                                | Claudio Airoidi  |
| Customer address                             | Chemistry institute, Unicamp, A1-100<br>Campinas, São Paulo 13083970   |
| License number                               | 3051910543208  |
| License date                                 | Dec 18, 2012   |
| Licensed content publisher                   | Elsevier   |
| Licensed content publication                 | Thermochimica Acta   |
| Licensed content title                       | Synthesized cellulose/succinic anhydride as an ion exchanger.<br>Calorimetry of divalent cations in aqueous suspension |
| Licensed content author                      | Júlio C.P. Melo, Edson C. Silva Filho, Sirlane A.A. Santana, Claudio Airoidi   |
| Licensed content date                        | 20 September 2011  |
| Licensed content volume number               | 524  |
| Licensed content issue number                | 1-2  |
| Number of pages                              | 6  |
| Start Page                                   | 29   |
| End Page                                     | 34   |
| Type of Use                                  | reuse in a thesis/dissertation   |
| Portion                                      | full article   |
| Format                                       | both print and electronic  |
| Are you the author of this Elsevier article? | Yes  |
| Will you be translating?                     | No   |
| Order reference number                       |  |
| Title of your thesis/dissertation            | Cellulose and Lignocellulosics as supports toward contaminants removal from liquids                                    |

## Anexo 1 - Artigos Publicados

|                                      |                   |
|--------------------------------------|-------------------|
| Expected completion date             | Dec 2012          |
| Estimated size (number of pages)     | 129               |
| Elsevier VAT number                  | GB 494 6272 12    |
| Permissions price                    | 0.00 USD          |
| VAT/Local Sales Tax                  | 0.0 USD / 0.0 GBP |
| Total                                | 0.00 USD          |
| <a href="#">Terms and Conditions</a> |                   |

### INTRODUCTION

1. The publisher for this copyrighted material is Elsevier. By clicking "accept" in connection with completing this licensing transaction, you agree that the following terms and conditions apply to this transaction (along with the Billing and Payment terms and conditions established by Copyright Clearance Center, Inc. ("CCC"), at the time that you opened your Rightslink account and that are available at any time at <http://myaccount.copyright.com>).

### GENERAL TERMS

2. Elsevier hereby grants you permission to reproduce the aforementioned material subject to the terms and conditions indicated.

3. Acknowledgement: If any part of the material to be used (for example, figures) has appeared in our publication with credit or acknowledgement to another source, permission must also be sought from that source. If such permission is not obtained then that material may not be included in your publication/copies. Suitable acknowledgement to the source must be made, either as a footnote or in a reference list at the end of your publication, as follows:

"Reprinted from Publication title, Vol /edition number, Author(s), Title of article / title of chapter, Pages No., Copyright (Year), with permission from Elsevier [OR APPLICABLE SOCIETY COPYRIGHT OWNER]." Also Lancet special credit - "Reprinted from The Lancet, Vol. number, Author(s), Title of article, Pages No., Copyright (Year), with permission from Elsevier."

4. Reproduction of this material is confined to the purpose and/or media for which permission is hereby given.

5. Altering/Modifying Material: Not Permitted. However figures and illustrations may be altered/adapted minimally to serve your work. Any other abbreviations, additions, deletions and/or any other alterations shall be made only with prior written authorization of Elsevier Ltd. (Please contact Elsevier at [permissions@elsevier.com](mailto:permissions@elsevier.com))

6. If the permission fee for the requested use of our material is waived in this instance, please be advised that your future requests for Elsevier materials may attract a fee.

7. Reservation of Rights: Publisher reserves all rights not specifically granted in the combination of (i) the license details provided by you and accepted in the course of this licensing transaction, (ii) these terms and conditions and (iii) CCC's Billing and Payment terms and conditions.

8. License Contingent Upon Payment: While you may exercise the rights licensed immediately upon issuance of the license at the end of the licensing process for the transaction, provided that you have

## Anexo 1 - Artigos Publicados

disclosed complete and accurate details of your proposed use, no license is finally effective unless and until full payment is received from you (either by publisher or by CCC) as provided in CCC's Billing and Payment terms and conditions. If full payment is not received on a timely basis, then any license preliminarily granted shall be deemed automatically revoked and shall be void as if never granted. Further, in the event that you breach any of these terms and conditions or any of CCC's Billing and Payment terms and conditions, the license is automatically revoked and shall be void as if never granted. Use of materials as described in a revoked license, as well as any use of the materials beyond the scope of an unrevoked license, may constitute copyright infringement and publisher reserves the right to take any and all action to protect its copyright in the materials.

9. **Warranties:** Publisher makes no representations or warranties with respect to the licensed material.

10. **Indemnity:** You hereby indemnify and agree to hold harmless publisher and CCC, and their respective officers, directors, employees and agents, from and against any and all claims arising out of your use of the licensed material other than as specifically authorized pursuant to this license.

11. **No Transfer of License:** This license is personal to you and may not be sublicensed, assigned, or transferred by you to any other person without publisher's written permission.

12. **No Amendment Except in Writing:** This license may not be amended except in a writing signed by both parties (or, in the case of publisher, by CCC on publisher's behalf).

13. **Objection to Contrary Terms:** Publisher hereby objects to any terms contained in any purchase order, acknowledgment, check endorsement or other writing prepared by you, which terms are inconsistent with these terms and conditions or CCC's Billing and Payment terms and conditions. These terms and conditions, together with CCC's Billing and Payment terms and conditions (which are incorporated herein), comprise the entire agreement between you and publisher (and CCC) concerning this licensing transaction. In the event of any conflict between your obligations established by these terms and conditions and those established by CCC's Billing and Payment terms and conditions, these terms and conditions shall control.

14. **Revocation:** Elsevier or Copyright Clearance Center may deny the permissions described in this License at their sole discretion, for any reason or no reason, with a full refund payable to you. Notice of such denial will be made using the contact information provided by you. Failure to receive such notice will not alter or invalidate the denial. In no event will Elsevier or Copyright Clearance Center be responsible or liable for any costs, expenses or damage incurred by you as a result of a denial of your permission request, other than a refund of the amount(s) paid by you to Elsevier and/or Copyright Clearance Center for denied permissions.

### LIMITED LICENSE

The following terms and conditions apply only to specific license types:

15. **Translation:** This permission is granted for non-exclusive world **English** rights only unless your license was granted for translation rights. If you licensed translation rights you may only translate this content into the languages you requested. A professional translator must perform all translations and reproduce the content word for word preserving the integrity of the article. If this license is to re-use 1 or 2 figures then permission is granted for non-exclusive world rights in all languages.

## Anexo 1 - Artigos Publicados

16. **Website:** The following terms and conditions apply to electronic reserve and author websites:  
**Electronic reserve:** If licensed material is to be posted to website, the web site is to be password-protected and made available only to bona fide students registered on a relevant course if:

This license was made in connection with a course,

This permission is granted for 1 year only. You may obtain a license for future website posting, All content posted to the web site must maintain the copyright information line on the bottom of each image,

A hyper-text must be included to the Homepage of the journal from which you are licensing at <http://www.sciencedirect.com/science/journal/xxxxx> or the Elsevier homepage for books at <http://www.elsevier.com> , and

Central Storage: This license does not include permission for a scanned version of the material to be stored in a central repository such as that provided by Heron/XanEdu.

17. **Author website** for journals with the following additional clauses:

All content posted to the web site must maintain the copyright information line on the bottom of each image, and the permission granted is limited to the personal version of your paper. You are not allowed to download and post the published electronic version of your article (whether PDF or HTML, proof or final version), nor may you scan the printed edition to create an electronic version.

A hyper-text must be included to the Homepage of the journal from which you are licensing at <http://www.sciencedirect.com/science/journal/xxxxx> . As part of our normal production process, you will receive an e-mail notice when your article appears on Elsevier's online service ScienceDirect ([www.sciencedirect.com](http://www.sciencedirect.com)). That e-mail will include the article's Digital Object Identifier (DOI). This number provides the electronic link to the published article and should be included in the posting of your personal version. We ask that you wait until you receive this e-mail and have the DOI to do any posting.

Central Storage: This license does not include permission for a scanned version of the material to be stored in a central repository such as that provided by Heron/XanEdu.

18. **Author website** for books with the following additional clauses:

Authors are permitted to place a brief summary of their work online only.

A hyper-text must be included to the Elsevier homepage at <http://www.elsevier.com> . All content posted to the web site must maintain the copyright information line on the bottom of each image. You are not allowed to download and post the published electronic version of your chapter, nor may you scan the printed edition to create an electronic version.

Central Storage: This license does not include permission for a scanned version of the material to be stored in a central repository such as that provided by Heron/XanEdu.

19. **Website** (regular and for author): A hyper-text must be included to the Homepage of the journal from which you are licensing at <http://www.sciencedirect.com/science/journal/xxxxx> . or for books to the Elsevier homepage at <http://www.elsevier.com>

20. **Thesis/Dissertation:** If your license is for use in a thesis/dissertation your thesis may be submitted to your institution in either print or electronic form. Should your thesis be published commercially, please reapply for permission. These requirements include permission for the Library and Archives of Canada to supply single copies, on demand, of the complete thesis and include permission for UMI to supply single copies, on demand, of the complete thesis. Should your thesis

## Anexo 1 - Artigos Publicados

---

be published commercially, please reapply for permission.

### 21. Other Conditions:

v1.6

**If you would like to pay for this license now, please remit this license along with your payment made payable to "COPYRIGHT CLEARANCE CENTER" otherwise you will be invoiced within 48 hours of the license date. Payment should be in the form of a check or money order referencing your account number and this invoice number RLNK500919371. Once you receive your invoice for this order, you may pay your invoice by credit card. Please follow instructions provided at that time.**

**Make Payment To:  
Copyright Clearance Center  
Dept 001  
P.O. Box 843006  
Boston, MA 02284-3006**

**For suggestions or comments regarding this order, contact RightsLink Customer Support: [customer@copyright.com](mailto:customer@copyright.com) or +1-877-622-5543 (toll free in the US) or +1-978-646-2777.**

**Gratis licenses (referencing \$0 in the Total field) are free. Please retain this printable license for your reference. No payment is required.**

## ELSEVIER LICENSE TERMS AND CONDITIONS

Dec 18, 2012

This is a License Agreement between Claudio Airoidi ("You") and Elsevier ("Elsevier") provided by Copyright Clearance Center ("CCC"). The license consists of your order details, the terms and conditions provided by Elsevier, and the payment terms and conditions.

**All payments must be made in full to CCC. For payment instructions, please see information listed at the bottom of this form.**

|  |  |
|--|--|
| Supplier                                     | Elsevier Limited<br>The Boulevard, Langford Lane<br>Kidlington, Oxford, OX5 1GB, UK                        |
| Registered Company Number                    | 1982084  |
| Customer name                                | Claudio Airoidi  |
| Customer address                             | Chemistry institute, Unicamp, A1-100<br>Campinas, São Paulo 13083970                                       |
| License number                               | 3051920789805  |
| License date                                 | Dec 18, 2012   |
| Licensed content publisher                   | Elsevier   |
| Licensed content publication                 | Carbohydrate Research  |
| Licensed content title                       | Exploring the favorable ion-exchange ability of phthalylated cellulose biopolymer using thermodynamic data |
| Licensed content author                      | Júlio C.P. de Melo, Edson C. da Silva Filho, Sirlane A.A. Santana, Claudio Airoidi                         |
| Licensed content date                        | 3 September 2010   |
| Licensed content volume number               | 345  |
| Licensed content issue number                | 13   |
| Number of pages                              | 8  |
| Start Page                                   | 1914   |
| End Page                                     | 1921   |
| Type of Use                                  | reuse in a thesis/dissertation   |
| Intended publisher of new work               | other  |
| Portion                                      | full article   |
| Format                                       | both print and electronic  |
| Are you the author of this Elsevier article? | Yes  |
| Will you be translating?                     | No   |
| Order reference number                       |  |

## Anexo 1 - Artigos Publicados

|                                      |   |
|--------------------------------------|---|
| Title of your thesis/dissertation    | Cellulose and Lignocellulosics as supports toward contaminants removal form liquids |
| Expected completion date             | Dec 2012  |
| Estimated size (number of pages)     | 129   |
| Elsevier VAT number                  | GB 494 6272 12  |
| Permissions price                    | 0.00 USD  |
| VAT/Local Sales Tax                  | 0.0 USD / 0.0 GBP   |
| Total                                | 0.00 USD  |
| <a href="#">Terms and Conditions</a> |   |

### INTRODUCTION

1. The publisher for this copyrighted material is Elsevier. By clicking "accept" in connection with completing this licensing transaction, you agree that the following terms and conditions apply to this transaction (along with the Billing and Payment terms and conditions established by Copyright Clearance Center, Inc. ("CCC"), at the time that you opened your Rightslink account and that are available at any time at <http://myaccount.copyright.com>).

### GENERAL TERMS

2. Elsevier hereby grants you permission to reproduce the aforementioned material subject to the terms and conditions indicated.

3. Acknowledgement: If any part of the material to be used (for example, figures) has appeared in our publication with credit or acknowledgement to another source, permission must also be sought from that source. If such permission is not obtained then that material may not be included in your publication/copies. Suitable acknowledgement to the source must be made, either as a footnote or in a reference list at the end of your publication, as follows:

"Reprinted from Publication title, Vol /edition number, Author(s), Title of article / title of chapter, Pages No., Copyright (Year), with permission from Elsevier [OR APPLICABLE SOCIETY COPYRIGHT OWNER]." Also Lancet special credit - "Reprinted from The Lancet, Vol. number, Author(s), Title of article, Pages No., Copyright (Year), with permission from Elsevier."

4. Reproduction of this material is confined to the purpose and/or media for which permission is hereby given.

5. Altering/Modifying Material: Not Permitted. However figures and illustrations may be altered/adapted minimally to serve your work. Any other abbreviations, additions, deletions and/or any other alterations shall be made only with prior written authorization of Elsevier Ltd. (Please contact Elsevier at [permissions@elsevier.com](mailto:permissions@elsevier.com))

6. If the permission fee for the requested use of our material is waived in this instance, please be advised that your future requests for Elsevier materials may attract a fee.

7. Reservation of Rights: Publisher reserves all rights not specifically granted in the combination of (i) the license details provided by you and accepted in the course of this licensing transaction, (ii) these terms and conditions and (iii) CCC's Billing and Payment terms and conditions.

8. License Contingent Upon Payment: While you may exercise the rights licensed immediately upon

issuance of the license at the end of the licensing process for the transaction, provided that you have disclosed complete and accurate details of your proposed use, no license is finally effective unless and until full payment is received from you (either by publisher or by CCC) as provided in CCC's Billing and Payment terms and conditions. If full payment is not received on a timely basis, then any license preliminarily granted shall be deemed automatically revoked and shall be void as if never granted. Further, in the event that you breach any of these terms and conditions or any of CCC's Billing and Payment terms and conditions, the license is automatically revoked and shall be void as if never granted. Use of materials as described in a revoked license, as well as any use of the materials beyond the scope of an unrevoked license, may constitute copyright infringement and publisher reserves the right to take any and all action to protect its copyright in the materials.

9. **Warranties:** Publisher makes no representations or warranties with respect to the licensed material.

10. **Indemnity:** You hereby indemnify and agree to hold harmless publisher and CCC, and their respective officers, directors, employees and agents, from and against any and all claims arising out of your use of the licensed material other than as specifically authorized pursuant to this license.

11. **No Transfer of License:** This license is personal to you and may not be sublicensed, assigned, or transferred by you to any other person without publisher's written permission.

12. **No Amendment Except in Writing:** This license may not be amended except in a writing signed by both parties (or, in the case of publisher, by CCC on publisher's behalf).

13. **Objection to Contrary Terms:** Publisher hereby objects to any terms contained in any purchase order, acknowledgment, check endorsement or other writing prepared by you, which terms are inconsistent with these terms and conditions or CCC's Billing and Payment terms and conditions. These terms and conditions, together with CCC's Billing and Payment terms and conditions (which are incorporated herein), comprise the entire agreement between you and publisher (and CCC) concerning this licensing transaction. In the event of any conflict between your obligations established by these terms and conditions and those established by CCC's Billing and Payment terms and conditions, these terms and conditions shall control.

14. **Revocation:** Elsevier or Copyright Clearance Center may deny the permissions described in this License at their sole discretion, for any reason or no reason, with a full refund payable to you. Notice of such denial will be made using the contact information provided by you. Failure to receive such notice will not alter or invalidate the denial. In no event will Elsevier or Copyright Clearance Center be responsible or liable for any costs, expenses or damage incurred by you as a result of a denial of your permission request, other than a refund of the amount(s) paid by you to Elsevier and/or Copyright Clearance Center for denied permissions.

### LIMITED LICENSE

The following terms and conditions apply only to specific license types:

15. **Translation:** This permission is granted for non-exclusive world **English** rights only unless your license was granted for translation rights. If you licensed translation rights you may only translate this content into the languages you requested. A professional translator must perform all translations and reproduce the content word for word preserving the integrity of the article. If this license is to re-use 1 or 2 figures then permission is granted for non-exclusive world rights in all

## Anexo 1 - Artigos Publicados

languages.

16. **Website:** The following terms and conditions apply to electronic reserve and author websites:

**Electronic reserve:** If licensed material is to be posted to website, the web site is to be password-protected and made available only to bona fide students registered on a relevant course if:

This license was made in connection with a course,

This permission is granted for 1 year only. You may obtain a license for future website posting,

All content posted to the web site must maintain the copyright information line on the bottom of each image,

A hyper-text must be included to the Homepage of the journal from which you are licensing at

<http://www.sciencedirect.com/science/journal/xxxxx> or the Elsevier homepage for books at

<http://www.elsevier.com>, and

Central Storage: This license does not include permission for a scanned version of the material to be stored in a central repository such as that provided by Heron/XanEdu.

17. **Author website** for journals with the following additional clauses:

All content posted to the web site must maintain the copyright information line on the bottom of each image, and the permission granted is limited to the personal version of your paper. You are not allowed to download and post the published electronic version of your article (whether PDF or HTML, proof or final version), nor may you scan the printed edition to create an electronic version.

A hyper-text must be included to the Homepage of the journal from which you are licensing at

<http://www.sciencedirect.com/science/journal/xxxxx>. As part of our normal production process,

you will receive an e-mail notice when your article appears on Elsevier's online service

ScienceDirect ([www.sciencedirect.com](http://www.sciencedirect.com)). That e-mail will include the article's Digital Object

Identifier (DOI). This number provides the electronic link to the published article and should be

included in the posting of your personal version. We ask that you wait until you receive this e-mail

and have the DOI to do any posting.

Central Storage: This license does not include permission for a scanned version of the material to be stored in a central repository such as that provided by Heron/XanEdu.

18. **Author website** for books with the following additional clauses:

Authors are permitted to place a brief summary of their work online only.

A hyper-text must be included to the Elsevier homepage at <http://www.elsevier.com>. All content

posted to the web site must maintain the copyright information line on the bottom of each image.

You are not allowed to download and post the published electronic version of your chapter, nor

may you scan the printed edition to create an electronic version.

Central Storage: This license does not include permission for a scanned version of the material to be stored in a central repository such as that provided by Heron/XanEdu.

19. **Website** (regular and for author): A hyper-text must be included to the Homepage of the journal from which you are licensing at <http://www.sciencedirect.com/science/journal/xxxxx>, or for books to the Elsevier homepage at <http://www.elsevier.com>

20. **Thesis/Dissertation:** If your license is for use in a thesis/dissertation your thesis may be submitted to your institution in either print or electronic form. Should your thesis be published commercially, please reapply for permission. These requirements include permission for the Library

## Anexo 1 - Artigos Publicados

---

and Archives of Canada to supply single copies, on demand, of the complete thesis and include permission for UMI to supply single copies, on demand, of the complete thesis. Should your thesis be published commercially, please reapply for permission.

### 21. Other Conditions:

v1.6

**If you would like to pay for this license now, please remit this license along with your payment made payable to "COPYRIGHT CLEARANCE CENTER" otherwise you will be invoiced within 48 hours of the license date. Payment should be in the form of a check or money order referencing your account number and this invoice number RLNK500919400. Once you receive your invoice for this order, you may pay your invoice by credit card. Please follow instructions provided at that time.**

**Make Payment To:  
Copyright Clearance Center  
Dept 001  
P.O. Box 843006  
Boston, MA 02284-3006**

**For suggestions or comments regarding this order, contact RightsLink Customer Support: [customercare@copyright.com](mailto:customercare@copyright.com) or +1-877-622-5543 (toll free in the US) or +1-978-646-2777.**

**Gratis licenses (referencing \$0 in the Total field) are free. Please retain this printable license for your reference. No payment is required.**

## Anexo 1 - Artigos Publicados

### ELSEVIER LICENSE TERMS AND CONDITIONS

Dec 18, 2012

This is a License Agreement between Claudio Airoidi ("You") and Elsevier ("Elsevier") provided by Copyright Clearance Center ("CCC"). The license consists of your order details, the terms and conditions provided by Elsevier, and the payment terms and conditions.

**All payments must be made in full to CCC. For payment instructions, please see information listed at the bottom of this form.**

|  |   |
|--|---|
| Supplier                                     | Elsevier Limited<br>The Boulevard, Langford Lane<br>Kidlington, Oxford, OX5 1GB, UK                     |
| Registered Company Number                    | 1982084   |
| Customer name                                | Claudio Airoidi   |
| Customer address                             | Chemistry institute, Unicamp, A1-100<br>Campinas, São Paulo 13083970                                    |
| License number                               | 3051920991829   |
| License date                                 | Dec 18, 2012  |
| Licensed content publisher                   | Elsevier  |
| Licensed content publication                 | Journal of Colloid and Interface Science  |
| Licensed content title                       | Cation removal using cellulose chemically modified by a Schiff base procedure applying green principles |
| Licensed content author                      | Edson C. da Silva Filho, Júlio C.P. de Melo, Maria G. da Fonseca, Claudio Airoidi                       |
| Licensed content date                        | 1 December 2009   |
| Licensed content volume number               | 340   |
| Licensed content issue number                | 1   |
| Number of pages                              | 8   |
| Start Page                                   | 8   |
| End Page                                     | 15  |
| Type of Use                                  | reuse in a thesis/dissertation  |
| Intended publisher of new work               | other   |
| Portion                                      | full article  |
| Format                                       | both print and electronic   |
| Are you the author of this Elsevier article? | Yes   |
| Will you be translating?                     | No  |
| Order reference number                       |   |

## Anexo 1 - Artigos Publicados

|                                      |   |
|--------------------------------------|---|
| Title of your thesis/dissertation    | Cellulose and Lignocellulosics as supports toward contaminants removal form liquids |
| Expected completion date             | Dec 2012  |
| Estimated size (number of pages)     | 129   |
| Elsevier VAT number                  | GB 494 6272 12  |
| Permissions price                    | 0.00 USD  |
| VAT/Local Sales Tax                  | 0.0 USD / 0.0 GBP   |
| Total                                | 0.00 USD  |
| <a href="#">Terms and Conditions</a> |   |

### INTRODUCTION

1. The publisher for this copyrighted material is Elsevier. By clicking "accept" in connection with completing this licensing transaction, you agree that the following terms and conditions apply to this transaction (along with the Billing and Payment terms and conditions established by Copyright Clearance Center, Inc. ("CCC"), at the time that you opened your Rightslink account and that are available at any time at <http://myaccount.copyright.com>).

### GENERAL TERMS

2. Elsevier hereby grants you permission to reproduce the aforementioned material subject to the terms and conditions indicated.

3. Acknowledgement: If any part of the material to be used (for example, figures) has appeared in our publication with credit or acknowledgement to another source, permission must also be sought from that source. If such permission is not obtained then that material may not be included in your publication/copies. Suitable acknowledgement to the source must be made, either as a footnote or in a reference list at the end of your publication, as follows:

"Reprinted from Publication title, Vol /edition number, Author(s), Title of article / title of chapter, Pages No., Copyright (Year), with permission from Elsevier [OR APPLICABLE SOCIETY COPYRIGHT OWNER]." Also Lancet special credit - "Reprinted from The Lancet, Vol. number, Author(s), Title of article, Pages No., Copyright (Year), with permission from Elsevier."

4. Reproduction of this material is confined to the purpose and/or media for which permission is hereby given.

5. Altering/Modifying Material: Not Permitted. However figures and illustrations may be altered/adapted minimally to serve your work. Any other abbreviations, additions, deletions and/or any other alterations shall be made only with prior written authorization of Elsevier Ltd. (Please contact Elsevier at [permissions@elsevier.com](mailto:permissions@elsevier.com))

6. If the permission fee for the requested use of our material is waived in this instance, please be advised that your future requests for Elsevier materials may attract a fee.

7. Reservation of Rights: Publisher reserves all rights not specifically granted in the combination of (i) the license details provided by you and accepted in the course of this licensing transaction, (ii) these terms and conditions and (iii) CCC's Billing and Payment terms and conditions.

8. License Contingent Upon Payment: While you may exercise the rights licensed immediately upon

issuance of the license at the end of the licensing process for the transaction, provided that you have disclosed complete and accurate details of your proposed use, no license is finally effective unless and until full payment is received from you (either by publisher or by CCC) as provided in CCC's Billing and Payment terms and conditions. If full payment is not received on a timely basis, then any license preliminarily granted shall be deemed automatically revoked and shall be void as if never granted. Further, in the event that you breach any of these terms and conditions or any of CCC's Billing and Payment terms and conditions, the license is automatically revoked and shall be void as if never granted. Use of materials as described in a revoked license, as well as any use of the materials beyond the scope of an unrevoked license, may constitute copyright infringement and publisher reserves the right to take any and all action to protect its copyright in the materials.

9. **Warranties:** Publisher makes no representations or warranties with respect to the licensed material.

10. **Indemnity:** You hereby indemnify and agree to hold harmless publisher and CCC, and their respective officers, directors, employees and agents, from and against any and all claims arising out of your use of the licensed material other than as specifically authorized pursuant to this license.

11. **No Transfer of License:** This license is personal to you and may not be sublicensed, assigned, or transferred by you to any other person without publisher's written permission.

12. **No Amendment Except in Writing:** This license may not be amended except in a writing signed by both parties (or, in the case of publisher, by CCC on publisher's behalf).

13. **Objection to Contrary Terms:** Publisher hereby objects to any terms contained in any purchase order, acknowledgment, check endorsement or other writing prepared by you, which terms are inconsistent with these terms and conditions or CCC's Billing and Payment terms and conditions. These terms and conditions, together with CCC's Billing and Payment terms and conditions (which are incorporated herein), comprise the entire agreement between you and publisher (and CCC) concerning this licensing transaction. In the event of any conflict between your obligations established by these terms and conditions and those established by CCC's Billing and Payment terms and conditions, these terms and conditions shall control.

14. **Revocation:** Elsevier or Copyright Clearance Center may deny the permissions described in this License at their sole discretion, for any reason or no reason, with a full refund payable to you. Notice of such denial will be made using the contact information provided by you. Failure to receive such notice will not alter or invalidate the denial. In no event will Elsevier or Copyright Clearance Center be responsible or liable for any costs, expenses or damage incurred by you as a result of a denial of your permission request, other than a refund of the amount(s) paid by you to Elsevier and/or Copyright Clearance Center for denied permissions.

### LIMITED LICENSE

The following terms and conditions apply only to specific license types:

15. **Translation:** This permission is granted for non-exclusive world **English** rights only unless your license was granted for translation rights. If you licensed translation rights you may only translate this content into the languages you requested. A professional translator must perform all translations and reproduce the content word for word preserving the integrity of the article. If this license is to re-use 1 or 2 figures then permission is granted for non-exclusive world rights in all

## Anexo 1 - Artigos Publicados

languages.

16. **Website:** The following terms and conditions apply to electronic reserve and author websites:

**Electronic reserve:** If licensed material is to be posted to website, the web site is to be password-protected and made available only to bona fide students registered on a relevant course if:

This license was made in connection with a course,

This permission is granted for 1 year only. You may obtain a license for future website posting.

All content posted to the web site must maintain the copyright information line on the bottom of each image,

A hyper-text must be included to the Homepage of the journal from which you are licensing at

<http://www.sciencedirect.com/science/journal/xxxxx> or the Elsevier homepage for books at

<http://www.elsevier.com>, and

Central Storage: This license does not include permission for a scanned version of the material to be stored in a central repository such as that provided by Heron/XanEdu.

17. **Author website** for journals with the following additional clauses:

All content posted to the web site must maintain the copyright information line on the bottom of each image, and the permission granted is limited to the personal version of your paper. You are not allowed to download and post the published electronic version of your article (whether PDF or HTML, proof or final version), nor may you scan the printed edition to create an electronic version.

A hyper-text must be included to the Homepage of the journal from which you are licensing at <http://www.sciencedirect.com/science/journal/xxxxx>. As part of our normal production process, you will receive an e-mail notice when your article appears on Elsevier's online service

ScienceDirect ([www.sciencedirect.com](http://www.sciencedirect.com)). That e-mail will include the article's Digital Object Identifier (DOI). This number provides the electronic link to the published article and should be included in the posting of your personal version. We ask that you wait until you receive this e-mail and have the DOI to do any posting.

Central Storage: This license does not include permission for a scanned version of the material to be stored in a central repository such as that provided by Heron/XanEdu.

18. **Author website** for books with the following additional clauses:

Authors are permitted to place a brief summary of their work online only.

A hyper-text must be included to the Elsevier homepage at <http://www.elsevier.com>. All content posted to the web site must maintain the copyright information line on the bottom of each image.

You are not allowed to download and post the published electronic version of your chapter, nor may you scan the printed edition to create an electronic version.

Central Storage: This license does not include permission for a scanned version of the material to be stored in a central repository such as that provided by Heron/XanEdu.

19. **Website** (regular and for author): A hyper-text must be included to the Homepage of the journal from which you are licensing at <http://www.sciencedirect.com/science/journal/xxxxx>. or for books to the Elsevier homepage at <http://www.elsevier.com>

20. **Thesis/Dissertation:** If your license is for use in a thesis/dissertation your thesis may be submitted to your institution in either print or electronic form. Should your thesis be published commercially, please reapply for permission. These requirements include permission for the Library

## Anexo 1 - Artigos Publicados

---

and Archives of Canada to supply single copies, on demand, of the complete thesis and include permission for UMI to supply single copies, on demand, of the complete thesis. Should your thesis be published commercially, please reapply for permission.

### 21. Other Conditions:

v1.6

**If you would like to pay for this license now, please remit this license along with your payment made payable to "COPYRIGHT CLEARANCE CENTER" otherwise you will be invoiced within 48 hours of the license date. Payment should be in the form of a check or money order referencing your account number and this invoice number RLNK500919403. Once you receive your invoice for this order, you may pay your invoice by credit card. Please follow instructions provided at that time.**

**Make Payment To:  
Copyright Clearance Center  
Dept 001  
P.O. Box 843006  
Boston, MA 02284-3006**

**For suggestions or comments regarding this order, contact RightsLink Customer Support: [customercare@copyright.com](mailto:customercare@copyright.com) or +1-877-622-5543 (toll free in the US) or +1-978-646-2777.**

**Gratis licenses (referencing \$0 in the Total field) are free. Please retain this printable license for your reference. No payment is required.**

# Anexo 1 - Artigos Publicados

## SPRINGER LICENSE TERMS AND CONDITIONS

5

Dec 18, 2012

This is a License Agreement between Claudio Airoldi ("You") and Springer ("Springer") provided by Copyright Clearance Center ("CCC"). The license consists of your order details, the terms and conditions provided by Springer, and the payment terms and conditions.

**All payments must be made in full to CCC. For payment instructions, please see information listed at the bottom of this form.**

|                                     |  |
|-------------------------------------|--|
| License Number                      | 3051921460048  |
| License date                        | Dec 18, 2012   |
| Licensed content publisher          | Springer   |
| Licensed content publication        | Journal of Thermal Analysis and Calorimetry  |
| Licensed content title              | X-ray diffraction and thermogravimetry data of cellulose, chlorodeoxycellulose and aminodeoxycellulose |
| Licensed content author             | Edson C. da Silva Filho  |
| Licensed content date               | Jan 1, 2009  |
| Volume number                       | 100  |
| Issue number                        | 1  |
| Type of Use                         | Thesis/Dissertation  |
| Portion                             | Full text  |
| Number of copies                    | 6  |
| Author of this Springer article     | Yes and you are a contributor of the new work  |
| Country of republication            | other  |
| Order reference number              |  |
| Title of your thesis / dissertation | Cellulose and Lignocellulosics as supports toward contaminants removal form liquids                    |
| Expected completion date            | Dec 2012   |
| Estimated size(pages)               | 129  |
| Total                               | 0.00 USD   |
| Terms and Conditions                |  |

### Introduction

The publisher for this copyrighted material is Springer Science + Business Media. By clicking "accept" in connection with completing this licensing transaction, you agree that the following terms and conditions apply to this transaction (along with the Billing and Payment terms and conditions established by Copyright Clearance Center, Inc. ("CCC"), at the time that you opened your Rightslink account and that are available at any time at <http://myaccount.copyright.com>).

### Limited License

## Anexo 1 - Artigos Publicados

With reference to your request to reprint in your thesis material on which Springer Science and Business Media control the copyright, permission is granted, free of charge, for the use indicated in your enquiry.

Licenses are for one-time use only with a maximum distribution equal to the number that you identified in the licensing process.

This License includes use in an electronic form, provided its password protected or on the university's intranet or repository, including UMI (according to the definition at the Sherpa website: <http://www.sherpa.ac.uk/romeo/>). For any other electronic use, please contact Springer at (permissions.dordrecht@springer.com or permissions.heidelberg@springer.com).

The material can only be used for the purpose of defending your thesis, and with a maximum of 100 extra copies in paper.

Although Springer holds copyright to the material and is entitled to negotiate on rights, this license is only valid, provided permission is also obtained from the (co) author (address is given with the article/chapter) and provided it concerns original material which does not carry references to other sources (if material in question appears with credit to another source, authorization from that source is required as well).

Permission free of charge on this occasion does not prejudice any rights we might have to charge for reproduction of our copyrighted material in the future.

#### Altering/Modifying Material: Not Permitted

You may not alter or modify the material in any manner. Abbreviations, additions, deletions and/or any other alterations shall be made only with prior written authorization of the author(s) and/or Springer Science + Business Media. (Please contact Springer at (permissions.dordrecht@springer.com or permissions.heidelberg@springer.com)

#### Reservation of Rights

Springer Science + Business Media reserves all rights not specifically granted in the combination of (i) the license details provided by you and accepted in the course of this licensing transaction, (ii) these terms and conditions and (iii) CCC's Billing and Payment terms and conditions.

#### Copyright Notice:Disclaimer

You must include the following copyright and permission notice in connection with any reproduction of the licensed material: "Springer and the original publisher /journal title, volume, year of publication, page, chapter/article title, name(s) of author(s), figure number(s), original copyright notice) is given to the publication in which the material was originally published, by adding; with kind permission from Springer Science and Business Media"

#### Warranties: None

Example 1: Springer Science + Business Media makes no representations or warranties with respect to the licensed material.

Example 2: Springer Science + Business Media makes no representations or warranties with respect to the licensed material and adopts on its own behalf the limitations and disclaimers established by CCC on its behalf in its Billing and Payment terms and conditions for this licensing transaction.

## Anexo 1 - Artigos Publicados

### Indemnity

You hereby indemnify and agree to hold harmless Springer Science + Business Media and CCC, and their respective officers, directors, employees and agents, from and against any and all claims arising out of your use of the licensed material other than as specifically authorized pursuant to this license.

### No Transfer of License

This license is personal to you and may not be sublicensed, assigned, or transferred by you to any other person without Springer Science + Business Media's written permission.

### No Amendment Except in Writing

This license may not be amended except in a writing signed by both parties (or, in the case of Springer Science + Business Media, by CCC on Springer Science + Business Media's behalf).

### Objection to Contrary Terms

Springer Science + Business Media hereby objects to any terms contained in any purchase order, acknowledgment, check endorsement or other writing prepared by you, which terms are inconsistent with these terms and conditions or CCC's Billing and Payment terms and conditions. These terms and conditions, together with CCC's Billing and Payment terms and conditions (which are incorporated herein), comprise the entire agreement between you and Springer Science + Business Media (and CCC) concerning this licensing transaction. In the event of any conflict between your obligations established by these terms and conditions and those established by CCC's Billing and Payment terms and conditions, these terms and conditions shall control.

### Jurisdiction

All disputes that may arise in connection with this present License, or the breach thereof, shall be settled exclusively by arbitration, to be held in The Netherlands, in accordance with Dutch law, and to be conducted under the Rules of the 'Netherlands Arbitrage Instituut' (Netherlands Institute of Arbitration). **OR:**

**All disputes that may arise in connection with this present License, or the breach thereof, shall be settled exclusively by arbitration, to be held in the Federal Republic of Germany, in accordance with German law.**

### Other terms and conditions:

v1.3

**If you would like to pay for this license now, please remit this license along with your payment made payable to "COPYRIGHT CLEARANCE CENTER" otherwise you will be invoiced within 48 hours of the license date. Payment should be in the form of a check or money order referencing your account number and this invoice number RLNK500919411. Once you receive your invoice for this order, you may pay your invoice by credit card. Please follow instructions provided at that time.**

**Make Payment To:  
Copyright Clearance Center  
Dept 001  
P.O. Box 843006  
Boston, MA 02284-3006**

**For suggestions or comments regarding this order, contact RightsLink Customer Support: [customercare@copyright.com](mailto:customercare@copyright.com) or +1-877-622-5543 (toll free in the US) or +1-978-646-2777.**

## Anexo 1 - Artigos Publicados

Gratis licenses (referencing \$0 in the Total field) are free. Please retain this printable license for your reference. No payment is required.

### ELSEVIER LICENSE TERMS AND CONDITIONS

Dec 18, 2012

This is a License Agreement between Claudio Airoidi ("You") and Elsevier ("Elsevier") provided by Copyright Clearance Center ("CCC"). The license consists of your order details, the terms and conditions provided by Elsevier, and the payment terms and conditions.

**All payments must be made in full to CCC. For payment instructions, please see information listed at the bottom of this form.**

|  |  |
|--|--|
| Supplier                                     | Elsevier Limited<br>The Boulevard, Langford Lane<br>Kidlington, Oxford, OX5 1GB, UK  |
| Registered Company Number                    | 1982084  |
| Customer name                                | Claudio Airoidi  |
| Customer address                             | Chemistry institute, Unicamp, A1-100<br>Campinas, São Paulo 13083970   |
| License number                               | 3051930180408  |
| License date                                 | Dec 18, 2012   |
| Licensed content publisher                   | Elsevier   |
| Licensed content publication                 | Chemical Engineering Journal   |
| Licensed content title                       | Copper sorption from aqueous solutions and sugar cane spirits by chemically modified babassu coconut ( <i>Orbignya speciosa</i> ) mesocarp   |
| Licensed content author                      | Adriana P. Vieira, Sirlane A.A. Santana, Cícero W.B. Bezerra, Hildo A.S. Silva, Júlio C.P. de Melo, Edson C. da Silva Filho, Claudio Airoidi |
| Licensed content date                        | 1 July 2010  |
| Licensed content volume number               | 161  |
| Licensed content issue number                | 1-2  |
| Number of pages                              | 7  |
| Start Page                                   | 99   |
| End Page                                     | 105  |
| Type of Use                                  | reuse in a thesis/dissertation   |
| Intended publisher of new work               | other  |
| Portion                                      | full article   |
| Format                                       | both print and electronic  |
| Are you the author of this Elsevier article? | Yes  |
| Will you be translating?                     | No   |
| Order reference number                       |  |

## Anexo 1 - Artigos Publicados

|                                      |   |
|--------------------------------------|---|
| Title of your thesis/dissertation    | Cellulose and Lignocellulosics as supports toward contaminants removal form liquids |
| Expected completion date             | Dec 2012  |
| Estimated size (number of pages)     | 129   |
| Elsevier VAT number                  | GB 494 6272 12  |
| Permissions price                    | 0.00 USD  |
| VAT/Local Sales Tax                  | 0.0 USD / 0.0 GBP   |
| Total                                | 0.00 USD  |
| <a href="#">Terms and Conditions</a> |   |

### INTRODUCTION

1. The publisher for this copyrighted material is Elsevier. By clicking "accept" in connection with completing this licensing transaction, you agree that the following terms and conditions apply to this transaction (along with the Billing and Payment terms and conditions established by Copyright Clearance Center, Inc. ("CCC"), at the time that you opened your Rightslink account and that are available at any time at <http://myaccount.copyright.com>).

### GENERAL TERMS

2. Elsevier hereby grants you permission to reproduce the aforementioned material subject to the terms and conditions indicated.

3. Acknowledgement: If any part of the material to be used (for example, figures) has appeared in our publication with credit or acknowledgement to another source, permission must also be sought from that source. If such permission is not obtained then that material may not be included in your publication/copies. Suitable acknowledgement to the source must be made, either as a footnote or in a reference list at the end of your publication, as follows:

"Reprinted from Publication title, Vol /edition number, Author(s), Title of article / title of chapter, Pages No., Copyright (Year), with permission from Elsevier [OR APPLICABLE SOCIETY COPYRIGHT OWNER]." Also Lancet special credit - "Reprinted from The Lancet, Vol. number, Author(s), Title of article, Pages No., Copyright (Year), with permission from Elsevier."

4. Reproduction of this material is confined to the purpose and/or media for which permission is hereby given.

5. Altering/Modifying Material: Not Permitted. However figures and illustrations may be altered/adapted minimally to serve your work. Any other abbreviations, additions, deletions and/or any other alterations shall be made only with prior written authorization of Elsevier Ltd. (Please contact Elsevier at [permissions@elsevier.com](mailto:permissions@elsevier.com))

6. If the permission fee for the requested use of our material is waived in this instance, please be advised that your future requests for Elsevier materials may attract a fee.

7. Reservation of Rights: Publisher reserves all rights not specifically granted in the combination of (i) the license details provided by you and accepted in the course of this licensing transaction, (ii) these terms and conditions and (iii) CCC's Billing and Payment terms and conditions.

## Anexo 1 - Artigos Publicados

8. License Contingent Upon Payment: While you may exercise the rights licensed immediately upon issuance of the license at the end of the licensing process for the transaction, provided that you have disclosed complete and accurate details of your proposed use, no license is finally effective unless and until full payment is received from you (either by publisher or by CCC) as provided in CCC's Billing and Payment terms and conditions. If full payment is not received on a timely basis, then any license preliminarily granted shall be deemed automatically revoked and shall be void as if never granted. Further, in the event that you breach any of these terms and conditions or any of CCC's Billing and Payment terms and conditions, the license is automatically revoked and shall be void as if never granted. Use of materials as described in a revoked license, as well as any use of the materials beyond the scope of an unrevoked license, may constitute copyright infringement and publisher reserves the right to take any and all action to protect its copyright in the materials.

9. Warranties: Publisher makes no representations or warranties with respect to the licensed material.

10. Indemnity: You hereby indemnify and agree to hold harmless publisher and CCC, and their respective officers, directors, employees and agents, from and against any and all claims arising out of your use of the licensed material other than as specifically authorized pursuant to this license.

11. No Transfer of License: This license is personal to you and may not be sublicensed, assigned, or transferred by you to any other person without publisher's written permission.

12. No Amendment Except in Writing: This license may not be amended except in a writing signed by both parties (or, in the case of publisher, by CCC on publisher's behalf).

13. Objection to Contrary Terms: Publisher hereby objects to any terms contained in any purchase order, acknowledgment, check endorsement or other writing prepared by you, which terms are inconsistent with these terms and conditions or CCC's Billing and Payment terms and conditions. These terms and conditions, together with CCC's Billing and Payment terms and conditions (which are incorporated herein), comprise the entire agreement between you and publisher (and CCC) concerning this licensing transaction. In the event of any conflict between your obligations established by these terms and conditions and those established by CCC's Billing and Payment terms and conditions, these terms and conditions shall control.

14. Revocation: Elsevier or Copyright Clearance Center may deny the permissions described in this License at their sole discretion, for any reason or no reason, with a full refund payable to you. Notice of such denial will be made using the contact information provided by you. Failure to receive such notice will not alter or invalidate the denial. In no event will Elsevier or Copyright Clearance Center be responsible or liable for any costs, expenses or damage incurred by you as a result of a denial of your permission request, other than a refund of the amount(s) paid by you to Elsevier and/or Copyright Clearance Center for denied permissions.

### LIMITED LICENSE

The following terms and conditions apply only to specific license types:

15. **Translation:** This permission is granted for non-exclusive world **English** rights only unless your license was granted for translation rights. If you licensed translation rights you may only translate this content into the languages you requested. A professional translator must perform all translations and reproduce the content word for word preserving the integrity of the article. If this

## Anexo 1 - Artigos Publicados

license is to re-use 1 or 2 figures then permission is granted for non-exclusive world rights in all languages.

16. **Website:** The following terms and conditions apply to electronic reserve and author websites:

**Electronic reserve:** If licensed material is to be posted to website, the web site is to be password-protected and made available only to bona fide students registered on a relevant course if:

This license was made in connection with a course,

This permission is granted for 1 year only. You may obtain a license for future website posting,

All content posted to the web site must maintain the copyright information line on the bottom of each image,

A hyper-text must be included to the Homepage of the journal from which you are licensing at

<http://www.sciencedirect.com/science/journal/xxxxx> or the Elsevier homepage for books at

<http://www.elsevier.com> , and

**Central Storage:** This license does not include permission for a scanned version of the material to be stored in a central repository such as that provided by Heron/XanEdu.

17. **Author website** for journals with the following additional clauses:

All content posted to the web site must maintain the copyright information line on the bottom of each image, and the permission granted is limited to the personal version of your paper. You are not allowed to download and post the published electronic version of your article (whether PDF or HTML, proof or final version), nor may you scan the printed edition to create an electronic version.

A hyper-text must be included to the Homepage of the journal from which you are licensing at <http://www.sciencedirect.com/science/journal/xxxxx> . As part of our normal production process, you will receive an e-mail notice when your article appears on Elsevier's online service ScienceDirect ([www.sciencedirect.com](http://www.sciencedirect.com)). That e-mail will include the article's Digital Object Identifier (DOI). This number provides the electronic link to the published article and should be included in the posting of your personal version. We ask that you wait until you receive this e-mail and have the DOI to do any posting.

**Central Storage:** This license does not include permission for a scanned version of the material to be stored in a central repository such as that provided by Heron/XanEdu.

18. **Author website** for books with the following additional clauses:

Authors are permitted to place a brief summary of their work online only.

A hyper-text must be included to the Elsevier homepage at <http://www.elsevier.com> . All content posted to the web site must maintain the copyright information line on the bottom of each image.

You are not allowed to download and post the published electronic version of your chapter, nor may you scan the printed edition to create an electronic version.

**Central Storage:** This license does not include permission for a scanned version of the material to be stored in a central repository such as that provided by Heron/XanEdu.

19. **Website** (regular and for author): A hyper-text must be included to the Homepage of the journal from which you are licensing at <http://www.sciencedirect.com/science/journal/xxxxx> . or for books to the Elsevier homepage at <http://www.elsevier.com>

20. **Thesis/Dissertation:** If your license is for use in a thesis/dissertation your thesis may be submitted to your institution in either print or electronic form. Should your thesis be published

## Anexo 1 - Artigos Publicados

---

commercially, please reapply for permission. These requirements include permission for the Library and Archives of Canada to supply single copies, on demand, of the complete thesis and include permission for UMI to supply single copies, on demand, of the complete thesis. Should your thesis be published commercially, please reapply for permission.

### 21. Other Conditions:

v1.6

**If you would like to pay for this license now, please remit this license along with your payment made payable to "COPYRIGHT CLEARANCE CENTER" otherwise you will be invoiced within 48 hours of the license date. Payment should be in the form of a check or money order referencing your account number and this invoice number RLNK500919416. Once you receive your invoice for this order, you may pay your invoice by credit card. Please follow instructions provided at that time.**

**Make Payment To:  
Copyright Clearance Center  
Dept 001  
P.O. Box 843006  
Boston, MA 02284-3006**

**For suggestions or comments regarding this order, contact RightsLink Customer Support: [customer care@copyright.com](mailto:customer care@copyright.com) or +1-877-622-5543 (toll free in the US) or +1-978-646-2777.**

**Gratis licenses (referencing \$0 in the Total field) are free. Please retain this printable license for your reference. No payment is required.**

---

# Anexo 1 - Artigos Publicados

## ELSEVIER LICENSE TERMS AND CONDITIONS

Dec 18, 2012

This is a License Agreement between Claudio Airoidi ("You") and Elsevier ("Elsevier") provided by Copyright Clearance Center ("CCC"). The license consists of your order details, the terms and conditions provided by Elsevier, and the payment terms and conditions.

**All payments must be made in full to CCC. For payment instructions, please see information listed at the bottom of this form.**

|  |  |
|--|--|
| Supplier                                     | Elsevier Limited<br>The Boulevard, Langford Lane<br>Kidlington, Oxford, OX5 1GB, UK                    |
| Registered Company Number                    | 1982084  |
| Customer name                                | Claudio Airoidi  |
| Customer address                             | Chemistry institute, Unicamp, A1-100<br>Campinas, São Paulo 13083970                                   |
| License number                               | 3051930539358  |
| License date                                 | Dec 18, 2012   |
| Licensed content publisher                   | Elsevier   |
| Licensed content publication                 | Journal of Hazardous Materials   |
| Licensed content title                       | Immobilization of ethylenesulfide on babassu coconut epicarp and mesocarp for divalent cation sorption |
| Licensed content author                      | Sirlane A.A. Santana, Adriana P. Vieira, Edson C. da Silva Filho, Júlio C.P. Melo, Claudio Airoidi     |
| Licensed content date                        | 15 February 2010   |
| Licensed content volume number               | 174  |
| Licensed content issue number                | 1-3  |
| Number of pages                              | 6  |
| Start Page                                   | 714  |
| End Page                                     | 719  |
| Type of Use                                  | reuse in a thesis/dissertation   |
| Intended publisher of new work               | other  |
| Portion                                      | full article   |
| Format                                       | both print and electronic  |
| Are you the author of this Elsevier article? | Yes  |
| Will you be translating?                     | No   |
| Order reference number                       |  |

## Anexo 1 - Artigos Publicados

|                                      |   |
|--------------------------------------|---|
| Title of your thesis/dissertation    | Cellulose and Lignocellulosics as supports toward contaminants removal form liquids |
| Expected completion date             | Dec 2012  |
| Estimated size (number of pages)     | 129   |
| Elsevier VAT number                  | GB 494 6272 12  |
| Permissions price                    | 0.00 USD  |
| VAT/Local Sales Tax                  | 0.0 USD / 0.0 GBP   |
| Total                                | 0.00 USD  |
| <a href="#">Terms and Conditions</a> |   |

### INTRODUCTION

1. The publisher for this copyrighted material is Elsevier. By clicking "accept" in connection with completing this licensing transaction, you agree that the following terms and conditions apply to this transaction (along with the Billing and Payment terms and conditions established by Copyright Clearance Center, Inc. ("CCC"), at the time that you opened your Rightslink account and that are available at any time at <http://myaccount.copyright.com>).

### GENERAL TERMS

2. Elsevier hereby grants you permission to reproduce the aforementioned material subject to the terms and conditions indicated.

3. Acknowledgement: If any part of the material to be used (for example, figures) has appeared in our publication with credit or acknowledgement to another source, permission must also be sought from that source. If such permission is not obtained then that material may not be included in your publication/copies. Suitable acknowledgement to the source must be made, either as a footnote or in a reference list at the end of your publication, as follows:

"Reprinted from Publication title, Vol /edition number, Author(s), Title of article / title of chapter, Pages No., Copyright (Year), with permission from Elsevier [OR APPLICABLE SOCIETY COPYRIGHT OWNER]." Also Lancet special credit - "Reprinted from The Lancet, Vol. number, Author(s), Title of article, Pages No., Copyright (Year), with permission from Elsevier."

4. Reproduction of this material is confined to the purpose and/or media for which permission is hereby given.

5. Altering/Modifying Material: Not Permitted. However figures and illustrations may be altered/adapted minimally to serve your work. Any other abbreviations, additions, deletions and/or any other alterations shall be made only with prior written authorization of Elsevier Ltd. (Please contact Elsevier at [permissions@elsevier.com](mailto:permissions@elsevier.com))

6. If the permission fee for the requested use of our material is waived in this instance, please be advised that your future requests for Elsevier materials may attract a fee.

7. Reservation of Rights: Publisher reserves all rights not specifically granted in the combination of (i) the license details provided by you and accepted in the course of this licensing transaction, (ii) these terms and conditions and (iii) CCC's Billing and Payment terms and conditions.

8. License Contingent Upon Payment: While you may exercise the rights licensed immediately upon

## Anexo 1 - Artigos Publicados

languages.

16. **Website:** The following terms and conditions apply to electronic reserve and author websites:

**Electronic reserve:** If licensed material is to be posted to website, the web site is to be password-protected and made available only to bona fide students registered on a relevant course if:

This license was made in connection with a course,

This permission is granted for 1 year only. You may obtain a license for future website posting.

All content posted to the web site must maintain the copyright information line on the bottom of each image,

A hyper-text must be included to the Homepage of the journal from which you are licensing at

<http://www.sciencedirect.com/science/journal/xxxxx> or the Elsevier homepage for books at

<http://www.elsevier.com>, and

Central Storage: This license does not include permission for a scanned version of the material to be stored in a central repository such as that provided by Heron/XanEdu.

17. **Author website** for journals with the following additional clauses:

All content posted to the web site must maintain the copyright information line on the bottom of each image, and the permission granted is limited to the personal version of your paper. You are not allowed to download and post the published electronic version of your article (whether PDF or HTML, proof or final version), nor may you scan the printed edition to create an electronic version.

A hyper-text must be included to the Homepage of the journal from which you are licensing at <http://www.sciencedirect.com/science/journal/xxxxx>. As part of our normal production process, you will receive an e-mail notice when your article appears on Elsevier's online service

ScienceDirect ([www.sciencedirect.com](http://www.sciencedirect.com)). That e-mail will include the article's Digital Object Identifier (DOI). This number provides the electronic link to the published article and should be included in the posting of your personal version. We ask that you wait until you receive this e-mail and have the DOI to do any posting.

Central Storage: This license does not include permission for a scanned version of the material to be stored in a central repository such as that provided by Heron/XanEdu.

18. **Author website** for books with the following additional clauses:

Authors are permitted to place a brief summary of their work online only.

A hyper-text must be included to the Elsevier homepage at <http://www.elsevier.com>. All content posted to the web site must maintain the copyright information line on the bottom of each image.

You are not allowed to download and post the published electronic version of your chapter, nor may you scan the printed edition to create an electronic version.

Central Storage: This license does not include permission for a scanned version of the material to be stored in a central repository such as that provided by Heron/XanEdu.

19. **Website** (regular and for author): A hyper-text must be included to the Homepage of the journal from which you are licensing at <http://www.sciencedirect.com/science/journal/xxxxx>, or for books to the Elsevier homepage at <http://www.elsevier.com>

20. **Thesis/Dissertation:** If your license is for use in a thesis/dissertation your thesis may be submitted to your institution in either print or electronic form. Should your thesis be published commercially, please reapply for permission. These requirements include permission for the Library

## Anexo 1 - Artigos Publicados

---

and Archives of Canada to supply single copies, on demand, of the complete thesis and include permission for UMI to supply single copies, on demand, of the complete thesis. Should your thesis be published commercially, please reapply for permission.

### 21. Other Conditions:

v1.6

**If you would like to pay for this license now, please remit this license along with your payment made payable to "COPYRIGHT CLEARANCE CENTER" otherwise you will be invoiced within 48 hours of the license date. Payment should be in the form of a check or money order referencing your account number and this invoice number RLNK500919420. Once you receive your invoice for this order, you may pay your invoice by credit card. Please follow instructions provided at that time.**

**Make Payment To:  
Copyright Clearance Center  
Dept 001  
P.O. Box 843006  
Boston, MA 02284-3006**

**For suggestions or comments regarding this order, contact RightsLink Customer Support: [customer care@copyright.com](mailto:customer care@copyright.com) or +1-877-622-5543 (toll free in the US) or +1-978-646-2777.**

**Gratis licenses (referencing \$0 in the Total field) are free. Please retain this printable license for your reference. No payment is required.**